frontiers | Research Topics

Epigenetic therapy against cancer: Toward new molecular targets and technologies

Edited by
Christiane Pienna Soares, Ângela Sousa, Chung Man Chin, Fatima Valdes-Mora and Daniela Trisciuoglio

Published in
Frontiers in Cell and Developmental Biology
Frontiers in Genetics

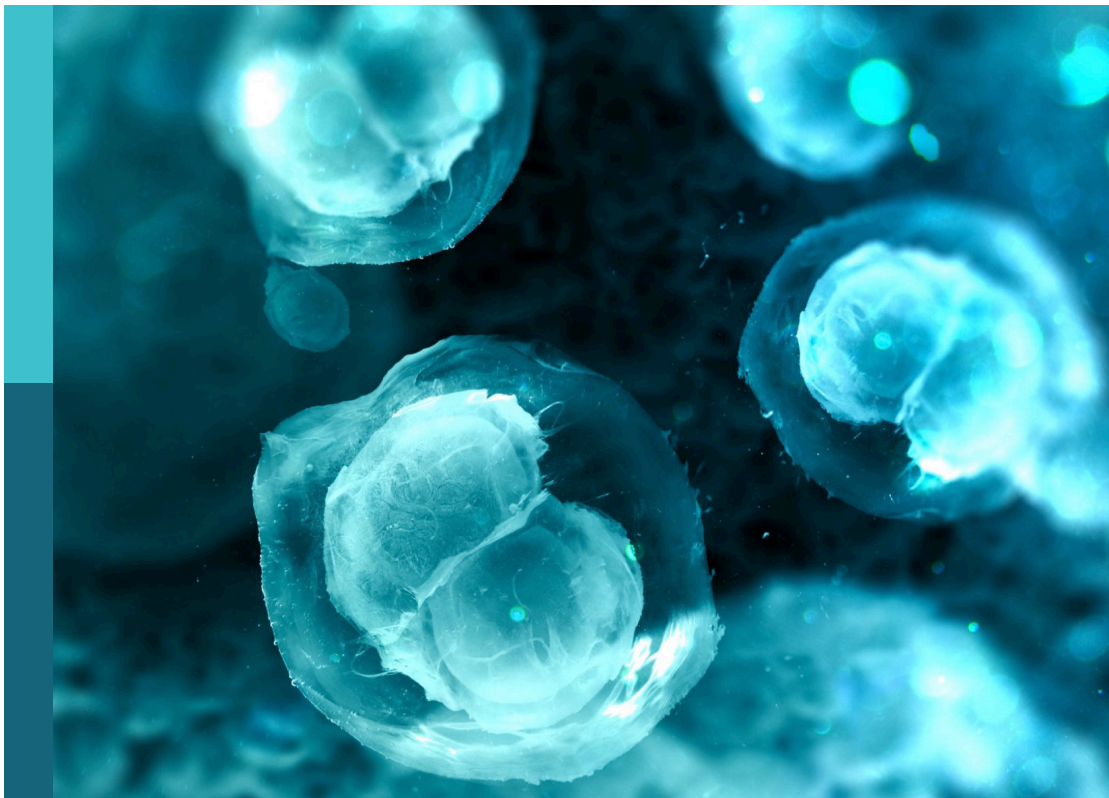

ISSN 1664-8714
ISBN 978-2-8325-2642-2
DOI 10.3389/978-2-8325-2642-2

About Frontiers

Frontiers is more than just an open access publisher of scholarly articles: it is a pioneering approach to the world of academia, radically improving the way scholarly research is managed. The grand vision of Frontiers is a world where all people have an equal opportunity to seek, share and generate knowledge. Frontiers provides immediate and permanent online open access to all its publications, but this alone is not enough to realize our grand goals.

Frontiers journal series

The Frontiers journal series is a multi-tier and interdisciplinary set of open-access, online journals, promising a paradigm shift from the current review, selection and dissemination processes in academic publishing. All Frontiers journals are driven by researchers for researchers; therefore, they constitute a service to the scholarly community. At the same time, the *Frontiers journal series* operates on a revolutionary invention, the tiered publishing system, initially addressing specific communities of scholars, and gradually climbing up to broader public understanding, thus serving the interests of the lay society, too.

Dedication to quality

Each Frontiers article is a landmark of the highest quality, thanks to genuinely collaborative interactions between authors and review editors, who include some of the world's best academicians. Research must be certified by peers before entering a stream of knowledge that may eventually reach the public - and shape society; therefore, Frontiers only applies the most rigorous and unbiased reviews. Frontiers revolutionizes research publishing by freely delivering the most outstanding research, evaluated with no bias from both the academic and social point of view. By applying the most advanced information technologies, Frontiers is catapulting scholarly publishing into a new generation.

What are Frontiers Research Topics?

Frontiers Research Topics are very popular trademarks of the *Frontiers journals series*: they are collections of at least ten articles, all centered on a particular subject. With their unique mix of varied contributions from Original Research to Review Articles, Frontiers Research Topics unify the most influential researchers, the latest key findings and historical advances in a hot research area.

Find out more on how to host your own Frontiers Research Topic or contribute to one as an author by contacting the Frontiers editorial office: frontiersin.org/about/contact

Epigenetic therapy against cancer: Toward new molecular targets and technologies

Topic editors

Christiane Pienna Soares — Sao Paulo State Universty, Brazil
Ângela Sousa — University of Beira Interior, Covilhã, Portugal
Chung Man Chin — School of Medicine, UNION of the Colleges of the GREAT LAKES (UNILAGO), Brazil
Fatima Valdes-Mora — Children's Cancer Institute Australia, Australia
Daniela Trisciuoglio — Institute of Molecular Biology and Pathology, Department of Biomedical Sciences, National Research Council (CNR), Italy

Citation

Soares, C. P., Sousa, Â., Chin, C. M., Valdes-Mora, F., Trisciuoglio, D., eds. (2023). *Epigenetic therapy against cancer: Toward new molecular targets and technologies*. Lausanne: Frontiers Media SA. doi: 10.3389/978-2-8325-2642-2

Table of contents

frontiers | Frontiers in Cell and Developmental Biology

TYPE Editorial
PUBLISHED 24 May 2023
DOI 10.3389/fcell.2023.1218986

OPEN ACCESS

EDITED AND REVIEWED BY
Michael E. Symonds,
University of Nottingham,
United Kingdom

*CORRESPONDENCE
Ângela Sousa,
angela@fcsaude.ubi.pt

†These authors have contributed equally to this work

RECEIVED 08 May 2023
ACCEPTED 11 May 2023
PUBLISHED 24 May 2023

CITATION
Sousa Â, Soares CP, Chin CM, Trisciuoglio D and Valdes-Mora F (2023), Editorial: Epigenetic therapy against cancer: toward new molecular targets and technologies.
Front. Cell Dev. Biol. 11:1218986.
doi: 10.3389/fcell.2023.1218986

Editorial: Epigenetic therapy against cancer: toward new molecular targets and technologies

Ângela Sousa[1*†], Christiane P. Soares[2†], Chung Man Chin[2,3†], Daniela Trisciuoglio[4†] and Fatima Valdes-Mora[5,6†]

[1]CICS-UBI—Health Science Research Centre, University of Beira Interior, Covilhã, Portugal, [2]School of Pharmaceutical Sciences, São Paulo State University (UNESP), Araraquara, Brazil, [3]School of Medicine, UNION of the Colleges of the GREAT LAKES (UNILAGO), Sao José do Rio Preto, Brazil, [4]IBPM Institute of Molecular Biology and Pathology, CNR National Research Council, C/o Department of Biology and Biotechnology "Charles Darwin", Sapienza University of Rome, Rome, Italy, [5]Children's Cancer Institute Australia Randwick, Randwick, NSW, Australia, [6]Garvan Institute of Medical Research Darlinghurst, Darlinghurst, NSW, Australia

KEYWORDS

cancer therapy, epigenetics, histone deacetylases, inhibitors, prognostic biomarker, tumor microenvironment

Editorial on the Research Topic
Epigenetic therapy against cancer: toward new molecular targets and technologies

Epigenetics is defined as a group of inheritable changes in gene expression without modifications to the DNA sequence. DNA methylation, histone deacetylation and non-coding RNA expression are examples of epigenetic control. Disruption of the epigenetic program of gene expression is a hallmark of cancer that initiates and propagates tumorigenesis. Considering that epigenetic modifications are reversible, the ability to restore the cancer epigenome through the inhibition of the epigenetic modifiers is a promising therapy for cancer treatment, by monotherapy or in combination with other anticancer therapies, including immunotherapies. Costa et al., summarized the main epigenetic alterations, their potential as a biomarker for early diagnosis and the epigenetic therapies approved for cancer treatment.

Anti-programmed cell death protein 1 (PD-1) or PD-ligand 1 (PD-L1) immune checkpoint therapy has shown exciting clinical outcomes in diverse human cancers. Shao et al., highlighted biological characteristics of exosome PD-L1 in tumor immunity, exosome PD-L1 detection methods and proposed that exosome PD-L1 can be a target for overcoming anti-PD-1/PD-L1 antibody treatment resistance. On the other hand, Jia and Wan, investigated the role and function of inositol-3-phosphate synthase 1 (ISYNA1) in pan-cancer, especially in colon adenocarcinoma (COAD). These authors found that ISYNA1 can be a potential prognostic biomarker in COAD, being positively correlated with the immunosuppressive tumor microenvironment (TME). In breast cancer (BC), the most common tumor in women, Zou et al., analyzed the expression, alteration, prognosis, and biological functions of various KCNKs genes. They verified that seven KCNKs genes can regulate breast cancer progression via modulating immune response and established a specific prognostic signature using these genes as ideal biomarkers for breast cancer patients.

Xiong et al., observed that DNA-methylation-based biomarker for body mass index (DM-BMI)-related genes were mostly involved in the process of cancer immunity, being positively correlated with immune checkpoint inhibitors (ICI) response markers in BC. In addition, Liu et al., found that NPY5R was frequently downregulated in BC tissues, due to its aberrant promoter CpG methylation, being considered a candidate biomarker. In consequence, ectopic expression of NPY5R significantly reduced breast tumor cell growth, induced cell apoptosis and G2/M arrest, acting as a tumor suppressor. Moreover, NPY5R also promoted the sensitivity of BC cells to chemotherapy by doxorubicin.

Multiple myeloma (MM) is an incurable clonal plasma cell malignancy, being fundamental its understanding and search for efficient therapeutic options. Vlummens et al., identified protein arginine methyltransferase 5 (PRMT5) as a promising prognostic target involved in DNA repair and epigenetics associated with high-risk myeloma, by using bioinformatic tools. They also verified that EPZ015938 strongly reduced the total symmetric-dimethyl arginine levels (PRMT5-inhibitor) in several human myeloma cell lines, leading to a decreased cellular growth and at later time points, apoptosis occurred. Mohammed et al., found that both H3K27 histone demethylases, namely, KDM6A/B, were highly expressed in epithelial cancer cells that lose attachment from the extracellular matrix (ECM) and their inhibition resulted in reduced sphere formation capacity and increased apoptosis.

Glioma is the most common and aggressive malignancy of the central nervous system. Li et al., identified deacetylases (HDACs) 1/2/3/4/5/7/9/10/11 as useful biomarkers for predicting the survival of patients with glioma. Furthermore, HDACs are considered putative precision therapy targets, since their expression are correlated with of immune cell infiltration in patients with glioma. He et al., studied the prognostic value and therapeutic perspectives of CXC chemokine receptor (CXCR) members, a complex of the immune-associated protein involved in tumor activation, invasion, migration, and angiogenesis through various chemical signals, in the glioma microenvironment. Zheng et al., identified a new n6-methyladenosine (m6A) methylation modification patterns and TME infiltration landscape that predict clinical outcomes for papillary renal cell carcinoma patients. In parallel, Luo et al., evaluated and characterized m6A regulator-mediated methylation modification patterns and verified that m6A modification plays an essential role in TME infiltration in ovarian cancer patients which can guide immunotherapy strategies with ICI. Moreover, Dai and Ye, developed and validated a novel histone acetylation-based gene signature that has a well predictive effect on the prognosis of ovarian cancer and can potentially be applied for clinical treatments.

Colorectal cancer can originate by a dysbiosis configuration, that results in the biofilm formation, production of toxic metabolites, DNA damage in intestinal epithelial cells through the secretion of genotoxins, and epigenetic regulation of oncogenes. Schemczssen-Graeff and Pileggi, highlighted the study of potential bacteria as a complement for cancer treatment, being considered the next-generation probiotics and live biotherapeutic products, can have a controlling action in epigenetic processes, changes in the regulation of genes of microbiome and host.

Author contributions

All authors listed have made a substantial, direct, and intellectual contribution to the work and approved it for publication.

Funding

ÂS was supported by CICS-UBI projects UIDB/00709/2020 and UIDP/00709/2020, financed by national funds through the Portuguese Foundation for Science and Technology/MCTES. CC is supported by Fundação de Amparo à Pesquisa do Estado de São Paulo (FAPESP) PROC. 2019/10746-6 and National Council for Scientific and Technological Development (CNPq) for productivity fellowship level 2 (CNPq process 306009/2022-6). DT was supported by Banca d'Italia Contributo liberale 2021and AIRCprojects under IG 2020-ID 24942.

Acknowledgments

We thank all the authors and reviewers for their contribution to the Research Topic.

Conflict of interest

The authors declare that the research was conducted in the absence of any commercial or financial relationships that could be construed as a potential conflict of interest.

Publisher's note

frontiers in Cell and Developmental Biology

REVIEW
published: 15 October 2021
doi: 10.3389/fcell.2021.760211

Effects of Tumor-Derived Exosome Programmed Death Ligand 1 on Tumor Immunity and Clinical Applications

Bo Shao[1,2†], Qin Dang[1†], Zhuang Chen[1], Chen Chen[2,3], Quanbo Zhou[1], Bingbing Qiao[4], Jinbo Liu[1], Shengyun Hu[1], Guixian Wang[1], Weitang Yuan[1] and Zhenqiang Sun[1,3]*

[1] Department of Colorectal Surgery, The First Affiliated Hospital of Zhengzhou University, Zhengzhou, China, [2] Academy of Medical Sciences, Zhengzhou University, Zhengzhou, China, [3] School of Life Sciences, Zhengzhou University, Zhengzhou, China, [4] Department of Hepatobiliary and Pancreatic Surgery, The First Affiliated Hospital of Zhengzhou University, Zhengzhou, China

Programmed death ligand 1 (PD-L1) is a typical immune surface protein that binds to programmed cell death 1 (PD-1) on T cells through its extracellular domain. Subsequently, T cell activity is inhibited, and tumor immune tolerance is enhanced. Anti-PD-1/PD-L1 immune checkpoint therapy blocks the combination of PD-1/PD-L1 and rejuvenates depleted T cells, thereby inhibiting tumor growth. Exosomes are biologically active lipid bilayer nanovesicles secreted by various cell types, which mediate signal communication between cells. Studies have shown that PD-L1 can not only be expressed on the surface of tumor cells, immune cells, and other cells in the tumor microenvironment, but also be released from tumor cells and exist in an extracellular form. In particular, exosome PD-L1 plays an unfavorable role in tumor immunosuppression. The immunomodulatory effect of exosome PD-L1 and its potential in fluid diagnosis have attracted our attention. This review aims to summarize the available evidence regarding the biological characteristics of exosome PD-L1 in tumor immunity, with a particular focus on the mechanisms in different cancers and clinical prospects. In addition, we also summarized the current possible and effective detection methods for exosome PD-L1 and proposed that exosome PD-L1 has the potential to become a target for overcoming anti-PD-1/PD-L1 antibody treatment resistance.

Keywords: exosome, PD-L1, PD-1, tumor immunity, biomarker

OPEN ACCESS

Edited by:
Christiane Pienna Soares, São Paulo State University, Brazil

Reviewed by:
Maria Eduarda Battistella, Federal University of Rio Grande do Sul, Brazil
Akbar Nawab, University of Florida, United States

***Correspondence:**
Zhenqiang Sun
fccsunzq@zzu.edu.cn

† These authors have contributed equally to this work and share first authorship

Specialty section:
This article was submitted to Epigenomics and Epigenetics, a section of the journal Frontiers in Cell and Developmental Biology

Received: *17 August 2021*
Accepted: *24 September 2021*
Published: *15 October 2021*

Citation:
Shao B, Dang Q, Chen Z, Chen C, Zhou Q, Qiao B, Liu J, Hu S, Wang G, Yuan W and Sun Z (2021) Effects of Tumor-Derived Exosome Programmed Death Ligand 1 on Tumor Immunity and Clinical Applications. Front. Cell Dev. Biol. 9:760211. doi: 10.3389/fcell.2021.760211

INTRODUCTION

Programmed cell death-1 (PD-1), also known as CD279, is expressed in a variety of immune cells, including peripheral activated T cells, B cells, and monocytes (Nishimura et al., 1996; Keir et al., 2008). The two known ligands of PD-1 are Programmed death-ligand 1 PD-L1 (B7-H1) and PD-L2 (B7-DC) (Blank et al., 2004). PD-L1 is a typical immune surface protein that binds to PD-1

Abbreviations: PD-L1, programmed death ligand 1; PD-1, programmed cell death 1; ILV, intraluminal vesicles; MVE, multiple vesicle endosomes; ESCRT, endosomal complex required for transportation; TAM, tumor-associated macrophages; sPD-L1, soluble PD-L1; DCs, dendritic cells; Tregs, regulatory T cells; NSCLC, non-small cell lung cancer; HNSCC, Head and neck squamous cell carcinoma; PD-L1 (KD) B16-F10, knockout of PD-L1-expressed B16-F10 cells; APCs, antigen presenting cells; CTL, cytotoxic T lymphocytes; HSCs, hematopoietic stem cells; SPR, surface plasmon resonance; PDAC, Pancreatic ductal adenocarcinoma; ELISA, enzyme-linked immunosorbent assay.

on T cells through its extracellular domain (Dong et al., 1999). PD-L1 inhibits the activity of T cells and enhances the immune tolerance of tumor cells, thereby preventing the immune response, which may damage the tumor, and leading to the immune escape of the tumor. PD-L1 was the first PD-1 ligand to be discovered. Numerous studies have shown that PD-L1 is abnormally expressed in many tumors, such as skin, brain, thyroid, esophageal, and colorectal tumors (Lin et al., 2015; Wang et al., 2016; Zhou et al., 2017). Therefore, PD-L1 is considered to be a critical factor involved in tumor immune escape.

Exosomes are biologically active extracellular vesicles approximately 30–120 nm in diameter with a lipid bilayer structure that are secreted by various cells (Théry et al., 2002). Exosomes are intraluminal vesicles (ILVs) formed by inward endosomal membrane budding during the maturation of multiple vesicular endosomes (MVEs; Colombo et al., 2014; Hessvik and Llorente, 2018). MVEs can fuse with lysosomes, leading to the degradation of extracellular vesicles and the recycling of their contents, which promotes cellular metabolism. MVEs also fuse with the cell membrane, causing ILVs to be released extracellularly, and these ILVs that are released from the cell are called exosomes (Colombo et al., 2014). Exosomes are released by various cell types and are stably present in all body fluids (Boukouris and Mathivanan, 2015). It has been widely validated that exosome facilitate communication between cells and the exchange of proteins, nucleic acids, and other substances (Lo Cicero et al., 2015; Cordonnier et al., 2017; Mashouri et al., 2019). Exosomes precisely transfer many biological components to target cells and are an effective way to affect gene expression in distant cells. These biological components are wrapped in a double membrane, which is stable even after being transferred to a remote location (Kourembanas, 2015; van Niel et al., 2018). Exosome biogenesis is a complex process. Lipid- and membrane-associated proteins accumulate in discrete membrane microdomains of the MVE, which then recruits soluble components such as cytoplasmic proteins, RNA, DNA, and cytokines (Nolte-'t Hoen et al., 2012; Villarroya-Beltri et al., 2013; Thakur et al., 2014). This process in turn involves important subunits of the endosomal complex required for transportation (ESCRT). Various subunits of ESCRT are involved in the formation of the entire ILV (Colombo et al., 2013). Recent experimental data indicate that interfering with the RNA of genes associated with ESCRT inactivating these proteins and components affect the secretion efficiency and composition of ILVs (Monypenny et al., 2018). However, some researchers have found that after knocking out the ESCRT complex, exosomes containing the marker CD63 are still present, which means that there may be ESCRT-independent ways to produce exosomes (Stuffers et al., 2009). Exosomes are involved in a wide range of processes, such as metabolic reprogramming (Thakur et al., 2020), macrophage M2 polarization (Ono et al., 2020), tissue repair (Roefs et al., 2020), osteogenic differentiation (Colletti et al., 2020), and hair regeneration (Hu et al., 2020). Emerging evidence suggests that tumor cells attenuate anti-tumor immunity by expressing biologically active PD-L1 on the surface of their secreted exosomes. In this review, we mainly summarize the mechanism of tumor-derived exosome PD-L1 in the context of tumor immunity and its potential significance in distinct tumor types.

BIOGENESIS AND MOLECULAR CHARACTERISTICS OF EXOSOME PD-L1

Programmed death ligand 1 is a protein that is expressed on the cell surface. Activation of the PD-1/PD-L1 pathway mainly leads to tumor immune escape and promotes tumor cell growth by affecting T cell tolerance, T cell apoptosis, and T cell failure and enhancing Treg cell functions (Ichikawa and Chen, 2005; Mittal et al., 2014; Zhang et al., 2015). PD-L1 is expressed on the surface of tumor cells (Wang et al., 2016) and promotes tumor immune escape (Daassi et al., 2020). However, the tumor immune escape mediated by PD-L1 on the cell surface is temporary and dependent on IFN-γ. Moreover, the expression time of PD-L1 on the surface of tumor cells is extremely short. PD-L1 is also expressed on the surface of host immune cells, especially tumor-associated macrophages (TAMs). While PD-L1 disappears from the surface of tumor cells, PD-L1 expression on host immune cells is maintained (Noguchi et al., 2017). Therefore, although PD-L1 on the surface of tumor cells plays a certain role in immune escape, the establishment of an immunosuppressive tumor microenvironment is mainly realized by the expression of PD-L1 on the surface of TAMs.

In addition to being expressed on the cell surface, PD-L1 is also released from tumor cells into the extracellular space to become free PD-L1, including exosome PD-L1 and soluble PD-L1 (sPD-L1; Frigola et al., 2011; Theodoraki et al., 2018). However, before the study of exosome PD-L1 received attention, the study of extracellular PD-L1 mainly focused on the effect of sPD-L1 on cancer (Xing et al., 2012; Shi et al., 2013; Nagato et al., 2017). Moreover, the total amount of PD-L1 in circulation did not distinguish between soluble and exosome forms. Recent studies have shown that exosome PD-L1 plays an important role in tumor immunosuppression (Ludwig et al., 2017; Chen et al., 2018; Ricklefs et al., 2018). Compared with sPD-L1, exosome PD-L1 is not easily degraded by extracellular proteolytic enzymes and can induce T cell dysfunction and improve stability (Fan et al., 2019). Therefore, it is important to understand how PD-L1 on cells is assembled into exosomes. Monypenny et al. (2018) showed that ALIX, a negative regulator of EGFR, regulates the assembly of certain exosome cargo and controls the balance between exosome PD-L1 and cell surface PD-L1. In ALIX-knockdown cells, the proportion of PD-L1 present in the MVEs was larger than that in ILVs, and MVEs were easily observed in the budded state, indicating that ALIX is required for the processing of PD-L1 from the MVE membrane into the ILV (**Figures 1A,B**). Cordonnier et al. (2020) showed that sPD-L1 may not be a reliable biomarker for melanoma compared to exosome PD-L1. In addition, macrophages and dendritic cells (DCs) release exosomes containing PD-L1 (Hong et al., 2016; Ricklefs et al., 2018; Cordonnier et al., 2020). Interestingly, exosomes in the plasma of patients with chronic lymphocytic leukemia were found to be rich in non-coding Y RNA hY4

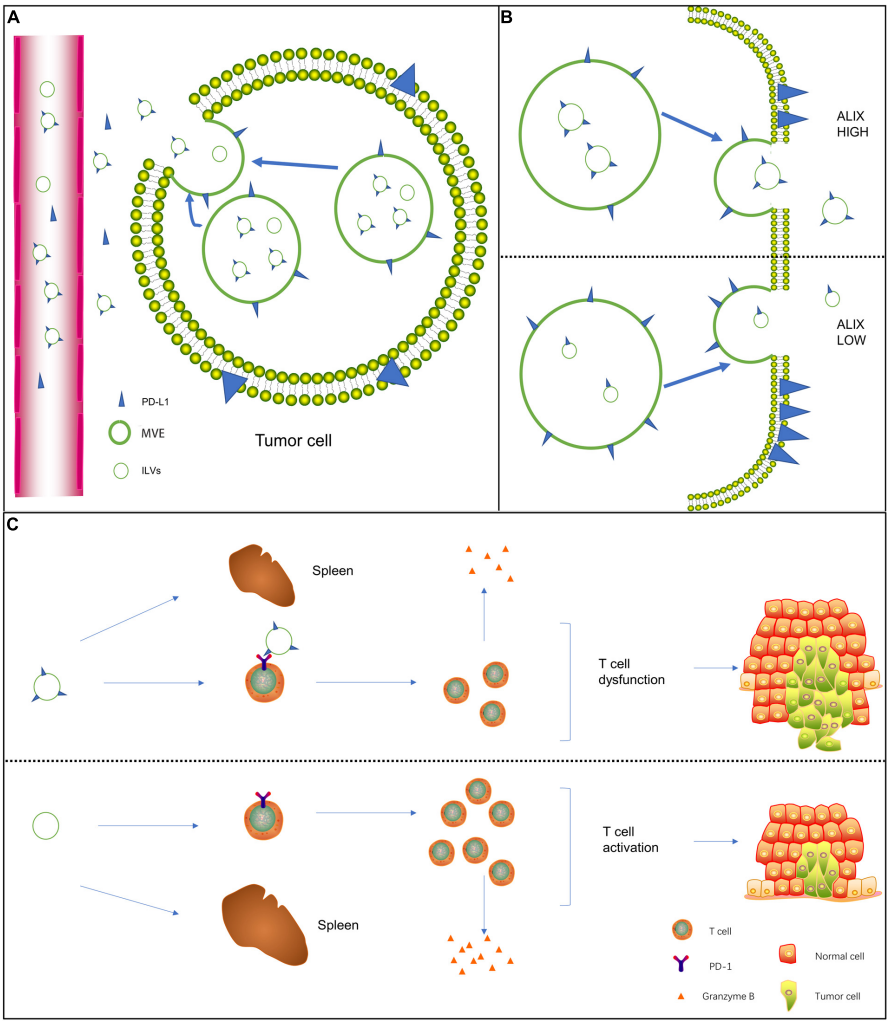

FIGURE 1 | Biogenesis of exosome PD-L1 and its mechanism of action on T cells. **(A)** In addition to being expressed on the cell surface, free PD-L1 is released from tumor cells to the extracellular space. Free PD-L1 can be divided into exosome PD-L1 and soluble PD-L1. **(B)** The negative EGFR regulator protein ALIX seems to regulate the assembly of certain exosome cargoes. In ALIX-knockdown cells, PD-L1 expression on the cell surface was strongly increased, but PD-L1 significantly entered exosomes. This decrease indicates that ALIX controls the balance between exosome PD-L1 and cell surface PD-L1. **(C)** In the presence of exosome PD-L1, the number of activated T cells decreased, the activity of these cells was significantly reduced, the spleen was reduced in size, the level of granzyme B secreted by T cells was significantly reduced, the killing ability of T cells was inhibited, and tumor growth was significantly promoted.

(Haderk et al., 2017). Additionally, transfer of CLL derived exosomes or hY4 alone to monocytes could lead to key CLL-associated phenotypes, which includes the release of cytokines as well as PD-L1 expression. In sum, the connection between tumor or immune cells and exosome PD-L1 may be highly intricate.

TUMOR-DERIVED EXOSOMES PD-L1 CAN REGULATE IMMUNE CELLS TO PROMOTE TUMOR GROWTH

Effect of Exosome PD-L1 on T Cells

Programmed death ligand 1 on the cell surface facilitates tumor immune escape by inducing activated T cell apoptosis, promoting T cell weakness, enhancing the function of regulatory T (Treg) cells, inhibiting T cell proliferation, activating damaged T cells, and stimulating the production of IL-2 (Zhang et al., 2015; Sun et al., 2018). Accumulating evidence has shown that exosome PD-L1 also plays a role in tumor immune escape and promotes tumor development by promoting T cell apoptosis and inhibiting the production of cytokines (Chen et al., 2018; Guo et al., 2019). Similarly, Kim et al. (2019) showed that exosomes containing PD-L1 could be isolated from the plasma of non-small cell lung cancer (NSCLC) patients. Tumor cell-derived exosome PD-L1 interacts with the PD-1 receptor on CD8 T cells, weakening the function of CD8 T cells, inducing their apoptosis, and promoting tumor immune escape (Kim et al., 2019). Therefore, membrane proteins on the surface of exosomes perform

functions in a variety of tumors through direct protein-protein interactions (**Table 1**).

Almost all previous studies on the interaction between PD-L1 and T cells were based on the surface PD-L1-mediated immunosuppression model of tumor cells (Iwai et al., 2002; Mittendorf et al., 2014). Whether exosome PD-L1 binds to PD-1 on T cells and inhibits the activity of CD8 T cells remains unknown. Yang et al. (2018) found that exosome PD-L1 was located on the surface of target cells and bound to PD-1, indicating that exosomes transfer functional PD-L1 to other cells. PD-1 and PD-L1 are part of the exosome cargo and modify the surface of exosomes in the serum of head and neck squamous cell carcinoma (HNSCC) patients (Theodoraki et al., 2019). Poggio et al. (2019) showed that in the presence of exosome PD-L1, T cells in tumor-draining lymph nodes expressed exhaustion markers, and the spleen was reduced in size (**Figure 1C**). The activation, proliferation, and killing potential of T cells is significantly enhanced by the removal of exosomes at the genetic level or by the deletion of PD-L1. When exogenous exosome PD-L1 was reintroduced, the effect was reversed (Poggio et al., 2019). Chen et al. (2018) established a mouse melanoma model with knockout of PD-L1 expression in B16-f10 cells [PD-L1 (KD) B16-F10 cells]. After the injection of exosomes derived from parental B16-F10 cells, the growth of tumors derived from PD-L1 (KD) B16-F10 cells was promoted, and the number of CD8 T lymphocytes invading the tumor was downregulated (Chen et al., 2018). The growth of tumor cells stimulated with exosomes containing PD-L1 was considerably increased compared with that of the control group in a constructed mouse breast cancer model (Yang et al., 2018).

Exosome PD-L1 Can Promote Tumor Immune Escape by Inducing Macrophage M2 Polarization

Macrophages are derived from monocytes, which in turn are derived from precursor cells in the bone marrow. Macrophages are usually used to maintain the homeostasis of the internal environment and resist the invasion of pathogens (Davies et al., 2013). Macrophages in different environments will produce corresponding polarization, such as common M1 macrophages and M2 macrophages (Martinez and Gordon, 2014). M1 macrophages can promote inflammation and release pro-inflammatory related factors, while M2 macrophages can resist inflammation, play important roles in immunity, tissue homeostasis, metabolism, and endocrine signal transduction, and can promote tumor metastasis and proliferation (Funes et al., 2018).

Previous studies have found that tumor-derived exosomes can induce M2 polarization of macrophages. For example, studies by Gabrusiewicz et al. (2018) have shown that exosomes derived from glioblastoma stem cells can pass through the monocyte cytoplasm and cause muscle activity. The recombination of protein skeleton transformed monocytes into immunosuppressive M2 type, and the expression of PD-L1 in macrophages increased. Haderk et al. (2017) found that when exosomes from chronic lymphocytic leukemia transfer to monocytes, they will cause inflammation, lead to cancer, and increase the expression of PD-L1, and make tumor immune escape. According to the above research, the focus of previous researchers is the change of PD-L1 in M2 macrophages and the impact on tumors. However, there is little research on whether PD-L1 in tumor-derived exosomes influences macrophage polarization. Tumor cells increase the release of glutamate through the cystine/glutamate transporter cystine-glutamate exchange (xCT) to balance the oxidation homeostasis in tumor cells and promote tumor progression (Okazaki et al., 2017). The latest study by Liu et al. (2021) found that inhibiting xCT in melanoma can cause the transcription factor IRF4/EGR1 to upregulate the expression of PD-L1, which leads to melanoma cells secreting many exosomes carrying PD-L1, which in turn induces M2 macrophages polarized and reduced the efficacy of anti-PD-1/PD-L1 in the treatment of melanoma. And it was further discovered that sulfasalazine (SAS) induced macrophage M2 polarization through exosome PD-L1, which weakened the anti-PD-1/PD-L1 curative effect, and finally led to anti-PD-1/PD-L1 treatment resistance (Liu et al., 2021).

In fact, it is not difficult to see that the expression of PD-L1 is upregulated in different tumor cells. The important mechanism of tumor immune escape is the combination

TABLE 1 | Tumor-derived exosome PD-L1 in cancers.

Tumor types	Target cell	Mechanisms	Tumor progression	References
NSCLC	T cell	Exosome PD-L1 inhibits cytokines (IL-2 and IFN-γ) and induces apoptosis of $CD8^+$ T-cells	↑	Kim et al., 2019
Melanoma	T cell	Exosome PD-L1 pass through T lymphocytes of secondary lymphoid organs and play a role through the immunosuppressive pathway of PD-1/PD-L1	↑	Cordonnier et al., 2020
Gastric cancer	T cell	Reduces the expression of CD69 and PD-1 on the surface of T cells, resulting in T cell dysfunction	↑	Fan et al., 2019
Breast cancer	T cell	Blocks phosphorylation of src family proteins, LAT and PLCγ in CD8 T cells, and promotes CD8 T cell dysfunction	↑	Chatterjee et al., 2020
HNSCC	T cell	Exosome PD-L1 inhibits and interferes $CD8^+$ effector T cell activation	↑	Theodoraki et al., 2018

↑, *tumor promotion; NSCLC, non-small cell lung cancer; HNSCC, head and neck squamous cell carcinoma.*

of PD-L1 with PD-1 of T cells, which causes an immune checkpoint response. With the increasing number of studies on exosome PD-L1 recently, its role in research has become more and more important. Related studies have found that the exosome PD-L1 and cell surface PD-L1 have the same membrane topology by using enzyme-linked immunosorbent assay (Chen et al., 2018). Exosomes containing PD-L1 secreted by tumors can effectively transfer exosomes PD-L1 to macrophages and weaken anti-tumor immunity in tumor microenvironment (Yang et al., 2018). However, the mechanism of how exosome PD-L1 induces immunosuppression has not yet been fully elucidated. Liu et al. (2021) confirmed that by increasing the expression of melanoma exosomes PD-L1, the M2 polarization of macrophages can be induced, which ultimately leads to resistance to anti-PD-1/PD-L1 treatment. In addition, this method is consistent with the results of tumor immune escape and anti-PD-L1 treatment caused by directly upregulating PD-L1 in macrophages (Zhang et al., 2017; Wen et al., 2018). All these indicate that tumor-derived exosomes PD-L1 can promote tumor immune escape by inducing the polarization of macrophages M2.

IMMUNOSUPPRESSIVE EFFECTS OF TUMOR-DERIVED EXOSOME PD-L1 ON DISTINCT CANCERS

Non-small Cell Lung Cancer

Lung cancer is the leading cause of cancer-related death worldwide (Siegel et al., 2012). Various targeted therapies and immunotherapies for NSCLC have been gradually and effectively applied (He et al., 2015; Grigg and Rizvi, 2016). Among them, PD-1/PD-L1 inhibitors are representative and have improved the clinical efficacy of NSCLC treatment to a certain extent (Herbst et al., 2016; Brahmer et al., 2017; Mok et al., 2019). Measurement of the expression level of exosome PD-L1 plays a fundamental role in the diagnosis and prognosis of NSCLC. However, there is still no expected response of NSCLC patients with positive immunohistochemical staining for PD-L1 to immunotherapy, and the reason remains elusive. Li et al. (2019) showed that exosome PD-L1 levels were significantly higher in NSCLC patients (especially in advanced-stage individuals) than in healthy controls. The level of exosome PD-L1 was obviously related to tumor size, positive lymph node status, distant metastasis and TNM stage (Li et al., 2019). Kim et al. (2019) found that exosomes containing PD-L1 could be isolated from the plasma of patients with NSCLC. Exosome PD-L1 plays an important role in tumor immune escape by inhibiting cytokines and inducing CD8 T cell apoptosis. Liu et al. measured exosome PD-L1 expression in NSCLC patients using a compact surface plasmon resonance (SPR) biosensor and found that exosome PD-L1 expression was significantly higher than that in healthy controls (Liu et al., 2018). Exosome PD-L1 from NSCLC cells has also been shown to mediate immune escape by inhibiting cytokines (IL-2 and IFN-γ) and inducing CD8 T cell apoptosis (Kim et al., 2019). In short, exosome PD-L1 may be a novel biomarker and a promising target for lung cancer.

Melanoma

Melanoma is a typical immunosuppressive malignant tumor with a high possibility of distant metastasis (Aubuchon et al., 2017). At present, immune checkpoint inhibitor therapy targeting PD-L1 has made remarkable achievements in the treatment of melanoma (Chen and Han, 2015; Topalian et al., 2016). However, the currently approved response rate of patients with advanced melanoma to monoclonal antibodies is still not satisfactory (Ribas et al., 2016; Zaretsky et al., 2016). Therefore, the identification of a typical biomarker is critical for the diagnosis and treatment of melanoma. The original intention was to focus on PD-L1 expression in tumors and blood samples; however, these test results were not necessarily reliable due to the inhibition of PD-L1 in tumors and the instability of PD-L1 in blood. Recently, exosome PD-L1 has been identified as a potential biomarker of melanoma. Cordonnier et al. (2020) further confirmed that circulating exosome PD-L1 in melanoma patients plays a role through T lymphocytes in secondary lymphoid organs and through the immunosuppressive PD-1/PD-L1 pathway. Moreover, a large increase in exosome PD-L1 is related to tumor progression (Cordonnier et al., 2020). Chen et al. (2018) demonstrated the presence of melanoma-associated exosome PD-L1 and its immunosuppressive effects and suggested that the exosome PD-L1 level is an indicator to distinguish clinical responders from non-responders.

Gastric Cancer

Gastric cancer is the fourth most common cancer in the world (Xiang et al., 2016). The efficacy of anti-PD-1 therapy in metastatic gastric cancer seems to be quite promising (Muro et al., 2016). A recent study have shown that exosome PD-L1 is required to predict the prognosis of gastric cancer patients. Fan et al. (2019) showed that there was a significant correlation between the level of exosome PD-L1 and the stage of gastric cancer, and the survival rate was worse in the group with higher exosome PD-L1 expression. The OS of patients with high exosome PD-L1 expression was significantly lower than that of patients in the low expression group with both stages I and II AJCC, demonstrating the predictive value of exosome PD-L1 for the OS of patients with early gastric cancer.

Breast Cancer

HER2 expression is elevated in 25% of breast cancer patients and is often accompanied by a poor prognosis (Slamon et al., 1989). At present, breast cancer treatments targeting HER2 have achieved some efficacy in clinical practice. However, not all breast cancer patients who overexpress HER2 respond to therapy, and many patients still develop treatment resistance (Nahta and Esteva, 2007). Notably, enhanced drug resistance is likely to cause the immune escape of cancer cells (Bruttel and Wischhusen, 2014). Chatterjee et al. (2020) reported that breast cancer cells secrete exosomes carrying PD-L1 and are highly immunosuppressive. Additionally, exosome PD-L1 is stimulated by TGF-β, which blocks the phosphorylation of src family proteins and promotes CD8 T cell dysfunction. Therefore,

exosome PD-L1 has considerable potential for the diagnosis and treatment of breast cancer patients (Martinez et al., 2017).

Pancreatic Cancer

Pancreatic cancer is one of the cancers with the highest mortality rate, and the detection of exosome PD-L1 in the blood is a good prognostic indicator of pancreatic cancer. Pancreatic ductal adenocarcinoma (PDAC) is the most common histological subtype of malignant pancreatic cancer (Rahbari et al., 2016), accounting for 90% of all cases. Because this type of malignant tumor is highly invasive and infiltrative, most diagnoses are made at the advanced tumor stage. The presence of a tumor immune escape mechanism leads to the rapid development of pancreatic cancer. To date, patients with pancreatic cancer have hardly responded to monotherapy with checkpoint inhibitors (Foley et al., 2016). PD-L1 is highly expressed in pancreatic cancer and is associated with poor prognosis (Geng et al., 2008; Chen et al., 2009; Wang et al., 2010). Therefore, the expression of tumor-derived exosome PD-L1 will greatly improve the diagnostic status of pancreatic cancer and immunotherapy. Lux et al. (2019) examined the expression of PD-L1 in blood samples and showed that the survival time of PD-L1-positive patients was significantly lower than that of PD-L1-negative patients. Therefore, the expression of PD-L1 in exosomes has profound significance for the prognosis of pancreatic cancer. However, since exosome PD-L1 expression in CP patients is higher than that in PDAC patients, exosome PD-L1 may not be suitable as a diagnostic indicator for pancreatic cancer (Lux et al., 2019).

Head and Neck Squamous Cell Carcinoma

Head and neck squamous cell carcinoma is a common and lethal disease with the highest diagnostic rate in the world (Ferlay et al., 2013; Mourad et al., 2017). The tumor microenvironment of HNSCC has strong immunosuppressive properties, and HNSCC is a highly immunosuppressive, malignant tumor (Ferris et al., 2006; Bergmann et al., 2007; Whiteside, 2018). The PD-1/PD-L1 immunosuppressive pathway has received great attention. A series of experimental studies showed that patients with excessive plasma exosome PD-L1 had higher disease activity than patients with lower exosome PD-L1 levels. Higher plasma levels of exosome PD-L1 were associated with stronger inhibition of CD8 effector T cell activation, and anti-PD-1 Abs significantly reduced the dose-dependent effect of exosome PD-L1 on T cell activity and sex-associated inhibition (Theodoraki et al., 2018). Therefore, in HNSCC, exosome PD-L1 binds to the PD-1 receptor on the surface of activated T cells to maintain their biological activity and effectively transmit signals, thereby affecting the function of immune cells and leading to immune escape. The level of tumor-derived exosomes can be used as an indicator to reflect the efficacy of patient treatment (Theodoraki et al., 2019). Theodoraki et al. (2018) isolated exosomes carrying PD-L1 from the plasma of HNSCC patients and inhibiting T cell function, demonstrating that circulating exosome PD-L1 may be a useful indicator of disease and immune activity in HNSCC patients.

Lymphoma

Lymphoma is a primary malignant tumor of lymph nodes or lymph tissues, and its occurrence may be related to gene mutations (Zahn et al., 2020), virus and other pathogen infections (Huang et al., 2021). Studies highlight the roles of clonally diverse CD4 T cells and innate effectors in the efficacy of PD-1 blockade in classical Hodgkin lymphomas (Cader et al., 2020). Additionally, study show that diffuse large B-cell lymphomas possess a self-organized infrastructure comprising side population (SP) and non-SP cells, where transitions between clonogenic states are modulated by exosome-mediated WNT signaling (Koch et al., 2014). Li et al. evaluated the prognostic value of pretreatment circulating sPD-L1 and exoPD-L1 in extranodal NK/T cell lymphoma patients (Li et al., 2020). Their study revealed that circulating exoPD-L1 and sPD-L1 levels were significantly elevated in extranodal NK/T cell lymphoma and might be promising biomarkers for evaluating the survival outcomes of extranodal NK/T cell lymphoma patients.

FUTURE CLINICAL APPLICATIONS OF EXOSOME PD-L1

Development of Exosome PD-L1 Detection Methods

Although the application of immunotherapy has shown considerable value in the diagnosis, treatment, and prediction of various cancers, the response rates of patients with positive PD-L1 pathology to immunotherapy is only 10–30% (Fehrenbacher et al., 2016; Eggermont et al., 2018). The level of exosome PD-L1 can reflect the occurrence of tumors in certain cancer types and has a strong correlation with the response to immunotherapy (Chen et al., 2018). Therefore, the detection of exosome PD-L1 levels can be used as a supplement to existing immune checkpoint measurements to increase the accuracy of diagnosis. At present, the accepted quantitative detection method for exosome PD-L1 is enzyme-linked immunosorbent assay (ELISA; Welton et al., 2010; Nawaz et al., 2014; Chen et al., 2018). However, this method has certain limitations. When exosome PD-L1 expression is too low (<200 pg/ml), it is impossible to distinguish between patients and healthy people (Ramirez et al., 2018). Furthermore, Huang et al. (2020) proposed a detection method called HOLMES-ExoPD-L1 that replaces ELISA to quantitatively detect exosome PD-L1. By applying an aptamer with a higher recognition efficiency than the PD-L1 antibody, the detection sensitivity is significantly improved. The uniformity of thermophoresis is used to promote faster binding of the aptamer to exosome PD-L1 (Huang et al., 2020). Pang et al. (2020) proposed an *in vitro* assay to detect plasma exosome PD-L1, which is undetectable by ELISA. The principle involves the use of nanoparticles to enrich exosomes by binding the TiO_2 shell and the hydrophilic phosphate head of exosome phospholipids. This method efficiently captures up to 96.5% of exosomes, which are then quantified by labeling exosome PD-L1 with a specifically labeled anti-PD-L1 antibody (Pang et al., 2020). Liu et al. (2018) developed a compact surface plasmon resonance (SPR) biosensor with the same principle as traditional SPR, which is a highly

sensitive, real-time, label-free optical detection method that does not require nanomaterials and effectively reduces the detection cost. Researchers analyzed NSCLC serum samples with this method and found that the expression of exosome PD-L1 in patients with NSCLC was increased. Surprisingly, this method has a higher detection sensitivity than the traditional ELISA detection method. With the same sample size, the researchers used this method to detect exosome PD-L1 levels that ELISA could not detect (Liu et al., 2018; **Table 2**).

Early Diagnosis and Prognosis of Cancer

Surgery is still the preferred method for radical treatment of tumors, but quite a lot of cancer patients are usually diagnosed at the advanced stage, thus missing the best opportunity for treatment. For example, most patients with gastric cancer are usually diagnosed at the advanced stage, and the 5-year survival rate is less than 20% (Price et al., 2012). 75% of lung cancer patients are already in the advanced stage when they are discovered (Steinman and Banchereau, 2007). Pancreatic ductal adenocarcinoma (PDAC) is highly aggressive and invasive, most of the diagnoses are performed in the advanced tumor stage (Rahbari et al., 2016). Therefore, exploring reliable indicators for early cancer diagnosis and prognostic factors has far-reaching significance for cancer diagnosis and treatment. Many reports show that PD-L1 is abnormally highly expressed in a variety of tumors (skin, brain, thyroid, esophagus, colorectal, etc.) (Iwai et al., 2002; Taube et al., 2014; Patel and Kurzrock, 2015). However, due to the inhibition of PD-L1 in tumors and the instability of PD-L1 in blood samples, some studies have shown that there is no difference in the concentration of sPD-L1 between NSCLC patients and healthy blood donors (Li et al., 2019). Therefore, simply detecting PD-L1 in tumors or blood is very unreliable for the early diagnosis of tumors. We know that exosomes have been widely regarded as a new type of crosstalk circuit between tumor cells and the tumor microenvironment (Li et al., 2015; Melo et al., 2015; Tang and Wong, 2015). Some studies have clarified that exosomes even represent the mechanism by which immunosuppressive agents in TME participate in the tumor progression cycle (Whiteside, 2016; Ludwig et al., 2017). Many current studies have shown that the detection of the expression level of exosomes PD-L1 is of great significance for the early diagnosis of tumors (Chen et al., 2018; Li et al., 2019). Li et al. (2019) showed that the level of exosome PD-L1 in NSCLC patients (especially advanced patients) was significantly higher than that in healthy controls. The level of exosome PD-L1 was significantly correlated with tumor size, lymph node positive status, distant metastasis and TNM stage (Li et al., 2019). However, the level of sPD-L1 is not related to clinicopathological features other than tumor size. Liu et al. (2018) measured the expression level of exosome PD-L1 in NSCLC patients by using a compact surface plasmon resonance (SPR) biosensor and found that the expression of exosome PD-L1 was significantly higher than that in healthy controls. The above studies show that exosome PD-L1 may become a promising biomarker for the diagnosis of lung cancer. In the plasma of melanoma patients, the level of exosome PD-L1 was significantly higher than that of sPD-L1, and exosome PD-L1 was detected in all patients. Although the level of exosome PD-L1 has no relationship to clinicopathological features, the change after treatment (ΔExoPD-L1) is related to tumor response to treatment, and it is verified that the increase of exosome PD-L1 is related to tumor progression (Cordonnier et al., 2020). Fan et al. (2019) showed that there was a significant correlation between the level of exosome PD-L1 and the stage of gastric cancer, and the survival rate was worse in the group with higher exosome PD-L1 expression. The OS of patients with high exosome PD-L1 expression was significantly lower than that of patients in the low expression group with both stages I and II AJCC, demonstrating the predictive value of exosome PD-L1 for the OS of patients with early gastric cancer (Fan et al., 2019). The above-mentioned studies show that the exosome PD-L1 is more reliable than tumor and serum

TABLE 2 | Exosome PD-L1 detection method.

Method	Mechanism	Advantage	Disadvantages
Enzyme-linked immunosorbent assay (ELISA)	The PD-L1 antigen and antibody are adsorbed on the surface of the solid phase carrier, allowing the antigen and antibody to react on the surface	Strong specificity, Fast Low cost	Low sensitivity, When the expression of PD-L1 in exosomes is too low (<200 pg/ml), it is impossible to distinguish patients from healthy people
HOLMES-ExoPD-L1	Due to the different depletion rates, the extracellular aptamers can observe strong fluorescence	Compared with PD-L1 antibody, the use of aptamers provides higher recognition efficiency, which can significantly improve the detection sensitivity, The operation is simple	The biological stability of aptamers is poor compared to antibodies, and the short half-life *in vivo* limits the development of aptamers in clinical applications
Based on Fe_3O_4@TiO_2 isolation and SERS immunoassay	Fe_3O_4@TiO_2 nanoparticles are used to enrich exosomes by combining the TiO_2 shell with the hydrophilic phosphate head of exosome phospholipids, followed by the addition of Au @ Ag @ MBA SERS tag modified with anti-PD-L1 antibody to mark the outside exosome PD-L1 for quantification	The speed is faster, Exosome PD-L1 can be captured and analyzed directly from the serum	With the use of nanomaterials, the cost may be higher
Compact surface plasmon resonance (SPR) biosensor	The same as the traditional SPR sensing mechanism	High-sensitivity, label-free, real-time optical detection method	Need to use its special equipment, there is a certain learning cost

PD-L1, and it is of great significance for the early diagnosis and prognosis of cancer.

Exosome PD-L1 as a Biomarker for Clinical Anti-PD-1/PD-L1 Therapy

Programmed death ligand 1 is rarely expressed on the cell surface of normal human tissues and is abundantly expressed on the surface of cancer cells (Dong et al., 2002). Additionally, IFN-γ upregulates PD-L1 on the surface of normal tissue cells and cancer cells. The use of an anti-human PD-L1 antibody prevents the effect of tumor cell PD-L1 on activated effector T cells and blocks the interaction of PD-L1 with T cells. This finding shows that the use of an anti-PD-L1 antibody inhibits the progressive growth of mouse tumors (Dong et al., 2002). PD-L1 inhibits the anti-tumor function of T cells by activating PD-1. The PD-L1 signaling pathway causes immune escape of tumor cells in the tumor microenvironment (TME; Mittal et al., 2014). Subsequent studies confirmed the accuracy of this concept (Iwai et al., 2002; Strome et al., 2003). These studies showed that tumors evade immune attack through the PD-1/PD-L1 pathway and provide an anti-PD-1/PD-L1 approach for cancer therapy (**Figure 2**).

Additionally, the FDA has approved two PD-1 antibodies for the treatment of human cancer. Multiple clinical studies have shown that anti-PD-1/PD-L1 therapy has exceedingly significant clinical importance for improving the survival rates of patients with advanced and metastatic tumors. Moreover, in a variety of cancers, especially solid tumors, anti-PD-1/PD-L1 therapy has a fairly long-lasting effect. Notably, the removal of exosome PD-L1 inhibits tumor growth, even in models that are resistant to anti-PD-L1 antibodies (Poggio et al., 2019). In some studies of metastatic melanoma, anti-PD-1/PD-L1 therapy showed profound application prospects (Ribas et al., 2016; Topalian et al., 2016). At present, immunohistochemical (IHC) staining of PD-L1 is routinely tested in clinical practice to predict the effect of anti-PD-1/PD-L1 immunotherapy (Martinez and Gordon, 2014). Compared with the PD-L1 negative/weak expression group, the remission rate of the PD-L1 high expression group increased from 8 to 30% (Funes et al., 2018). But even so, a considerable number of NSCLC patients with positive PD-L1 IHC staining have unsatisfactory immunotherapy effects (Gabrusiewicz et al., 2018). Among them, PD-1/PD-L1 inhibitors are represented, which have improved the clinical efficacy of NSCLC and other tumors to a certain extent (Okazaki et al., 2017; Chen et al., 2018; Liu et al., 2021). However, many tumor patients with positive immunohistochemical staining for PD-L1 still have no expected response after receiving immunotherapy.

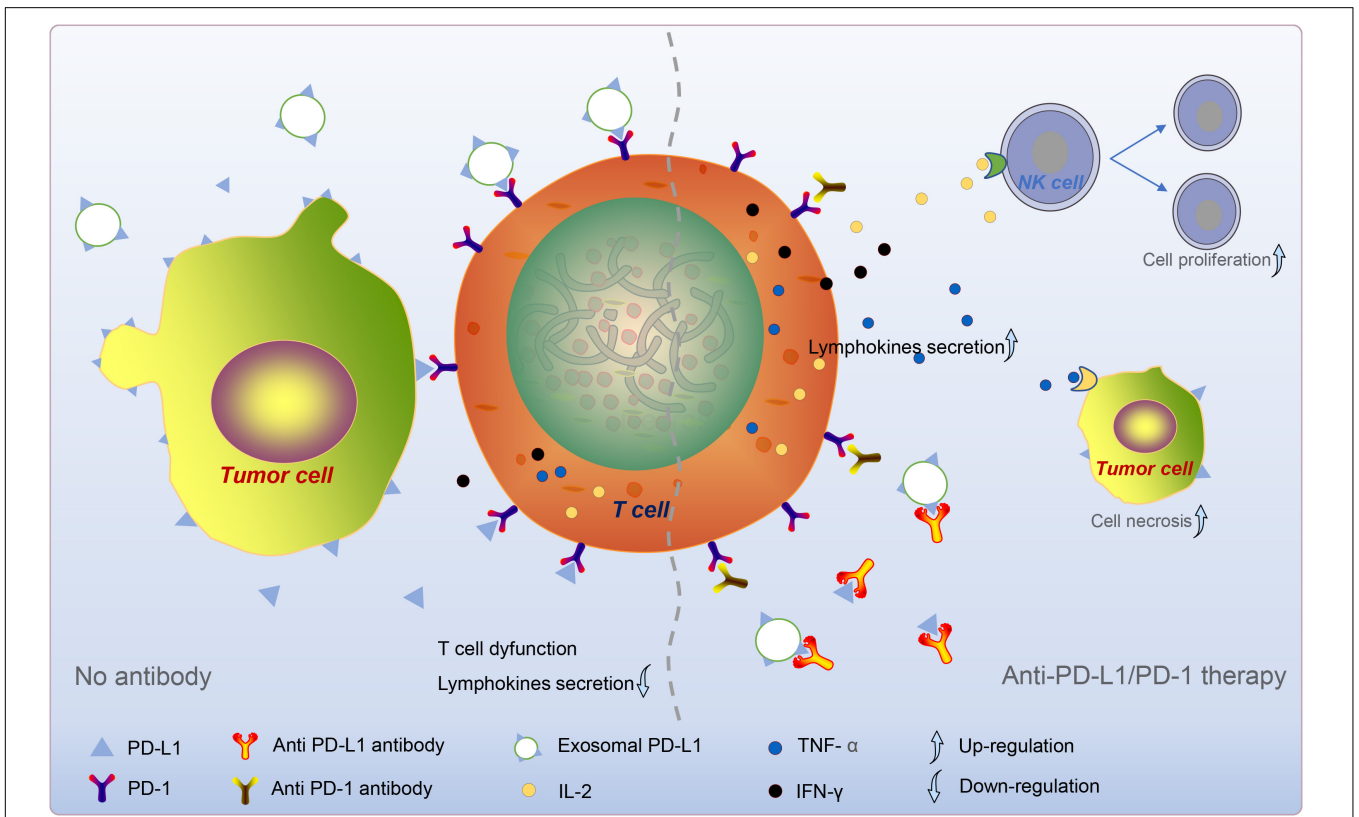

FIGURE 2 | Tumor cell-derived exosome PD-L1-mediated immune escape. Exosome PD-L1, which synergizes with sPD-L1 and PD-L1 on the surface of tumor cells, binds to PD-1 on T cells and reduces T cell activity and lymphokine secretion. In anti-PD-L1/PD-1 therapy, the antibody specifically binds to PD-L1/PD-1, prevents the coupling of circulating PD-L1 to PD-1, increases the secretion of cytokines. Subsequently, these cytokines, such as IL-2, TNF-α, and IFN-γ, could give rise to the division and proliferation of NK cells and the death of tumor cells. The dotted line divides the picture into left and right sides. The left part mainly describes the "No antibodies" situation, and the right part mainly talks about the "anti-pd-1/PD-L1 therapy" situation.

In gastric cancer patients, not all PD-L1 positive patients respond to anti-PD-1, and even PD-L1-negative patients respond (Wen et al., 2018). The reason for this disappointing result is not yet clear, but it is likely that the integrated mechanism of the PD-L1 pathway in TME is not fully understood. Therefore, we need to have a deeper understanding of the immunosuppressive pathway of PD-1/PD-L1 to better improve the treatment efficacy in patients. Recent studies have shown that circulating exosome PD-L1 promotes activated T cell apoptosis and inhibits the production of cytokines (Chen et al., 2018). Antibodies against PD-L1 or PD-1 block the inhibitory effect of exosome PD-L1 on T cells. Exosome PD-L1 may reflect the dynamic interaction between tumors and immune cells (Chen et al., 2018). In treated patients, the recovery of T cell activity was negatively correlated with an increase in exosome PD-L1. Exosome PD-L1 reflected whether anti-PD-1 therapy successfully triggered anti-tumor immunity. Currently, circulating exosome PD-L1 has been used as a predictive biomarker of the clinical response to anti-PD-1 therapy. However, given that the dynamic expression of tumor PD-L1 is lower than that of exosome PD-L1 and the detection of tumor PD-L1 requires invasive tumor biopsies, exosome PD-L1 may be a promising blood-based biomarker. Subsequent confirmation of the clinical application potential of exosome PD-L1 in multiple cancer types is required. For example, Theodoraki et al. (2018) showed that in HNSCC patients, higher plasma levels of exosome PD-L1 were associated with stronger inhibition of CD8 effector T cell activation. Anti-PD-1 Abs significantly reduced the dose-dependent inhibition of T cell activity by exosome PD-L1 (Theodoraki et al., 2019). Poggio et al. (2019) found that exosome PD-L1 seems to be resistant to anti-PD-L1 treatment. At the same time, inhibiting exosome PD-L1 helps maintain long-lasting anti-tumor immunity (Zhang et al., 2017). A study by Del Re et al. (2018) explored the relationship between exosome PD-L1 mRNA expression and response to anti-PD-1 treatment in melanoma (n = 18) and non-small cell lung cancer (n = 8). They emphasized that exosome PD-L1 should be considered when predicting the outcome of anti-PD-1 treatment (Siegel et al., 2012). This may also be the reason why the PD-L1 IHC profile of the tumor is not an ideal biomarker for the selection of anti-PD-1/PD-L1 immunotherapy candidates. Based on the above conclusions, we know that we cannot simply detect the tumor PD-L1 for verification. But if there is a serological marker that can provide reliable information on the expression status of tumor PD-L1, this situation can be greatly improved. The exosome PD-L1 is very likely to be this serological marker.

CONCLUSION

Tumor-derived exosomes PD-L1 play a key role in tumor immune escape of tumors. At present, there are several mechanisms by which cell surface or exosome PD-L1 mediates tumor immunity to achieve immune escape, such as by inducing activated T cell apoptosis, promoting T cell weakness, enhancing the function of Tregs, inhibiting T cell proliferation, and inhibiting impaired T cell activation and IL-2 production.

Many studies have confirmed that PD-L1 on tumor cells mediates immunosuppressive effects. Similarly, PD-L1 secreted by tumor cells on the surface of exosomes binds to PD-1 on T cells and exerts biological effects. However, further exploration of the molecular mechanisms is needed. Exosome PD-L1 has been shown to be of clinical value in the diagnosis, treatment and prognosis of various cancers, such as NSCLC, melanoma, gastric cancer, breast cancer and HNSCC. The measurement of PD-L1 levels in exosomes complements existing immune checkpoint measurements, facilitating the accuracy of immune-related tumor diagnosis. In addition, exosome PD-L1 contributes to anti-PD-L1/PD-1 therapy and enhances the sensitivity of tumor patients to treatment. Nevertheless, more work remains to be done to apply tumor-derived exosome PD-L1 in clinical practice.

AUTHOR CONTRIBUTIONS

ZS provided direction and guidance throughout the preparation of this manuscript. BS and QD wrote and edited the manuscript. ZC, CC, QZ, and SH reviewed and made significant revisions of the manuscript. BQ, JL, GW, and WY collected and prepared the related manuscript. All authors read and approved the final manuscript.

FUNDING

This study was supported by the National Natural Science Foundation of China (81972663), Key Scientific Research Projects of Institutions of Higher Education in Henan Province (19A310024), Medical Scientific and Technological Research Project of Henan Province (201702027), National Natural Science Foundation of Henan Province (182300410342), and Health Commission Technology Talents Overseas Training Project of Henan Province (2018140).

REFERENCES

Aubuchon, M., Bolt, L., Janssen-Heijnen, M., Verleisdonk-Bolhaar, S., van Marion, A., and van Berlo, C. (2017). Epidemiology, management and survival outcomes of primary cutaneous melanoma: a ten-year overview. *Acta Chir. Belg.* 117, 29–35.

Bergmann, C., Strauss, L., Zeidler, R., Lang, S., and Whiteside, T. L. (2007). Expansion of human T regulatory type 1 cells in the microenvironment of cyclooxygenase 2 overexpressing head and neck squamous cell carcinoma. *Cancer Res.* 67, 8865–8873. doi: 10.1158/0008-5472.Can-07-0767

Blank, C., Brown, I., Peterson, A. C., Spiotto, M., Iwai, Y., Honjo, T., et al. (2004). PD-L1/B7H-1 inhibits the effector phase of tumor rejection by T cell receptor (TCR) transgenic CD8+ T cells. *Cancer Res.* 64, 1140–1145.

Boukouris, S., and Mathivanan, S. (2015). Exosomes in bodily fluids are a highly stable resource of disease biomarkers. *Proteomics Clin. Appl.* 9, 358–367.

Brahmer, J. R., Rodríguez-Abreu, D., Robinson, A. G., Hui, R., Csőszi, T., Fülöp, A., et al. (2017). Health-related quality-of-life results for pembrolizumab versus chemotherapy in advanced, PD-L1-positive NSCLC (KEYNOTE-024): a multicentre, international, randomised, open-label phase 3 trial. *Lancet Oncol.* 18, 1600–1609. doi: 10.1016/s1470-2045(17)30690-3

Bruttel, V. S., and Wischhusen, J. (2014). Cancer stem cell immunology: key to understanding tumorigenesis and tumor immune escape? *Front. Immunol.* 5:360. doi: 10.3389/fimmu.2014.00360

Cader, F. Z., Hu, X., Goh, W. L., Wienand, K., Ouyang, J., Mandato, E., et al. (2020). A peripheral immune signature of responsiveness to PD-1 blockade in patients with classical Hodgkin lymphoma. *Nat. Med.* 26, 1468–1479. doi: 10.1038/s41591-020-1006-1

Chatterjee, S., Chatterjee, A., Jana, S., Dey, S., Roy, H., Das, M. K., et al. (2020). Transforming growth factor beta orchestrates PD-L1 enrichment in tumor derived exosomes and mediates CD8 T cell dysfunction regulating early phosphorylation of TCR signalome in breast cancer. *Carcinogenesis* 42, 38–47. doi: 10.1093/carcin/bgaa092

Chen, G., Huang, A. C., Zhang, W., Zhang, G., Wu, M., Xu, W., et al. (2018). Exosome PD-L1 contributes to immunosuppression and is associated with anti-PD-1 response. *Nature* 560, 382–386. doi: 10.1038/s41586-018-0392-8

Chen, L., and Han, X. (2015). Anti–PD-1/PD-L1 therapy of human cancer: past, present, and future. *J. Clin. Invest.* 125, 3384–3391.

Chen, X. L., Yuan, S. X., Chen, C., Mao, Y. X., Xu, G., and Wang, X. Y. (2009). [Expression of B7-H1 protein in human pancreatic carcinoma tissues and its clinical significance]. *Ai Zheng* 28, 1328–1332. doi: 10.5732/cjc.009.10245

Colletti, M., Tomao, L., Galardi, A., Paolini, A., Di Paolo, V., De Stefanis, C., et al. (2020). Neuroblastoma-secreted exosomes carrying miR-375 promote osteogenic differentiation of bone-marrow mesenchymal stromal cells. *J. Extracell. Vesicles* 9:1774144. doi: 10.1080/20013078.2020.1774144

Colombo, M., Moita, C., van Niel, G., Kowal, J., Vigneron, J., Benaroch, P., et al. (2013). Analysis of ESCRT functions in exosome biogenesis, composition and secretion highlights the heterogeneity of extracellular vesicles. *J. Cell Sci.* 126(Pt 24), 5553–5565. doi: 10.1242/jcs.128868

Colombo, M., Raposo, G., and Théry, C. (2014). Biogenesis, secretion, and intercellular interactions of exosomes and other extracellular vesicles. *Annu. Rev. Cell Dev. Biol.* 30, 255–289. doi: 10.1146/annurev-cellbio-101512-122326

Cordonnier, M., Chanteloup, G., Isambert, N., Seigneuric, R., Fumoleau, P., Garrido, C., et al. (2017). Exosomes in cancer theranostic: diamonds in the rough. *Cell Adh. Migr.* 11, 151–163. doi: 10.1080/19336918.2016.1250999

Cordonnier, M., Nardin, C., Chanteloup, G., Derangere, V., Algros, M. P., Arnould, L., et al. (2020). Tracking the evolution of circulating exosome-PD-L1 to monitor melanoma patients. *J. Extracell. Vesicles* 9:1710899. doi: 10.1080/20013078.2019.1710899

Daassi, D., Mahoney, K. M., and Freeman, G. J. (2020). The importance of exosome PDL1 in tumour immune evasion. *Nat. Rev. Immunol.* 20, 209–215. doi: 10.1038/s41577-019-0264-y

Davies, L. C., Jenkins, S. J., Allen, J. E., and Taylor, P. R. (2013). Tissue-resident macrophages. *Nat. Immunol.* 14, 986–995. doi: 10.1038/ni.2705

Del Re, M., Marconcini, R., Pasquini, G., Rofi, E., Vivaldi, C., Bloise, F., et al. (2018). PD-L1 mRNA expression in plasma-derived exosomes is associated with response to anti-PD-1 antibodies in melanoma and NSCLC. *Br. J. Cancer* 118, 820–824. doi: 10.1038/bjc.2018.9

Dong, H., Strome, S., Salomao, D., Tamura, H., Hirano, F., Flies, D., et al. (2002). Tumor-associated B7-H1 promotes T-cell apoptosis: a potential mechanism of immune evasion. *Nat. Med.* 8, 793–800. doi: 10.1038/nm730

Dong, H., Zhu, G., Tamada, K., and Chen, L. (1999). B7-H1, a third member of the B7 family, co-stimulates T-cell proliferation and interleukin-10 secretion. *Nat. Med.* 5, 1365–1369. doi: 10.1038/70932

Eggermont, A. M. M., Blank, C. U., Mandala, M., Long, G. V., Atkinson, V., Dalle, S., et al. (2018). Adjuvant pembrolizumab versus placebo in resected stage III melanoma. *N. Engl. J. Med.* 378, 1789–1801. doi: 10.1056/NEJMoa1802357

Fan, Y., Che, X., Qu, J., Hou, K., Wen, T., Li, Z., et al. (2019). Exosome PD-L1 retains immunosuppressive activity and is associated with gastric cancer prognosis. *Ann. Surg. Oncol.* 26, 3745–3755. doi: 10.1245/s10434-019-07431-7

Fehrenbacher, L., Spira, A., Ballinger, M., Kowanetz, M., Vansteenkiste, J., Mazieres, J., et al. (2016). Atezolizumab versus docetaxel for patients with previously treated non-small-cell lung cancer (POPLAR): a multicentre, open-label, phase 2 randomised controlled trial. *Lancet* 387, 1837–1846. doi: 10.1016/s0140-6736(16)00587-0

Ferlay, J., Steliarova-Foucher, E., Lortet-Tieulent, J., Rosso, S., Coebergh, J.-W. W., Comber, H., et al. (2013). Cancer incidence and mortality patterns in Europe: estimates for 40 countries in 2012. *Eur. J. Cancer* 49, 1374–1403.

Ferris, R. L., Whiteside, T. L., and Ferrone, S. (2006). Immune escape associated with functional defects in antigen-processing machinery in head and neck cancer. *Clin. Cancer Res.* 12, 3890–3895. doi: 10.1158/1078-0432.Ccr-05-2750

Foley, K., Kim, V., Jaffee, E., and Zheng, L. (2016). Current progress in immunotherapy for pancreatic cancer. *Cancer Lett.* 381, 244–251.

Frigola, X., Inman, B. A., Lohse, C. M., Krco, C. J., Cheville, J. C., Thompson, R. H., et al. (2011). Identification of a soluble form of B7-H1 that retains immunosuppressive activity and is associated with aggressive renal cell carcinoma. *Clin. Cancer Res.* 17, 1915–1923. doi: 10.1158/1078-0432.Ccr-10-0250

Funes, S. C., Rios, M., Escobar-Vera, J., and Kalergis, A. M. (2018). Implications of macrophage polarization in autoimmunity. *Immunology* 154, 186–195. doi: 10.1111/imm.12910

Gabrusiewicz, K., Li, X., Wei, J., Hashimoto, Y., Marisetty, A. L., Ott, M., et al. (2018). Glioblastoma stem cell-derived exosomes induce M2 macrophages and PD-L1 expression on human monocytes. *Oncoimmunology* 7:e1412909. doi: 10.1080/2162402x.2017.1412909

Geng, L., Huang, D., Liu, J., Qian, Y., Deng, J., Li, D., et al. (2008). B7-H1 up-regulated expression in human pancreatic carcinoma tissue associates with tumor progression. *J. Cancer Res. Clin. Oncol.* 134, 1021–1027. doi: 10.1007/s00432-008-0364-8

Grigg, C., and Rizvi, N. A. (2016). PD-L1 biomarker testing for non-small cell lung cancer: truth or fiction? *J. Immunother. Cancer* 4:48.

Guo, Y., Ji, X., Liu, J., Fan, D., Zhou, Q., Chen, C., et al. (2019). Effects of exosomes on pre-metastatic niche formation in tumors. *Mol. Cancer* 18:39. doi: 10.1186/s12943-019-0995-1

Haderk, F., Schulz, R., Iskar, M., Cid, L. L., Worst, T., Willmund, K. V., et al. (2017). Tumor-derived exosomes modulate PD-L1 expression in monocytes. *Sci. Immunol.* 2:eaah5509. doi: 10.1126/sciimmunol.aah5509

He, J., Hu, Y., Hu, M., and Li, B. (2015). Development of PD-1/PD-L1 pathway in tumor immune microenvironment and treatment for non-small cell lung cancer. *Sci. Rep.* 5, 1–9.

Herbst, R. S., Baas, P., Kim, D. W., Felip, E., Pérez-Gracia, J. L., Han, J. Y., et al. (2016). Pembrolizumab versus docetaxel for previously treated, PD-L1-positive, advanced non-small-cell lung cancer (KEYNOTE-010): a randomised controlled trial. *Lancet* 387, 1540–1550. doi: 10.1016/s0140-6736(15)01281-7

Hessvik, N., and Llorente, A. (2018). Current knowledge on exosome biogenesis and release. *Cell. Mol. Life Sci.* 75, 193–208. doi: 10.1007/s00018-017-2595-9

Hong, C. S., Funk, S., Muller, L., Boyiadzis, M., and Whiteside, T. L. (2016). Isolation of biologically active and morphologically intact exosomes from plasma of patients with cancer. *J. Extracell. Vesicles* 5:29289. doi: 10.3402/jev.v5.29289

Hu, S., Li, Z., Lutz, H., Huang, K., Su, T., Cores, J., et al. (2020). Dermal exosomes containing miR-218-5p promote hair regeneration by regulating β-catenin signaling. *Sci. Adv.* 6:eaba1685. doi: 10.1126/sciadv.aba1685

Huang, H. H., Hsiao, F. Y., Chen, H. M., Wang, C. Y., and Ko, B. S. (2021). Antiviral prophylaxis for hepatitis B carriers improves the prognosis of diffuse large B-cell lymphoma in Taiwan-a population-based study. *Br. J. Haematol.* 192, 110–118. doi: 10.1111/bjh.17142

Huang, M., Yang, J., Wang, T., Song, J., Xia, J., Wu, L., et al. (2020). Homogeneous, low-volume, efficient and sensitive quantitation of circulating exosome PD-L1 for cancer diagnosis and immunotherapy response prediction. *Angewandte Chemie* 59, 4800–4805.

Ichikawa, M., and Chen, L. (2005). Role of B7-H1 and B7-H4 molecules in down-regulating effector phase of T-cell immunity: novel cancer escaping mechanisms. *Front. Biosci.* 10:2856–2860. doi: 10.2741/1742

Iwai, Y., Ishida, M., Tanaka, Y., Okazaki, T., Honjo, T., and Minato, N. (2002). Involvement of PD-L1 on tumor cells in the escape from host immune system and tumor immunotherapy by PD-L1 blockade. *Proc. Natl. Acad. Sci. U.S.A.* 99, 12293–12297. doi: 10.1073/pnas.192461099

Keir, M., Butte, M., Freeman, G., and Sharpe, A. (2008). PD-1 and its ligands in tolerance and immunity. *Annu. Rev. Immunol.* 26, 677–704. doi: 10.1146/annurev.immunol.26.021607.090331

Kim, D. H., Kim, H., Choi, Y. J., Kim, S. Y., Lee, J.-E., Sung, K. J., et al. (2019). Exosome PD-L1 promotes tumor growth through immune escape in non-small cell lung cancer. *Exp. Mol. Med.* 51, 1–13.

Koch, R., Demant, M., Aung, T., Diering, N., Cicholas, A., Chapuy, B., et al. (2014). Populational equilibrium through exosome-mediated Wnt signaling in

tumor progression of diffuse large B-cell lymphoma. *Blood* 123, 2189–2198. doi: 10.1182/blood-2013-08-523886

Kourembanas, S. (2015). Exosomes: vehicles of intercellular signaling, biomarkers, and vectors of cell therapy. *Annu. Rev. Physiol.* 77, 13–27. doi: 10.1146/annurev-physiol-021014-071641

Li, C., Li, C., Zhi, C., Liang, W., Wang, X., Chen, X., et al. (2019). Clinical significance of PD-L1 expression in serum-derived exosomes in NSCLC patients. *J. Transl. Med.* 17:355. doi: 10.1186/s12967-019-2101-2

Li, J-W., Wei, P., Guo, Y., Shi, D., Yu, B-H., Su, Y-F., et al. (2020). Clinical significance of circulating exosomal PD-L1 and soluble PD-L1 in extranodal NK/T-cell lymphoma, nasal-type. *Am. J. Cancer Res.* 10, 4498–4512.

Li, Y., Zheng, Q., Bao, C., Li, S., Guo, W., Zhao, J., et al. (2015). Circular RNA is enriched and stable in exosomes: a promising biomarker for cancer diagnosis. *Cell Res.* 25, 981–984. doi: 10.1038/cr.2015.82

Lin, Y., Sung, W., Hsieh, M., Tsai, S., Lai, H., Yang, S., et al. (2015). High PD-L1 expression correlates with metastasis and poor prognosis in oral squamous cell carcinoma. *PLoS One* 10:e0142656. doi: 10.1371/journal.pone.0142656

Liu, C., Zeng, X., An, Z., Yang, Y., Eisenbaum, M., Gu, X., et al. (2018). Sensitive detection of exosome proteins via a compact surface plasmon resonance biosensor for cancer diagnosis. *ACS Sens.* 3, 1471–1479. doi: 10.1021/acssensors.8b00230

Liu, N., Zhang, J., Yin, M., Liu, H., Zhang, X., Li, J., et al. (2021). Inhibition of xCT suppresses the efficacy of anti-PD-1/L1 melanoma treatment through exosome PD-L1-induced macrophage M2 polarization. *Mol. Ther.* 29, 2321–2334. doi: 10.1016/j.ymthe.2021.03.013

Lo Cicero, A., Stahl, P., and Raposo, G. (2015). Extracellular vesicles shuffling intercellular messages: for good or for bad. *Curr. Opin. Cell Biol.* 35, 69–77. doi: 10.1016/j.ceb.2015.04.013

Ludwig, S., Floros, T., Theodoraki, M. N., Hong, C. S., Jackson, E. K., Lang, S., et al. (2017). Suppression of lymphocyte functions by plasma exosomes correlates with disease activity in patients with head and neck cancer. *Clin. Cancer Res.* 23, 4843–4854. doi: 10.1158/1078-0432.Ccr-16-2819

Lux, A., Kahlert, C., Grützmann, R., and Pilarsky, C. (2019). C-met and PD-L1 on circulating exosomes as diagnostic and prognostic markers for pancreatic Cancer. *Int. J. Mol. Sci.* 20:3305.

Martinez, F. O., and Gordon, S. (2014). The M1 and M2 paradigm of macrophage activation: time for reassessment. *F1000Prime Rep.* 6:13. doi: 10.12703/p6-13

Martinez, V. G., O'Neill, S., Salimu, J., Breslin, S., Clayton, A., Crown, J., et al. (2017). Resistance to HER2-targeted anti-cancer drugs is associated with immune evasion in cancer cells and their derived extracellular vesicles. *Oncoimmunology* 6:e1362530.

Mashouri, L., Yousefi, H., Aref, A., Ahadi, A., Molaei, F., and Alahari, S. (2019). Exosomes: composition, biogenesis, and mechanisms in cancer metastasis and drug resistance. *Mol. Cancer* 18:75. doi: 10.1186/s12943-019-0991-5

Melo, S. A., Luecke, L. B., Kahlert, C., Fernandez, A. F., Gammon, S. T., Kaye, J., et al. (2015). Glypican-1 identifies cancer exosomes and detects early pancreatic cancer. *Nature* 523, 177–182. doi: 10.1038/nature14581

Mittal, D., Gubin, M. M., Schreiber, R. D., and Smyth, M. J. (2014). New insights into cancer immunoediting and its three component phases-elimination, equilibrium and escape. *Curr. Opin. Immunol.* 27, 16–25. doi: 10.1016/j.coi.2014.01.004

Mittendorf, E. A., Philips, A. V., Meric-Bernstam, F., Qiao, N., Wu, Y., Harrington, S., et al. (2014). PD-L1 expression in triple-negative breast cancer. *Cancer Immunol. Res.* 2, 361–370. doi: 10.1158/2326-6066.Cir-13-0127

Mok, T. S. K., Wu, Y. L., Kudaba, I., Kowalski, D. M., Cho, B. C., Turna, H. Z., et al. (2019). Pembrolizumab versus chemotherapy for previously untreated, PD-L1-expressing, locally advanced or metastatic non-small-cell lung cancer (KEYNOTE-042): a randomised, open-label, controlled, phase 3 trial. *Lancet* 393, 1819–1830. doi: 10.1016/s0140-6736(18)32409-7

Monypenny, J., Milewicz, H., Flores-Borja, F., Weitsman, G., Cheung, A., Chowdhury, R., et al. (2018). ALIX Regulates tumor-mediated immunosuppression by controlling EGFR activity and PD-L1 presentation. *Cell Rep.* 24, 630–641. doi: 10.1016/j.celrep.2018.06.066

Mourad, M., Jetmore, T., Jategaonkar, A. A., Moubayed, S., Moshier, E., and Urken, M. L. (2017). Epidemiological trends of head and neck cancer in the United States: a SEER population study. *J. Oral Maxillofac. Surg.* 75, 2562–2572.

Muro, K., Chung, H. C., Shankaran, V., Geva, R., Catenacci, D., Gupta, S., et al. (2016). Pembrolizumab for patients with PD-L1-positive advanced gastric cancer (KEYNOTE-012): a multicentre, open-label, phase 1b trial. *Lancet Oncol.* 17, 717–726.

Nagato, T., Ohkuri, T., Ohara, K., Hirata, Y., Kishibe, K., Komabayashi, Y., et al. (2017). Programmed death-ligand 1 and its soluble form are highly expressed in nasal natural killer/T-cell lymphoma: a potential rationale for immunotherapy. *Cancer Immunol. Immunother.* 66, 877–890. doi: 10.1007/s00262-017-1987-x

Nahta, R., and Esteva, F. J. (2007). Trastuzumab: triumphs and tribulations. *Oncogene* 26, 3637–3643.

Nawaz, M., Camussi, G., Valadi, H., Nazarenko, I., Ekström, K., Wang, X., et al. (2014). The emerging role of extracellular vesicles as biomarkers for urogenital cancers. *Nat. Rev. Urol.* 11, 688–701. doi: 10.1038/nrurol.2014.301

Nishimura, H., Agata, Y., Kawasaki, A., Sato, M., Imamura, S., Minato, N., et al. (1996). Developmentally regulated expression of the PD-1 protein on the surface of double-negative (CD4-CD8-) thymocytes. *Int. Immunol.* 8, 773–780. doi: 10.1093/intimm/8.5.773

Noguchi, T., Ward, J. P., Gubin, M. M., Arthur, C. D., Lee, S. H., Hundal, J., et al. (2017). Temporally distinct PD-L1 expression by tumor and host cells contributes to immune escape. *Cancer Immunol. Res.* 5, 106–117. doi: 10.1158/2326-6066.Cir-16-0391

Nolte-'t Hoen, E., Buermans, H., Waasdorp, M., Stoorvogel, W., Wauben, M., and Hoen, P. A. (2012). Deep sequencing of RNA from immune cell-derived vesicles uncovers the selective incorporation of small non-coding RNA biotypes with potential regulatory functions. *Nucleic Acids Res.* 40, 9272–9285. doi: 10.1093/nar/gks658

Okazaki, F., Matsunaga, N., Hamamura, K., Suzuki, K., Nakao, T., Okazaki, H., et al. (2017). Administering xCT inhibitors based on circadian clock improves antitumor effects. *Cancer Res.* 77, 6603–6613. doi: 10.1158/0008-5472.Can-17-0720

Ono, K., Sogawa, C., Kawai, H., Tran, M., Taha, E., Lu, Y., et al. (2020). Triple knockdown of CDC37, HSP90-alpha and HSP90-beta diminishes extracellular vesicles-driven malignancy events and macrophage M2 polarization in oral cancer. *J. Extracell. Vesicles* 9:1769373. doi: 10.1080/20013078.2020.1769373

Pang, Y., Shi, J., Yang, X., Wang, C., Sun, Z., and Xiao, R. (2020). Personalized detection of circling exosome PD-L1 based on Fe3O4@ TiO2 isolation and SERS immunoassay. *Biosens. Bioelectron.* 148:111800.

Patel, S. P., and Kurzrock, R. (2015). PD-L1 expression as a predictive biomarker in cancer immunotherapy. *Mol. Cancer Ther.* 14, 847–856. doi: 10.1158/1535-7163.Mct-14-0983

Poggio, M., Hu, T., Pai, C. C., Chu, B., Belair, C. D., Chang, A., et al. (2019). Suppression of exosome PD-L1 induces systemic anti-tumor immunity and memory. *Cell* 177, 414–427.e13. doi: 10.1016/j.cell.2019.02.016

Price, T. J., Shapiro, J. D., Segelov, E., Karapetis, C. S., Pavlakis, N., Van Cutsem, E., et al. (2012). Management of advanced gastric cancer. *Expert Rev. Gastroenterol. Hepatol.* 6, 199–209.

Rahbari, M., Rahbari, N., Reissfelder, C., Weitz, J., and Kahlert, C. (2016). Exosomes: novel implications in diagnosis and treatment of gastrointestinal cancer. *Langenbecks Arch. Surg.* 401, 1097–1110.

Ramirez, M. I., Amorim, M. G., Gadelha, C., Milic, I., Welsh, J. A., Freitas, V. M., et al. (2018). Technical challenges of working with extracellular vesicles. *Nanoscale* 10, 881–906.

Ribas, A., Hamid, O., Daud, A., Hodi, F. S., Wolchok, J. D., Kefford, R., et al. (2016). Association of pembrolizumab with tumor response and survival among patients with advanced melanoma. *JAMA* 315, 1600–1609. doi: 10.1001/jama.2016.4059

Ricklefs, F. L., Alayo, Q., Krenzlin, H., Mahmoud, A. B., Speranza, M. C., Nakashima, H., et al. (2018). Immune evasion mediated by PD-L1 on glioblastoma-derived extracellular vesicles. *Sci. Adv.* 4:eaar2766. doi: 10.1126/sciadv.aar2766

Roefs, M., Sluijter, J., and Vader, P. (2020). Extracellular vesicle-associated proteins in tissue repair. *Trends Cell Biol.* 30, 990–1013. doi: 10.1016/j.tcb.2020.09.009

Shi, M. H., Xing, Y. F., Zhang, Z. L., Huang, J. A., and Chen, Y. J. (2013). [Effect of soluble PD-L1 released by lung cancer cells in regulating the function of T lymphocytes]. *Zhonghua Zhong Liu Za Zhi* 35, 85–88. doi: 10.3760/cma.j.issn.0253-3766.2013.02.002

Siegel, R., Naishadham, D., and Jemal, A. (2012). Cancer statistics, 2012. *CA Cancer J. Clin.* 62, 10–29.

Slamon, D. J., Godolphin, W., Jones, L. A., Holt, J. A., Wong, S. G., Keith, D. E., et al. (1989). Studies of the HER-2/neu proto-oncogene in human breast and ovarian cancer. *Science* 244, 707–712.

Steinman, R. M., and Banchereau, J. (2007). Taking dendritic cells into medicine. *Nature* 449, 419–426.

Strome, S. E., Dong, H., Tamura, H., Voss, S. G., Flies, D. B., Tamada, K., et al. (2003). B7-H1 blockade augments adoptive T-cell immunotherapy for squamous cell carcinoma. *Cancer Res.* 63, 6501–6505.

Stuffers, S., Sem Wegner, C., Stenmark, H., and Brech, A. (2009). Multivesicular endosome biogenesis in the absence of ESCRTs. *Traffic* 10, 925–937. doi: 10.1111/j.1600-0854.2009.00920.x

Sun, C., Mezzadra, R., and Schumacher, T. N. (2018). Regulation and function of the PD-L1 checkpoint. *Immunity* 48, 434–452. doi: 10.1016/j.immuni.2018.03.014

Tang, M. K., and Wong, A. S. (2015). Exosomes: emerging biomarkers and targets for ovarian cancer. *Cancer Lett.* 367, 26–33. doi: 10.1016/j.canlet.2015.07.014

Taube, J. M., Klein, A., Brahmer, J. R., Xu, H., Pan, X., Kim, J. H., et al. (2014). Association of PD-1, PD-1 ligands, and other features of the tumor immune microenvironment with response to anti-PD-1 therapy. *Clin. Cancer Res.* 20, 5064–5074. doi: 10.1158/1078-0432.Ccr-13-3271

Thakur, A., Qiu, G., Xu, C., Han, X., Yang, T., Ng, S. P., et al. (2020). Label-free sensing of exosome MCT1 and CD147 for tracking metabolic reprogramming and malignant progression in glioma. *Sci. Adv.* 6:eaaz6119. doi: 10.1126/sciadv.aaz6119

Thakur, B., Zhang, H., Becker, A., Matei, I., Huang, Y., Costa-Silva, B., et al. (2014). Double-stranded DNA in exosomes: a novel biomarker in cancer detection. *Cell Res.* 24, 766–769. doi: 10.1038/cr.2014.44

Theodoraki, M. N., Yerneni, S. S., Hoffmann, T. K., Gooding, W. E., and Whiteside, T. L. (2018). Clinical significance of PD-L1(+) exosomes in plasma of head and neck cancer patients. *Clin. Cancer Res.* 24, 896–905. doi: 10.1158/1078-0432.Ccr-17-2664

Theodoraki, M. N., Yerneni, S., Gooding, W. E., Ohr, J., Clump, D. A., Bauman, J. E., et al. (2019). Circulating exosomes measure responses to therapy in head and neck cancer patients treated with cetuximab, ipilimumab, and IMRT. *Oncoimmunology* 8:1593805. doi: 10.1080/2162402x.2019.1593805

Théry, C., Zitvogel, L., and Amigorena, S. (2002). Exosomes: composition, biogenesis and function. *Nat. Rev. Immunol.* 2, 569–579. doi: 10.1038/nri855

Topalian, S. L., Taube, J. M., Anders, R. A., and Pardoll, D. M. (2016). Mechanism-driven biomarkers to guide immune checkpoint blockade in cancer therapy. *Nat. Rev. Cancer* 16:275.

van Niel, G., D'Angelo, G., and Raposo, G. (2018). Shedding light on the cell biology of extracellular vesicles. *Nat. Rev. Mol. Cell Biol.* 19, 213–228. doi: 10.1038/nrm.2017.125

Villarroya-Beltri, C., Gutiérrez-Vázquez, C., Sánchez-Cabo, F., Pérez-Hernández, D., Vázquez, J., Martin-Cofreces, N., et al. (2013). Sumoylated hnRNPA2B1 controls the sorting of miRNAs into exosomes through binding to specific motifs. *Nat. Commun.* 4:2980. doi: 10.1038/ncomms3980

Wang, L., Ma, Q., Chen, X., Guo, K., Li, J., and Zhang, M. (2010). Clinical significance of B7-H1 and B7-1 expressions in pancreatic carcinoma. *World J. Surg.* 34, 1059–1065. doi: 10.1007/s00268-010-0448-x

Wang, X., Teng, F., Kong, L., and Yu, J. (2016). PD-L1 expression in human cancers and its association with clinical outcomes. *OncoTargets Ther.* 9, 5023–5039. doi: 10.2147/ott.S105862

Welton, J. L., Khanna, S., Giles, P. J., Brennan, P., Brewis, I. A., Staffurth, J., et al. (2010). Proteomics analysis of bladder cancer exosomes. *Mol. Cell. Proteomics* 9, 1324–1338. doi: 10.1074/mcp.M000063-MCP201

Wen, Z. F., Liu, H., Gao, R., Zhou, M., Ma, J., Zhang, Y., et al. (2018). Tumor cell-released autophagosomes (TRAPs) promote immunosuppression through induction of M2-like macrophages with increased expression of PD-L1. *J. Immunother. Cancer* 6:151. doi: 10.1186/s40425-018-0452-5

Whiteside, T. L. (2016). Exosomes and tumor-mediated immune suppression. *J. Clin. Invest.* 126, 1216–1223. doi: 10.1172/jci81136

Whiteside, T. L. (2018). Head and neck carcinoma immunotherapy: facts and hopes. *Clin. Cancer Res.* 24, 6–13. doi: 10.1158/1078-0432.Ccr-17-1261

Xiang, S. Y., Yu, C., Aggarwal, A., and Reinhard, C. (2016). Genomic alterations and molecular subtypes of gastric cancers in Asians. *Chin. J. Cancer* 35:42.

Xing, Y. F., Zhang, Z. L., Shi, M. H., Ma, Y., and Chen, Y. J. (2012). [The level of soluble programmed death-1 in peripheral blood of patients with lung cancer and its clinical implications]. *Zhonghua Jie He He Hu Xi Za Zhi* 35, 102–106.

Yang, Y., Li, C.-W., Chan, L.-C., Wei, Y., Hsu, J.-M., Xia, W., et al. (2018). Exosome PD-L1 harbors active defense function to suppress T cell killing of breast cancer cells and promote tumor growth. *Cell Res.* 28, 862–864.

Zahn, M., Kaluszniak, B., Möller, P., and Marienfeld, R. (2020). The PTP1B mutant PTP1BΔ2-4 is a positive regulator of the JAK/STAT signalling pathway in Hodgkin lymphoma. *Carcinogenesis* 42, 517–527. doi: 10.1093/carcin/bgaa144

Zaretsky, J. M., Garcia-Diaz, A., Shin, D. S., Escuin-Ordinas, H., Hugo, W., Hu-Lieskovan, S., et al. (2016). Mutations associated with acquired resistance to PD-1 blockade in melanoma. *N. Engl. J. Med.* 375, 819–829. doi: 10.1056/NEJMoa1604958

Zhang, J., Gao, J., Li, Y., Nie, J., Dai, L., Hu, W., et al. (2015). Circulating PD-L1 in NSCLC patients and the correlation between the level of PD-L1 expression and the clinical characteristics. *Thorac. Cancer* 6, 534–538. doi: 10.1111/1759-7714.12247

Zhang, Y., Du, W., Chen, Z., and Xiang, C. (2017). Upregulation of PD-L1 by SPP1 mediates macrophage polarization and facilitates immune escape in lung adenocarcinoma. *Exp. Cell Res.* 359, 449–457. doi: 10.1016/j.yexcr.2017.08.028

Zhou, Y., Miao, J., Wu, H., Tang, H., Kuang, J., Zhou, X., et al. (2017). PD-1 and PD-L1 expression in 132 recurrent nasopharyngeal carcinoma: the correlation with anemia and outcomes. *Oncotarget* 8, 51210–51223. doi: 10.18632/oncotarget.17214

Conflict of Interest: The authors declare that the research was conducted in the absence of any commercial or financial relationships that could be construed as a potential conflict of interest.

Publisher's Note: All claims expressed in this article are solely those of the authors and do not necessarily represent those of their affiliated organizations, or those of the publisher, the editors and the reviewers. Any product that may be evaluated in this article, or claim that may be made by its manufacturer, is not guaranteed or endorsed by the publisher.

frontiers in Cell and Developmental Biology

ORIGINAL RESEARCH
published: 11 January 2022
doi: 10.3389/fcell.2021.794801

Characterization of m6A Regulator-Mediated Methylation Modification Patterns and Tumor Microenvironment Infiltration in Ovarian Cancer

*Yihong Luo, Xiang Sun and Jian Xiong**

Department of Gynaecology and Obstetrics, Guangzhou Women and Children's Medical Center, Guangzhou Medical University, Guangzhou, China

Introduction: Studies have demonstrated the epigenetic regulation of immune responses in various cancers. However, little is known about the RNA N6-methyladenosine (m6A) modification patterns of the microenvironment (TME) cell infiltration in ovarian cancer (OC).

Methods: We evaluated the correlation between m6A modification patterns and TME cell infiltration based on 459 OC samples from the Cancer Genome Atlas and Gene-Expression Omnibus database. We constructed an m6Ascore system to quantify m6A modification patterns using principal component analysis.

Results: Based on unsupervised clustering, three m6A modification patterns were identified. Gene set variation analysis showed that the antigen presentation signal pathway, the NOTCH signaling pathway, and the metabolism-related pathway differed significantly across m6A modificaiton patterns. The m6Ascore is closely correlated with TME cell infiltration. OC patients with lower m6Ascores had worse outcomes. There was better risk stratification with combined m6Ascore and tumor mutation burden. The responses to immune checkpoint inhibitor treatment significantly differed between high and low m6Ascore groups.

Conclusion: M6A modification plays an essential role in TME cell infiltration in OC. Evaluating the m6A modification patterns in OC patients could enhance our understanding of TME infiltration characterization and guide immunotherapy strategies.

Keywords: ovairan cancer, N6-methyladenosine, microenvironment, RNA methylation, immunotherapy

OPEN ACCESS

Edited by:
Daniela Trisciuoglio, Institute of Molecular Biology and Pathology, Italy

Reviewed by:
Qinglv Wei, Third Affiliated Hospital of Chongqing Medical University, China
Christiane Pienna Soares, Sao Paulo State Universty, Brazil
Yutao Wang, China Medical University, China

****Correspondence:***
Jian Xiong
xiongjian0817@outlook.com

Specialty section:
This article was submitted to Epigenomics and Epigenetics, a section of the journal Frontiers in Cell and Developmental Biology

Received: *19 October 2021*
Accepted: *17 December 2021*
Published: *11 January 2022*

Citation:
Luo Y, Sun X and Xiong J (2022) Characterization of m6A Regulator-Mediated Methylation Modification Patterns and Tumor Microenvironment Infiltration in Ovarian Cancer. Front. Cell Dev. Biol. 9:794801. doi: 10.3389/fcell.2021.794801

INTRODUCTION

Ovarian cancer (OC) is the third most common cancer in the female reproductive system and the leading cause of cancer-related death among gynecological cancers (Siegel et al., 2018). Patients with OC are often diagnosed at an advanced stage because of a lack of early diagnosis methods. There remains a lack of satisfactory treatment for patients with advanced OC. Thus, OC patients suffer poor outcomes and high relapse rates. The 5-year survival for most OC patients is less than 40% despite the advances in therapies such as adjuvant chemotherapy and cytoreductive surgery (Armstrong et al., 2020). Therefore, understanding the molecular mechanisms underlying the pathogenesis and development of OC may advance the diagnosis and treatment of OC.

Several lines of evidence suggested that epigenetics plays an essential role in ovarian carcinogenesis. N6-methyladenosine (m6A) RNA methylation, one of the most dominant drivers of eukaryotic mRNA modification, is a common form of epigenetic regulation (Liu and Pan, 2016). Many proteins defined as m6A "writers" (METTL3, METTL14, WTAP, et al.), "readers" (YTHDF1, YTHDF2, YTHDC2, HNRNPA2B1, et al.) and "erasers" (ALKBH5 and FTO) participate in the modification of m6A methylation (Roundtree et al., 2017). An in-depth understanding of these m6A regulators would contribute to uncover the mechanism of m6A RNA modification in post-transcriptional regulation. Evidence revealed that m6A regulators are implicated in disorders of diverse biological processes, including cell proliferation and death, embryonic

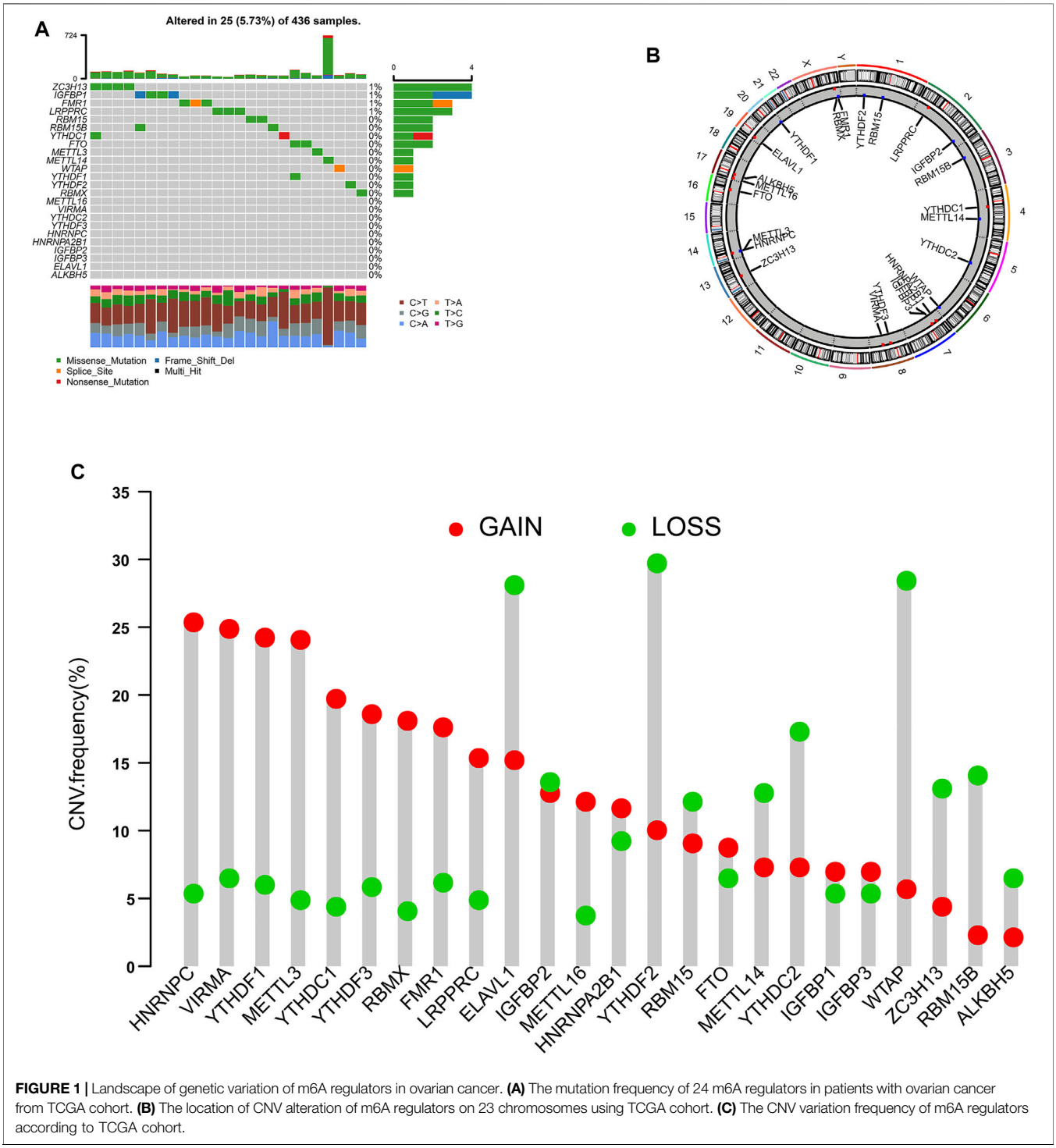

FIGURE 1 | Landscape of genetic variation of m6A regulators in ovarian cancer. **(A)** The mutation frequency of 24 m6A regulators in patients with ovarian cancer from TCGA cohort. **(B)** The location of CNV alteration of m6A regulators on 23 chromosomes using TCGA cohort. **(C)** The CNV variation frequency of m6A regulators according to TCGA cohort.

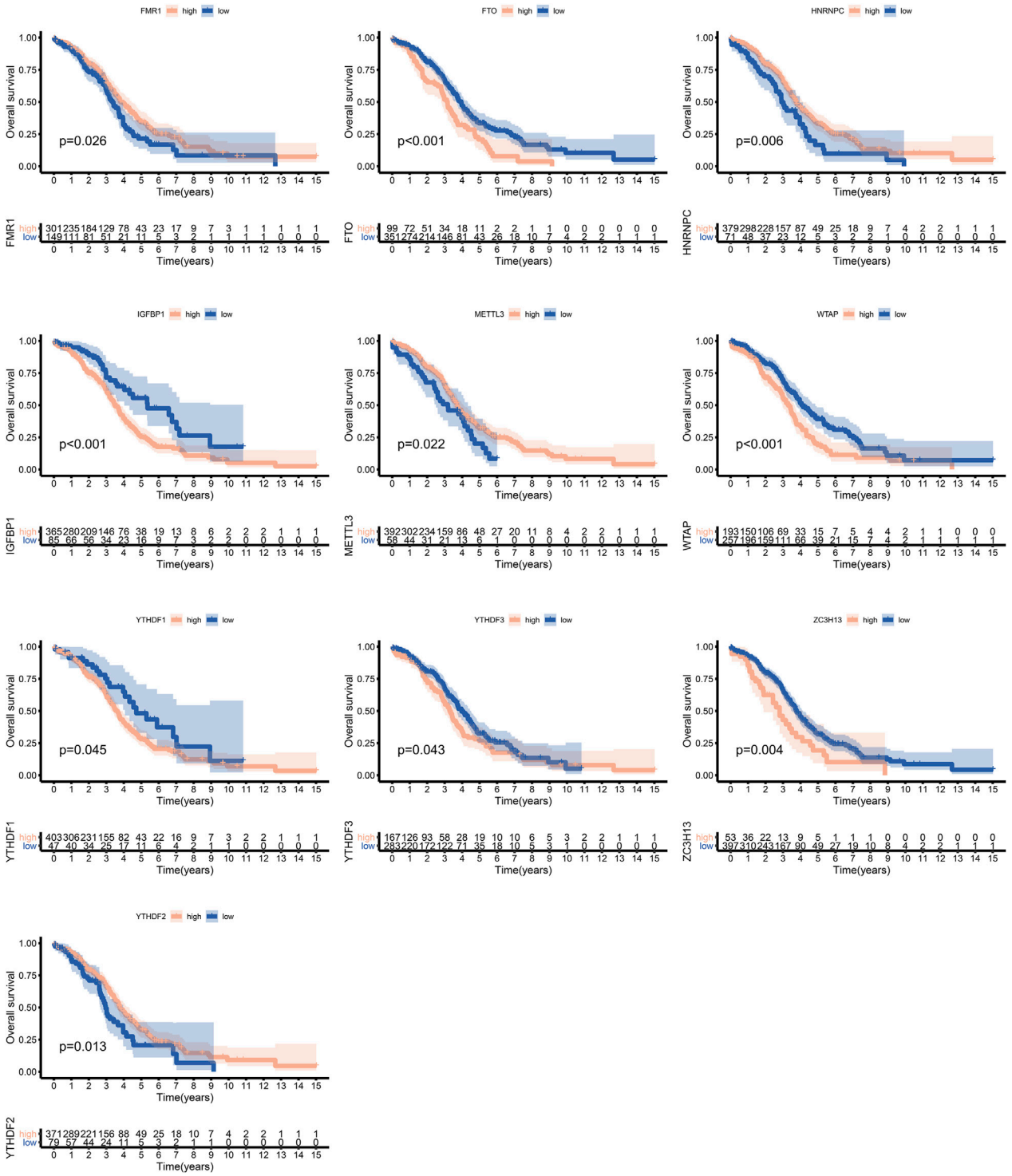

FIGURE 2 | Survival analysis of m6A regulators in ovarian cancer according to TCGA and GSE14764 cohorts.

stem cell self-renewal, fate determination, cancer progression, and immunomodulatory abnormalities (Yue et al., 2015; Deng et al., 2018). For instance, the m6A writer METTL3 can promote the growth and invasion of OC via stimulating AXL translation (Hua et al., 2018). The m6A reader YTHDF1 promotes the progression of OC via augmenting the translation of EIF3C in

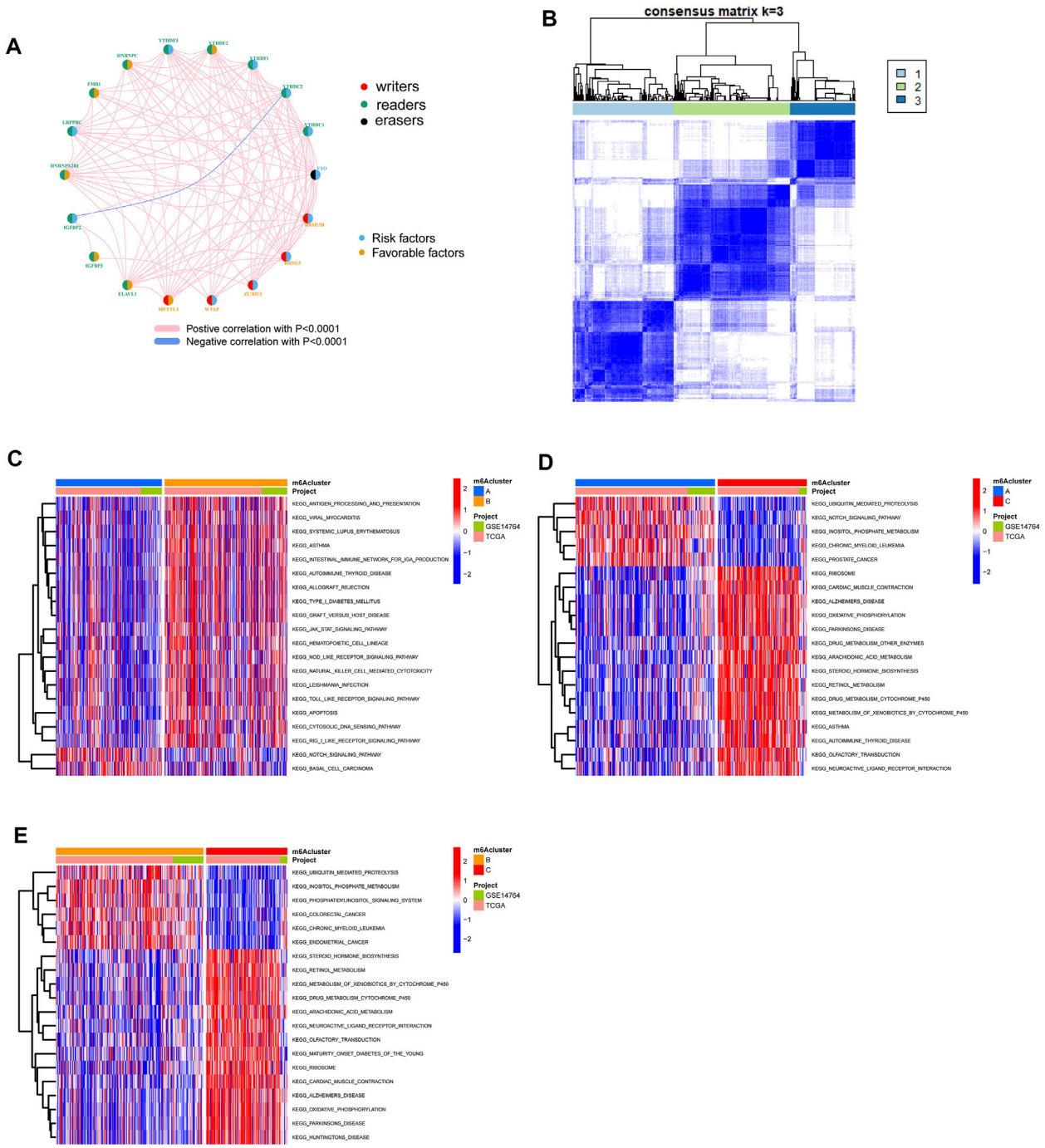

FIGURE 3 | Patterns of m6A methylation modification and biological characteristics of each pattern. **(A)** The interaction between m6A regulators in ovarian cancer. **(B)** Consensus matrices of m6A regulators according to TCGA and GSE14764 cohort for k = 3. **(C–E)**. GSVA enrichment analysis showing the activation states of biological pathways in distinct m6A modification patterns.

a m6A dependent manner (Liu et al., 2020). The m6A eraser FTO can inhibit the self-renewal of OC cancer stem cell via blocking cAMP signaling (Huang et al., 2020).

Studies demonstrated that the tumor microenvironment (TME) plays an essential role in tumor progression. TME is constructed by stromal cells, containing fibroblasts, mesenchymal stem cells, and immune cells (Quail and Joyce, 2013). Innate immune cells (neutrophils, dendritic cells, macrophages, innate lymphoid cells, natural killer cells, and myeloid-derived suppressor cells) and adaptive immune cells

(B cells and T cells) in the TME contribute to tumor progression (Hinshaw and Shevde, 2019). TME components directly and indirectly affect multiple biological behaviors of cancer cells such as inhibiting apoptosis, inducing proliferation, avoiding hypoxia, inducing immune tolerance, et al. (Binnewies et al., 2018). The evidence suggests that m6A modification could build a TME favorable for the growth of cancer cells (Zhu et al., 2021). For instance, Yi Jian et al. found that ALKBH5 could promote the progression of OC in a simulated TME via NF-κB signaling (Jiang et al., 2020). Therefore, a comprehensive understanding of the correlation between TME and m6A regulators might help elucidate the mechanisms of TME immune regulation. In the present study, we integrated the genomic data of OC samples from the Cancer Genome Atlas (TCGA) and Gene-Expression Omnibus (GEO) to evaluate the m6A modification pattern and its correlation with TME, which would enhance our understanding of how m6A modification participates in shaping TME in OC.

METHODS

Data Source

The mRNA expression profiles and clinical data containing 379 OC samples were downloaded from TCGA (http://cancergenome.nih.gov/). GSE14764 (Denkert et al., 2009) containing 80 OC samples was downloaded from GEO (http://www.ncbi.nlm.nih.gov/geo/). Samples without survival data were removed from further analysis. The "ComBat" algorithm of the sva package was used to correct the batch effects from non-biological technical biases. The somatic mutation data were downloaded from TCGA. Data in this study were analyzed using R software (version 3.6.1) and R Bioconductor packages.

Unsupervised Clustering for 24 m6A Regulators

A total of 24 m6A regulators were extracted to identify distinct m6A modification patterns. Based on the expression of these 24 m6A regulators, unsupervised clustering analysis was used to identify different m6A modification patterns, and classify OC patients for further analysis. A consensus clustering algorithm was used to determine the number of clusters and their stability (Wong, 1979). The ConsensusClusterPlus package was used to perform this algorithm, and we conducted 1000 times repetitions to guarantee the stability of clusters (Hayes, 2010).

Gene Set Variation Analysis

GSVA enrichment analysis was performed to investigate the biological processes between different m6A clusters. GSVA is commonly used to estimate the variation in biological processes in an expression dataset (Hänzelmann et al., 2013). We downloaded the gene set of "c2.cp.kegg.v6.2.symbols" from MSigDB for GSVA analysis. The clusterProfiler R package was used to conduct functional annotation for m6A-related genes. The cut-off value of FDR was 0.05. Adjusted $p < 0.05$ was represented statistical significance.

Tumor Microenvironment Cell Infiltration

We used single-sample gene set enrichment analysis (ssGSEA) to quantify the relative abundance of each immune cell infiltration in the OC TME. The gene set for marking each immune cell type was as described previously (Charoentong et al., 2017). The relative abundance of each immune infiltrating cell in each sample was represented with enrichment scores.

Construction of the m6A Gene Signature

To identify m6A-related genes, the OC samples were classified into three m6A modification patterns according to the expression of m6A regulators. Differentially expressed genes (DEGs) between m6A modification patterns were identified using the empirical Bayesian approach of the limma package. DEGs with adjusted $p < 0.001$ were considered significant.

We constructed an m6A gene signature (the m6Ascore) to quantify m6A modification patterns. The overlap of DEGs from various m6A clusters was extracted. We classified the OC patients into several groups using an unsupervised clustering method to analyze the overlap DEGs. The number of gene clusters and their stability were defined using the consensus clustering algorithm. Then, we extracted the genes with significant outcomes using a univariate Cox regression model. Principal component analysis (PCA) was performed to construct an m6A gene signature. The m6Ascore is defined as: m6Ascore = $\sum(PC1_i + PC2_i)$, where i represents each of the m6A-related genes (Zhang et al., 2020).

The Association Between m6A Gene Signature and Immunotherapy

The immunophenoscores (IPSs) of OC patients were downloaded from the cancer-immune group atlas (TCIA, https://tcia.at/home). The IPS was obtained according to four categories of immunogenicity-related genes (effector cells, MHC molecules, immunosuppressor cells, and immune modulators). The value of IPS ranges from 0 to 10, calculated based on z-scores, representing the expression of genes in cell types. The values of IPS are positively correlated with immunogenicity. A correlation analysis was also conducted to reveal the association between m6Ascore and TME.

Cell Culture and Transfection

Human ovarian cancer cell lines, A2780 and OVCAR3, were both obtained from the Chinese Academy of Sciences Cell Bank (China). A2780 and OVCAR3 were cultured in RPMI 1640 (Hyclone) and DMEM (High-Glucose) medium (Hyclone) supplemented with 10% serum. Both cells were cultured at 37°C in an atmosphere of 5% CO2.

Transwell Assay

Migration and invasion of ovarian cancer cells were measured by transwell chamber with 8-μm pores (Corning Costar, Corning, NY, United States) using 24-well plates. Briefly, A2780 and OVCAR3 cells (5 × 104) in 300 μl serum-free culture media were added into the upper chamber with 10% FBS in the lower chamber inserted in 24-well plates and cultured for 8 h. The

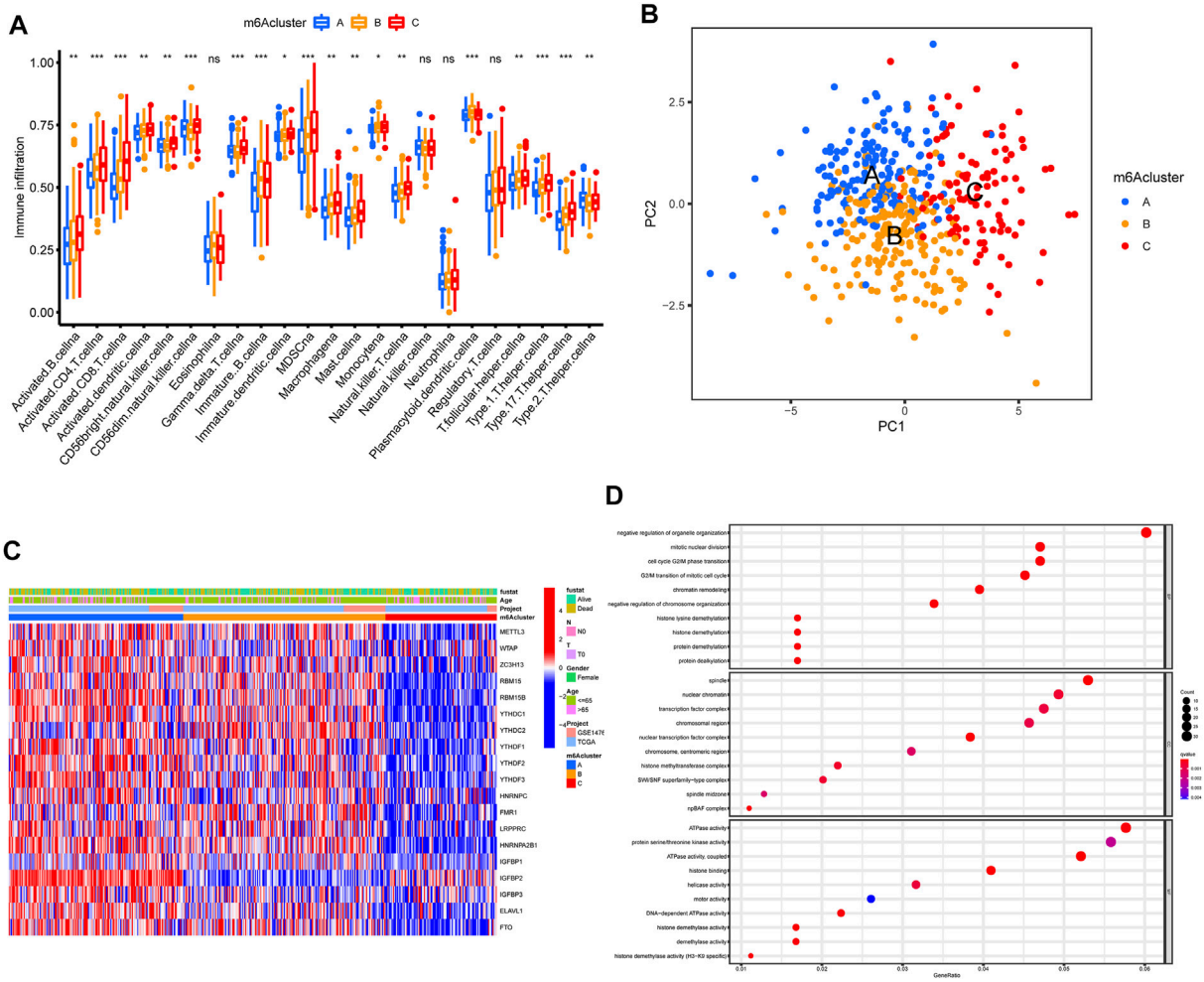

FIGURE 4 | TME cell infiltration characteristics and transcriptome traits in distinct m6A modification patterns. **(A)** The abundance of each TME infiltrating cell in three m6A modification patterns. **(B)** Principal component analysis for the transcriptome profiles of three m6A modification patterns, showing a remarkable difference on transcriptome between different modification patterns. **(C)** Unsupervised clustering of m6A regulators according to TCGA and GSE14764 cohort. **(D)** Functional annotation for m6A-related genes using GO enrichment analysis.

migrated cells on the lower side of the membranes were fixed with methanol and then stained with crystal violet and counted.

Wound-Healing Migration Assay

Wound-healing assay was used to measure the migration ability of cells. Cells were seeded into six-well plates and a straight line was drawn with a 1,000-μl sterile pipette when the density was 90–100%. Incubate for 48 h after the addition of serum-free medium. A microscope was used to make photography of scratch at 0 and 48 h.

Statistical Analysis

Spearman and distance correlation analyses were used to compute the correlation coefficients between the expression of m6A regulators and TME infiltrating immune cells. The *t*-test and Kruskal-Wallis tests were used for comparisons between two groups. Comparisons of three or more groups were conducted using one-way ANOVA or Kruskal-Wallis tests. The Kaplan-Meier method was used to generate the survival curves for predictive analysis, and the significance of differences was identified using the log-rank test. The survminer R package was used to determine the cut-off point for each subgroup. A multivariable Cox regression analysis was conducted to identify the independent prognostic factors. The waterfall function of the maftools package was used to generate the mutation landscape. The copy number variation landscape was plotted using the RCircos R package. All data were processed in R 3.6.1 software with a p-value < 0.05, indicating statistical significance.

RESULTS

Genetic Variation and Survival Analysis of m6A Regulators in Ovarian Cancer

We identified 24 m6A regulators in this study. The incidences of somatic mutations and copy number variations (CNVs) of the 24

m6A regulators are summarized in **Figure 1**. Twenty-five of 436 samples experienced mutations of m6A regulators. ZC3H13 and IGFBP1 exhibited the highest mutation frequency, while METTL16, VIRMA, YTHDC2, YTHDF3, HNRNPC, HNRNPA2B1, IGFBP2, IGFBP3, ELAVL1, and ALKBH5 showed no mutations in OC samples (**Figure 1A**). **Figure 1B** shows the location of CNV alteration of the 24 m6A regulators on chromosomes. HNRNPC, VRMA, YTHDF1, METTL3, YTHDC1, YTHDF3, RBMX, FMR1, and LRPPPC were focused on the amplification in copy number, while ELAVL1, YTHDF2, and WTAP had a widespread frequency of CNV deletion. Among these m6A regulators, the expressions of FMR1, FTO, HNRNPC, IGFBP1, METTL3, WTAP, YTHDF1, YTHDF3, ZC3H13, and YTHDF2 were significantly correlated with the outcome of OC, according to TCGA and GSE14764 cohorts (**Figure 2**).

Tumor Microenvironment Cell Infiltration in Different m6A Modification Patterns

The OC patients were classified with different m6A modification patterns based on the expression of m6A regulators using the ConsensusClusterPlus R package. Unsupervised clustering was used to identify three distinct m6A modification patterns, called m6Acluster A–C (**Figure 3B**, **Figure 4C**). GSVA enrichment analysis was performed to analyze the biological process among different m6Aclusters (**Figures 3C–3E**). Subsequent analysis of TME cell infiltration showed that m6Acluster-C was significantly rich in activated CD4/8 T cell, MDSC, macrophage, regulatory T cells, et al. (**Figure 4A**). The M6A score and the results of six different immune infiltration assessments are presented in **Supplementary Figure S1**.

Construction of an m6A Gene Signature

To further explore the m6A modification pattern, 572 m6A phenotype-related DEGs were extracted from three distinct m6Aclusters (**Figure 5A**). A multivariable Cox regression was conducted to identify genes with independently prognostic values (**Figure 5D**). GO enrichment analysis was performed to identify the biological processes related to 572 DEGs (**Figure 4D**). Then, we classified the OC patients into different genomic subtypes based on the 572 m6A phenotype-related DEGs using unsupervised clustering analysis. The OC patients were classified into three m6A modification genomic phenotypes, called genecluster A–C (**Figure 5B**, **Figure 6A**). This indicated that three distinct m6A modification patterns did exist in OC. The three geneclusters were closely associated with m6Aclusters (**Figure 6A**). The expression levels of m6A regulators differed significantly in the three geneclusters, following our expectation based on the m6A modification patterns.

Considering the complexity and heterogeneity of m6A modification, we constructed a scoring system to quantify m6A modifications based on the 572 m6A phenotype-related genes, termed as the m6Ascore. To better illustrate m6Ascore characteristics, we tested the correlations between the m6Ascore and TME cell infiltration (**Figure 6B**). The expression difference of M6A regulators in the three subgroups were shown in **Figure 6C**. A survival analysis revealed that patients with lower m6Ascores suffered from worse outcomes (**Figure 6D**). The m6Ascores significantly differed across m6Aclusters and geneClusters (**Figures 6E,F**).

Characteristics of m6A Modification and Tumor Somatic Mutation

According to OC samples in TCGA, we found that OC patients with a lower tumor mutation burden had worse outcomes (**Figure 7B**). However, the m6Ascore was not correlated with tumor mutation burden (**Figure 7A**). Interestingly, it provided a better risk stratification combining m6Ascore with tumor mutation burden (**Figure 7B**). We further analyzed the distribution of somatic mutation between high and low m6Ascore groups, showing that the tumor mutation burden was of no significant difference between high and low m6Ascore groups (**Figure 7C**).

The Association Between m6A Gene Signature and Immunotherapy

A correlation analysis was also conducted to reveal the associations between m6Ascore and immunotherapy. The OC patients with higher m6Ascore had higher IPS in all of the CTLA4_neg_PD1_neg, CTLA4_neg_PD1_pos, CTLA4_pos_PD1_neg, and CTLA4_pos_PD1_pos groups, indicating that these patients would have a better response to immunotherapy.

Knockout of YTHDF2 Significantly Inhibits Ovarian Cancer Cell Migration and Invasion

To further explore the relationship between YTHDF2 and cell proliferation and invasion phenotype in ovarian cancer cell lines, we conducted a series experiments *in vitro*. Transwell experiment proved that the migration ability of YTHDF2-knockdown group was significantly lower than that of NC group (**Figures 8A–C**). The wound healing test is used to study the effect of YTHDF2 on the migration of ovarian cancer cells. The results showed that the reduction of YTHDF2 led to the weakening of the migration ability of ovarian cancer cells (**Figure 8D**). Later, we gave the TCGA cohort and found that the expression level of YTHDF2 has a close positive correlation with common cell proliferation-related proteins, such as MKI67, PCNA, CTNNB1, TPX2 (**Figure 8E**).

DISCUSSION

It appears that m6A modification participates in the occurrence and development of tumors by interacting with a variety of m6A regulatory factors. A variety of m6A regulatory factors have been reported in the literature. Therefore, we identified groups of m6A regulatory modes in OC using transcriptional sequencing data and determined the biological functions of groups of various m6A regulatory modes using functional analysis. Adjust the difference in pathways. We then identified DEGs of m6A regulators using

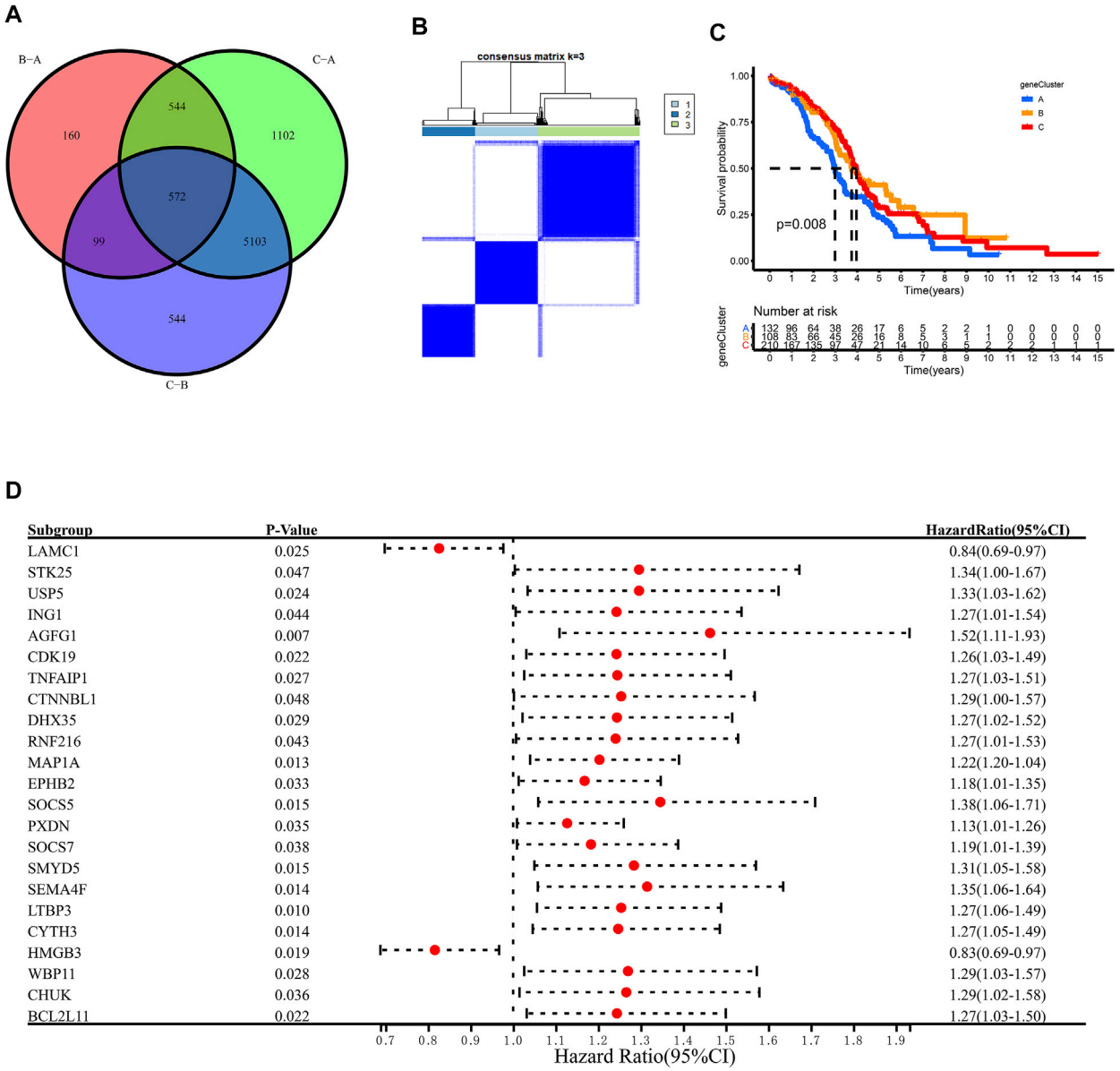

FIGURE 5 | Unsupervised clustering of 572 m6A phenotye-related genes according to TCGA and GSE14764 cohort. **(A)** 572 m6A phenotype-related genes shown in venn diagram. **(B)** Consensus matrices of 572 m6A phenotye-related genes according to TCGA and GSE14764 cohort for k = 3. **(C)** Survial analysis for the three m6A modification patterns in TCGA and GSE14764 cohort. **(D)** The prognostic analysis for m6A phenotye-related genes in TCGA and GSE14764 cohort using a multivariate Cox regression model.

pairwise difference analysis. These genes were later used to construct the m6Ascore.

We identified three m6A regulatory expression patterns based on unsupervised clustering. The GSVA score of the antigen presentation signal pathway in the C1 group is relatively low, suggesting that m6A in OC may affect the process of antigen presentation in the immune system. Han et al. found that mRNA m6A methylation mediates durable neoantigen-specific immunity after being regulated by the m6A binding protein YTHDF15 (Han et al., 2019). Compared with wild-type mice, ythdf1-deficient mice showed a higher antigen-specific $CD8^+$ T cell anti-tumor response. The deletion of YTHDF1 in classical dendritic cells enhances the cross-presentation of tumor antigens and the cross-priming of $CD8^+$ T cells *in vivo*. The NOTCH signaling pathway GSVA score was higher in the C1 group, suggesting that m6A significantly affects the NOTCH signaling pathway in OC. Zhang et al. found that continuous activation of Notch signal in METTL3-deficient embryonic arterial endothelial cells blocked the endothelial-to-haematopoietic transition (EHT) and inhibited the production of the earliest hematopoietic stem and progenitor cells (Zhang et al., 2017).

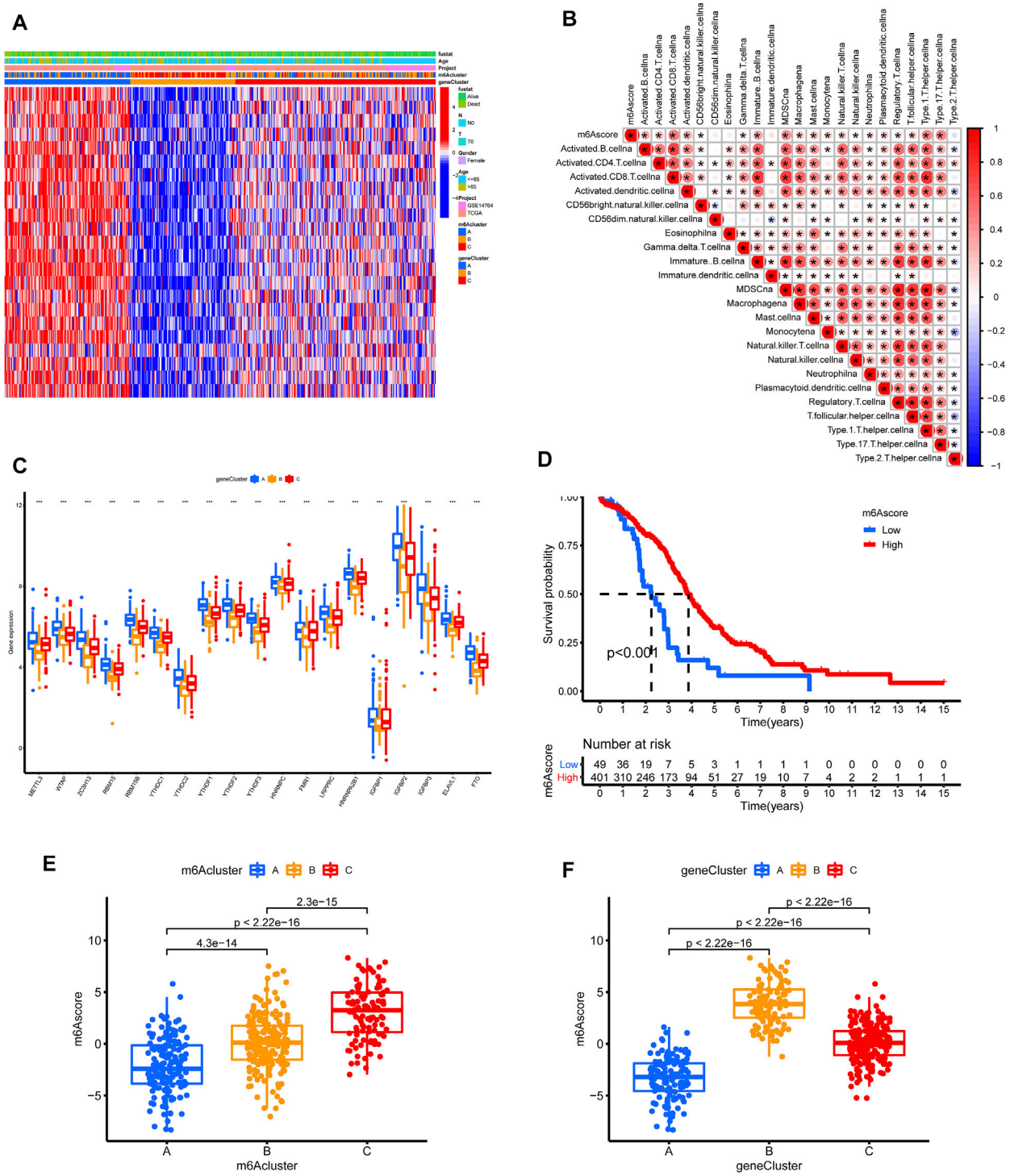

FIGURE 6 | Construction of m6A signature according to TCGA and GSE14764 cohort. **(A)** Unsupervised clustering of the m6A phenotype-related genes to classify patients into different genomic subtypes. **(B)** Correlations between m6Ascore and the TME infiltrating cell using Spearman analysis. **(C)** The expression of m6A regulators in three gene clusters. **(D)** Survival analysis for low and high m6Ascore patient groups using Kaplan-Meier curves. **(E,F)** Comparison of m6Ascores in different m6Aclusters and geneclusters.

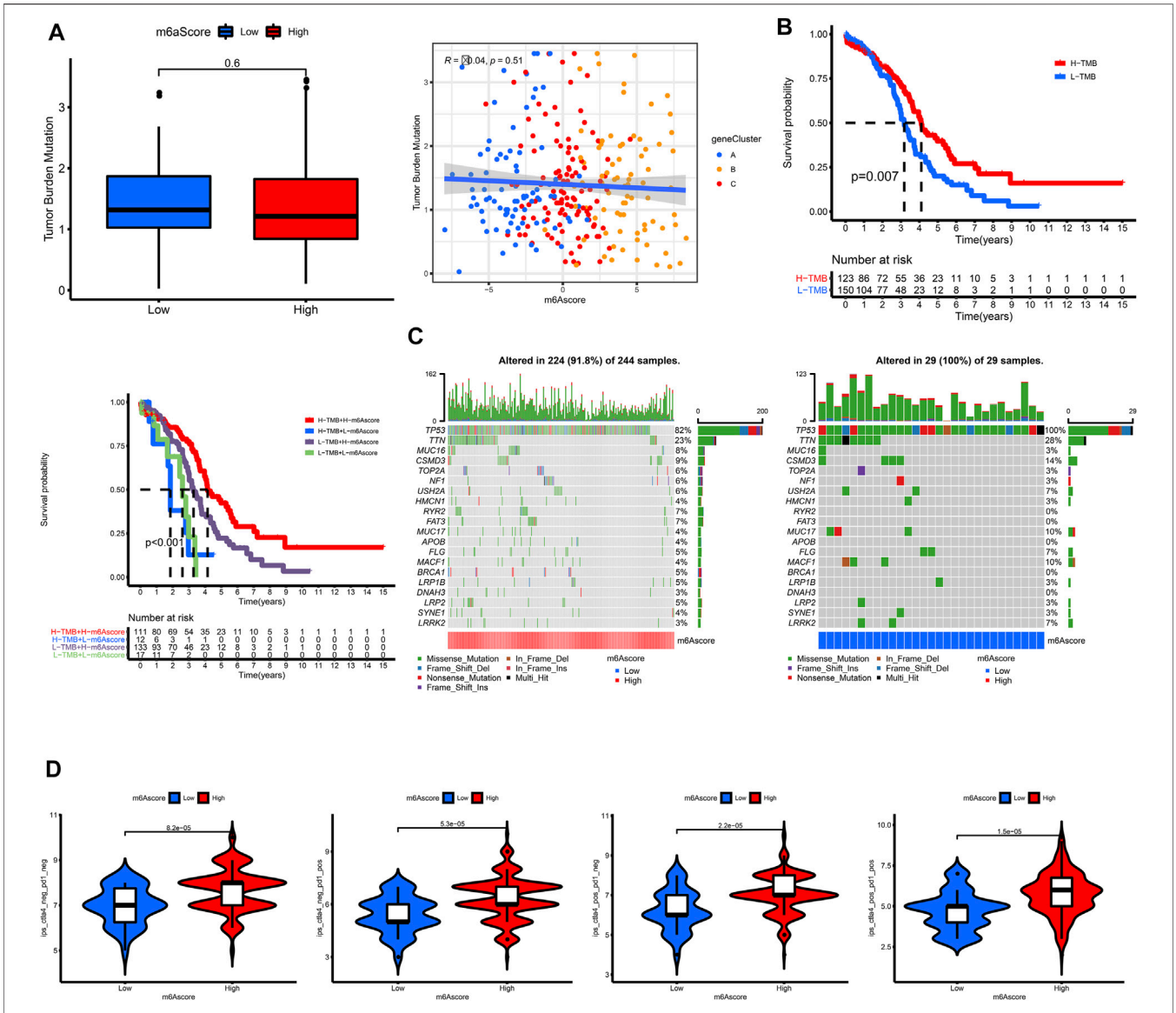

FIGURE 7 | Characteristics of m6A modification and tumor somatic mutation in TCGA. **(A)** The correlation of TMB and m6Ascore. **(B)** Survival analysis for subgroup patients stratified by both TMB and m6Ascore using Kaplan-Meier curves. **(C)** The waterfall plot of tumor somatic mutation established by those with high m6Ascore and low m6Ascore. **(D)** The association between m6Ascore and immunotherapy.

Colon cancer and endometrial cancer in the C2 group have higher GSVA scores, suggesting that m6A in OC may affect the regulation process of colon cancer and endometrial cancer pathways. IGF2BP3, METTL3, ALKBH5, et al. have been shown to be related to the proliferation and invasion of colon cancer tumor cells (Xu et al., 2020; Yang et al., 2020; Guo et al., 2020)–(Guo et al., 2020; Xu et al., 2020; Yang et al., 2020). IGF2BP and FTO are associated with tumorigenesis of endometrial epithelial carcinoma (Zhang et al., 2021a; Zhang et al., 2021b). In addition, the GSVA score of the oxidative phosphorylation signaling pathway in the C2 group is lower, suggesting that m6A may significantly affect the oxidative phosphorylation signaling pathway in OC. Pastò et al. Found that oxidative phosphorylation in stem cells of patients with epithelial OC (Pastò et al., 2014). Later, oxidative phosphorylation was also confirmed as a therapeutic target for OC (Burnett, 2019).

The GSAV scores of metabolism-related pathways in the C3 group are relatively high, suggesting that m6A may affect the metabolic process in the body in OC. Dongjun Dai et al. believe that m6A modification affects almost every step of RNA metabolism, including mRNA processing, mRNA output from the nucleus to the cytoplasm, mRNA translation, mRNA decay, and the biogenesis of long non-coding RNA (lncRNA) and microRNA (miRNA) (Zhao et al., 2017; Dai et al., 2018).

We found that m6Ascore is related to immune microinfiltration, and there are differences in different immune checkpoint inhibitor treatment response groups, suggesting that M6A plays an essential role in the tumor microenvironment. The

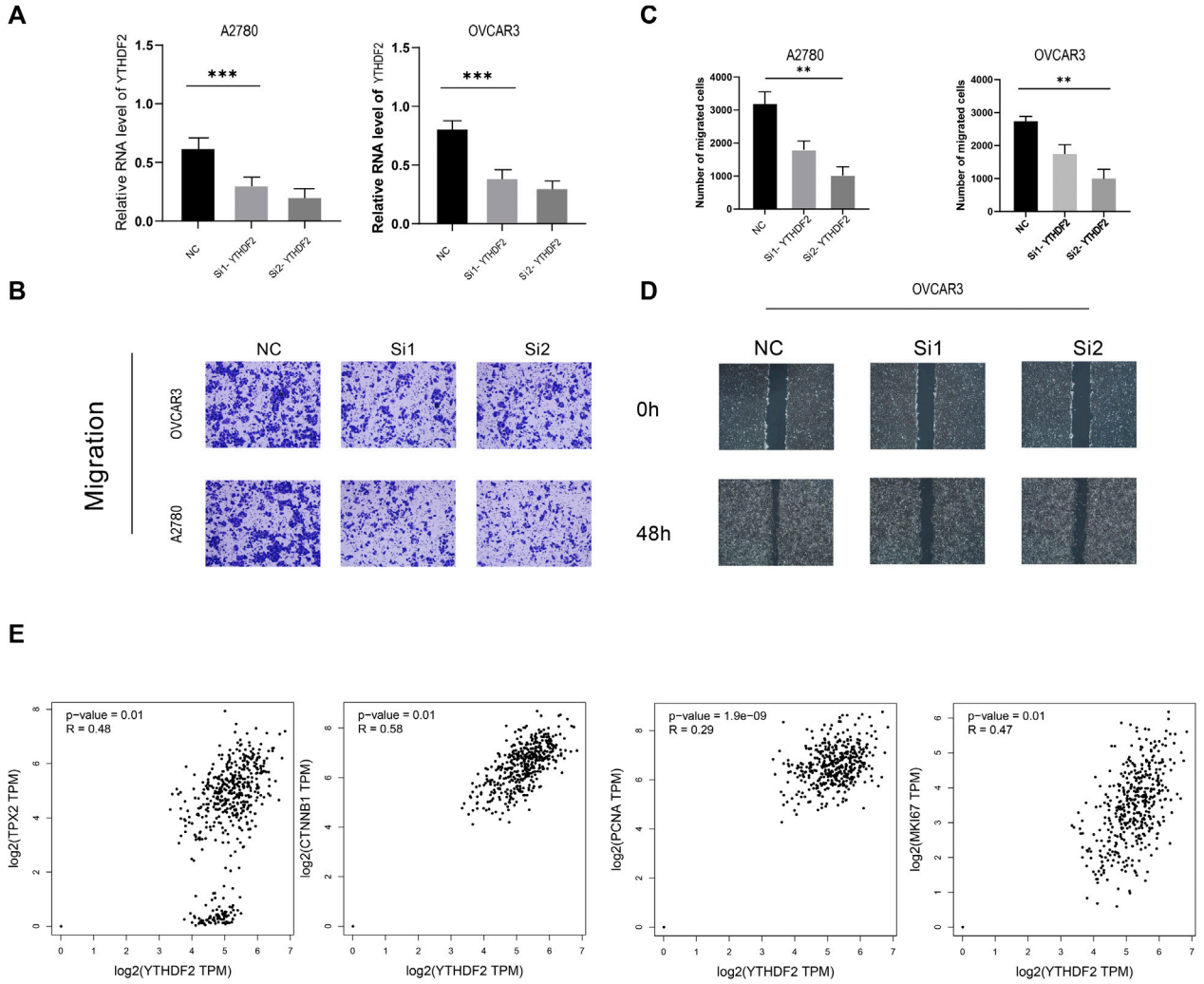

FIGURE 8 | A2780 and OVCAR3 Cell experiments. **(A)** RNA level of YTHDF2 in A2780 and OVCAR3 Cell experiments following YTHDF2 knockdown. **(B,C)** Knockdown of YTHDF2 decreased cell migration as detected by Transwell assays. **(D)** Knockdown of YTHDF2 decreased cell migration as detected by Wound-healing migration assays. **(E)**. YTHDF2 shows positive correlation with TPX2, MKI67, PCNA and CTNNB1.

role of m6A in dendritic cells (DCs) has been elucidated. DNA and RNA trigger innate immune responses by activating toll-like receptors (TLRs) on the surface of DCs. However, when DCs were exposed to m6A-modified RNA, compared with unmodified RNA, cytokines and activation markers were significantly produced, indicating that m6A modification hindered the activation of DCs. In addition, the innate immune system can detect RNA lacking m6A as a means of selectively responding to bacteria or necrotic tissue (Karikó et al., 2005). In addition, the methylation of m6A on mRNA controls the homeostasis of T cells. Studies showed that reduced m6A levels (caused by Mettl3-KO) lead to reduced Socs mRNA degradation, leading to inactivation of the IL-7/STAT5/Socs pathway. IL-7 stimulation activates the JAK/STAT pathway through m6A regulation, and downregulates the expression of SOCS family genes, and initiates the reprogramming of naive T cells to achieve differentiation and proliferation (Li et al., 2017).

There are some limitations to this article. Although the two cohorts were combined for data analysis, our findings of the article have not been verified by basic experiments and clinical trials. These limitations will be addressed in our future work.

CONCLUSION

There are three m6A mediation modes with significantly different representative pathways. We identified these representative genes according to the grouping results of these genes, an m6Ascore was constructed. The m6Ascore was closely related to the immune microenvironment and immunotherapy response. We provided a comprehensive analysis of the m6A regulation mode and biological effects in OC. These findings may provide support for the study of the mechanism of m6A mediation mode in OC.

DATA AVAILABILITY STATEMENT

The datasets presented in this study can be found in online repositories. The names of the repository/repositories and accession number(s) can be found in the article/**Supplementary Material**.

AUTHOR CONTRIBUTIONS

All authors wrote, revised, and approved the manuscript. All authors read and approved the final manuscript.

ACKNOWLEDGMENTS

JX wants to thank his parents for the love and support over the years.

SUPPLEMENTARY MATERIAL

The Supplementary Material for this article can be found online at: https://www.frontiersin.org/articles/10.3389/fcell.2021.794801/full#supplementary-material

REFERENCES

Armstrong, D. K., Alvarez, R. D., Bakkum-Gamez, J. N., Barroilhet, L., Behbakht, K., Berchuck, A., et al. (2020). Ovarian Cancer, Version 2.2020, NCCN Clinical Practice Guidelines in Oncology. *J. Natl. Compr. Cancer Netw.* 19 (2), 191–226.

Binnewies, M., Roberts, E. W., Kersten, K., Chan, V., Fearon, D. F., Merad, M., et al. (2018). Understanding the Tumor Immune Microenvironment (TIME) for Effective Therapy. *Nat. Med.* 24 (5), 541–550. doi:10.1038/s41591-018-0014-x

Burnett, A. L. (2019). The Science and Practice of Erection Physiology: Story of a Revolutionary Gaseous Molecule. *Trans. Am. Clin. Climatol Assoc.* 130, 51–59.

Charoentong, P., Finotello, F., Angelova, M., Mayer, C., Efremova, M., Rieder, D., et al. (2017). Pan-cancer Immunogenomic Analyses Reveal Genotype-Immunophenotype Relationships and Predictors of Response to Checkpoint Blockade. *Cel. Rep.* 18 (1), 248–262. doi:10.1016/j.celrep.2016.12.019

Dai, D., Wang, H., Zhu, L., Jin, H., and Wang, X. (2018). N6-methyladenosine Links RNA Metabolism to Cancer Progression. *Cell Death Dis* 9 (2), 124. doi:10.1038/s41419-017-0129-x

Deng, X., Su, R., Weng, H., Huang, H., Li, Z., and Chen, J. (2018). RNA N6-Methyladenosine Modification in Cancers: Current Status and Perspectives. *Cell Res* 28 (5), 507–517. doi:10.1038/s41422-018-0034-6

Denkert, C., Budczies, J., Darb-Esfahani, S., Györffy, B., Sehouli, J., Könsgen, D., et al. (2009). A Prognostic Gene Expression index in Ovarian Cancer-Validation across Different Independent Data Sets. *J. Pathol.* 218 (2), 273–280. doi:10.1002/path.2547

Guo, T., Liu, D. F., Peng, S. H., and Xu, A. M. (2020). ALKBH5 Promotes colon Cancer Progression by Decreasing Methylation of the lncRNA NEAT1. *Am. J. Transl Res.* 12 (8), 4542–4549.

Han, D., Liu, J., Chen, C., Dong, L., Liu, Y., Chang, R., et al. (2019). Anti-tumour Immunity Controlled through mRNA m6A Methylation and YTHDF1 in Dendritic Cells. *Nature* 566 (7743), 270–274. doi:10.1038/s41586-019-0916-x

Hänzelmann, S., Castelo, R., and Guinney, J. (2013). GSVA: Gene Set Variation Analysis for Microarray and RNA-Seq Data. *bmc bioinformatics* 14 (1), 7.

Hayes, D. N. (2010). ConsensusClusterPlus: a Class Discovery Tool with Confidence Assessments and Item Tracking. *Bioinformatics* 26 (12), 1572–1573.

Hinshaw, D. C., and Shevde, L. A. (2019). The Tumor Microenvironment Innately Modulates Cancer Progression. *Cancer Res.* 79 (18), 4557–4566. doi:10.1158/0008-5472.can-18-3962

Hua, W., Zhao, Y., Jin, X., Yu, D., He, J., Xie, D., et al. (2018). METTL3 Promotes Ovarian Carcinoma Growth and Invasion through the Regulation of AXL Translation and Epithelial to Mesenchymal Transition. *Gynecol. Oncol.* 151 (2), 356–365. doi:10.1016/j.ygyno.2018.09.015

Huang, H., Wang, Y., Kandpal, M., Zhao, G., Cardenas, H., Ji, Y., et al. (2020). FTO-dependent N6-Methyladenosine Modifications Inhibit Ovarian Cancer Stem Cell Self-Renewal by Blocking cAMP Signaling. *Cancer Res.* 80 (16), 3200–3214. doi:10.1158/0008-5472.can-19-4044

Jiang, Y., Wan, Y., Gong, M., Zhou, S., Qiu, J., and Cheng, W. (2020). RNA Demethylase ALKBH5 Promotes Ovarian Carcinogenesis in a Simulated Tumour Microenvironment through Stimulating NF- κ B Pathway. *J. Cel Mol Med* 24 (11), 6137–6148. doi:10.1111/jcmm.15228

Karikó, K., Buckstein, M., Ni, H., and Weissman, D. (2005). Suppression of RNA Recognition by Toll-like Receptors: the Impact of Nucleoside Modification and the Evolutionary Origin of RNA. *Immunity* 23 (2), 165–175. doi:10.1016/j.immuni.2005.06.008

Li, H.-B., Tong, J., Zhu, S., Batista, P. J., Duffy, E. E., Zhao, J., et al. (2017). m6A mRNA Methylation Controls T Cell Homeostasis by Targeting the IL-7/STAT5/SOCS pathwaysA mRNA Methylation Controls T Cell Homeostasis by Targeting the IL-7/STAT5/SOCS Pathways. *Nature* 548 (7667), 338–342. doi:10.1038/nature23450

Liu, N., and Pan, T. (2016). N6-methyladenosine-encoded Epitranscriptomics. *Nat. Struct. Mol. Biol.* 23 (2), 98–102. doi:10.1038/nsmb.3162

Liu, T., Wei, Q., Jin, J., Luo, Q., Liu, Y., Yang, Y., et al. (2020). The m6A Reader YTHDF1 Promotes Ovarian Cancer Progression via Augmenting EIF3C Translation. *Nucleic Acids Res.* 48 (7), 3816–3831. doi:10.1093/nar/gkaa048

Pastò, A., Bellio, C., Pilotto, G., Ciminale, V., Silic-Benussi, M., Guzzo, G., et al. (2014). Cancer Stem Cells from Epithelial Ovarian Cancer Patients Privilege Oxidative Phosphorylation, and Resist Glucose Deprivation. *Oncotarget* 5 (12), 4305–4319. doi:10.18632/oncotarget.2010

Quail, D. F., and Joyce, J. A. (2013). Microenvironmental Regulation of Tumor Progression and Metastasis. *Nat. Med.* 19 (11), 1423–1437. doi:10.1038/nm.3394

Roundtree, I. A., Evans, M. E., Pan, T., and He, C. (2017). Dynamic RNA Modifications in Gene Expression Regulation. *cell* 169 (7), 1187–1200. doi:10.1016/j.cell.2017.05.045

Siegel, R. L., Miller, K. D., and Jemal, A. (2018). Cancer Statistics, 2018. *CA: A Cancer J. Clinicians* 68 (1), 7–30. doi:10.3322/caac.21442

Wong, J. A. H. A. (1979). Algorithm AS 136: A K-Means Clustering Algorithm. *J. R. Stat. Soc.* 28 (1), 100–108.

Xu, J., Chen, Q., Tian, K., Liang, R., Chen, T., Gong, A., et al. (2020). m6A Methyltransferase METTL3 Maintains colon Cancer Tumorigenicity by Suppressing SOCS2 to Promote Cell Proliferation. *Oncol. Rep.* 44 (3), 973–986. doi:10.3892/or.2020.7665

Yang, Z., Wang, T., Wu, D., Min, Z., Tan, J., and Yu, B. (2020). RNA N6-Methyladenosine Reader IGF2BP3 Regulates Cell Cycle and Angiogenesis in colon Cancer. *J. Exp. Clin. Cancer Res.* 39 (1), 203. doi:10.1186/s13046-020-01714-8

Yue, Y., Liu, J., and He, C. (2015). RNA N6-Methyladenosine Methylation in post-transcriptional Gene Expression Regulation. *Genes Dev.* 29 (13), 1343–1355. doi:10.1101/gad.262766.115

Zhang, B., Wu, Q., Li, B., Wang, D., Wang, L., and Zhou, Y. L. (2020). m6A Regulator-Mediated Methylation Modification Patterns and Tumor Microenvironment Infiltration Characterization in Gastric Cancer. *Mol. Cancer* 19, 53. doi:10.1186/s12943-020-01170-0

Zhang, C., Chen, Y., Sun, B., Wang, L., Yang, Y., Ma, D., et al. (2017). m6A Modulates Haematopoietic Stem and Progenitor Cell specificationA Modulates Haematopoietic Stem and Progenitor Cell Specification. *Nature* 549 (7671), 273–276. doi:10.1038/nature23883

Zhang, L., Wan, Y., Zhang, Z., Jiang, Y., Lang, J., Cheng, W., et al. (2021). FTO Demethylates m6A Modifications in HOXB13 mRNA and Promotes Endometrial Cancer Metastasis by Activating the WNT Signalling Pathway. *RNA Biol.* 18 (9), 1265–1278. doi:10.1080/15476286.2020.1841458

Zhang, L., Wan, Y., Zhang, Z., Jiang, Y., Gu, Z., Ma, X., et al. (2021). IGF2BP1 Overexpression Stabilizes PEG10 mRNA in an m6A-dependent Manner and Promotes Endometrial Cancer Progression. *Theranostics* 11 (3), 1100–1114. doi:10.7150/thno.49345

Zhao, B. S., Roundtree, I. A., and He, C. (2017). Post-transcriptional Gene Regulation by mRNA Modifications. *Nat. Rev. Mol. Cel Biol* 18 (1), 31–42. doi:10.1038/nrm.2016.132

Zhu, J., Xiao, J., Wang, M., and Hu, D. (2021). Pan-Cancer Molecular Characterization of m6A Regulators and Immunogenomic Perspective on the Tumor Microenvironment. *Front. Oncol.* 10, 618374. doi:10.3389/fonc.2020.618374

Conflict of Interest: The authors declare that the research was conducted in the absence of any commercial or financial relationships that could be construed as a potential conflict of interest.

Publisher's Note: All claims expressed in this article are solely those of the authors and do not necessarily represent those of their affiliated organizations, or those of the publisher, the editors and the reviewers. Any product that may be evaluated in this article, or claim that may be made by its manufacturer, is not guaranteed or endorsed by the publisher.

frontiers in Cell and Developmental Biology

ORIGINAL RESEARCH
published: 11 January 2022
doi: 10.3389/fcell.2021.798221

The Novel Methylation Biomarker NPY5R Sensitizes Breast Cancer Cells to Chemotherapy

Jiazhou Liu[1,2†], Xiaoyu Wang[1,2†], Jiazheng Sun[1,2], Yuru Chen[1,2], Jie Li[1,2], Jing Huang[3], Huimin Du[4], Lu Gan[4], Zhu Qiu[1], Hongzhong Li[1,2], Guosheng Ren[1,2] and Yuxian Wei[1,2]**

[1]Chongqing Key Laboratory of Molecular Oncology and Epigenetics, The First Affiliated Hospital of Chongqing Medical University, Chongqing, China, [2]Department of Endocrine and Breast Surgery, The First Affiliated Hospital of Chongqing Medical University, Chongqing, China, [3]Department of Respiratory, The First Affiliated Hospital of Chongqing Medical University, Chongqing, China, [4]Department of Oncology, The First Affiliated Hospital of Chongqing Medical University, Chongqing, China

OPEN ACCESS

Edited by:
Dhirendra Kumar,
National Institute of Environmental Health Sciences (NIEHS), United States

Reviewed by:
Apiwat Mutirangura,
Chulalongkorn University, Thailand
Satish Sati,
University of Pennsylvania, United States

***Correspondence:**
Guosheng Ren
rengs726@126.com
Yuxian Wei
saltish0301@163.com

†These authors have contributed equally to this work

Specialty section:
This article was submitted to Epigenomics and Epigenetics, a section of the journal Frontiers in Cell and Developmental Biology

Received: 19 October 2021
Accepted: 15 December 2021
Published: 11 January 2022

Citation:
Liu J, Wang X, Sun J, Chen Y, Li J, Huang J, Du H, Gan L, Qiu Z, Li H, Ren G and Wei Y (2022) The Novel Methylation Biomarker NPY5R Sensitizes Breast Cancer Cells to Chemotherapy. Front. Cell Dev. Biol. 9:798221. doi: 10.3389/fcell.2021.798221

Breast cancer (BC) is the most common tumor in women, and the molecular mechanism underlying its pathogenesis remains unclear. In this study, we aimed to investigate gene modules related to the phenotypes of BC, and identify representative candidate biomarkers for clinical prognosis of BC patients. Using weighted gene co-expression network analysis, we here identified NPY5R as a hub gene in BC. We further found that NPY5R was frequently downregulated in BC tissues compared with adjacent tumor-matched control tissues, due to its aberrant promoter CpG methylation which was confirmed by methylation analysis and treatment with demethylation agent. Higher expression of NPY5R was closely associated with better prognosis for BC patients. Gene set enrichment analysis showed that transcriptome signatures concerning apoptosis and cell cycle were critically enriched in specimens with elevated NPY5R. Ectopic expression of NPY5R significantly curbed breast tumor cell growth, induced cell apoptosis and G2/M arrest. Moreover, NPY5R also promoted the sensitivity of BC cells to doxorubicin. Mechanistically, we found that NPY5R restricted STAT3 signaling pathway activation through interacting with IL6, which may be responsible for the antitumor activity of NPY5R. Collectively, our findings indicate that NPY5R functions as a tumor suppressor but was frequently downregulated in BC.

Keywords: breast cancer, NPY5R, WGCNA, IL6, stat3, CpG methylation

INTRODUCTION

Breast cancer (BC) is one of the most common malignant tumors in women, which seriously affects women's physical and mental health (Sung et al., 2021). Globally, its morbidity and mortality have long occupied the first place among female malignant tumors. Although treatments based on molecular subtype have achieved striking breakthrough in BC, there are still many patients suffering from recurrence and metastasis, leading to unsatisfactory long-term survival (Desantis et al., 2014). Therefore, a more in-depth study of the etiology and pathogenesis of BC is urgently needed to find more reliable diagnostic and prognostic markers, which may provide a promising targetable therapy for BC.

Neuropeptide Y receptor type 5 (NPY5R) is a G-protein coupled receptor which belongs to the subfamily of neuropeptide Y (NPY) receptors mediating the action of endogenous NPY (Kumar et al., 2016). NPY5R is located on human chromosome 4q31-q32 region, encoding 456

amino acids (Kim and Kim, 2018), it is widely distributed in human brain, mostly in cortex, putamen and caudate nucleus, and can inhibit the activity of adenylate cyclase and the appetite (Dumont et al., 1998; Jacques et al., 1998). Mice lacking the NPY5R gene failed to prefer food odors over pheromones after fasting (Horio and Liberles, 2021). Additionally, it was reported that NPY5R was involved in regulating the proliferation and apoptosis of granulosa cells (Urata et al., 2020). More recently, NPY5R was found to be a molecular marker for tumorigenesis of HR (+)/HER2 (−) BC in adolescents and young adults (Yi and Zhou, 2020). However, the function of NPY5R remains poorly characterized and its pathological significance needs to be investigated.

In this study, we harnessed Gene Expression Profiling Interactive Analysis (GEPIA), Gene Expression Omnibus (GEO) and The Cancer Genome Atlas (TCGA) databases to analyze the expression of NPY5R in BC and normal breast tissues and elucidate the relationship between NPY5R expression and prognosis of BC patients. Interestingly, we found that NPY5R expression was silenced by promoter methylation in BC. Our study sheds light on the critical role of NPY5R in inhibiting BC cell growth and increasing the sensitivity of BC cells to doxorubicin (DOX) *in vitro*. Further mechanistic studies showed that the IL6-STAT3 pathway was implicated in NPY5R-mediated antitumor effects. Thus, NPY5R may serve as a biomarker for BC diagnosis and a potential target for BC treatment.

MATERIALS AND METHODS

Data and Resources

The clinical characteristics and RNA-seq data included 113 normal samples and 1109 tumor samples were retrieved from the Breast Invasive Carcinoma (BRCA) project of TCGA database (https://portal.gdc.cancer.gov/). The microarray datasets were collected from the GEO database (https://www.ncbi.nlm.nih.gov/geo/). Datasets TCGA-BRCA and GSE29431 were used to construct the co-expression networks and identify hub genes in this study. The R package of "limma" was used to identify differentially expressed genes (DEGs) according to the criteria of false discovery rate (FDR) < 0.05 and absolute of log2 fold change >1. We explored the expression of NPY5R in BC using GEPIA database (http://gepia.cancer-pku.cn/). Datasets GSE37751 and GSE5364 were utilized to validate the expression of NPY5R in BC.

Weighted Gene Co-Expression Network Analysis (WGCNA)

Gene co-expression network analysis was performed with the R package "WGCNA" (Langfelder and Horvath, 2008). First, the similarity matrix was constructed by using the expression data by calculating the Pearson correlation coefficient between two genes. Next, the similarity matrix was transformed into an adjacency matrix with a network type of signed. Six and five were set as the soft power using the pickSoftThreshold function in the Datasets TCGA-BRCA and GSE29431, respectively. Then, the gene expression matrix was converted into the Topological Overlap Matrix (TOM). 1-TOM was used as the distance to cluster the genes, and then the dynamic pruning tree was built to identify the modules. Finally, intersection genes of significantly related modules (the blue and brown modules) and DEGs were visualized by Cytoscape software (v3.8.0). The top 10 hub genes, identified by the plug-in cytoHubba of the Cytoscape software with maximal clique centrality (MCC) algorithm.

Functional Enrichment Analysis

The functional enrichment of NPY5R-coexpressed genes was analyzed by Gene Ontology (GO) classification and Kyoto Encyclopedia of Genes and Genomes (KEGG) pathways from the SHBIO (http://enrich.shbio.com/). Adjust p value <0.05 was considered as statistically significant.

Gene Set Enrichment Analysis (GSEA)

GSEA 4.1.0 software (downloaded from http://www.gsea-msigdb.org/gsea/downloads.jsp) was employed to dissect the signaling pathways significantly associated with NPY5R expression levels. The pathways with the following criteria were regarded to be significantly enriched: nominal p-value < 0.05, false discovery rate (FDR) q-value < 0.25, and normalized enrichment score (NES) > 1 (Liu et al., 2021).

Cell Lines and Tissue Specimens

The human BC cell lines MCF-7, BT-549, BT-474, MDA-MB-231, MDA-MB-468, T47D, ZR-75-1, and SK-BR-3, the normal mammary epithelial cell line MCF-10A were obtained from American Type Culture Collection (ATCC, Manassas, VA, United States). Cell lines were cultured in RPMI-1640 medium (Gibco BRL, Karlsruhe, Germany) containing 10% fetal bovine serum at 37°C with 5% CO_2. Human BC samples and matched adjacent non-tumor tissue samples used for immunohistochemistry (IHC) staining and quantitative real-time PCR (qRT-PCR) were collected from the First Affiliated Hospital of Chongqing Medical University. This research was authorized by the Institutional Ethics Committees of the First Affiliated Hospital of Chongqing Medical University.

5-Aza-2-deoxycytidine (Aza) and Trichostatin A (TSA) Treatment

Cells were treated with 10 μM Aza (Sigma-Aldrich, St. Louis, MO, United States) for 72 h and then treated with 100 nM TSA (Cayman Chemical Co., Ann Arbor, MI, United States) for an additional 24 h.

Cell Proliferation, Clonogenic Assay, Cell Cycle Analysis, and Apoptosis Assay

These experiments were performed as described previously (Li X. et al., 2018; He et al., 2020). DOX (HANHUI,

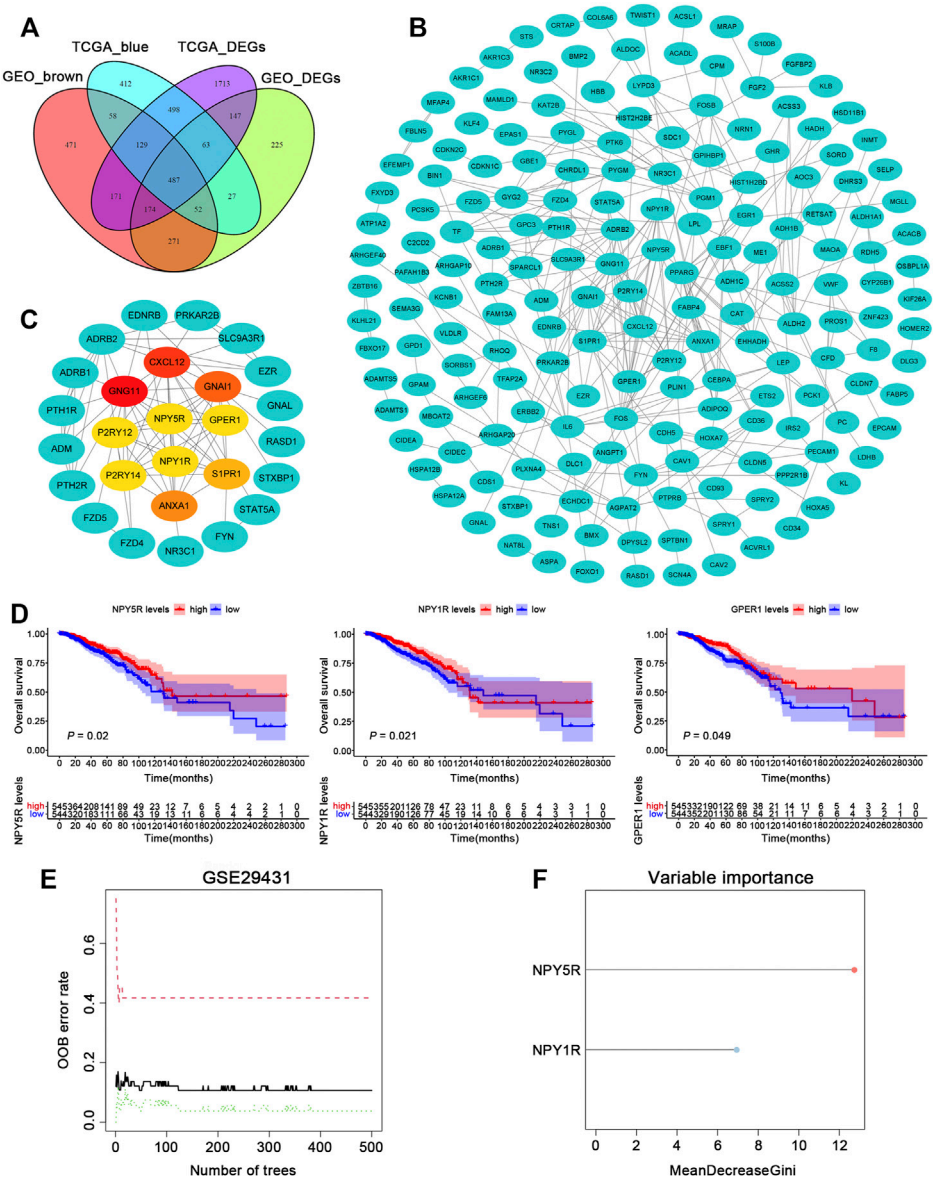

FIGURE 1 | Identification of gene modules during BC development using WGCNA. **(A)** Venn diagram depicting the overlap between DEGs and WGCNA gene modules that are the most relevant to tumorigenesis. **(B)** PPI network of overlapping genes was selected from the Venn diagram. **(C)** According to the MCC score, the Top 10 genes were selected as the hub genes. **(D)** The Kaplan–Meier survival analysis of ten hub genes in TCGA-BRCA cohort. **(E)** The influence of the number of decision trees on the error rate. The *x*-axis is the number of decision trees and the *y*-axis is the OOB error rate. **(F)** Results of the Gini coefficient method in random forest classifier. The gene (red lollipop) that ranked in the top list according to the prognostic importance was chosen for further analyses.

19052011) was applied at various concentrations (4, 8, 12, and 16 μM) for 48 h and DMSO was used as control (Yang et al., 2021).

Western Blotting

Western blot analysis was performed as described previously (Li Y. et al., 2018). Western blot analysis was performed with anti-cleaved PARP (#5625), anti-cleaved-caspase9 (#9501), anti-β-Tubulin (#2146), anti-p-STAT3 (#9145), and anti-STAT3 (#9139) antibodies purchased from Cell Signaling Technology (Danvers, MA, United States). An anti-NPY5R (#PA5-106850) antibody was purchased from Invitrogen (Waltham, MA, United States). Anti- cyclin B1 (sc-245) antibody was obtained from Santa Cruz Biotechnology., Inc. (Santa Cruz, CA, United States). Anti-cdc25c (#A5133) antibody was purchased from Bimake (Houston, TX, United States).

qRT-PCR

Total RNA was extracted from cells using the TRIzol extraction kit (Invitrogen). qRT-PCR was carried out as described previously (Li Y. et al., 2018). All the primers

used for qRT-PCR were listed in Additional file: **Supplementary Table S1**.

Immunofluorescence Assay

Immunofluorescence staining was performed as described in our previous study (Li Y. et al., 2018). The cells were incubated with anti-STAT3 (1:800, CST, #9139). After incubating with secondary antibody, DNA was counterstained with diamidino phenylindole (DAPI, Sigma–Aldrich, 32670). Imagines were obtained under a confocal laser scanning microscope (Leica, Hilden, Germany).

Immunohistochemistry

The IHC protocol was performed as described previously (Li Y. et al., 2018). IHC staining was performed from human BC and adjacent tissues using anti-NPY5R (1:50, Invitrogen, #PA5-106850). Based on the immunoreactive score method, the intensity of human BC tissue staining (protein expression) was scored range from 0-10, indicating negative staining to strong staining.

Plasmids and Cell Transfection

A NPY5R-expressing plasmid was purchased from GeneChem (Shanghai, China). pcDNA3.1 and NPY5R-containing plasmid (4 μg) were transfected with Lipofectamine 2000 (Invitrogen, Carlsbad, United States) into MDA-MB-231 and SK-BR-3 cells. After 6 h of transfection, cells were changed fresh cell culture medium for subsequent experiments.

Random Forest Screening for Important Genes

Random forest algorithm was leveraged to evaluate the impact of the expression of select genes on patient OS with the R package "randomForest", and to provide variable importance value for each gene (Tian et al., 2020).

Statistical Analysis

All experiments were repeated three times. Data analysis was performed by GraphPad Prism 7 and in the R version 4.1.0. We used the *t*-test and Wilcox test to calculate the difference between high-NPY5R and low-NPY5R groups. Survival curves were calculated using the Kaplan-Meier method and were compared with the log-rank test. (*$p < 0.05$; **$p < 0.01$; ***$p < 0.001$; ****$p < 0.0001$. p values <0.05 were considered statistically significant).

RESULTS

Key Gene Module Related to Breast Cancer is identified *via* WCGNA

To dig out relevant genes contributing potentially to the pathogenesis of BC, we analyzed the TCGA-BRCA and GSE29431 datasets to examine differentially expressed genes (DEGs). 3381 and 1445 DEGs were extracted from the expression profiles in the two datasets, respectively (**Supplementary Figures S1A,B**). To further identify BC phenotype-related modules, we performed WGCNA based on gene expression profiles in the above datasets. The co-expression modules were generated with Dynamic tree cutting. 19 and 11 genes co-expression modules were recognized in the TCGA-BRCA and GSE29431 datasets, respectively (**Supplementary Figures S1C,E**). By performing a module trait relationship analysis, the blue module and the brown module were identified in datasets TCGA-BRCA and GSE29431, respectively, for their significantly negative correlation with tumor development (**Supplementary Figures S1D,F**). The list of genes in blue and brown modules is provided in **Supplementary Table S2**. Finally, we obtained intersection genes of blue and brown modules genes and DEGs in datasets TCGA-BRCA and GSE29431 (**Figure 1A**).

NPY5R has the Potential to Act as a Regulatory Hub in Breast Cancer

To identify putative novel targets in BC, 487 overlapped genes were selected for further analysis. Based on the STRING database (https://www.string-db.org/), we built and presented a PPI network through Cytoscape app, and then calculated the hub genes of the protein network using the cytoHubba plugin (**Figure 1B**). As shown in **Figure 1C**, we obtained the top 10 hub genes (CXCL12, GNG11, GNAI1, P2RY12, P2RY14, ANXA1, S1PR1, NPY5R, NPY1R, and GPER1) by MCC values. To investigate the relationship between the 10 hub genes and patient prognosis, the patients in TCGA-BRCA cohort were assigned to groups based on high or low expression of the 10 genes. The expression of 3 hub genes (NPY5R, NPY1R and GPER1) was found closely correlated with BC patients' overall survival (OS) as determined by K–M analysis, shown in **Figure 1D** ($p < 0.05$, log-rank test). In the GSE29431 dataset, a machine learning algorithm called random forest (RF) classifier identified a model combining two genes (NPY5R, NPY1R; **Figure 1E**). One gene (NPY5R) that has rarely been reported among most cancers ranked at the top of the list according to the prognostic importance (**Figure 1F**). Therefore, NPY5R was selected for in-depth investigation.

NPY5R is Downregulated in Human Breast Cancer

To explore the significance of NPY5R in BC, we first analyzed publicly available TCGA-BRCA dataset. A significantly decreased NPY5R expression was observed in tumor tissues compared with tumor-free tissues (**Figure 2A**). As predicted, same trend was demonstrated in two independent datasets (GSE37751, GSE5364) from GEO (**Figure 2B**). IHC further confirmed that NPY5R protein levels in BC tissues were lower than those in adjacent non-tumor tissue (**Figures 2C,D**). Furthermore, we also showed that all (7/8 cases) of BC tissues (tumor) exhibited lower NPY5R

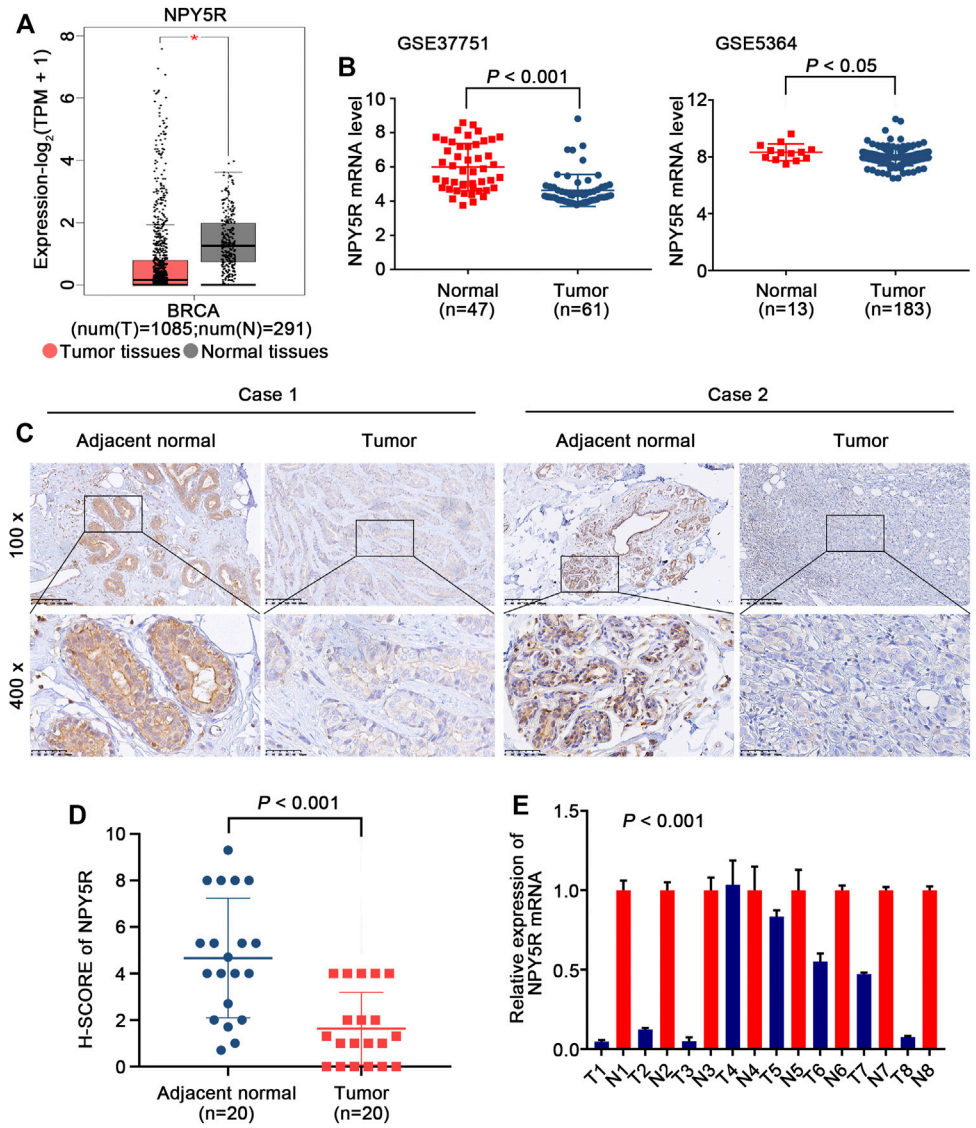

FIGURE 2 | The expression levels of NPY5R in BC tissues. **(A)** NPY5R mRNA expression in BC and normal breast tissues from TCGA database (*$p < 0.05$). **(B)** Analysis of NPY5R expression in BC and normal breast tissues using the GEO database. Statistical significance was evaluated using Wilcoxon rank sum test. **(C)** Immunohistochemical staining of NPY5R in BC tissues and adjacent non-tumor tissues. Typical images are shown at 200× and 400× magnifications. Scale bars, 50 μm. **(D)** H-SCORE of the two groups ($p < 0.001$). **(E)** 8 pairs of primary BRCA and adjacent tissues are tested by q-PCR ($p < 0.001$).

expression compared to their corresponding non-cancerous controls (normal) by qPCR (**Figure 2E**).

Promoter Hypermethylation Contributes to the Decreased Expression of NPY5R in Breast Cancer

To explore the possible mechanism leading to the low expression of NPY5R in BC tissues, we studied the correlation between NPY5R methylation state and its expression levels. Based on SMART (Shiny Methylation Analysis Resource Tool) App (http://www.bioinfo-zs.com/smartapp/), we found that the NPY5R methylation level is significantly higher in BC tissues compared to normal breast tissues (**Figure 3A**). Furthermore, SurvivalMeth (http://bio-bigdata.hrbmu.edu.cn/survivalmeth) was utilized to explore the DNA methylation-related functional elements. There were 13 CpG sites located in promoter and non-promoter region of NPY5R, twelve of which were differential and one was not (**Figure 3B**). The average value of twelve differential CpG sites was higher in tumor samples (0.29) than in normal samples (0.22, $p < 0.01$). We also found NPY5R mRNA expression was markedly negatively associated with the methylation levels of the cg15586439, cg13975625, cg11784623, cg21748223, cg04961466, cg20618622, cg01002253, cg08346159, cg10341154, and cg18438777 probes (**Figure 3C**). Given the close relationship between the methylation of NPY5R promoter and NPY5R expression, we suspected that CpG methylation may regulate NPY5R expression. The precise genomic location of

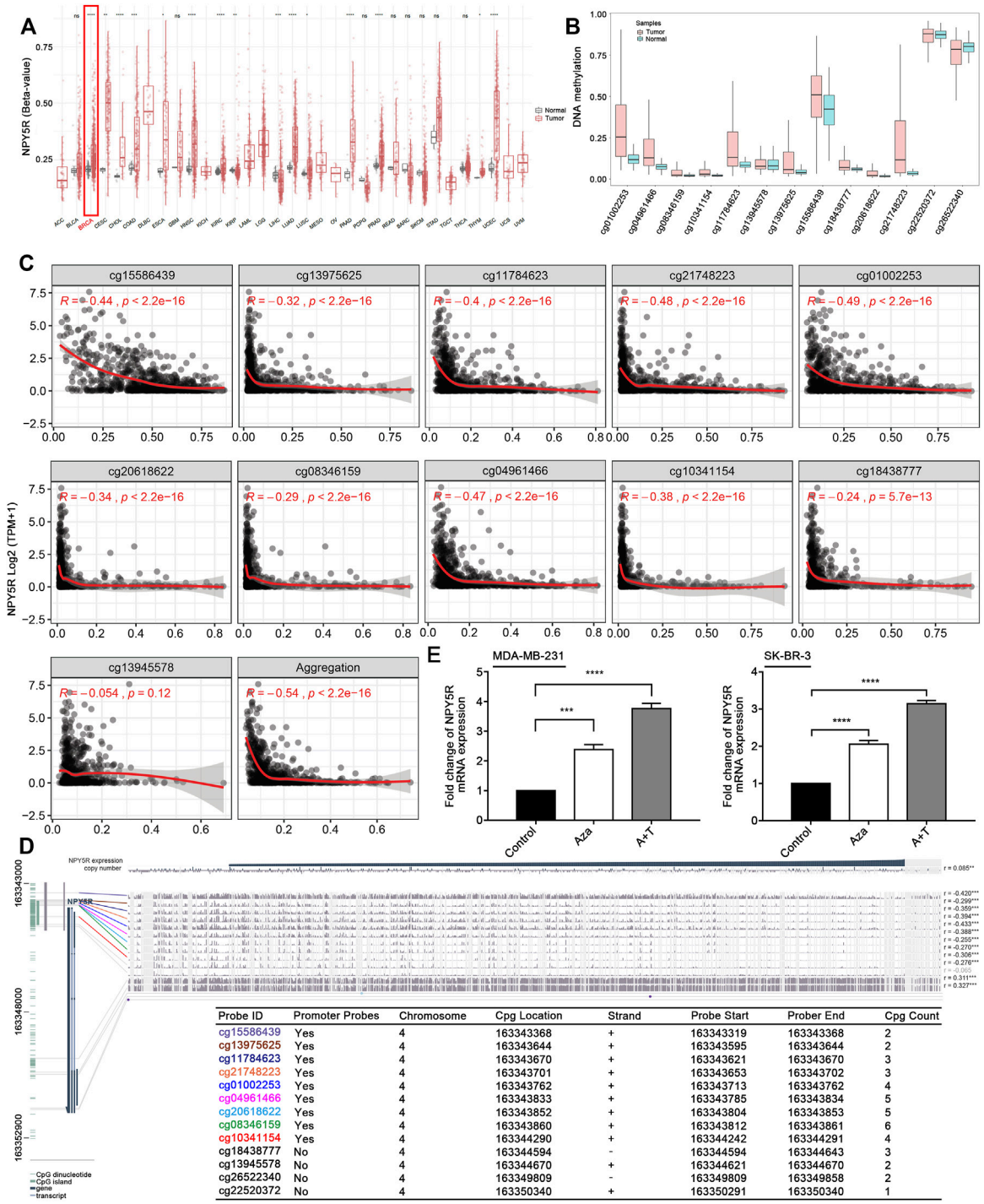

Probe ID	Promoter Probes	Chromosome	Cpg Location	Strand	Probe Start	Prober End	Cpg Count
cg15586439	Yes	4	163343368	+	163343319	163343368	2
cg13975625	Yes	4	163343644	+	163343595	163343644	2
cg11784623	Yes	4	163343670	+	163343621	163343670	3
cg21748223	Yes	4	163343701	+	163343653	163343702	3
cg01002253	Yes	4	163343762	+	163343713	163343762	4
cg04961466	Yes	4	163343833	+	163343785	163343834	5
cg20618622	Yes	4	163343852	+	163343804	163343853	5
cg08346159	Yes	4	163343860	+	163343812	163343861	6
cg10341154	Yes	4	163344290	+	163344242	163344291	4
cg18438777	No	4	163344594	-	163344594	163344643	3
cg13945578	No	4	163344670	+	163344621	163344670	2
cg26522340	No	4	163349809	-	163349809	163349858	2
cg22520372	No	4	163350340	+	163350291	163350340	1

FIGURE 3 | Methylation of NPY5R in BRCA. **(A)** The methylation β values of NPY5R in various types of tumoral and their paracancerous tissues in TCGA datasets. **(B)** The methylation level of different probes in breast tumor and normal groups. **(C)** Correlation between NPY5R expression and methylated sites. Spearman's correlation coefficient (r) was used for the significance test. **(D)** The left aquamarine column represents the sequence of NPY5R, and each probe is marked in the sequence. The statistics on the right hand side show how NPY5R expression and promoter DNA methylation are negatively correlated (Pearson correlation coefficient). The relative position of each probe in NPY5R gene is indicated in the bottom panel. **(E)** Detection of NPY5R expression by RT-PCR after Aza treatment without or with TSA (T) in MDA-MB-231 and SK-BR-3 cells. Data represent the mean ± SD of three independent experiments; *$p < 0.05$; **$p < 0.01$; ***$p < 0.001$; ****$p < 0.0001$.

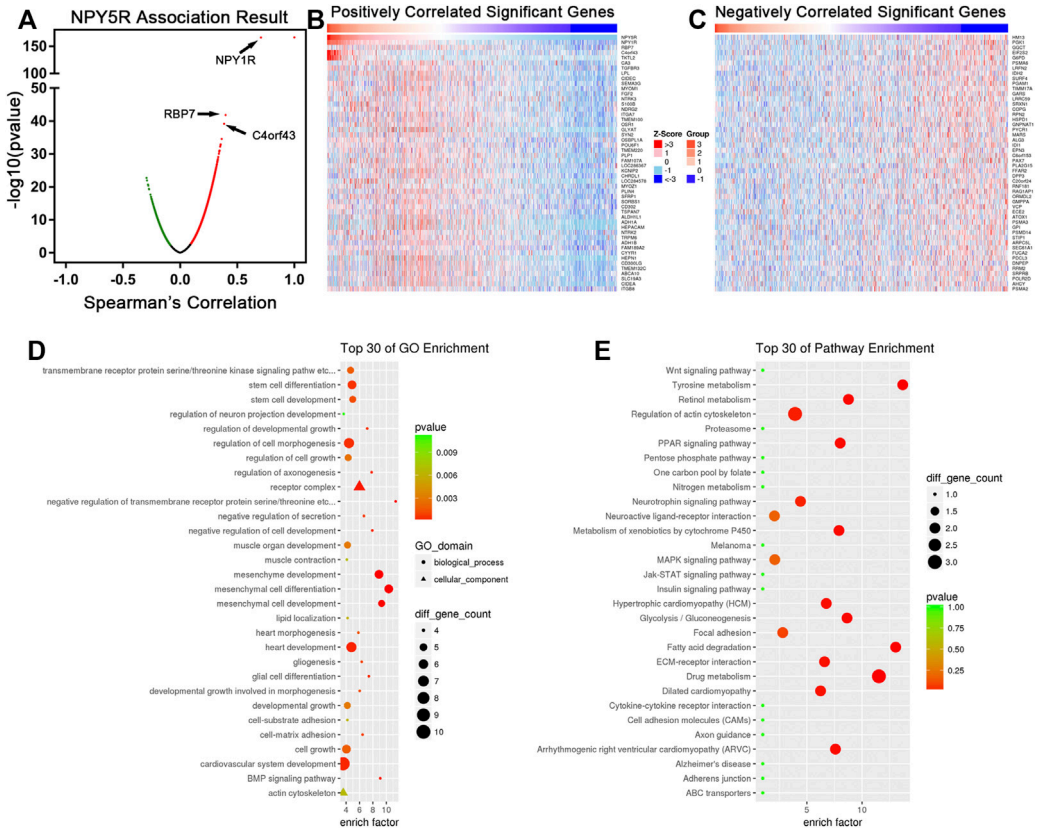

FIGURE 4 | The co-expression genes of NPY5R in BC. **(A)** Strongly co-expressed genes of NPY5R identified by Spearman correlation test in the TCGA BRCA cohort. **(B,C)** Heat maps showing genes positively and negatively correlated with NPY5R in the TCGA BRCA cohort (TOP 50). Red indicates positively correlated genes, and blue indicates negatively correlated genes. **(D,E)** Significantly enriched GO terms and KEGG pathways of NPY5R co-expression genes. FDR, false discovery rate.

DNA methylation is one of the most important factors in the regulatory effect of DNA methylation on gene expression. We explored the available TCGA DNA methylation data at individual CpGs relating to their precise genomic location using the MEXPRESS tool (https://mexpress.be/). As indicated in **Figure 3D**, we found the methylation of NPY5R distributed in different regions of the gene using 13 probes (the localization of each probe is presented in the figure, and those localized in the promoter region are highlighted in different colors). Based on the above bioinformatic analyses, we next investigated whether DNA methylation affects NPY5R gene expression. Indeed, it was upregulated after treatment with the DNA methyltransferase inhibitor Aza alone or in combination with the HDAC inhibitor TSA (**Figure 3E**). These results indicated that alterations in the DNA methylation levels could be the underlying mechanisms responsible for the downregulation of NPY5R.

Furthermore, we analyzed the correlations of NPY5R expression and methylation with clinicopathological features (**Supplementary Figures S2A–L**), and found that decreased NPY5R expression was correlated with lymph node metastasis (N1 vs. N0, $p = 0.04$) and depth of invasion (T4/T2 vs. T1, $p < 0.05$) (**Supplementary Figures S2D,F**). In addition, tumors with high NPY5R methylation had significantly lymph node metastasis (N3 vs. N1, $p < 0.05$), depth of invasion (T3 vs. T1, $p < 0.01$), and higher TNM stage (III vs. I/II, $p < 0.05$) (**Supplementary Figures S2J–L**).

The Biological Function of Co-expression Genes Related to NPY5R in Breast Cancer

To investigate the mechanism of NPY5R regulating BC progression, the co-expression network of NPY5R in the TCGA-BRCA cohort was constructed with functional module of the LinkedOmics database (http://www.linkedomics.org). As shown in the volcano plot (**Figure 4A**), 5340 genes (dark red dots) were significantly positively correlated with NPY5R, and 2370 genes (dark green dots) were significantly negatively correlated (FDR<0.01, *t*-test followed by multiple testing correction).

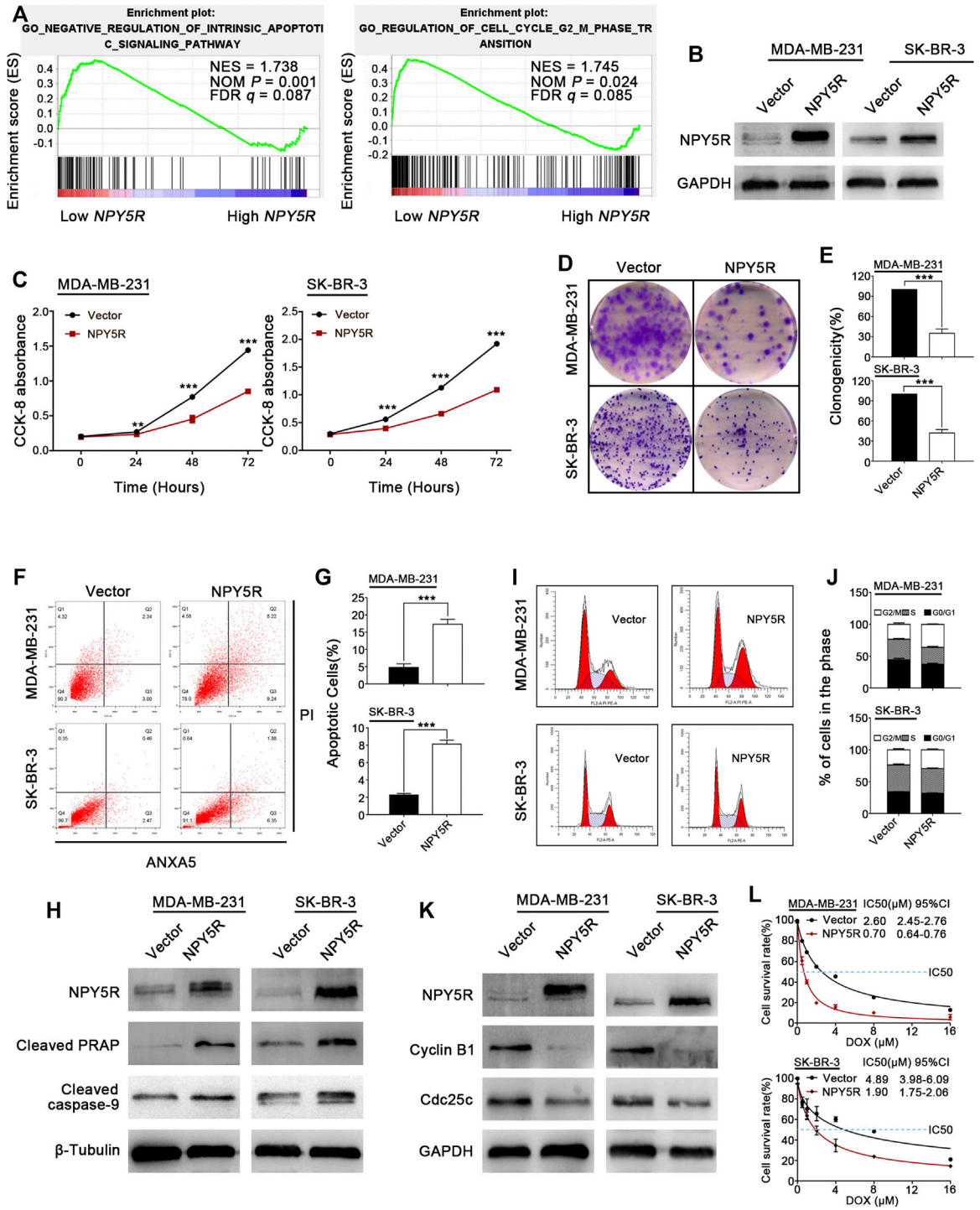

FIGURE 5 | Tumor suppressive functions of NPY5R in BC cells. **(A)** Gene enrichment plots showed that a series of gene sets including GO NEGATIVE REGULATION OF INTRINSIC APOPTOTIC SIGNALING PATHWAY (apoptosis) and GO REGULATION OF CELL CYCLE G2 M PHASE TRANSITION (cell cycle) were enriched in the NPY5R-high subgroup. **(B)** Overexpression of NPY5R in MDA-MB-231 and SK-BR-3 cells were confirmed by western blot. **(C–E)** The effects of transient NPY5R overexpression, the control vector, on cell proliferation and colony formation ability, as measured by CCK-8 **(C)** and colony formation **(D,E)**. Data represent the mean ± SD of three independent experiments; $^{*}p < 0.05$; $^{**}p < 0.01$; $^{***}p < 0.001$. **(F)** The proportion of apoptotic cells in transiently transfected MDA-MB-231 and SK-BR-3 cells. **(G)** Quantification of apoptosis changes. **(I,J)** Flow cytometry analysis of cell cycle of transiently transfected MDA-MB-231 and SK-BR-3 cells by PI staining. **(H,K)** The expression of apoptosis-related proteins and cell cycle-related proteins in NPY5R-expressing cells was determined by western blot analysis. **(L)** CCK8 was performed to analyze effect of NPY5R expression on chemosensitivity of BC cells to DOX.

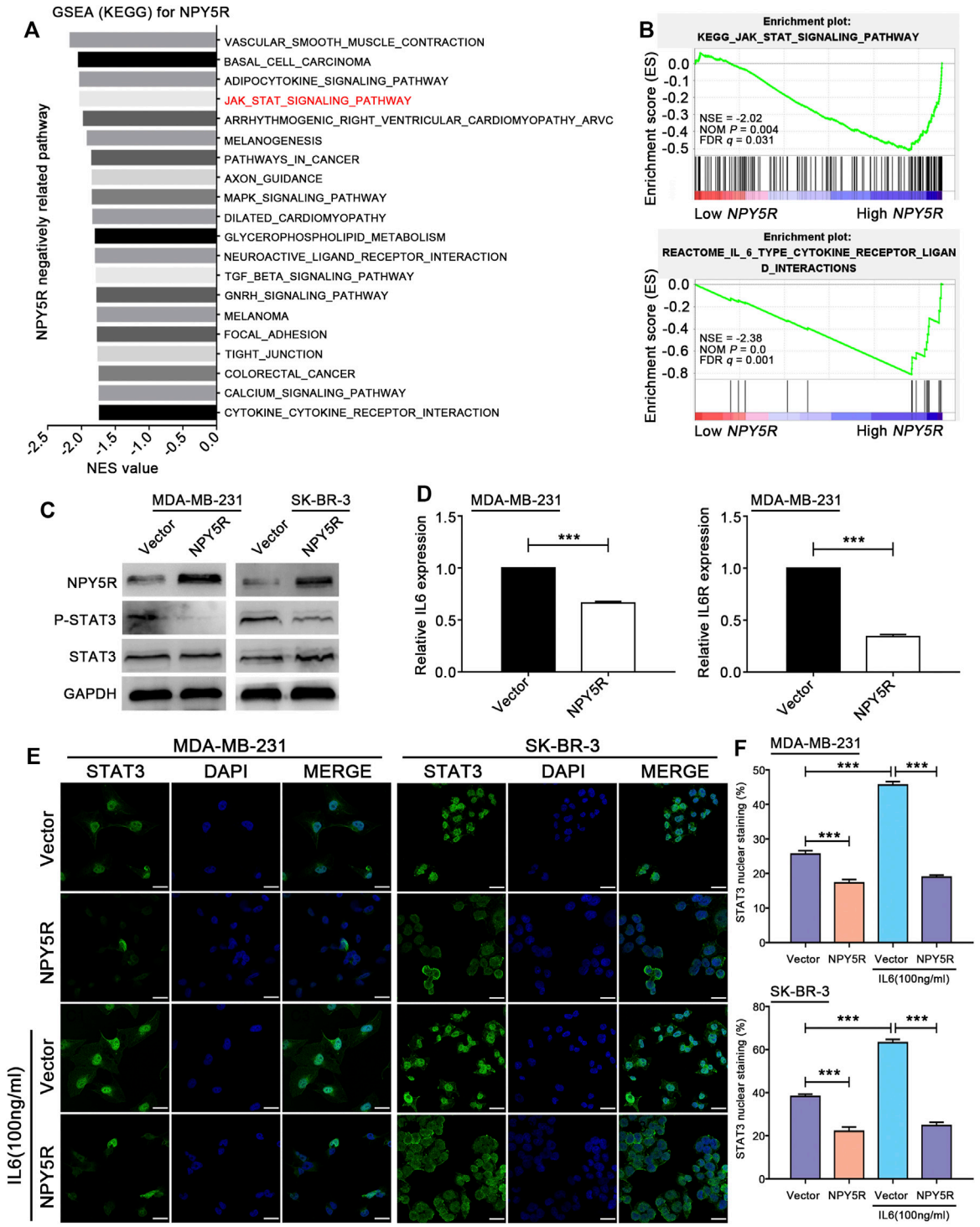

FIGURE 6 | NPY5R antagonizes STAT3 signaling through downregulating IL6. **(A)** GSEA analysis showed NPY5R-related KEGG pathways in BRCA tissue of TCGA database (Low expression group (n = 555) vs High expression group (n = 554), $p < 0.05$). **(B)** GSEA plots of KEGG JAK-STAT signaling and Reactome IL6 type cytokine receptor ligand interactions showing negatively correlation with higher expression of NPY5R in the BC. NES, normalized enrichment score; NOM, nominal; FDR, false discovery rate. **(C)** The expression of p-STAT3 and STAT3 in NPY5R-expressed MDA-MB-231 and SK-BR-3 cells was detected by western blot analysis. **(D)** The mRNA-expression levels of IL6 and IL6R after NPY5R overexpression in MDA-MB-231 cells. **(E)** Confocal immunofluorescence analysis of STAT3 expression in NPY5R- and empty vector-transfected cells. Cells were cultured and treated with or without IL6 (100 ng ml^{-1}). Nuclear localization of STAT3 is shown in green (arrows). DAPI (blue) was used as a nuclear counterstain. Scale bars, 25 μm. **(F)** Quantification of nuclear STAT3-positive staining. Results are presented as means ± S.D.

The top 50 significant genes were presented in heatmaps (**Figures 4B,C**). Among those, NPY5R was extremely negative associated with HM13 gene expression (negative rank #1, p = 2.05e−23). NPY5R also showed strong positive correlations with NPY1R (positive rank #2, p = 1.94e−166) and RBP7 (positive rank #3, p = 1.42e−42). Furthermore, GO analysis indicated that NPY5R-coexpressed genes were mainly enriched in the developmental growth, cell growth, and stem cell development (**Figure 4D**), and KEGG analysis demonstrated several enrichment pathways including Jak-STAT, Wnt, and MAPK signaling pathways (**Figure 4E**).

NPY5R Suppresses Breast Cancer *via* Inhibiting Cell Proliferation and Inducing Apoptosis and Cell Cycle Arrest

To investigate potential biological functions of NPY5R in BC, GSEA was performed with the TCGA-BRCA dataset. The results showed that GO NEGATIVE REGULATION OF INTRINSIC APOPTOTIC SIGNALING PATHWAY (apoptosis) and GO REGULATION OF CELL CYCLE G2 M PHASE TRANSITION (cell cycle) were significantly enriched in the NPY5R-high group (**Figure 5A**). Next, gain-of-function studies were performed to validate these findings. We transfected pcDNA3.1 (+) framework plasmid or pcDNA-NPY5R plasmid into BC cell lines MDA-MB-231 and SK-BR-3 which lack endogenous NPY5R expression (**Supplementary Figure S3**). Re-expression of NPY5R mRNA and protein in these cells was evidenced by RT-PCR and western blot analysis (**Figure 5B**; **Supplementary Figure S4**). The effects of NPY5R on cell proliferation and viability were further examined *via* CCK8 and colony formation assays. NPY5R overexpression significantly suppressed cell proliferation and viability (**Figures 5C–E**). To dig out the molecular mechanism by which NPY5R inhibits cell growth, we investigated the effect of NPY5R on cell cycle distribution and apoptosis by flow cytometry. NPY5R increased the proportion of both early and late apoptotic cells in MDA-MB-231 and SK-BR-3 (**Figures 5F,G**). As cell apoptosis was activated through caspase cascade, the enhanced level of cleaved caspase-9, and poly ADP-ribose polymerase (PARP) was also observed in NPY5R-overexpression cells (**Figure 5H**). Furthermore, overexpressing NPY5R induced G2/M phase cell cycle arrest, which was confirmed by decreased key G2/M cell cycle regulators, cyclin B1 and cdc25c (**Figures 5I–K**). To determine the effect of NPY5R expression on the sensitivity of BRCA cells to chemotherapeutic agents, NPY5R-overexpressing cells were treated with DOX at different concentrations for 48 h. Clearly, overexpression of NPY5R enhanced the sensitivity of BC cells to DOX (**Figure 5L**).

NPY5R Inhibits IL6-Mediated STAT3 Activation

Next, to investigate which signaling pathways underlie the biological effects of NPY5R, GSEA was performed based on the mRNA expression profiles of NPY5R, and identified 20 gene signatures that were negatively correlated with higher expression of NPY5R. Among them, two established gene signatures KEGG JAK STAT signaling (ranking 4th) and REACTOME IL6 TYPE CYTOKINE RECEPTOR LIGAND INTERACTIONS (ranking 1st) were skewed toward high expression of NPY5R (**Figures 6A,B**). Therefore, we further examined the effect of NPY5R on these signaling pathways in BC. As shown in **Figure 6C**, overexpression of NPY5R inhibited the activation of STAT3 signaling. Then, qRT-PCR showed that IL6 and IL6 receptor (IL6R) expressions were downregulated in NPY5R-overexpressed MDA-MB-231 cells (**Figure 6D**). Since IL6 is a putative activator of STAT3 pathway, we next examined if NPY5R can interfere with IL6-mediated activation of STAT3. Our data indicated that overexpression of NPY5R significantly attenuated the expression of nuclear STAT3. Stimulating MDA-MB-231 and SK-BR-3 cells with IL6 (100 ng ml^{-1}) for 6 h led to a significant increase in nuclear localization of STAT3, whereas overexpression of NPY5R significantly abolished this phenomenon (**Figure 6E**). Taken together, these results showed that IL6-STAT3 presents as an important functional node in mediating the biological effects of NPY5R in BC cells.

DISCUSSION

Nowadays, the abnormal expression of genes is considered to be one of the factors in occurrence and development of BC, and increasing research has demonstrated that some dysregulated genes in BC might be candidate biomarkers for diagnosis and prognosis. Therefore, we analyzed the datasets TCGA-BRCA and GSE29431 to examine DEGs markedly related to BC pathogenesis. The gene sets (modules) of the WGCNA were constructed from the differential gene expression profiles data *via* using unsupervised clustering, which directly focuses on the relationship between modules and tumorigenesis. Among the modules, we mainly focused on the blue module and the brown module, and the results showed that it was strongly correlated with the tumor phenotype. Using Cytoscape app analysis (Lotia et al., 2013), we obtained the ten most highly connected hub genes (CXCL12, GNG11, GNAI1, P2RY12, P2RY14, ANXA1, S1PR1, NPY5R, NPY1R, and GPER1) in the two modules. Consistent with our results, all these genes have been reported to be related to the development of BRCA (Cooke et al., 2015; Zhu et al., 2017; Shah et al., 2018; Liu et al., 2019; Feng et al., 2020; Zhang H. et al., 2021; Zhang N. et al., 2021; Correia et al., 2021; Xiong et al., 2021). Among them, NPY5R, NPY1R and GPER1 were positively associated with the OS. We further combined the strengths of machine learning techniques to improve the statistical power of our BC predictive model. As a form of an ensemble algorithm, RF has an outstanding performance on the processing of multiple-featured data with high accuracy and precision. RF classifier screening results identified NPY5R as the best-characterized gene. Thus, these data highlight the potential of NPY5R as a clinical prognostic marker in BC.

NPY5R is the major subtype of NPY receptors that mediate the biological functions of NPY (Herzog et al., 1997). NPY and its receptor NPY5R play an essential role in hunger-dependent odour preference (Horio and Liberles, 2021). Notably, the effect of the NPY or NPY receptors on tumor cell growth is controversially discussed (Korner and Reubi, 2007). Y5R agonist had no effect on the growth of this

MCF-7 (Memminger et al., 2012). Y5R agonist induced SK-N-MC cell death (Kitlinska et al., 2005). Y2R antagonist prevented the anti-proliferative effects of NPY on cholangiocarcinoma growth (DeMorrow et al., 2011). Overexpressed NPY1R inhibited prostate cancer progression (Li et al., 2020). Moreover, NPY5R in granulosa cells varies among follicular stage and its response is strong at early antral (EA) stage. NPY5R regulates granulosa cell proliferation in a follicular stage-dependent manner, with an induction at EA and suppression at late antral follicles (Urata et al., 2020). Conversely, NPY-induced increases in VEGF expression in 4T1 cells were attenuated only under Y5R antagonism (Medeiros and Jackson, 2013). Y5R antagonist inhibited the proliferative effect of NPY in the 4T1 BC cell line (Medeiros et al., 2012). However, the mechanism of action of NPY5R in the development and progression of BC remains unclear. GEPIA and datasets (GSE37751, GSE5364) were exploited to evaluate the expression of NPY5R in BC tissues compared with normal breast tissues. The results of IHC staining and RT-qPCR further verified that the level of NPY5R was significantly lower in tissues from BC patients than in normal breast tissues. Epigenetic modifications, including DNA methylation, acetylation, etc., can alter gene expression (Jones and Takai, 2001; Cavalli and Heard, 2019). The average β values for promoter methylation were significantly higher in the head and neck squamous cell carcinoma (HNSCC) samples than in the normal samples (Misawa et al., 2017). NPY5R promoter methylation correlated inversely with its respective mRNA level in the HNSCC samples (Misawa et al., 2017). Thus, a possible link between promoter methylation and downregulation of NPY5R expression in BC was investigated. Here, we first correlated the expression level of NPY5R and its methylation status. We found an increase in the DNA methylation level of NPY5R in a variety of tumoral samples, and NPY5R mRNA expression was strongly negatively associated with the methylation levels of multiple CpG sites. We further showed that demethylation treatment effectively restored NPY5R expression, confirming that promoter methylation contributes to suppression of NPY5R expression in silenced BC cells. A series of *in vitro* functional experiments revealed that NPY5R possesses a tumor-suppressive function in BC. Although recent report revealed that NPY5R plays a promotive role in the proliferation in high NPY5R-expressing 4T1 cells (Medeiros et al., 2012; Medeiros and Jackson, 2013), our findings indicated that NPY5R overexpression significantly suppressed cell proliferation in MDA-MB-231 and SK-BR-3 cells with the lowest endogenous levels of NPY5R. The divergent effects of NPY5R on tumor cell proliferation may depend on the tumor cell line used, the NPY5R expressed in the cell line, and different experimental conditions such as different NPY5R concentrations.

GSEA suggested that a number of gene sets were found to be negatively correlated with higher expression of NPY5R, including the top-ranking KEGG_VASCULAR_SMOOTH_MUSCLE_CONTRACTION (ranking 1st), KEGG _BASAL_CELL_CARCINOMA (ranking 2nd), KEGG _ADIPOCYTOKINE_SIGNALING_PATHWAY (ranking 3rd), KEGG _JAK_STAT_SIGNALING_PATHWAY (ranking 4th), and REACTOME_IL_6_TYPE_CYTOKINE_RECEPTOR_LIGAND_INTERACTIONS (ranking 1st). The IL6/JAK/STAT3 pathway is aberrantly hyperactivated in many types of cancer (Yu et al., 2014; Johnson et al., 2018), and is important for human BC development as well as BC metastasis (Wang et al., 2017; Siersbaek et al., 2020). Our results demonstrated that re-expression of NPY5R significantly inhibited the phosphorylation and nuclear localization of STAT3. Furthermore, qRT-PCR showed that the expressions of IL6 and IL6R were downregulated in NPY5R-overexpressed cells, indicating a close link between NPY5R and IL6/STAT3.

Together, these data warrant that the potential of NPY5R as a diagnostic and prognostic marker in cancer treatment. Remarkably, the analysis of the methylation levels of NPY5R would help evaluate patient prognosis and efficacy of clinical chemotherapy.

DATA AVAILABILITY STATEMENT

The original contributions presented in the study are included in the article/**Supplementary Material**, further inquiries can be directed to the corresponding authors.

ETHICS STATEMENT

Written informed consent was obtained from the individual(s) for the publication of any potentially identifiable images or data included in this article.

AUTHOR CONTRIBUTIONS

YW, GR and HL led study design and prepared the manuscript; JL, XW and JS carried out the experiments; JL and JH performed data analysis and interpretation; HD, LG, ZQ, and YC assisted in tissue sample collection; All authors read and approved the final manuscript.

FUNDING

This work was supported by the National Natural Science Foundation of China (Nos 82173166, 81472475 and 31420103915), and the Chongqing medical scientific research project (Joint project of Chongqing Health Commission and Science and Technology Bureau) (No. 2019MSXM019).

ACKNOWLEDGMENTS

We thank HL for suggestions and discussion, Ke Xu for technical support in DNA Methylation Analysis.

SUPPLEMENTARY MATERIAL

The Supplementary Material for this article can be found online at: https://www.frontiersin.org/articles/10.3389/fcell.2021.798221/full#supplementary-material

REFERENCES

Cavalli, G., and Heard, E. (2019). Advances in Epigenetics Link Genetics to the Environment and Disease. *Nature* 571, 489–499. doi:10.1038/s41586-019-1411-0

Cooke, N. M., Spillane, C. D., Sheils, O., O'Leary, J., and Kenny, D. (2015). Aspirin and P2Y12 Inhibition Attenuate Platelet-Induced Ovarian Cancer Cell Invasion. *BMC Cancer* 15, 627. doi:10.1186/s12885-015-1634-x

Correia, A. L., Guimaraes, J. C., Auf Der Maur, P., Auf der Maur, D., Trefny, M. P., Okamoto, R., et al. (2021). Hepatic Stellate Cells Suppress NK Cell-Sustained Breast Cancer Dormancy. *Nature* 594, 566–571. doi:10.1038/s41586-021-03614-z

Demorrow, S., Onori, P., Venter, J., Invernizzi, P., Frampton, G., White, M., et al. (2011). Neuropeptide Y Inhibits Cholangiocarcinoma Cell Growth and Invasion. *Am. J. Physiology-Cell Physiol.* 300, C1078–C1089. doi:10.1152/ajpcell.00358.2010

Desantis, C., Ma, J., Bryan, L., and Jemal, A. (2014). Breast Cancer Statistics, 2013. *CA. Cancer. J. Clin.* 64, 52–62.

Dumont, Y., Jacques, D., Bouchard, P., and Quirion, R. m. (1998). Species Differences in the Expression and Distribution of the Neuropeptide Y Y1, Y2, Y4, and Y5 Receptors in Rodents, guinea Pig, and Primates Brains. *J. Comp. Neurol.* 402, 372–384. doi:10.1002/(sici)1096-9861(19981221)402:3<372:aid-cne6>3.0.co;2-2

Feng, J., Lu, S.-S., Xiao, T., Huang, W., Yi, H., Zhu, W., et al. (2020). ANXA1 Binds and Stabilizes EphA2 to Promote Nasopharyngeal Carcinoma Growth and Metastasis. *Cancer Res.* 80, 4386–4398. doi:10.1158/0008-5472.can-20-0560

He, J., Wu, M., Xiong, L., Gong, Y., Yu, R., Peng, W., et al. (2020). BTB/POZ Zinc finger Protein ZBTB16 Inhibits Breast Cancer Proliferation and Metastasis through Upregulating ZBTB28 and Antagonizing BCL6/ZBTB27. *Clin. Epigenet* 12, 82. doi:10.1186/s13148-020-00867-9

Herzog, H., Darby, K., Ball, H., Hort, Y., Beck-Sickinger, A., and Shine, J. (1997). Overlapping Gene Structure of the Human Neuropeptide Y Receptor Subtypes Y1 and Y5 Suggests Coordinate Transcriptional Regulation. *Genomics* 41, 315–319. doi:10.1006/geno.1997.4684

Horio, N., and Liberles, S. D. (2021). Hunger Enhances Food-Odour Attraction through a Neuropeptide Y Spotlight. *Nature* 592, 262–266. doi:10.1038/s41586-021-03299-4

Jacques, D., Tong, Y., Shen, S. H., and Quirion, R. (1998). Discrete Distribution of the Neuropeptide Y Y5 Receptor Gene in the Human Brain: an *In Situ* Hybridization Study. *Mol. Brain Res.* 61, 100–107. doi:10.1016/s0169-328x(98)00208-3

Johnson, D. E., O'keefe, R. A., and Grandis, J. R. (2018). Targeting the IL-6/JAK/STAT3 Signalling axis in Cancer. *Nat. Rev. Clin. Oncol.* 15, 234–248. doi:10.1038/nrclinonc.2018.8

Jones, P. A., and Takai, D. (2001). The Role of DNA Methylation in Mammalian Epigenetics. *Science* 293, 1068–1070. doi:10.1126/science.1063852

Kim, E. J., and Kim, Y.-K. (2018). Panic Disorders: The Role of Genetics and Epigenetics. *AIMS Genet.* 05, 177–190. doi:10.3934/genet.2018.3.177

Kitlinska, J., Abe, K., Kuo, L., Pons, J., Yu, M., Li, L., et al. (2005). Differential Effects of Neuropeptide Y on the Growth and Vascularization of Neural Crest-Derived Tumors. *Cancer Res.* 65, 1719–1728. doi:10.1158/0008-5472.can-04-2192

Körner, M., and Reubi, J. C. (2007). NPY Receptors in Human Cancer: a Review of Current Knowledge. *Peptides* 28, 419–425. doi:10.1016/j.peptides.2006.08.037

Kumar, J. S. D., Walker, M., Packiarajan, M., Jubian, V., Prabhakaran, J., Chandrasena, G., et al. (2016). Radiosynthesis and *In Vivo* Evaluation of Neuropeptide Y5 Receptor (NPY5R) PET Tracers. *ACS Chem. Neurosci.* 7, 540–545. doi:10.1021/acschemneuro.5b00315

Langfelder, P., and Horvath, S. (2008). WGCNA: an R Package for Weighted Correlation Network Analysis. *BMC Bioinformatics* 9, 559. doi:10.1186/1471-2105-9-559

Li, X., Huang, J., Luo, X., Yang, D., Yin, X., Peng, W., et al. (2018). Paired Box 5 Is a Novel Marker of Breast Cancers that Is Frequently Downregulated by Methylation. *Int. J. Biol. Sci.* 14, 1686–1695. doi:10.7150/ijbs.27599

Li, X., Lv, J., and Liu, S. (2020). MCM3AP-AS1 KD Inhibits Proliferation, Invasion, and Migration of PCa Cells via DNMT1/DNMT3 (A/B) Methylation-Mediated Upregulation of NPY1R. *Mol. Ther. - Nucleic Acids* 20, 265–278. doi:10.1016/j.omtn.2020.01.016

Li, Y., Huang, J., Zeng, B., Yang, D., Sun, J., Yin, X., et al. (2018). PSMD2 Regulates Breast Cancer Cell Proliferation and Cell Cycle Progression by Modulating P21 and P27 Proteasomal Degradation. *Cancer Lett.* 430, 109–122. doi:10.1016/j.canlet.2018.05.018

Liu, J., Wei, Y., Wu, Y., Li, J., Sun, J., Ren, G., et al. (2021). ATP2C2 Has Potential to Define Tumor Microenvironment in Breast Cancer. *Front. Immunol.* 12, 657950. doi:10.3389/fimmu.2021.657950

Liu, Y., Zhi, Y., Song, H., Zong, M., Yi, J., Mao, G., et al. (2019). S1PR1 Promotes Proliferation and Inhibits Apoptosis of Esophageal Squamous Cell Carcinoma through Activating STAT3 Pathway. *J. Exp. Clin. Cancer Res.* 38, 369. doi:10.1186/s13046-019-1369-7

Lotia, S., Montojo, J., Dong, Y., Bader, G. D., and Pico, A. R. (2013). Cytoscape App Store. *Bioinformatics* 29, 1350–1351. doi:10.1093/bioinformatics/btt138

Medeiros, P. J., Al-Khazraji, B. K., Novielli, N. M., Postovit, L. M., Chambers, A. F., and Jackson, D. N. (2012). Neuropeptide Y Stimulates Proliferation and Migration in the 4T1 Breast Cancer Cell Line. *Int. J. Cancer* 131, 276–286. doi:10.1002/ijc.26350

Medeiros, P. J., and Jackson, D. N. (2013). Neuropeptide Y Y5-Receptor Activation on Breast Cancer Cells Acts as a Paracrine System that Stimulates VEGF Expression and Secretion to Promote Angiogenesis. *Peptides* 48, 106–113. doi:10.1016/j.peptides.2013.07.029

Memminger, M., Keller, M., Lopuch, M., Pop, N., Bernhardt, G., Von Angerer, E., et al. (2012). The Neuropeptide Y Y1 Receptor: A Diagnostic Marker? Expression in MCF-7 Breast Cancer Cells Is Down-Regulated by Antiestrogens *In Vitro* and in Xenografts. *PLoS One* 7, e51032. doi:10.1371/journal.pone.0051032

Misawa, K., Imai, A., Mochizuki, D., Misawa, Y., Endo, S., Hosokawa, S., et al. (2017). Genes Encoding Neuropeptide Receptors Are Epigenetic Markers in Patients with Head and Neck Cancer: a Site-specific Analysis. *Oncotarget* 8, 76318–76328. doi:10.18632/oncotarget.19356

Tian, Y., Yang, J., Lan, M., and Zou, T. (2020). Construction and Analysis of a Joint Diagnosis Model of Random Forest and Artificial Neural Network for Heart Failure. *Aging (Albany NY)* 12, 26221–26235.

Shah, K., Moharram, S. A., and Kazi, J. U. (2018). Acute Leukemia Cells Resistant to PI3K/mTOR Inhibition Display Upregulation of P2RY14 Expression. *Clin. Epigenet* 10, 83. doi:10.1186/s13148-018-0516-x

Siersbæk, R., Scabia, V., Nagarajan, S., Chernukhin, I., Papachristou, E. K., Broome, R., et al. (2020). IL6/STAT3 Signaling Hijacks Estrogen Receptor α Enhancers to Drive Breast Cancer Metastasis. *Cancer Cell* 38, 412–e9. doi:10.1016/j.ccell.2020.06.007

Sung, H., Ferlay, J., Siegel, R. L., Laversanne, M., Soerjomataram, I., Jemal, A., et al. (2021). Global Cancer Statistics 2020: GLOBOCAN Estimates of Incidence and Mortality Worldwide for 36 Cancers in 185 Countries. *CA A. Cancer J. Clin.* 71, 209–249. doi:10.3322/caac.21660

Urata, Y., Salehi, R., Lima, P. D. A., Osuga, Y., and Tsang, B. K. (2020). Neuropeptide Y Regulates Proliferation and Apoptosis in Granulosa Cells in a Follicular Stage-dependent Manner. *J. Ovarian Res.* 13, 5. doi:10.1186/s13048-019-0608-z

Wang, S., Liang, K., Hu, Q., Li, P., Song, J., Yang, Y., et al. (2017). JAK2-binding Long Noncoding RNA Promotes Breast Cancer Brain Metastasis. *J. Clin. Invest.* 127, 4498–4515. doi:10.1172/jci91553

Xiong, W., Zhang, B., Yu, H., Zhu, L., Yi, L., and Jin, X. (2021). RRM2 Regulates Sensitivity to Sunitinib and PD-1 Blockade in Renal Cancer by Stabilizing ANXA1 and Activating the AKT Pathway. *Adv. Sci. (Weinh)* 8, (18), e2100881. doi:10.1002/advs.202100881

Yang, Q., Zhao, S., Shi, Z., Cao, L., Liu, J., Pan, T., et al. (2021). Chemotherapy-elicited Exosomal miR-378a-3p and miR-378d Promote Breast Cancer Stemness and Chemoresistance via the Activation of EZH2/STAT3 Signaling. *J. Exp. Clin. Cancer Res.* 40, 120. doi:10.1186/s13046-021-01901-1

Yi, S., and Zhou, W. (2020). Tumorigenesis-related Key Genes in Adolescents and Young Adults with HR(+)/HER2(-) Breast Cancer. *Int. J. Clin. Exp. Pathol.* 13, 2701–2709.

Yu, H., Lee, H., Herrmann, A., Buettner, R., and Jove, R. (2014). Revisiting STAT3 Signalling in Cancer: New and Unexpected Biological Functions. *Nat. Rev. Cancer* 14, 736–746. doi:10.1038/nrc3818

Zhang, H., Zheng, Z., Zhang, R., Yan, Y., Peng, Y., Ye, H., et al. (2021). SMYD3 Promotes Hepatocellular Carcinoma Progression by Methylating S1PR1 Promoters. *Cell Death Dis* 12, 731. doi:10.1038/s41419-021-04009-8

Zhang, N., Sun, P., Xu, Y., Li, H., Liu, H., Wang, L., et al. (2021). The GPER1/SPOP axis Mediates Ubiquitination-dependent Degradation of ERα to Inhibit the Growth of Breast Cancer Induced by Oestrogen. *Cancer Lett.* 498, 54–69. doi:10.1016/j.canlet.2020.10.019

Zhu, C., Kros, J. M., Van Der Weiden, M., Zheng, P., Cheng, C., and Mustafa, D. A. M. (2017). Expression Site of P2RY12 in Residential Microglial Cells in Astrocytomas Correlates with M1 and M2 Marker Expression and Tumor Grade. *Acta Neuropathol. Commun.* 5, 4. doi:10.1186/s40478-016-0405-5

Conflict of Interest: The authors declare that the research was conducted in the absence of any commercial or financial relationships that could be construed as a potential conflict of interest.

Publisher's Note: All claims expressed in this article are solely those of the authors and do not necessarily represent those of their affiliated organizations, or those of the publisher, the editors and the reviewers. Any product that may be evaluated in this article, or claim that may be made by its manufacturer, is not guaranteed or endorsed by the publisher.

frontiers in Cell and Developmental Biology

ORIGINAL RESEARCH
published: 02 February 2022
doi: 10.3389/fcell.2022.780176

The Histone H3K27me3 Demethylases KDM6A/B Resist Anoikis and Transcriptionally Regulate Stemness-Related Genes

Mohammed Razeeth Shait Mohammed[1,2], *Mazin Zamzami*[1], *Hani Choudhry*[1,2], *Firoz Ahmed*[3,4], *Bushra Ateeq*[5] *and Mohammad Imran Khan*[1,2]*

[1]Department of Biochemistry, Faculty of Science, King Abdulaziz University, Jeddah, Saudi Arabia, [2]Centre of Artificial Intelligence in Precision Medicines, King Abdulaziz University, Jeddah, Saudi Arabia, [3]Department of Biochemistry, College of Science, University of Jeddah, Jeddah, Saudi Arabia, [4]University of Jeddah Centre for Scientific and Medical Research (UJ-`CSMR), University of Jeddah, Jeddah, Saudi Arabia, [5]Molecular Oncology Lab, Department of Biological Sciences and Bioengineering, Indian Institute of Technology-Kanpur (IIT-K), Kanpur, India

OPEN ACCESS

Edited by:
Fatima Valdes-Mora,
Children's Cancer Institute Australia, Australia

Reviewed by:
Naoko Hattori,
National Cancer Center Research Institute, Japan
Souvik Dey,
Manipal Center for Biotherapeutics Research (MCBR), India

***Correspondence:**
Mohammad Imran Khan
mikhan@kau.edu.sa

Specialty section:
This article was submitted to Epigenomics and Epigenetics, a section of the journal Frontiers in Cell and Developmental Biology

Received: 20 September 2021
Accepted: 10 January 2022
Published: 02 February 2022

Citation:
Shait Mohammed MR, Zamzami M, Choudhry H, Ahmed F, Ateeq B and Khan MI (2022) The Histone H3K27me3 Demethylases KDM6A/B Resist Anoikis and Transcriptionally Regulate Stemness-Related Genes. Front. Cell Dev. Biol. 10:780176. doi: 10.3389/fcell.2022.780176

Epithelial cancer cells that lose attachment from the extracellular matrix (ECM) to seed in a distant organ often undergo anoikis's specialized form of apoptosis. Recently, KDM3A (H3K9 demethylase) has been identified as a critical effector of anoikis in cancer cells. However, whether other histone demethylases are involved in promoting or resisting anoikis remains elusive. We screened the major histone demethylases and found that both H3K27 histone demethylases, namely, KDM6A/B were highly expressed during ECM detachment. Inhibition of the KDM6A/B activity by using a specific inhibitor results in reduced sphere formation capacity and increased apoptosis. Knockout of KDM6B leads to the loss of stem cell properties in solitary cells. Furthermore, we found that KDM6B maintains stemness by transcriptionally regulating the expression of stemness genes *SOX2*, *SOX9*, and *CD44* in detached cells. KDM6B occupies the promoter region of both *SOX2* and *CD44* to regulate their expression epigenetically. We also noticed an increased occupancy of the HIF1α promoter by KDM6B, suggesting its regulatory role in maintaining hypoxia in detached cancer cells. This observation was further strengthened as we found a significant positive association in the expression of both KDM6B and HIF1α in various cancer types. Overall, our results reveal a novel transcriptional program that regulates resistance against anoikis and maintains stemness-like properties.

Keywords: anoikis, histone demethylases, *CD44*, *SOX2*, HIF1α

INTRODUCTION

Normal epithelial cells are non-tumorigenic and are anchorage-dependent, i.e., attach well with the matrix for obtaining nutrition and physiological cues. However, tumorigenic epithelial cells require detachment from the matrix and move to different body sites to initiate metastasis (Simpson et al., 2008; Chaffer and Weinberg, 2011; Buchheit et al., 2014). Several studies described that loss of matrix detachment leads to massive changes throughout both molecular and cellular levels. These modifications are attributed to matrix-detached cells to become anoikis-resistant (Paoli et al., 2013; Buchheit et al., 2014). Matrix-detached cells overcome the anoikis condition through several

pathways; one of them is related to the epithelial–mesenchymal transition of ECM-detached epithelial cells (Polyak and Weinberg, 2009; Kim et al., 20122012).

ECM-detached cells overcome the anoikis condition through several pathways. One of them is related to the EMT (epithelial–mesenchymal transition) (Heerboth et al., 2015). Circulating cancer cells activate some genes responsible for activating anti-apoptotic and differentiation pathways; it activates the EMT and downregulates the mechanism depending upon the cell to cell attachment and stimulates the cell adhesion molecule and cell displacement. ECM-detached cancer cells undergo diverging epigenetic changes (Heerboth et al., 2015). ECM-detached cells, to aid in the hypoxic environment of circulating tumor cells, alter cell proliferation, anaerobic glycolysis, and metastasis. HIF-1 alpha (Hypoxia-inducible factor 1 alpha) is the main regulatory factor of hypoxia (Chen and Lou, 2017). Several studies revealed hypoxia modulates the chromatin epigenetic landscape. HIF-1 α prompts the expression of several JmjC- Jumonji-domain histone demethylases (KDMs) and histone methylases under hypoxic conditions (Yamane et al., 2006).

The HIF alters the chromatin in different ways by changing the expression level of different KDMs and DNA methyltransferase and increases transcription factors to promote EMTs (Mohyeldin et al., 2010; Tyrakis et al., 2016).

In addition to this, the transcriptomic adjustment of the circulating, matrix-detached tumorigenic cells is also documented due to diverging epigenetic changes at DNA and histone levels (Aceto et al., 2014; Gkountela et al., 2019).

Therefore, in the current study, we aimed to explore the impact of matrix detachment on the epigenome, mainly KDM(s), in various cancer types. Furthermore, we aimed to assess the role of identified KDM(s) in maintaining the stemness and survival of matrix-detached cancer cells.

MATERIALS AND METHODS

Cell Lines and Culture

Various cancer cell lines were maintained in the Dulbecco's modified Eagle's medium (DMEM) supplemented with 10% FBS and 1% penicillin–streptomycin (Invitrogen) at 37°C in 5% CO_2. All the cell lines, namely, HCT116, HeLa, and 22Rυ1 used in the current study, were obtained from ATCC (United States). The cells were grown to 70–90% confluence, and the media was changed every two days. In addition, the cell lines were routinely checked for any *Mycoplasma* contamination.

Anoikis (Matrix Detachment) Model

We have followed the well-established method of the cell detachment model in our experiments (Khan et al., 2021). Briefly, cells were grown in an ultra-low attachment plate obtained from Corning (Sigma) in a CO_2 incubator at 37°C. The assessments of matrix detachment were performed in a cell suspension culture. First, cells were dislodged by simple agitation in the presence of trypsin, followed with washing with PBS, resuspended at 0.5×10^6 cells/ml in serum-free culture media containing BSA, and finally were cultured in an ultra-low attachment plate at 37°C for various time points, which resulted in the formation of spheroids. The spheroids were treated with either a vehicle control (0.1% DMSO) or with different concentrations of GSK J4 (Abcam-144396, Cambridge, MA United States) for five days. The images were captured by using a Nikon (United States) inverted light microscope. Images were analyzed for size measurement by ImageJ software (https://imagej.net/Invasion_assay).

Real-Time qPCR Analysis for the mRNA Expression

Briefly, RNA was extracted from all the cell lines at the end of different experimental conditions using the RNAeasy kit (Qiagen) and reverse-transcribed with a high-capacity cDNA reverse transcription kit (applied biosystems). cDNA (1–100 ng) was amplified in triplicates using gene-specific primers (**Table 1**). Threshold cycle (C_T) values obtained from the instrument's software were used to calculate the respective mRNAs' fold change. ΔC_T was calculated by subtracting the C_T value of the housekeeping gene from that of the mRNA of interest. $\Delta\Delta C_T$ for each mRNA was then calculated by subtracting the control's CT value from the experimental value. The fold change was calculated by formula $2^{-\Delta\Delta CT}$.

Histone Demethylase Activity Assay

Histone H3K27 demethylase KDM6A/B activity was measured by using the Abcam- KDM6A/B activity quantification kit (ab156910). The protocol was performed based on the Kit guidelines. 15 µg of the nuclear extract was used. The nuclear protein was extracted without using detergent. The ECM-detached cells with and without treatment of GSK J4 and ECM-attached cells 2×10^6 were obtained. They were washed with ice-cold PBS three times in 500 g for 10 min in 500 µL of lysis buffer 10 mM HEPES, pH 7.9, with 1.5 mM $MgCl_2$ and 10 mM KCl (add 5 µL of 0.1 M DTT and 5 µL of protease inhibitor cocktail) and incubated for 15 min in ice. The supernatant was removed after spinning, and the pellets were resuspended in 200 µL of the lysis buffer, and five gentle strokes were performed using a glass homogenizer. It was allowed to spin for 20 min at 12,000 g. The cytosolic fraction (supernatant) was removed, and 150 µL of nuclear extraction buffer 20 mM HEPES, pH 7.9, with 1.5 mM $MgCl_2$, 0.42 M NaCl, 0.2 mM EDTA, and 25% (v/v) glycerol was added with the addition of 1.5 µL of 0.1 M DTT and 1.5 µL of protease inhibitor cocktail. It was incubated in ice for 30 min with a gentle shake every 2 min and allowed to spin at 21,000 g for 10 min to obtain the supernatant (Nuclear protein).

H3K27 Methyltransferase Activity Assay

The H3K27-specific methyltransferase activity was performed using a commercially available kit from Abcam [H3K27 methylation Assay Kit (Colorimetric) # ab156910]. The assay kit could measure the activity or inhibition of H3K27 mono/di/tri subtypes and required cellular nuclear extracts. Briefly, equal amounts of protein samples were added in each independent experiment; however, the overall protein concentration ranged

TABLE 1 | List of primers for real-time PCR.

hJARID1A	5′-TGTGTTGAGCCAGCGTATGG-3′	5′-CCACCCGGTTAAAAGCAGACT-3′
hJARID2	5′-TGTTCACAACGGGCATGTTT-3′	5′-TTGTGTTTTTGAACAGGTTCCTTCT-3′
hKDM3A	5′-GTGGTTTTCAGCAACCGTTATAAA-3′	5′-CAGTGACGGATCAACAATTTTCA-3′
hKDM3B	5′-TGCCCTTGTATCAGTCGACAGA-3′	5′GCACTAGGGTTTATGCTAGGAAGCT-3′
hKDM4A	5′-TGCAGATGTGAATGGTACCCTCTA-3′	5′-CACCAAGTCCAGGATTGTTCTCA-3′
hKDM4B	5′-GGCCTCTTCACGCAGTACAATAT-3′	5′-CCAGTATTTGCGTTCAAGGTCAT-3′
hKDM4C	5′-GAATGCTGTCTCTGCAATTTGAGA-3′	5′-CAACGGCGCACATGACAT-3′
hKDM6B	5′-CGGAGACACGGGTGATGATT-3′	5′-CAGTCCTTTCACAGCCAATTCC-3′
hSOX2	5′- TGATCATGTCCCGGAGGT-3′	5′- CATGGGTTCGGTGGTCAAG-3′
hSOX9	5′- TCTACTCCACCTTCACCTACAT-3′	5′-CTGTGTGTAGACGGGTTGTT-3′
hCD44	5′- CAGCACTTCAGGAGGTTACAT-3′	5′- GTAGCAGGGATTCTGTCTGTG-3′
LinVEGFA	5′-GCCTCCGAAACCATGAACTTT-3′	5′-CCATGAACTTCACCACTTCGT-3′
Lin HIF 2α	5′-CTGAACGTCTCAAAGGGCCA-3′	5′-CCTTCCTCCTCTCCGAGCTA-3′
Lin HIF 1α	5′-ATGCTTTAACTTTGCTGGCCC-3′	5′-TCTGTGTCGTTGCTGCCAAA-3′
hKDM6A	5′-CACAGTACCAGGCCTCCTCATT-3′	5′-TCACTATCTGAGTGGTCTTTATGATGACT-3′

from 100 to 300 ng H3K27 modifications were calculated according to the manufacturer's instructions, which also accounts for protein amounts, and the final values for each modification were presented as the percentage over untreated control.

Protein Extraction and Western Blot Analysis

Various cancer cells (HCT116, HeLa, and 22Rv1) were cultured in a T_{75} flask (1×10^6/flask). After 24 h, plating cells in ultra-low attachment plates were treated with GSK J4 for the indicated dose for five consecutive days. The new treatment was added every 48 h; following completion of treatment, media was aspirated, and cells were washed with cold PBS (pH 7.4) and pelleted in 15-ml falcon tubes. Ice-cold lysis buffer was added to the pellet. The composition of the lysis buffer was 50 mM Tris–HCl, 150 mM NaCl, 1 mM ethylene glycol-bis(aminoethyl ether)-tetraacetic acid, 1 mM ethylenediaminetetraacetic acid, 20 mM NaF, 100 mM Na_3VO_4, 0.5% NP-40, 1% Triton X-100, and 1 mM phenylmethylsulfonyl fluoride, pH 7.4 with freshly added protease inhibitor cocktail (Protease Inhibitor Cocktail Set III, Calbiochem, La Jolla, CA). Then, cells were passed through the needle of the syringe to break up the cell aggregates. The lysate was cleared by centrifugation at 14,000 *g* for 30 min at 4 °C, and the supernatant (nuclear lysate) was used or immediately stored at −80°C. For western blotting, 4–12% polyacrylamide gels were used to resolve 30 μg of protein, transferred onto a nitrocellulose membrane, probed with appropriate monoclonal primary antibodies, and detected by chemiluminescence after incubation with specific secondary antibodies (Shait Mohammed et al., 2020).

Flow Cytometry Analysis

HeLa, HCT116, and 22Rυ1 cells were grown in an ultra-low attachment plate for six days with and without treatment of GSK J4. Cells were washed two times in ice-cold PBS and resuspended in 100 μL of staining solution (5 μL PE-conjugated anti-CD 70 (BD Bioscience), CD 133 (Miltenyibiotec-130-090-853), and FITC-conjugated anti-CD 105(BD Bioscience- 56143) and anti-CD44(Miltenyibiotec -130-098-210), 1% FBS, in 1X PBS and incubated at room temperature under the dark condition for 2 h. Then, cells were washed three times in a wash buffer (1% FBS in 1X PBS) and then analyzed by using a Guava Easy-Cyte flow cytometer. For all assays, 10,000 cells were taken for measurement and also for analysis. For each plot, 1000 cells were displayed.

Immunofluorescence

For immunofluorescence assay, cells were grown in ultra-low attachment plates for six days with and without treatment of GSK J4. Then, cells were collected and washed two times with ice-cold PBS, and cells were stained with a staining solution containing (5 μL, CD 133 and FITC anti-CD 105, and anti-CD44) 1% FBS in 1X PBS and incubated at room temperature in the dark for 2 h. Then, cells were washed two times in ice-cold PBS, and cells were analyzed using a Amins image stream flow cytometer.

Apoptosis Assay

The apoptotic cells were detected by using Annexin V-FITC and propidium iodide. The cells were grown in an ultra-low attachment plate for six days with and without treatment with GSK J4. After treatment, spheroids were harvested and washed with PBS (ice-cold) three times. The spheroids were broken down by multiple pipetting and resuspended in 100 μL 1X binding buffer, 10 μL Annexin V-FITC, and 5 μL *p*I. After incubation for 20 min in RT (dark condition), the cells were analyzed by using The Guava® easy, yet 5 flow cytometer, and the percentage of apoptosis cells was calculated (Alzahrani et al., 2021).

TABLE 2 | List of primers for CHIP-q PCR.

Chip-CD44	5′- CTGGCAGCCCCGATTATT-3′	5- AGCGAGCGAAGGACACAC-3′
Chip-Sox9	5′- GCTCTAAGCATTTCGTGTAA-3′	5′- TACGAAACACCTGAAGGG-3′
Chip-SOX2	5′- CGACAACAAGAGAAACAAAAC-3′	5′- CCAGCAAGGCCCGGGTTA-3′
Chip-HIF1α	5′ GAAGTTTACAGCAACAGGAG-3′	5′- TTACAACGGGGTCTTTCCTTAC-3′

CHIP PCR

The CHIP experiments were performed by using the Abcam (ab185913) chip kit. The protocol was followed as per standard guidelines of the manual with minor modifications. The spheroids (ECM detached), ECM-attached cells, and ECM-detached cells were harvested and washed with ice with 3 ml PBS. Cells were resuspended in 1% formaldehyde in the DMEM and incubated at RT for 10 min with the minor rocking platform, and 300 μL of 1.25 M glycine was added for crosslinking washed with ice-cold PBS. The pellet was resuspended in 300 μL lysis buffer, and the chromatin was sheared using a water bath sonicator (15 cycles on and 15 cycles off for 20 min). Three micrograms of the sheared chromatin were taken to the well coated with KDM6B antibodies, input (negative control) along with nonimmune IgG and incubated overnight at 4°C. The unbounded chromatins were removed and washed with the

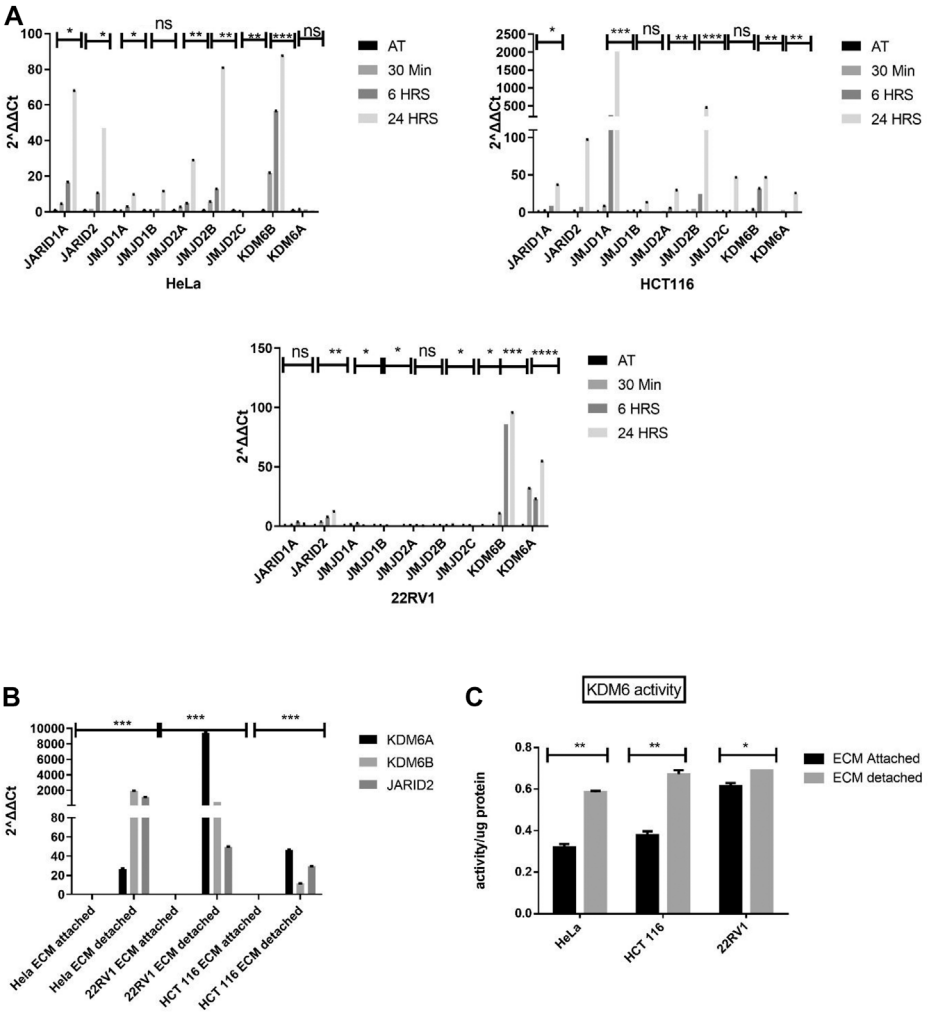

FIGURE 1 | Matrix detachment induces the KDM6B expression and activity. **(A)** Expression of various hypoxia-regulated histone demethylases in HeLa, HCT116, and 22Rv1 cell lines during matrix detachment at shorter time points (30 min, 6, and 24 h). **(B)** JARID2 and KDM6B/A in HeLa, HCT116, and 22Rυ1 cell lines during matrix detachment for six days. The values were normalized with the housekeeping gene *RPLP0*, and other gene expression values were calculated. **(C)** KDM6 demethylase activity was measured in the nuclear extract of HeLa, HCT116, and 22Rv1 cells grown in matrix-detached conditions. ***p*.value > 0.001, **p*.value > 0.01, ****p*.value > 0.0001.

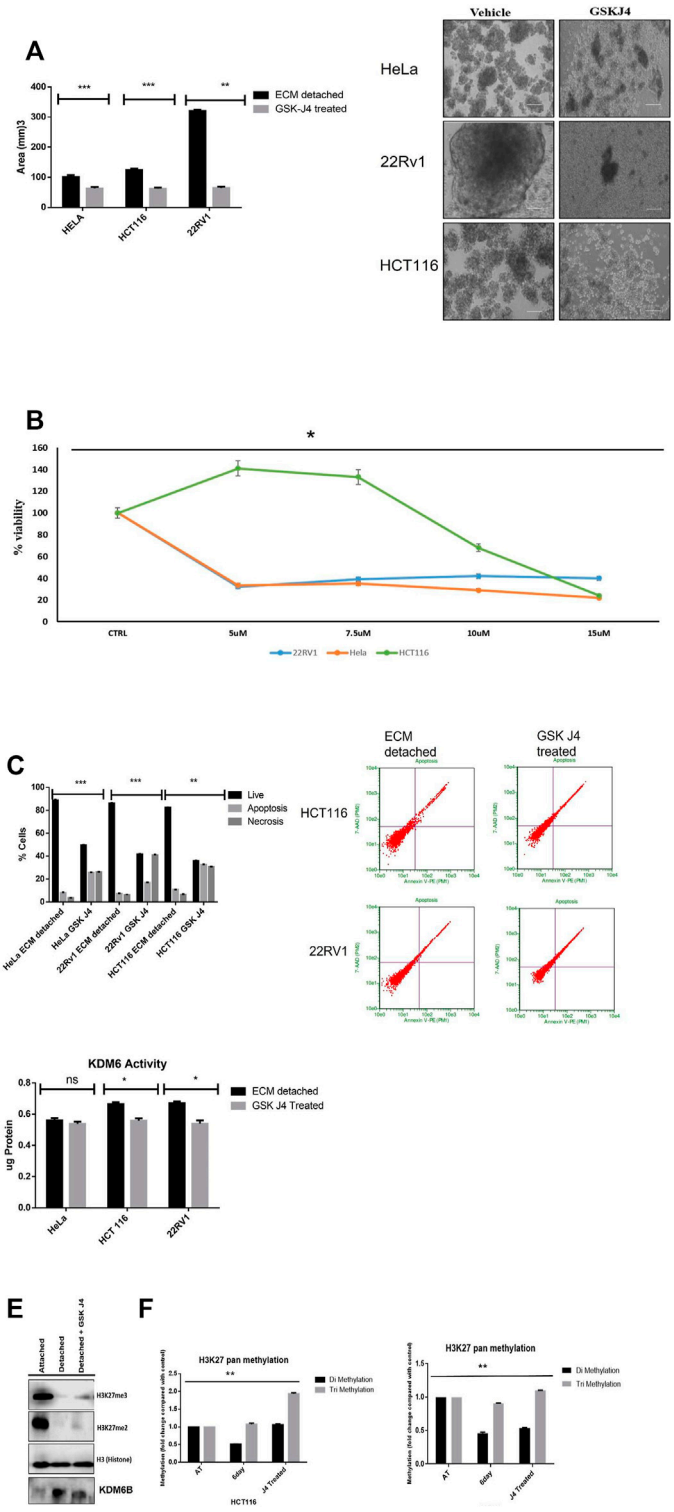

FIGURE 2 | KDM6A/B inhibition reduces the spheroid size and induces apoptosis. **(A)** Sphere formation assay HeLa, HCT116, and 22Rv1 cell lines were cultured in matrix detachment for six days and simultaneously treated either with GSK J4 (5 μM for HeLa and 22Rv1, 10 μM for HCT116) or with vehicle 0.1% DMSO (control). At the end of the treatment schedule, sphere images were captured using a Nikon inverted light microscope, and images were analyzed for size measurement by ImageJ software $N = 8$. Histogram plots were plotted for average size in all conditions. **(B)** HeLa, HCT116, and 22Rv1 cell lines were cultured in matrix detachment for six days and simultaneously treated with different GSK J4 or with vehicle 0.1% DMSO (control). Cell proliferation was measured using WST-1, and IC 50 was calculated. **(C)** Apoptosis assay HeLa, HCT116, and 22Rv1 cell lines were cultured in matrix detachment for six days and simultaneously treated either with GSK J4 (5 μM for HeLa and

(*Continued*)

FIGURE 2 | 22Rv1,10 μM for HCT116) or with vehicle 0.1% DMSO (control). As mentioned above, a similar treatment strategy was used, and apoptosis assay was performed using Annexin V and *p*I. The histogram data were plotted for % cells showing live or apoptotic populations. **(D)** KDM6B/A demethylase activity was measured from the nuclear extract of HeLa, HCT116, and 22Rv1 cell lines and were cultured in matrix detachment for six days and simultaneously treated either with GSK J4 (5 μM for HeLa and 22Rv1,10 μM for HCT116 KDM6B/A) or with vehicle control. The activity was measured using the KDM6 activity assay kit. **(E)** Histone was extracted from ECM-attached and ECM-detached cells. ECM-detached cells treated with GSK-J4 using a histone extraction kit (ab113476) and 10 μg of histone protein loaded for Western blot; Western blot showing GSK J4 treatment for six days significantly induces the expression of H3K27me2/3 in 22RV1 during matrix detachment conditions. **(F)** pan H3k27 me2 and me3 was measured from histone extracted as previous conditions mentioned above. *p*.value $^{**}p$.value > 0.001, $^{*}p$.value > 0.01, $^{***}p$.value > 0.0001.

wash buffer. DNA was released using the DNA release buffer and incubated at 60°C for 45 min in a water bath; subsequently, the solution was transferred to PCR tubes heated at 95°C for 15 min at a thermocycler. The DNA was purified by using the column provided in the kit. The PCR was performed by using the targeted primers (**Table 2**) of specific genes.

Gene Expression Correlation Analysis

For the correlation analysis of gene expressions among *KDM6B*, *SOX2*, *CD44*, and HIF1α, a gene expression profile was taken from two different studies. 1) A metastatic melanoma sample was taken from Hugo et al., 2016 (PMID: 26997480). The study provided the normalized gene expression data in FPKM values from 27 samples. 2) Metastatic breast cancer data of the Metastatic Breast Cancer Project (www.mbcproject.org). The study provided the normalized gene expression data in RSEM values from 146 samples. The normalized expression values were transformed into log2 (x+0.1), and then, the Pearson correlation coefficient was measured with the ggpubr package.

Statistical Analysis

Data were analyzed using GraphPad Prism (version 5; GraphPad Software). The two-tailed, unpaired *t*-test was used. Data points in graphs represent mean ± SD, and p values <0.05 were considered significant.

CRISPR Knockout of KDM6B

CRISPR case-based gene knockout experiments, the plasmid-containing CRISPR double nickase was constructed by SANTA CRUZ biotechnology sc-401883-NIC for KDM6B and non-targeted + ve control (sc-437281). For plasmid transfection, 1×10^5 per HeLa cells were plated at a 6-well plate. First, 1 μg plasmid was transfected by using Lipofectamine 3000. After transfection, at 48 h, the cells were collected for extraction of total protein. The knockout efficiency was verified by Western blotting.

RESULTS

KDM6A/B Expression and Demethylase Activity Are Increased During Anoikis

To investigate key histone demethylase, promote or regulate anoikis resistance. We measured the expression of various histone demethylases in detachment conditions of different cancer cell types (HeLa, HCT116, and 22Rv1). Quantitative gene transcript analysis at early time points (from 30 min to 24 h) showed statistically significant induction of various histone demethylases such as JARID1A, JARID2, JMJD1A, and KDM6A/B in all the three cancer cell types grown in detached conditions (**Figure 1A**). We decided to investigate the above-tested histone demethylases' expression pattern in long-term detachment conditions (6 days). Only histone demethylase, namely KDM6A/B, stands out as its expression was consistently upregulated in all three cell lines during detached conditions compared with attached (**Figure 1B**).

Since both KDM6A/B are H3K27 me3 demethylases and were most consistently upregulated at all time points in all cell types, we decided to focus our further work on KDM6A/B. We performed quantitative activity assay for KDM6A/B demethylases and found a statistically significant increase in the KDM6A/B demethylase activity in HeLa, 22Rv1, and HCT116 cell lines in detached conditions when compared with the attached. (**Figure 1C**). Based on the above data, ECM detachment of cancer induces the expression and activity of KDM6A/B histone demethylases, removing the repressive H3K27me3 mark across the genome, thereby facilitating transcription.

Targeting KDM6A/B Demethylases Reduces Sphere-Forming Capabilities and Induces Apoptosis of Cancer Cells During Anoikis

Matrix detachment of cancer cells tends to form spheroids. Therefore, to investigate the effect of KDM6A/B inhibition in spheroid formation, we treated spheroids of HeLa, HCT116, and 22Rv1 that formed during matrix detachment with GSK J4 (Heinemann et al., 2014), a highly specific inhibitor of KDM6A/B. Results showed that GSK J4 significantly reduced the size of spheroids of all cancer cell lines tested compared to untreated, respectively (**Figure 2A**), and IC50 for different dose concentrations was measured before treatment (**Figure 2B**).

The reduction in the spheroid size is associated with cell death. So we measure the percentage of cell death that might have occurred in ECM-detached cancer cells during GSK J4 treatment. As expected, GSK J4 significantly induces apoptosis in all the ECM-detached cancer cells. Among them, 22Rv1 showed the maximum percentage of apoptotic cells (57.7%) when compared with HeLa (34.4%) and HCT116 (22.8%) (**Figure 2C**). Overall, we observed that reducing the KDM6A/B activity significantly reduces the sphere-forming capacity and invokes apoptosis in ECM-detached cancer cells.

We observed that GSK J4 treatment significantly reduces the KDM6A/B activity in all cell lines and KDM6B expression (**Figures 2D,E**), along with GSK J4 treatment which induces global H3K27me2/3 methylation (**Figures 2E,F**).

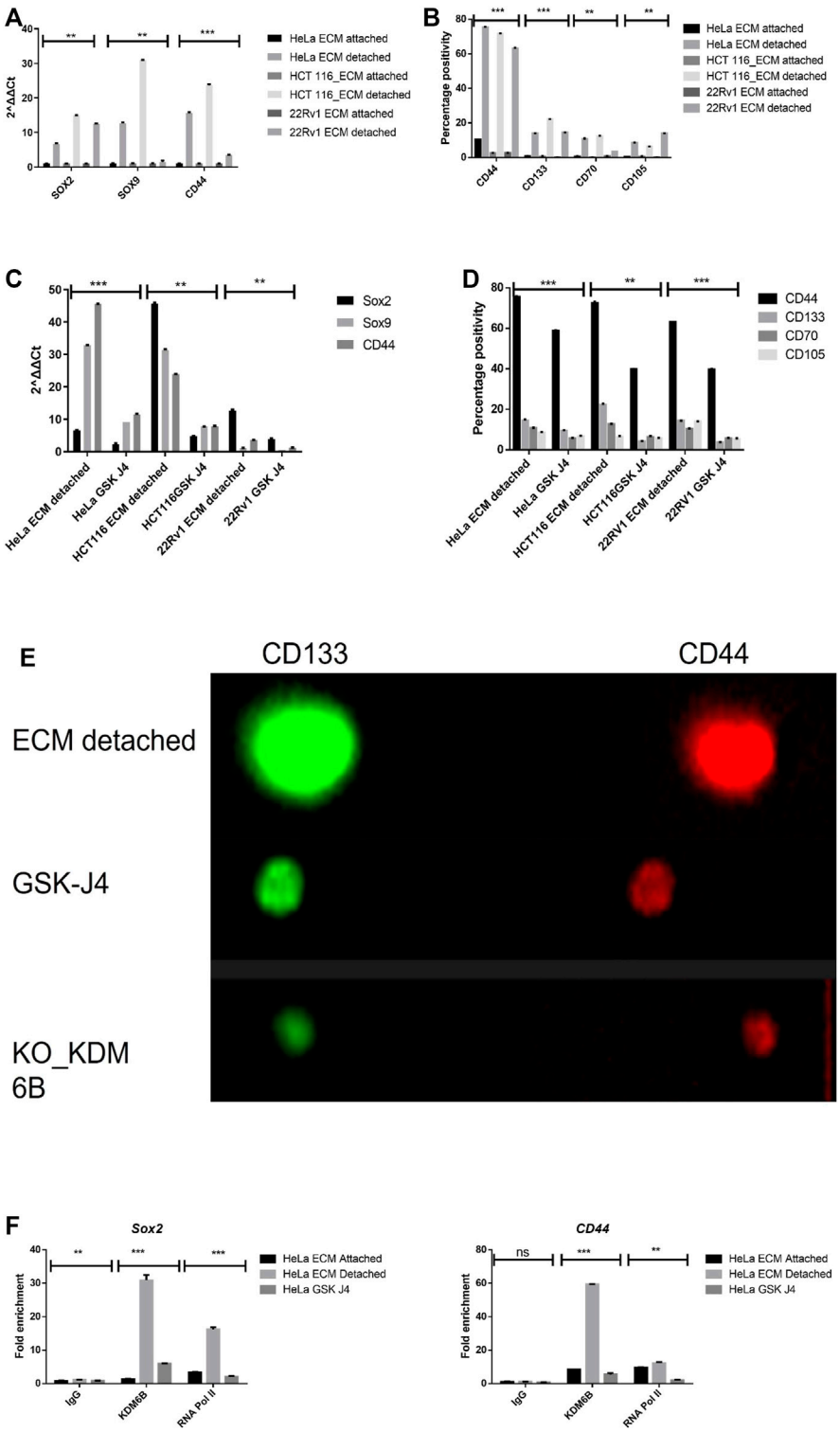

FIGURE 3 | Matrix detachment induces the expression of stemness markers that are repressed by the KDM6B-specific inhibitor. **(A)** mRNA expression of various stemness-related genes (*SOX2*, *SOX9*, and *CD44*) in HeLa, HCT116, and 22Rv1 cell lines during matrix detachment at six days. The values were normalized with the housekeeping gene *RPLP0*, and other gene expression values were calculated. **(B)** Flow cytometry–based expression of various surface markers of stemness in HeLa, HCT116, and 22Rv1 cell lines during matrix detachment for six days. **(C)** Spheroids were treated with GSK-J4 (5 μM for HeLa and 22Rv1,10 μM for HCT116), a specific inhibitor of KDM6 histone demethylases. Moreover, the mRNA expression of various stemness-related genes (*SOX2*, *SOX9*, and *CD44*) in HeLa, HCT116, and 22Ru1 cell lines were measured as explained

(*Continued*)

FIGURE 3 | above. **(D)** Spheroids were treated with GSK-J4 (5 μM for HeLa and 22Rv1,10 μM for HCT116). In addition, the flow cytometry–based expression of various surface markers of stemness was measured. **(E)** Immunofluorescence for various stemness surface markers was measured in spheroids and spheroids treated with GSK-J4 in HeLa. **(F)** Enrichment of KDM6B and RNA Pol II on the promoters of *SOX2* and *CD44* genes in the presence and absence of GSK J4 in ECM-detached (spheroids) cells; nonimmune IgG was used as the input control. ***p*.value > 0.001, **p*.value > 0.01, ****p*.value > 0.0001.

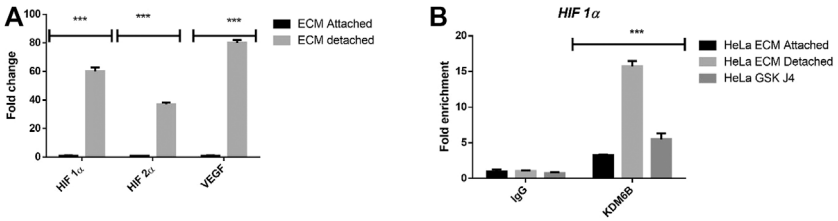

FIGURE 4 | Matrix detachment induces the hypoxia-regulated KDM6B expression and activity. **(A)** mRNA expression of various stemness-related genes HIF1α, HIF2 α, and target gene VEGF in HeLa cell lines during matrix detachment for six days. The values were normalized with the housekeeping gene *RPLP0*, and other gene expression values were calculated. **(B)** Enrichment of KDM6B on the promoters of HIF 1α both in the presence and absence of GSK J4 (5 μM) in HeLa cells during matrix detachment for six days; nonimmune IgG was used as the input control. ***p*.value > 0.001, **p*.value > 0.01, ****p*.value > 0.0001.

Targeting KDM6A/B Demethylases Reduces the Expression of Stemness-Related Genes During Anoikis

During matrix detachment, cancer cells often present with induced expression of stemness genes; therefore, we quantified the expression of genes related to stemness such as *SOX2*, *SOX9*, and *CD44* and found significantly increased levels of these stemness-related genes in all matrix-detached cancer cell lines when compared to their attached counterparts (**Figure 3A**). Furthermore, we further validated the stemness by measuring the surface protein marker of stemness such as CD44, CD133, and mesenchymal markers, namely, CD70 and CD105, by flow cytometry. As expected, we observed statistically significant upregulation of surface stemness and mesenchymal markers in all detached cancer cells compared to attached cells. Thus, our data represent that detachment induces stemness (**Figure 3B**).

To investigate the role of KDM6A/B demethylases in the transcriptional regulation of stemness genes, we treated all the detached cancer cell types with GSK J4 (a KDM6A/B) for a total period of 5 days after the initial 24 h of anoikis (detachment). Our data showed that GSK J4 treatment significantly reduces the transcript levels of *SOX2*, *SOX9*, and *CD44* genes in detached cancer cells compared to the untreated control (**Figure 3C**). Next, we assess the impact of GSK J4 treatment on the expression of stemness-related surface proteins by using both flow cytometry and immunofluorescence and found that GSK J4 significantly reduced the expression of *CD44*, *CD133*, *CD70*, and *CD105* in detached cells when compared to untreated (**Figures 3D,E**; **Supplementary Figure S1**).

We next aimed to investigate the KDM6B occupancy on stemness genes' promoters during anoikis conditions. For this, we performed a CHIP-RT PCR assay. As a result, we observed significant enrichment of KDM6B on promoter regions of *SOX2* and *CD44* but not on *SOX9* in detached cancer cells. Furthermore, GSK J4 treatment significantly reduces the occupancy of KDM6B on promoters of both *SOX2* and *CD44*, suggesting the KDM6B-driven regulation of these stemness genes in detached cancer cells (**Figure 3F**).

Targeting KDM6A/B Demethylases Reduces the HIF-1α Expression During Anoikis

Hypoxia-driven regulation of the histone demethylase expression and activity is a well-established phenomenon. Recent studies have shown that various histone methyltransferases such as SET7/9, G9a, and GLP can methylate HIF1A and regulate and repress its expression (Bao et al., 2018). It prompted us to investigate whether induction in the KDM6B activity during ECM detachment might positively regulate the hypoxia-related transcription factors HIF1α and HIF2α expressions and reduce KDM6B activity (using GSKJ4) negatively regulate its expression (**Figure 4A**). Thus, we investigated whether KDM6B occupies hypoxic transcription factors' promoters and regulates their expression. Results showed a clear enrichment of KDM6B on the HIF1α promoter and a subsequent reduction in the enrichment by GSK J4, further confirming the transcriptional regulation of HIF1α in matrix-detached conditions (**Figure 4B**).

The KDM6B Knockout by CRISPR Reduces the Spheroid Size and Stem Cell Markers

To investigate the role of KDM6B in the expression regulation of stem cell markers, we used the CRISPR Double Nickase KDM6B plasmid, which can inhibit the gene expression level of KDM6B. Our results showed that CRISPR, **Figure 5A** completely removed the protein level of KDM6B in HeLa cells. The spheroid size was decreased (**Figure 5B**).To examine the KDM6B role in maintaining stem cell markers, we cultured the HeLa KDM6B-knockout cells in the ECM-detached condition. After six days, we examined for stem cell surface markers by flow cytometry. We found that KDM6B knockout significantly reduced the

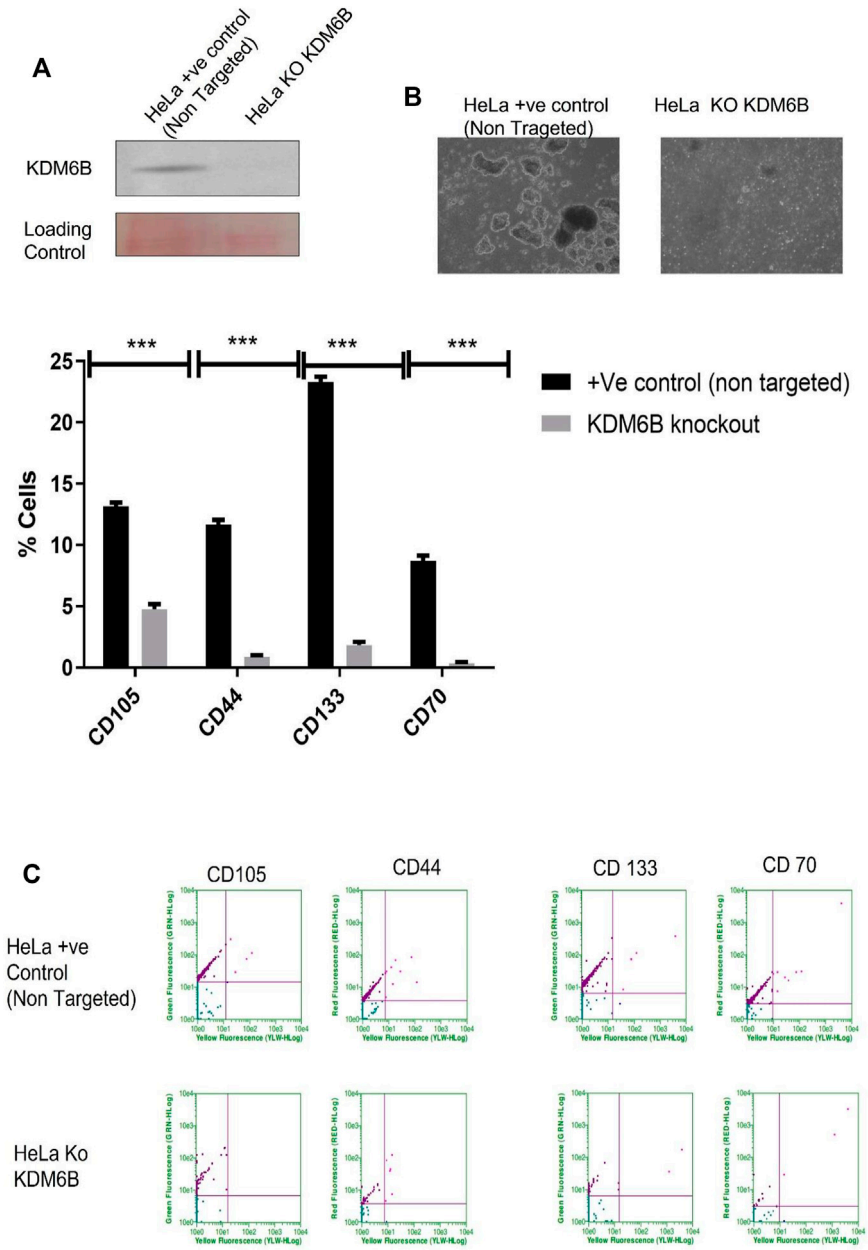

FIGURE 5 | CRISPR knockout KDM6B and reduce stemness in ECM-detached cells. **(A)** Total protein was isolated from +ve control empty CRISPR Cas-transfected cell line and CRISPR KDM6B-knockout cell lines. Western blot was performed as previously mentioned, and the blot was probed with anti-human KDM6B antibodies; the loading control was blot stained with Ponceau staining. **(B)** Sphere formation assay HeLa + ve Control (non-targeted) and HeLa KDM6B-knockout cell lines were cultured in matrix detachment for six days. At the end of the treatment schedule, sphere images were captured by using a Nikon inverted light microscope. **(C)** HeLa + ve Control (non-targeted) and HeLa KDM6B-knockout cell lines were cultured in matrix detachment for six days in the end for time duration. The flow cytometry–based expression of various surface markers of stemness was measured.

expression of *CD44*, *CD133*, *CD70*, and *CD105* in detached cells when compared to a positive control (**Figure 5C**).

Clinical mRNA Expression Association of KDM6B and HIF1α

Based on our results that KDM6B transcriptionally regulates the expression of HIF1α, we next investigated the positive association between KDM6B and HIF1α in clinical samples using TCGA datasets. We found a positive association between KDM6B and HIF1α in various cancer types. In metastatic melanoma and breast cancer samples, a significantly high positive correlation was observed between KDM6B and HIF1α mRNA (R = 0.45, p-value = 0.018; R = 0.26, p-value = 0.0014) (**Figures 6A,B**). Similarly, we found a significant positive association between HIF1α and *SOX2*

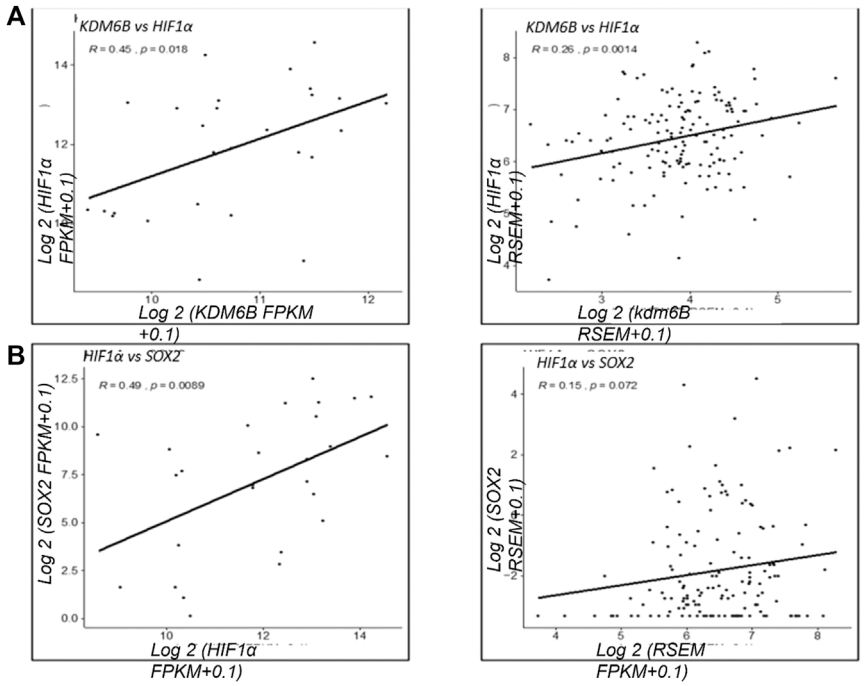

FIGURE 6 | Clinical correlation of KDM6B and HIF 1α in various cancer types. Correlation analysis of the gene expression between KDM6B and HIF 1α from metastatic samples. **(A)** Gene expression in metastatic melanoma samples. **(B)** Gene expression in metastatic breast samples ***p*.value > 0.001, **p*.value > 0.01, ****p*.value > 0.0001.

(R = 0.49, *p*-value = 0.0089) along with *CD44* and *SOX2* (R = 0.39, *p*-value = 0.045) in melanoma cancers. We also found that metastatic breast samples had a significantly high positive correlation between CD44 and HIF1α (R = 0.24, *p*-value = 0.0031) (**Supplementary Figure S2**).

DISCUSSION

Anoikis (matrix detachment) can be regulated by histone demethylases such as KDM3B (Pedanou et al., 2016). However, whether other histone demethylases regulate this process is not well explored yet. In the current work, we found that 1) During anoikis, matrix detachment induces the expression of KDM6A/B, a histone H3K27me2/3 demethylase in all cell types tested. 2) Inhibition of the KDM6A/B activity reduces the expression of stemness-related genes, namely, SOX2 and CD44 and were found to be highly expressed during matrix detachment. 3) Mechanistically, KDM6B occupies the promoter regions of stemness-related genes, thereby regulating their expression. 4) We also noticed that HIF1α was transcriptionally regulated by KDM6B during anoikis conditions. 5) Finally, we observed a positive association between KDM6B, HIF1α, and SOX2 mRNA in various cancer types. Overall, we found that matrix detachment modulates the epigenome during anoikis, inducing KDM6A/B that positively regulates the expression of *SOX2*, *CD44*, and HIF1α to regulate survival and stemness of cancer cells.

KDM6B was shown to regulate epithelial to mesenchymal (EMT) conversion of cancer cells by regulating the expression of the EMT process's essential transcription factors (Ramadoss et al., 20122012; Liu et al., 2018). Our results suggest KDM6B as a critical regulator of metastasis in different cancer types. Our findings that increased the KDM6B expression and activity are essential for spheroid maintenance during matrix detachment and align well with these previous studies.

Various histone methylases, including KDM6B, regulate normal and cancer stem cells (Jeong et al., 2010; Akiyama et al., 2016; Tang et al., 2016). This study found that blocking the KDM6B activity showed a dramatic reduction in the expression of stemness marker genes, mainly *SOX2*, *SOX9*, and *CD44*, suggesting their epigenetic regulation in matrix-detached conditions. The post-translational modifications of *SOX2* are shown to regulate its protein stability and transcriptional activity. Akt-mediated phosphorylation at Thr118 promotes the transcriptional activity of *SOX2* in ESCs (Burchfield et al., 2015). Furthermore, Mallaney et al., (2019) showed that Set7 methylates *SOX2* at K119, inhibiting Sox2 transcriptional activity and inducing Sox2 ubiquitination and degradation. Our study found that KDM6B occupies the SOX2 promoter in matrix-detached conditions, probably reduces the repressive H3K27me3 from its promoter, and increases its expression. Previous research by Fang et al., (2014) had shown that GSK J4 treatment reduces the expression of stemness genes, i.e., SOX2, Nanog, and OCT4 in breast cancer stem cells;

however, they did not present direct evidence that KDM6B occupies the promoter of these genes in cancer cells.

CD44 is a prominent and well-established marker of stem cells, and its expression can be regulated at epigenetic levels. DNA methylation of the CD44 promoter by DNA methyltransferases (DNMTs), MBD1, MBD2, and MeCP2 is well-reported (Eberth et al., 2010; Müller et al., 2010). Our work found that KDM6B occupies the promoter of CD44 during matrix detachment of cancer cells. Our finding of KDM6B-mediated transcriptional regulation of CD44 is in apparent agreement with (Eberth et al., 2010; Li et al., 2014; Itoh et al., 2019), who showed *CD44* as a bonafide target of KDM6B in immune and leukemic cells. However, we firmly believe this is the first report to show epigenetic regulation of *CD44* by KDM6B in various concrete cancer types. Furthermore, a positive correlation of the gene expression from two different metastatic cancer data suggesting the involvement of KDM6B in regulating HIF1α, *SOX2*, and *CD44* further indicates the stemness regulatory function of KDM6B in various cancer types.

Hypoxia has been recently associated with the matrix detachment of cancer cells and can regulate the matrix-detached cancer cells (Mohammed and Razeeth, 2021). Our results are in explicit agreement with this study as we also found a clear induction in the expression of HIF and its target genes. . We found that KDM6B occupies the promoter HIF1α and regulates its expression in matrix-detached cancer cells Hypoxia regulates global transcription in multiple ways, and regulation of the expression and activity of histone demethylases is one of them (Heinemann et al., 2014). Therefore, we target to explore the expression pattern of hypoxia-regulated histone demethylases in matrix-detached cancer cells. Our study showed significant and consistent upregulation of KDM6B in all cell lines at the time points tested. Thus, KDM6B plays a crucial and dual role in cancer initiation and progression through binding to promoters of oncogenes or suppressor genes. Furthermore, KDM6B was associated with aggressiveness and enhanced migratory properties of various cancer types (Burchfield et al., 2015; Fu et al., 2019).

CONCLUSION

Our data suggest that the rapid and sustained upregulation of KDM6B following matrix detachment is necessary for *SOX2* and *CD44*-mediated stemness to enhance anchorage-independent survival of various cancer patients' cells. Additional consequences of the context-specific increase and regulation of HIF1α by KDM6B might be likely to further aid in survival in response to changing nutrient microenvironments. Our study highlights an essential role of KDM6B in cancer and has important implications for targeting this protein for anticancer therapies.

DATA AVAILABILITY STATEMENT

The original contributions presented in the study are included in the article/**Supplementary Material**; further inquiries can be directed to the corresponding author.

AUTHOR CONTRIBUTIONS

MS designed and performed the experiments and analyzed the data. BA, MS, and FA carried out the bioinformatics analysis. MK, MZ, and HC designed the study and supervised all aspects of data collection. MK, MS, and FA wrote the manuscript. All authors read and approved the final manuscript.

FUNDING

Under grant no, this project was funded by the Deanship of Scientific Research (DSR), King Abdulaziz University, Jeddah. (KEP-15-130-38).

ACKNOWLEDGMENTS

The authors would like to thank DSR technical and financial support. A preprint has previously been published (Razeeth et al., 2021).

SUPPLEMENTARY MATERIAL

The Supplementary Material for this article can be found online at: https://www.frontiersin.org/articles/10.3389/fcell.2022.780176/full#supplementary-material

REFERENCES

Aceto, N., Bardia, A., Miyamoto, D. T., Donaldson, M. C., Wittner, B. S., Spencer, J. A., et al. (2014). Circulating Tumor Cell Clusters Are Oligoclonal Precursors of Breast Cancer Metastasis. *Cell* 158 (5), 1110–1122. doi:10.1016/j.cell.2014.07.013

Akiyama, T., Wakabayashi, S., Soma, A., Sato, S., Nakatake, Y., Oda, M., et al. (2016). Transient Ectopic Expression of the Histone Demethylase JMJD3 Accelerates the Differentiation of Human Pluripotent Stem Cells. *Development* 143 (20), 3674–3685. doi:10.1242/dev.139360

Alzahrani, A. M., Shait Mohammed, M. R., Alghamdi, R. A., Ahmad, A., Zamzami, M. A., Choudhry, H., et al. (2021). Urolithin A and B Alter Cellular Metabolism and Induce Metabolites Associated with Apoptosis in Leukemic Cells. *Ijms* 22 (11), 5465. doi:10.3390/ijms22115465

Bao, L., Chen, Y., Lai, H.-T., Wu, S.-Y., Wang, J. E., Hatanpaa, K. J., et al. (2018). Methylation of Hypoxia-Inducible Factor (HIF)-1α by G9a/GLP Inhibits HIF-1 Transcriptional Activity and Cell Migration. *Nucleic Acids Res.* 46 (13), 6576–6591. doi:10.1093/nar/gky449

Buchheit, C. L., Weigel, K. J., and Schafer, Z. T. (2014). Cancer Cell Survival during Detachment from the ECM: Multiple Barriers to Tumour Progression. *Nat. Rev. Cancer* 14 (9), 632–641. doi:10.1038/nrc3789

Burchfield, J. S., Li, Q., Wang, H. Y., and Wang, R.-F. (2015). JMJD3 as an Epigenetic Regulator in Development and Disease. *Int. J. Biochem. Cel Biol.* 67, 148–157. doi:10.1016/j.biocel.2015.07.006

Chaffer, C. L., and Weinberg, R. A. (2011). A Perspective on Cancer Cell Metastasis. *Science* 25331 (6024), 1559–1564. doi:10.1126/science.1203543

Chen, C., and Lou, T. (2017). Hypoxia Inducible Factors in Hepatocellular Carcinoma. *Oncotarget* 8 (28), 46691–46703. doi:10.18632/oncotarget.17358

Eberth, S., Schneider, B., Rosenwald, A., Hartmann, E. M., Romani, J., Zaborski, M., et al. (2010). Epigenetic Regulation of CD44in Hodgkin and Non-hodgkin Lymphoma. *BMC Cancer* 10, 517. doi:10.1186/1471-2407-10-517

Fang, L., Zhang, L., Wei, W., Jin, X., Wang, P., Tong, Y., et al. (2014). A Methylation-Phosphorylation Switch Determines Sox2 Stability and Function in ESC Maintenance or Differentiation. *Mol. Cel* 55 (4), 537–551. doi:10.1016/j.molcel.2014.06.018

Fu, C., Li, Q., Zou, J., Xing, C., Luo, M., Yin, B., et al. (2019). JMJD3 Regulates CD4+ T Cell Trafficking by Targeting Actin Cytoskeleton Regulatory Gene Pdlim4. *J. Clin. Invest.* 129 (11), 4745–4757. doi:10.1172/jci128293

Gkountela, S., Castro-Giner, F., Szczerba, B. M., Vetter, M., Landin, J., Scherrer, R., et al. (2019). Circulating Tumor Cell Clustering Shapes DNA Methylation to Enable Metastasis Seeding. *Cell* 176 (1-2), 98–e14. doi:10.1016/j.cell.2018.11.046

Heerboth, S., Housman, G., Leary, M., Longacre, M., Byler, S., Lapinska, K., et al. (2015). EMT and Tumor Metastasis. *Clin. Transl Med.* 4, 6. doi:10.1186/s40169-015-0048-3

Heinemann, B., Nielsen, J. M., Hudlebusch, H. R., Lees, M. J., Larsen, D. V., Boesen, T., et al. (2014). Inhibition of Demethylases by GSK-J1/j4. *Nature* 514 (7520), E1–E2. doi:10.1038/nature13688

Itoh, Y., Golden, L. C., Itoh, N., Matsukawa, M. A., Ren, E., Tse, V., et al. (2019). The X-Linked Histone Demethylase Kdm6a in CD4+ T Lymphocytes Modulates Autoimmunity. *J. Clin. Invest.* 129 (9), 3852–3863. doi:10.1172/jci126250

Jeong, C. H., Cho, Y. Y., Kim, M. O., Kim, S. H., Cho, E. J., Lee, S. Y., et al. (2010). Phosphorylation of Sox2 Cooperates in Reprogramming to Pluripotent Stem Cells. *Stem Cells* 28 (12), 2141–2150. doi:10.1002/stem.540

Khan, M. I., Zamzami, M. A., Ahmad, A., and Choudhry, H. (2021). Molecular Profiling of Epigenetic Landscape of Cancer Cells during Extracellular Matrix Detachment. *Sci. Rep.* 11, 2784. doi:10.1038/s41598-021-82431-w

Kim, Y.-N., Koo, K. H., Sung, J. Y., Yun, U.-J., and Kim, H. (20122012). Anoikis Resistance: An Essential Prerequisite for Tumor Metastasis. *Int. J. Cel Biol.* 2012, 1–11. doi:10.1155/2012/306879

Li, Q., Zou, J., Wang, M., Ding, X., Chepelev, I., Zhou, X., et al. (2014). Critical Role of Histone Demethylase Jmjd3 in the Regulation of CD4+ T-Cell Differentiation. *Nat. Commun.* 5, 5780. doi:10.1038/ncomms6780

Liu, X., Li, C., Zhang, R., Xiao, W., Niu, X., Ye, X., et al. (2018). The EZH2-H3K27me3-DNMT1 Complex Orchestrates Epigenetic Silencing of the Wwc1 Gene, a Hippo/YAP Pathway Upstream Effector, in Breast Cancer Epithelial Cells. *Cell Signal.* 51, 243–256. doi:10.1016/j.cellsig.2018.08.011

Mallaney, C., Ostrander, E. L., Celik, H., Kramer, A. C., Martens, A., Kothari, A., et al. (2019). Kdm6b Regulates Context-dependent Hematopoietic Stem Cell Self-Renewal and Leukemogenesis. *Leukemia* 33 (10), 2506–2521. doi:10.1038/s41375-019-0462-4

Mohammed, S., and Razeeth, M. (2021). Compound C, a Broad Kinase Inhibitor Alters Metabolic Fingerprinting of Extra Cellular Matrix Detached Cancer Cells. *Front. Oncol.* 11, 244. doi:10.3389/fonc.2021.612778

Mohyeldin, A., Garzón-Muvdi, T., and Quiñones-Hinojosa, A. (2010). Oxygen in Stem Cell Biology: a Critical Component of the Stem Cell Niche. *Cell Stem Cell* 7 (2), 150–161. doi:10.1016/j.stem.2010.07.007

Müller, I., Wischnewski, F., Pantel, K., and Schwarzenbach, H. (2010). Promoter- and Cell-specific Epigenetic Regulation of CD44, Cyclin D2, GLIPR1 and PTEN by Methyl-CpG Binding Proteins and Histone Modifications. *BMC Cancer* 10, 297. doi:10.1186/1471-2407-10-297

Paoli, P., Giannoni, E., and Chiarugi, P. (2013). Anoikis Molecular Pathways and its Role in Cancer Progression. *Biochim. Biophys. Acta (Bba) - Mol. Cel Res.* 1833 (12), 3481–3498. doi:10.1016/j.bbamcr.2013.06.026

Pedanou, V. E., Gobeil, S., Tabariès, S., Simone, T. M., Zhu, L. J., Siegel, P. M., et al. (2016). The Histone H3K9 Demethylase KDM3A Promotes Anoikis by Transcriptionally Activating Pro-apoptotic Genes BNIP3 and BNIP3L. *Elife* 5, e16844. doi:10.7554/eLife.16844

Polyak, K., and Weinberg, R. A. (2009). Transitions between Epithelial and Mesenchymal States: Acquisition of Malignant and Stem Cell Traits. *Nat. Rev. Cancer* 9 (4), 265–273. doi:10.1038/nrc2620

Ramadoss, S., Chen, X., and Wang, C.-Y. (20122012). Histone Demethylase KDM6B Promotes Epithelial-Mesenchymal Transition. *J. Biol. Chem.* 287 (53), 44508–44517. doi:10.1074/jbc.m112.424903

Razeeth, M., Zamzami, M., Choudhry, H., Ahmed, F., Ateeq, B., and Khan, M. I. (2021). *Histone H3K27me3 Demethylase Act as Key Regulator of Stem Cell Markers in Matrix Detached Cancer Cells*. PREPRINT (Version 1) available at Research Square. doi:10.21203/rs.3.rs-193530/v1

Shait Mohammed, M. R., Krishnan, S., Amrathlal, R. S., Jayapal, J. M., Namperumalsamy, V. P., Prajna, L., et al. (2020). Local Activation of the Alternative Pathway of Complement System in Mycotic Keratitis Patient Tear. *Front. Cel. Infect. Microbiol.* 10, 205. doi:10.3389/fcimb.2020.00205

Simpson, C. D., Anyiwe, K., and Schimmer, A. D. (2008). Anoikis Resistance and Tumor Metastasis. *Cancer Lett.* 18272 (2), 177–185. doi:10.1016/j.canlet.2008.05.029

Tang, B., Qi, G., Tang, F., Yuan, S., Wang, Z., Liang, X., et al. (2016). Aberrant JMJD3 Expression Upregulates Slug to Promote Migration, Invasion, and Stem Cell-like Behaviors in Hepatocellular Carcinoma. *Cancer Res.* 76 (22), 6520–6532. doi:10.1158/0008-5472.can-15-3029

Tyrakis, P. A., Palazon, A., Macias, D., Lee, K. L., Phan, A. T., Veliça, P., et al. (2016). S-2-hydroxyglutarate Regulates CD8+ T-Lymphocyte Fate. *Nature* 540 (7632), 236–241. doi:10.1038/nature20165

Yamane, K., Toumazou, C., Tsukada, Y.-i., Erdjument-Bromage, H., Tempst, P., Wong, J., et al. (2006). JHDM2A, a JmjC-Containing H3K9 Demethylase, Facilitates Transcription Activation by Androgen Receptor. *Cell* 125 (3), 483–495. doi:10.1016/j.cell.2006.03.027

Conflict of Interest: The authors declare that the research was conducted in the absence of any commercial or financial relationships that could be construed as a potential conflict of interest.

Publisher's Note: All claims expressed in this article are solely those of the authors and do not necessarily represent those of their affiliated organizations, or those of the publisher, the editors, and the reviewers. Any product that may be evaluated in this article, or claim that may be made by its manufacturer, is not guaranteed or endorsed by the publisher.

frontiers in Cell and Developmental Biology

ORIGINAL RESEARCH
published: 14 February 2022
doi: 10.3389/fcell.2022.792564

ISYNA1: An Immunomodulatory-Related Prognostic Biomarker in Colon Adenocarcinoma and Pan-Cancer

*Zeming Jia and Xiaoping Wan**

Department of General Surgery, Xiangya Hospital, Central South University, Changsha, China

Background: Colon adenocarcinoma (COAD) is a common digestive system tumor in the world. However, the role and function of ISYNA1 (inositol-3-phosphate synthase 1) in COAD remain unclear. We aim to explore the role of ISYNA1 in pan-cancer, especially in COAD.

Methods: The expression, clinical characteristic, and prognosis of ISYNA1 in pan-cancer were evaluated using the TCGA (the Cancer Genome Atlas), GTEx (the Genotype-Tissue Expression), and CCLE (Cancer Cell Line Encyclopedia). Pathway enrichment analysis of ISYNA1 was conducted using the R package "clusterProfiler." We analyzed the correlation between the immune cell infiltration level and ISYNA1 expression using two sources of immune cell infiltration data, including the TIMER online database and ImmuCellAI database.

Results: ISYNA1 was highly expressed in COAD and other cancer types compared with respective normal tissues. High ISYNA1 expression predicted poorer survival in COAD. We also found that ISYNA1 expression was positively correlated with the infiltration level of tumor-associated macrophages and tumor-associated fibroblasts in COAD.

Conclusion: In conclusion, our findings revealed ISYNA1 to be a potential prognostic biomarker in COAD. High ISYNA1 expression indicates the immunosuppressive microenvironment.

Keywords: TCGA, ISYNA1, colon adenocarcinoma, prognostic biomarker, macrophages, immunosuppressive microenvironment

OPEN ACCESS

Edited by:
Christiane Pienna Soares, Sao Paulo State Universty, Brazil

Reviewed by:
Qiming Wang, Tongji University, China
Li Liu, Southern Medical University, China
Carolina Panis, Universidade Estadual do Oeste do Paraná, Brazil

****Correspondence:***
Xiaoping Wan
13548571977@163.com

Specialty section:
This article was submitted to Epigenomics and Epigenetics, a section of the journal Frontiers in Cell and Developmental Biology

Received: *10 October 2021*
Accepted: *17 January 2022*
Published: *14 February 2022*

Citation:
Jia Z and Wan X (2022) ISYNA1: An Immunomodulatory-Related Prognostic Biomarker in Colon Adenocarcinoma and Pan-Cancer. Front. Cell Dev. Biol. 10:792564. doi: 10.3389/fcell.2022.792564

INTRODUCTION

Colon adenocarcinoma (COAD) is a global common gastrointestinal tumor, which presents a fatal factor to the health of humans (Wei et al., 2020). The early stage of COAD has no obvious symptoms, leading to the diagnosis of many patients at an advanced stage (Zhou W et al., 2020). Thus, it is pressing to explore the potential mechanisms and identify crucial biomarkers for diagnosis, prognosis, and treatment in COAD.

A body of work have found that the tumor microenvironment (TME), especially the tumor immune microenvironment (TIME), plays an important role in the development of COAD and weakens the response of COAD patients for treatment (Lin et al., 2020). The immune system in the TME was always rebuilt by tumor cells and accelerated tumor progression. For example, tumor-

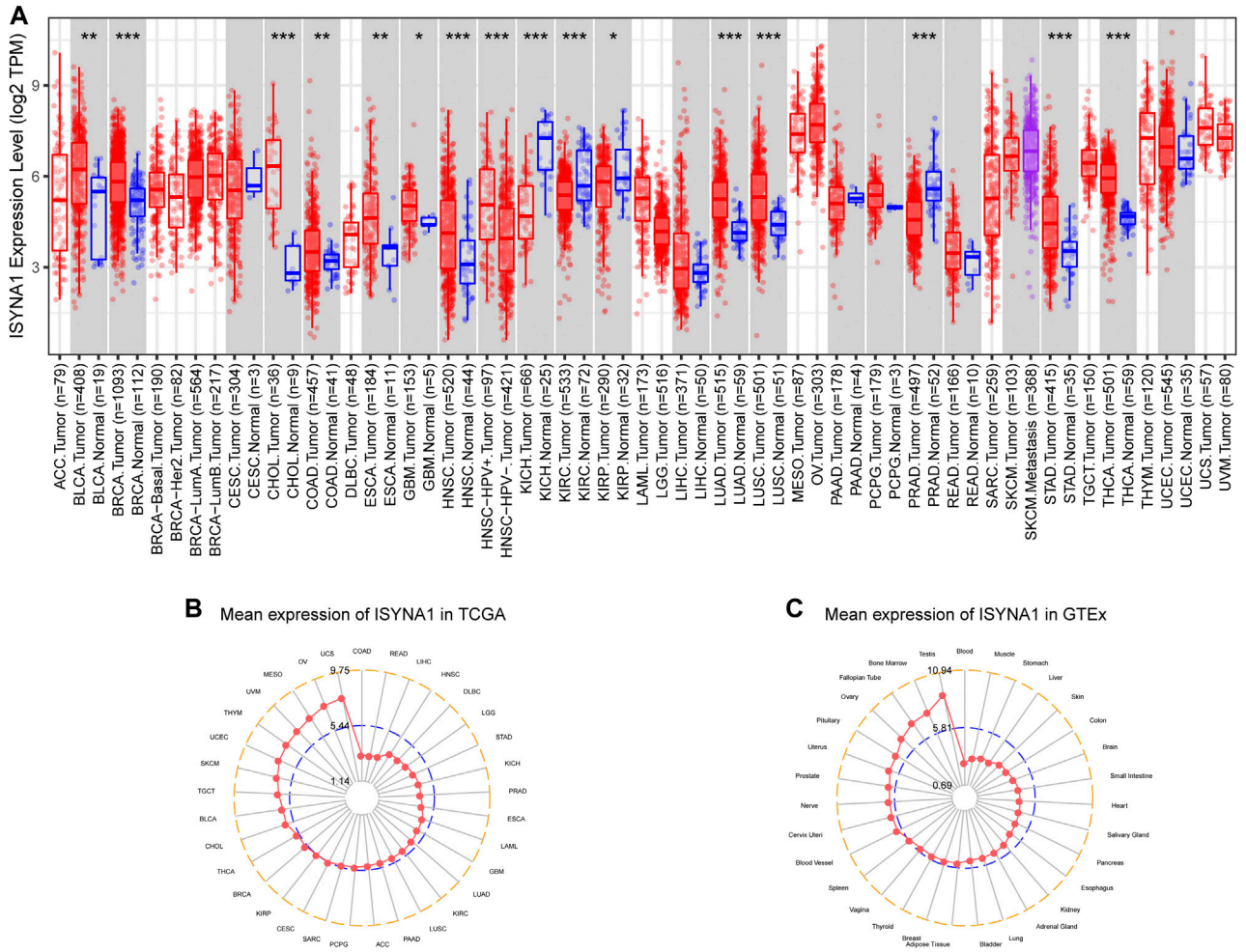

FIGURE 1 | (A) Pan-cancer expression of ISYNA1. **(B)** ISYNA1 expression in tumor tissues from TCGA cohort. **(C)** ISYNA1 expression in normal tissues from GTEx cohort. *$p < 0.05$, **$p < 0.01$, ***$p < 0.001$, ****$p < 0.0001$.

associated macrophages (TAMs) were rebuilt directly or indirectly by tumor cells, and in turn play an immunosuppressive and tumor-promoting role in the process of tumor development (Choi et al., 2018; Qiu et al., 2018; Deepak et al., 2020; Liu et al., 2021). Except for the immune cells, stromal cells in TME were also an accomplice in tumor progression. Stromal cells like cancer-associated fibroblasts (CAFs) could release cytokines, such as TGFB1, IL6, and IL8, and accelerate tumor progression.

ISYNA1 (inositol-3-phosphate synthase 1) encodes the rate-limiting enzyme inositol-3-phosphate synthase. Until now, there are few studies on ISYNA1 in tumor research. In our study, we comprehensively analyzed the role of ISYNA1 using multi-omics data from the TCGA database for 33 cancers, including expression, clinical features, prognostic values, DNA methylation, copy number alteration (CNA), and mutation status of ISYNA1. The correlation between ISYNA1 expression and immune cell infiltration was further assessed. The high expression of ISYNA1 predicted the immunosuppressive TIME, which may lead to poorer survival of tumor patients with a high ISYNA1 expression in COAD. Therefore, targeting ISYNA1 may be a potential cancer therapy method in COAD.

MATERIALS AND METHODS

RNA Extraction and qRT-PCR

Tumor and adjacent normal tissues of COAD, rectum adenocarcinoma (READ), and liver hepatocellular carcinoma (LIHC) were obtained from the Department of General Surgery, Xiangya Hospital. The research protocols were approved by the Research Ethics Committee of Xiangya Hospital. All participants gave written consent of their tissue samples and medical information to be analyzed for scientific research. The total RNA of tissues was isolated and purified by AG RNAex Pro Reagent, AG21101 (Accurate Biology, China),

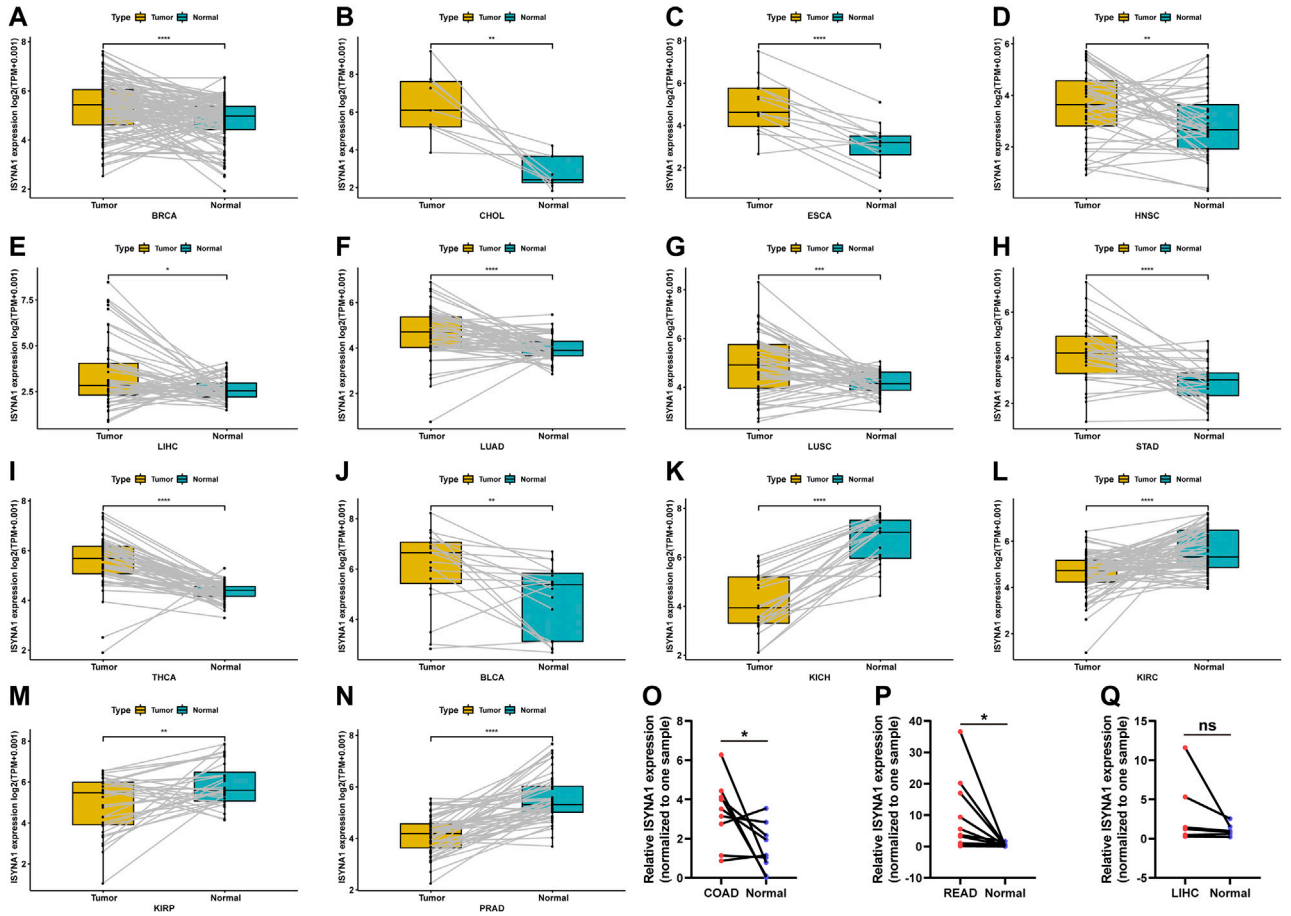

FIGURE 2 | (A–N) ISYNA1 expression in paired tumor and adjacent normal tissues from TCGA in indicated tumor types. **(O–Q)** ISYNA1 expression in COAD, READ, and LIHC based on the qRT-PCR assay. *$p < 0.05$, **$p < 0.01$, ***$p < 0.001$, ****$p < 0.0001$.

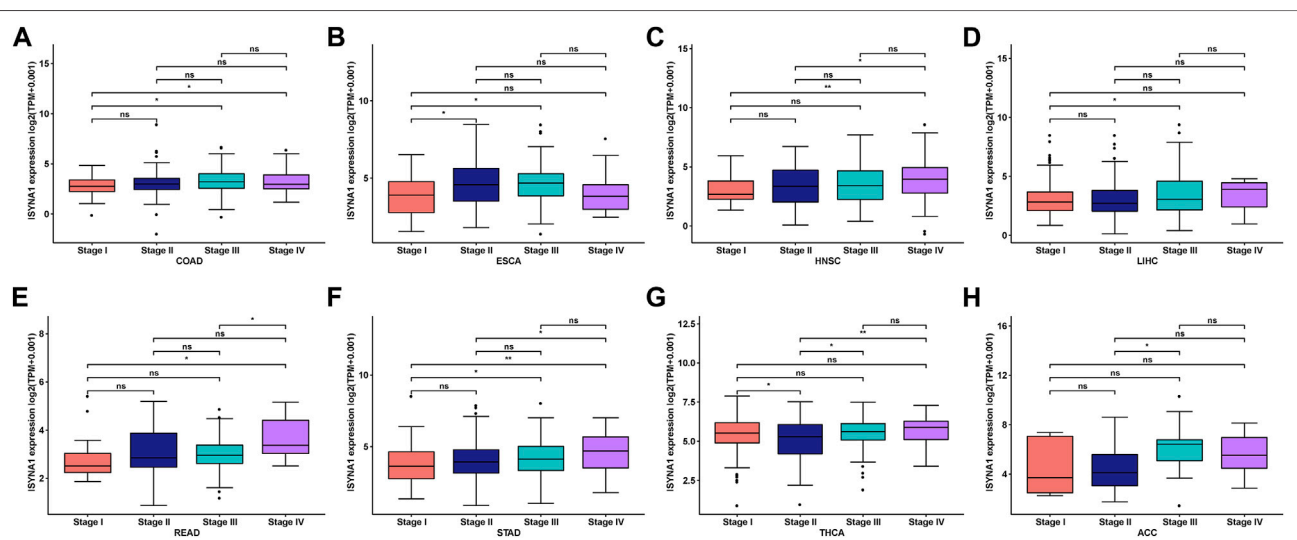

FIGURE 3 | (A–H) ISYNA1 expression in various tumor stages in indicated tumor types. *$p < 0.05$, **$p < 0.01$, ***$p < 0.001$, ****$p < 0.0001$.

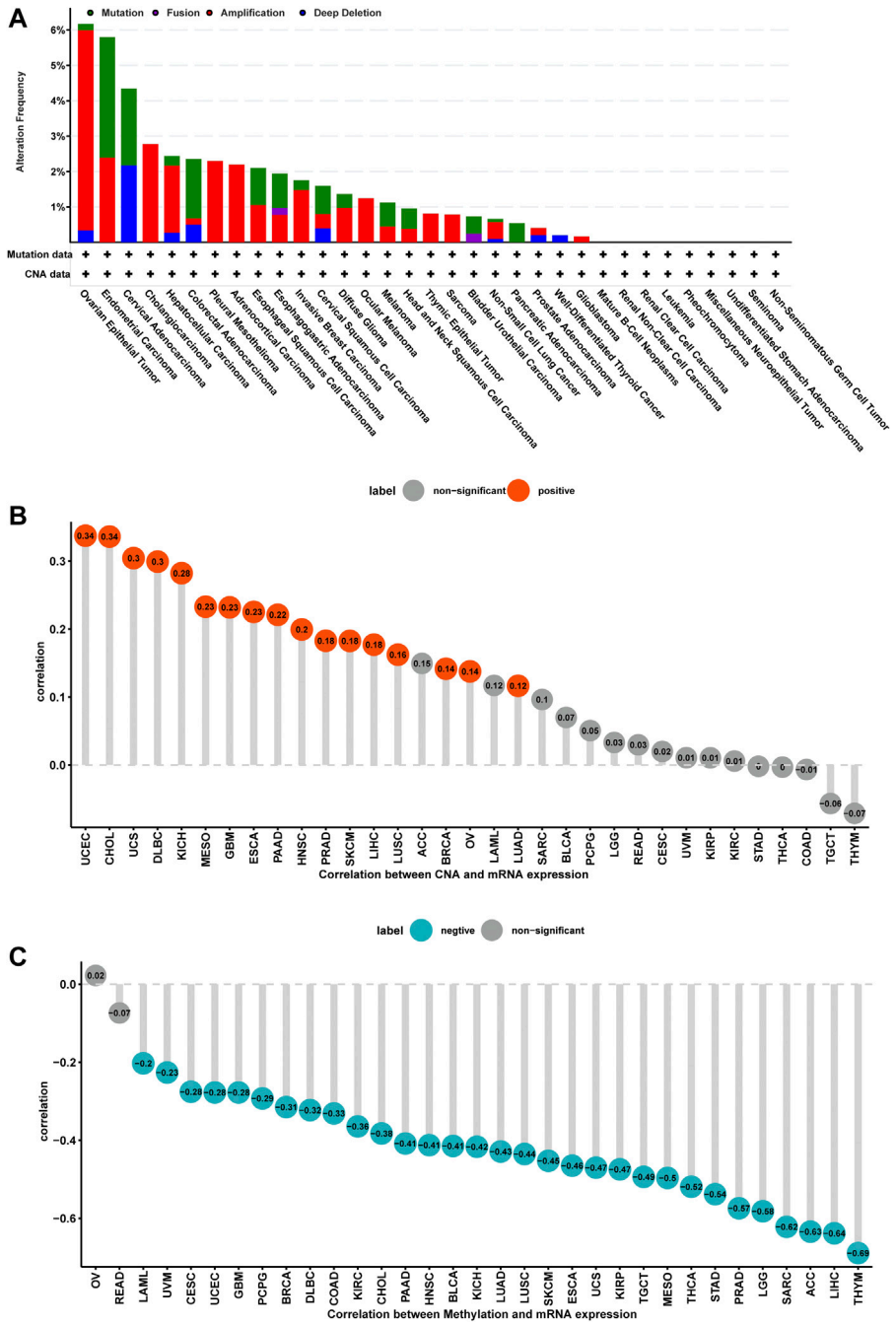

FIGURE 4 | Gene alteration of ISYNA1. **(A)** The mutation and CNA status of ISYNA1 in TCGA pan-cancer. **(B)** The correlation between ISYNA1 expression and CNA. **(C)** The correlation between ISYNA1 expression and DNA methylation.

following the manufacturer's instructions. Quantitative PCR (qPCR) analysis of samples was performed using EvoM-MLV RT Kit, AG11711 (Accurate Biology, China) following the manufacturer's instructions. ACTB1 was used as the internal control. The primers were designed as follows:

ACTB1:
Forward 5′-GGCATTCACGAGACCACCTAC-3′.
Reverse 5′-CGACATGACGTTGTTGGCATAC-3′.
ISYNA1:
Forward 5′-CAGCACCGGGTTTTTGTGG-3′.
Reverse 5′-TCCTTAGAGCGGAACTGCAAT-3′.
CD274 (PDL1):
Forward 5′-TGGCATTTGCTGAACGCATTT-3′.
Reverse 5′- TGCAGCCAGGTCTAATTGTTTT-3′.

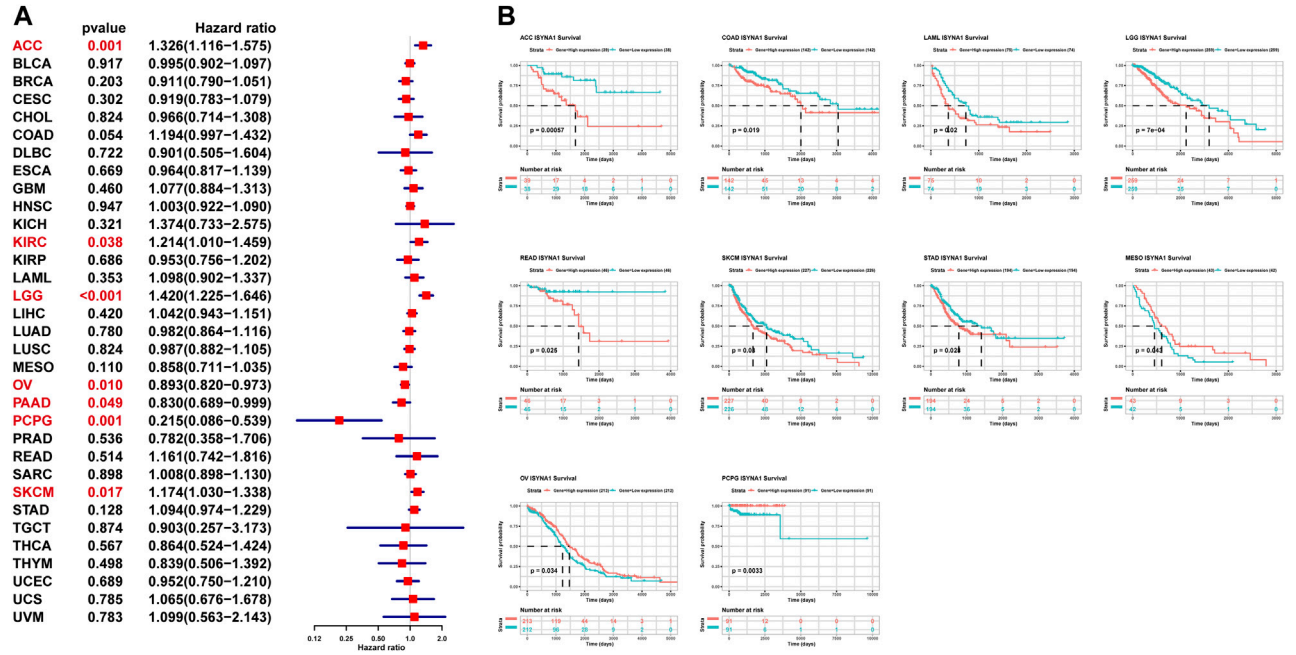

FIGURE 5 | Prognostic value of ISYNA1. **(A)** The UniCox OS analysis of ISYNA1 in TCGA pan-cancer. Red represents significant results ($p < 0.05$). **(B)** Kaplan–Meier OS analysis of ISYNA1 in TCGA pan-cancer in indicated tumor types.

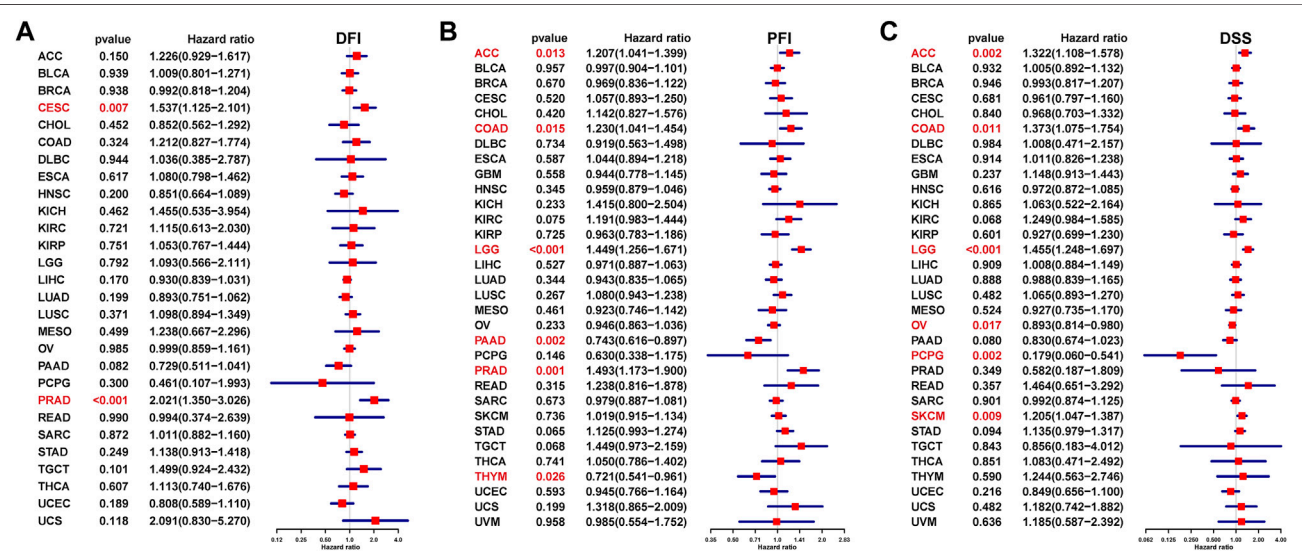

FIGURE 6 | Prognostic value of ISYNA1 in predicting DFI, PFI, and DSS. **(A)** The UniCox results of DFI were shown using forest plots. **(B)** The UniCox results of PFI were shown using forest plots. **(C)** The UniCox results of DSS were shown using forest plots.

Data Collection

The expression profiles and clinical information of the Cancer Genome Atlas (TCGA) and Cancer Cell Line Encyclopedia (CCLE) were downloaded from the UCSC Xena (https://xenabrowser.net/datapages/) database. The infiltration level of different immune cells in TCGA was downloaded from the ImmuCellAI database (http://bioinfo.life.hust.edu.cn/ImmuCellAI#!/).

Online Website

The pan-cancer expression of ISYNA1 in TCGA cohort was performed using the TIMER2 database (http://timer.comp-genomics.org/). The cBioPortal database was used to analyze the CNA and mutation status of ISYNA1. The correlation between ISYNA1 expression and infiltration level CAFs/TAMs was performed using the TIMER2 database.

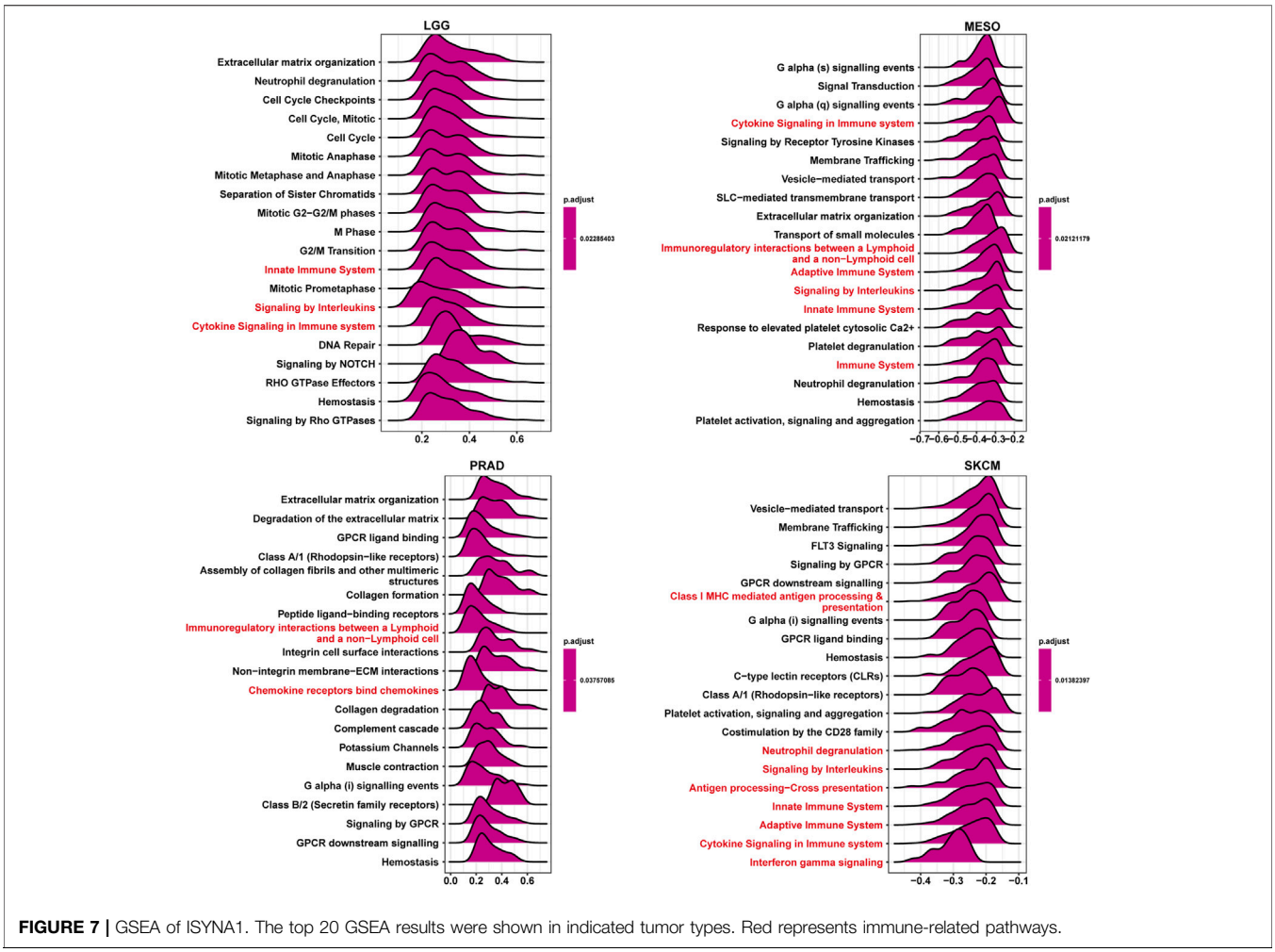

FIGURE 7 | GSEA of ISYNA1. The top 20 GSEA results were shown in indicated tumor types. Red represents immune-related pathways.

Correlation and Gene Set Enrichment Analysis

The association between the ISYNA1 expression level and all mRNAs was analyzed using TCGA RNAseq data, and Pearson's correlation coefficient was calculated. The mRNAs correlated with ISYNA1 ($p < 0.05$) were ranked and subjected to the GSEA. The analysis was conducted using the R package "clusterProfiler."

Relationship Between ISYNA1 Expression and TME

The TME gene sets were downloaded, and the scores of each gene set in TCGA pan-cancer were calculated using the method from this published study (Zeng et al., 2019).

Correlation Between ISYNA1 Expression and Immune Cell Infiltration

First, the correlation between ISYNA1 expression and infiltration level CAFs/TAMs was performed using the TIMER2 database. Second, we downloaded the immune cell infiltration data of TCGA pan-cancer from the ImmuCellAI database and performed a correlation analysis between ISYNA1 expression and infiltration levels of 24 immune cells.

Correlation Between ISYNA1 Expression and Half Maximal Inhibitory Concentration (IC50) of Anticancer Drugs

We downloaded the RNA expression profiles of cancer cell lines and IC50 information of 192 anticancer drugs from the GDSC database (https://www.cancerrxgene.org/). Then, we calculated the association between ISYNA1 expression and IC50 of anticancer drugs.

RESULTS

Expression of ISYNA1 in Pan-Cancer

First, we investigated ISYNA1 expression using the TIMER2 database. We found that ISYNA1 was highly expressed in 12 among 33 cancers types, including BLCA, BRCA, CHOL, COAD, ESCA, GBM, HNSC, LIHC, LUAD, LUSC, STAD, and THCA. In addition, ISYNA1 was lowly expressed in only four cancer types, such as KICH, KIRC, KIRP, and PRAD (**Figure 1A**). To evaluate

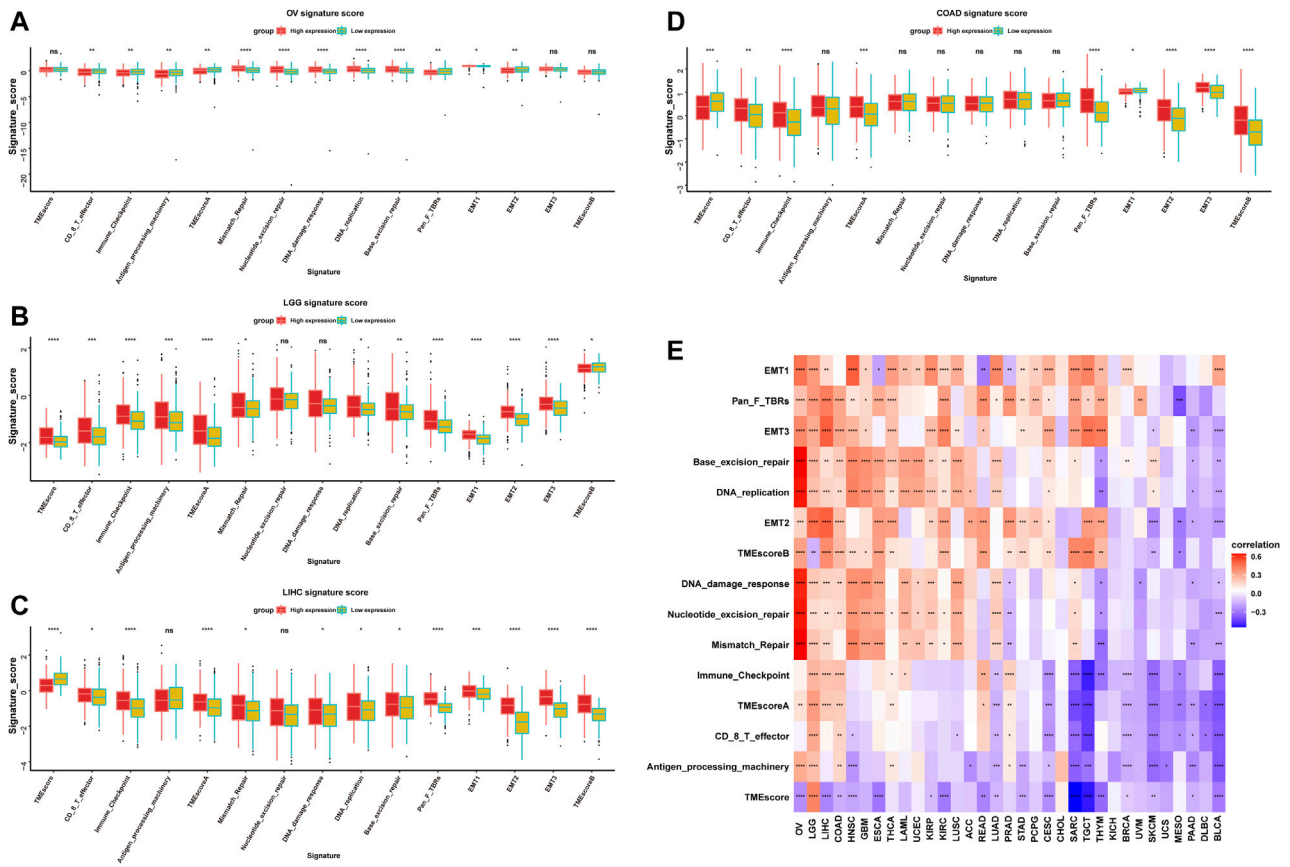

FIGURE 8 | TME-related pathway analysis. **(A–D)** The scores of TME-related pathways in high- and low-ISYNA1 groups in indicated tumor types. **(E)** The correlation analysis between ISYNA1 expression and TME-related pathways in pan-cancer. Red represents positive correlation, and blue represents negative correlation. The darker the color, the stronger the correlation.

the expression of ISYNA1 only in tumor tissues from TCGA cohort, we found that ISYNA1 expression was highest in tumor tissues of UCS and lowest in tumor tissues of COAD compared with other tumor tissues (**Figure 1B**). In normal tissues from GTEx database, we found that ISYNA1 expression was highest in testis tissue and lowest in blood (**Figure 1C**).

Regarding the paired tumor and adjacent normal tissues in TCGA cohort, we observed that ISYNA1 was over-expressed in 10 cancers, such as BRCA, CHOL, ESCA, HNSC, LIHC, LUAD, LUSC, STAD, THCA, and BLCA (**Figures 2A–J**). In addition, ISYNA1 was lowly expressed in KICH, KIRC, KIRP, and PRAD (**Figures 2K–N**), which was consistent with the above results. In addition, we verified the expression of ISYNA1 by qRT-PCR in COAD, READ, and LIHC. Results revealed that ISYNA1 was highly expressed in COAD and READ (**Figures 2O–Q**).

We further investigated ISYNA1 expression at different tumor stages. The results revealed that ISYNA1 expression was different in the various tumor stages in COAD, ESCA, HNSC, LIHC, READ, STAD, THCA, and ACC (**Figures 3A–H**).

Gene Alteration of ISYNA1 in Pan-Cancer

Mutation, DNA methylation, and CNA are main factors that influence gene expression. Thus, we assessed the mutations, DNA methylation, and CNA of ISYNA1. We revealed that the highest alteration frequency of ISYNA1 (>6%) was observed in OV patients, in which the "amplification" was the primary type (**Figure 4A**). For the correlation between ISYNA1 and CNA, we found that ISYNA1 expression was positively correlated with CNA in 17 among 33 cancers types (**Figure 4B**), indicating that the high CNA was one of the main causes of high ISYNA1 expression in pan-cancer, except in COAD. In addition, we also found that the promoter methylation level of ISYNA1 was negatively correlated with ISYNA1 expression in 31 among 33 cancers types (**Figure 4C**), including COAD ($r = -0.33$), indicating that the promoter methylation level of ISYNA1 mainly affects ISYNA1 mRNA expression in OCAD.

Prognostic Value of ISYNA1

To assess the prognostic value of ISYNA1 in pan-cancer, the univariate Cox regression analysis (UniCox) and Kaplan–Meier survival analysis were conducted. Results of the UniCox indicated that ISYNA1 acts as a risk factor for overall survival (OS) of patients with ACC, KIRC, LGG, and SKCM, and acts as a protective factor for OS in patients with OV, PAAD, and PCPG (**Figure 5A**). The Kaplan–Meier OS analysis proved

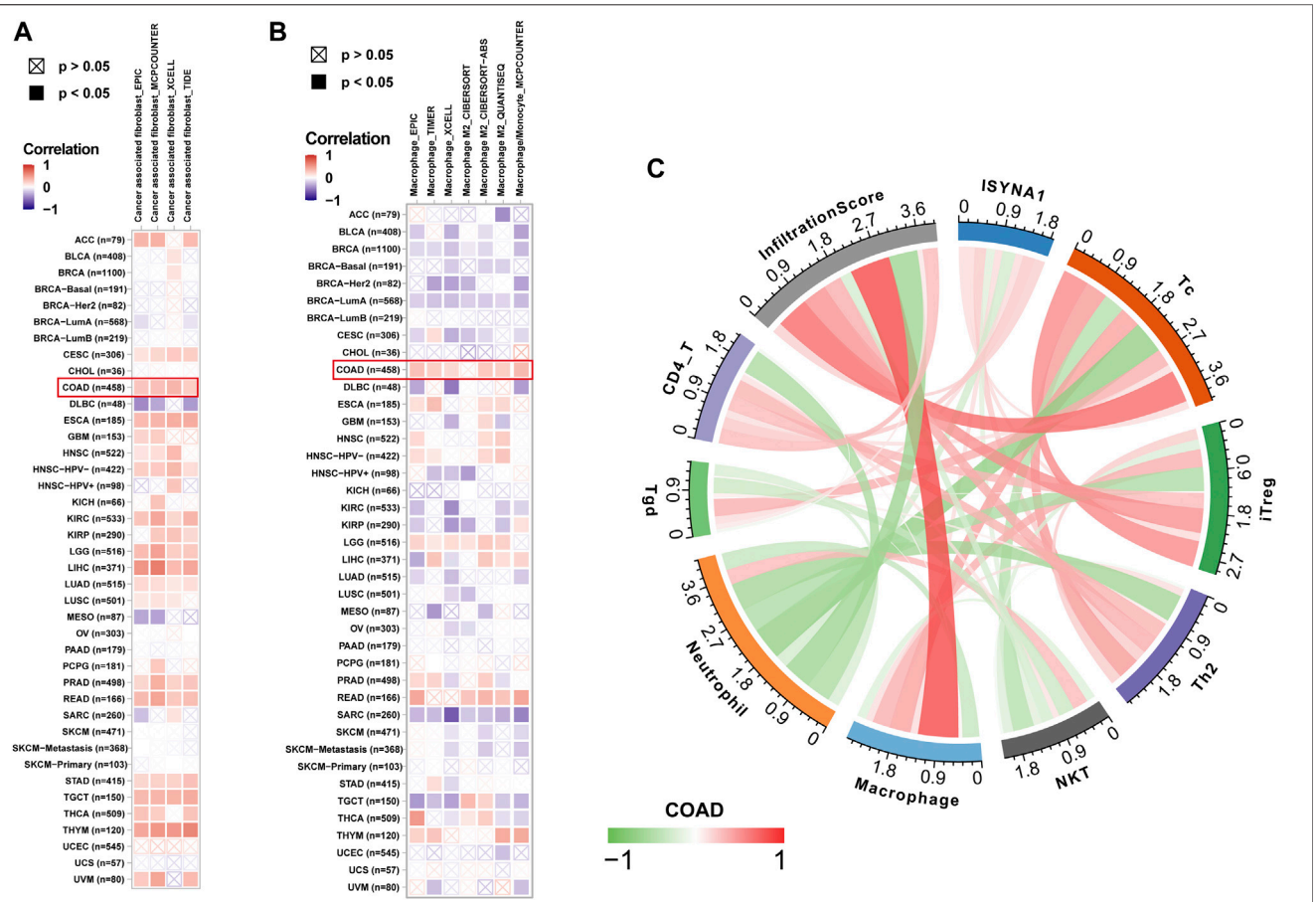

FIGURE 9 | Immune infiltration analysis. **(A)** The relationship between ISYNA1 expression and infiltration levels of CAFs in pan-cancer using the TIMER2 database. **(B)** The relationship between ISYNA1 expression and infiltration levels of TAMs in pan-cancer using the TIMER2 database. **(C)** The correlation between ISYNA1 expression and infiltration levels of 22 immune cells using data from the ImmuCellAI database. Significant results were shown (correlation $p < 0.05$).

that the elevated expression of ISYNA1 predicted worse OS of patients with ACC, COAD, LAML, LGG, READ, SKCM, and STAD. In contrast, a high ISYNA1 expression predicted longer OS time in patients with MESO, OV, and PCPG (**Figure 5B**).

We also assessed the prognostic value of ISYNA1 in predicting disease-free interval (DFI), progression-free interval (PFI), and disease-specific survival (DSS) of tumor patients using univariate Cox regression analysis. For DFI, a high ISYNA1 expression predicted shorter DFI times in patients with CESC and PRAD (**Figure 6A**). For PFI, a high ISYNA1 expression predicted shorter PFI times in patients with ACC, COAD, LGG, and PRAD, and longer PFI time in patients with PAAD and THYM (**Figure 6B**). For DSS, a high ISYNA1 expression predicted a worse DSS status in patients with ACC, COAD, LGG, and SKCM, and a better DSS status in patients with OV and PCPG (**Figure 6C**).

GSEA of ISYNA1

To explore the potential pathways for the potential involvement of ISYNA1 in tumor progression, we further conducted the GSEA of ISYNA1 using TCGA pan-cancer data. Interestingly, we found common GSEA results for various tumor types. The immune regulation relevant pathways, such as "adaptive immune system," "innate immune system," "signaling by interleukins," and "cytokine signaling in immune system," were simultaneously enriched in LGG, MESO, PRAD, and SKCM (**Figure 7**).

Relationship Between ISYNA1 Expression and Immune Cell Infiltration

We further analyzed the role of ISYNA1 in TME. Through difference analysis and correlation analysis, we found that ISYNA1 was positively correlated with TME-related pathways mainly in OV, LGG, LIHC, and COAD (**Figures 8A–E**). For example, the scores of immune system-related pathways and tumor stroma-related pathways were higher in the high-ISYNA1 expression group in COAD (**Figure 8E**). By analyzing the association between ISYNA1 expression and immune cell infiltration using the TIMER2 database, we found that ISYNA1 expression was positively associated with the infiltration of CAFs and TAMs in COAD (**Figures 9A,B**). Using immune cell infiltration data from the ImmuCellAI database, we found that ISYNA1 expression was positively correlated with immunosuppressive cells, such as TAMs and iTreg

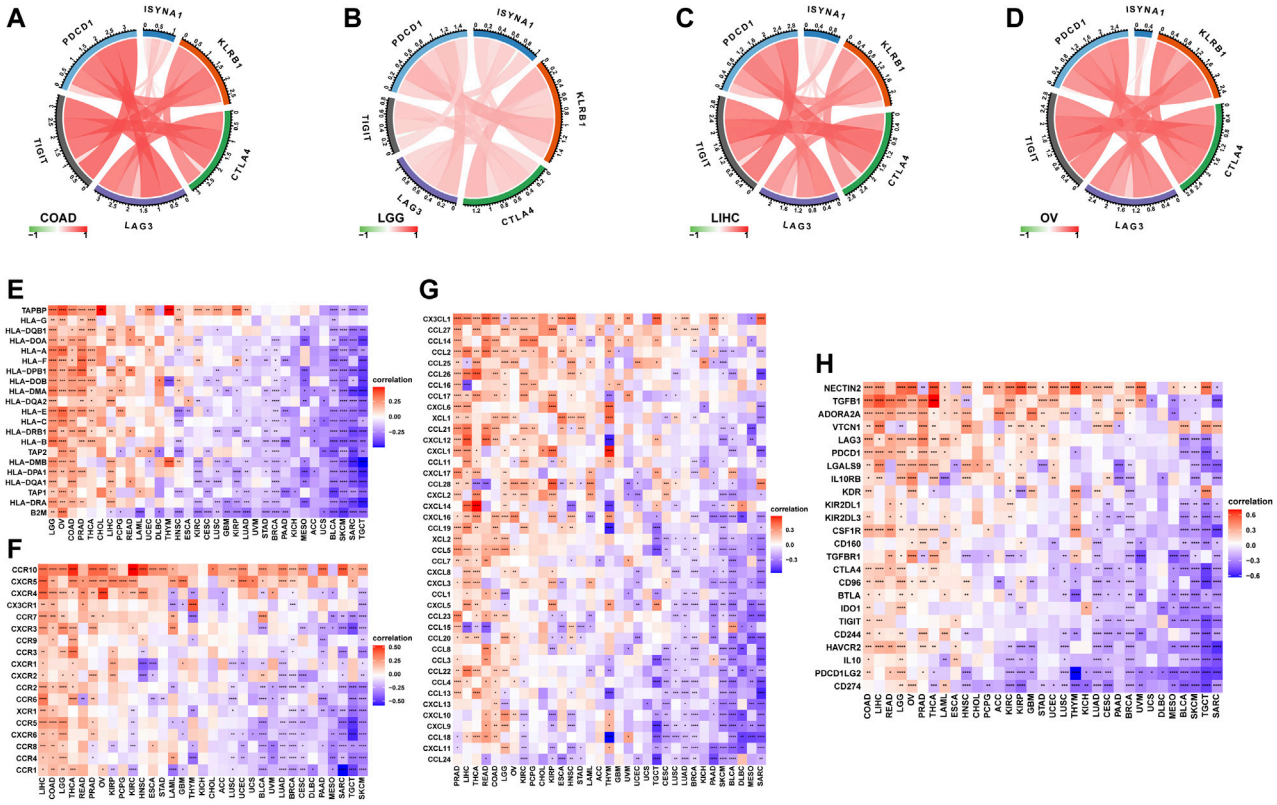

FIGURE 10 | Correlation between ISYNA1 expression and immunosuppressive genes. **(A–D)** The correlation between ISYNA1 expression and immune checkpoints. Red lines represent positive correlation, and blue lines represent negative correlation. The darker the color, the stronger the correlation. **(E)** The correlation between ISYNA1 expression and MHC genes in pan-cancer. **(F)** The correlation between ISYNA1 expression and chemokine receptors in pan-cancer. **(G)** The correlation between ISYNA1 expression and chemokines in pan-cancer. **(H)** The correlation between ISYNA1 expression and immunosuppressive genes in pan-cancer. Red represents positive correlation, and blue represents negative correlation. The darker the color, the stronger the correlation. $^{*}p < 0.05$, $^{**}p < 0.01$, $^{***}p < 0.001$, $^{****}p < 0.0001$.

(**Figure 9C**). These results indicated that high ISYNA1 expression may contribute to the tumor immunosuppressive microenvironment. To further explore the relationship between ISYNA1 and TIME, we conducted a correlation analysis among immunosuppressive genes, immune checkpoints, and ISYNA1. The results showed that ISYNA1 expression was positively correlated with immune checkpoints, such as PDCD1, TIGIT, LAG3, CTLA4, and KLRB1, in COAD, LGG, LIHC, and OV (**Figures 10A–D**). We also observed that ISYNA1 was positively correlated with MHC genes (**Figure 10E**), chemokines and chemokine receptors (**Figures 10F,G**), and immunosuppressive genes (**Figure 10H**) in COAD. Interestingly, there was no correlation between ISYNA1 and CD274 (PD-L1) expression, which was validated by qRT-PCR in COAD, READ, and LIHC (**Supplementary Figures S1A–C**). These results revealed that ISYNA1 expression predicted the immunosuppressive microenvironment.

Correlation Analysis of ISYNA1 Expression and Drug Response

We downloaded half-inhibitory concentration (IC50) values of 192 drugs and gene expression profiles of 809 cell lines from the Genomics of Drug Sensitivity in Cancer database (GDSC: https://www.cancerrxgene.org/) and analyzed Spearman's correlation between ISYNA1 expression and IC50 values. Among 192 anticancer drugs, the IC50 values of 26 drugs were positively correlated with ISYNA1 expression, while only the IC50 values of three drugs were negatively correlated with ISYNA1 expression (**Supplementary Table S1**, **Figures 11A–D**). These results revealed that patients with high ISYNA1 expression were predicted to be resistant to most anticancer drugs.

DISCUSSION

COAD is one of the most common cancers and is a fatal factor in the health of humans globally (Simon, 2016; Thanikachalam and Khan, 2019). A body of studies have shown that the reconstruction of TIME by colorectal cancer cells plays a key role in the progression of COAD, weakening the response of patients with COAD to the treatment and leading to worse survival status (Becht et al., 2016; Franke et al., 2019; Ganesh et al., 2019; Lichtenstern et al., 2020). Thus, the identification of essential genes that could affect TIME in COAD is urgently needed.

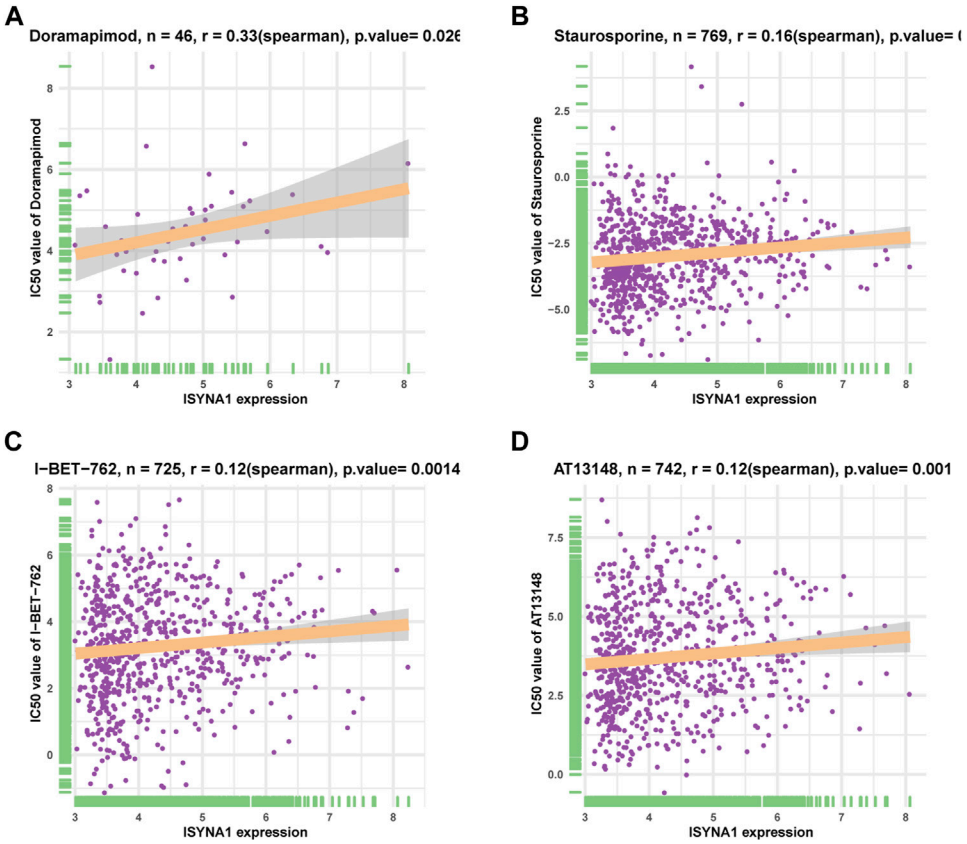

FIGURE 11 | Correlation analysis of ISYNA1 expression and drug response. **(A–D)** The correlation between ISYNA1 expression and IC50 of indicated anticancer drugs.

ISYNA1 encodes the rate-limiting enzyme inositol-3-phosphate synthase. Until now, there are few studies on ISYNA1 in tumor research. It was reported that ISYNA1 functions as an oncogene in several tumors (Azimi et al., 2014). For example, ISYNA1 was observed as highly expressed in BLCA, regulating the proliferation and apoptosis of BLCA cells (Guo et al., 2019). In pancreatic cancer, the ISYNA1-p21/ZEB-1 pathway could contribute to tumor progression (Zhou L et al., 2020).

In our study, we first assessed the expression of ISYNA1 and found the elevated ISYNA1 expression in 12 among 33 cancers types, including BLCA, BRCA, CHOL, COAD, ESCA, GBM, HNSC, LIHC, LUAD, LUSC, STAD, and THCA. In addition, decreased ISYNA1 expression was observed in four cancer types, such as KICH, KIRC, KIRP, and PRAD. To determine the prognostic value of ISYNA1, we conducted the UniCox and Kaplan–Meier survival analysis in TCGA cohort. Results of the UniCox indicated that ISYNA1 acts as a risk factor for OS in patients with ACC, KIRC, LGG, and SKCM and acts as a protective factor for OS in patients with OV, PAAD, and PCPG. The Kaplan–Meier OS analysis revealed that an elevated ISYNA1 expression indicated worse survival of patients with ACC, COAD, LAML, LGG, READ, SKCM, and STAD. In contrast, a high ISYNA1 expression predicted longer OS time in patients with MESO, OV, and PCPG.

GSEA results predicted the immune regulatory function of ISYNA1 in COAD. Through the analysis of the correlation between ISYNA1 expression and TME, we found that the scores of immune system-related pathways and tumor stroma-related pathways were higher in the high-ISYNA1 expression group in COAD. Furthermore, the association among immune cell infiltration, stroma cell infiltration, and ISYNA1 expression was analyzed. Results revealed that the infiltration levels of TAMs and CAFs were positively correlated with ISYNA1 expression in COAD. We further validated the results using immune cell infiltration data from the ImmuCellAI database. The results also revealed that ISYNA1 expression was positively associated with the infiltration of TAMs in COAD. Moreover, we found that ISYNA1 expression was positively correlated with iTreg cells in COAD. Through the correlation analysis between ISYNA1 expression and immunosuppressive genes, we found that ISYNA1 expression was positively correlated with most immunosuppressive genes and immune checkpoints in COAD, such as TGFBR1, IL10, IL10RB, CTLA4, CD274, PDCD1, TIGIT, and LAG3.

In conclusion, our findings revealed that ISYNA1 is an oncogene and a prognostic marker in COAD. High ISYNA1 expression may contribute to the immunosuppressive

microenvironment in COAD. Targeting ISYNA1 may be a potential method for COAD therapy.

DATA AVAILABILITY STATEMENT

The datasets presented in this study can be found in online repositories. The names of the repository/repositories and accession number(s) can be found in the article/ **Supplementary Material**.

AUTHOR CONTRIBUTIONS

ZJ contributed to conceptualization, methodology, software, formal analysis, writing–original draft, and visualization. XW contributed to formal analysis, software, visualization, investigation, and validation. All authors contributed to the article and approved the submitted version.

FUNDING

This work was supported by the Natural Science Foundation of Hunan Province, China (grant no: 2020JJ4880) and the National Special Program for International Cooperation, China (grant no: 2013DFA32150)

SUPPLEMENTARY MATERIAL

The Supplementary Material for this article can be found online at: https://www.frontiersin.org/articles/10.3389/fcell.2022.792564/full#supplementary-material

REFERENCES

Azimi, A., Pernemalm, M., Frostvik Stolt, M., Hansson, J., Lehtiö, J., Egyházi Brage, S., et al. (2014). Proteomics Analysis of Melanoma Metastases: Association between S100a13 Expression and Chemotherapy Resistance. *Br. J. Cancer* 110 (10), 2489–2495. doi:10.1038/bjc.2014.169

Becht, E., de Reyniès, A., Giraldo, N. A., Pilati, C., Buttard, B., Lacroix, L., et al. (2016). Immune and Stromal Classification of Colorectal Cancer Is Associated with Molecular Subtypes and Relevant for Precision Immunotherapy. *Clin. Cancer Res.* 22 (16), 4057–4066. doi:10.1158/1078-0432.CCR-15-2879

Choi, J., Gyamfi, J., Jang, H., and Koo, J. S. (2018). The Role of Tumor-Associated Macrophage in Breast Cancer Biology. *Histol. Histopathol.* 33 (2), 133–145. doi:10.14670/HH-11-916

Deepak, K. G. K., Vempati, R., Nagaraju, G. P., Dasari, V. R., S., N., Rao, D. N., et al. (2020). Tumor Microenvironment: Challenges and Opportunities in Targeting Metastasis of Triple Negative Breast Cancer. *Pharmacol. Res.* 153, 104683. doi:10.1016/j.phrs.2020.104683

Franke, A. J., Skelton, W. P., Starr, J. S., Parekh, H., Lee, J. J., Overman, M. J., et al. (2019). Immunotherapy for Colorectal Cancer: a Review of Current and Novel Therapeutic Approaches. *J. Natl. Cancer Inst.* 111 (11), 1131–1141. doi:10.1093/jnci/djz093

Ganesh, K., Stadler, Z. K., Cercek, A., Mendelsohn, R. B., Shia, J., Segal, N. H., et al. (2019). Immunotherapy in Colorectal Cancer: Rationale, Challenges and Potential. *Nat. Rev. Gastroenterol. Hepatol.* 16 (6), 361–375. doi:10.1038/s41575-019-0126-x

Guo, X., Li, H.-H., Hu, J., Duan, Y.-X., Ren, W.-G., Guo, Q., et al. (2019). Isyna1 Is Overexpressed in Bladder Carcinoma and Regulates Cell Proliferation and Apoptosis. *Biochem. Biophys. Res. Commun.* 519 (2), 246–252. doi:10.1016/j.bbrc.2019.08.129

Lichtenstern, C. R., Ngu, R. K., Shalapour, S., and Karin, M. (2020). Immunotherapy, Inflammation and Colorectal Cancer. *Cells* 9 (3), 618. doi:10.3390/cells9030618

Lin, A., Zhang, J., and Luo, P. (2020). Crosstalk between the Msi Status and Tumor Microenvironment in Colorectal Cancer. *Front. Immunol.* 11, 2039. doi:10.3389/fimmu.2020.02039

Liu, C., Zhou, X., Zeng, H., Wu, D., and Liu, L. (2021). Hilpda Is a Prognostic Biomarker and Correlates with Macrophage Infiltration in Pan-Cancer. *Front. Oncol.* 11, 597860. doi:10.3389/fonc.2021.597860

Qiu, S.-Q., Waaijer, S. J. H., Zwager, M. C., de Vries, E. G. E., van der Vegt, B., and Schröder, C. P. (2018). Tumor-associated Macrophages in Breast Cancer: Innocent Bystander or Important Player? *Cancer Treat. Rev.* 70, 178–189. doi:10.1016/j.ctrv.2018.08.010

Balchen, V., and Simon, K. (2016). Colorectal Cancer Development and Advances in Screening. *Clin. Interv. Aging* 11, 967–976. doi:10.2147/CIA.S109285

Thanikachalam, K., and Khan, G. (2019). Colorectal Cancer and Nutrition. *Nutrients* 11 (1), 164. doi:10.3390/nu11010164

Wei, S., Chen, J., Huang, Y., Sun, Q., Wang, H., Liang, X., et al. (2020). Identification of Hub Genes and Construction of Transcriptional Regulatory Network for the Progression of colon Adenocarcinoma Hub Genes and Tf Regulatory Network of colon Adenocarcinoma. *J. Cel. Physiol.* 235 (3), 2037–2048. doi:10.1002/jcp.29067

Zeng, D., Li, M., Zhou, R., Zhang, J., Sun, H., Shi, M., et al. (2019). Tumor Microenvironment Characterization in Gastric Cancer Identifies Prognostic and Immunotherapeutically Relevant Gene Signatures. *Cancer Immunol. Res.* 7 (5), 737–750. doi:10.1158/2326-6066.CIR-18-0436

Zhou L, L., Sheng, W., Jia, C., Shi, X., Cao, R., Wang, G., et al. (2020). Musashi2 Promotes the Progression of Pancreatic Cancer through a Novel ISYNA1-p21/ZEB-1 Pathway. *J. Cel. Mol. Med.* 24 (18), 10560–10572. doi:10.1111/jcmm.15676

Zhou W, W., Zhang, S., Li, H.-b., Cai, Z., Tang, S., Chen, L.-x., et al. (2020). Development of Prognostic Indicator Based on Autophagy-Related Lncrna Analysis in colon Adenocarcinoma. *Biomed. Res. Int.* 2020, 1–14. doi:10.1155/2020/9807918

Conflict of Interest: The authors declare that the research was conducted in the absence of any commercial or financial relationships that could be construed as a potential conflict of interest.

Publisher's Note: All claims expressed in this article are solely those of the authors and do not necessarily represent those of their affiliated organizations, or those of the publisher, the editors, and the reviewers. Any product that may be evaluated in this article, or claim that may be made by its manufacturer, is not guaranteed or endorsed by the publisher.

GLOSSARY

ACC adrenocortical carcinoma
BLCA bladder urothelial carcinoma
BRCA breast invasive carcinoma
CESC cervical squamous cell carcinoma and endocervical adenocarcinoma
CHOL cholangiocarcinoma
COAD colon adenocarcinoma
DLBC lymphoid neoplasm diffuse large b-cell lymphoma
ESCA esophageal carcinoma
GBM glioblastoma multiforme
HNSC head and neck squamous cell carcinoma
KICH kidney chromophobe
KIRC kidney renal clear cell carcinoma
KIRP kidney renal papillary cell carcinoma
LAML acute myeloid leukemia
LGG lower-grade glioma
LIHC liver hepatocellular carcinoma
LUAD lung adenocarcinoma
LUSC lung squamous cell carcinoma
MESO mesothelioma
OV ovarian serous cystadenocarcinoma
PAAD pancreatic adenocarcinoma
PCPG pheochromocytoma and paraganglioma
PRAD prostate adenocarcinoma
READ rectum adenocarcinoma
SARC sarcoma
SKCM skin cutaneous melanoma
STAD stomach adenocarcinoma
TGCT testicular germ cell tumor
THCA thyroid carcinoma
THYM thymoma
UCEC uterine corpus endometrial carcinoma
UCS uterine carcinosarcoma
UVM uveal melanoma

frontiers in Cell and Developmental Biology

ORIGINAL RESEARCH
published: 18 February 2022
doi: 10.3389/fcell.2022.793425

Development and Validation of a Novel Histone Acetylation-Related Gene Signature for Predicting the Prognosis of Ovarian Cancer

Qinjin Dai[1] *and Ying Ye*[2]*

[1]Guangzhou Women and Children's Medical Center, Guangzhou Medical University, Guangzhou, China, [2]Department of Cardiothoracic Surgery, The Second Affiliated Hospital of Chongqing Medical University, Chongqing, China

Histone acetylation is one of the most common epigenetic modifications, which plays an important role in tumorigenesis. However, the prognostic role of histone acetylation-regulators in ovarian cancer (OC) remains little known. We compared the expression levels of 40 histone acetylation-related genes between 379 OC samples and 88 normal ovarian tissues and identified 37 differently expressed genes (DEGs). We further explored the prognostic roles of these DEGs, and 8 genes were found to be correlated with overall survival ($p < 0.1$). In the training stage, an 8 gene-based signature was conducted by the least absolute shrinkage and selector operator (LASSO) Cox regression. Patients in the training cohort were divided into two risk subgroups according to the risk score calculated by the 8-gene signature, and a notable difference of OS was found between the two subgroups ($p < 0.001$). The 8-gene risk model was then verified to have a well predictive role on OS in the external validation cohort. Combined with the clinical characteristics, the risk score was proved to be an independent risk factor for OS. In conclusion, the histone acetylation-based gene signature has a well predictive effect on the prognosis of OC and can potentially be applied for clinical treatments.

Keywords: ovarian cancer, histone acetylation, gene signature, overall survival, predictive model

OPEN ACCESS

Edited by:
Ângela Sousa,
University of Beira Interior, Portugal

Reviewed by:
Kazim Yalcin Arga,
Marmara University, Turkey
Shanshan Li,
Hubei University, China

***Correspondence:**
Ying Ye
yey1227@hospital.cqmu.edu.cn

Specialty section:
This article was submitted to Epigenomics and Epigenetics, a section of the journal Frontiers in Cell and Developmental Biology

Received: *12 October 2021*
Accepted: *26 January 2022*
Published: *18 February 2022*

Citation:
Dai Q and Ye Y (2022) Development and Validation of a Novel Histone Acetylation-Related Gene Signature for Predicting the Prognosis of Ovarian Cancer. Front. Cell Dev. Biol. 10:793425. doi: 10.3389/fcell.2022.793425

INTRODUCTION

Ovarian cancer (OC) owns the highest mortality rate among all gynecological tumors (Kuroki and Guntupalli, 2020). Generally, most of the OC patients were at an advanced stage when being diagnosed, due to the lack of typical clinical symptoms and available screening biomarkers in the early stages (Krzystyniak et al., 2016). In the treatment phase, chemotherapy resistance is easy to develop, causing a high rate of recurrence (Christie and Bowtell, 2017). In spite of the therapeutic regimens that have been rapidly developed, the 5-years survival rate of OC has been poorly improved in decades. As the limited treatment methods, researchers have been searching for reliable markers to predict the prognosis of ovarian cancer and the therapeutic targets. Recently, human epididymis protein 4 (HE4) has been found to have a better predict role on recurrence in comparison to CA-125

Abbreviations: OC, ovarian cancer; LASSO, least absolute shrinkage and selection operator; TCGA, The Cancer Genome Atlas database; GEO, gene expression omnibus; GTEx, genotype-tissue expression; GO, gene ontology; KEGG, kyoto encyclopedia of genes and genomes; DEGs, differentially expressed genes; PCA, principal component analysis; t-SNE, t-distributed stochastic neighbor embedding.

(Scaletta et al., 2017). However, in clinical practice, either CA-125 or HE4 can only be used as a monitoring/predictive indicator while not as a therapeutic target; In addition, single-gene predictive models tend to have low specificities. Conversely, predictive models based on multiple genes often showed better predicting efficacies. With the increasing data of next-generation sequencing (NGS), a few systematic predictive models based on multiple genes have been established and revealed favorable accuracy. In recent years, a growing number of studies have found that multi-targeted combination therapies can help to improve the prognosis of tumor patients, thus it remains essential to identify new potential anti-tumor targets.

Epigenetic modifications are genetic modifications that cause heritable phenotypic changes in the expression of a gene without altering its DNA sequence, which has been proved to regulate the expression of tumor-related genes, and could be potential therapeutic targets (Cao and Yan, 2020). In eukaryotes, histones are bound to DNA to form chromatin, and the terminal amino acid residues can be covalently modified by methylation, acetylation, phosphorylation, ubiquitination, and adenosine diphosphate (ADP) glycosylation (Bennett and Licht, 2018). Among them, acetylation modification of the N-terminus of histone H3 and H4 lysine residues is the main histone modification associated with transcription, chromatin remodeling, and DNA expression and repair. Histone acetylation is a reversible dynamic equilibrium process, mediated by histone acetyltransferases (HAT) and histone deacetylases (HDAC) (Kaypee et al., 2016). In the presence of HAT, the acetyl is transferred to the N-terminal lysine residue of the histone, which counteracts the positive charge of the residue and allows the DNA conformation to unfold, resulting in the relaxation of the nucleosome structure and the activation of the transcription of the specific genes, whereas the function of HDAC is the opposite (Shen et al., 2015). HATs have been proved to be involved in the transformation of malignant tumors, not as direct tumor suppressors or oncogenes, but as acetyltransferases and transcriptional co-activators regulating the expression of key genes and proteins (Ell and Kang, 2013). HDACs include several family members and are currently one of the most studied anti-cancer targets. By inhibiting HDACs' activity and promoting histone acetylation, histone deacetylase inhibitors (HDACis) can inhibit cancer cell growth, induce differentiation and apoptosis (Autin et al., 2019). Normally, HATs and HDACs dynamically regulate the processes in the histone acetylation, while the unbalance of acetylation level could contribute to cancer development. The HAT/HDAC inhibitors can affect gene expression by altering the acetylation level of histones in specific regions of chromatin, making them a new class of antitumor drugs with promising development and application, therefore, exploring the prognostic value of these histone deacetylase-related regulators is essential for the development of highly selective targeted drugs for a specific type of cancer.

However, most studies preferred to explore one single histone acetylation site or the specific role of HDACs (Zhou et al., 2018), ignoring the importance of HATs and sirtuin family proteins. For this reason, we performed a study to make a comprehensive understanding of the expression levels of the histone acetylation-related genes between OC and normal ovarian tissues and to explore the prognostic value of these regulators.

MATERIALS AND METHODS

Data Sources

The transcriptome sequencing data of 379 OC patients and the corresponding clinical information were acquired from The Cancer Genome Atlas (TCGA) database (downloaded at https://portal.gdc.cancer.gov/). As lacking data of normal group, we combined the Genotype-Tissue Expression (GTEx) database to get the RNA sequencing data of ovarian tissue from 88 normal women (downloaded at https://xenabrowser.net). The GTEx Research Consortium study collected more than 7,000 autopsy samples from 449 humans, and the 88 normal ovarian tissues were all obtained from previously healthy human donors. A validation cohort with the RNA-seq data and the clinical features of 380 OC patients were obtained from the Gene Expression Omnibus (GEO) database (https://www.ncbi.nlm.nih.gov/geo/, GSE140082). The read count values in each database were all downloaded as fragments per kilobase million (FPKM), and to minimize the batch effects, we applied the "Combat" function in the "SVA" R package. Moreover, we employed the "Scale" function to further normalize the expression level of each gene before cross-validations.

The 40 histone acetylation-related regulators were retrieved from a review (Cheng et al., 2019), and they were shown in **Supplementary Table S1**.

Identification of Differently Expressed Genes Between Tumor and Normal Tissues

In this phase, the TCGA and the GTEx datasets were merged, and before comparisons, the expression data were both normalized by FPKM. The DEGs between tumor and normal tissues were identified by applying the "limma" R package (with $FDR < 0.05$). The heatmaps of DEGs were accomplished by using the "heatmap" R package and the spearman correlation analysis was conducted by the "reshape2" R package.

Development and Validation of the Histone Acetylation-Related Gene Signature

To assess the prognostic value of each histone acetylation-related DEG, we combined the gene expression data and the corresponding overall survival time and survival status information of each patient in the TCGA cohort (training cohort). The univariate Cox regression model was utilized to screen the prognosis-related genes. Those genes with $p < 0.1$ were chosen for developing the prognostic signature by applying the Least absolute shrinkage and selection operator (LASSO) cox regression model provided from the "glmnet" R package. Finally, 8 genes with nonzero coefficients were decided by the minimum criteria and the risk score of the gene signature was calculated by the formula: $Risk\,Score = \sum_{i}^{n} X_i \times Y_i$ (X: coefficient of each gene, Y: gene expression level). Referred to the median risk score of the

training cohort, patients were divided into low- and high-risk groups. The Kaplan-Meier analysis was utilized to compare the OS time and survival possibility between the low- and high-risk populations. The principal components analysis (PCA) and the t-distributed stochastic neighbor embedding (t-SNE) were performed based on the 8-gene signature by applying the "ggpolt2" and the "Rtsne" R packages. To assess the sensitivity and the specificity of the risk score, we constructed a 3-years ROC curve by applying the "survival", "survminer" and "timeROC" R packages. In the validation phase, patients from the GEO cohort were also classified into low- and high-risk populations according to the median risk score from the training cohort, and the two populations were compared to validate the gene signature.

Independent Prognostic Analysis

We employed the univariate and multivariable cox regression models (applying the "survival" R package) to assess the independent prognostic value of the risk score. Moreover, clinical features of age and tumor stage were carried out into the regression models to identify whether the risk score was independently correlated with OS. The Nomogram conducted by the "survival" and the "rms" packages were presented to show the results of the predicting model. Besides, the calibration curve was plotted to evaluate the consistency between ideal and actual predicting outcomes.

Functional Enrichment Analysis

Based on the risk score, patients in the TCGA cohort were stratified into low- and high-risk groups. According to the criteria of $|\log_2 FC|>1$, FDR<0.05, the DEGs between the two risk groups were screened out. The Gene Ontology (GO) and the Kyoto Encyclopedia of Genes and Genomes (KEGG) analyses were performed by the "cluster Profiler" R package. Moreover, to make comparisons of the infiltrating scores of immune cells and the activities of immune pathways between low- and high-risk groups, we employed the single-sample gene set enrichment analysis (ssGSEA), which was accomplished by the "gsva" R package. The full workflow diagram is shown in **Figure 1**.

Statistical Analysis

When comparing the gene expression level between two groups, the Student's t-test was utilized, while the Pearson chi-square test was applied to compare the categorical variables. The Kaplan-Meier analysis was used for comparing the OS time and survival possibilities between low- and high-risk subgroups. To assess the independent prognostic value of the risk model, the univariate and multivariable cox regression models were applied. All statistical analyses were completed by the R software (version 4.0.2).

RESULTS

Identification of Differently Expressed Genes Between Normal and Tumor Tissues

We combined the TCGA and the GTEx datasets and got the gene expression data of 379 tumors and 88 normal ovarian tissues. The gene expression levels of the 40-histone acetylation regulators were all compared and finally 37 DEGs were identified. Among them, 25genes were at a lower expression level in the tumor group, while the other 12 genes were enriched. The heatmap for each DEG and the violin plot for all 40 genes were presented in **Figures 2A,B**. To better understand the correlations of these DEGs, a spearman correlation analysis was performed (**Figure 2C**).

Development of a Prognostic Gene Signature in the Training Set

In the training cohort (TCGA cohort), we analyzed the prognostic value of each histone acetylation-related DEG by applying the univariate cox regression model. Totally, 8 survival-related genes were picked out (with the p value < 0.1) for further analysis, they were *SIRT5*, *BRD4*, *OGA*, *SIRT2*, *HDAC4*, *NCOA3*, *HDAC1*, and *HDAC11* (**Figure 3A**). We employed the least absolute shrinkage and selection operator (LASSO) Cox regression model to construct a risk signature and ultimately, 8 genes were all retained according to the optimum λ value (**Figures 3B,C**). According to each gene's coefficient, the risk score was calculated as follow: risk score = -0.173* *SIRT5(exp)* + 0.185**BRD4(exp)* + 0.038**OGA(exp)* + 0.159**SIRT2(exp)* + 0.059**HDAC4(exp)* + 0.014**NCOA3(exp)* + 0.106**HDAC1(exp)* + 0.140**HDAC11(exp)*. To explore the interactions of the 8 genes, a protein-protein interactions (PPI) network was conducted by the Search Tool for the Retrieval of Interacting Genes (STRING), version 11.0 (https://string-db.org/) (**Figure 3D**). According to the median risk score, 187 patients were treated as the low-risk group, while the other 187 were regarded as the high-risk group (5 patients without corresponding survival information were excluded) (**Figure 4A**). The PCA and the t-SNE analysis revealed that patients with different risks were tended to separate in two directions (**Figures 4B,C**). We can observe from the distribution graph that high-risk patients were at lower survival rates and shorter survival times than those with low-risk (**Figure 4D**). Similarly, the Kaplan-Meier curve also demonstrated a notable shorter OS time and lower survival possibility in the high-risk population (HR: 1.75, 95% CI: 1. 32–2.31, $p < 0.001$, **Figure 4E**). The predictive accuracy of the risk score was assessed by the time-dependent receiver operating characteristic (ROC) analysis, and we found the area under the curve (AUC) was 0.711 for 1 year, 0.707 for 2 years, and 0.633 for 3 years (**Figure 4F**).

Validation of the Gene Signature in a Gene Expression Omnibus Cohort

In this phase, 380 OC patients from a GEO cohort were regarded as the validation set. By applying the median risk score of the training cohort, 199 patients were treated as the low-risk group, while the other 181 were at high risk (**Figure 5A**). Consistently, the different risk populations could also be separated into two clusters when applying the PCA and the t-SNE analysis (**Figures 5B,C**). Notable higher mortality and a shorter OS time were discovered in the high-risk patients (**Figure 5D**); Besides, the

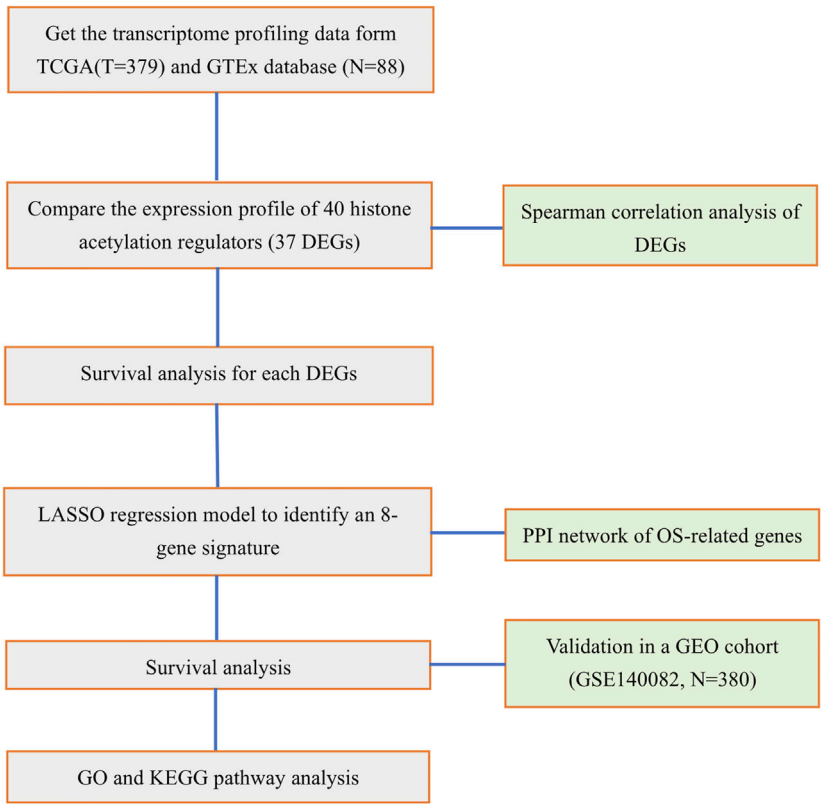

FIGURE 1 | Workflow diagram for the study.

survival analysis also indicated a lower survival possibility in the high-risk group (HR: 1.78, 95% CI: 1.19–2.68, $p < 0.01$, **Figure 5E**). The ROC curve showed the risk score could be a favorable predictor in the external dataset as well, and the AUC was 0.609 for 1 year, 0.639 for 2 years, and 0.649 for 3 years.

Independent Prognostic Value of the Risk Score

To explore whether the gene signature-based risk score could be an independent prognostic factor, we applied the univariate and multivariable Cox regression models. In the training cohort, univariate analysis showed the age and the risk score were correlated with the prognosis (**Figure 6A**), furthermore, in the multivariable model, it indicated that the 2 factors could be independent predictors for prognosis (HR for risk score: 2.910, 95% CI: 1.942–4.360, $p < 0.001$, **Figure 6B**). In the validation cohort, the risk score was also found to be an independent risk factor (HR: 2.298, 95% CI: 1.376–3,840, $p = 0.001$, **Figures 6C,D**). Moreover, a heatmap combined with the clinical features in the training cohort implied that the age and the survival status were significantly different between low- and high-risk subgroups (**Figure 6E**). These independently associated risk factors were used to build a risk estimation nomogram in both the training and the validation cohort (**Figures 7A,B**). The calibration curve for the survival status at 3 years showed that the nomogram performed well in the two cohorts (**Figures 7C,D**).

Functional Analyses of Differently Expressed Genes Between the Two Risk Groups

The DEGs between the low- and high-risk subgroups were identified by the screening criteria with p-value < 0.05 and $|\log_2 FC| > 1$. In total, 55 DEGs were screened out, and 18 of them were negatively correlated with the risk scores (**Supplementary Table S2**). To explore the potential functions of these DEGs, the GO (bubble plot) and KEGG pathway (bar plot) analyses were performed (**Figures 8A,B**). The results indicated that these DEGs were correlated with the development of organs, chemotaxis of immune cells, and regulation of signaling pathways. Notably, it's worth exploring the associations between OC and Wnt signaling pathway, as some of the DEGs (*RSPO4*, *NOTUM*, and *SFRP5*) were involved in this canonical signaling pathway.

Comparison of Immune Activity Between the Two Risk Groups

As the functional analyses revealed that lots of DEGs were related to the chemotaxis of immune cells, we next compared the

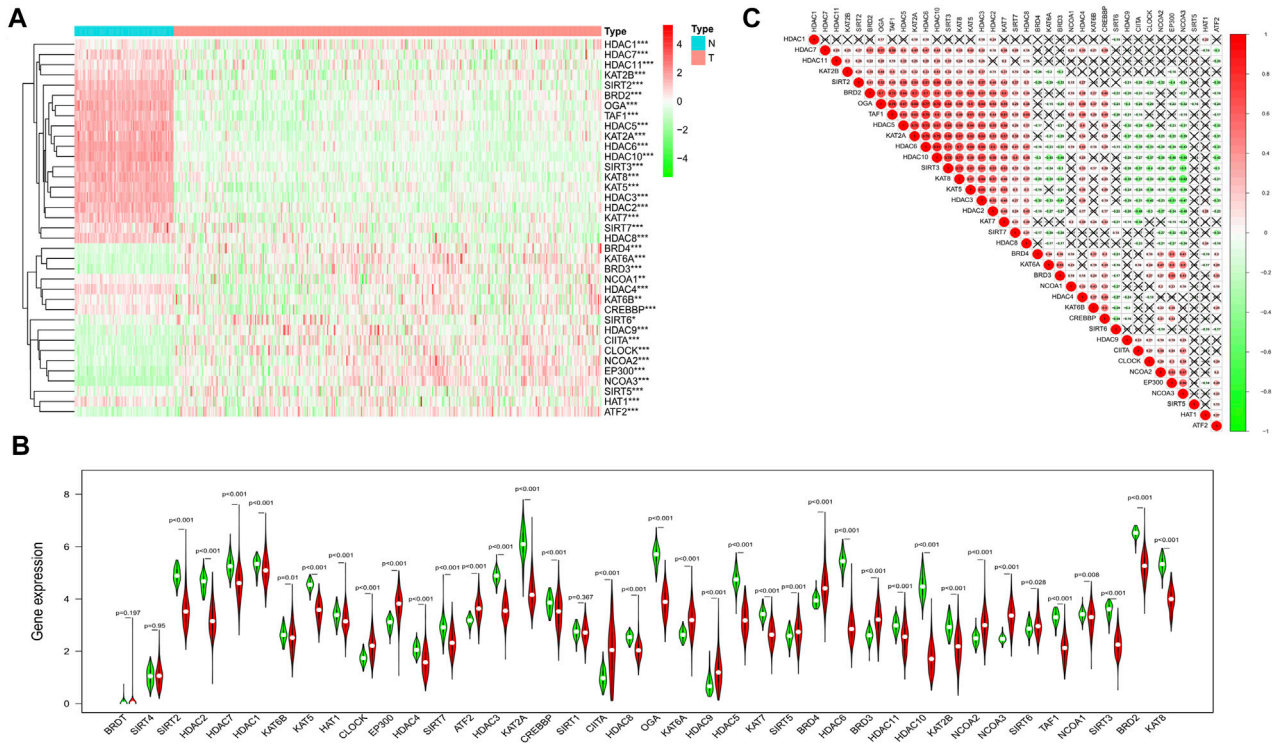

FIGURE 2 | Identification of the DEGs between the normal and ovarian cancer tissues. **(A)** Heatmap of all the DEGs in normal and tumor tissues (green: low-expression; Red: high expression). **(B)** The violin plot for all the histone acetylation-related regulators (Red: tumor tissues; Green: normal ovarian tissues). **(C)** Spearman correlation analysis for the 37 DEGs (Red: positive correlation, Green: negative correlation, the absolute values of correlation coefficient less than 0.10 were marked with "×").

infiltrating scores of 16 types of immune cells and the activity of 13 immune pathways. The results indicated that the dendritic cells (DCs), induced dendritic cells (iDCs), neutrophils, natural killer cells (NK cells), plasmacytoid dendritic cells (pDCs), follicular helper T cells (Tfh), and T-help 1/2 cells were at lower levels of infiltrations in the high-risk subgroup (**Figure 9A**). Meanwhile, we discovered that most of the immune pathways were with decreased activity in the high-risk population (**Figure 9B**).

DISCUSSION

In this study, we systematically investigated the gene expression levels of the currently known 40 histone acetylation-related regulators in ovarian cancer and found most of them expressed differently between tumor and normal tissues, indicating that these regulators play important roles in the genesis and development of OC. We applied the LASSO Cox regression model to construct an 8-gene signature, which was validated to be an independent risk factor for the OS of OCs. The functional analyses manifested that the DEGs between the two groups which were divided by the signature were enriched in the organ development, immune cell chemotaxis, and regulation of signaling pathways.

Histone acetylation modifications can affect the cell cycle, cell differentiation, and apoptosis. An imbalance in acetylation will lead to abnormal gene expression and alterations in important physiological functions, leading to tumorigenesis (Farria et al., 2015). According to the specific functions, these histone acetylation regulators could be divided into 3 categories: the "writers", act as histone acetyltransferases; the "readers", help to recognize acetyl-lysine sites; and the "erasers", in charge of histone deacetylation (Cheng et al., 2019). However, their interactions and the correlations with OC patients' OS remain largely unknown. In the 8-gene based risk signature, *OGA* and *NCOA3* belong to the "writers", *BRD4* functioned as the "readers" and the "erasers" contain *SIRT2*, *SIRT5*, *HDAC1*, *HDAC4*, *HDAC11*. Except for *SIRT5*, other 7 genes were identified as the risk factor in predicting the OS of OC patients (with HR > 1). *OGA* owns the ability to acetylate histones, as the carboxyl terminus contains the structural domain of histone acetyltransferase. *OGA* was reported to have a higher expression level in poorly differentiated laryngeal tumor cells and was associated with a poor prognosis (Starska et al., 2015). While *OGA* was found to be negatively correlated with tumor progression in breast cancer (Krześlak et al., 2012). In ovarian cancer, inhibition of *OGA* would lead to *p53* stabilization and increase its nuclear localization and indicated *OGA* is a potential therapeutic target (de Queiroz et al., 2016). *NCOA3* (*KAT13B*) is a member of the Src/p160 nuclear receptor co-activation family, owning the histone

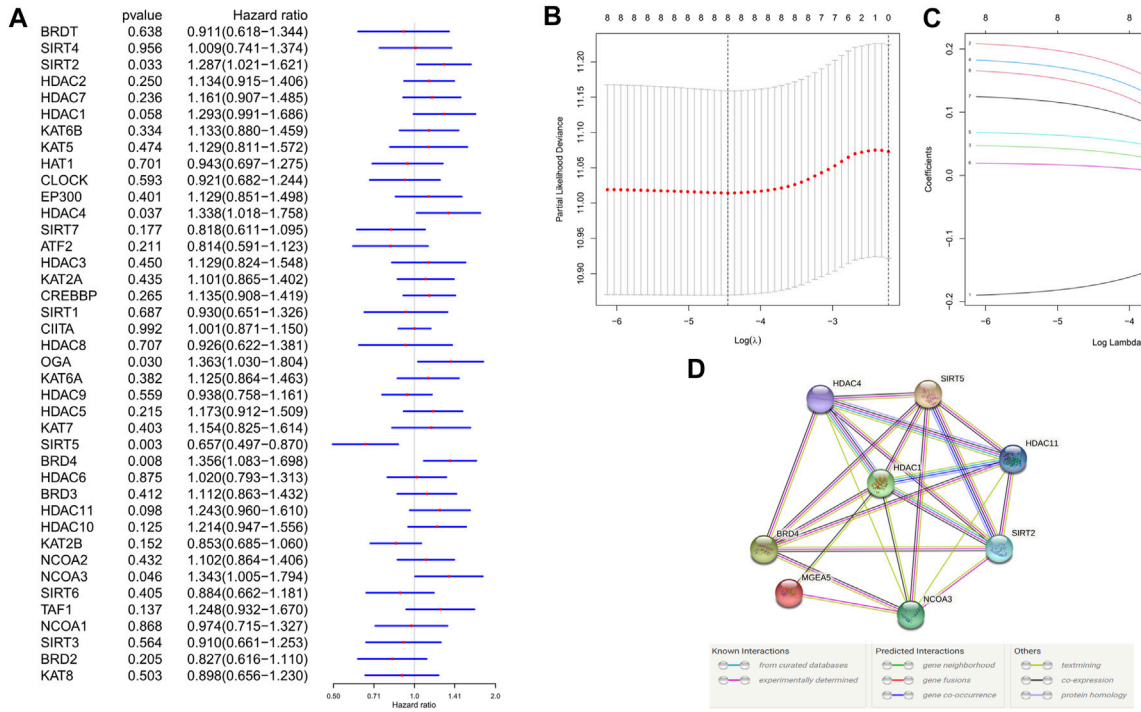

FIGURE 3 | Development of risk signature in the training cohort. **(A)** Univariate cox regression analysis of OS for each histone acetylation-related regulator, and 8 genes were identified with $p < 0.1$. **(B)** Cross-validation for tuning the parameter selection in the LASSO regression. **(C)** LASSO regression and the coefficients of the 8 OS-related genes. **(D)** PPI network showing the interactions between the OS-related genes.

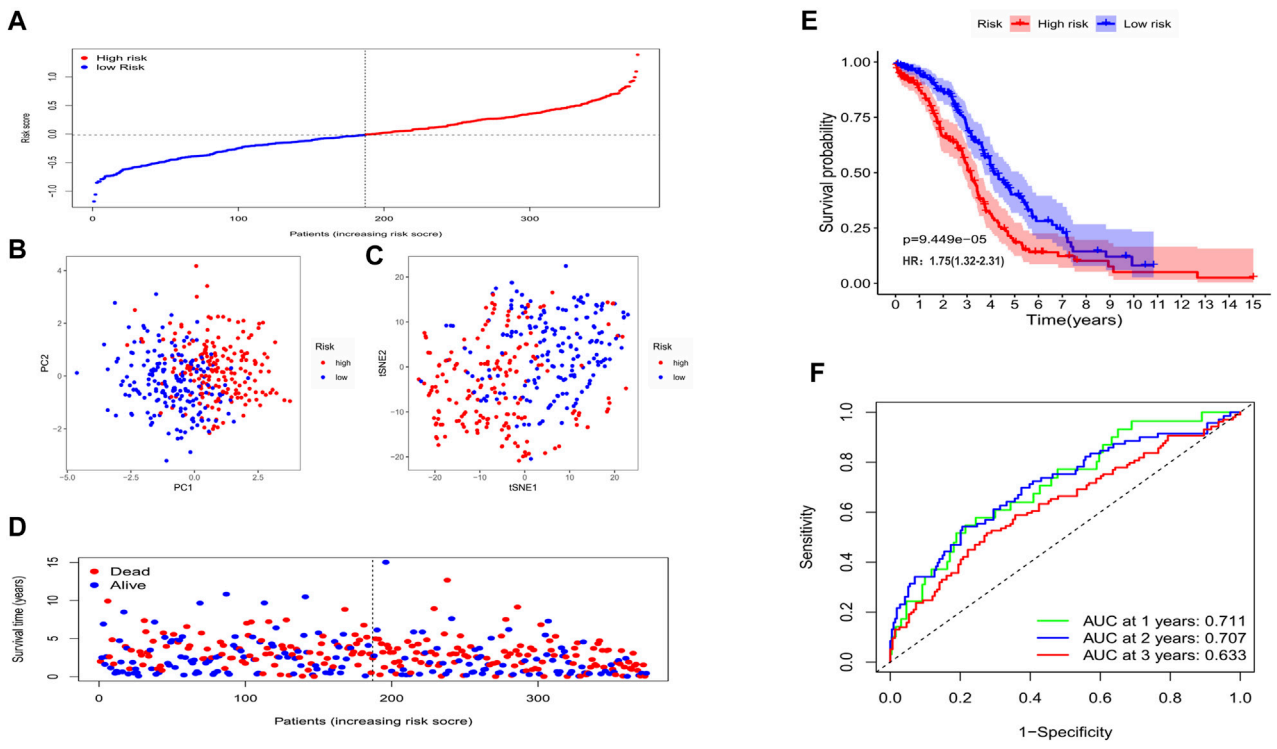

FIGURE 4 | The prognostic value of the gene signature in the training set. **(A)** The distribution of patients based on the median risk score. **(B)** PCA plot for OCs based on the risk score. **(C)** The t-SNE analysis based on the risk score. **(D)** The survival status for each individual (left of the dotted line: low-risk population; right of the dotted line: high-risk population). **(E)** Kaplan-Meier curves for the OS of patients between the high- and low-risk groups. **(F)** Time-dependent ROC curves demonstrated the predictive efficiency.

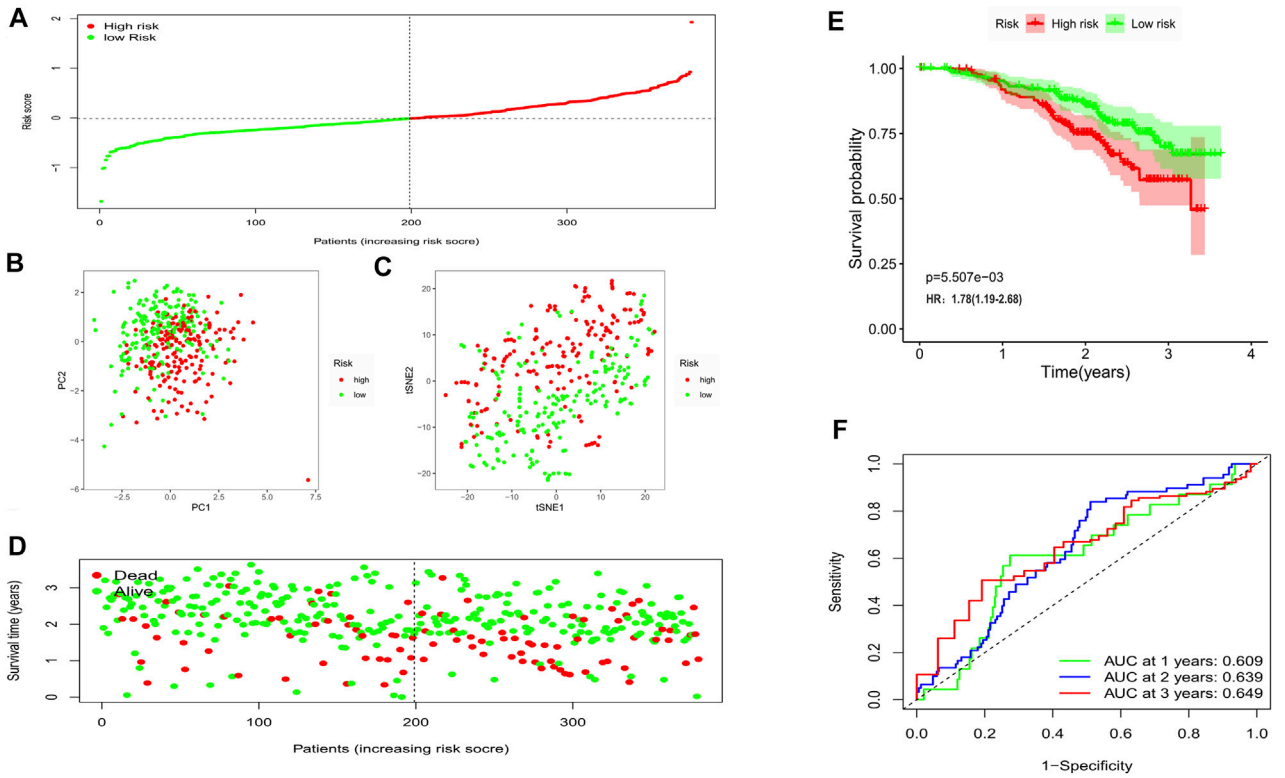

FIGURE 5 | Validation of the risk model in the external cohort. **(A)** Distribution of patients in the validation cohort based on the median risk score of the training cohort. **(B)** The PCA plot for OCs. **(C)** The t-SNE analysis based on the risk score. **(D)** The survival status for each patient (left of the dotted line: low-risk population; right of the dotted line: high-risk population). **(E)** Kaplan-Meier curves for the OS. **(F)** Time-dependent ROC curves for OCs.

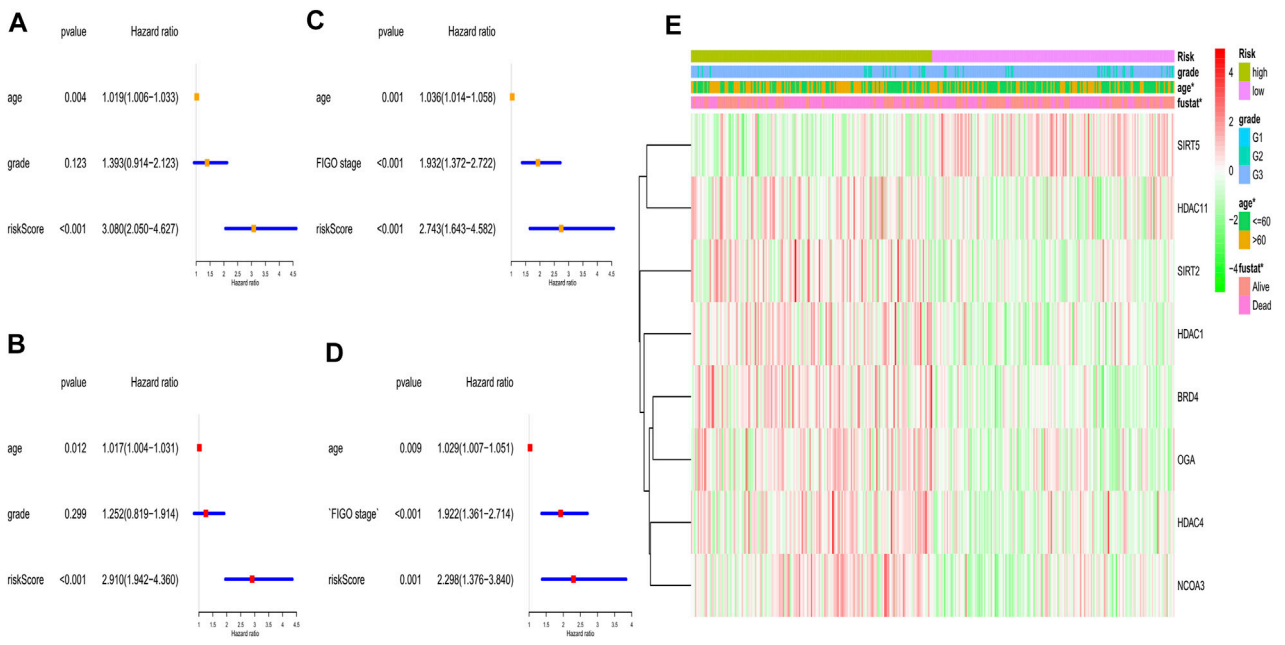

FIGURE 6 | Univariate and multivariate Cox regression analyses for the risk score. **(A)** Univariate analysis for the TCGA (training) cohort. **(B)** Multivariate analysis for the TCGA (training) cohort. **(C)** Univariate analysis for the GEO (validation) cohort. **(D)** Multivariate analysis for the GEO (validation) cohort. **(E)** Heatmap for the gene expression combined with clinical features in the TCGA (training) cohort.

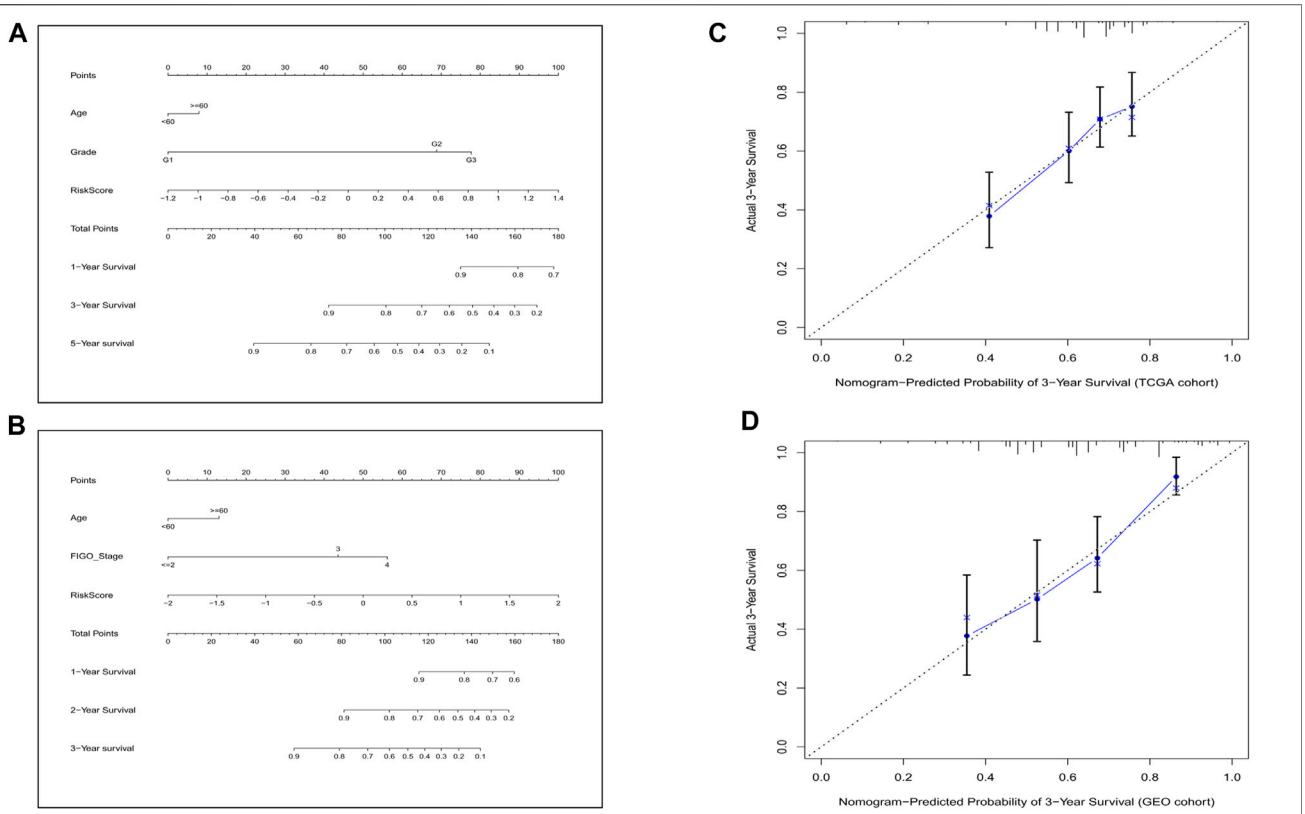

FIGURE 7 | Construction of the predictive model. **(A)** The prognostic model to predict the OS in the training cohort. **(B)** The prognostic model to predict the OS in the validation cohort. **(C)** Calibration curves for the OS nomogram model in the training set. **(D)** Calibration curves for the OS nomogram model in the validation set.

acetyltransferase activity and promoting gene transcription. *NCOA3* was initially found to be highly expressed in breast cancer, and it was later discovered to be amplified in many other malignant diseases (Gojis et al., 2010). *NCOA3* was also found to be a marker for platinum resistance in ovarian cancer (Palmieri et al., 2013). *BRD4* is a histone acetylation site reader, binds in hyper-acetylated chromatin regions, acts as a nucleation center for the assembly of large protein complexes, promotes RNA-PolII activity, and stimulates transcription initiation and elongation (Devaiah et al., 2016). The inhibitor of *BRD4* has great promise for cancer therapy, it competes with acetylated residues to bind to the *BRD4* bromodomain, thereby reducing RNA-PolII flux and blocking transcription of key oncogenes (Donato et al., 2017). In dealing with ovarian cancer, *BRD4* inhibitors could re-sensitize drug-resistant cancer cells to anti-cancer drugs (Andrikopoulou et al., 2021). *SIRT2* can catalyze the deacetylation of histone H3 and H4, leading to dense chromatin curl and consequent inhibition of gene transcription and expression (Budayeva and Cristea, 2016). *SIRT2* up-regulation may contribute to cisplatin sensitivity in OC cell lines and may be positively correlated with longer OS time (Wang et al., 2020; Zeng et al., 2020). However, our study implied that *SIRT2* is a risk factor for OC patients, and the conclusion is consistent with Teng's study (Teng and Zheng, 2017). Thus, the specific mechanisms of *SIRT2* in ovarian cancer still need further exploration. *SIRT5* has a weaker ability to deacetylate histones compared to other members of the sirtuins family (He et al., 2012). *SIRT5* was the unique gene identified in this study that was positively associated with a better prognosis. As the multiple protein modification functions of *SIRT5*, the protective role on ovarian cancer remains for further investigations. *HDAC1* is mainly involved in the deacetylation of histones. The correlations between *HDAC1* and the prognosis of malignant diseases are not clear since the controversial role of *HDAC1* in diverse types of cancer. *HDAC1* over-expression was discovered to prolong the OS time in Asian breast cancer patients (Qiao et al., 2018), while it was a risk factor for patients with lung cancer (Cao et al., 2017). Knocking down of *HDAC1* has been reported to enhance the sensitivity to cisplatin-based chemotherapy in ovarian cancer (Liu et al., 2018), indicating that *HDAC1* is a potential therapeutic target. *HDAC4* can deacetylate lysine residues at sites K9, K14, K18, and K23 of histone H3 and sites K5, K8, K12, and K16 of H4 (Wang et al., 2014). *HDAC4* is aberrantly expressed in a variety of cancer cells and tissues and may play a role in cancer development. Besides, *HDAC4* was also found to be involved in the process of platinum resistance in ovarian cancer (Stronach et al., 2011). *HDAC11* is responsible for the deacetylation of core histones and is a key factor in the regulation of transcription and the cell cycle (Licciardi et al., 2013; Liu et al., 2020). It has been reported that the deletion of *HDAC11* leads to cell death in colon, prostate, breast, and ovarian cancer cell lines (Deubzer et al., 2013). However, a recent study indicated that down-regulation of *HDAC11* would promote tumor metastasis from lymph nodes in breast cancer (Leslie et al., 2019). As the double-edged roles of *HDAC11*, and the little evidence in ovarian cancer treatment, furthermore in-depth

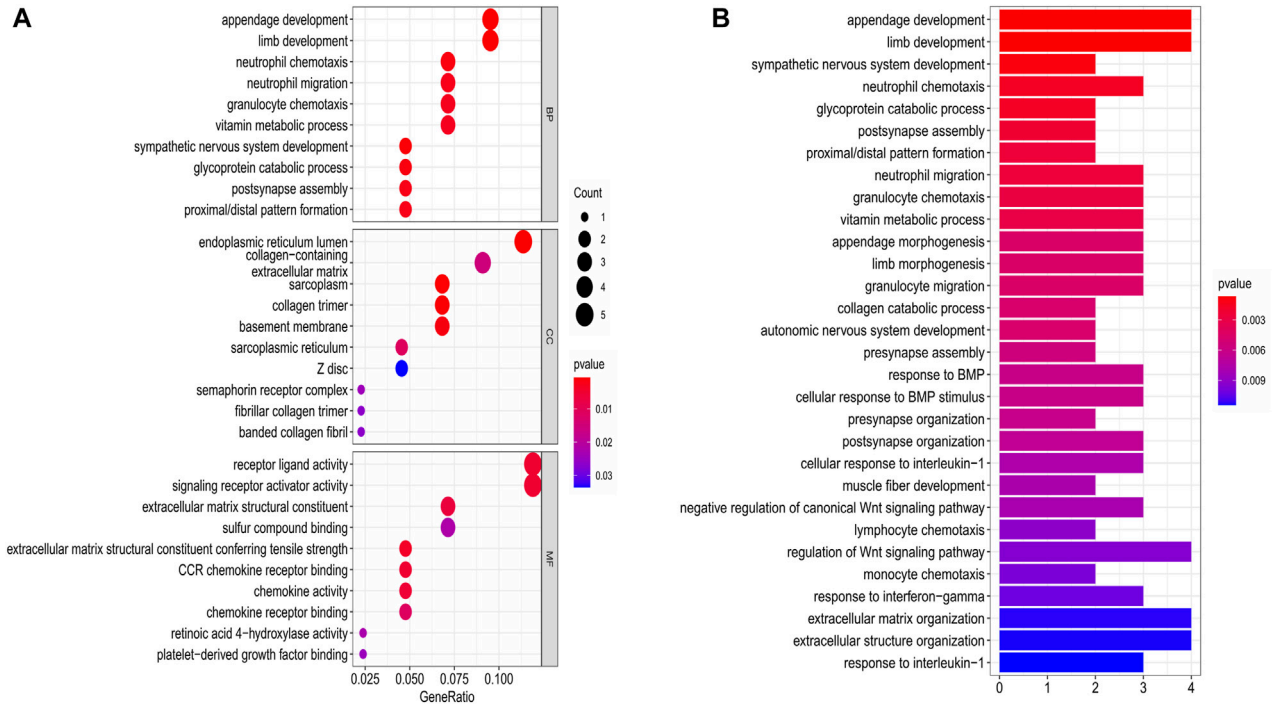

FIGURE 8 | Functional analysis based on the DEGs between the two-risk groups in the training cohort. **(A)** Bubble graph for GO enrichment. **(B)** Bar plot for KEGG pathways (the length of the bar presents the amount of gene enrichment).

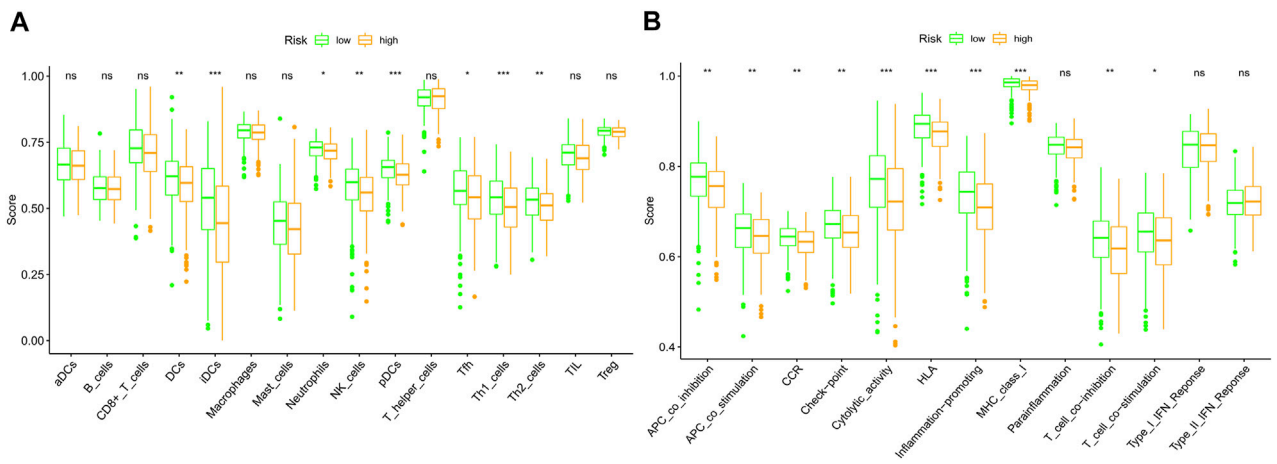

FIGURE 9 | Comparison of the immune cells and immune pathways between low (green)- and high (orange)-risk subgroups based on the ssGSEA. **(A)** Compare the enrichment scores of immune cells. **(B)** Compare of the immune-related pathways. (ns: not significant; *$p < 0.05$; **$p < 0.01$; ***$p < 0.001$).

studies about *HDAC11* should be taken into consideration. Notably, half of the poor prognosis-related genes own the ability of histone deacetylation (*SIRT2*, *HDAC1*, *HDAC4*, *HDAC11*). As a prior study reported, HDACs and the sirtuins family proteins are often over-expressed in malignancies, and promote tumor progression (Hai et al., 2021). However, the specific mechanisms of HDACs or sirtuins were quite different among tumors, thus to identify survival-related HDACs would help to facilitate targeted therapies towards ovarian cancer. Moreover, HDACs and HATs dynamically regulated the processes in the histone acetylation, thereby co-influencing transcription of oncogenes and tumor suppressor genes, while lots of studies only focused on the predictive roles of HDACs, neglecting the importance of HATs. Our work made a systematic study on the prognostic roles of these histone acetylation regulators, providing insights and novel molecular targets of epigenetic therapy towards ovarian cancer.

When the GO and KEGG pathway analyses were performed, we found that a variety of receptor-ligand interactions, as well as the immune cells-chemotaxis biological processes and pathways, were enriched. Moreover, lots of DEGs were correlated with the regulation of the Wnt signaling pathway, and this signal pathway was proved to contribute to the cisplatin resistance and weaken the anti-tumor immunity in OC (Doo et al., 2020; He et al., 2021). In this study, the top 3 Wnt signaling pathway-related genes were *RSPO4*, *NOTUM*, and *SFRP5*. R-spondin 4 (*RSPO4*) is an agonist of the Wnt signaling pathway, and was elevated about 2.5 folds in the high-risk population in our study, indicating that *RSPO4* may promote ovarian cancer progression through activation of the Wnt pathway. *NOTUM* (notum palmitoleoyl-protein carboxylesterase) acts as a negative regulator of the Wnt pathway, however, it was highly enriched in the high-risk group (about 6-folds up-regulated). A recent study demonstrated that *NOTUM* may be a novel efficacious target in treating colorectal cancer (Flanagan et al., 2021), so it's worth initiating explorations of *NOTUM* in ovarian cancer as lacking data. *SFRP5* (secreted frizzled related protein 5) can negatively regulate the Wnt pathway, and is regarded as a tumor suppressor. Our study found that *SFRP5* was unexpectedly up-regulated (3-folds) in the high-risk group, and the reason may be caused by the epigenetic silencing of *SFRP5* in the high-risk group (Su et al., 2010). In addition, as the Wnt pathway plays a pivotal role in organ development (Liu et al., 2022), it is not difficult to explain why lots of the DEGs are associated with organ development in our study.

According to the analyses of immune cells and pathways, we can speculate that these histone acetylation-related genes may affect the components of the tumor immune microenvironment and could regulate the immune-related signaling pathways. These findings may provide new targets for anti-tumor immunotherapies.

CONCLUSION

In conclusion, our study implied that histone acetylation is closely correlated with ovarian cancer and we developed a novel prognostic model of 8 histone acetylation-related genes. This model was proved to be independently associated with OS in OC patients, supplying a new strategy for predicting the prognosis and treating with OC.

DATA AVAILABILITY STATEMENT

The datasets presented in this study can be found in online repositories. The names of the repository/repositories and accession number(s) can be found in the article/ **Supplementary Material**.

AUTHOR CONTRIBUTIONS

YY performed study concept and design, revised the manuscript and make final approval of the version. QD analyzed data and wrote the manuscript.

FUNDING

This research did not receive any specific grant from funding agencies in the public, commercial, or not-for-profit sectors.

ACKNOWLEDGMENTS

We like to acknowledge the TCGA, GTEx and the GEO (GSE140082) network for providing data.

SUPPLEMENTARY MATERIAL

The Supplementary Material for this article can be found online at: https://www.frontiersin.org/articles/10.3389/fcell.2022.793425/full#supplementary-material

REFERENCES

Andrikopoulou, A., Liontos, M., Koutsoukos, K., Dimopoulos, M., and Zagouri, F. (2021). Clinical Perspectives of BET Inhibition in Ovarian Cancer. *Cell Oncol. (Dordrecht)* 44 (2), 237–249. doi:10.1007/s13402-020-00578-6

Autin, P., Blanquart, C., and Fradin, D. (2019). Epigenetic Drugs for Cancer and microRNAs: A Focus on Histone Deacetylase Inhibitors. *Cancers (Basel)* 11 (10). doi:10.3390/cancers11101530

Bennett, R. L., and Licht, J. D. (2018). Targeting Epigenetics in Cancer. *Annu. Rev. Pharmacol. Toxicol.* 58, 187–207. doi:10.1146/annurev-pharmtox-010716-105106

Budayeva, H. G., and Cristea, I. M. (2016). Human Sirtuin 2 Localization, Transient Interactions, and Impact on the Proteome Point to its Role in Intracellular Trafficking. *Mol. Cell Proteomics* 15 (10), 3107–3125. doi:10.1074/mcp.m116.061333

Cao, J., and Yan, Q. (2020). Cancer Epigenetics, Tumor Immunity, and Immunotherapy. *Trends Cancer* 6 (7), 580–592. doi:10.1016/j.trecan.2020.02.003

Cao, L.-L., Song, X., Pei, L., Liu, L., Wang, H., and Jia, M. (2017). Histone Deacetylase HDAC1 Expression Correlates with the Progression and Prognosis of Lung Cancer. *Medicine* 96 (31), e7663. doi:10.1097/md.0000000000007663

Cheng, Y., He, C., Wang, M., Ma, X., Mo, F., Yang, S., et al. (2019). Targeting Epigenetic Regulators for Cancer Therapy: Mechanisms and Advances in Clinical Trials. *Sig Transduct Target. Ther.* 4, 62. doi:10.1038/s41392-019-0095-0

Christie, E. L., and Bowtell, D. D. L. (2017). Acquired Chemotherapy Resistance in Ovarian Cancer. *Ann. Oncol.* 28, viii13–viii15. doi:10.1093/annonc/mdx446

de Queiroz, R. M., Madan, R., Chien, J., Dias, W. B., and Slawson, C. (2016). Changes in O-Linked N-Acetylglucosamine (O-GlcNAc) Homeostasis Activate the P53 Pathway in Ovarian Cancer Cells. *J. Biol. Chem.* 291 (36), 18897–18914. doi:10.1074/jbc.m116.734533

Deubzer, H. E., Schier, M. C., Oehme, I., Lodrini, M., Haendler, B., Sommer, A., et al. (2013). HDAC11 Is a Novel Drug Target in Carcinomas. *Int. J. Cancer* 132 (9), 2200–2208. doi:10.1002/ijc.27876

Devaiah, B. N., Gegonne, A., and Singer, D. S. (2016). Bromodomain 4: a Cellular Swiss Army Knife. *J. Leukoc. Biol.* 100 (4), 679–686. doi:10.1189/jlb.2ri0616-250r

Donato, E., Croci, O., Sabò, A., Muller, H., Morelli, M. J., Pelizzola, M., et al. (2017). Compensatory RNA Polymerase 2 Loading Determines the Efficacy and

Transcriptional Selectivity of JQ1 in Myc-Driven Tumors. *Leukemia* 31 (2), 479–490. doi:10.1038/leu.2016.182

Doo, D. W., Meza-Perez, S., Londoño, A. I., Goldsberry, W. N., Katre, A. A., Boone, J. D., et al. (2020). Inhibition of the Wnt/β-Catenin Pathway Enhances Antitumor Immunity in Ovarian Cancer. *Ther. Adv. Med. Oncol.* 12, 1758835920913798. doi:10.1177/1758835920913798

Ell, B., and Kang, Y. (2013). Transcriptional Control of Cancer Metastasis. *Trends Cell Biology* 23 (12), 603–611. doi:10.1016/j.tcb.2013.06.001

Farria, A., Li, W., and Dent, S. Y. R. (2015). KATs in Cancer: Functions and Therapies. *Oncogene* 34 (38), 4901–4913. doi:10.1038/onc.2014.453

Flanagan, D. J., Pentinmikko, N., Luopajärvi, K., Willis, N. J., Gilroy, K., Raven, A. P., et al. (2021). NOTUM from Apc-Mutant Cells Biases Clonal Competition to Initiate Cancer. *Nature* 594 (7863), 430–435. doi:10.1038/s41586-021-03525-z

Gojis, O., Rudraraju, B., Alifrangis, C., Krell, J., Libalova, P., and Palmieri, C. (2010). The Role of Steroid Receptor Coactivator-3 (SRC-3) in Human Malignant Disease. *Eur. J. Surg. Oncol. (Ejso)* 36 (3), 224–229. doi:10.1016/j.ejso.2009.08.002

Hai, R., He, L., Shu, G., and Yin, G. (2021). Characterization of Histone Deacetylase Mechanisms in Cancer Development. *Front. Oncol.* 11, 700947. doi:10.3389/fonc.2021.700947

He, S., Wang, W., Wan, Z., Shen, H., Zhao, Y., You, Z., et al. (2021). FAM83B Inhibits Ovarian Cancer Cisplatin Resistance through Inhibiting Wnt Pathway. *Oncogenesis* 10 (1), 6. doi:10.1038/s41389-020-00301-y

He, W., Newman, J. C., Wang, M. Z., Ho, L., and Verdin, E. (2012). Mitochondrial Sirtuins: Regulators of Protein Acylation and Metabolism. *Trends Endocrinol. Metab.* 23 (9), 467–476. doi:10.1016/j.tem.2012.07.004

Kaypee, S., Sudarshan, D., Shanmugam, M. K., Mukherjee, D., Sethi, G., and Kundu, T. K. (2016). Aberrant Lysine Acetylation in Tumorigenesis: Implications in the Development of Therapeutics. *Pharmacol. Ther.* 162, 98–119. doi:10.1016/j.pharmthera.2016.01.011

Krześlak, A., Forma, E., Bernaciak, M., Romanowicz, H., and Bryś, M. (2012). Gene Expression of O-GlcNAc Cycling Enzymes in Human Breast Cancers. *Clin. Exp. Med.* 12 (1), 61–65. doi:10.1007/s10238-011-0138-5

Krzystyniak, J., Ceppi, L., Dizon, D., and Birrer, M. (2016). Epithelial Ovarian Cancer: the Molecular Genetics of Epithelial Ovarian Cancer. *Ann. Oncol.* 27 (Suppl. 1), i4–i10. doi:10.1093/annonc/mdw083

Kuroki, L., and Guntupalli, S. R. (2020). Treatment of Epithelial Ovarian Cancer. *Bmj* 371, m3773. doi:10.1136/bmj.m3773

Leslie, P. L., Chao, Y. L., Tsai, Y.-H., Ghosh, S. K., Porrello, A., Van Swearingen, A. E. D., et al. (2019). Histone Deacetylase 11 Inhibition Promotes Breast Cancer Metastasis from Lymph Nodes. *Nat. Commun.* 10 (1), 4192. doi:10.1038/s41467-019-12222-5

Licciardi, P. V., Ververis, K., Tang, M. L., El-Osta, A., and Karagiannis, T. C. (2013). Immunomodulatory Effects of Histone Deacetylase Inhibitors. *Cmm* 13 (4), 640–647. doi:10.2174/1566524011313040013

Liu, J., Xiao, Q., Xiao, J., Niu, C., Li, Y., Zhang, X., et al. (2022). Wnt/β-catenin Signalling: Function, Biological Mechanisms, and Therapeutic Opportunities. *Sig Transduct Target. Ther.* 7 (1), 3. doi:10.1038/s41392-021-00762-6

Liu, S.-S., Wu, F., Jin, Y.-M., Chang, W. Q., and Xu, T.-M. (2020). HDAC11: a Rising star in Epigenetics. *Biomed. Pharmacother.* 131, 110607. doi:10.1016/j.biopha.2020.110607

Liu, X., Yu, Y., Zhang, J., Lu, C., Wang, L., Liu, P., et al. (2018). HDAC1 Silencing in Ovarian Cancer Enhances the Chemotherapy Response. *Cell Physiol Biochem* 48 (4), 1505–1518. doi:10.1159/000492260

Palmieri, C., Gojis, O., Rudraraju, B., Stamp-Vincent, C., Wilson, D., Langdon, S., et al. (2013). Expression of Steroid Receptor Coactivator 3 in Ovarian Epithelial Cancer Is a Poor Prognostic Factor and a Marker for Platinum Resistance. *Br. J. Cancer* 108 (10), 2039–2044. doi:10.1038/bjc.2013.199

Qiao, W., Liu, H., Liu, R., Liu, Q., Zhang, T., Guo, W., et al. (2018). Prognostic and Clinical Significance of Histone Deacetylase 1 Expression in Breast Cancer: A Meta-Analysis. *Clinica Chim. Acta* 483, 209–215. doi:10.1016/j.cca.2018.05.005

Scaletta, G., Plotti, F., Luvero, D., Capriglione, S., Montera, R., Miranda, A., et al. (2017). The Role of Novel Biomarker HE4 in the Diagnosis, Prognosis and Follow-Up of Ovarian Cancer: a Systematic Review. *Expert Rev. Anticancer Ther.* 17 (9), 827–839. doi:10.1080/14737140.2017.1360138

Shen, Y., Wei, W., and Zhou, D.-X. (2015). Histone Acetylation Enzymes Coordinate Metabolism and Gene Expression. *Trends Plant Science* 20 (10), 614–621. doi:10.1016/j.tplants.2015.07.005

Starska, K., Forma, E., Brzezińska-Błaszczyk, E., Lewy-Trenda, I., Bryś, M., Jóźwiak, P., et al. (2015). Gene and Protein Expression of O-GlcNAc-Cycling Enzymes in Human Laryngeal Cancer. *Clin. Exp. Med.* 15 (4), 455–468. doi:10.1007/s10238-014-0318-1

Stronach, E. A., Alfraidi, A., Rama, N., Datler, C., Studd, J. B., Agarwal, R., et al. (2011). HDAC4-regulated STAT1 Activation Mediates Platinum Resistance in Ovarian Cancer. *Cancer Res.* 71 (13), 4412–4422. doi:10.1158/0008-5472.can-10-4111

Su, H.-Y., Lai, H.-C., Lin, Y.-W., Liu, C.-Y., Chen, C.-K., Chou, Y.-C., et al. (2010). Epigenetic Silencing of SFRP5 Is Related to Malignant Phenotype and Chemoresistance of Ovarian Cancer through Wnt Signaling Pathway. *Int. J. Cancer* 127 (3), 555–567. doi:10.1002/ijc.25083

Teng, C., and Zheng, H. (2017). Low Expression of microRNA-1908 Predicts a Poor Prognosis for Patients with Ovarian Cancer. *Oncol. Lett.* 14 (4), 4277–4281. doi:10.3892/ol.2017.6714

Wang, W., Im, J., Kim, S., Jang, S., Han, Y., Yang, K. M., et al. (2020). ROS-induced SIRT2 Upregulation Contributes to Cisplatin Sensitivity in Ovarian Cancer. *Antioxidants (Basel)* 9 (11), 1137. doi:10.3390/antiox9111137

Wang, Z., Qin, G., and Zhao, T. C. (2014). HDAC4: Mechanism of Regulation and Biological Functions. *Epigenomics* 6 (1), 139–150. doi:10.2217/epi.13.73

Zeng, Z., Huang, Y., Li, Y., Huang, S., Wang, J., Tang, Y., et al. (2020). Gene Expression and Prognosis of Sirtuin Family Members in Ovarian Cancer. *Medicine* 99 (24), e20685. doi:10.1097/md.0000000000020685

Zhou, L., Xu, X., Liu, H., Hu, X., Zhang, W., Ye, M., et al. (2018). Prognosis Analysis of Histone Deacetylases mRNA Expression in Ovarian Cancer Patients. *J. Cancer* 9 (23), 4547–4555. doi:10.7150/jca.26780

Conflict of Interest: The authors declare that the research was conducted in the absence of any commercial or financial relationships that could be construed as a potential conflict of interest.

Publisher's Note: All claims expressed in this article are solely those of the authors and do not necessarily represent those of their affiliated organizations, or those of the publisher, the editors, and the reviewers. Any product that may be evaluated in this article, or claim that may be made by its manufacturer, is not guaranteed or endorsed by the publisher.

frontiers in Cell and Developmental Biology

ORIGINAL RESEARCH
published: 08 March 2022
doi: 10.3389/fcell.2022.818082

Integrative Analysis of Gene Expression and DNA Methylation Depicting the Impact of Obesity on Breast Cancer

Zhenchong Xiong[1†], *Xing Li*[1†], *Lin Yang*[2†], *Linyu WU*[1], *Yi Xie*[1], *Fei Xu*[1*] *and Xinhua Xie*[1*]

[1]*Department of Breast Oncology, Sun Yat-sen University Cancer Center, State Key Laboratory of Oncology in South China, Collaborative Innovation Center of Cancer Medicine, Guangzhou, China,* [2]*Department of Radiation Oncology, Nanfang Hospital, Southern Medical University, Guangzhou, China*

Obesity has been reported to be a risk factor for breast cancer, but how obesity affects breast cancer (BC) remains unclear. Although body mass index (BMI) is the most commonly used reference for obesity, it is insufficient to evaluate the obesity-related pathophysiological changes in breast tissue. The purpose of this study is to establish a DNA-methylation-based biomarker for BMI (DM-BMI) and explore the connection between obesity and BC. Using DNA methylation data from The Cancer Genome Atlas (TCGA) and Gene Expression Omnibus (GEO), we developed DM-BMI to evaluate the degree of obesity in breast tissues. In tissues from non-BC and BC population, the DM-BMI model exhibited high accuracy in BMI prediction. In BC tissues, DM-BMI correlated with increased adipose tissue content and BC tissues with increased DM-BMI exhibited higher expression of pro-inflammatory adipokines. Next, we identified the gene expression profile relating to DM-BMI. Using Gene Ontology (GO) and the Kyoto Encyclopedia of Genes and Genomes (KEGG) database, we observed that the DM-BMI-related genes were mostly involved in the process of cancer immunity. DM-BMI is positively correlated with T cell infiltration in BC tissues. Furthermore, we observed that DM-BMI was positively correlated with immune checkpoint inhibitors (ICI) response markers in BC. Collectively, we developed a new biomarker for obesity and discovered that BC tissues from obese individuals exhibit an increased degree of immune cell infiltration, indicating that obese BC patients might be the potential beneficiaries for ICI treatment.

Keywords: obesity, breast cancer, immune checkpoint inhibitor, DNA methylation, biomarker

OPEN ACCESS

Edited by:
Christiane Pienna Soares, Sao Paulo State University, Brazil

Reviewed by:
Chuanjun Shu, Nanjing Medical University, China
Chang Gong, Sun Yat-sen University, China
Jie Li, The First Affiliated Hospital of Sun Yat-sen University, China

****Correspondence:***
Fei Xu
xufei@sysucc.org.cn
Xinhua Xie
xiexh@sysucc.org.cn

†These authors have contributed equally to this work and share first authorship

Specialty section:
This article was submitted to Epigenomics and Epigenetics, a section of the journal Frontiers in Cell and Developmental Biology

Received: *19 November 2021*
Accepted: *01 February 2022*
Published: *08 March 2022*

Citation:
Xiong Z, Li X, Yang L, WU L, Xie Y, Xu F and Xie X (2022) Integrative Analysis of Gene Expression and DNA Methylation Depicting the Impact of Obesity on Breast Cancer. Front. Cell Dev. Biol. 10:818082. doi: 10.3389/fcell.2022.818082

Abbreviations: BC, Breast Cancer; HR, Hormone Receptor; BMI, Body Mass Index; DM-BMI, DNA Methylation-Based BMI Index; TCGA, The Cancer Genome Atlas; GO, Gene Ontology; KEGG, Kyoto Encyclopedia of Genes and Genomes; ICI, Immune Checkpoint Inhibitor; GEO, Gene Expression Omnibus; knn, k-nearest neighbors; SNPs, Single Nucleotide Polymorphisms; TMB, Tumour Mutation Burden; Treg, Regulatory T Cells; IFNG, IFN-γ Signature; IFNG.GS, IFNG Hallmark Gene Set; TIDE, Tumour Immune Dysfunction and Exclusion; MDSCs, Myeloid-Derived Suppressor Cells; CAFs, Cancer-Associated Fibroblasts; TAM-M2, M2 Subtype of Tumour-Associated Macrophages; Chr, Chromosome; DMP, Differentially Methylated Probes; GSEA, Gene Set Enrichment Analysis.

INTRODUCTION

Breast cancer (BC) is the most commonly diagnosed cancer and the second leading cause of cancer death for women in the world (Bray et al., 2018). It was reported in previous studies that obesity, characterized by excess adipose tissues, is a risk factor for BC (Pierobon and Frankenfeld, 2013; Sung et al., 2019). For premenopausal women, obesity is connected with increased risk of hormone receptor (HR) negative BC, while for postmenopausal women, it is connected with increased risk of HR positive BC (Suzuki et al., 2009; Picon-Ruiz et al., 2017). Moreover, several studies showed that obese patients exhibited more aggressive tumor features (such as larger tumor size, lymph node metastasis, shorter disease-free survival, and greater risk of mortality) compared with non-obese patients in BC (Copson et al., 2015; Jiralerspong and Goodwin, 2016). Although it has been observed in previous studies that the adipose tissue in obese individuals increasingly secrets adipokines (including hormones, growth factors, and cytokines) and contributes to an environment promoting cancer proliferation and metastasis (Khandekar et al., 2011; Maguire et al., 2021), how obesity impacts BC requires further studies.

Body mass index (BMI), defined as a person's weight in kilograms divided by the square of height in meters, is the most commonly used method for obesity evaluation. However, it is more like a surrogate measure for body fatness for obesity should be calculated using the excess accumulation of adipose tissues rather than body mass (Prentice and Jebb, 2001). As there is heterogeneity in the body distribution, function, and tissue composition of adipose tissue among BC patients, a total body mass index is insufficient to evaluate the degree of obesity in local tissue. Moreover, BMI is only able to reflect the gaining of weight, with no indication in pathophysiological changes during the process of obesity (Bosello et al., 2016). Thus, developing new biomarkers to evaluate the obesity status of BC tissues is helpful to assess the impact of obesity on BC.

It is well known that obesity is affected by multiple factors (including environmental factors, genetic predisposition, and the individual lifestyle) (Conway and Rene, 2004; Bray et al., 2016). Recently, increased evidences showed that DNA methylation is also involved in the process of obesity (Ling and Rönn, 2019; Samblas et al., 2019). DNA methylation is an epigenetic mechanism which regulates gene expression through chromatin structure changes. Equally influenced by environmental factors, genetic predisposition and the individual lifestyle, the level of gene methylation is dynamically changing in setting up stable gene expression profiles to adapt to the process of obesity (Samblas et al., 2019; Cabre et al., 2021). A previous study analyzing the whole genome methylation and gene expression in non-diseased breast showed that obesity is connected with the genome-wide methylation changes in human tissue (Hair et al., 2015a). In addition, Hair et al. observed that obesity is significantly correlated with genome-wide hyper-methylation in ER-positive BCs (Hair et al., 2015b). Thus, changes of genome-wide DNA methylation could be a reflection of the biological changes in breast tissue during the process of obesity. The goal of our study is to capture the obesity-related genomic changes and explore the impact of obesity on BC tissues. We developed DNA methylation-based BMI index (DM-BMI) to evaluate the degree of obesity in breast tissues and validated the accuracy of DM-BMI in breast tissues from non-BC and BC population. Furthermore, we assessed the correlation among DM-BMI, obesity adipose tissue content, and the expression of adipokines in BC tissues. Next, we identified the DM-BMI-related gene expression profile. Using Gene Ontology (GO) and Kyoto Encyclopedia of Genes and Genomes (KEGG) database, we observed that the DM-BMI-related genes are significantly involved in the process of cancer immunity. Using Estimate and Cibersort algorithm, we observed a positive correlation between DM-BMI and immune cell infiltration. Finally, we assessed the correlation between DM-BMI and biomarkers of response to immune checkpoint inhibitors (ICI) (Shah et al., 2012) and observed that DM-BMI positively correlated with ICI response in BC.

TABLE 1 | Clinicopathological features for TCGA-BRCA cases

	Unmatched BC cases (n = 775)	Matched BC cases (n = 76)
ER status (%)		
+	155 (20%)	12 (15.8%)
–	512 (66.1%)	53 (69.7%)
Unknown	108 (13.9%)	11 (14.5%)
PR status (%)		
+	216 (27.9%)	19 (25%)
-	449 (57.9%)	45 (59.2%)
Unknown	110 (14.2%)	12 (15.8%)
HER2 status (%)		
+	469 (60.5%)	41 (53.9%)
-	93 (12%)	12 (15.8%)
Unknown	213 (27.5%)	23 (30.3%)
T stage (%)		
T1	199 (25.7%)	17 (22.4%)
T2	442 (57%)	46 (60.5%)
T3	108 (13.9%)	8 (10.5%)
T4	23 (3%)	5 (6.6%)
Unknown	3 (0.4%)	0 (0%)
N stage (%)		
N1	346 (44.6%)	26 (34.3%)
N2	268 (34.6%)	34 (44.7%)
N3	95 (12.3%)	9 (11.8%)
N4	55 (7.1%)	4 (5.3%)
Unknown	11 (11.4%)	3 (3.9%)
M stage (%)		
M0	610 (78.7%)	70 (92.1%)
M1	13 (1.7%)	1 (1.3%)
MX	152 (19.6%)	5 (6.6%)
Molecular subtype (%)		
Normal-like	33 (4.3%)	1 (1.3%)
Luminal A	370 (47.7%)	41 (53.9%)
Luminal B	120 (15.5%)	20 (26.4%)
Her-2	39 (5%)	6 (7.9%)
TNBC	125 (16.1%)	8 (10.5%)
Unknown	88 (11.4%)	0 (0%)
Vital status (%)		
Alive	672 (86.7%)	45 (59.2%)
Death	103 (13.3%)	31 (40.8%)

***Abbreviation**: ER = Estrogen receptor; PR = Progesterone receptor*

MATERIALS AND METHODS

Data collection and processing

The training set includes genome-wide methylation data of 221 normal breast tissues in GEO (GSE88883 and GSE101961) while the validation sets includes data of 44 normal breast tissues (Validation Set 1). Data of 70 tumor-adjacent breast tissues (Validation Set 2) in GEO (GSE67919 and GSE74214) were used to develop the DM-BMI score. BMI data of the above cases are listed in **Supplementary Materials S1, S2**. The DNA methylation and expression data of 76 cases with matched tumor and tumor-adjacent breast tissues and the data of 775 cases with unmatched tumor tissues were collected from The Cancer Genome Atlas (TCGA) database (https://portal.gdc.cancer.gov/). Clinical features of BC patients in TCGA-BRCA are listed in **Table 1**.

Genome-wide methylation data was profiled using Illumina Infinium HumanMethylation450 BeadChips Assay. For DNA methylation data, β value ranging from 0 (no DNA methylation) to 1 (complete DNA methylation) was used to define the methylation level of each probe. Probes with missing value in over 50% samples were removed while the probes with missing value in less than 50% of samples were imputed with the k-nearest neighbors (knn) imputation method. Probes located on the sex chromosome and probes containing known single nucleotide polymorphisms (SNPs) were removed. Eventually, 301,998 probes were included in this study. BMIQ normalization for type I and II probe correction was performed. Data from multiple studies was integrated and the Combat algorithm was performed to remove the batch effects. The above processes were carried out using the R package ChAMP (Tian et al., 2017).

For gene expression data, background correction and normalization were carried out using the R package limma (Ritchie et al., 2015).

Calculation of DNA-methylation based body mass index

To improve the predictive accuracy of the model, the BMI value was transformed to F(BMI) before further analysis, which is shown as follows:

$$\mathrm{F(BMI)} = \log(\mathrm{BMI}+1) - \log(\mathrm{healthy.BMI}+1) \text{ if BMI} < \\ = \mathrm{healthy.BMI} \quad (1)$$

$$\mathrm{F(BMI)} = (\mathrm{BMI} - \mathrm{healthy.BMI})/(\mathrm{healthy.BMI}+1) \text{ if BMI} > \mathrm{healthy.BMI} \quad (2)$$

The parameter healthy.BMI was set to 25, referring to the upper limit of BMI in healthy population.

A lasso regression was used to regress the DM-BMI in the form of F(BMI) based on the BMI data and DNA methylation data with 301,998 probes; 42 probes were selected in the lasso regression model as BMI predictors according to the lambda.min value (**Supplementary Figure S1A**). The coefficient values of each probe are shown in **Supplementary Figure S1B**. The lasso regression analysis was carried out using R package glmnet (alpha was set to 1, and the lambda value was identified by performing a 10-fold cross validation to the training data).

Analysis of intra-sample adipose tissue content

Adipose tissue accounts for a large proportion of breast tissue composition. Based on DNA methylation, we used a deconvolution algorithm to calculate the proportion of adipose tissue in breast and BC tissues. Teschendorff et al. (2016) provided a deconvolution algorithm to model cell subpopulations in breast tissues based on DNA methylation data. Illumina 450k DNA methylation data of human mammary epithelial cells (GSE40699) and adipose tissue (GSE48472) were used as reference profiles. Data were processed as previously described. Probes with an absolute difference in beta-value between the human mammary epithelial cells and the averaged adipose tissue >0.7 were selected for the evaluation of intra-sample adipose tissue content. Data for adipose tissue content are listed in **Supplementary Material S3**.

Characteristics analyses of body mass index predictors

Forty-two probes were selected in the lasso regression model as BMI predictors. The distribution of 42 probes on chromosome, CpG island, and TSS regions was assessed using the R package ChAMP. BMI predictors, differentially methylated between BC tissues and tumor-adjacent breast tissues in the TCGA database, were identified using the R package Champ. The survival correlation of BMI predictors was assessed using TCGA BRCA data. Correlation between the methylation level of BMI predictors and DM-BMI was assessed.

Functional and clinical characteristics analysis of DM-BMI-related gene profile

DM-BMI of TCGA-BC tissues were calculated using DNA methylation data. Spearman correlation coefficient was used to assess the correlation of DM-BMI and clinical characteristics (menopause status, hormone status, copy number variation and gene mutation) in BC. Gene expression profile related to DM-BMI was identified; functional analysis of the related genes was process by GO and KEGG analysis. Besides, we performed gene set variation analysis (GSVA) to identify DM-BMI related gene signature using gene expression data in TCGA (Hänzelmann et al., 2013). The above procedures were performed using the R software.

Evaluation of correlations between DM-BMI and the immune microenvironment in breast cancer

Tumor mutation burden (TMB) was defined as the number of non-synonymous mutations/Mb of genome. As previously

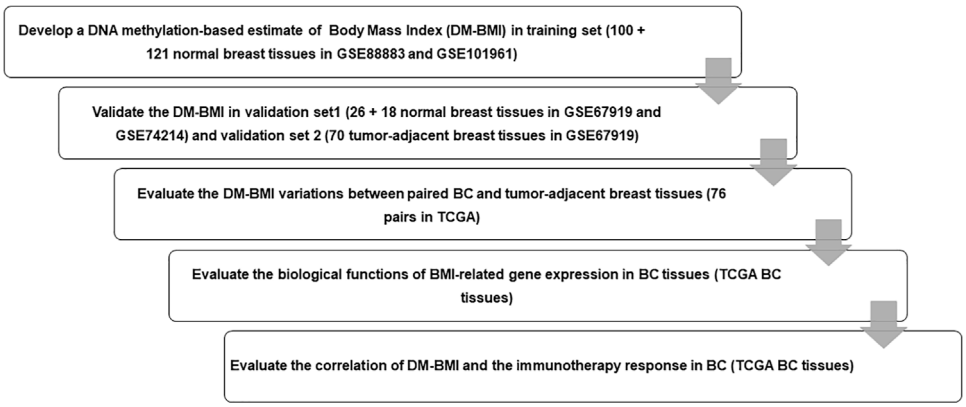

FIGURE 1 | Flow chart of the study design. We enrolled 221 normal breast tissues as training set to develop a lasso regression to predict DM-BMI and validated the accuracy of the model with data from normal breast tissues and tumor-adjacent breast tissues. Then, we predicted DM-BMI in 775 BC tissues and 76 matched tumor-adjacent breast tissues. The correlation between DM-BMI and clinical characteristics was assessed in BC tissues. Further, we identified the DM-BMI related gene profile and evaluated the relationships between DN-BMI and tumor immune response in BC tissues.

reported (Chalmers et al., 2017), TMB of BC tissues in TCGA was calculated as (whole exome non-synonymous mutations)/ 38 (Mb).

The level of tumor-infiltrating immune cells and stromal cells in each tissue were evaluated by ESTIMATE algorithm (Yoshihara et al., 2013). The proportion of 22 immune cells in each tissue was evaluated using the CIBERSORT algorithm (http://cibersort.stanford.edu/) (Gentles et al., 2015). Correlations between DM-BMI and ESTIMATE/CIBERSORT scores were calculated using Spearman correlation coefficient. The data for TMB, ESTIMATE, and CIBERSORT analysis are listed in **Supplementary Material S4**.

Evaluation of correlations between DM-BMI and the cancer immunotherapy response

Biomarkers used to predict the immunotherapy response includes: IFN-γ signature (IFNG) (Ayers et al., 2017), IFNG hallmark gene set (IFNG.GS) (Benci et al., 2019), antigen processing and presenting machinery (APM) score (Leone et al., 2013), CD274, CD8, Tumour Immune Dysfunction and Exclusion (TIDE) (Jiang et al., 2018), myeloid-derived suppressor cells (MDSCs), cancer-associated fibroblasts (CAFs), and the M2 subtype of tumor-associated macrophages (TAM-M2) (Joyce and Fearon, 2015). IFNG was calculated by averaging six genes (IFNG, STAT1, IDO1, CXCL9, CXCL10, HLA-DRA) (Ayers et al., 2017). IFNG.GS was calculated as the average expression of all genes in the set (Benci et al., 2019). APS was defined as the mRNA expression status of APM genes (PSMB5, PSMB6, PSMB7, PSMB8, PSMB9, PSMB10, TAP1, TAP2, ERAP1, ERAP2, CANX, CALR, PDIA3, TAPBP, B2M, HLA-A, HLA-B, and HLA-C) (Leone et al., 2013). CD274, CD8, TIDE, MDSCs, CAFs, and TAM-M2 were calculated using the web application (http://tide.dfci.harvard.edu). The relevant data are listed in **Supplementary Material S4**.

RESULTS

Development and validation of DM-BMI in breast, tumor-adjacent, and breast cancer tissues

A total of 221 breast tissues from non-BC cases (GEO database) were selected as the training cohort to develop the DNA-methylation-based BMI (DM-BMI) prediction model (**Figure 1**). The median BMI and median age of the training cohort were 28.24 (6.07–53.74) and 37 (17–82). Fifty lasso regression models based on DNA methylation data of the training cohort (301,998 probes per sample) were constructed. A model with minimum mean-squared error was selected based on the Lambda value (**Supplementary Figure S1A**). Forty-two probes were included and their coefficients are shown in **Supplementary Figure S1B** and **Supplementary Material S5**. We used Spearman correlation coefficient and paired *t*-test to assess the predictive accuracy of the DM-BMI model. DM-BMI showed a significant correlation with BMI (**Figure 2A**) while paired *t*-test revealed that there was no significant difference between DM-BMI and BMI ($t = -0.384$, df = 220, p-value = 0.702). Using a deconvolution algorithm, we evaluated the breast tissue composition and observed that the increased DM-BMI was significantly correlated with higher proportion of adipose tissue (**Figure 2B**). These results showed the high accuracy of DM-BMI for BMI prediction.

Next, 44 normal breast cases (Validation Set 1) and 70 tumor-adjacent breast tissues (Validation Set 2) were enrolled for external validation (**Figure 1**). The median BMI and median age of Validation Set 1 were 27.1 (14.6–62.7) and 44 (13–80); median BMI and median age of Validation Set 2 were 28.65 (16.5–53.4) and 56 (29–84). In both Validation Sets 1 and 2, DM-BMI showed positive correlation with BMI (**Figures 2C,E**). Paired *t*-test revealed that there was no significant difference between DM-BMI and BMI ($t = -0.253$, $df = 43$, p-value = 0.801,

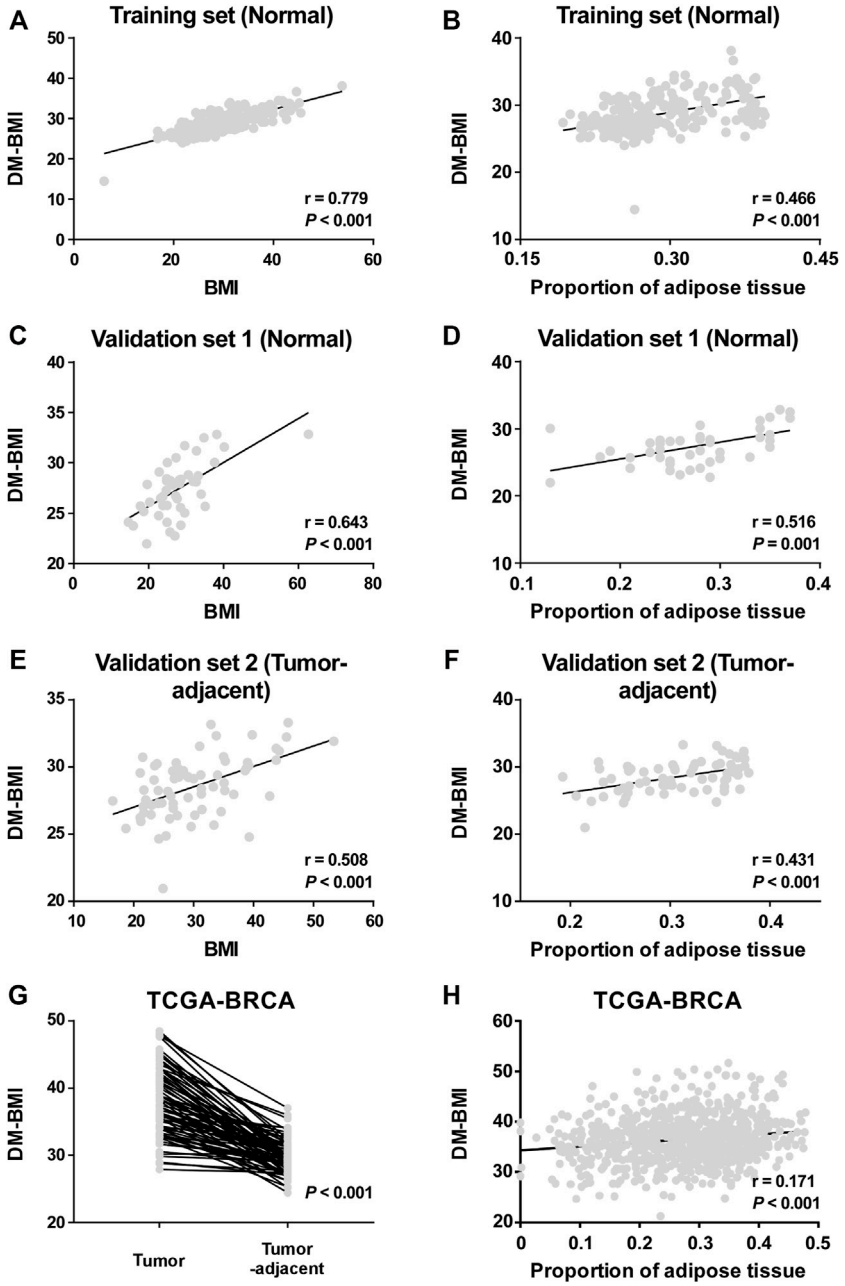

FIGURE 2 | Development and validation of the DA-BMI predicting model. **(A,B)** Correlation of DM-BMI with **(A)** BMI and **(B)** proportion of adipose tissue in normal breast tissues based on the training set (GSE88883 and GSE101961). **(C,D)** Correlation of DM-BMI with **(C)** BMI and **(D)** proportion of adipose tissue in normal breast tissues based on Validation Set 1 (GSE67919 and GSE74214). **(E,F)** Correlation of DM-BMI with **(E)** BMI and **(F)** proportion of adipose tissue in tumor-adjacent breast tissues based on Validation Set 2 (GSE67919). **(G)** Analyzing the differences of DM-BMI between tumor tissues (n = 76) and matched tumor-adjacent breast tissues (n = 76) based on the TCGA-BRCA dataset. **(H)** Correlation of DM-BMI with proportion of adipose tissue in BC tissues based on the TCGA-BRCA dataset (n = 775). (A-F and H) *r*, Spearman correlation coefficient. **(G)** p-values were determined by paired *t*-test.

Validation Set 1; $t = -1.87$, $df = 69$, p-value = 0.066, Validation Set 2). Moreover, DM-BMI is significantly correlated with adipose tissue proportion in both normal and tumor-adjacent breast tissues (**Figures 2D,F**). The above results showed a high prediction accuracy of DM-BMI model in normal and tumor-adjacent breast tissues.

Furthermore, we assessed the DM-BMI of paired tumor and tumor-adjacent breast tissues in TCGA database. The tumor tissues exhibited a higher level of DM-BMI compared with its paired tumor-adjacent tissues (**Figure 2G**). In BC tissues, DM-BMI is positively correlated with adipose tissue proportion (**Figure 2H**).

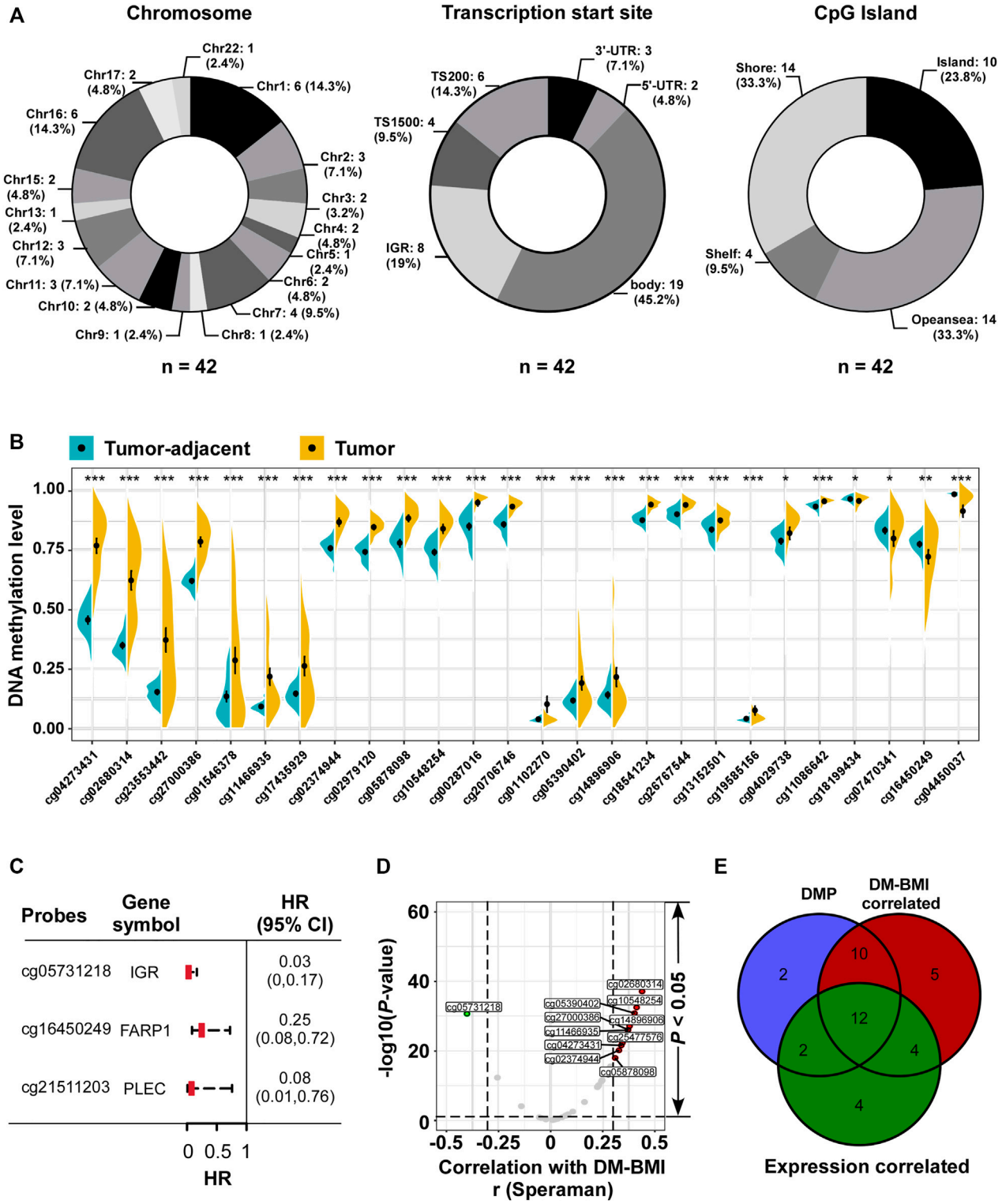

FIGURE 3 | Characteristic analyses of BMI predictors. **(A)** Distribution of 42 BMI predictors referring to (Left) chromosome and (Middle) transcription Start Sites; CpG islands were listed as number (proportion). For chromosome, no BMI predictors were located in Chr14, 18, 19, 20, and 21. **(B)** Identification of differential methylation BMI predictors between tumor tissues and matched tumor-adjacent breast tissues in TCGA dataset (n = 76). *p < 0.05, **p < 0.01, ***p < 0.001. **(C)** Forest plot of the prognostic related BMI predictors referring to DNA methylation level from TCGA BC tissues (*n* = 774): three BMI predictors (mapping to FARP1, PLEC, and cg05731218 located in the intergenic region/IGR) negatively correlated with overall survival. **(D)** Volcano plot of the correlation analysis between DM-BMI and

(*Continued*)

FIGURE 3 | methylation level of BMI predictors. *r*, Spearman correlation coefficient; 39 BMI predictors positively correlated with DM-BMI (BMI predictors with correlation coefficient >0.3 were marked as red dot; n = 10), and five BMI predictors negatively correlated with DM-BMI (BMI predictors with Spearman correlation coefficient < –0.3 were marked as green dot; n = 1). **(E)** Venn diagram of DMP; DM-BMI-correlated and expression-correlated BMI predictors. BMI predictors differentially methylated between tumor and tumor-adjacent tissues were labeled as blue; methylation levels of the BMI predictors correlated with DM-BMI were labeled as red; methylation levels of BMI predictors negatively correlated with gene expression were labeled as green.

What is known about the 42 body mass index predictors?

As DM-BMI was significantly correlated with obesity status, which has been suggested to regard as a risk factor for BC, we further assessed the relevance between BMI predictors and BC. As hyper-methylation of CpG island at gene promoter regions often causes gene silencing, we first evaluated the distribution of BMI predictors. Among 22 pairs of chromosomes (Chr), Chr1 and 16 are the most common region for BMI predictor distribution; 45.2% of BMI predictors were located at the gene body regions while only 23.8% of them were located at the promoter regions (TS1500 and TS200). Furthermore, we observed that only a few parts of BMI predictors were located at CpG islands (**Figure 3A**).

Next, we assessed the methylation variation of BMI predictors between tumor and tumor-adjacent breast tissues. Twenty-six differentially methylated probes (DMP) were identified: 22 BMI predictors were hyper-methylated in tumor tissues compared with the tumor-adjacent breast tissues; 4 were hypo-methylated in tumor (**Figure 3B**). Three of 42 BMI predictors were correlated with better OS for BC patients, while 2 of them were located at gene-coding regions (**Figure 3C**). In BC tissues, the correlation between the methylation level of 42 BMI predictors and DM-BMI was evaluated. Eleven of them were significantly correlated with DM-BMI (correlation coefficient >0.3 or < –0.3; **Figures 3D,E**); 35 of 42 BMI predictors were matched to the human gene region. Through the integrative analysis of DNA methylation and expression data, the negative correlation between methylation level and gene expression was observed in 22 of 42 BMI predictors (**Figure 3E**).

Functional and clinical characteristics analysis of DM-BMI related gene profile in breast cancer

Later we explored the biological significance of DM-BMI in breast cancer tissues. The survival correlation of DM-BMI was evaluated in BCs and the subgroup of BCs with cancer therapy (chemotherapy, endocrine-therapy, anti-HER2 therapy, and radiation-therapy). DM-BMI was consistently correlated with higher mortality risk in the whole cohort of BC patients and subgroups of patients with chemotherapy, endocrine-therapy or radiation-therapy, respectively (**Table 2**). Tissues from patients with postmenopausal status and TP53-mutation exhibited a significantly higher level of DM-BMI (**Figures 4A,B**). Apart from that, an increasing level of DM-BMI was correlated with an increased proportion of ERBB2 and MYC amplification (**Figures 4C,D**).

TABLE 2 | Survival analysis of DM-BMI in BC with systemic therapy

Subgroup	Hazard ratio (high vs. Low)	95%CI	p-Value
Overall	1.046329459	1.005–1.089	0.027924058
Chemotherapy	1.100065801	1.029–1.176	0.00529122
Hormone therapy	1.087123098	1.009–1.171	0.027857745
Anti-HER2 therapy	1.048120675	0.832–1.320	0.689677033
Radiation therapy	1.0775886	1.003–1.158	0.041331982

Previous studies showed that adipokines produced by obese adipose tissues leads to obesity-mediated inflammation and BC progression. In BC tissues, sections of adipose tissue were positively correlated with DM-BMI. Expression of six pro-inflammatory adipokines was positively correlated with DM-BMI while the expression of two anti-inflammatory adipokines was negatively correlated with DM-BMI (**Figure 4E**). These results indicated that obesity increased the expression of pro-inflammatory adipokines in BC tissues.

Furthermore, we assessed the DM-BMI (obesity)-related gene expression profile and mRNA expression of 10,032 genes significantly correlated with DM-BMI. To evaluate the biological effect of obesity on BC, we performed a GSEA analysis of DM-BMI-related genes using KEGG and GO database. GO analysis showed that gens positively correlated with DM-BMI were significantly involved in antigen process and presentation, immune cell activation, MHC protein binding, and immune receptor activity in BC (**Figure 4F**). KEGG consistently showed that DM-BMI-related genes were significantly enriched in tumor-immunity-related pathway (which includes antigen processing and presentation, NK cell-mediated cytotoxicity, T cell differentiation, and PD-1 checkpoint pathway) (**Figure 4G**). These results indicated that the obesity-related gene profile is involved in the regulation of immune response in BC.

DM-BMI correlated with T-cell infiltration and immune checkpoint inhibitor response markers in breast cancer

We evaluated the correlation between obesity and immune response to BC. Gene mutation which changes the protein-coding sequence and leads to the expression of abnormal proteins was suggested to be the driving factor for cancer development. Also, the abnormal protein derived from tumor mutation might rouse immune response. In BC tissues, we observed a positive correlation between DM-BMI and TMB (**Figure 5A**). Using the Estimate algorithm, we evaluated the degree of immune cell infiltration in TCGA BC tissues.

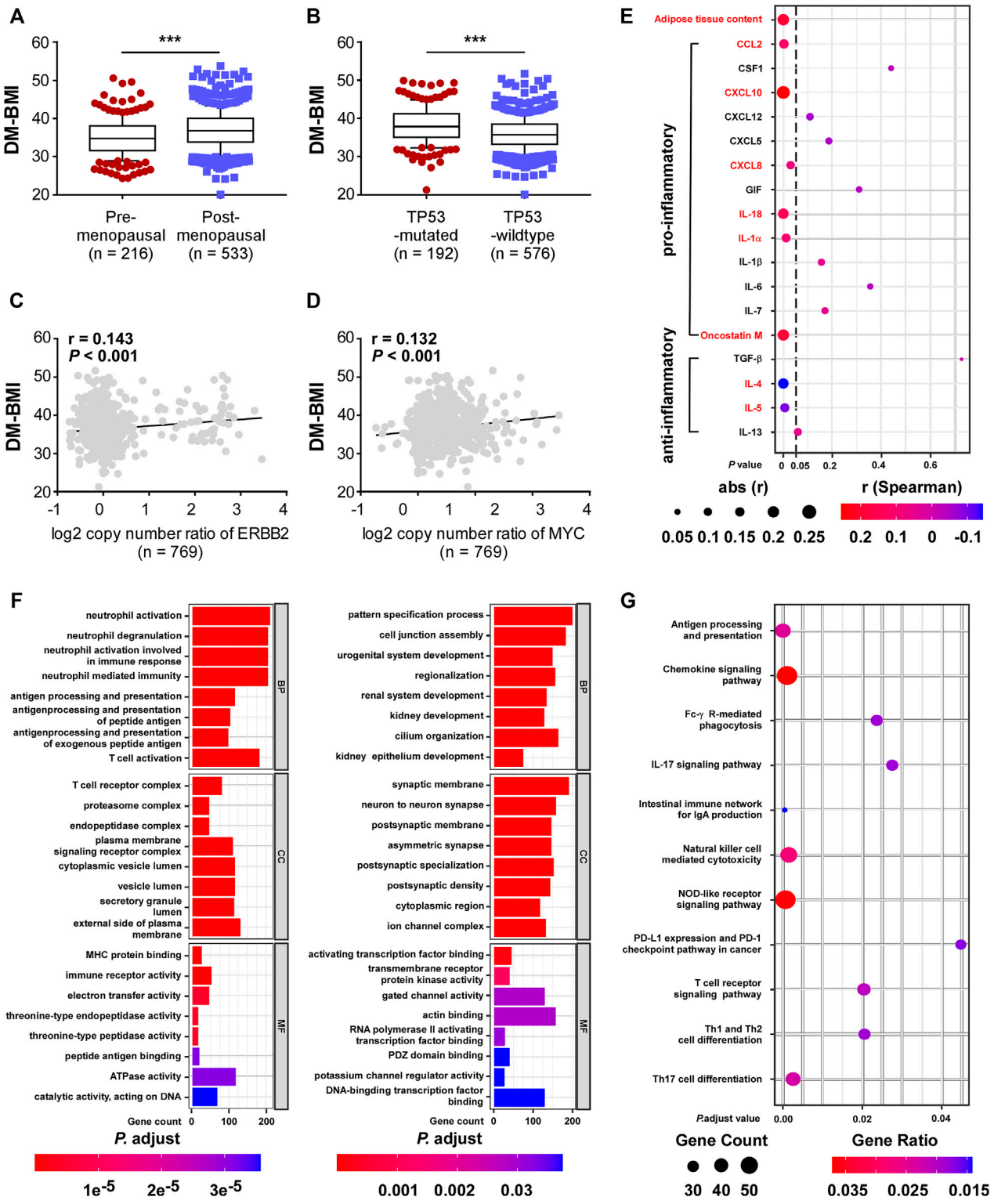

FIGURE 4 | Functional and clinical characteristics analysis of DM-BMI-related gene profile in BC. **(A,B)** Analyzing the differences of DM-BMI based on **(A)** menopause status of patients (n = 749) or TP53 mutation status (n = 768) based on TCGA-BRCA dataset. **(C,D)** Correlation of DM-BMI with copy number of **(C)** ERBB2 and **(D)** MYC. *r*, Spearman correlation coefficient. **(E)** Correlation of DM-BMI and expression of pro/anti-inflammatory adipokines in BC tissues (n = 771). Expressions of adipokines significantly correlated with DM-BMI were labeled as red. **(F)** GO function analysis of DM-BMI related gene. (Left) Analysis of gene whose mRNA expression positively correlated with DM-BMI (Ayers et al., 2017); analysis of gene whose mRNA expression negatively correlated with DM-BMI. **(G)** Analysis of DM-BMI-related gene enrichment in immunologic pathway based on KEGG database. Gene ratio was defined as: number of genes enriched to target pathway/number of DM-BMI related genes included in the KEGG dataset.

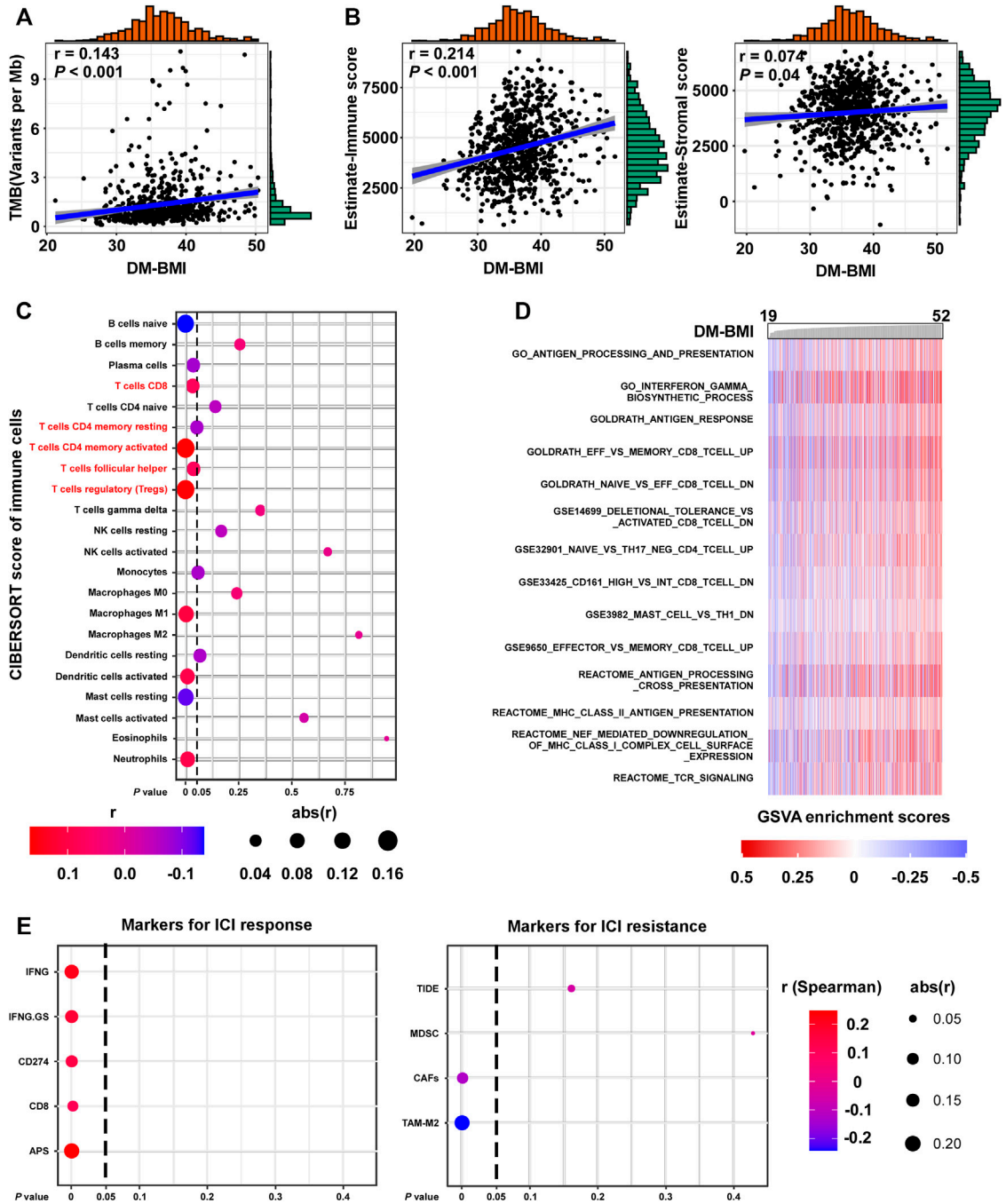

FIGURE 5 | DM-BMI correlated with T cell infiltration and ICI response in BC. **(A)** Correlation of DM-BMI with tumor mutation burden (TMB) in BC tissues (TCGA-BRCA, n = 775). Numerical distribution of DM-BMI and TMB is shown on the above *x*- and the right *y*-axis, respectively. **(B)** Correlation of DM-BMI with the level of infiltrating immune cells (Left, estimate-immune score) and the level of stromal cells (Right, estimate-stromal score) in BC tissues (TCGA-BRCA, n = 772). Numerical distribution of DM-BMI and estimate-immune/stromal score is shown on the above *x*- and the right *y*-axis, respectively. **(C)** Correlation of DM-BMI with 22 types of immune cell components is shown by dotplot. Five of 7 T-cell contents correlated with DM-BMI, which were labeled in red. **(D)** GSVA analysis identified an immunologic pathway which positively correlated with DM-BMI. Enrichment scores of pathways from the GSEA-Molecular Signatures Database were calculated using GSVA in BC tissues (TCGA-BRCA-mRNA data, *n* = 771). Immunologic gene sets which significantly correlated with DM-BMI are displayed (*r* > 0.3). **(E)** Correlation of DM-BMI with markers for ICI response/resistance is shown by dotplot. For **(A,B)**, *r*, Spearman correlation coefficient.

Interestingly, we found a positive correlation between DM-BMI and Estimate-immune score while no significant correlation was observed between DM-BMI and Estimate-Stromal score (**Figure 5B**). Next, we calculated the relative abundance of 22 immune cell types in TCGA BC tissues. Among them, the content of CD8-T, CD4 memory-activated T, T follicular helper, and regulatory T cells (Treg) were positively correlated with DM-BMI, indicating a more intense T cell-mediated immune response in BC tissues with increased DM-BMI (**Figures 5C,D**). As the representative of immunotherapy, the ICI therapy suppressed BC progression by activating T cell-mediated immune response. Thus, we examined whether DM-BMI predicted the tumor response to ICI. Five markers for ICI response and four markers for ICI resistance were selected to evaluate the tumor response. In BC tissues, DM-BMI is positively correlated with IFNG, IFNG.GS, CD274, CD8, and APS, indicating that BC tissues with increased DM-BMI exhibited a better response to ICI (**Figures 5A,E**). Moreover, DM-BMI was negatively correlated with two ICI resistance markers (CAFs and TAM-M2). All those results indicated that BC tissue at obesity status might exhibit a more intense response to ICI based on markers of ICI response.

DISCUSSION

Based on the DNA methylation pattern, we developed an obesity evaluation model (DM-BMI) in the study. We then further identified the obesity-related gene expression profile based on the DM-BMI model. Although obesity has been shown to be a BC risk factor for many years, most studies have been focusing on the correlation between obesity and clinical prognosis while studies about the biological and genomic impact of obesity on breast cancer were limited. The adipose tissue, as the major agent mediating obesity-related biological effects, is an important starting point for the study of the obesity impact. In both breast and BC tissue, we observed a positive correlation between the proportion adipose tissue content and the DM-BMI. Previous studies reported that the expansion of adipose tissue, accompanied by the dysregulation of the endocrine function (adipokine secretion) of the adipose cells, was driven by an increase in size of adipose or by a formation of a new adipose cell (Ghaben and Scherer, 2019; Quail and Dannenberg, 2019). As the DM-BMI increased, we observed an increased expression of pro-inflammatory adipokines but a decreased expression of anti-inflammatory adipokines which might synergistically induce obesity-mediated inflammation through the activation of the NF-κB pathway and a pro-oncogenic environment.

In addition to the expansion of adipose tissue, we also observed a promoting effect of obesity on immune response in BC tissue. For those obese individuals, adipose tissue expands with the increasing demand of oxygen, which induces the development of the hypoxia environment (Iwamoto et al., 2018). The activation of hypoxia signaling increases the expression of adipokines, especially the pro-inflammation adipokines (including CCL2, CXCL8, CXCL10, IL-18, IL-1α and Oncostatin M), which is involved in the recruitment of tumor-associated immune cells (Taylor and Colgan, 2017; Hou et al., 2020; McGettrick and O'Neill, 2020). Moreover, previous studies showed that adipocytes could fuel immune cells by releasing exosome-sized and lipid-filled vesicles (Flaherty et al., 2019; Zhang et al., 2020). In BC tissues, we observed that DM-BMI is positively correlated with the degree of M1 macrophages and activated dendritic cell and T cell infiltration, indicating an increase activity of tumor immune response. As T cell exhaustion is the key for tumor immune escape, previous studies have indicated that T cell exhaustion could be reversed by immune checkpoint inhibition (such as PD-1 inhibition) and replenishing activated T cells (such as CAR-T) (Bajgain et al., 2018; Bassez et al., 2021). Interestingly, in obese BC tissues, we found an increase content of CD4 +CD8 + and follicular helper T cells, which may be the result of an increased secretion of immune chemokines in adipose tissue. Although we observed a positive correlation between DM-BMI and regulatory T cell (Treg), coupled with a subset of immune cell with immunosuppressive activity, they can be interpreted as a negative feedback regulation by the immune system to maintain the stability of the immune environment after the activation of the immune response (von Boehmer and Daniel, 2013). Furthermore, our study revealed that DM-BMI is positively correlated with ICI response markers in BC tissues. These results suggest that obese BC patients may benefit from ICI. Recently, Wang et al. consistently reported that obesity is concerned with increased response of PD-1/PD-L1 blockade in an animal melanoma tumor model (Wang et al., 2019). However, as our findings were mainly supported by database analysis, data from clinical samples treated with ICI treatment are still required to validate the correlation between DM-BMI and ICI response.

With the increasing number of obese patients, the impact of obesity on the treatment of breast cancer has aroused more and more attention. We observed that the increased DM-BMI was correlated with higher mortality risk in patients with chemotherapy, hormone therapy, and radiation therapy. Although no evidence pointed out that obesity will induce drug-resistance in cancer cell, dose of chemotherapy and radiation might still be routinely reduced in obese individuals as doctors usually limit body surface area under 2 m^2 to reduce toxicity when calculating the dose of chemotherapy (Lyman, 2012; Picon-Ruiz et al., 2017). As is highly expressed of aromatase, adipose tissue is an endocrine organ, which is an important site for estrogen biosynthesis, especially for postmenopausal women (Liedtke et al., 2012). For obese BC patients, increased expression of aromatase might cause the resistance to endocrine-therapy.

Because of the limitation of BMI in obesity evaluation, several imaging methods have been developed for obesity evaluation (including: bioimpedance analysis instruments, dual-energy x-ray absorptiometry, computed tomography, and magnetic resonance imaging) (Karlsson et al., 2013; Neamat-Allah et al., 2014). Although these new methods enabled the precise quantification of adipose tissue, the operational complexity did limit their application (Nimptsch et al., 2019). Developing new methods to evaluate the degree of obesity is of great value.

Recently, an increased number of studies indicated that environmental factors (such as dietary pattern and lifestyle) will induce changes in the DNA methylation pattern predisposing to obesity and obesity and, likewise, results in genome-wide methylation variation (Wahl et al., 2017; Samblas et al., 2019). Moreover, biomarkers based on DNA methylation have been shown to be effective in obesity evaluation while most of them were only applied in blood samples (Samblas et al., 2019). Thus, we developed a DNA-methylation-based biomarker (DM-BMI) for obesity evaluation in breast tissue. In both normal breast and tumor-adjacent breast tissue, DM-BMI showed a significant correlation in both BMI and the content of adipose tissue. In addition, we also observed that DM-BMI was positively correlated with the degree of pro-inflammatory adipokine and immune cell infiltration in BC tissues. All those data indicated that DM-BMI is an effective biomarker to evaluate the biological changes in tumor tissues of obese patients.

The identification of BMI predictors naturally causes the assumption that these CpGs are critical regulators of obesity. In our study, only 11 of 42 BMI predictors were significantly correlated with DM-BMI while the others exhibited negligible correlation with DM-BMI. Although DNA methylation level was negatively correlated with gene expression in over half of BMI predictors, 45.2% of BMI predictors were located at the body region of gene sequence. How the CpGs located at the body region regulate gene expression remains unclear. As a previous study reported, the variations of DNA methylation pattern are the consequence, rather than cause, of adiposity (Wahl et al., 2017). Whether these BMI predictors are regulators of obesity or imprints of the biological process remained to be further investigated.

CONCLUSION

Collectively, we established a new biomarker for obesity evaluation and discovered that BC tissues of obese individuals exhibit an increased degree of immune cell infiltration, indicating that obese BC patients might be the potential beneficiaries for ICI treatment.

DATA AVAILABILITY STATEMENT

The datasets presented in this study can be found in online repositories. The names of the repository/repositories and accession number(s) can be found in the article/ **Supplementary Material**.

AUTHOR CONTRIBUTIONS

XH and FX designed the overall project; ZX and XL analyzed the data and wrote the manuscript; ZX and LY collected and analyzed the data; XL, LW, and YX did the statistical analysis. All the authors have read and approved the final manuscript.

FUNDING

The study was supported by funds from the National Natural Science Foundation of China (81974444 to XX).

ACKNOWLEDGMENTS

We thank Qian Chen for helping us with polishing the manuscript.

SUPPLEMENTARY MATERIAL

The Supplementary Material for this article can be found online at: https://www.frontiersin.org/articles/10.3389/fcell.2022.818082/full#supplementary-material

REFERENCES

Ayers, M., Lunceford, J., Nebozhyn, M., Murphy, E., Loboda, A., Kaufman, D. R., et al. (2017). IFN-γ-related mRNA Profile Predicts Clinical Response to PD-1 Blockade. *J. Clin. Invest.* 127 (8), 2930–2940. doi:10.1172/jci91190

Bajgain, P., Tawinwung, S., D'Elia, L., Sukumaran, S., Watanabe, N., Hoyos, V., et al. (2018). CAR T Cell Therapy for Breast Cancer: Harnessing the Tumor Milieu to Drive T Cell Activation. *J. Immunotherapy Cancer* 6 (1), 34. doi:10.1186/s40425-018-0347-5

Bassez, A., Vos, H., Van Dyck, L., Floris, G., Arijs, I., Desmedt, C., et al. (2021). A Single-Cell Map of Intratumoral Changes during Anti-PD1 Treatment of Patients with Breast Cancer. *Nat. Med.* 27 (5), 820–832. doi:10.1038/s41591-021-01323-8

Benci, J. L., Johnson, L. R., Choa, R., Xu, Y., Qiu, J., Zhou, Z., et al. (2019). Opposing Functions of Interferon Coordinate Adaptive and Innate Immune Responses to Cancer Immune Checkpoint Blockade. *Cell* 178 (4), 933–948. e914. doi:10.1016/j.cell.2019.07.019

Bosello, O., Donataccio, M. P., and Cuzzolaro, M. (2016). Obesity or Obesities? Controversies on the Association between Body Mass index and Premature Mortality. *Eat. Weight Disordewd* 21 (2), 165–174. doi:10.1007/s40519-016-0278-4

Bray, F., Ferlay, J., Soerjomataram, I., Siegel, R. L., Torre, L. A., and Jemal, A. (2018). Global Cancer Statistics 2018: GLOBOCAN Estimates of Incidence and Mortality Worldwide for 36 Cancers in 185 Countries. *CA: a Cancer J. clinicians* 68 (6), 394–424. doi:10.3322/caac.21492

Bray, G. A., Frühbeck, G., Ryan, D. H., and Wilding, J. P. H. (2016). Management of Obesity. *The Lancet* 387 (10031), 1947–1956. doi:10.1016/s0140-6736(16)00271-3

Cabre, N., Luciano-Mateo, F., Chapski, D. J., Baiges-Gaya, G., Fernandez-Arroyo, S., Hernandez-Aguilera, A., et al. (2021). Glutaminolysis-induced mTORC1 Activation Drives Non-alcoholic Steatohepatitis Progression. *J. Hepatol.*. doi:10.1016/j.jhep.2021.04.037

Chalmers, Z. R., Connelly, C. F., Fabrizio, D., Gay, L., Ali, S. M., Ennis, R., et al. (2017). Analysis of 100,000 Human Cancer Genomes Reveals the Landscape of Tumor Mutational burden. *Genome Med.* 9 (1), 34. doi:10.1186/s13073-017-0424-2

Conway, B., and Rene, A. (2004). Obesity as a Disease: No Lightweight Matter. *Obes. Rev.* 5 (3), 145–151. doi:10.1111/j.1467-789x.2004.00144.x

Copson, E. R., Cutress, R. I., Maishman, T., Eccles, B. K., Gerty, S., Stanton, L., et al. (2015). Obesity and the Outcome of Young Breast Cancer Patients in the UK: the POSH Study. *Ann. Oncol.* 26 (1), 101–112. doi:10.1093/annonc/mdu509

Flaherty, S. E., 3rd, Grijalva, A., Xu, X., Ables, E., Nomani, A., and Ferrante, A. W., Jr. (2019). A Lipase-independent Pathway of Lipid Release and Immune

Modulation by Adipocytes. *Science* 363 (6430), 989–993. doi:10.1126/science.aaw2586

Gentles, A. J., Newman, A. M., Liu, C. L., Bratman, S. V., Feng, W., Kim, D., et al. (2015). The Prognostic Landscape of Genes and Infiltrating Immune Cells across Human Cancers. *Nat. Med.* 21 (8), 938–945. doi:10.1038/nm.3909

Ghaben, A. L., and Scherer, P. E. (2019). Adipogenesis and Metabolic Health. *Nat. Rev. Mol. Cel Biol* 20 (4), 242–258. doi:10.1038/s41580-018-0093-z

Hair, B. Y., Troester, M. A., Edmiston, S. N., Parrish, E. A., Robinson, W. R., Wu, M. C., et al. (2015). Body Mass index Is Associated with Gene Methylation in Estrogen Receptor-Positive Breast Tumors. *Cancer Epidemiol. Biomarkers Prev.* 24 (3), 580–586. doi:10.1158/1055-9965.epi-14-1017

Hair, B. Y., Xu, Z., Kirk, E. L., Harlid, S., Sandhu, R., Robinson, W. R., et al. (2015). Body Mass index Associated with Genome-wide Methylation in Breast Tissue. *Breast Cancer Res. Treat.* 151 (2), 453–463. doi:10.1007/s10549-015-3401-8

Hänzelmann, S., Castelo, R., and Guinney, J. (2013). GSVA: Gene Set Variation Analysis for Microarray and RNA-Seq Data. *BMC bioinformatics* 14, 7. doi:10.1186/1471-2105-14-7

Hou, J., Zhao, R., Xia, W., Chang, C.-W., You, Y., Hsu, J.-M., et al. (2020). PD-L1-mediated Gasdermin C Expression Switches Apoptosis to Pyroptosis in Cancer Cells and Facilitates Tumour Necrosis. *Nat. Cel Biol* 22 (10), 1264–1275. doi:10.1038/s41556-020-0575-z

Iwamoto, H., Abe, M., Yang, Y., Cui, D., Seki, T., Nakamura, M., et al. (2018). Cancer Lipid Metabolism Confers Antiangiogenic Drug Resistance. *Cel Metab.* 28 (1), 104–117. doi:10.1016/j.cmet.2018.05.005

Jiang, P., Gu, S., Pan, D., Fu, J., Sahu, A., Hu, X., et al. (2018). Signatures of T Cell Dysfunction and Exclusion Predict Cancer Immunotherapy Response. *Nat. Med.* 24 (10), 1550–1558. doi:10.1038/s41591-018-0136-1

Jiralerspong, S., and Goodwin, P. J. (2016). Obesity and Breast Cancer Prognosis: Evidence, Challenges, and Opportunities. *Jco* 34 (35), 4203–4216. doi:10.1200/jco.2016.68.4480

Joyce, J. A., and Fearon, D. T. (2015). T Cell Exclusion, Immune Privilege, and the Tumor Microenvironment. *Science* 348 (6230), 74–80. doi:10.1126/science.aaa6204

Karlsson, A.-K., Kullberg, J., Stokland, E., Allvin, K., Gronowitz, E., Svensson, P.-A., et al. (2013). Measurements of Total and Regional Body Composition in Preschool Children: A Comparison of MRI, DXA, and Anthropometric Data. *Obesity* 21 (5), 1018–1024. doi:10.1002/oby.20205

Khandekar, M. J., Cohen, P., and Spiegelman, B. M. (2011). Molecular Mechanisms of Cancer Development in Obesity. *Nat. Rev. Cancer* 11 (12), 886–895. doi:10.1038/nrc3174

Leone, P., Shin, E.-C., Perosa, F., Vacca, A., Dammacco, F., and Racanelli, V. (2013). MHC Class I Antigen Processing and Presenting Machinery: Organization, Function, and Defects in Tumor Cells. *JNCI J. Natl. Cancer Inst.* 105 (16), 1172–1187. doi:10.1093/jnci/djt184

Liedtke, S., Schmidt, M. E., Vrieling, A., Lukanova, A., Becker, S., Kaaks, R., et al. (2012). Postmenopausal Sex Hormones in Relation to Body Fat Distribution. *Obesity (Silver Spring, Md)* 20 (5), 1088–1095. doi:10.1038/oby.2011.383

Ling, C., and Rönn, T. (2019). Epigenetics in Human Obesity and Type 2 Diabetes. *Cel Metab.* 29 (5), 1028–1044. doi:10.1016/j.cmet.2019.03.009

Lyman, G. H. (2012). Weight-based Chemotherapy Dosing in Obese Patients with Cancer: Back to the Future. *Jop* 8 (4), e62–e64. doi:10.1200/jop.2012.000606

Maguire, O. A., Ackerman, S. E., Szwed, S. K., Maganti, A. V., Marchildon, F., Huang, X., et al. (2021). Creatine-mediated Crosstalk between Adipocytes and Cancer Cells Regulates Obesity-Driven Breast Cancer. *Cel Metab.* 33 (3), 499–512. e496. doi:10.1016/j.cmet.2021.01.018

McGettrick, A. F., and O'Neill, L. A. J. (2020). The Role of HIF in Immunity and Inflammation. *Cel Metab.* 32 (4), 524–536. doi:10.1016/j.cmet.2020.08.002

Neamat-Allah, J., Wald, D., Hüsing, A., Teucher, B., Wendt, A., Delorme, S., et al. (2014). Validation of Anthropometric Indices of Adiposity against Whole-Body Magnetic Resonance Imaging - A Study within the German European Prospective Investigation into Cancer and Nutrition (EPIC) Cohorts. *PloS one* 9 (3), e91586. doi:10.1371/journal.pone.0091586

Nimptsch, K., Konigorski, S., and Pischon, T. (2019). Diagnosis of Obesity and Use of Obesity Biomarkers in Science and Clinical Medicine. *Metabolism* 92, 61–70. doi:10.1016/j.metabol.2018.12.006

Picon-Ruiz, M., Morata-Tarifa, C., Valle-Goffin, J. J., Friedman, E. R., and Slingerland, J. M. (2017). Obesity and Adverse Breast Cancer Risk and Outcome: Mechanistic Insights and Strategies for Intervention. *CA: a Cancer J. clinicians* 67 (5), 378–397. doi:10.3322/caac.21405

Pierobon, M., and Frankenfeld, C. L. (2013). Obesity as a Risk Factor for Triple-Negative Breast Cancers: a Systematic Review and Meta-Analysis. *Breast Cancer Res. Treat.* 137 (1), 307–314. doi:10.1007/s10549-012-2339-3

Prentice, A. M., and Jebb, S. A. (2001). Beyond Body Mass index. *Obes. Rev.* 2 (3), 141–147. doi:10.1046/j.1467-789x.2001.00031.x

Quail, D. F., and Dannenberg, A. J. (2019). The Obese Adipose Tissue Microenvironment in Cancer Development and Progression. *Nat. Rev. Endocrinol.* 15 (3), 139–154. doi:10.1038/s41574-018-0126-x

Ritchie, M. E., Phipson, B., Wu, D., Hu, Y., Law, C. W., Shi, W., et al. (2015). Limma powers Differential Expression Analyses for RNA-Sequencing and Microarray Studies. *Nucleic Acids Res.* 43 (7), e47. doi:10.1093/nar/gkv007

Samblas, M., Milagro, F. I., and Martínez, A. (2019). DNA Methylation Markers in Obesity, Metabolic Syndrome, and Weight Loss. *Epigenetics* 14 (5), 421–444. doi:10.1080/15592294.2019.1595297

Shah, S. P., Roth, A., Goya, R., Oloumi, A., Ha, G., Zhao, Y., et al. (2012). The Clonal and Mutational Evolution Spectrum of Primary Triple-Negative Breast Cancers. *Nature* 486 (7403), 395–399. doi:10.1038/nature10933

Sung, H., Siegel, R. L., Torre, L. A., Pearson-Stuttard, J., Islami, F., Fedewa, S. A., et al. (2019). Global Patterns in Excess Body Weight and the Associated Cancer burden. *CA Cancer J. Clin.* 69 (2), 88–112. doi:10.3322/caac.21499

Suzuki, R., Orsini, N., Saji, S., Key, T. J., and Wolk, A. (2009). Body Weight and Incidence of Breast Cancer Defined by Estrogen and Progesterone Receptor Status-A Meta-Analysis. *Int. J. Cancer* 124 (3), 698–712. doi:10.1002/ijc.23943

Taylor, C. T., and Colgan, S. P. (2017). Regulation of Immunity and Inflammation by Hypoxia in Immunological Niches. *Nat. Rev. Immunol.* 17 (12), 774–785. doi:10.1038/nri.2017.103

Teschendorff, A. E., Gao, Y., Jones, A., Ruebner, M., Beckmann, M. W., Wachter, D. L., et al. (2016). DNA Methylation Outliers in normal Breast Tissue Identify Field Defects that Are Enriched in Cancer. *Nat. Commun.* 7, 10478. doi:10.1038/ncomms10478

Tian, Y., Morris, T. J., Webster, A. P., Yang, Z., Beck, S., Feber, A., et al. (2017). ChAMP: Updated Methylation Analysis Pipeline for Illumina BeadChips. *Bioinformatics* 33 (24), 3982–3984. doi:10.1093/bioinformatics/btx513

von Boehmer, H., and Daniel, C. (2013). Therapeutic Opportunities for Manipulating TReg Cells in Autoimmunity and Cancer. *Nat. Rev. Drug Discov.* 12 (1), 51–63. doi:10.1038/nrd3683

Wahl, S., Drong, A., Lehne, B., Loh, M., Scott, W. R., Kunze, S., et al. (2017). Epigenome-wide Association Study of Body Mass index, and the Adverse Outcomes of Adiposity. *Nature* 541 (7635), 81–86. doi:10.1038/nature20784

Wang, Z., Aguilar, E. G., Luna, J. I., Dunai, C., Khuat, L. T., Le, C. T., et al. (2019). Paradoxical Effects of Obesity on T Cell Function during Tumor Progression and PD-1 Checkpoint Blockade. *Nat. Med.* 25 (1), 141–151. doi:10.1038/s41591-018-0221-5

Yoshihara, K., Shahmoradgoli, M., Martínez, E., Vegesna, R., Kim, H., Torres-Garcia, W., et al. (2013). Inferring Tumour Purity and Stromal and Immune Cell Admixture from Expression Data. *Nat. Commun.* 4, 2612. doi:10.1038/ncomms3612

Zhang, C., Yue, C., Herrmann, A., Song, J., Egelston, C., Wang, T., et al. (2020). STAT3 Activation-Induced Fatty Acid Oxidation in CD8+ T Effector Cells Is Critical for Obesity-Promoted Breast Tumor Growth. *Cel Metab.* 31 (1), 148–161. e145. doi:10.1016/j.cmet.2019.10.013

Conflict of Interest: The authors declare that the research was conducted in the absence of any commercial or financial relationships that could be construed as a potential conflict of interest.

Publisher's Note: All claims expressed in this article are solely those of the authors and do not necessarily represent those of their affiliated organizations, or those of the publisher, the editors, and the reviewers. Any product that may be evaluated in this article, or claim that may be made by its manufacturer, is not guaranteed or endorsed by the publisher.

frontiers in Cell and Developmental Biology

ORIGINAL RESEARCH
published: 10 March 2022
doi: 10.3389/fcell.2022.840759

Comprehensive Analysis of the Differential Expression and Prognostic Value of Histone Deacetylases in Glioma

Jinwei Li[1], Xianlei Yan[1], Cong Liang[1], Hongmou Chen[1], Meimei Liu[1], Zhikang Wu[1], Jiemin Zheng[1], Junsun Dang[1], Xiaojin La[2] and Quan Liu[1]**

[1]Department of Neurosurgery, The Fourth Affliated Hospital of Guangxi Medical University, Liuzhou, China, [2]College of Traditional Chinese Medicine, North China University of Science and Technology, Tangshan, China

OPEN ACCESS

Edited by:
Ângela Sousa,
University of Beira Interior, Portugal

Reviewed by:
Vijay Thakur,
University of Miami Hospital, United States
Yinyan Wang,
Capital Medical University, China

***Correspondence:**
Quan Liu
liuq0928@163.com
Xiaojin La
laxiaojin@ncst.edu.cn

Specialty section:
This article was submitted to Epigenomics and Epigenetics, a section of the journal Frontiers in Cell and Developmental Biology

Received: *21 December 2021*
Accepted: *31 January 2022*
Published: *10 March 2022*

Citation:
Li J, Yan X, Liang C, Chen H, Liu M, Wu Z, Zheng J, Dang J, La X and Liu Q (2022) Comprehensive Analysis of the Differential Expression and Prognostic Value of Histone Deacetylases in Glioma. Front. Cell Dev. Biol. 10:840759. doi: 10.3389/fcell.2022.840759

Gliomas are the most common and aggressive malignancies of the central nervous system. Histone deacetylases (HDACs) are important targets in cancer treatment. They regulate complex cellular mechanisms that influence tumor biology and immunogenicity. However, little is known about the function of HDACs in glioma. The Oncomine, Human Protein Atlas, Gene Expression Profiling Interactive Analysis, Broad Institute Cancer Cell Line Encyclopedia, Chinese Glioma Genome Atlas, OmicShare, cBioPortal, GeneMANIA, STRING, and TIMER databases were utilized to analyze the differential expression, prognostic value, and genetic alteration of HDAC and immune cell infiltration in patients with glioma. *HDAC1/2* were considerable upregulated whereas HDAC11 was significantly downregulated in cancer tissues. *HDAC1/2/3/4/5/7/8/11* were significantly correlated with the clinical glioma stage. *HDAC1/2/3/10* were strongly upregulated in 11 glioma cell lines. High *HDCA1/3/7* and low *HDAC4/5/11* mRNA levels were significantly associated with overall survival and disease-free survival in glioma. *HDAC1/2/3/4/5/7/9/10/11* are potential useful biomarkers for predicting the survival of patients with glioma. The functions of HDACs and 50 neighboring genes were primarily related to transcriptional dysregulation in cancers and the Notch, cGMP-PKG, and thyroid hormone signaling pathways. HDAC expression was significantly correlated with the infiltration of B cells, $CD4^+$ T cells, $CD8^+$ T cells, macrophages, neutrophils, and dendritic cells in glioma. Our study indicated that HDACs are putative precision therapy targets and prognostic biomarkers of survival in glioma patients.

Keywords: bioinformatics analysis, HDACs, immune infiltration, CGGA, Chinese Glioma Genome Atlas, biomarker, glioma

Abbreviations: CNS, central nervous system; GBM, glioblastoma; IHC, immunohistochemistry; HDAC, histone deacetylase; GEPIA, gene expression profiling interactive analysis; TCGA, The Cancer Genome Atlas; CCLE, Cancer Cell Line Encyclopedia; KEGG, Kyoto Encyclopedia of Genes and Genomes; LGG, lower-grade glioma; TIMER, Tumor Immune Estimation Resource.

INTRODUCTION

Glioma is the most common tumor of the central nervous system (CNS). It accounts for 30% of all CNS tumors and 80% of all malignant brain tumors (Ostrom et al., 2019). Progress has been made in glioblastoma (GBM) treatment by combining maximal surgical resection with radiotherapy and concurrent and adjuvant temozolomide chemotherapy. Nevertheless, the two- and five-year survival rates are only 25 and 10%, respectively, (Stupp et al., 2005; Stupp et al., 2009). Tumor heterogeneity is a major challenge in precise glioma diagnosis and therapy (Neftel et al., 2019). Hence, molecular signatures for glioma are urgently required (Song et al., 2014).

Growing evidence suggests that epigenetic and genetic changes are pivotal in malignant disease onset and progression (Jones and Baylin, 2007). Histone deacetylases (HDACs) are important regulators of gene expression and control a broad array of physiological processes such as differentiation, apoptosis, survival, proliferation, and autophagy. They are also involved in cancer pathogenesis (Glozak and Seto, 2007; Wilson et al., 2008; Kang et al., 2014). There are four HDAC families and 18 individual HDACs. The zinc-dependent HDAC family comprises 11 isoforms divided into class I (HDAC1–3 and 8), class IIa (HDAC4, 5, 7, and 9), class IIb (HDAC6 and 10), and class IV (HDAC11) (Kashyap and Kakkar, 2020). Class III HDACs are homologous to yeast Sir2 and participate in transcriptional silencing. However, they have a deoxyhypusine synthase-like NAD/FAD-binding domain that is distinct from those of the other HDAC classes (Park et al., 2021). HDAC1 and two act mainly via nucleosome remodeling and deacetylase, switch independent 3, mitotic deacetylase, and corepressor of REST complexes. HDAC3 is recruited only by the nuclear receptor corepressor complex (Millard et al., 2017). HDAC6 regulates Hsp90, tau, and the cytoskeleton by interacting with tubulin and cortactin. It recognizes ubiquitinated proteins and induces aggregate formation (Hubbert et al., 2002; Kovacs et al., 2005; Dompierre et al., 2007; Zhang et al., 2007; Cohen et al., 2011; Simões-Pires et al., 2013). HDAC10 is a polyamine deacetylase (Ho et al., 2020), and HDAC11 has limited homology to class I and II enzymes (Li et al., 2015).

HDACs play important roles in many diseases. HDAC1 promotes medulloblastoma growth and affects cell cycle progression, microtubule dynamics, and DNA damage response (Abdelfattah et al., 2018). Preclinical studies suggest a role for HDAC1 in the epigenetic regulation of sarcoma tumorigenesis (Bennani-Baiti and Idriss, 2011). HDAC2 is highly expressed in sarcomas (Pacheco and Nielsen, 2012). HDAC3 is a target of the HDAC inhibitors approved by the US Food and Drug Administration to treat lymphoid malignancies (Stengel et al., 2019). HDAC4 overexpression has been observed in acute promyelocytic leukemia (Chauchereau et al., 2004), B cell lymphoma (Sandhu et al., 2012), and multiple myeloma (Kikuchi et al., 2015). HDAC6 is protective in tauopathy and suppresses aberrant tau accumulation. Chronic HDAC6 loss results in accelerated tau pathology, cognitive dysfunction, and reduced survival (Trzeciakiewicz et al., 2020). HDAC7 is a bona fide transcriptional repressor vital to B cell development (Azagra et al., 2016). HDAC8 modulates p53 activity and ensures long-term hematopoietic stem cell maintenance and survival under stress (Hua et al., 2017). HDAC5, HDAC7, and HDAC9 play protective roles during cardiac hypertrophy (Mckinsey, 2011). HDAC11 performs a key function in oncogene-induced, non-homeostatic hematopoiesis (11 deficiency disrupt, 2020).

Nevertheless, the mechanisms by which HDACs are inhibited or promoted in glioma development and progression are unclear. No comprehensive bioinformatics analysis has been conducted to identify the putative role of HDACs in glioma. In the present study, we mined numerous large databases to analyze HDAC expression, mutation, and function and immune infiltration and determine their potential oncogenic and prognostic value in glioma.

MATERIALS AND METHODS

Oncomine Database

Oncomine (https://www.oncomine.org) contains 715 gene expression datasets and 86,733 samples. It is the largest oncogene chip database and incorporated data mining platform (§ et al., 2007). Transcriptional mRNA expression data for 11 HDACs in various cancers and their corresponding normal adjacent tissues were retrieved from Oncomine. The search content and threshold values were as follows: keywords, HDAC1–HDAC11; primary filter, cancer vs. normal; cancer type, absolute value of log2 $|$Fold Change$|$ > 1.5 and $p < 0.05$; and gene rank, 10%. p-values were calculated using the Student's t-test.

Human Protein Atlas

The Human Protein Atlas (https://www.proteinatlas.org) is an online tool including immunohistochemistry (IHC) expression data for protein distribution and expression in 20 cancer tissues, 48 human healthy tissues, 47 cell lines, and 12 blood cell types (Asplund et al., 2012). IHC images were used to compare HDAC protein expression levels among normal and cancer tissues. Localization of HDAC immunofluorescence expression in glioma cell lines was explored.

Gene Expression Profiling Interactive Analysis

GEPIA (http://gepia.cancer-pku.cn/detail.php) is a new online interactive web server enabling users to examine RNA sequencing expression data for tumors, normal tissues, and samples in the Genotype-Tissue Expression projects and The Cancer Genome Atlas (TCGA). GEPIA is based on a criterion processing pipeline. It provides customizable functions such as tumor/normal differential expression analysis, profiling by cancer type or pathological stage, similar gene detection, and patient survival, correlation, and dimensionality reduction analyses (Tang et al., 2017). In the present study, differential gene expression analysis was used to compare tumors and normal tissues using GEPIA. The Student's t-test was used to generate p-values for the expression analysis. A Kaplan–Meier curve for the patient survival analysis was also plotted.

Broad Institute Cancer Cell Line Encyclopedia Database

The CCLE (https://www.broadinstitute.org/ccle) project conducts detailed genetic and pharmacologic characterizations of large panels of human cancer models. It develops integrated computational analyses linking distinct pharmacologic vulnerability to genomic patterns and provides public access to genomic data for the analysis and visualization of approximately 1,000 cell lines (Ghandi et al., 2019). The mRNA expression levels of 11 HDACs in multiple glioma cell lines were compared. The RNA expression dataset for 12 glioma cell lines was retrieved from CCLE and the HDAC expression levels were plotted in heat maps.

Chinese Glioma Genome Atlas Database

CGGA (http://www.cgga.org.cn) is the largest glioma genome database in China. It provides multiple omics and matches clinical data for >2,000 primary and recurrent samples excised from Chinese cohorts (Zhao et al., 2020). In the present study, online tools and the mRNAseq_693 dataset were used to analyze the pathological stages associated with HDAC expression in patients with glioma.

GeneMANIA Database and OmicShare

GeneMANIA (http://www.genemania.org) is a well maintained, user-friendly gene list analysis web interface used to derive hypotheses based on gene functions (Max et al., 2018). Here, GeneMANIA was utilized to construct a gene–gene interaction network of HDAC family members based on their physical interactions, predictions, co-expression levels, co-localizations, genetic interactions, drug-interactions-2020, transcriptional-factor-targets-2020, and so on. GeneMANIA was also used to evaluate HDAC functions. OmicShare (http://www.omicshare.com/tools) is a comprehensive platform for data processing and analysis, learning biological information, and sharing scientific research knowledge. Gene Ontology (GO) and Kyoto Encyclopedia of Genes and Genomes (KEGG) pathway enrichment analyses were performed using the free online data analysis platform OmicShare Tools (https://www.omicshare.com/tools).

cBioPortal Databases

The cBioPortal (http://cbioportal.org) is a free asset that downloads large-scale cancer genomics datasets incorporating 245 cancer studies. The cBioPortal was used to explore genetic alterations in HDACs in glioma (Cerami et al., 2012). Here, the cBioPortal database was applied to explore 804 mutations in the brain lower-grade glioma (LGG; TCGA, and PanCancer Atlas) and glioblastoma multiforme (TCGA and Firehose Legacy) datasets for nerve center tumors. The distribution of HDAC mutations in glioma was calculated.

STRING

STRING (https://string-db.org/) is a protein interaction website providing a comprehensive, objective global network. It presents its data using a unique set of computational predictions (Szklarczyk et al., 2019). A protein–protein interaction (PPI) network analysis was conducted through STRING to collect and integrate the expression of HDACs and their potential interactions.

Tumor Immune Estimation Resource Analysis

The TIMER (https://cistrome.shinyapps.io/timer/) (Li et al., 2017) was used to evaluate the infiltration of $CD8^+$ T cells, B cells, $CD4^+$ T cells, macrophages, neutrophils, and dendritic cells in tumors and correlate them with HDAC expression in GBM and LGG. The survival module was used to establish prognostic relevance. $p < 0.01$ was considered statistically significant.

Quantitative Real-Time Polymerase Chain Reaction of Tissues

Total RNA was extracted from tissue specimens using Animal RNA Isolation Kit (Invitrogen, Beyotime, Shanghai, China) according to the manufacturer's instructions, and RNA was reversely transcribed into cDNA using Transcription First Strand cDNA synthesis kit (Beyotime, Shanghai, China). Quantitative real-time PCR (qRT-PCR) analyses were quantified with BeyoFast™ SYBR Green (Beyotime, Shanghai, China). The relative expression of HDACs were calculated based on the 2-ΔΔCt method with GADPH as an internal reference. qRT-PCR primers used in the present study were as follows:

HDAC1 forward primer, 5′- TCAAGATGGCCTGAGCAA GG-3'; HDAC1 reverse primer, 5′-TGTGCGCTGGTCCCTATC TA-3′; HDAC2 forward primer, 5′- TTCCAAGCCCGACTG TGAGA-3′; HDAC2 reverse primer, 5′-ACCTGTTAGAGC CAGTAAGCAC-3′; HDAC3 forward primer, 5′- GGCCGA TGCTGAAGAGAGAG-3′; HDAC3 reverse primer, 5′-GGG GATACCCAGTTCAGACC-3′; HDAC4 forward primer, 5′-CCTGTGGCCACTGCTCTAAA-3′; HDAC4 reverse primer, 5′-AATGCCATTCTCGGTGCTGA-3′; HDAC5 forward primer, 5′- CAGGCTGCTGCCACTCAAGA-3′; HDAC5 reverse primer, 5′-CACAATGATGAAGCCCAGAGGG-3′; HDAC6 forward primer, 5′- AGCTAGTCCTGTGCCGCTA-3′; HDAC6 reverse primer, 5′-TGTAGGTAATGCCGCTGT GG-3′; HDAC7 forward primer, 5′- ACCTGCGAGTGGGCC AAAG-3′; HDAC7 reverse primer, 5′-TACGGCACTTCGCTT GCTC-3′; HDAC8 forward primer, 5′- AATGAGCCCCATCGA ATCCAG-3′; HDAC8 reverse primer, 5′-GATATCCTCCCT CTTTCCCCCTA-3′; HDAC9 forward primer, 5′- ACTTGG TTACCCCAAGGAGC-3′; HDAC9 reverse primer, 5′-ATG CAGTGGAGGTCAGATGC-3′; HDAC10 forward primer, 5′-TCACTGGACAAGCCTCCAC-3′; HDAC10 reverse primer, 5′-GGCAAGATCGTCGTCCTGAA-3′; HDAC11 forward primer, 5′- TGCTAAAGAGGCCATCAGGC′; HDAC10 reverse primer, 5′-TGAGGATGGAGTCGGCGATA-3′; GAPDH forward primer, 5′- CCGCATCTTCTTGTGCAGTG′; GAPDH reverse primer, 5′- TCCCGTTGATGACCAGCTTC -3′

RESULTS

Comparison of HDAC Expression Levels in Glioma and Normal Tissue Samples

To explore the potential prognostic and therapeutic values of various HDACs, we used the Oncomine and HPA databases to

TABLE 1 | Significant changes in histone deacetylase transcription between various types of glioma and normal tissues (Oncomine database).

	Database type	Tumor type	*p*-value	*t*-test	Fold change
HDAC1	TCGA Brain Statistics	Brain Glioblastoma vs. Normal	3.08E-8	14.612	3.131
HDAC2	Pomeroy Brain Statistics (Ostrom et al., 2019)	Desmoplastic Medulloblastoma vs. Normal	5.47E-5	6.188	3.133
HDAC3	Gutmann Brain Statistics (Stupp et al., 2009)	Pilocytic Astrocytoma vs. Normal	0.021	3.649	2.483
HDAC6	Sun Brain Statistics (Stupp et al., 2005)	Glioblastoma vs. Normal	6.66E-13	8.831	3.221
	Sun Brain Statistics	Anaplastic Astrocytoma vs. Normal	2.34E-6	5.48	2.608

Differences in transcriptional expression were compared by Students' t-test. Cut-off of *p*-value and fold-change were as follows: *p*-value: 0.01,fold-change: 1.5, gene rank: 10%

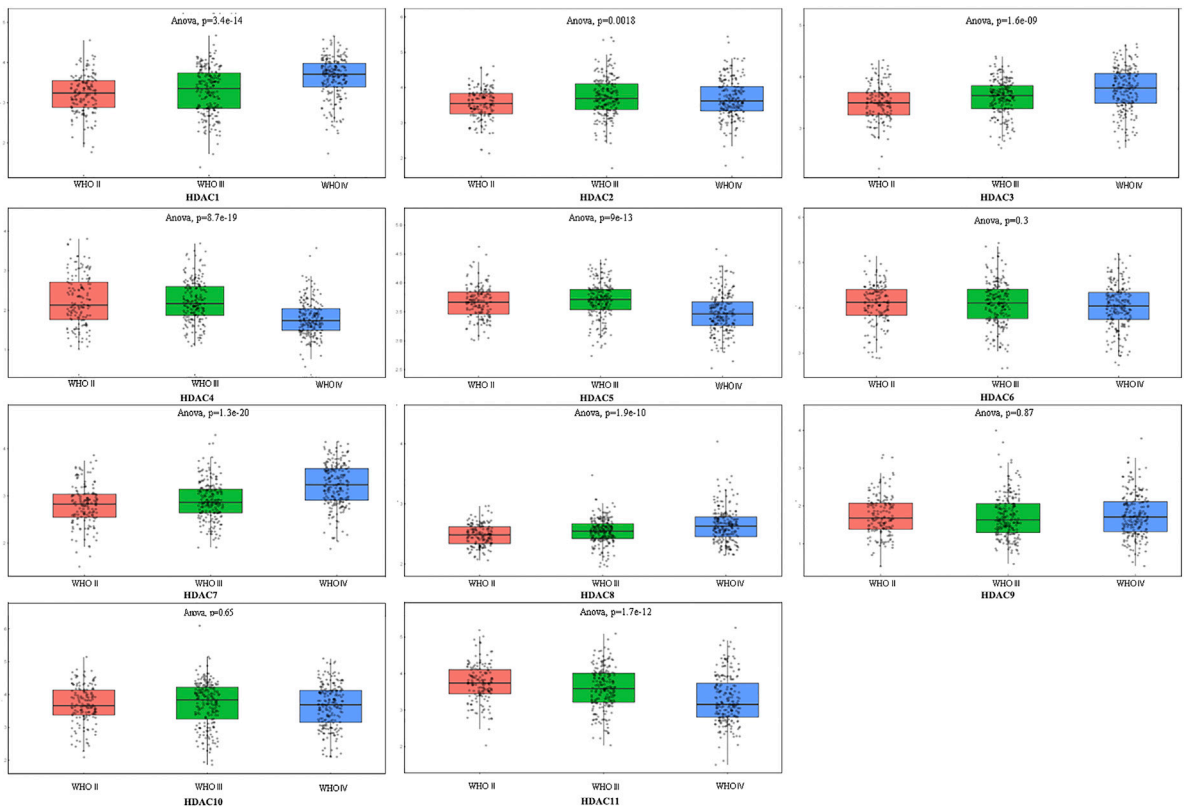

FIGURE 1 | Comprehensive analysis of prognosis and histone deacetylase expression in glioma. HDAC1/2/3/4/5/7/8/11 expression levels were correlated with pathological stage of glioma patients ($p < 0.05$).

analyze their mRNA and protein expression levels in patients with glioma. TCGA statistics revealed that *HDAC1* expression was 3.131-fold higher (p = 3.08E-8) in ductal brain glioblastoma than in normal tissues (**Table 1**). Pomeroy (Pomeroy et al., 2002) has reported a 3.133-fold increase in *HDAC2* in desmoplastic medulloblastoma than in normal tissue samples (p = 5.47E-5). Gutmann has (Gutmann et al., 2002) observed a 2.483-fold increase in *HDAC3* in pilocytic astrocytoma than in normal samples (p = 0.021). Sun Brain Statistics (Sun et al., 2006) disclosed *HDAC6* overexpression in glioblastoma tissues compared with normal tissues and the fold change was 3.221 (p = 6.66E-13). The database search returned a 2.608-fold increase in *HDAC6* mRNA expression in anaplastic astrocytoma compared with normal tissues (p = 2.34E-6).

We also explored protein-level HDAC expression using the Human Protein Atlas database. Low and medium HDAC1/4/8/9/10 protein expression levels were determined for normal tissues, and high HDAC1/4/8/9/10 protein expression levels were found in glioma tissues (**Figures 1A,D,G,H**). **Figures 2C,E,F** show that HDAC3/5/6 proteins are not expressed in normal gastric tissues but are detected at low and medium levels in glioma tissues.

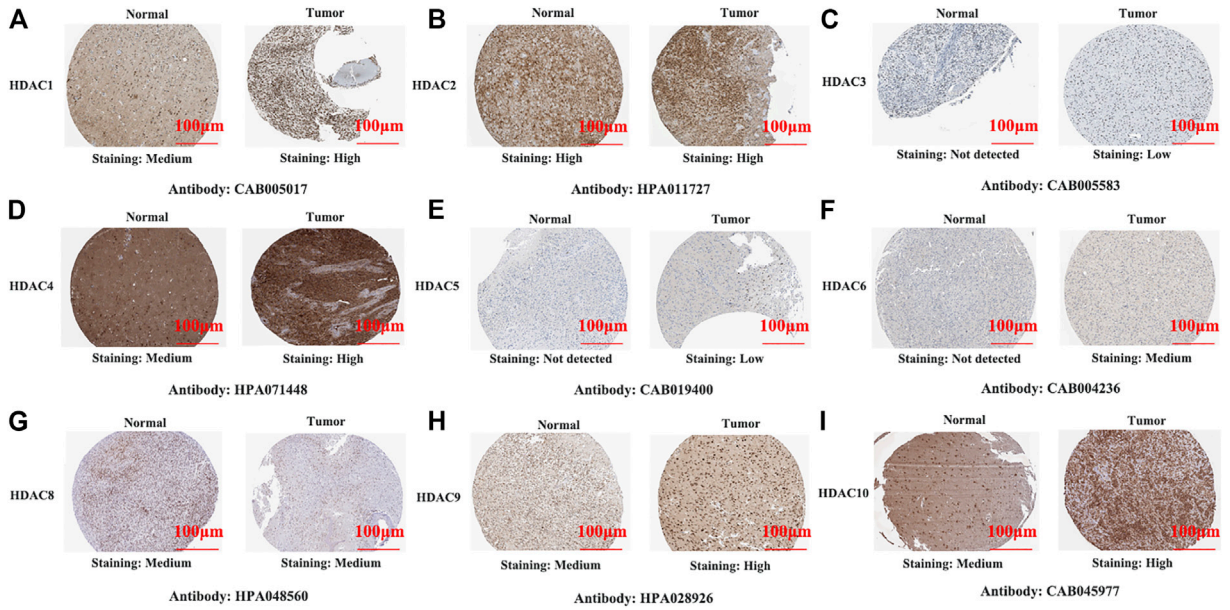

FIGURE 2 | Representative immunohistochemistry images of histone deacetylase family members in glioma and normal tissues (Human Protein Atlas Database). All tissues were observed at ×100 magnification.

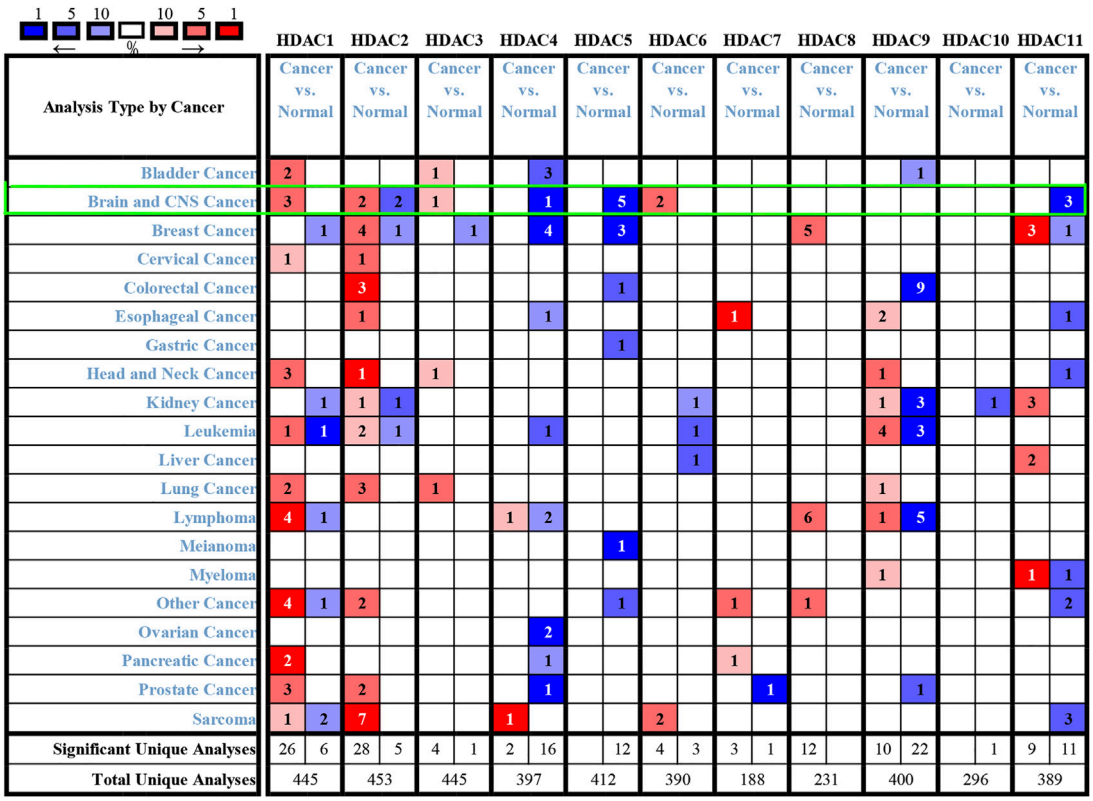

FIGURE 3 | Histone deacetylase transcription levels in various cancers (Oncomine). Numbers in colored cells show quantities of datasets with statistically significant target gene mRNA upregulation (red) or downregulation (blue). The following criteria were used: *p*-value, 0.01; fold change, two; gene rank, 10%; data type, mRNA; analysis type, cancer vs. normal tissue. CNS: central nervous system.

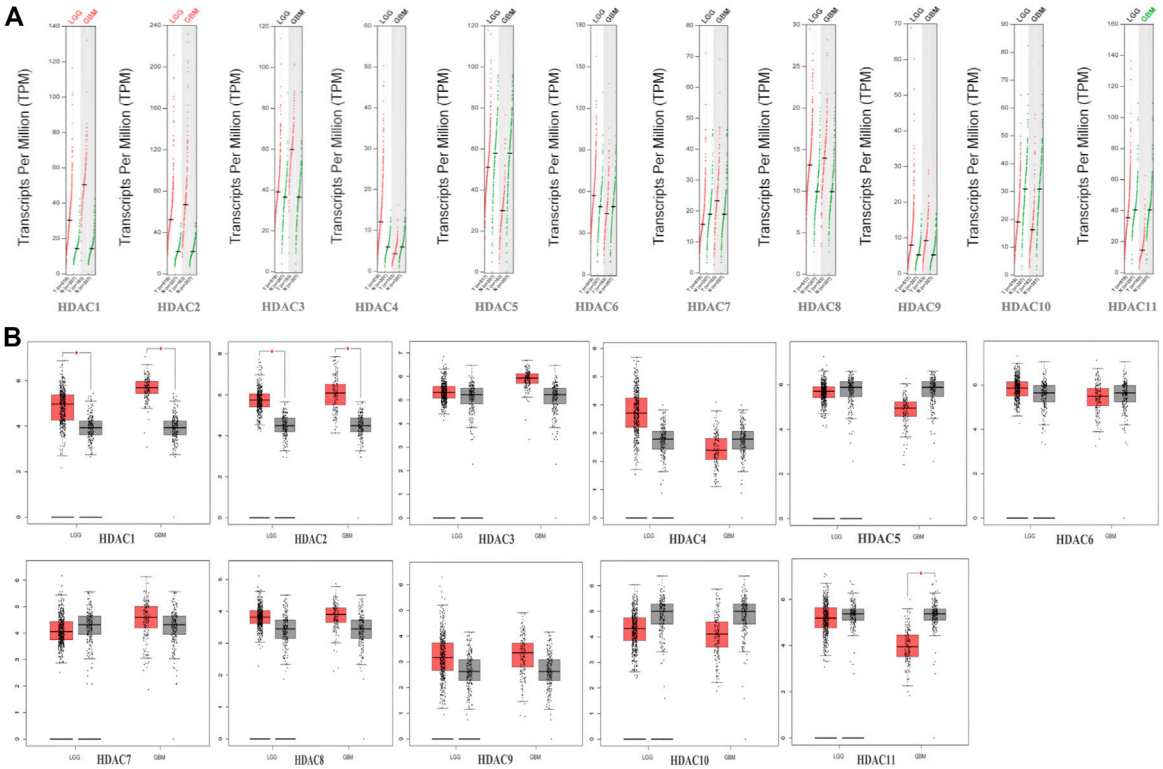

FIGURE 4 | Gene expression profiling interactive analysis data for histone deacetylase (HDAC) mRNA expression in glioma including glioblastoma (GBM) and lower-grade glioma (LGG) compared with NB tissue **(A,B)** Scatter diagram and Box plot showing that HDAC1/2 expression levels in GBM (n = 163) and LGG (n = 518) tumor tissues were higher than those in normal tissues (n = 207). HDAC11 expression levels were lower in GBM tumor tissues than in normal tissues ($p < 0.05$).

Relationships Between HDAC mRNA Levels and Clinicopathological Parameters of Patients with Glioma

To explore distinct HDAC expression in patients with glioma, HDAC mRNA expression was analyzed using the Oncomine database (**Figure 3**). The Oncomine data revealed that compared with normal tissues, the *HDAC1/2/3/6* transcriptional levels were significantly elevated and those of *HDAC2/4/5/11* were significantly decreased in CNS cancer tissues. The GEPIA dataset was used to compare HDAC mRNA expression between glioma and normal tissues. *HDAC1* and *HDAC2* were relatively upregulated and HDAC11 was downregulated in LGG and GBM tumor tissues (**Figure 4**). We also compared HDAC expression levels across glioma tumor stages. *HDAC1/2/3/4/5/7/8/11* expression significantly varied across glioma stages, whereas *HDAC6/9/10* expression did not (**Figure 1**). Therefore, qRT-PCR was performed to verify the expression of HDAC family gene mRNA in glioma tumor tissues. *HDAC1/2/3/4/5/8/11* expression levels were correlated with pathological stage of glioma patients ($p < 0.05$) (**Figure 5**).

HDACs mRNA Expression and Immunofluorescence in Glioma Cells

We compared HDAC expression levels among the foregoing databases and used CCLE to explore HDAC1/2 expression levels in glioma cell lines. All HDACs were strongly upregulated in glioma cell lines (**Figure 6C**). We also found that *HDAC1/2/3/10* were highly expressed in 11 glioma cell lines from the CCLE database, namely, SW1783, TM31, KNS60, M059K, GOS3, SF126, KALS1, LN229, GI1, KNS81, KG1C, and AM38 (**Figure 6B**). We searched the cell atlas of the HDAC family in glioma and observed immunofluorescence of *HDAC1/2/3/4/5/7/9* (**Figure 6A**). In the human protein map, most HDAC proteins were localized to and upregulated in human glioma cell nuclei.

Prognostic Significance of HDACs in Patients with Glioma

We evaluated the prognostic significance of HDACs in patients with glioma using the GEPIA and CGGA databases. A log-rank test analysis revealed that high *HDCA1/3/7* and low *HDAC4/5/11* mRNA levels were significantly associated with overall survival (OS) and disease-free survival (DFS) ($p < 0.05$) (**Figure 7**). *HDAC9* mRNA downregulation and *HDAC10* mRNA upregulation had prognostic value in DFS, whereas *HDAC2* mRNA upregulation had prognostic value in OS ($p < 0.05$). The GEPIA database showed that *HDAC1/2/3/4/5/7/9/10/11* mRNA expression levels were significantly associated with

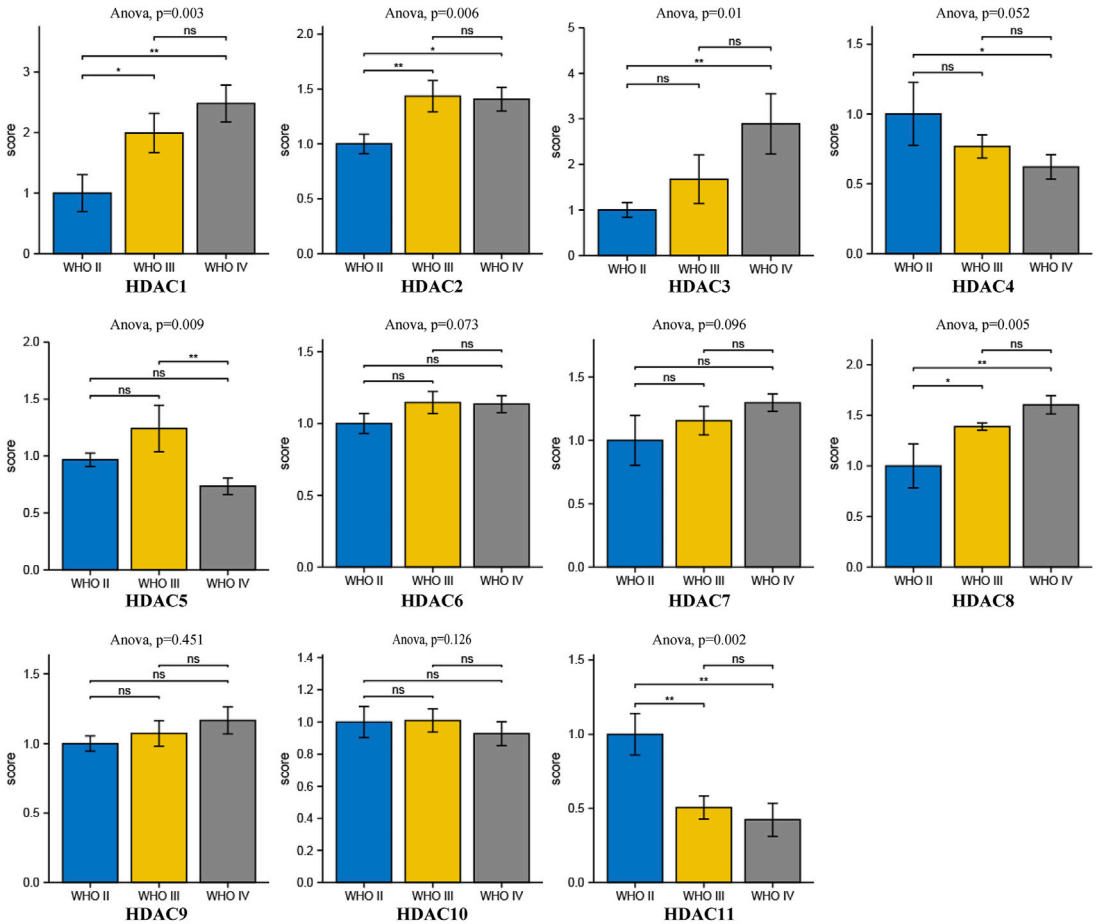

FIGURE 5 | Comprehensive analysis of prognosis and histone deacetylase expression in glioma. HDAC *HDAC1/2/3/4/5/8/11* expression levels were correlated with pathological stage of glioma patients ($p < 0.05$).

glioma patient prognosis and could, therefore, be exploited as biomarkers for the prediction of glioma patient survival.

Genetic HDAC Alteration Analysis in Glioma Patients

Genetic alterations in the HDACs of glioma patients were examined using TCGA database and the cBioPortal online tool. HDACs were altered in 804 samples from 1,118 glioma patients in TCGA databases of brain LGG and GBM. The alteration rates were 12.05% (62/514) and 5.52% (16/290), respectively. Deep deletion accounted for most of the observed changes (**Figure 8A**). **Figure 8B** shows that genetic HDAC alterations occurred in 78 (10%) of queried samples and that the alteration rates in the individual sequence were in the range of 0.1–3%. HDAC4, HDAC6, and HDAC10 were ranked as the top three of the eleven HDAC members and their deep deletion rates were 3, 1.4, and 1.4%, respectively, (**Figure 8B**). The "Survival" tab, the Kaplan–Meier plot, and the log-rank test plotted survival curves indicated that cases with or without HDAC alterations had no correlation with OS or DFS (**Figures 8C,D**).

Predicted HDAC and HDAC-Related Neighboring Gene Functions and Pathways in Patients with Glioma

We analyzed 50 neighboring genes significantly related to HDACs and used GeneMANIA to construct an integrated network. **Figure 8A** shows that according to the weight analysis, HDACs were associated with ubiquitinase-related genes, including USP3/5/13/16/20/22/33/39/44/49/45/51. Gene-related drugs acting on HDACs included panobinostat, vorinostat, romidepsin, SB939, valproic acid, and MGCD-0103. The transcription factors HMEF2_Q6, RSRFC4_Q2, MEF2_02, and MEF2_03 were associated with HDAC-related genes. The LGG and GBM mRNA data in TCGA and the Spearman's correlation analyses were used to calculate correlations among HDAC family members. The STRING database was used to build a PPI network for the HDAC family (**Figures 9A,B**). There were significant positive correlations between the following HDACs: HDAC1 with HDAC3; HDAC2 with HDAC3 and HDAC8; HDAC4 with HDAC5 and HDAC6; HDAC5 with HDAC6; HDAC6 with HDAC10; HDAC7 with HDAC1, HDAC3, HDAC6, and HDAC10; HDAC8 with

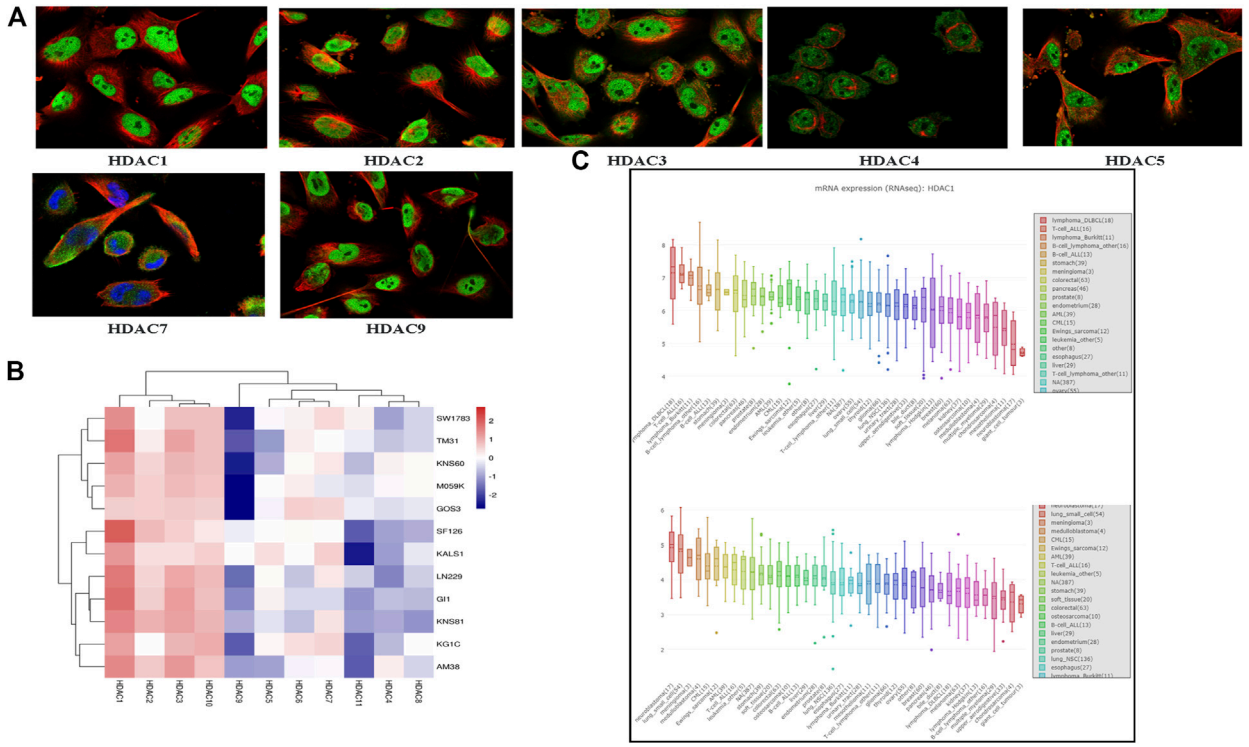

FIGURE 6 | Cell line histone deacetylase (HDCA) mRNA expression levels (Cancer Cell Line Encyclopedia) **(A)** HDAC1/2/3/4/5/7/9 immunofluorescence was expressed in glioma U-251 MG cell nuclei **(B)** HDAC1/2/3/10 mRNA was highly expressed in 12 glioma cell lines **(C)** Box plot was sorted and colored according to average distribution of HDAC1 and HDAC2 expression in various tumor cell lines. Immunofluorescence analysis of HDAC1/2/3/4/5/7/9 in U-251 MG.

HDAC3 and HDAC6; HDAC9 with HDAC2; and HDAC11 with HDAC4 and HDAC5. There were also significant negative correlations between the following HDACs: HDAC4 with HDAC1 and HDAC3; and HDAC5 with HDAC1 and HDAC3 (**Figure 9C**).

GO enrichment and KEGG pathway analyses of the HDACs and 50 neighboring genes were performed using OmicShare. The top ten most highly enriched GO items were identified (**Figures 10A–C**). The GO term analysis showed that differentially expressed genes correlated with the HDACs were localized mainly with the histone deacetylase complex, nuclear part, nucleus, nucleoplasm, nuclear lumen, and intracellular organelle lumen; HDACs negatively regulate RNA biosynthesis and transcription, DNA templates, RNA metabolism, histone H3 deacetylation, and histone modification at these sites. HDACs have histone deacetylase-binding, H3-K14-specific NAD-dependent histone deacetylase and histone deacetylase activity, protein deacetylase activity, NAD-dependent histone deacetylase activity, and so on. The KEGG pathway analysis disclosed viral carcinogenesis, apelin signaling, arginine and proline metabolism, transcriptional misregulation in cancer, Notch signaling, and cGMP-PKG signaling. The thyroid hormone signaling pathway and arginine biosynthesis were significantly associated with glioma tumorigenesis and progression (**Figure 10D**).

HDAC Expression and Immune Infiltration in Glioma

The TIMER database was used to investigate associations among the HDACs family members and immune cell infiltration. The immune cell count is correlated with cancer cell proliferation and progression (**Figure 11**). *HDAC1* expression in LGG was positively correlated with the infiltration of B cells ($p < 0.001$), $CD4^+$ T cells ($p < 0.01$), macrophages ($p < 0.01$), neutrophils ($p < 0.001$), and dendritic cells ($p < 0.01$). *HDAC2/8* expression levels in LGG and GBM were positively correlated with purity infiltration ($p < 0.01$).

HDAC3 expression in LGG was positively correlated with the infiltration of B cells ($p < 0.01$), neutrophils ($p < 0.01$), and dendritic cells ($p < 0.01$). *HDAC7* expression in LGG was positively correlated with the infiltration of $CD4^+$ T cells ($p < 0.01$), macrophages ($p < 0.01$), and dendritic cells ($p < 0.001$). *HDAC9* expression in LGG was positively correlated with $CD8^+$ T cell infiltration ($p < 0.001$). *HDAC11* expression in LGG was positively correlated with purity infiltration ($p < 0.01$) and negatively correlated with neutrophil infiltration ($p < 0.01$). A Cox proportional hazard model of HDACs and clinical factors in glioma was also evaluated. *HDAC3/4* expression, patient age, and $CD4^+$ T cell density were significantly associated with clinical outcomes in GBM (**Table 2**). *HDAC1* expression and patient age were significantly associated with the clinical prognosis of LGG (**Table 3**).

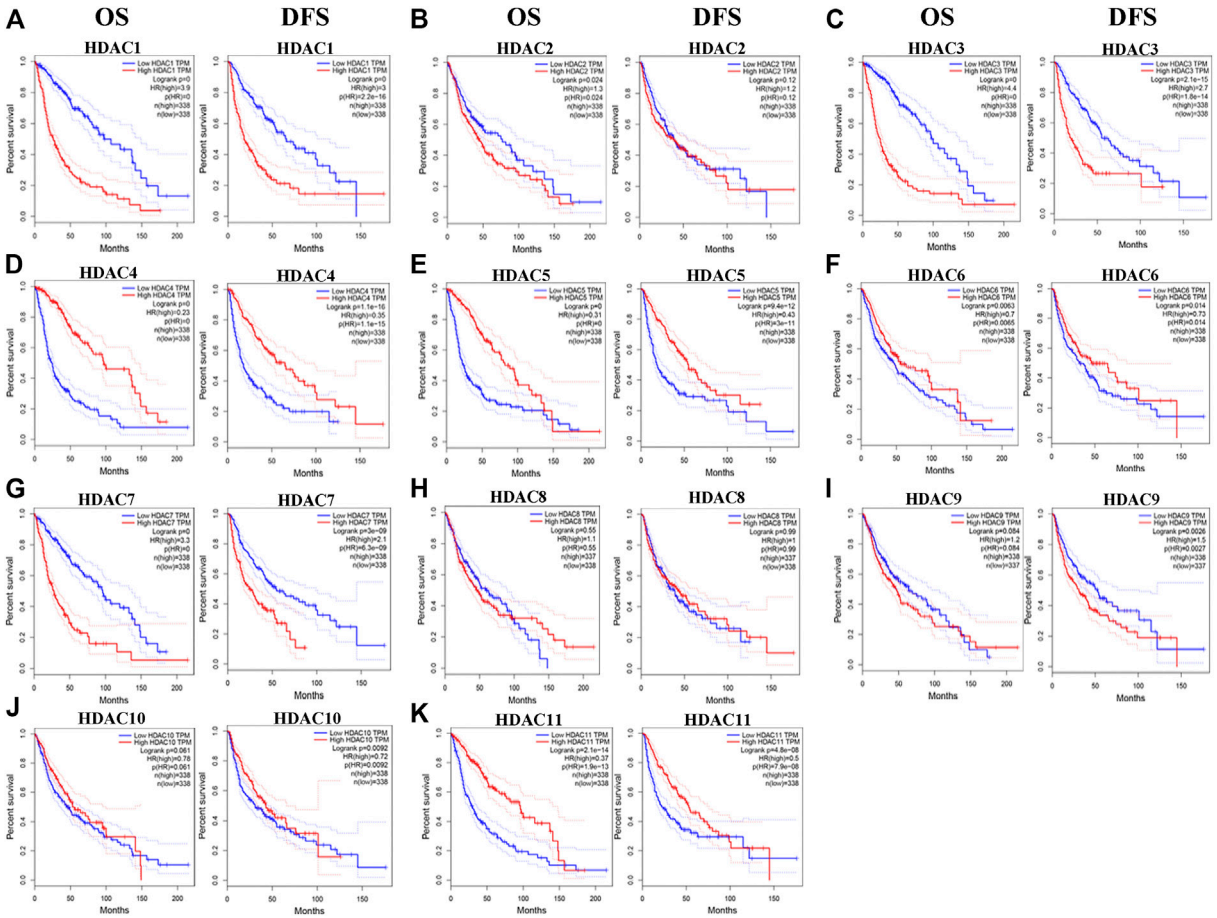

FIGURE 7 | Prognostic value of histone deacetylase mRNA expression in patients with glioma (Gene expression profiling interactive analysis). *$p < 0.05$. HR, hazard ratio; OS, overall survival; DFS, disease-free survival.

DISCUSSION

Epigenetic modifications are heritable, reversible genetic changes that do not involve DNA mutation. HDACs are epigenetic regulators that remove the acetyl moieties from acetylated lysine residues of post-translationally modified histone proteins that form the core of the chromatin network. This mechanism compresses chromatin, compromises DNA accessibility, and represses transcription and gene silencing (Sengupta and Seto, 2004). However, distinct roles of each HDAC family member in glioma remain to be clarified. In the present study, we analyzed HDAC expression, mutation, prognostic value, functional enrichment, and immune cell infiltration in patients with glioma. To this end, we consulted various public databases including Oncomine, Human Protein Atlas, GEPIA, cBioPortal, CCLE, GeneMANIA, String, and CGGA. GO enrichment and KEGG pathway were analyzed with OmicShare Tools.

Previous studies have evaluated the roles of certain HDAC family members in glioma (Lodrini et al., 2013; Wang et al., 2017; Lo Cascio et al., 2019; Song et al., 2020). A previous study has indicated that the NFAT2-HDAC1 pathway may maintain the malignant phenotype and promote mesenchymal transition in glioma stem-like cells (GSCs). Hence, GSCs are potential molecular targets for GBM therapy (Song et al., 2020). HDAC1 ablation significantly decreased stemness and proliferation in patient-derived GSCs in a p53-dependent manner. By contrast, it had only minimal impact on normal human neural stem cells and astrocytes (Lo Cascio et al., 2019). HDAC1 knockdown inhibited the epithelial–mesenchymal transition transcription factors TWIST1 and SNAIL, downregulated the mesenchymal marker matrix metalloprotein-9, and upregulated the epithelial marker E-cadherin 34. Hence, HDAC1 may contribute to epithelial–mesenchymal transition in glioma cells (Wang et al., 2017). Our results showed that HDAC1 was highly expressed in glioma tumor tissue and significantly correlated with patient survival and immune infiltrate density. Moreover, *HDAC1* had the highest mRNA expression level of all HDACs in 12 glioma cell lines. A Cox proportional hazard model of HDACs and clinical factors disclosed that *HDAC1* expression was significantly correlated with clinical outcome in LGG. *HDAC1* upregulation was significantly correlated with poor OS and DFS in patients with glioma patients. The foregoing associations merit further

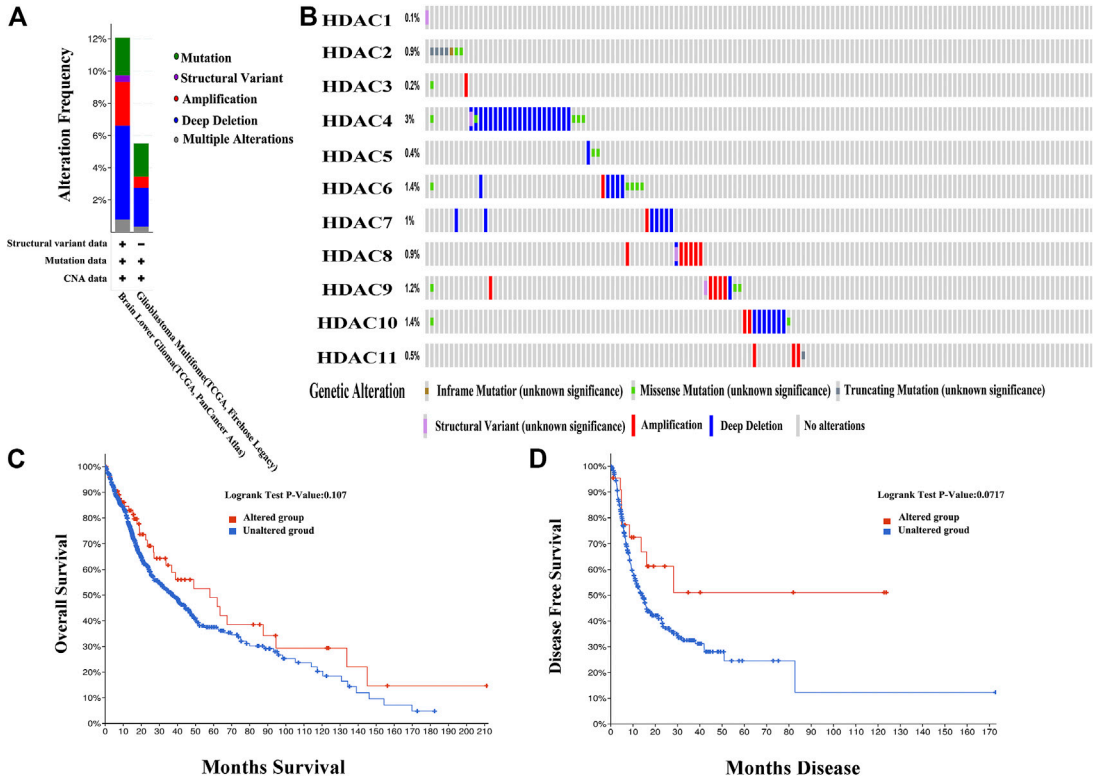

FIGURE 8 | Genetic histone deacetylase (HDAC) alteration analysis in patients with OS (cBioPortal) **(A)** HDAC alterations **(B)** OncoPrint tab summary of query of HDAC alterations. Kaplan–Meier plots comparing **(C)** overall survival (OS) and **(D)** disease-free survival (DFS) in patients with and without HDAC gene alterations.

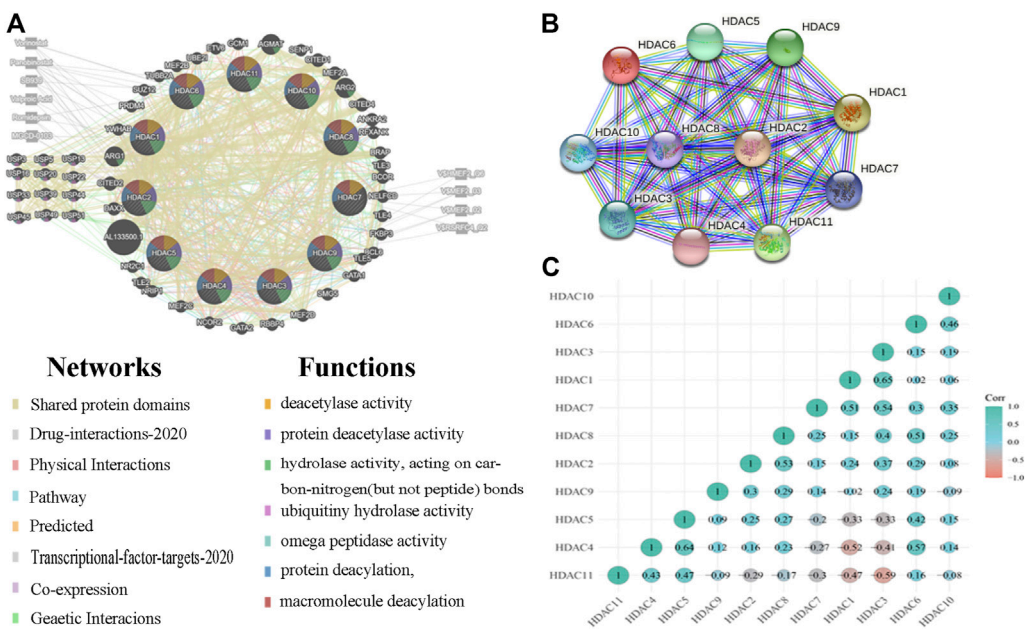

FIGURE 9 | Protein–protein interactions (PPI) among histone deacetylases (HDACs) **(A)** Network of HDACs and their 50 neighboring genes was constructed using GeneMANIA **(B)** PPI network of various HDACs **(C)** Pearson correlation coefficients among HDACs.

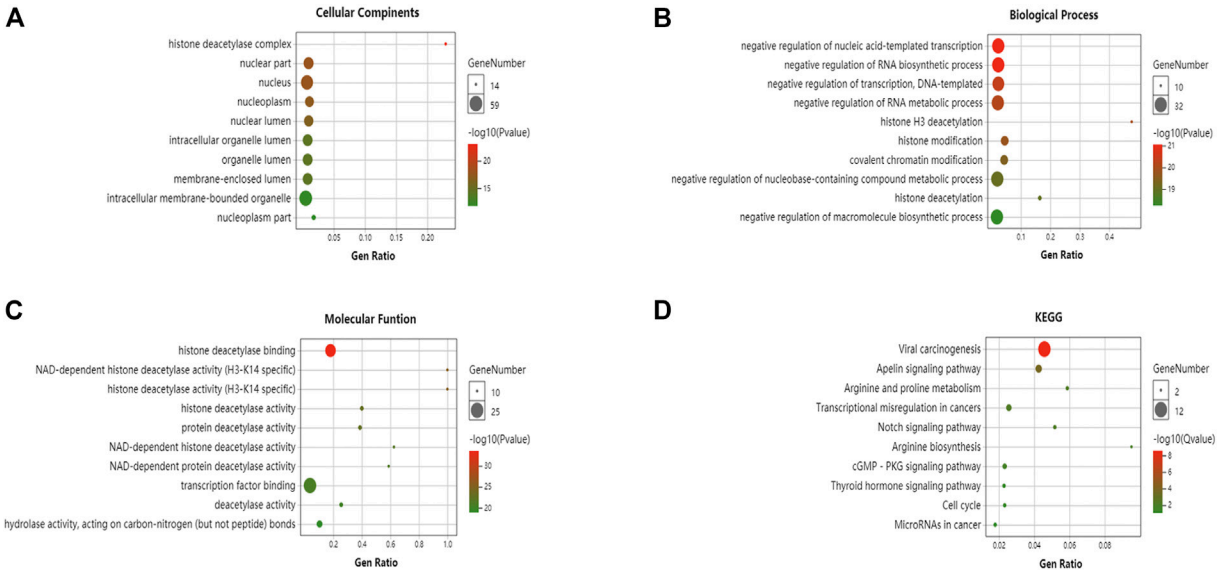

FIGURE 10 | Gene ontology (GO) enrichment and Kyoto Encyclopedia of Genes and Genomes (KEGG) pathway analyses of HDACs and their interactions (OmicShare). GO enrichment analysis of target genes based on **(A)** cellular component, **(B)** biological process, and **(C)** molecular function **(D)** KEGG pathway enrichment analysis of target genes.

investigation. We plan to knock out or use the expression of protease inhibitor *HDAC1* in glioma cell lines to observe tumor cell invasion and migration in functional experiments. Besides use tumor-bearing nude mice to further verify whether its *HDAC1* can inhibit tumor growth.

Recent observations demonstrated that class I HDACs (HDAC1, HDAC2, and HDAC3) modulate DNA damage signaling (Miller et al., 2010; Thurn et al., 2013), maintain genomic stability, and prevent tumorigenesis *in vivo* (Dovey et al., 2013; Heideman et al., 2013; Santoro et al., 2013). The mammalian class I deacetylase HDAC2 has been extensively studied. HDAC2 downregulation markedly inhibits tumor growth. Thus, HDAC2 may be an oncogene in tumorigenesis (Zhu et al., 2004). HDAC2 protein overexpression was detected in human gastric, prostate, and breast cancers (Nakagawa et al., 2007; Jinwon et al., 2014). HDAC2 represses gene expression by deacetylating H4K16ac (Ma et al., 2013), determines transcription repression, and participates in the nucleosome remodeling deacetylase complex. *In vitro* and *in vivo* experiments demonstrated that silencing TRPS1 inhibited tumor growth, whereas HDAC2 overexpression promoted it (Wang et al., 2018). The results of the present study corroborated these findings. *HDAC2* expression was higher in glioma tumor than in normal tissues. *HDAC2* expression was also significantly correlated with glioma grade and positively correlated with purity infiltration. However, we found that unlike mRNA expression, immune combination expression was elevated in both glioma and normal tissues possibly because of gene regulation during transcription and translation.

During thymocyte development, HDAC3 is required for positive selection and CD4 lineage development (Stengel et al., 2015). HDAC3 represses CD8 lineage genes to keep double-positive thymocytes in a bipotential state (Philips et al., 2019). Here, *HDAC3* expression in LGG was positively correlated with the infiltration of B cells, neutrophils, and dendritic cells. *HDAC3* mRNA expression was significantly associated with clinical outcome in GBM. Hence, immunity-related cells may be implicated in glioma pathogenesis.

HDAC4 is a key member of class IIa HDACs and performs a wide variety of functions (Seto and Yoshida, 2014). In various cells, HDAC4 is post-transcriptionally regulated by several microRNAs such as miR-1, miR-29, miR-140, miR-155, miR-200a, miR-206, and miR-365 (Wang et al., 2014). Some studies have shown that the molecular mechanism of glioma formation involved HDAC4-mediated SP1 and KLF5 deacetylation in selective MKK7 transcription and oncogenic JNK/c-Jun cascade activation. These findings were consistent with the findings of our research. The results of the immune combination showed that HDAC4 is highly expressed in glioma tumor tissues. KEGG enrichment analysis has revealed that in cancers, HDAC and its neighboring 50 genes are enriched in microRNAs. *HDAC4* upregulation was significantly correlated with poor OS and DFS in all patients with glioma. A Cox proportional hazard model of HDAC and its clinical factors disclosed that *HDAC4* expression was significantly correlated with clinical GBM outcome.

HDAC5 is a class II HDAC. Aberrant HDAC5 expression has been observed in multiple cancer types. HDAC5 participates in cell proliferation and invasion, immune response, and maintenance of stemness (Yang et al., 2021). In the present study, *HDAC5* expression was low in tumor cell lines and in glioma and normal tissues. However, *HDAC5* upregulation was significantly correlated with tumor stage, poor OS, and DFS in all patients with glioma.

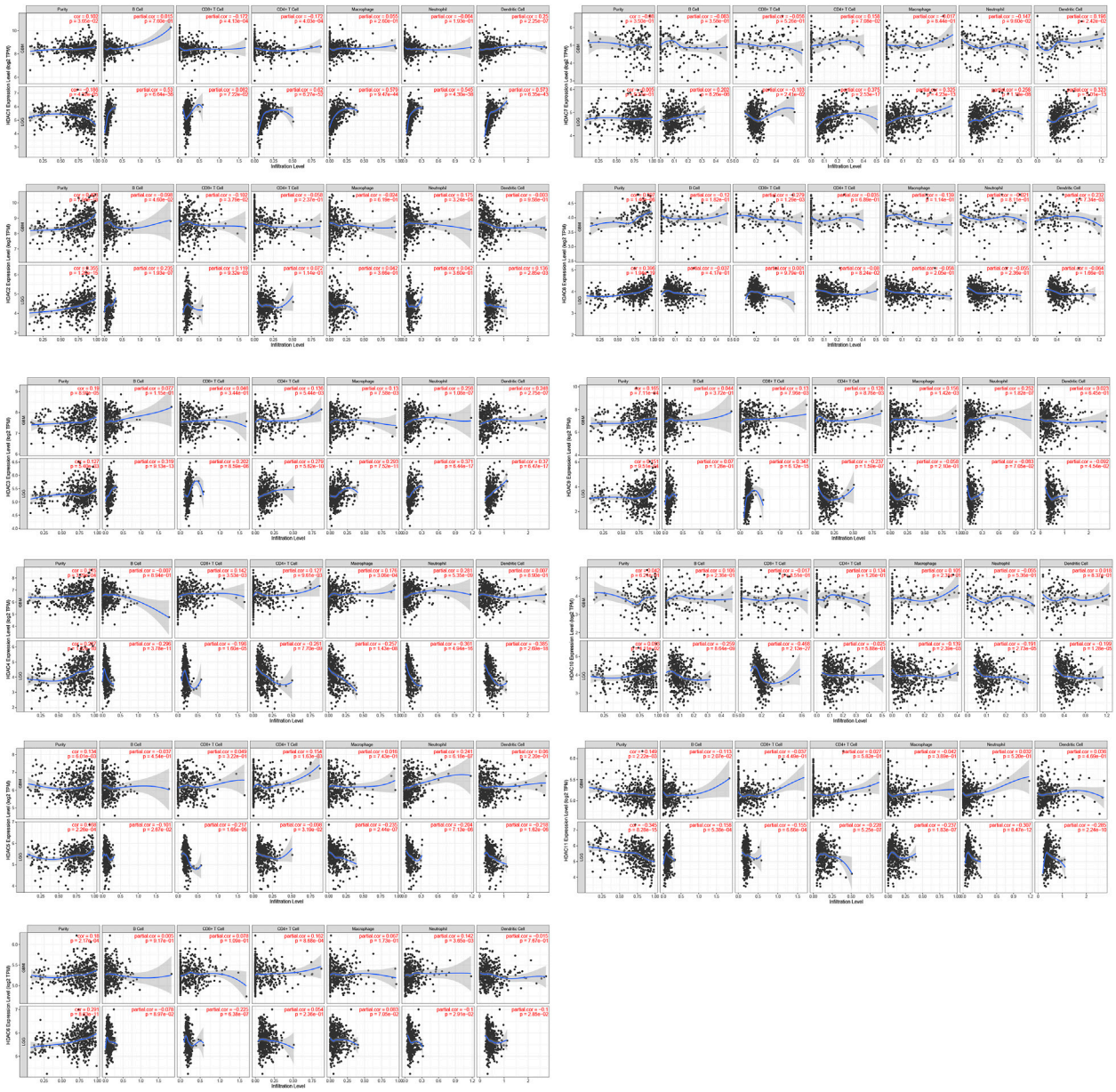

FIGURE 11 | Correlations among differentially expressed HDACs and immune cell infiltration (TIMER). Correlations between immune cell abundance and HDAC1–11 expression.

HDAC6 and 10 are class IIb HDACs based on their subcellular localizations and expression patterns (Haberland et al., 2009). Previous research has shown that HDAC6-selective inhibitors delayed tumor initiation and progression *in vivo* without causing any significant adverse effects (Auzmendi-Iriarte et al., 2019). HDAC6 inhibition induces an *in vivo* delay in tumor growth and downregulates PD-L1 expression. Several key immunological checkpoint modulators are regulated by HDAC6 (Lienlaf et al., 2016). *HDAC10* expression is positively associated with PD-L1 expression and may predict the outcome of patients with non-small cell lung carcinoma. HDAC10 inhibition combined with doxorubicin administration kills neuroblastoma but not non-malignant cells by impeding drug efflux and enhancing DNA damage. This novel mechanism targets chemotherapy resistance (Johannes et al., 2018). In this study, *HDAC6* expression was higher in glioma tumor than in normal tissues. Low *HDAC6* mRNA expression was significantly correlated with OS and DFS in patients with glioma. *HDAC10* expression is moderate in LGG and elevated in high-grade gliomas. However, low *HDAC10* mRNA expression was not significantly correlated with DFS in patients with glioma.

HDAC7 sustains human mammary epithelial cell proliferation and favors the establishment of stem-like cell populations by

TABLE 2 | Multivariate survival model analysis based on TIMER online tool (glioblastoma).

	Coef	HR	95%CI_l	95%CI_u	*p*.value	Sig
Age	0.033	1.033	1.007	1.060	0.012	*
Gender male	0.414	1.512	0.881	2.596	0.133	—
Race Black	−0.156	0.855	0.150	4.892	0.860	—
Race White	−0.510	0.600	0.150	2.406	0.471	—
Purity	−0.850	0.427	0.072	2.530	0.349	—
B_cells	−0.376	0.686	0.082	5.725	0.728	—
CD8+Tcell	0.114	1.121	0.271	4.632	0.875	—
CD4+Tcell	4.274	71.838	3.371	1,530.896	0.006	**
Macrophage	2.002	7.405	0.507	108.057	0.143	—
Neutrophil	−1.933	0.145	0.005	4.585	0.273	—
Dendritic	0.932	2.539	0.842	7.656	0.098	
HDAC1	−0.741	0.476	0.206	1.101	0.083	—
HDAC2	0.242	1.274	0.721	2.251	0.405	—
HDAC3	1.272	3.569	1.322	9.633	0.012	*
HDAC4	−1.340	0.262	0.111	0.618	0.002	**
HDAC5	0.469	1.598	0.650	3.925	0.307	—
HDAC6	0.763	2.144	0.814	5.650	0.123	
HDAC7	−0.293	0.746	0.400	1.390	0.356	—
HDAC8	−0.211	0.810	0.276	2.372	0.700	—
HDAC9	0.132	1.141	0.792	1.644	0.479	—
HDAC10	0.017	1.017	0.576	1.796	0.954	—
HDAC11	0.236	1.267	0.747	2.147	0.380	—

*Coef: coefficient, HR: hazard ratio, CI: confidence interval, sig: significance. *p < 0.05.*

maintaining a proficient microenvironment. High HDAC8 expression levels in human GBM tissues and GBM-R cell lines were correlated with *O*-methylguanine-DNA methyltransferase levels (Cutano et al., 2019). An inhibitor of HDAC8 combined with temozolomide administration induced WT-p53-mediated apoptosis via WT-p53-mediated *O*-methylguanine-DNA methyltransferase inhibition in GBM-R cell lines (Tsai et al., 2021). Elevated HDAC9 expression is associated with poor prognosis and promotes malignancy (Huang et al., 2018; Linares et al., 2019; Li et al., 2020). *HDAC9* deficiency promoted tumor progression by decreasing $CD8^+$ dendritic cell (DC) infiltration in the tumor microenvironment. *HDAC9* expression was significantly positively correlated with $CD8^+$ cell counts in human lung cancer stroma samples (Ning et al., 2020). In the present study, immune cell infiltration was associated with HDACs in glioma. *HDAC9* expression in LGG was positively correlated with $CD8^+$ cell infiltration. *HDAC7* expression in LGG was positively correlated with the infiltration of $CD4^+$ T cells, macrophages, and dendritic cells. *HDAC8* expression in LGG and GBM was positively correlated with purity infiltration. *High HDAC7* mRNA expression was significantly correlated with OS and DFS in patients with glioma. However, *HDAC8* mRNA expression levels were not meaningful for prognostic survival analyses of patients with glioma. *HDAC9* mRNA expression levels were not associated with OS in patients with glioma.

HDAC11 is the only member of the class IV HDACs (Seto and Yoshida, 2014). There is limited information regarding its functions. Using a novel class of highly selective HDAC inhibitors and genetically deficient mouse models, the foregoing study revealed that HDAC11 was necessary for oncogenic JAK2-driven myeloproliferative neoplasm cell and tissue proliferation and survival (Yue et al., 2020). Other data demonstrated a significant role of HDAC11 in mitotic cell cycle progression and survival of MYCN-amplified neuroblastoma cells and suggested that HDAC11 is potentially a valuable drug target (Thole et al., 2017). The present study arrived at the same conclusions. KEGG enrichment analysis disclosed that enrichment of HDAC and its neighboring 50 genes was

TABLE 3 | Multivariate survival model analysis based on TIMER online tool (lower-grade glioma).

	Cof	HR	95%CI_l	95%CI_u	*p*.value	Sig
Age	0.059	1.061	1.043	1.079	0.000	***
Gender male	0.245	1.277	0.827	1.973	0.270	—
Race Black	16.758	18,961,194.043	0	Inf	0.995	—
Race White	17.125	27,383,645.009	0	Inf	0.994	—
Purity	−0.225	0.799	0.269	2.372	0.686	—
B_cell	0.932	2.540	0.001	4,482.746	0.807	—
CD8_Tcell	1.699	5.466	0.003	9,731.339	0.656	—
CD4_Tcel	−2.442	0.087	0.000	1,089.174	0.612	—
Macrophage	4.756	116.240	0.842	16,038.885	0.059	—
Neutrophil	−6.479	0.002	0.000	11.959	0.156	—
Dendritic	1.393	4.025	0.036	454.222	0.564	—
HDAC1	0.815	2.260	1.408	3.627	0.001	**
HDAC2	0.209	1.233	0.715	2.126	0.451	—
HDAC3	0.148	1.160	0.510	2.636	0.723	—
HDAC4	−0.098	0.907	0.597	1.378	0.647	—
HDAC5	−0.342	0.710	0.377	1.338	0.290	—
HDAC6	−0.353	0.703	0.312	1.583	0.395	—
HDAC7	0.215	1.240	0.618	2.489	0.544	—
HDAC8	0.521	1.685	0.732	3.878	0.220	—
HDAC9	0.113	1.119	0.833	1.504	0.455	—
HDAC10	0.245	1.278	0.833	1.959	0.261	—
HDAC11	0.265	1.304	0.833	2.041	0.245	—

*Coef: coefficient, HR: hazard ratio, CI: confidence interval, sig: significance. *p < 0.05.*

associated with the cell cycle. *HDAC11* expression was lower in glioma tumor than in normal tissues. *HDAC11* downregulation was significantly correlated with tumor stage, poor OS, and DFS in patients with glioma.

There are several limitations to our study. Firstly, we only analyzed data retrieved from online databases, we must validate our findings using large cohorts. Secondly, our HDAC IHC and immunofluorescence data were incomplete. Third, we did not use our cell lines or tissues to further verify the results. Although HDAC family expression data are similar for glioma cell lines and pancancer analyses. Perhaps, Basic experiments must be conducted to elucidate the mechanisms of HDAC family members and determine their impact on epigenetics. At present, a large number of HDAC inhibitors have been used in other tumors, and we can use HDAC inhibitors to act on cells or animals to further observe their inhibition of tumors. The conventional histone acetylases show lack of blood-brain barrier permeability in the treatment of brain diseases, but through the development of new small molecule probes and carriers, they can penetrate the blood-brain barrier well. we may use nano-encapsulation to further break through the blood-brain barrier (Dang, 2014). In the actual human clinical safety and effectiveness test, we can observe the immunohistochemical expression of HDAC in clinical work and combine with traditional glioma gene diagnosis to analyze and judge the prognosis of glioma diseases.

CONCLUSION

Most of these histone Acetylases are usually adjunctive to other chemoradiotherapy drugs such as temozolomide/bevacizumab. However, most of the current clinical trials are phase I/II clinical trials, and further phase III trials are needed to demonstrate the role of histone acetylases in gliomas. In a phase two Study of Concurrent Radiation Therapy, Temozolomide, and the Histone Deacetylase Inhibitor Valproic Acid for Patients With Glioblastoma, histone inhibitors may improve outcomes for patients with glioma compared with historical data (Krave, 2015). In the present study, we systematically analyzed HDAC expression and prognostic value in glioma and revealed the heterogeneity and complexity of the molecular mechanisms associated with these cancers. We also investigated the mRNA expression patterns, prognostic values, genetic alterations, GO enrichment, and PPI networks of HDACs in patients with glioma. According to the immune prognosis analysis, the age and *HDAC1* mRNA expression of patients with LGG were related to disease prognosis. Patient age, $CD4^+$ T cell density, and *HDAC3* and *HDAC4* mRNA expression were associated with high-grade glioma prognosis. *HDAC1* and *HDAC2* were relatively upregulated whereas *HDAC11* was downregulated in LGG and GBM tumor tissues. *High HDCA1* and low *HDAC11* mRNA expression levels were significantly related to glioma OS and DFS. HDAC2 mRNA upregulation had prognostic value in OS. The foregoing results indicate that HDAC1/2 are potential prognostic biomarkers for patients with glioma. The present study may facilitate the discovery of novel prognostic biomarkers for glioma among other HDAC family members.

DATA AVAILABILITY STATEMENT

The original contributions presented in the study are included in the article/Supplementary Materials, further inquiries can be directed to the corresponding authors.

ETHICS STATEMENT

The studies involving human participants were reviewed and approved by the Ethics Committee of Liuzhou Workers' Hospital. The patients/participants provided their written informed consent to participate in this study.

AUTHOR CONTRIBUTIONS

JL and HC participated in the manuscript of the article and the conception of the article, ML, XL, ZW, and JD edited the picture and data analysis, and QL participated in the review of the article. LC and LX for experimental verification and article revision.

FUNDING

This study was supported by the Science and Technology Department of Guangxi Zhuang Autonomous Region, Grant No. 2018GXNSFAA294026 and by Guangxi Natural Science Foundation, Grant No. 2018GXNSFAA294026.

REFERENCES

Abdelfattah, N., Rajamanickam, S., Panneerdoss, S., Timilsina, S., Yadav, P., Onyeagucha, B. C., et al. (2018). MiR-584-5p Potentiates Vincristine and Radiation Response by Inducing Spindle Defects and DNA Damage in Medulloblastoma. *Nat. Commun.* 9, 4541. doi:10.1038/s41467-018-06808-8

Asplund, A., Edqvist, P.-H. D., Schwenk, J. M., and Pontén, F. (2012). Antibodies for Profiling the Human Proteome-The Human Protein Atlas as a Resource for Cancer Research. *Proteomics* 12, 2067–2077. doi:10.1002/pmic.201100504

Auzmendi-Iriarte, J., Saenz-Antoñanzas, A., Andermatten, J., Elua-Pinin, A., Aldaba, E., Vara, Y., et al. (2019). P11.46 Discovery of a New HDAC6 Inhibitor for the Treatment of Glioblastoma. *Neuro Oncol.* 21, iii53–iii54. doi:10.1093/neuonc/noz126.192

Azagra, A., Román-González, L., Collazo, O., Rodríguez-Ubreva, J., de Yébenes, V. G., Barneda-Zahonero, B., et al. (2016). *In Vivo* conditional Deletion of HDAC7 Reveals its Requirement to Establish Proper B Lymphocyte Identity and Development. *J. Exp. Med.* 213, 2591–2601. doi:10.1084/jem.20150821

Bennani-Baiti, I. M., and Idriss, M. (2011). Epigenetic and Epigenomic Mechanisms Shape Sarcoma and Other Mesenchymal Tumor Pathogenesis. *Epigenomics* 3, 715–732. doi:10.2217/epi.11.93

Cerami, E., Gao, J., Dogrusoz, U., Gross, B. E., Sumer, S. O., Aksoy, B. A., et al. (2012). The cBio Cancer Genomics Portal: An Open Platform for Exploring

Multidimensional Cancer Genomics Data: Figure 1. *Cancer Discov.* 2, 401–404. doi:10.1158/2159-8290.cd-12-0095

Chauchereau, A., Mathieu, M., Saintignon, J. D., Ferreira, R., Pritchard, L. L., Mishal, Z., et al. (2004). HDAC4 Mediates Transcriptional Repression by the Acute Promyelocytic Leukaemia-Associated Protein PLZF. *Oncogene* 23 (54), 8777. doi:10.1038/sj.onc.120812

Cohen, T. J., Guo, J. L., Hurtado, D. E., Kwong, L. K., Mills, I. P., Trojanowski, J. Q., et al. (2011). The Acetylation of Tau Inhibits its Function and Promotes Pathological Tau Aggregation. *Nat. Commun.* 2, 252. doi:10.1038/ncomms1255

Cutano, V., Di Giorgio, E., Minisini, M., Picco, R., Dalla, E., and Brancolini, C. (2019). HDAC7-mediated Control of Tumour Microenvironment Maintains Proliferative and Stemness Competence of Human Mammary Epithelial Cells. *Mol. Oncol.* 13, 1651–1668. doi:10.1002/1878-0261.12503

Dang, Junsun. (2014). Image-Guided Synthesis Reveals Potent Blood-Brain Barrier Permeable Histone Deacetylase Inhibitors. *Acs Chem. Neurosci.* 5, 588.

Dompierre, J. P., Godin, J. D., Charrin, B. C., Cordelières, F. P., King, S. J., Humbert, S., et al. (2007). Histone Deacetylase 6 Inhibition Compensates for the Transport Deficit in Huntington's Disease by Increasing Tubulin Acetylation. *J. Neurosci.* 27, 3571–3583. doi:10.1523/jneurosci.0037-07.2007

Dovey, O. M., Foster, C. T., Conte, N., Edwards, S. A., Edwards, J. M., Singh, R., et al. (2013). Histone Deacetylase 1 and 2 Are Essential for normal T-Cell Development and Genomic Stability in Mice. *Blood* 121, 1335–1344. doi:10.1182/blood-2012-07-441949

Ghandi, M., Huang, F. W., Jané-Valbuena, J., Kryukov, G. V., Lo, C. C., McDonald, E. R., et al. (2019). Next-generation Characterization of the Cancer Cell Line Encyclopedia. *Nature* 569, 503–508. doi:10.1038/s41586-019-1186-3

Glozak, M. A., and Seto, E. (2007). Histone Deacetylases and Cancer. *Oncogene* 26, 5420–5432. doi:10.1038/sj.onc.1210610

Gutmann, D. H., Hedrick, N. M., Li, J., Nagarajan, R., Perry, A., and Watson, M. A. (2002). Comparative Gene Expression Profile Analysis of Neurofibromatosis 1-associated and Sporadic Pilocytic Astrocytomas. *Cancer Res.* 62, 2085–2091.

Haberland, M., Montgomery, R. L., and Olson, E. N. (2009). The many Roles of Histone Deacetylases in Development and Physiology: Implications for Disease and Therapy. *Nat. Rev. Genet.* 10, 32–42. doi:10.1038/nrg2485

HDAC11 Deficiency Disrupts Oncogene-Induced Hematopoiesis in Myeloproliferative Neoplasms. (2020).

Heideman, M. R., Wilting, R. H., Yanover, E., Velds, A., de Jong, J., Kerkhoven, R. M., et al. (2013). Dosage-dependent Tumor Suppression by Histone Deacetylases 1 and 2 through Regulation of C-Myc Collaborating Genes and P53 Function. *Blood* 121, 2038–2050. doi:10.1182/blood-2012-08-450916

Ho, T. C. S., Chan, A. H. Y., and Ganesan, A. (2020). Thirty Years of HDAC Inhibitors: 2020 Insight and Hindsight. *J. Med. Chem.* 63, 12460–12484. doi:10.1021/acs.jmedchem.0c00830

Hua, W. K., Qi, J., Cai, Q., Carnahan, E., Ramirez, M. A., Li, L., et al. (2017). HDAC8 Regulates Long-Term Hematopoietic Stem Cell Maintenance under Stress by Modulating P53 Activity. *Blood* 130 (24), 2619. doi:10.1182/blood-2017-03-771386

Huang, Y., Jian, W., Zhao, J., and Wang, G. (2018). Overexpression of HDAC9 Is Associated with Poor Prognosis and Tumor Progression of Breast Cancer in Chinese Females. *Ott* Vol. 11, 2177–2184. doi:10.2147/ott.s164583

Hubbert, C., Guardiola, A., Shao, R., Kawaguchi, Y., Ito, A., Nixon, A., et al. (2002). HDAC6 Is a Microtubule-Associated Deacetylase. *Nature* 417, 455–458. doi:10.1038/417455a

Jinwon, S., Min, S. K., Hye-Rim, P., Hoon, K. D., Jung, K. M., Su, K. L., et al. (2014). Expression of Histone Deacetylases HDAC1, HDAC2, HDAC3, and HDAC6 in Invasive Ductal Carcinomas of the Breast. *J. Breast Cancer* 17, 323.

Johannes, R., Emily, K., Kolbinger, F. R., Katharina, K., Siavosh, M., Lars, H., et al. (2018). Dual Role of HDAC10 in Lysosomal Exocytosis and DNA Repair Promotes Neuroblastoma Chemoresistance. *Scientific Rep.* 8, 10039.

Jones, P. A., and Baylin, S. B. (2007). The Epigenomics of Cancer. *Cell* 128, 683–692. doi:10.1016/j.cell.2007.01.029

Kang, Z.-H., Wang, C.-Y., Zhang, W.-L., Zhang, J.-T., Yuan, C.-H., Zhao, P.-W., et al. (2014). Histone Deacetylase HDAC4 Promotes Gastric Cancer SGC-7901 Cells Progression via P21 Repression. *PLoS ONE* 9, e98894. doi:10.1371/journal.pone.0098894

Kashyap, K., and Kakkar, R. (2020). Exploring Structural Requirements of Isoform Selective Histone Deacetylase Inhibitors: a Comparative In Silico Study. *J. Biomol. Struct. Dyn.* 39, 1–16. doi:10.1080/07391102.2019.1711191

Kikuchi, S., Suzuki, R., Ohguchi, H., Yoshida, Y., Lu, D., Cottini, F., et al. (2015). Class IIa HDAC Inhibition Enhances ER Stress-Mediated Cell. Death in Multiple Myeloma. *Leukemia* 29 (9), 1918. doi:10.1038/leu.2015.83

Kovacs, J. J., Murphy, P. J. M., Gaillard, S., Zhao, X., Wu, J.-T., Nicchitta, C. V., et al. (2005). HDAC6 Regulates Hsp90 Acetylation and Chaperone-dependent Activation of Glucocorticoid Receptor. *Mol. Cel.* 18, 601–607. doi:10.1016/j.molcel.2005.04.021

Krave, A. V. (2015). A Phase 2 Study of Concurrent Radiation Therapy, Temozolomide, and the Histone Deacetylase Inhibitor Valproic Acid for Patients with Glioblastoma. *Int. J. Radiat. Oncol. Biol. Phys.* 92, 986–992.

Li, H., Li, X., Lin, H., and Gong, J. (2020). High HDAC9 Is Associated with Poor Prognosis and Promotes Malignant Progression in Pancreatic Ductal Adenocarcinoma. *Mol. Med. Rep.* 21, 822–832. doi:10.3892/mmr.2019.10869

Li, T., Fan, J., Wang, B., Traugh, N., Chen, Q., Liu, J. S., et al. (2017). TIMER: A Web Server for Comprehensive Analysis of Tumor-Infiltrating Immune Cells. *Cancer Res.* 77, e108–e110. doi:10.1158/0008-5472.can-17-0307

Li, Y., Peng, L., and Seto, E. (2015). Histone Deacetylase 10 Regulates the Cell Cycle G2/M Phase Transition via a Novel Let-7-HMGA2-Cyclin A2 Pathway. *Mol. Cel. Biol.* 35, 3547–3565. doi:10.1128/MCB.00400-15

Lienlaf, M., Perez-Villarroel, P., Knox, T., Pabon, M., Sahakian, E., Powers, J., et al. (2016). Essential Role of HDAC6 in the Regulation of PD-L1 in Melanoma. *Mol. Oncol.* 10, 735–750. doi:10.1016/j.molonc.2015.12.012

Linares, A., Assou, S., Lapierre, M., Thouennon, E., Duraffourd, C., Fromaget, C., et al. (2019). Increased Expression of the HDAC 9 Gene Is Associated with Antiestrogen Resistance of Breast Cancers. *Mol. Oncol.* 13, 1534–1547. doi:10.1002/1878-0261.12505

Lo Cascio, C., Mcnamara, J., Luna Melendez, E., and Mehta, S. (2019). STEM-25. HDAC1 IS ESSENTIAL FOR GLIOMA STEM CELL SURVIVAL. *Neuro-Oncology* 21, vi239. doi:10.1093/neuonc/noz175.998

Lodrini, M., Oehme, I., Schroeder, C., Milde, T., Schier, M. C., Kopp-Schneider, A., et al. (2013). MYCN and HDAC2 Cooperate to Repress miR-183 Signaling in Neuroblastoma. *Nucleic Acids Res.* 41, 6018–6033. doi:10.1093/nar/gkt346

Ma, P., Schultz, R. M., and Matzuk, M. M. (2013). Histone Deacetylase 2 (HDAC2) Regulates Chromosome Segregation and Kinetochore Function via H4K16 Deacetylation during Oocyte Maturation in Mouse. *Plos Genet.* 9, e1003377. doi:10.1371/journal.pgen.1003377

Max, F., Harold, R., Christian, L., Khalid, Z., Jason, M., Bader, G. D., et al. (2018). GeneMANIA Update 2018. *Nucl. Acids Res.* 46, W60–W64. doi:10.1093/nar/gky311

Mckinsey, T. A. (2011). *The Biology and Therapeutic Implications of HDACs in the Heart, Histone Deacetylases: The Biology and Clinical Implication*.

Millard, C. J., Watson, P. J., Fairall, L., and Schwabe, J. W. R. (2017). Targeting Class I Histone Deacetylases in a "Complex" Environment. *Trends Pharmacol. Sci.* 38, 363–377. doi:10.1016/j.tips.2016.12.006

Miller, K. M., Tjeertes, J. V., Coates, J., Legube, G., Polo, S. E., Britton, S., et al. (2010). Human HDAC1 and HDAC2 Function in the DNA-Damage Response to Promote DNA Nonhomologous End-Joining. *Nat. Struct. Mol. Biol.* 17, 1144–1151. doi:10.1038/nsmb.1899

Nakagawa, M., Oda, Y., Eguchi, T., Aishima, S.-I., Yao, T., Hosoi, F., et al. (2007). Expression Profile of Class I Histone Deacetylases in Human Cancer Tissues. *Oncol. Rep.* 18, 769–774. doi:10.3892/or.18.4.769

Neftel, C., Laffy, J., Filbin, M. G., Hara, T., Shore, M. E., Rahme, G. J., et al. (2019). An Integrative Model of Cellular States, Plasticity, and Genetics for Glioblastoma. *Cell* 178, 835–e21. doi:10.1016/j.cell.2019.06.024

Ning, Y., Ding, J., Sun, X., Xie, Y., Su, M., Ma, C., et al. (2020). HDAC9 Deficiency Promotes Tumor Progression by Decreasing the CD8+ Dendritic Cell Infiltration of the Tumor Microenvironment. *J. Immunother. Cancer* 8. doi:10.1136/jitc-2020-000529

Ostrom, Q. T., Gino, C., Haley, G., Nirav, P., Kristin, W., Carol, K., et al. (2019). CBTRUS Statistical Report: Primary Brain and Other Central Nervous System Tumors Diagnosed in the United States in 2012–2016. *Neuro Oncol.* 21, v1–v100. doi:10.1093/neuonc/noz150

Pacheco, M., and Nielsen, T. O. (2012). Histone Deacetylase 1 and 2 in Mesenchymal Tumors. *Mod. Pathol.* 25, 222–230. doi:10.1038/modpathol.2011.157

Park, H., Kim, J., Ahn, S., and Ryu, H. (2021). Epigenetic Targeting of Histone Deacetylases in Diagnostics and Treatment of Depression. *Int. J. Mol. Sci.* 22. doi:10.3390/ijms22105398

Philips, R. L., Lee, J. H., Gaonkar, K., Chanana, P., Chung, J. Y., Romero Arocha, S. R., et al. (2019). HDAC3 Restrains CD8-Lineage Genes to Maintain a Bi-potential State in CD4+CD8+ Thymocytes for CD4-Lineage Commitment. *Elife* 8. doi:10.7554/eLife.43821

Pomeroy, S. L., Tamayo, P., Gaasenbeek, M., Sturla, L. M., Angelo, M., Mclaughlin, M. E., et al. (2002). Prediction of central Nervous System Embryonal Tumour Outcome Based on Gene Expression. *Nature* 415, 436–442. doi:10.1038/415436a

Sandhu, S. K., Volinia, S., Costinean, S., Galasso, M., Neinast, R., Santhanam, R., et al. (2012). miR-155 Targets Histone Deacetylase 4 (HDAC4) and Impairs Transcriptional Activity of B-Cell Lymphoma 6 (BCL6) in the Eμ-miR-155 Transgenic Mouse Model. *Proc. Natl. Acad. Sci. U S A.* 109, 20047–20052. doi:10.1073/pnas.1213764109

Santoro, F., Botrugno, O. A., Dal Zuffo, R., Pallavicini, I., Matthews, G. M., Cluse, L., et al. (2013). A Dual Role for Hdac1: Oncosuppressor in Tumorigenesis, Oncogene in Tumor Maintenance. *Blood* 121, 3459–3468. doi:10.1182/blood-2012-10-461988

Sengupta, N., and Seto, E. (2004). Regulation of Histone Deacetylase Activities. *J. Cel. Biochem.* 93, 57–67. doi:10.1002/jcb.20179

Seto, E., and Yoshida, M. (2014). Erasers of Histone Acetylation: the Histone Deacetylase Enzymes. *Cold Spring Harbor Perspect. Biol.* 6, a018713. doi:10.1101/cshperspect.a018713

Simões-Pires, C., Zwick, V., Nurisso, A., Schenker, E., Carrupt, P.-A., Cuendet, M., et al. (2013). HDAC6 as a Target for Neurodegenerative Diseases: what Makes it Different from the Other HDACs. *Mol. Neurodegeneration* 8, 7. doi:10.1186/1750-1326-8-7

Song, Y., Luo, Q., Long, H., Hu, Z., Que, T., Zhang, X., et al. (2014). Alpha-enolase as a Potential Cancer Prognostic Marker Promotes Cell Growth, Migration, and Invasion in Glioma. *Mol. Cancer* 13, 65. doi:10.1186/1476-4598-13-65

Song, Y., Jiang, Y., Tao, D., Wang, Z., Wang, R., Wang, M., et al. (2020). NFAT2-HDAC1 Signaling Contributes to the Malignant Phenotype of Glioblastoma. *Neuro-Oncology* 22, 46–57. doi:10.1093/neuonc/noz136

Stengel, K. R., Zhao, Y., Klus, N. J., Kaiser, J. F., Gordy, L. E., Joyce, S., et al. (2015). Histone Deacetylase 3 Is Required for Efficient T Cell Development. *Mol. Cel. Biol.* 35, 3854–3865. doi:10.1128/mcb.00706-15

Stengel, K. R., Bhaskara, S., Jing, W., Qi, L., Ellis, J. D., Sampathi, S., et al. (2019). Histone Deacetylase 3 Controls a Transcriptional Network Required for B Cell. Maturation. *Nucleic Acids Res.* 47 (20), 10612–10627. doi:10.1093/nar/gkz816

Szklarczyk, D., Gable, A. L., Lyon, D., Junge, A., Wyder, S., Huerta-Cepas, J., et al. (2019). STRING V11: Protein-Protein Association Networks with Increased Coverage, Supporting Functional Discovery in Genome-wide Experimental Datasets. *Nucleic Acids Res.* 47, D607–D613. doi:10.1093/nar/gky1131

Stupp, R., Hegi, M. E., Mason, W. P., van den Bent, M. J., Taphoorn, M. J., Janzer, R. C., et al. (2009). Effects of Radiotherapy with Concomitant and Adjuvant Temozolomide versus Radiotherapy Alone on Survival in Glioblastoma in a Randomised Phase III Study: 5-year Analysis of the EORTC-NCIC Trial. *Lancet Oncol.* 10, 459–466. doi:10.1016/S1470-2045(09)70025-7

Stupp, R., Mason, W. P., van den Bent, M. J., Weller, M., Fisher, B., and Taphoorn, M. J. B. (2005). Radiotherapy Plus Concomitant and Adjuvant Temozolomide for Glioblastoma. *New Engl. J. Med.* 352, 987–996. doi:10.1056/NEJMoa043330

Sun, L., Hui, A.-M., Su, Q., Vortmeyer, A., Kotliarov, Y., Pastorino, S., et al. (2006). Neuronal and Glioma-Derived Stem Cell Factor Induces Angiogenesis within the Brain. *Cancer Cell* 9, 287–300. doi:10.1016/j.ccr.2006.03.003

Tang, Z., Li, C., Kang, B., Gao, G., Li, C., and Zhang, Z. (2017). GEPIA: A Web Server for Cancer and Normal Gene Expression Profiling and Interactive Analyses. *Nucleic Acids Res.* 45, W98–W102. doi:10.1093/nar/gkx247

Thole, T. M., Lodrini, M., Fabian, J., Wuenschel, J., Pfeil, S., Hielscher, T., et al. (2017). Neuroblastoma Cells Depend on HDAC11 for Mitotic Cell Cycle Progression and Survival. *Cell Death Dis.* 8, e2635. doi:10.1038/cddis.2017.49

Thurn, K. T., Thomas, S., Raha, P., Qureshi, I., and Munster, P. N. (2013). Histone Deacetylase Regulation of ATM-Mediated DNA Damage Signaling. *Mol. Cancer Ther.* 12, 2078–2087. doi:10.1158/1535-7163.mct-12-1242

Trzeciakiewicz, H., Ajit, D., Tseng, J.-H., Chen, Y., Ajit, A., Tabassum, Z., et al. (2020). An HDAC6-dependent Surveillance Mechanism Suppresses Tau-Mediated Neurodegeneration and Cognitive Decline. *Nat. Commun.* 11, 5522. doi:10.1038/s41467-020-19317-4

Tsai, C., Ko, H., Chiou, S., Lai, Y., Hou, C., Javaria, T., et al. (2021). NBM-BMX, an HDAC8 Inhibitor, Overcomes Temozolomide Resistance in Glioblastoma Multiforme by Downregulating the β-Catenin/c-Myc/SOX2 Pathway and Upregulating P53-Mediated MGMT Inhibition. *Int. J. Mol. Sci.* 22. doi:10.3390/ijms22115907

Wang, X.-Q., Bai, H.-M., Li, S.-T., Sun, H., Min, L.-Z., Tao, B.-B., et al. (2017). Knockdown of HDAC1 Expression Suppresses Invasion and Induces Apoptosis in Glioma Cells. *Oncotarget* 8, 48027–48040. doi:10.18632/oncotarget.18227

Wang, Y., Zhang, J., Wu, L., Liu, W., Wei, G., Gong, X., et al. (2018). Tricho-rhino-phalangeal Syndrome 1 Protein Functions as a Scaffold Required for Ubiquitin-specific Protease 4-directed Histone Deacetylase 2 De-ubiquitination and Tumor Growth. *Breast Cancer Res.* 20, 83. doi:10.1186/s13058-018-1018-7

Wang, Z., Qin, G., and Zhao, T. C. (2014). HDAC4: Mechanism of Regulation and Biological Functions. *Epigenomics* 6, 139–150. doi:10.2217/epi.13.73

Wilson, A. J., Byun, D.-S., Nasser, S., Murray, L. B., Ayyanar, K., Arango, D., et al. (2008). HDAC4 Promotes Growth of Colon Cancer Cells via Repression of P21. *MBoC* 19, 4062–4075. doi:10.1091/mbc.e08-02-0139

Yang, J., Gong, C., Ke, Q., Fang, Z., Chen, X., Ye, M., et al. (2021). Insights into the Function and Clinical Application of HDAC5 in Cancer Management. *Front. Oncol.* 11, 661620. doi:10.3389/fonc.2021.661620

Yue, L., Sharma, V., Horvat, N. P., Akuffo, A. A., Beatty, M. S., Murdun, C., et al. (2020). HDAC11 Deficiency Disrupts Oncogene-Induced Hematopoiesis in Myeloproliferative Neoplasms. *Blood* 135, 191–207. doi:10.1182/blood.2019895326

Zhang, X., Yuan, Z., Zhang, Y., Yong, S., Salas-Burgos, A., Koomen, J., et al. (2007). HDAC6 Modulates Cell Motility by Altering the Acetylation Level of Cortactin. *Mol. Cel.* 27, 197–213. doi:10.1016/j.molcel.2007.05.033

Zhao, Z., Zhang, K., Wang, Q., Li, G., and Jiang, T. (2020). *Chinese Glioma Genome Atlas (CGGA): A Comprehensive Resource with Functional Genomic Data for Chinese Glioma Patients*.

Zhu, P., Martin, E., Mengwasser, J., Schlag, P., Janssen, K.-P., and Göttlicher, M. (2004). Induction of HDAC2 Expression upon Loss of APC in Colorectal Tumorigenesis. *Cancer Cell* 5, 455–463. doi:10.1016/s1535-6108(04)00114-x

§, D. R. R., Kalyana-Sundaram, S., Mahavisno, V., Varambally, R., Yu, J., Briggs, B. B., et al. (2007). Oncomine 3.0: Genes, Pathways, and Networks in a Collection of 18,000 Cancer Gene Expression Profiles. *Neoplasia* 9, 166–180. doi:10.1593/neo.07112

Conflict of Interest: The authors declare that the research was conducted in the absence of any commercial or financial relationships that could be construed as a potential conflict of interest.

Publisher's Note: All claims expressed in this article are solely those of the authors and do not necessarily represent those of their affiliated organizations, or those of the publisher, the editors and the reviewers. Any product that may be evaluated in this article, or claim that may be made by its manufacturer, is not guaranteed or endorsed by the publisher.

frontiers in Cell and Developmental Biology

ORIGINAL RESEARCH
published: 17 March 2022
doi: 10.3389/fcell.2022.818194

Identification of New m^{6}A Methylation Modification Patterns and Tumor Microenvironment Infiltration Landscape that Predict Clinical Outcomes for Papillary Renal Cell Carcinoma Patients

Bin Zheng[1,2,3†], *Fajuan Cheng*[4,5†], *Zhongshun Yao*[1,2], *Yiming Zhang*[1,2], *Zixiang Cong*[1,2,3], *Jianwei Wang*[6], *Zhihong Niu*[1,2*] *and Wei He*[1,2*]

[1]Department of Urology, Shandong Provincial Hospital Affiliated to Shandong University, Jinan, China, [2]Department of Urology, Shandong Provincial Hospital Affiliated to Shandong First Medical University, Jinan, China, [3]Cheeloo College of Medicine, Shandong University, Jinan, China, [4]Department of Nephrology, Shandong Provincial Hospital Affiliated to Shandong University, Jinan, China, [5]Department of Nephrology, Shandong Provincial Hospital Affiliated to Shandong First Medical University, Jinan, China, [6]Department of Urology, Shandong Provincial ENT Hospital Affiliated to Shandong University, Jinan, China

OPEN ACCESS

Edited by:
Ângela Sousa,
University of Beira Interior, Portugal

Reviewed by:
Yan Chun Li,
University of Chicago, United States
Xiuli Liu,
University of Texas Southwestern Medical Center, United States

***Correspondence:**
Zhihong Niu
nzh1789@163.com
Wei He
Hewei@bjmu.edu.cn

†These authors have contributed equally to this work

Specialty section:
This article was submitted to Epigenomics and Epigenetics, a section of the journal Frontiers in Cell and Developmental Biology

Received: 19 November 2021
Accepted: 11 February 2022
Published: 17 March 2022

Citation:
Zheng B, Cheng F, Yao Z, Zhang Y, Cong Z, Wang J, Niu Z and He W (2022) Identification of New m^{6}A Methylation Modification Patterns and Tumor Microenvironment Infiltration Landscape that Predict Clinical Outcomes for Papillary Renal Cell Carcinoma Patients. Front. Cell Dev. Biol. 10:818194. doi: 10.3389/fcell.2022.818194

N6-methyladenosine (m^{6}A) is the product of the most prevalent mRNA modification in eukaryotic cells. Accumulating evidence shows that tumor microenvironment (TME) plays a pivotal role in tumor development. However, the underlying relationship between m^{6}A modification and the TME of a papillary renal cell carcinoma (PRCC) is still unclear. To investigate the relationship between m^{6}A modification and prognosis and immunotherapeutic efficacy for PRCC, we looked for distinct m^{6}A modification patterns based on 23 m^{6}A-related genes. Next, the correlation between m^{6}A modification patterns and TME-related characteristics was investigated. Then, the intersected differentially expressed genes were selected and the scoring system, denoted as m^{6}A score, was established to evaluate m^{6}A modification, prognosis, and immunotherapeutic efficacy. In this study, three distinct m^{6}A expression clusters were identified. Based on the results of immune cell infiltration analysis and functional analysis, carcinogenic pathways, TME-related immune cells, and pathways were identified as well. More importantly, the established m^{6}A score showed good value in predicting clinical outcomes according to results using external cohorts. Specifically, PRCC patients with low m^{6}A score value showed better survival, immunotherapeutic response, and higher tumor mutation burden. Furthermore, immunohistochemistry using PRCC clinical samples from our medical center was carried out and verified our results. In conclusion, this study highlights the underlying correlation between m^{6}A modification and the immune landscape

Abbreviations: ccRCC, clear cell renal cell carcinoma; CNV, Copy number variation; DEGs, Differentially expressed genes; GEO, Gene-Expression Omnibus; GSVA, Gene set variation analysis; ICI, Immunological checkpoint inhibitor; m^{6}A, N6-methyladenosine; PCA, Principal component analysis; PRCC, papillary renal cell carcinoma; ssGSEA, Single-sample gene-set enrichment analysis; TCGA, The Cancer Genome Atlas; TCIA, The Cancer Immunome Atlas; TMB, Tumor mutation burden; TME, tumor microenvironment.

and, hence, enhances our understanding of the TME and improved the therapeutic outlook for PRCC patients.

Keywords: m 6 A, tumor microenvironment, immunotherapy, mutation burden, survival

INTRODUCTION

Kidney cancer is a heterogenous disease for which several subtypes with different genetic and morphologic characteristics are identified. Renal cell carcinoma (RCC) accounts for the vast majority of histological types of kidney cancer with clear cell renal cell carcinoma (ccRCC) making up 70%–80% and papillary renal cell carcinoma (PRCC) 15%–20% of RCCs (Linehan et al., 2016; Barata and Rini, 2017; Vuong et al., 2019). Although most cases of PRCC are indolent with limited risk of mortality, the overall prognosis for PRCC remains limited (Steffens et al., 19902012).

The tumor microenvironment TME is a cellular environment in which tumor cells and other nonmalignant cells exist, and it is composed of various immune cells and related materials, including lymphocytes, fibroblasts, stromal cells, blood vessels, and so on (Wu and Dai, 2017). The TME acts as the soil of tumor cells, and the great impact of TME on tumorigenesis and tumor immunotherapy has become increasingly evident (Li et al., 2021). In an abnormal TME, immune cells become significantly remodeled, which affects their normal functions, such as proliferation, migration, and differentiation (Binnewies et al., 2018). Therefore, immunosuppression is the essential characteristic of TME. Currently, RCC tumors are considered to be immunogenic, and many studies find that various immune cells could infiltrate into RCC TMEs. However, these immune cells block the effective antitumor responses. Owing to the immunosuppressed state of RCC tumors and the immune-tolerance of TMEs, the response of RCC to immune checkpoint inhibitors (ICIs) is unsatisfactory (Syn et al., 2017).

Due to the advances in RNA sequencing, N6-methyladenosine (m^6A), the product of the most common type of mRNA modification in eukaryotic cells, has garnered great interest (Qi et al., 2016; Ke et al., 2017). The m^6A modification is regulated by three types of molecules, known as "writer," "eraser," and "reader" molecules (Yang et al., 2018). It is reported that m^6A modification plays multifaceted roles in tumor development and metastasis (Xiao et al., 2018). Various research investigation indicates that abnormal m^6A modification occurs in most immune cells, including dendritic cells, regulatory T cells, macrophages, $CD4^+$ T cells, and $CD8^+$ T cells, and results in tumor escape or immune disorder (Chen et al., 2018; Han et al., 2019; Li et al., 2021). However, it is still unclear whether m^6A modification in diverse immune cells in the TME is responsible for tumor progression and the effectiveness of ICIs. Therefore, it is essential to determine the potential effects of m^6A modification on the TME and to explore its clinic value as a new therapeutic tool for treatment of PRCC.

MATERIALS AND METHODS

Data Collection and Processing

The expression data and clinical information for kidney renal papillary cell carcinoma (KIRP) were downloaded directly from the Cancer Genome Atlas (TCGA) (https://cancergenome.nih.gov/), Gene Expression Omnibus (https://www.ncbi.nlm.nih.gov/geo/), and the Cancer Immunome Atlas (TCIA) (https://tcia.at/home). Specific data from 289 KIRP patients and 32 tumor-free patients were obtained from these databases. Copy number variation (CNV) and somatic mutation data were downloaded from TCGA as well. Samples without survival data were removed. The "limma" package was used to normalize gene expression data and transform fragments per kilobase per million (FPKM) values to transcripts per kilobase per million (TPM) value. R (R version 4.0.1) was used to extract and analyze expression data and clinical information. After conducting a comprehensive literature review (Zhang et al., 2020; Gu et al., 2021; Zhong et al., 2021), we identified 23 m^6A regulators, including *METTL3*, *METTL14*, *METTL16*, *WTAP*, *VIRMA*, *ZC3H13*, *RBM15*, *RBM15B*, *YTHDC1*, *YTHDC2*, *YTHDF1*, *YTHDF2*, *YTHDF3*, *HNRNPC*, *FMR1*, *LRPPRC*, *HNRNPA2B1*, *IGFBP1*, *IGFBP2*, *IGFBP3*, *RBMX*, *FTO*, and *ALKBH5*, representing m^6A writers, readers, and erasers.

Identification of Differentially Expressed Genes and Functional Analysis

The "limma" and "ggplot2" packages were used to assess and visualize the differentially expressed genes (DEGs) in KIRP samples and nontumor tissues. Difference with adjust $p < .01$ were considered to be significant. Gene Ontology (GO) and Kyoto Encyclopedia of Genes and Genomes (KEGG) analyses were performed through the "clusterProfiler" package. To determine the differences in biological processes between various m^6A expression clusters, specifically to estimate the variation in biological processes, gene set variation analysis (GSVA) was conducted by using the "GSVA" package (Hänzelmann et al., 2013). We utilized the gene set "c2.cp.kegg.v6.2-symbols" from the MSigDB database (Liberzon et al., 2011). Here, adjusted $p < .05$ was considered as the threshold.

Estimation of TME Immune Cell Infiltration and Tumor Mutation Burden

Single-sample gene-set enrichment analysis (ssGSEA) was used to quantify the level of immune infiltration into the PRCC TME (Barbie et al., 2009; Charoentong et al., 2017). The relevant gene set, which marks various TME-infiltrated immune cell subtypes, was collected from previous studies (Barbie et al., 2009; Charoentong et al., 2017). The ssGSEA scores represented the enrichment of different immune cell subtypes in each sample. Tumor mutation burden (TMB) was analyzed with the KIRP somatic mutation data by using the "maftools" R package (Chen and Mellman, 2017). Two TMB sets (high and low TMB) were constructed by using an optimal cutoff value of TMB. We evaluated the difference between the m6Ascore values of two TMB sets.

Unsupervised Clustering and the Construction of an m^{6}A Regulators Model

Owing to relatively small sizes of the KIRP data sets in the Gene-Expression Omnibus (GEO) database, we used the GSE2748 cohort and TCGA KIRP data set to perform unsupervised clustering analysis with the "ConsensusClusterPlus" package (Wilkerson and Hayes, 2010). Here, 1000 repetitions were performed. The expression data of 23 m^{6}A genes were extracted from GSE2748. The clustering analysis was performed to classify the KIRP samples into distinct m^{6}A expression clusters based on the expression of 23 m^{6}A regulators.

To quantify the m^{6}A expression cluster of each KIRP sample, the m^{6}A score was applied and established as follows. First, we identified intersected DEGs from the constructed m^{6}A expression clusters. All KIRP patients were divided into diverse groups *via* unsupervised clustering analysis. Then, the univariate Cox regression analysis was utilized to assess the prognosis of each selected gene. $p < .05$ was considered as the significance criterion. After extracting the prognosis-related regulators, we applied principal component analysis to establish the m^{6}A gene model, and the principal components 1 and 2 were selected as signature scores. Finally, m^{6}A score was calculated using following formula: m^{6}A score = Σ ($PC1_i$ + $PC2_i$) (where i is the expression of the selected m^{6}A related DEGs from the m^{6}A expression cluster) (Sotiriou et al., 2006; Zeng et al., 2019).

Genomic and Clinical Data for ICI Therapy

Then, we investigated whether the established m^{6}A expression cluster could predict the response of PRCC to ICI therapy based on two immunotherapy cohorts. After a comprehensive search for gene expression data and complete clinical information of patients treated with ICIs, we finally included two related cohorts. The first cohort involved metastatic melanoma patients treated with the anti-PD-1 drug (pembrolizumab) from the GEO database (GSE78220). Moreover, genomic and clinical data for mTOR inhibitor (everolimus) therapy was downloaded from the **Supplementary File** appended to published study (Barbie et al., 2009; Charoentong et al., 2017). All raw expression data were normalized using the "limma" package and transformed into the more comparable TPM value.

Immunohistochemistry

Five pairs of PRCC and adjacent normal tissues were collected from May 2021 to October 2021 from Shandong Provincial Hospital affiliated with Shandong First University. The study was approved by the Ethics Committee of Shandong Provincial Hospital (Approval No. SWYX: NO. 2021-491). IHC was performed according to published method (Wang et al., 2020). All samples were incubated with rabbit polyclonal anti-CD8 (ab101500), anti-CD69 (ab233396), anti-CD163 (ab182422), anti-YTHDF1 (ab252346), anti-YTHDF2 (ab220163), anti-YTHDF3 (ab220161), anti-ZC3H13 (IHC0104123), anti-HNRNPA2B1 (ab31645), and anti-IGFBP2 (ab188200) antibodies overnight at 4°C and then washed. Two pathologists independently assessed the IHC slides.

Statistical Analysis

The Kruskal–Wallis test was used to estimate the significance of differences between values of three or more groups. Spearman's correlation analysis was applied to calculate the correlation coefficient between number of TME-infiltrated immune cells and the expression level of m^{6}A regulators. We employed the "survminer" package to determine the optimal cutoff value. Based on the optimal cutoff point, all PRCC patients were grouped into high or low m^{6}A score sets. Then, the Kaplan–Meier analysis with a log-rank test was conducted to test the prognosis of patients. The mutation landscape of KIRP cohorts was depicted by using the "maftools" package (Mayakonda et al., 2018). Statistical analysis was performed with R packages (version 4.0.1). A two-tailed $p < .05$ was considered to be significant.

RESULTS

Genetic Variation and Clinical Relevance of m^{6}A Genes in PRCC

Based on the transcriptomic profiles of 23 m^{6}A regulators, we investigated the expression pattern of all m^{6}A regulators in PRCC and normal samples from TCGA (**Figure 1A**). Then, we integrated CNV as well as somatic mutations and illustrated the prevalence of alteration of m^{6}A genes in PRCC. Only 22 of 281 samples (7.83%) showed m^{6}A regulator mutations. Specifically, 8 out of 23 m^{6}A regulators experienced mutations (**Figure 1B**). Afterward, we investigated the CNV frequency of 23 m^{6}A genes, which identified that most CNV alterations in 23 genes were focused on the CNV deletion (**Figure 1C**). Moreover, we determined the locations of the CNV alteration on human chromosomes as well (**Figure 1D**). These results indicate that genetic variation commonly occurs in PRCC cells and is heterogeneous between PRCC and normal tissues, exhibiting the potential role for the aberrant expression of m^{6}A genes in tumorigenesis and development as well as progression. Finally, when investigating the potential clinical relevance of 23 m^{6}A regulators, we found that three types of m^{6}A regulators were positively correlated with patient prognosis and interacted with each other (**Figure 1E** and **Supplementary Figure S1A**). In addition, most of the genes were indicated to be risk factors for overall survival (OS) of PRCC patients; only *YTHDC1*, *ALKBH5*, *FTO*, *RBM15B*, *METTL14*, and *METTL16* were out.

We also determined whether genetic variations of "writer," "reader," and "eraser" genes were associated with the expression other m^{6}A regulators' (**Supplementary Figures S1B–L**). The results demonstrate that only *YTHDF1* was upregulated in *METTL14* mutated PRCC samples while other m^{6}A genes highly expressed in wild-type *ALKBH5*, *HNRNPC*, *METTL14*, *YTHDC1*, and *YTHDC2*.

Different m^{6}A Modification Patterns Mediated by 23 m^{6}A Genes and Its Clinical Relevance

Based on the expression levels of the 23 m^{6}A genes, we classified the PRCC patients by carrying out unsupervised clustering analysis (**Supplementary Figures S2A–E**). We finally identified three

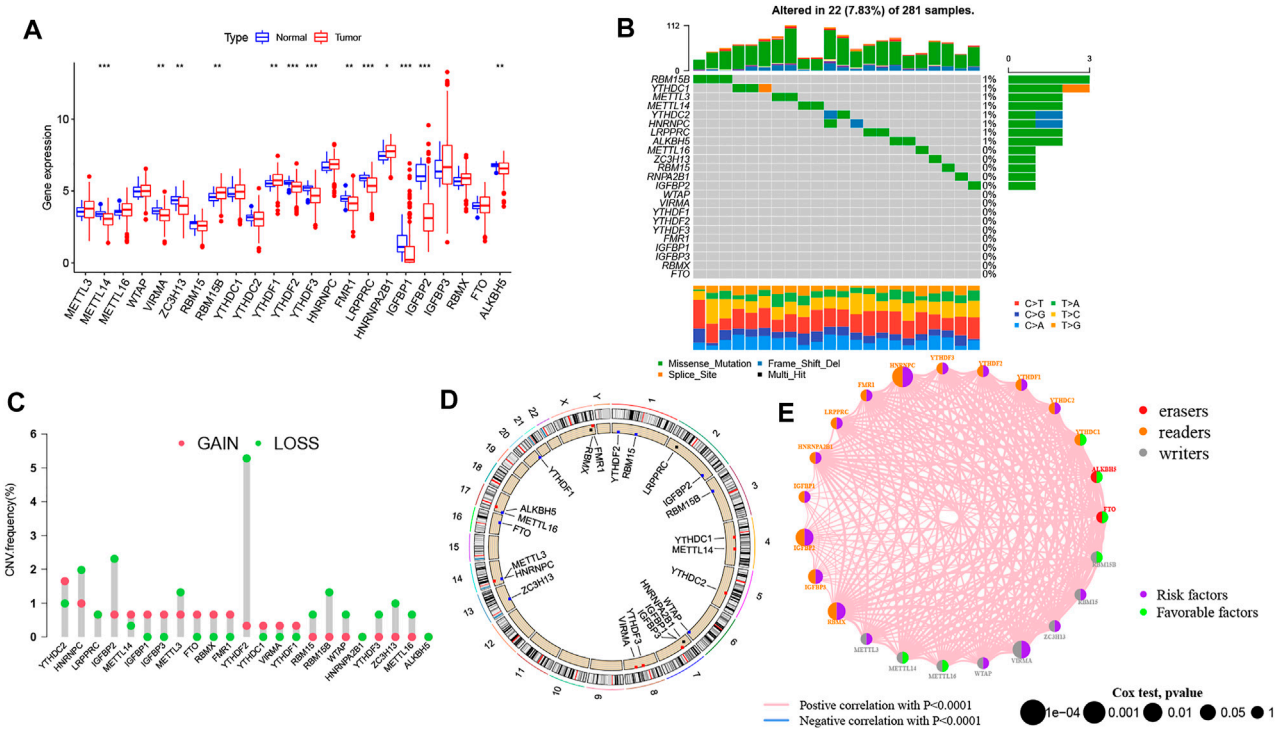

FIGURE 1 | Characteristics of genetic and variation of m^{6}A genes in pRCC. **(A)** Transcriptomic profile of 23 m6A genes among normal and PRCC tumor tissues. The upper and lower ends of the boxes indicate interquartile range (IQR) of values. The lines in the boxes represent each the median value. The asterisks represented the *p* value. (*p < .05; **p < .01; ***p < .001) **(B)** Mutation frequency of 23 m^{6}A genes in in 289 PRCC patients. The bar plot at the upper part of the figure shows TMB. Numbers on the right part of the figure represent the mutation frequency. **(C)** CNV alteration frequency of 23 m^{6}A genes in the 289-patient PRCC cohort. The height of each column indicates the alteration frequency. The red dot represents the amplification frequency; the green dot represents the deletion frequency. **(D)** Location of CNV alterations of 23 m^{6}A genes on human chromosomes in PRCC cohort. **(E)** Interaction network of 23 m^{6}A genes in the PRCC cohort. The size of each circle is indicative of the magnitude of the effect on the prognosis. The green dots mean the protective factors, and the purple dots represent the risk factors. The thickness of each line indicates the degree of correlation between each gene.

patterns, termed as m^{6}A expression clusters A, B and C, which included 56 cases in m^{6}A expression cluster A, 128 cases in m^{6}A expression cluster B, and 127 cases in m^{6}A expression cluster C (**Figure 2A**). Then, we determined the prognostic values of the three m^{6}A modification patterns. According to this analysis, m^{6}A expression cluster A showed the most favorable survival (**Figure 2B**). After combing the TCGA and GEO data sets for comprehensive clinical data from PRCC patients, we made a heat map to visualize the correlation between the three m^{6}A expression clusters and clinical characteristics. As shown in the **Figure 2A**, m^{6}A expression cluster C was associated with poor prognosis and enriched in metastatic tumors as well as being associated with patient old age. By comparison, m^{6}A expression clusters A and B showed relatively better prognose. We also noted that 23 m^{6}A-related genes had relatively high expression levels in m^{6}A expression cluster C, followed by m^{6}A expression clusters B and A (**Figure 2C**).

Biological and TME Cell Infiltration Characteristics in Three m^{6}A Modification Patterns

To investigate the biological processes associated with the three types of m^{6}A modification patterns, we performed a GSVA analysis. The m^{6}A expression cluster A was found to be associated with immune activation processes, such as complement and coagulation cascades. The m^{6}A expression cluster B was found to be associated with oncogenic and stromal signaling pathways, including mTOR signaling pathways, ERBB signaling pathways, and adherens junction. The m^{6}A expression cluster C was also found to be related with immune-related pathways, such as the Notch signaling pathway (**Figures 2D,E**). Then, we explored the TME cell infiltration for the different m^{6}A expression clusters. The ssGSEA analysis presented that activated CD8$^+$ T cells, myeloid-derived suppressor cells, and several innate immune cells, such as macrophages and monocytes, were enriched in m^{6}A expression cluster A (**Figure 3A**). Moreover, m^{6}A expression cluster C was associated with natural killer cells, plasmacytoid dendritic cells, and type 2 T helper cells. Afterward, we determined the proportion of immune cells in the three m^{6}A expression clusters by using the CIBERSORT algorithm (**Figure 3B**). However, a significant difference between the different immune cells was not observed. Finally, we used principal component analysis (PCA), which verified significant differences between the three distinct clusters of PRCC patients (**Figure 3C**).

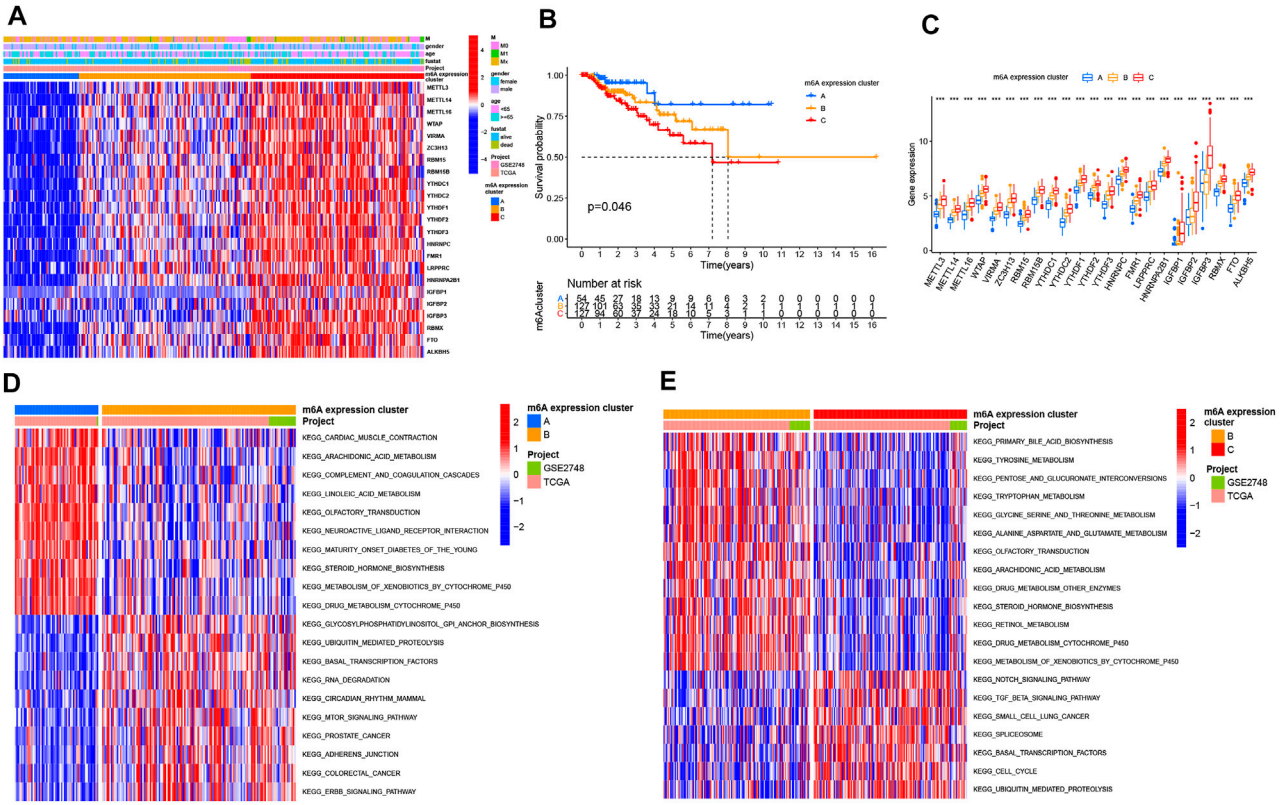

FIGURE 2 | Distinct m^{6}A modification patterns and biological features of each cluster. **(A)** Unsupervised clustering of 23 m^{6}A genes in TCGA PRCC and GSE2748 data sets. The m^{6}A expression cluster, tumor M stage, survival status, gender, and age were used as annotations. Red means high expression of m^{6}A genes, and blue represents low expression. The M means metastasis. **(B)** Kaplan–Meier survival analysis showing the OS for the three m^{6}A expression clusters based on TCGA PRCC and GSE2748 data sets. A log-rank test was performed. **(C)** Expression pattern of 23 m^{6}A genes among three m^{6}A expression clusters. The upper and lower ends of the boxes mean interquartile range (IQR) of the values. The lines in the boxes represent each the median value. The asterisks represent the *p* value. (*$p < .05$; **$p < .01$; ***$p < .001$) **(D,E)** GSVA enrichment analysis depicting the activation states of the biological processes in three m^{6}A expression clusters. In the heat map, red means activated pathways, and blue means inhibited pathways. **(D)** m^{6}A expression clusters B vs. A **(E)** m^{6}A expression clusters B vs. C.

Model and Biological Characteristics of the m^{6}A Regulators

To further describe the features of the three m^{6}A expression clusters, we identified 4780 intersected m^{6}A DEGs among the three clusters (**Supplementary Figure S2E**). Afterward, we analyzed these phenotype-related genes by carrying out KEGG and GO enrichment analyses. The GO analysis revealed a significant enrichment (FDR <0.01) of the methyltransferase complex, RNA methyltransferase activity, and activation of innate immune response (**Figure 3D** and **Supplementary Table S1**). The KEGG pathway analysis also indicated that RCC, PD-L1 expression, and the PD-1 checkpoint pathway in cancer were enriched in these selected m^{6}A DEGs (**Figure 3E** and **Supplementary Table S2**). The above analysis further confirmed the pivotal role played by m^{6}A modification in immune regulation as well as RCC. Next, univariate Cox regression analysis was carried out to determine the prognosis-related m^{6}A genes. Here, 1285 prognosis-related m^{6}A regulators were extracted for unsupervised clustering analysis. With the optimal $k = 3$, three genomic clusters were constructed and named m^{6}A-based gene expression clusters A–C (**Supplementary Figures S3A–E**). A PCA analysis found difference between these three m^{6}A-based gene expression clusters as well (**Figure 3F**). Once again, these results confirmed that diverse m^{6}A modification patterns occurred for PRCC.

To determine the clinical relevance of these clusters, we evaluated the healthy status among the three m^{6}A-based gene expression clusters. The m^{6}A-based gene cluster C showed a worse prognosis than did m^{6}A-based gene expression clusters A and B (**Figure 4A**). As shown in **Figure 4B**, m^{6}A-based gene expression cluster C was mainly enriched in metastatic tumors. However, the other clusters were related with alive status as well as nonmetastatic tumor (**Figure 4B**). The results of the differential analysis of the three clusters validated the pattern of m^{6}Agene signatures as well (**Figure 4C**).

Evaluation of the m^{6}A Modification Patterns Among the m^{6}A Regulator Signatures

We employed m^{6}A score (a scoring methodology) to quantify and evaluate m^{6}A modification patterns. Alterations of each of the PRCC

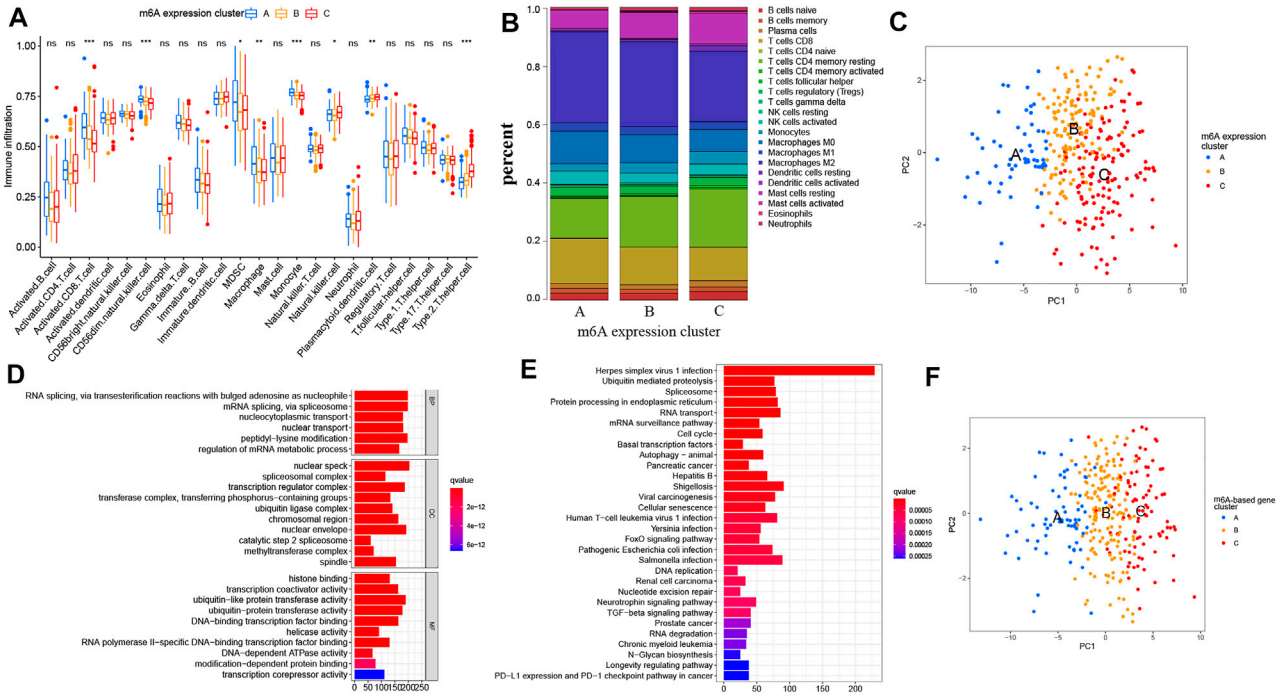

FIGURE 3 | Characteristics of TME cell infiltration in diverse m^{6}A expression clusters and the construction of m^{6}A gene signatures. **(A)** Abundance of TME-related immune cells in three m^{6}A patterns. The histogram shows the expression difference of 23 kinds of immune cells between m^{6}A expression cluster A, B, and C. The upper and lower ends of the boxes mean interquartile range (IQR) of the values. The lines in the boxes represent each the median value. The asterisks represent the *p* value. (*$p < .05$; **$p < .01$; ***$p < .001$) **(B)** Proportion of different TME-related immune cells in the three m^{6}A patterns as analyzed by CIBERSORT. **(C)** Principal component analysis of PRCC patients in three m^{6}A expression clusters, which indicates a remarkable difference between the different modification patterns. **(D**,**E)** Functional analysis for m^{6}A-related genes. **(D)** GO enrichment analysis. **(E)** KEGG enrichment analysis. MF means molecular function, CC means cellular component, and BP means biological process. **(F)** Principal component analysis of PRCC patients for the three m^{6}A-based gene expression clusters. The left part of each figure indicates the biological functions and signaling pathways. The degree of enrichment is represented by the color depth of each bar plot.

patient's attributes were visualized by producing and inspecting an alluvial diagram. The results suggest that most of the PRCC samples showing the m6A-based gene expression cluster C were marked with a high m^{6}A score and showed poor patient survival (**Figure 4D**). Then, we assessed the correlations between m^{6}A score and biological processes. The m^{6}A score was only positively associated with processes involving type 2 T helper cells but negatively correlated with processes involving other immune cells (**Figure 4E**). Significant differences in the m^{6}A score were observed between the three m^{6}A-based gene expression clusters as well as between the m^{6}A expression clusters. Both of these results presented that m6A expression cluster C and m6A-based gene expression cluster C have the highest m^{6}Ascore (**Figures 4F,G**). Afterward, PRCC patients were divided into two distinct groups with an optimal cutoff value. As shown in **Figure 4H**, patients with low m^{6}A scores showed relatively good survival compared with the high m^{6}A score group.

The m^{6}A Modification Model in the Role of Tumor Somatic Mutation and Immunotherapy

We also analyzed and visualized the somatic mutation profiles of PRCC patients of the high and low m^{6}A score groups by using the "maftools" package. Compared with the high m^{6}A score set, the low m^{6}A score group showed a higher percentage of somatic mutations (**Figures 5A,B**). A previous study shows an association of high TMB with better survival for most cancers (Xie et al., 2020). Still, a high TMB could improve the prognosis for patients treated with ICIs (Samstein et al., 2019). Considering the significant role of TMB, we tested its prognosis value for PRCC. As observed in the survival plot, the high-TMB set presented improved survival (**Figure 5C**). Moreover, we found the worst survival for the PRCC patients with both a low-TMB and high m^{6}A score (**Figure 5D**). The above outcome implies that TMB as well as m^{6}A score could potentially be used as predictive biomarkers.

Next, we interrogated the clinical value of the m^{6}A modification model in immunotherapy (including PD-1 blockade and mTOR inhibitor). In the PD-1 blockade cohort (GSE78220), patients with low m^{6}A scores showed improved overall survival (OS) (**Figure 6A**). In addition, in the anti-mTOR group, there was a significant difference in OS as well as progression free survival (PFS) between low and high m^{6}A score groups. The therapeutic advantages of the mTOR inhibitor was observed in the low m^{6}A score group (**Figures 6B,C**). Moreover, in light of unsatisfactory outcomes from tumor therapy, we queried whether m^{6}A score could affect the

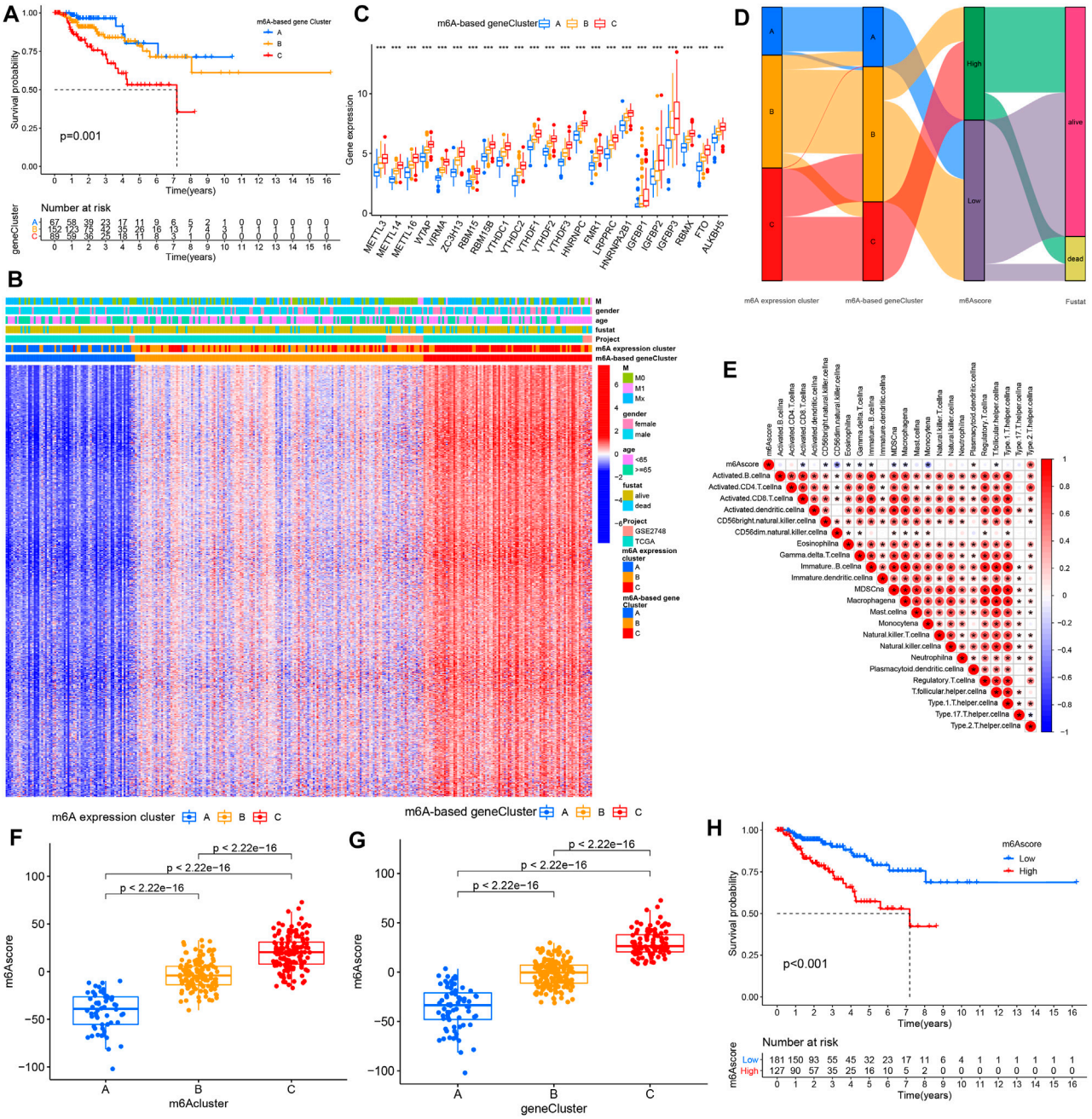

FIGURE 4 | Characteristics of diverse m^{6}A-based gene expression clusters. **(A)** Kaplan–Meier survival analysis showed the OS for the three m^{6}A-based gene expression clusters based on TCGA PRCC and GSE2748 data set with PRCC. **(B)** Unsupervised clustering of the intersected m^{6}A phenotype-related genes in PRCC, which classifies patients into several clusters, termed m^{6}A-based gene expression clusters. The m^{6}A cluster, tumor M stage, survival status, gender, and age are used as annotations. Red means high expression of m^{6}A genes, and blue represents low expression. The M means metastasis. **(C)** Expression pattern of 23 m^{6}A genes for the three m^{6}A-based gene expression clusters. The histogram indicates the expression level of 23 m^{6}A genes between m^{6}A-based gene cluster A, B, and C. The upper and lower ends of the boxes mean each the interquartile range (IQR) of values. The lines in the boxes represent median value. The asterisks represented the *p* value. (**p* < .05; ***p* < .01; ****p* < .001). **(D)** Alluvial diagram displaying the differences in m^{6}A expression clusters, m^{6}A-based gene expression clusters, and m^{6}Ascore. **(E)** Spearman analyses of the correlations between m^{6}Ascore and biological characteristics in the PRCC cohort. **(F,G)** Differential analysis of m^{6}A score values among **(F)** m^{6}A expression clusters and **(G)** m^{6}A-based gene expression clusters in TCGA PRCC and GSE2748 data sets. **(H)** K–M analyses for the OS of PRCC patients in high and low m^{6}A score groups.

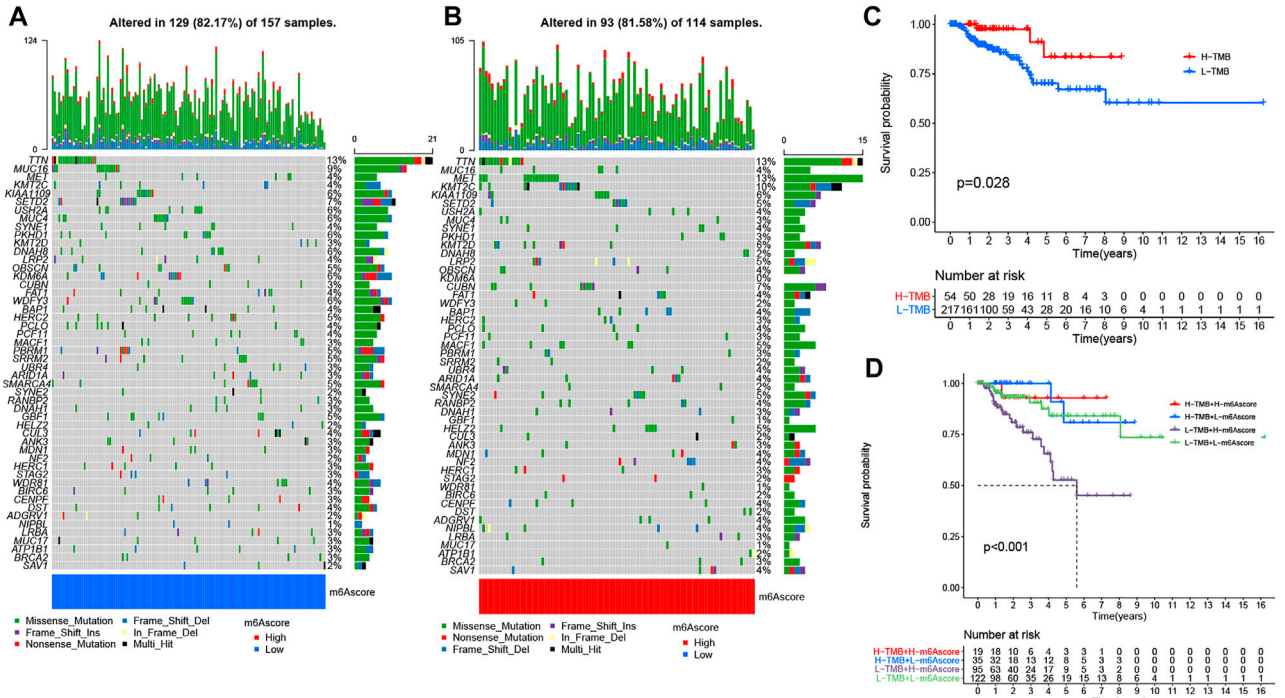

FIGURE 5 | The changes of somatic mutations among distinct m^{6}A score groups. **(A,B)** Waterfall plot showing The changes of somatic mutations in **(A)** the low-m6A score set and **(B)** high-m6A score group. The bar plot at the upper part of the figure shows TMB. The numbers on the right part of the figure represent the mutation frequency. **(C)** Survival analysis for the OS of patients in high- and low-TMB groups. **(D)** K-M analysis for PRCC patients stratified by both m^{6}A score and TMB. MSI-H, high microsatellite instability; MSI-L, low microsatellite instability.

therapeutic efficacy. The poor outcome of overall response rate and clinical benefit was correlated with high m^{6}A score (**Figures 6D,E**). Finally, we used the m^{6}A score to predict the reaction to immunotherapy efficacy. After downloading the immunotherapy fraction data from the Cancer Immunome Database (TCIA), we compared the predictive abilities of the m^{6}A scores of the two m^{6}A score groups. Patients with low m^{6}A score values showed significantly better reactions to anti-CTLA-4 and anti-PD-1 therapy (**Figures 6F–I**).

Biological Validation of Significant m^{6}A Regulators and Immune Cell Markers

The robustness of m^{6}A regulators as biomarkers was verified using primary PRCC clinical samples from the Shandong Provincial Hospital affiliated with Shandong First Medical University. We selected six m^{6}A genes from the DEGs and five immune cell markers for the following validation. The IHC images acquired of immune cell markers showed weak staining for CD8, CD69, and CD163 in normal renal tissue (**Figures 7G–I**). Tumor tissue staining of YTHDF1 and HNRNPA2B1 showed moderate staining in the nucleus, and negative staining was observed in the normal tissues (**Figures 7A,D**). In normal kidney samples, moderate staining for ZC3H13 and YTHDF2 were observed in the nucleus. Regarding the YTHDF3 and IGFBP2, strong staining was positive on the cytoplasm (**Figures 7B,C,E,F**). However, weak staining patterns for ZC3H13, YTHDF2, YTHDF3, and IGFBP2 were observed in PRCC tissues (**Figures 7B,C,E,F**). These unique IHC staining patterns further confirmed the above results and illustrated that these selected m^{6}A regulators could be used to predict clinical outcomes.

DISCUSSION

The m^{6}A modification plays a pivotal role in tumorigenesis, tumor development, progression, and prognosis (He et al., 2019). Previous studies show the m^{6}A modification displaying dual suppressive and promotive functions in various tumors (He et al., 2018; Wang et al., 2018). However, there are few studies of the m^{6}A modification for RCC (especially PRCC) initiation, progression, and therapy. The TME is a potential regulator of cancer progression and a source of therapeutic targets. In the complex TME, immune and stromal cells play significant roles in cancer development (Quail and Joyce, 2013; Ho et al., 2020). Currently, knowledge of the kidney TME is restricted to only a few different tumor types and lacks comprehensive analysis. Therefore, in this study, we focused our attention on the role of m^{6}A modification in the TME of PRCC and aimed to unravel the potential functions of this modification and contribute to

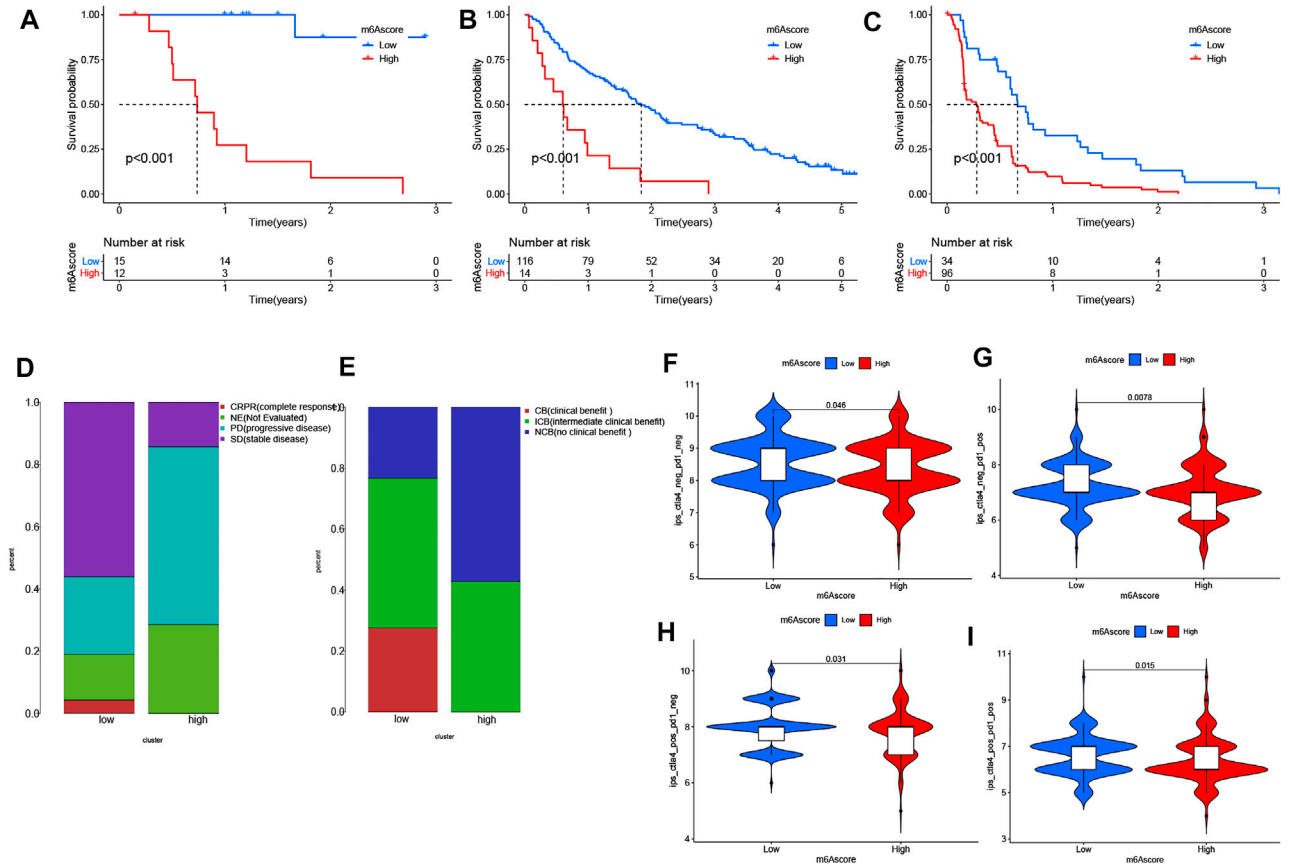

FIGURE 6 | The role of distinct m^{6}A modification patterns in immunotherapy. **(A–C)** Results showing the associations of m6A score was negatively associated with OS and PFS following **(A**,**B)** anti-PD-1 therapy or **(C)** use of mTOR inhibitors. Negative associations were observed in both cases. **(D**,**E)** Proportions of PRCC patients with **(D)** an immunotherapy response and **(E)** clinical benefit in the two m6Ascore sets. **(F–I)** Relationship between m6A score and immunotherapeutic response under PD-1 and CTLA-4 expressions: **(F)** negative PD-1 and CTLA-4. **(G)** positive PD-1 and negative CTLA-4. **(H)** positive CTLA-4 and negative PD-1. **(I)** positive PD-1 and CTLA-4.

obtaining a deeper understanding of antitumor immune effects of the TME in PRCC.

CNV is one of the most important somatic aberrations in cancer, and several studies find significant associations between CNVs and cancers (Speleman et al., 2008; Shlien and Malkin, 2009; Beroukhim et al., 2010). Based on 23 m^{6}A genes and PRCC copy-number profiles, we explored the alteration of m^{6}A genes in PRCC. The mutations of the m^{6}A regulators occurred relatively infrequently in PRCC, but CNV deletion was a common event. Then, on the basis of clustering analysis, we identified three different m^{6}A expression clusters in PRCC. In 2017, Chen DS et al. proposed three types of cancer-immune phenotypes, namely, immune-inflamed, immune-excluded, and immune-desert phenotypes (Speleman et al., 2008; Shlien and Malkin, 2009; Beroukhim et al., 2010). The immune-inflamed phenotype is characterized by the presence of CD4$^+$ T, CD8$^+$ T, myeloid, and monocytc cells in the TME, which is positioned near the tumor cells (Herbst et al., 2014; Turley et al., 2015). The immune-excluded phenotype also involves the presence of many immune cells, but with these cell, located mainly surrounding the stroma instead of the nest of the tumor (Joyce and Fearon, 2015; Hegde et al., 2016). The immune-desert phenotype presents a paucity of CD8$^+$ T cells in both tumor parenchyma and stroma with this paucity being a feature of a noninflamed TME (Gajewski et al., 2013; Kim and Chen, 2016). In our current study, we found an enrichment of activated CD8$^+$ T cells, myeloid-derived suppressor cells, macrophages, and monocytes in m^{6}A expression cluster A, an association of the m^{6}A expression cluster B with adherens junction, and m^{6}A expression cluster C showing the presence of natural killer and plasmacytoid dendritic cells. Due to the presence of CD8 expressing T cells and other myeloid cells as well as monocytes, the m^{6}A expression cluster A showed improved survival.

Then, we identified the intersected DEGs between diverse m^{6}A expression clusters and assessed the potential biological functions of these genes and the pathways used by them. Our results show a significant enrichment of these DEGs in m^{6}A-, immune- and immunotherapy-related biological functions and pathways. Moreover, we chose T cell (CD8, CD69) and macrophage markers (CD163) as well as differentially expressed m^{6}A regulators to validate the clinical application using primary PRCC samples from our hospital, and the results further

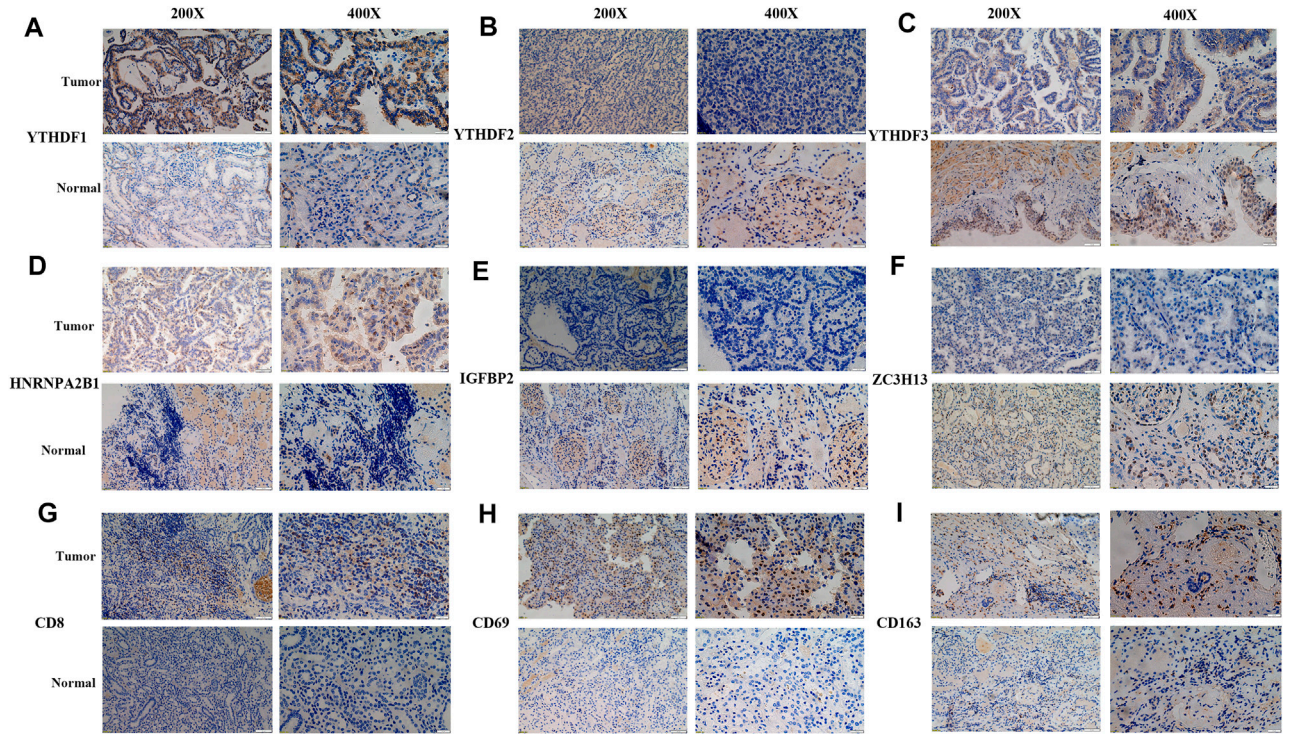

FIGURE 7 | Representative IHC images of significant m^{6}A regulators and immune cell markers in PRCC samples. **(A–F)** IHC patterns for selected m^{6}A regulators in normal and tumor samples. **(G–I)** IHC patterns for three immune cell markers in normal and tumor samples. Bar, 50 and 200 μm.

confirm the prognostic value in clinical application. To limit the individual heterogeneity, we utilized m^{6}A score to quantify and evaluate m^{6}A modification patterns. Similar to the results of previous research, the m^{6}A expression cluster C and m^{6}A expression cluster A in the current work presented, respectively, the highest and lowest m^{6}A score in PRCC. The K-M survival curve illustrates a better OS and better prognosis associated with m^{6}A-based gene expression cluster A than with m^{6}A-based gene expression cluster C. These results suggest that the m^{6}A scoring system could be applied to determine distinct immune phenotypes and m^{6}A modification patterns.

Somatic mutation was detected between high- and low-m^{6}A score groups as well. The low m^{6}A score group had a high TMB with high TMB associated with better survival for PRCC patients. A similar trend was found in studies involving melanoma and osteosarcoma (Aoude et al., 2020; Xie et al., 2020). Still, a high TMB appears to indicate a better prognosis for patients receiving ICIs for treating various types of tumors (Snyder et al., 2014; Rizvi et al., 2015; Van Allen et al., 2015; Rosenberg et al., 2016). These findings suggest better immunotherapeutic outcomes for the low m^{6}A score group than for the high m^{6}A score group. In light of the disappointing outcomes from immunotherapy (including anti-PD-1 therapy and mTOR inhibitors) to date (Larkin et al., 2015; Postow et al., 2015; Rotte et al., 2018; de Vries-Brilland et al., 2020), we sought to determine whether m^{6}A score could serve as a biomarker to stratify patients with different levels of immune-responsiveness to tumors. By utilizing GSE78220 (PD-1 blockade cohort) and the anti-mTOR group (Hugo et al., 2016; Braun et al., 2020), we showed an association between a low m^{6}A score and improve OS and PFS time. Thus, distinct m^{6}A modification patterns may impact the efficacy of immunotherapy, and m^{6}A score has potential clinical value in evaluating the efficacy of therapeutic.

To improve the outcome for PRCC patients, access to accurate and efficient biomarkers is indispensable. Therefore, we investigated the TME and m^{6}A-related genes to reveal the associated immune cells and molecular mechanism as well as clinical value. This investigation suggests that diverse m^{6}A modification patterns could affect the complexity of the PRCC TME. Moreover, the established m^{6}A score was indicated by our results to have great potential as a predictive indicator to assess the distinct m^{6}A modification patterns and prognose of PRCC patients. More importantly, given the high variety of responses to immunotherapy, the m^{6}A score may be utilized to evaluate how tumors might react to being exposed to an immunotherapy (including anti-PD-1 therapy and mTOR inhibitors). We do note that the relatively small number of PRCC patients receiving immunotherapy may affect the predictive ability of m^{6}A score. Therefore, in future investigations, expression data and clinical information from our medical center will be collected. Further experiments *in vivo* and *in vitro* will also be implemented to confirm the molecular mechanism of m^{6}A-related regulators in the PRCC TME. Nevertheless, the study we carried out has enhanced our understanding of TME characteristics and improved the therapeutic landscape for PRCC patients.

DATA AVAILABILITY STATEMENT

The original contributions presented in the study are included in the article/**Supplementary Material**, further inquiries can be directed to the corresponding authors.

ETHICS STATEMENT

The studies involving human participants were reviewed and approved by the Ethics Committee of Shandong Provincial Hospital. The patients/participants provided their written informed consent to participate in this study.

AUTHOR CONTRIBUTIONS

BZ and WH contributed to the study conception; FC, BZ, JW, ZY, YZ, and ZC conducted the data analysis and were responsible for writing the first draft of the paper. WH, FC, and ZN revised the paper; and all authors read and approved the final version of the manuscript.

SUPPLEMENTARY MATERIAL

The Supplementary Material for this article can be found online at: https://www.frontiersin.org/articles/10.3389/fcell.2022.818194/full#supplementary-material

REFERENCES

Aoude, L. G., Bonazzi, V. F., Brosda, S., Patel, K., Koufariotis, L. T., Oey, H., et al. (2020). Pathogenic Germline Variants Are Associated with Poor Survival in Stage III/IV Melanoma Patients. *Sci. Rep.* 10 (1), 17687. doi:10.1038/s41598-020-74956-3

Barata, P. C., and Rini, B. I. (2017). Treatment of Renal Cell Carcinoma: Current Status and Future Directions. *CA: a Cancer J. clinicians* 67 (6), 507–524. doi:10.3322/caac.21411

Barbie, D. A., Tamayo, P., Boehm, J. S., Kim, S. Y., Moody, S. E., Dunn, I. F., et al. (2009). Systematic RNA Interference Reveals that Oncogenic KRAS-Driven Cancers Require TBK1. *Nature* 462 (7269), 108–112. doi:10.1038/nature08460

Beroukhim, R., Mermel, C. H., Porter, D., Wei, G., Raychaudhuri, S., Donovan, J., et al. (2010). The Landscape of Somatic Copy-Number Alteration across Human Cancers. *Nature* 463 (7283), 899–905. doi:10.1038/nature08822

Binnewies, M., Roberts, E. W., Kersten, K., Chan, V., Fearon, D. F., Merad, M., et al. (2018). Understanding the Tumor Immune Microenvironment (TIME) for Effective Therapy. *Nat. Med.* 24 (5), 541–550. doi:10.1038/s41591-018-0014-x

Braun, D. A., Hou, Y., Bakouny, Z., Ficial, M., Sant' Angelo, M., Forman, J., et al. (2020). Interplay of Somatic Alterations and Immune Infiltration Modulates Response to PD-1 Blockade in Advanced clear Cell Renal Cell Carcinoma. *Nat. Med.* 26 (6), 909–918. doi:10.1038/s41591-020-0839-y

Charoentong, P., Finotello, F., Angelova, M., Mayer, C., Efremova, M., Rieder, D., et al. (2017). Pan-cancer Immunogenomic Analyses Reveal Genotype-Immunophenotype Relationships and Predictors of Response to Checkpoint Blockade. *Cel Rep.* 18 (1), 248–262. doi:10.1016/j.celrep.2016.12.019

Chen, D. S., and Mellman, I. (2017). Elements of Cancer Immunity and the Cancer-Immune Set point. *Nature* 541 (7637), 321–330. doi:10.1038/nature21349

Chen, M., Wei, L., Law, C.-T., Tsang, F. H.-C., Shen, J., Cheng, C. L.-H., et al. (2018). RNA N6-Methyladenosine Methyltransferase-like 3 Promotes Liver Cancer Progression through YTHDF2-dependent Posttranscriptional Silencing of SOCS2. *Hepatology* 67 (6), 2254–2270. doi:10.1002/hep.29683

de Vries-Brilland, M., Gross-Goupil, M., Seegers, V., Boughalem, E., Beuselinck, B., Thibault, C., et al. (2020). *Are Immune Checkpoint Inhibitors a Valid Option for Papillary Renal Cell Carcinoma? A Multicentre Retrospective Study*, 136. Oxford, United Kingdom: European journal of cancer, 76–83.

Gajewski, T. F., Woo, S.-R., Zha, Y., Spaapen, R., Zheng, Y., Corrales, L., et al. (2013). Cancer Immunotherapy Strategies Based on Overcoming Barriers within the Tumor Microenvironment. *Curr. Opin. Immunol.* 25 (2), 268–276. doi:10.1016/j.coi.2013.02.009

Gu, Y., Wu, X., Zhang, J., Fang, Y., Pan, Y., Shu, Y., et al. (2021). The Evolving Landscape of N6-Methyladenosine Modification in the Tumor Microenvironment. *Mol. Ther.* 29 (5), 1703–1715. doi:10.1016/j.ymthe.2021.04.009

Han, D., Liu, J., Chen, C., Dong, L., Liu, Y., Chang, R., et al. (2019). Anti-tumour Immunity Controlled through mRNA m6A Methylation and YTHDF1 in Dendritic Cells. *Nature* 566 (7743), 270–274. doi:10.1038/s41586-019-0916-x

Hänzelmann, S., Castelo, R., and Guinney, J. (2013). GSVA: Gene Set Variation Analysis for Microarray and RNA-Seq Data. *BMC bioinformatics* 14, 7. doi:10.1186/1471-2105-14-7

He, L., Li, H., Wu, A., Peng, Y., Shu, G., and Yin, G. (2019). Functions of N6-Methyladenosine and its Role in Cancer. *Mol. Cancer* 18 (1), 176. doi:10.1186/s12943-019-1109-9

He, L., Li, J., Wang, X., Ying, Y., Xie, H., Yan, H., et al. (2018). The Dual Role of N6-methyladenosine Modification of RNAs Is Involved in Human Cancers. *J. Cel Mol Med* 22 (10), 4630–4639. doi:10.1111/jcmm.13804

Hegde, P. S., Karanikas, V., and Evers, S. (2016). The where, the when, and the How of Immune Monitoring for Cancer Immunotherapies in the Era of Checkpoint Inhibition. *Clin. Cancer Res.* 22 (8), 1865–1874. doi:10.1158/1078-0432.ccr-15-1507

Herbst, R. S., Soria, J.-C., Kowanetz, M., Fine, G. D., Hamid, O., Gordon, M. S., et al. (2014). Predictive Correlates of Response to the Anti-PD-L1 Antibody MPDL3280A in Cancer Patients. *Nature* 515 (7528), 563–567. doi:10.1038/nature14011

Ho, W. J., Jaffee, E. M., and Zheng, L. (2020). The Tumour Microenvironment in Pancreatic Cancer - Clinical Challenges and Opportunities. *Nat. Rev. Clin. Oncol.* 17 (9), 527–540. doi:10.1038/s41571-020-0363-5

Hugo, W., Zaretsky, J. M., Sun, L., Song, C., Moreno, B. H., Hu-Lieskovan, S., et al. (2016). Genomic and Transcriptomic Features of Response to Anti-PD-1 Therapy in Metastatic Melanoma. *Cell* 165 (1), 35–44. doi:10.1016/j.cell.2016.02.065

Joyce, J. A., and Fearon, D. T. (2015). T Cell Exclusion, Immune Privilege, and the Tumor Microenvironment. *Science* 348 (6230), 74–80. doi:10.1126/science.aaa6204

Ke, S., Pandya-Jones, A., Saito, Y., Fak, J. J., Vågbø, C. B., Geula, S., et al. (2017). m6A mRNA Modifications Are Deposited in Nascent Pre-mRNA and Are Not Required for Splicing but Do Specify Cytoplasmic turnoverA mRNA Modifications Are Deposited in Nascent Pre-mRNA and Are Not Required for Splicing but Do Specify Cytoplasmic Turnover. *Genes Dev.* 31 (10), 990–1006. doi:10.1101/gad.301036.117

Kim, J. M., and Chen, D. S. (2016). Immune Escape to PD-L1/pd-1 Blockade: Seven Steps to success (Or Failure). *Ann. Oncol.* 27 (8), 1492–1504. doi:10.1093/annonc/mdw217

Larkin, J., Chiarion-Sileni, V., Gonzalez, R., Grob, J. J., Cowey, C. L., Lao, C. D., et al. (2015). Combined Nivolumab and Ipilimumab or Monotherapy in Untreated Melanoma. *N. Engl. J. Med.* 373 (1), 23–34. doi:10.1056/nejmoa1504030

Li, M., Zha, X., and Wang, S. (2021). The Role of N6-Methyladenosine mRNA in the Tumor Microenvironment. *Biochim. Biophys. Acta (Bba) - Rev. Cancer* 1875 (2), 188522. doi:10.1016/j.bbcan.2021.188522

Liberzon, A., Subramanian, A., Pinchback, R., Thorvaldsdóttir, H., Tamayo, P., and Mesirov, J. P. (2011). Molecular Signatures Database (MSigDB) 3.0. *Bioinformatics* 27 (12), 1739–1740. doi:10.1093/bioinformatics/btr260

Linehan, W. M., Linehan, W. M., Spellman, P. T., Ricketts, C. J., Creighton, C. J., Fei, S. S., et al. (2016). Comprehensive Molecular Characterization of Papillary Renal-Cell Carcinoma. *N. Engl. J. Med.* 374 (2), 135–145. doi:10.1056/NEJMoa1505917

Mayakonda, A., Lin, D.-C., Assenov, Y., Plass, C., and Koeffler, H. P. (2018). Maftools: Efficient and Comprehensive Analysis of Somatic Variants in Cancer. *Genome Res.* 28 (11), 1747–1756. doi:10.1101/gr.239244.118

Postow, M. A., Chesney, J., Pavlick, A. C., Robert, C., Grossmann, K., McDermott, D., et al. (2015). Nivolumab and Ipilimumab versus Ipilimumab in Untreated Melanoma. *N. Engl. J. Med.* 372 (21), 2006–2017. doi:10.1056/nejmoa1414428

Qi, S. T., Ma, J. Y., Wang, Z. B., Guo, L., Hou, Y., Sun, Q. Y., et al. (2016). N6-Methyladenosine Sequencing Highlights the Involvement of mRNA Methylation in Oocyte Meiotic Maturation and Embryo Development by Regulating Translation in *Xenopus laevis*. *J. Biol. Chem.* 291 (44), 23020–23026. doi:10.1074/jbc.m116.748889

Quail, D. F., and Joyce, J. A. (2013). Microenvironmental Regulation of Tumor Progression and Metastasis. *Nat. Med.* 19 (11), 1423–1437. doi:10.1038/nm.3394

Rizvi, N. A., Hellmann, M. D., Snyder, A., Kvistborg, P., Makarov, V., Havel, J. J., et al. (2015). Mutational Landscape Determines Sensitivity to PD-1 Blockade in Non-small Cell Lung Cancer. *Science* 348 (6230), 124–128. doi:10.1126/science.aaa1348

Rosenberg, J. E., Hoffman-Censits, J., Powles, T., van der Heijden, M. S., Balar, A. V., Necchi, A., et al. (2016). Atezolizumab in Patients with Locally Advanced and Metastatic Urothelial Carcinoma Who Have Progressed Following Treatment with Platinum-Based Chemotherapy: a Single-Arm, Multicentre, Phase 2 Trial. *The Lancet* 387 (10031), 1909–1920. doi:10.1016/s0140-6736(16)00561-4

Rotte, A., Jin, J. Y., and Lemaire, V. (2018). Mechanistic Overview of Immune Checkpoints to Support the Rational Design of Their Combinations in Cancer Immunotherapy. *Ann. Oncol.* 29 (1), 71–83. doi:10.1093/annonc/mdx686

Samstein, R. M., Lee, C.-H., Shoushtari, A. N., Hellmann, M. D., Shen, R., Janjigian, Y. Y., et al. (2019). Tumor Mutational Load Predicts Survival after Immunotherapy across Multiple Cancer Types. *Nat. Genet.* 51 (2), 202–206. doi:10.1038/s41588-018-0312-8

Shlien, A., and Malkin, D. (2009). Copy Number Variations and Cancer. *Genome Med.* 1 (6), 62. doi:10.1186/gm62

Snyder, A., Makarov, V., Merghoub, T., Yuan, J., Zaretsky, J. M., Desrichard, A., et al. (2014). Genetic Basis for Clinical Response to CTLA-4 Blockade in Melanoma. *N. Engl. J. Med.* 371 (23), 2189–2199. doi:10.1056/nejmoa1406498

Sotiriou, C., Wirapati, P., Loi, S., Harris, A., Fox, S., Smeds, J., et al. (2006). Gene Expression Profiling in Breast Cancer: Understanding the Molecular Basis of Histologic Grade to Improve Prognosis. *J. Natl. Cancer Inst.* 98 (4), 262–272. doi:10.1093/jnci/djj052

Speleman, F., Kumps, C., Buysse, K., Poppe, B., Menten, B., and De Preter, K. (2008). Copy Number Alterations and Copy Number Variation in Cancer: Close Encounters of the Bad Kind. *Cytogenet. Genome Res.* 123 (1-4), 176–182. doi:10.1159/000184706

Steffens, S., Janssen, M., Roos, F. C., Becker, F., Schumacher, S., Seidel, C., et al. (19902012)., 48. Oxford, England, 2347–2352. doi:10.1016/j.ejca.2012.05.002Incidence and Long-Term Prognosis of Papillary Compared to clear Cell Renal Cell Carcinoma-Aa Multicentre Study*Eur. J. Cancer*15

Syn, N. L., Teng, M. W. L., Mok, T. S. K., and Soo, R. A. (2017). De-novo and Acquired Resistance to Immune Checkpoint Targeting. *Lancet Oncol.* 18 (12), e731–e741. doi:10.1016/s1470-2045(17)30607-1

Turley, S. J., Cremasco, V., and Astarita, J. L. (2015). Immunological Hallmarks of Stromal Cells in the Tumour Microenvironment. *Nat. Rev. Immunol.* 15 (11), 669–682. doi:10.1038/nri3902

Van Allen, E. M., Miao, D., Schilling, B., Shukla, S. A., Blank, C., Zimmer, L., et al. (2015). Genomic Correlates of Response to CTLA-4 Blockade in Metastatic Melanoma. *Science* 350 (6257), 207–211. doi:10.1126/science.aad0095

Vuong, L., Kotecha, R. R., Voss, M. H., and Hakimi, A. A. (2019). Tumor Microenvironment Dynamics in Clear-Cell Renal Cell Carcinoma. *Cancer Discov.* 9 (10), 1349–1357. doi:10.1158/2159-8290.cd-19-0499

Wang, Q., Chen, C., Ding, Q., Zhao, Y., Wang, Z., Chen, J., et al. (2020). METTL3-mediated m6A Modification of HDGF mRNA Promotes Gastric Cancer Progression and Has Prognostic Significance. *Gut* 69 (7), 1193–1205. doi:10.1136/gutjnl-2019-319639

Wang, S., Chai, P., Jia, R., and Jia, R. (2018). Novel Insights on m6A RNA Methylation in Tumorigenesis: a Double-Edged Sword. *Mol. Cancer* 17 (1), 101. doi:10.1186/s12943-018-0847-4

Wilkerson, M. D., and Hayes, D. N. (2010). ConsensusClusterPlus: a Class Discovery Tool with Confidence Assessments and Item Tracking. *Bioinformatics (Oxford, England)* 26 (12), 1572–1573. doi:10.1093/bioinformatics/btq170

Wu, T., and Dai, Y. (2017). Tumor Microenvironment and Therapeutic Response. *Cancer Lett.* 387, 61–68. doi:10.1016/j.canlet.2016.01.043

Xiao, C.-L., Zhu, S., He, M., Chen, D., Zhang, Q., Chen, Y., et al. (2018). N6-Methyladenine DNA Modification in the Human Genome. *Mol. Cel.* 71 (2), 306–318. doi:10.1016/j.molcel.2018.06.015

Xie, L., Yang, Y., Guo, W., Che, D., Xu, J., Sun, X., et al. (2020). The Clinical Implications of Tumor Mutational Burden in Osteosarcoma. *Front. Oncol.* 10, 595527. doi:10.3389/fonc.2020.595527

Yang, Y., Hsu, P. J., Chen, Y.-S., and Yang, Y.-G. (2018). Dynamic Transcriptomic m6A Decoration: Writers, Erasers, Readers and Functions in RNA Metabolism. *Cell Res* 28 (6), 616–624. doi:10.1038/s41422-018-0040-8

Zeng, D., Li, M., Zhou, R., Zhang, J., Sun, H., Shi, M., et al. (2019). Tumor Microenvironment Characterization in Gastric Cancer Identifies Prognostic and Immunotherapeutically Relevant Gene Signatures. *Cancer Immunol. Res.* 7 (5), 737–750. doi:10.1158/2326-6066.cir-18-0436

Zhang, B., Wu, Q., Li, B., Wang, D., Wang, L., and Zhou, Y. L. (2020). m6A Regulator-Mediated Methylation Modification Patterns and Tumor Microenvironment Infiltration Characterization in Gastric cancerA Regulator-Mediated Methylation Modification Patterns and Tumor Microenvironment Infiltration Characterization in Gastric Cancer. *Mol. Cancer* 19 (1), 53. doi:10.1186/s12943-020-01170-0

Zhong, J., Liu, Z., Cai, C., Duan, X., Deng, T., and Zeng, G., (2021). m6A Modification Patterns and Tumor Immune Landscape in clear Cell Renal Carcinoma. *J. Immunother. Cancer* 9 (2), 646. doi:10.1136/jitc-2020-001646

Conflict of Interest: The authors declare that the research was conducted in the absence of any commercial or financial relationships that could be construed as a potential conflict of interest.

Publisher's Note: All claims expressed in this article are solely those of the authors and do not necessarily represent those of their affiliated organizations, or those of the publisher, the editors and the reviewers. Any product that may be evaluated in this article, or claim that may be made by its manufacturer, is not guaranteed or endorsed by the publisher.

frontiers | Frontiers in Genetics

ORIGINAL RESEARCH
published: 27 April 2022
doi: 10.3389/fgene.2022.787141

Prognostic Value and Therapeutic Perspectives of CXCR Members in the Glioma Microenvironment

*Jiarong He[1], Zhongzhong Jiang[1], Jiawei Lei[2], Wen Zhou[1], Yan Cui[1], Biao Luo[1] and Mingming Zhang[1]**

[1]Department of Neurosurgery, The Second Xiangya Hospital, Central South University, Changsha, China, [2]Department of General Surgery, The Second Xiangya Hospital, Central South University, Changsha, China

Background: CXCR (CXC Chemokine Receptor) is a complex of the immune-associated protein involved in tumor activation, invasion, migration, and angiogenesis through various chemical signals in the tumor microenvironment (TME). However, significant prognostic characteristics of CXCR members and their impact on the occurrence and progression of glioma have not yet been fully elucidated.

Methods: In this research, we used Oncomine, TCGA, GTEx, and CGGA databases to analyze the transcription and survival data of glioma patients. Afterward, the influence of CXCR members on the TME was explored using comprehensive bioinformatics analysis.

Results: The mRNA expression levels of CXCR1/2/3/4/7 were significantly up-regulated in glioma than in normal samples, whereas the mRNA expression level of CXCR5 was decreased. We then summarized the genetic alteration landscape of CXCR and identified two molecular subtypes based on CXCR expression patterns in glioma. The characteristics of CXCRs were also investigated, including the clinicopathological parameters, TME cell infiltration, and prognosis of patients with glioma. After Lasso and multivariable Cox regression, a CR-Score for predicting overall survival (OS) was constructed and the predictive performance of the signature was validated. The high-risk group was a significantly poorer prognostic group than the low-risk group as judged by the CR-Score (TCGA cohort, $p < 0.001$, CGGA cohort, $p < 0.001$). Moreover, the CR-Score was significantly correlated to the tumor-immune infiltration and cancer stem cell (CSC) index. A risk scale-based nomogram incorporating clinical factors for individual risk estimation was established thereby.

Conclusion: These findings may pave the way for enhancing our understanding of CXCR modification patterns and developing better immune therapeutic approaches for glioma.

Keywords: CXCR, tumor microenvironment, glioma, mutation burden, prognosis

OPEN ACCESS

Edited by:
Ângela Sousa,
University of Beira Interior, Portugal

Reviewed by:
Zhi-Qiang Li,
Wuhan University, China
Quan Cheng,
Central South University, China
Christiane Pienna Soares,
Sao Paulo State Universty, Brazil

****Correspondence:***
Mingming Zhang
zhangmm@csu.edu.cn

Specialty section:
This article was submitted to Epigenomics and Epigenetics, a section of the journal Frontiers in Genetics

Received: *30 September 2021*
Accepted: *30 March 2022*
Published: *27 April 2022*

Citation:
He J, Jiang Z, Lei J, Zhou W, Cui Y, Luo B and Zhang M (2022) Prognostic Value and Therapeutic Perspectives of CXCR Members in the Glioma Microenvironment. Front. Genet. 13:787141. doi: 10.3389/fgene.2022.787141

Abbreviations: GBM, Glioblastoma; LGG, Low-grade glioma; TCGA, The Cancer Genome Atlas; CSC, Cancer stem cell; CNV, Copy number variation; TME, Tumor microenvironment; TILs, Tumor-infiltrating lymphocytes; ICIs, Immune Checkpoint Inhibitors; GO, Gene Ontology; KEGG, Kyoto Encyclopedia of Genes and Genomes; OS, Overall survival; TIICs, Tumor-infiltrating immune cells; ROC, Receiver Operating Characteristic; AUC, Area Under the Curve.

INTRODUCTION

Despite recent advances in therapeutic options such as surgery, radiotherapy, and chemotherapy, the prognosis of glioma patients remains unsatisfactory (Sung et al., 2021). The introduction of immune checkpoint inhibitors (ICIs) has become a breakthrough in tumor immunotherapy in recent years. Unfortunately, only a minority of glioma patients respond to ICIs (Romani et al., 2018), and the incidence of anti-PD-L1 treatment-related adverse events is up to 16% (Marin-Acevedo et al., 2019). Therefore, there is a need for the development of more effective regimens that are better tolerated and more efficient. The efficacy of checkpoint blockade immunotherapy largely depends on the composition and proportion of tumor-infiltrating lymphocytes (TILs) (Curran et al., 2010). Tumors with high TIL content are called immunologically active "inflamed" tumors and usually respond to ICI (Pitt et al., 2016; Cristescu et al., 2018), while immunologically inactive " non-inflamed" TIL (-) tumors do not benefit from immune checkpoint blockade. The interaction of tumor cells with the tumor microenvironment plays a critical role in cancer progression, aggressiveness, and response to immunotherapy (Wang et al., 2017).

In the last decades, the chemokine system has been widely studied in multiple cancer cell lines (Mollica Poeta et al., 2019). CXC chemokine receptors, a diverse group of 7-transmembrane domains G protein-coupled receptor, are frequently involved in tumorigenesis and tumor progression (Mollica Poeta et al., 2019). CXCR1 and CXCR2 are cellular membrane receptors for Interleukin-8 receptor A (IL-8RA) and Interleukin-8 receptor B (IL-8RB), respectively, mainly expressed on the surface of T cells, monocytes, and neutrophils, belonging to the GPCR superfamily (Jin et al., 2019). CXCL8/CXCR1 performs as drug receptors and signal transduction, while CXCL8/CXCR2 promotes inflammation and angiogenesis (Park et al., 2012). Overexpression of CXCR1 and CXCR2 strengthened the invasion capability of tumor cells. Jin et al. reported that CXCR1 and CXCR2 modified CARs significantly enhanced the persistence and migration of T cells in tumors, inducing tumor degeneration and persistent immunologic memory in preclinical models of malignancies such as glioblastoma, pancreatic and ovarian cancer (Jin et al., 2019).

CXCR3 is a crucial molecule in tumorigenesis and neuroinflammatory. Zhou Y et al. discovered that CXCR3 was also involved in the pathogenesis of glioma, chronic pain, bipolar disorder, MS, AD, and HAM/TSP (Zhou et al., 2019). Previous studies have found that the dysregulation of CXCR3 was negatively correlated with tumor invasion depth (Hu et al., 2015). Meanwhile, it regulates the activation of TILs and resident immune cells (Zhou et al., 2019). CXCR4 as the most common type of GPCR member stands out for its involvement in several pathological conditions, including immune diseases and cancer (Pozzobon et al., 2016). The expression levers of the CXCR4 and its ligand stromal cell-derived factor-1(SDF-1, CXCL12) are maintained by chemokine signaling pathways via positive feedback loops. Recently, the expression of CXCR4 was found to be involved in cancer stem cells self-renewal and the generation and maintenance of the perivascular stem cell niche (Richardson, 2016). Moreover, extracellular regulated kinase (ERK) pathway, transforming growth factor (TGF)-alpha and matrix metalloproteinase (MMP)-7, MMP-9 were found closely associated with the expression of CXCR4 (Fanelli et al., 2012). CXCR5 was closely related to tumor progression. Yang et al. discovered that glioblastoma cells target CXCR5 by releasing exosome miR-214-5p to regulate lipopolysaccharide stimulation to modulate microglia inflammatory response (Yang et al., 2019). CXCL16/CXCR6 axis acts a pivotal part in the pro-tumor microenvironment, and the silencing of CXCR6 reduced the proliferation rate on glioma cells (Lepore et al., 2018), indicating that CXCR6 plays an oncogenic role in glioma. In addition, CXCR7, also known as ACKR3, a new functional receptor for CXCL12 with a higher affinity than CXCR4, mediates resistance to drug-induced apoptosis. Previous studies have also shown that CXCR7 is significantly associated with adverse outcomes (Hattermann et al., 2010).

To date, the dysregulated expression of CXCR members and their significant prognostic role have been partly studied in some researches. Most of the previous studies evaluate the performance of one or two CXCRs due to technical limitations, while the immune response is characterized by multiple genes interacting in a highly coordinated manner. Thus, a comprehensive analysis of the characteristics of multiple CXCR-mediated cell infiltrates may provide additional insights into the prediction of immunotherapy responses and the underlying mechanisms of glioma tumorigenesis. In this report, we identified the expression and potential prognostic value of CXCRs for glioma patients through computational analysis. The genome information from 1,360 glioma samples was incorporated to correlate the chemokine system with the immunity characteristics of the tumor-associated microenvironment. Our study concludes that the CR-Score is a reliable prognostic predictive value for glioma and can inform special immunotherapy treatment.

MATERIALS AND METHODS

Data Collection and Preprocessing

The workflow diagram of this research was shown in **Supplementary Figure S1**. Gene expression data for normal brain tissues were obtained from the Genotype-Tissue Expression (GTEx) Data Portal (https://xenabrowser.net/datapages/). Original RNA-sequencing (RNA-seq) data (fragments per kilobase per million fragments mapped, FPKM) and corresponding clinicopathological features of 1,360 glioma patients were downloaded from The Cancer Genome Atlas (TCGA) database (http://Cancegenome.nih.gov/) and Chinese Glioma Genome Atlas (CGGA) platform (http://www.cgga.org.cn/). The detailed information on the samples is presented in **Table 1**. Patients without survival information were excluded from the corresponding analysis. The FPKM values were converted into transcripts per kilobase per million (TPM) before further investigation (Conesa et al., 2016). All the datasets were retrieved from the published literature and the ethics statement confirmed that all written informed consent was obtained.

Consensus Clustering of Differentially Expressed Genes

In this study, we used the "edger" R package to normalize the transcriptome sequencing data of the two cohorts before

TABLE 1 | Clinical characteristics of patients with glioma.

Characteristics	CGGA Cohort (n=693)	TCGA Cohort (n=667)
Age		
≤65	661 (95.4)	535 (80.2)
>65	31 (4.5)	132 (19.8)
NA	1 (0.1)	0
Gender		
Male	398 (57.4)	390 (58.5)
Female	295 (42.6)	277 (41.5)
Histologic grade		
2	188 (27.2)	149 (22.4)
3	255 (36.8)	159 (23.8)
4	249 (35.9)	359 (53.8)
NA	1 (0.1)	0
Survival status		
OS years (median)	3.28	1.95
Alive	266 (38.4)	371 (55.6)
Dead	397 (57.3)	296 (44.4)
NA	30 (4.3)	0
PRS-type		
Primary	422 (60.9)	647 (97.1)
Recurrent	271 (39.1)	20 (2.9)
Radio-status		
treated	510 (73.6)	493 (73.9)
un-treated	136 (19.6)	151 (22.7)
NA	47 (6.8)	23 (3.4)
Chemo_status		
TMZ-treated	486 (70.2)	-
un-treated	161 (23.2)	-
NA	46 (6.6)	-

comparison. Limma package was utilized for differential expression analysis with $|\log2FC| \geq 1$ and FDR <0.05. p values were denoted as follows: *, $p < 0.05$; **, $p < 0.01$; ***, $p < 0.001$. Clustered analysis of CXCR-mediated patterns was employed using the Genesis K-means method. The "ConsensuClusterPlus" package was used to control the stability and optimal of clusters. In addition, the differences in overall survival rates between the two subtypes were evaluated by the Log-rank test using the survminer R package.

Association of Two Clusters With Tumor Microenvironment and Immune Checkpoint Blockade in Glioma

ESTIMATE algorithm was utilized to evaluate the stromal/immune scores of each glioma sample. Furthermore, we used the CIBERSORT algorithm to calculate the abundance of 22 immune cell subsets for each tumor specimen (Newman et al., 2015). Also, the expression of immune checkpoint blockade between the two clusters was analyzed.

Analysis of Mutation and Copy Number Variation

We used the R package "maftools" to generate waterfall maps of genomic mutations and copy number variations (CNVs) in the TCGA-glioma cohort (VarScan2). For copy number variation analysis, GISTIC.2 was used to identify missing gene sequences and amplified genomes, including deep deletion, shallow deletion, high amplification, and low-level gain. The gain or loss in copy number was determined by the total number of genes with copy number alterations at the focal and arm levels. The tumor mutation burden (TMB) was calculated as the number of all somatic copy number alterations (SCNAs) using the two-sample t-test.

Development and Validation of the Prognostic Model

Univariate and multivariate Cox proportional hazard analyses were performed to assess the prognostic factors, including CR-Score, patient age, gender, and tumor grade. Hazard ratios (HR) and corresponding 95% confidence intervals (CI) were estimated using the R package "forestplot". The R package "glmnet" was used for Lasso-penalized Cox regression analysis to construct a prognostic model. We set the significance cut-off p-value as 0.05, and five CXCRs were selected and used for further analysis.

The CR-Score was calculated using the following equation:

$$\text{CR-Score} = \sum \left(\text{Exp}\left(\text{Xi}\right)^{*} \text{Coef}\left(\text{Xi}\right) \right)$$

where Exp (Xi) and Coef (Xi) represented the expression and coefficient of each gene Xi, respectively. Principal component analysis (PCA) was conducted in R using the "prcomp" function. The predictive capability of the CR-Score was evaluated using Receiver Operating Characteristic (ROC) curve analysis.

Functional Annotation and Immune Infiltration Analysis

For gene ontology (GO) pathway and Kyoto Encyclopedia of Genes and Genomes (KEGG) analysis, we used the clusterProfiler R package. In addition, we performed the Single-sample gene set enrichment analysis (ssGSEA) to quantify the relative abundance of immune infiltration levels using the "GSVA" R package (Rooney et al., 2015). The Timer, Quantiseq, Mcpcounter, Xcell, and Epic databases were used to calculate the fractions of infiltrating immune cells in glioma.

Establish a Predictive Nomogram Scoring Model

Based on the results of the independent prognostic analysis, the "rms" R package was used to construct a nomogram to predict personalized survival probability. Each clinicopathologic variable was assigned an integer-weighted score in the nomogram scoring model. The sum of all variables scores was added up to get the total score. Clinical ROC was performed to assess the predictive efficiency of the nomogram model. The calibration plot was used to evaluate the accuracy of the prediction for the probability of survival events at 1-, 3-, and 5- year.

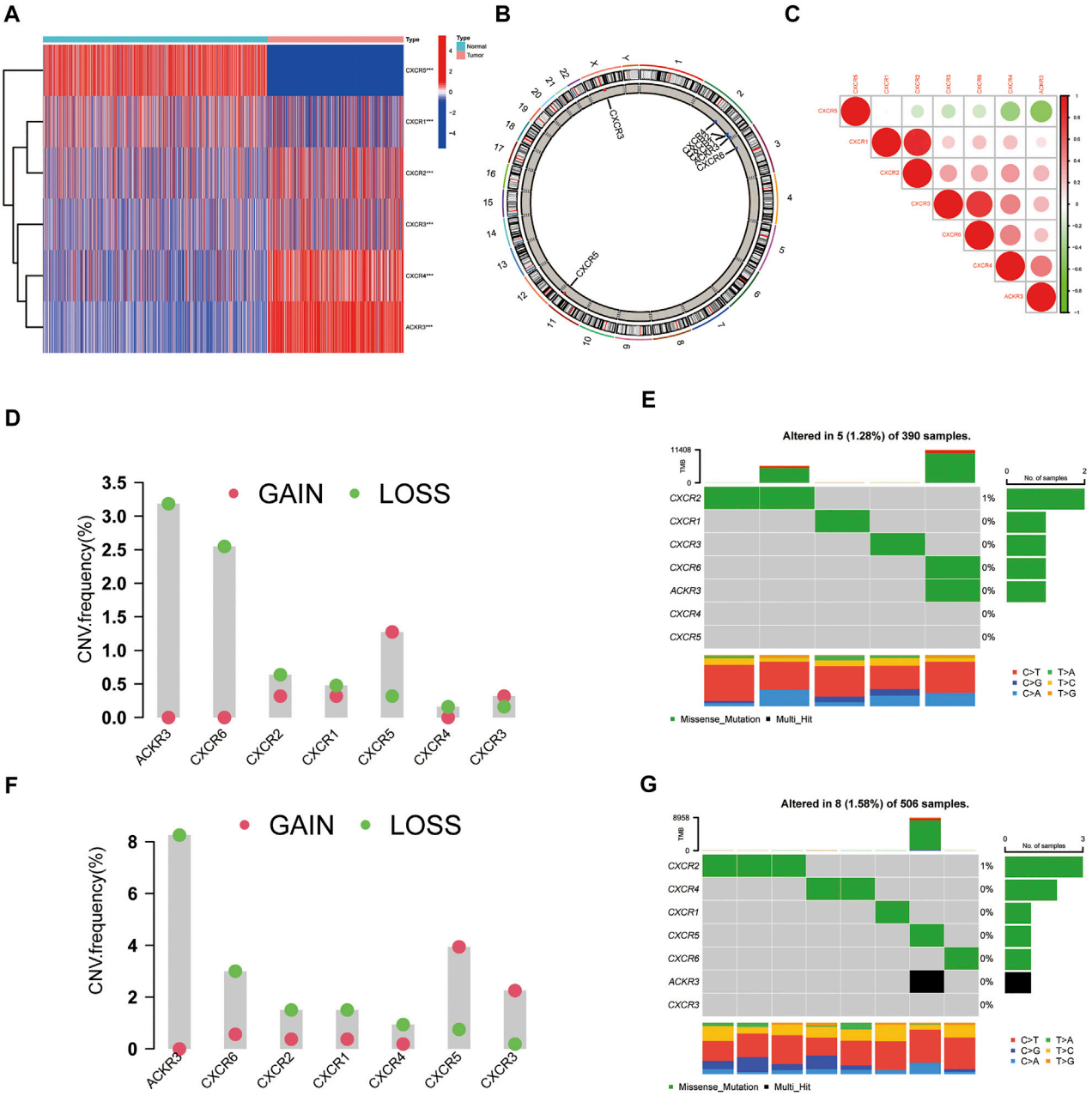

FIGURE 1 | Transcriptional and Genetic alterations of CXCRs in glioma. **(A)** Heatmap of six differential expression CXCRs in glioma tissues and normal brain tissues (red: high expression; blue: low expression). Asterisk indicates: t test, $^{*}p < 0.05$, $^{**}p < 0.01$ and $^{***}p < 0.001$ compared to the normal brain tissues. **(B)** The location of CNV alteration of seven CXCR molecules on 23 chromosomes. **(C)** Correlations between seven CXCR genes. The darker the blue, the stronger the negative correlation, and the darker the red, the stronger the positive correlation. CNV distribution of CXCRs in GBM **(D)** and LGG **(F)** tumor samples. The height of the bar represented the total alteration frequency. The landscape of somatic mutation frequency of CXCRs in GBM cohort **(E)** and LGG cohort **(G)**. The somatic mutation landscape of the GBM cohort **(E)** and LGG cohort **(G)**. Each column represented an individual sample. The bar graph on the right indicated the mutation frequency of each gene. The upper barplot showed the mutations.

Statistical Analysis

Pearson and Spearman correlation coefficients were used to determine the correlation between two variables. We used the unpaired student's t-test to assess the statistical significance for normally distributed variables, and the Mann-Whitney U test was used to analyze non-normally distributed continuous variables. A one-way ANOVA test was used to compare two or more groups. Survival curves of the two subgroups in each data set were estimated by Kaplan-Meier method and compared by the log-rank (Mantel-Cox) test. All statistical analyses were accomplished with R software (v4.0.2, https://www.r-project.org/), with a p-value < 0.05 (two-tailed test) indicating statistical significance.

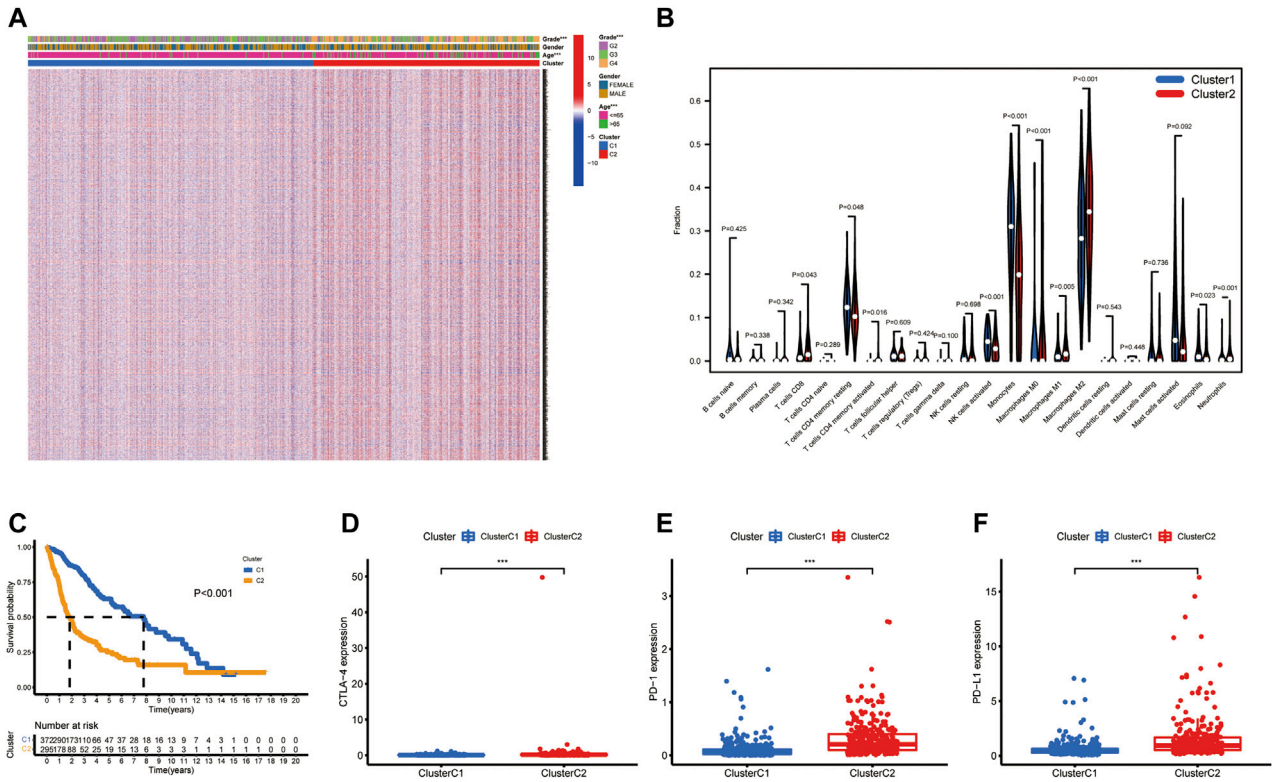

FIGURE 2 | The clinicopathological and TME characteristics of the two molecular subtypes. **(A)** Heatmap showing clinicopathologic features of the two clusters. **(B)** The proportions of 22 immune cells among the clusters. **(C)** Kaplan–Meier curves for OS of the two clusters (log-rank tests, $p < 0.001$). **(D–F)** Histograms representing CTLA-4, PD-1, and PD-L1 expression. Data are shown as the mean ± SD; t test, $^{*}p < 0.05$, $^{**}p < 0.01$ and $^{***}p < 0.001$ compared to the cluster C2 in **(D–F)**.

RESULTS

Identification of Transcriptional Variations and Genetic Alterations of CXCRs in Glioma

Gene expression levels of seven CXCRs were measured between 667 tumor and 1,431 normal brain tissues from TCGA-Glioma and GTEx-Brain data. A total of six CXCRs were either downregulated or upregulated in glioma (**Figure 1A**). Among them, one gene (CXCR5) was downregulated while five other genes (CXCR1, CXCR2, CXCR3, CXCR4, and ACKR3) were enriched in glioma compared with normal brain tissues (**Supplementary Table S1**). Oncomine platform was used to compare the mRNA expression levels of CXCRs in pan-cancer tissues and normal tissues (**Supplementary Figure S2**).

Furthermore, we identified the distributions of copy number variation in the chromosomes (**Figure 1B**). The correlation network analysis of seven CXCR molecules was presented in **Figure 1C**. We also investigated the frequency of CNV alterations and found that more than half of the seven CXCRs had copy number deletions (**Figures 1D–F**). At the genetic level, five of 390 (1.28%) glioblastoma (GBM) samples and eight of 506 (1.58%) low-grade glioma (LGG) samples confirmed genetic mutations (**Figures 1E–G**). **Figure 1D** demonstrated that ACKR3 with the highest frequency of variants in GBM, followed by CXCR6. Compared to the LGG cohort, ACKR3 also showed the highest mutation frequency, among the seven CXCRs. We further found that the mRNA expression of ACKR3 was up-regulated, showing CNV loss, while the down-regulation of CXCR5 showed CNV gain, indicating that CNV alteration might regulate the transcriptional activity of CXCRs.

The Characteristics of CXC Chemokine Receptor Subtypes in Glioma

To investigate the relationship between the expression of these seven CXCR genes and glioma subtypes, we performed a consensus clustering analysis in glioma patients. By applying the standard K-means clustering algorithm, when k = 2, the inter-group correlation is low and the intra-group correlation is the highest. The results showed that 667 glioma patients were divided into two separate clusters (C1, n = 372; C2, n = 295). Gene expression profiles (GEPs) and corresponding clinicopathological parameters including gender (male or female), age (≤65 or >65 years), and tumor histological differentiation (G2-G4) were presented in a heatmap (**Figure 2A**). To examine the effect of CXCRs on the TME of glioma, we used the CIBERSORT algorithm to assess the diversities between the two subtypes from cell level (**Supplementary Table S2**). Among them, the infiltration levels of T cells CD4 memory resting, NK cells activated, Monocytes, and Eosinophils were

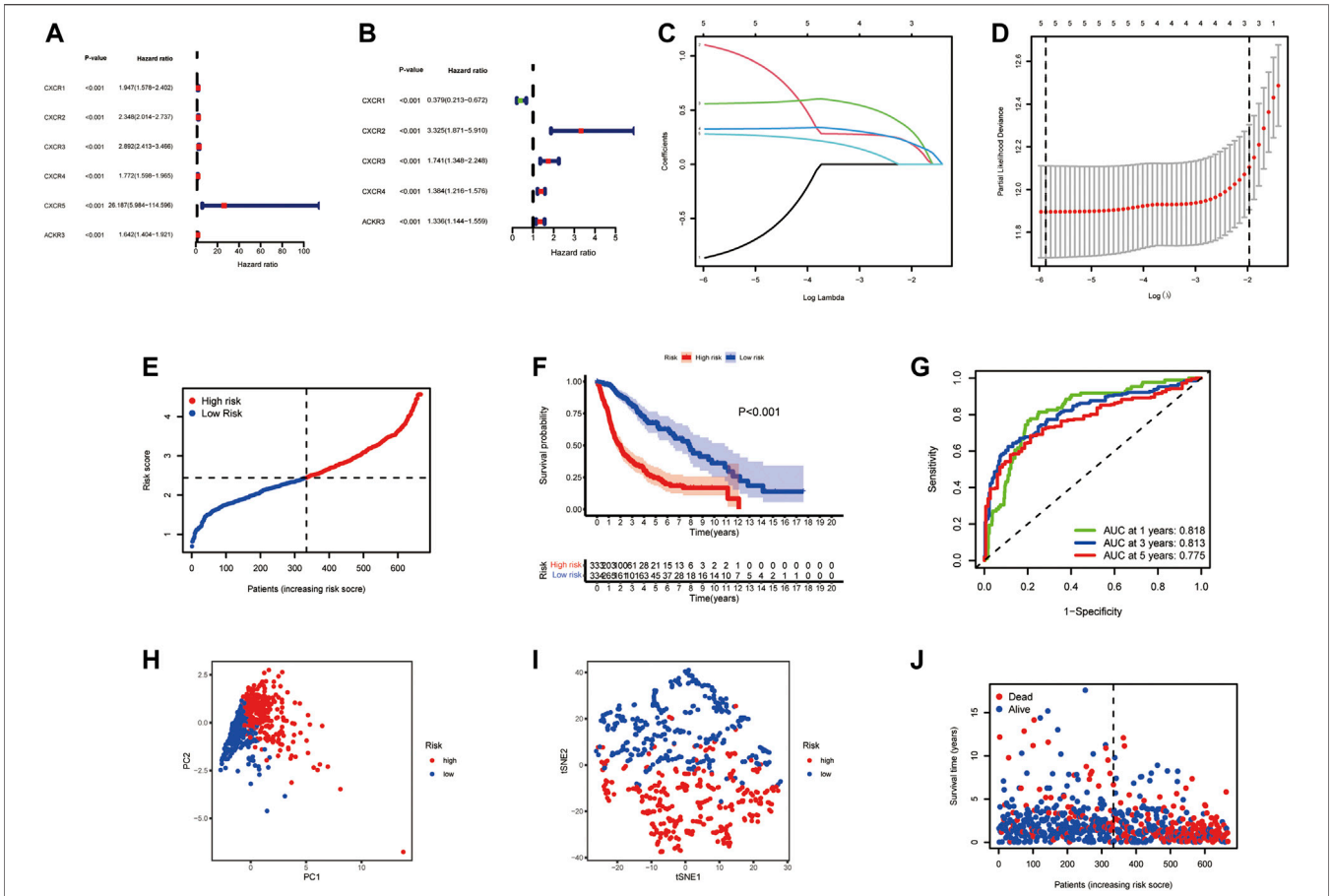

FIGURE 3 | Prognostic value of the risk signature model. Forest plot of prognostic CXCR genes based on univariate **(A)** and multivariable **(B)** Cox regression analysis. **(C)** Lasso coefficient profiles of the five survival-related CXCRs. **(D)** Ten-fold cross-validation for tuning parameter selection in the Lasso model. **(E)** The distribution of CR-Score in the TCGA dataset. **(F)** Kaplan-Meier curve of OS in the high- (red) and low-(blue) risk groups. **(G)** ROC curves for the predictive model. **(H)** PCA plot of the TCGA cohort. **(I)** t-SNE plot for patients. **(J)** Distribution of the survival data and CR-Score.

significantly higher in cluster C1 than in cluster C2 (**Figure 2B**). Moreover, a significant difference for OS was found in the two clusters (**Figure 2C**). The results showed that the expression levels of immune checkpoints in cluster C2 were significantly higher than those in cluster C1 (**Figures 2D–F**).

Construction and Evaluation of a Prognostic Model

To construct a CXCR-related prognostic model, univariate and multivariable Cox regression analyses were used to screen for survival-related genes. Univariate Cox regression analysis revealed the prognostic value of the six CXCRs in glioma patients (**Figure 3A** and **Supplementary Table S3**). Subsequently, five genes with independent prognostic value (CXCR1, CXCR2, CXCR3, CXCR4, and ACKR3) were identified by multivariate Cox regression, of which 4 genes (CXCR2, CXCR3, CXCR4, and ACKR3) had an increased probability of death (HR > 1), while the remaining CXCR1 gene was a protective factor for HR < 1 (**Figure 3B** and **Supplementary Table S3**). The 5-gene signature was identified by Lasso penalized Cox regression analysis based on the optimum λ value (**Figures 3C,D**). The CR-Score of the CXCR-based model was calculated as follows: CR-Score = (−0.9711 * CASP1 exp.) + (1.2015 * CXCR2 exp.) + (0.5543 * CXCR3 exp.) + (0.3252 * CXCR4 exp.) + (0.2893 * ACKR3 exp.). Patients were divided into the high-risk group (n = 333) and the low-risk group (n = 334) according to the median cut-off value (**Figure 3E**). Kaplan-Meier survival analysis of glioma patients showed that high CR-Scores were associated with significantly worse patient survival (**Figure 3F**, $p < 0.001$). In addition, the effectiveness of the model was assessed by time-correlated ROC analysis, and the area under the curve (AUC) for the signature was 0.818 at 1 year, 0.813 at 3 years, and 0.775 at 5 years for survival (**Figure 3G**). Through principal component analysis and t-distributed Stochastic Neighbor Embedding (t-SNE), it was found that patients with different CR-Scores had different directions of distribution (**Figures 3H,I**), and patients in the low-risk group had better OS than those in the high-risk group (**Figure 3J**).

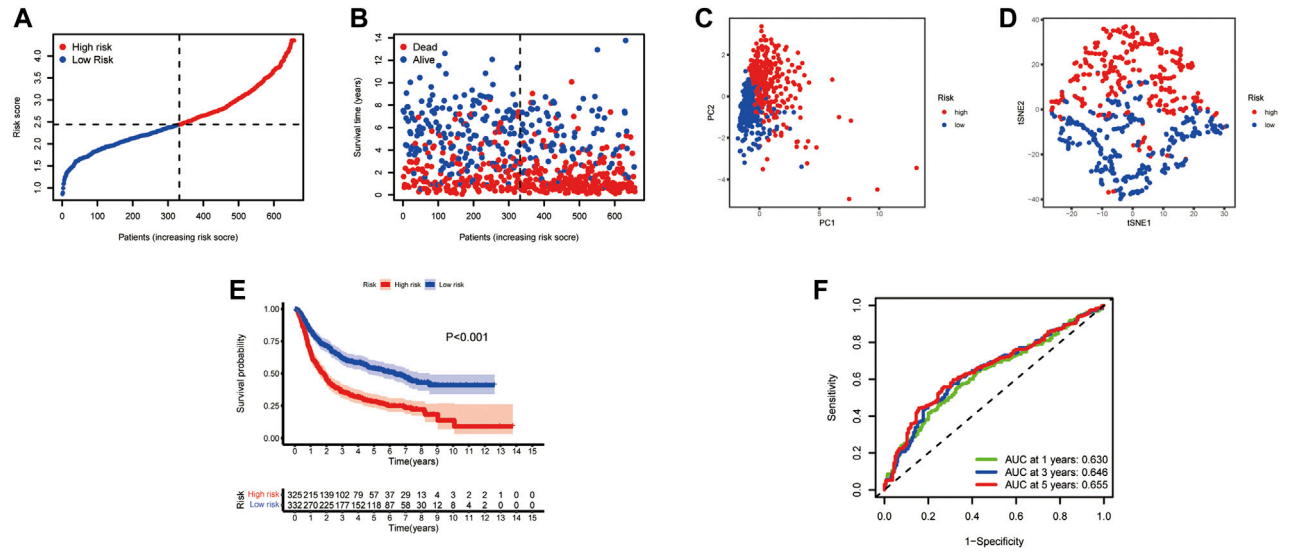

FIGURE 4 | Validation of the risk signature in the CGGA testing set. **(A)** Patient distribution and median value of CR-Score. **(B)** Survival time and status distribution by CR-Score. **(C)** PCA plot of the CGGA cohort. **(D)** t-SNE plot of the dataset. **(E)** Kaplan-Meier survival analysis of OS for glioma patients. **(F)** Time-dependent ROC curves.

Validation of the Prognostic Model

In this study, 693 glioma samples from the CGGA cohort were used as the test set. Before proceeding further, we used the same formula to normalize the RNA sequencing expression data. Patients were divided into high-risk groups (n = 325) and low-risk groups (n = 332) according to the median cutoff value of the TCGA cohort (**Figure 4A**). Our analysis indicated that the high-risk group had a worse survival than the low-risk group (**Figures 4B–E**). The PCA and t-SNE results also showed a satisfactory separation between the two groups (**Figures 4C,D**). Our model predicted 1-, 3-, and 5-year OS with AUCs were 0.630, 0.646, and 0.655, respectively (**Figure 4F**). Analysis of the five CXCR-based prognostic signature showed that the CR-Score was still comparatively performing well, suggesting that the CR-Score can accurately predict the clinical outcome of glioma patients.

Independent Prognostic Value of the CXC Chemokine Receptor Molecules

We then performed a univariate and multivariable Cox proportional hazard analysis to determine whether the CXCR signature model could be used as an independent prognostic indicator for glioma patients. Univariate Cox regression analysis showed that age, grade, and CR-Score were significantly associated with prognosis. The higher the CR-Score, the worse the prognosis (HR: 2.765, 95%CI: 2.401–3.184, $p < 0.001$ **Figure 5A**; HR: 1.729, 95% CI: 1.510–1.980, $p < 0.001$ **Figure 5C**). After adjusting for potential confounding factors, the CR-Score also showed significance in multivariate Cox regression (HR: 1.441, 95% CI: 1.211–1.714, $p < 0.001$, **Figure 5B**; HR: 1.302, 95% CI: 1.131–1.498, $p < 0.001$, **Figure 5D**). Moreover, we conducted a heatmap to interpret the possible associations between the clinicopathological parameters of the TCGA cohort and five genes (**Figure 5E**). Wilcoxon signed-rank tests compared differences in CR-Score among different groups for these clinicopathological features, indicating that age, clinical stage, and tumor PRS status were positively associated with CR-Score (**Figures 5F–K**).

Functional Enrichment and Immune Infiltrating

To elucidate the functions of CXCR-related genes between the two subgroups classified from the risk model, we extracted DEGs in the TCGA cohort with the "limma" R package with $|\log2FC| \geq 1$ and FDR<0.05. A total of 470 DEGs were identified between the high- and low-risk groups. Among them, 261 genes were upregulated and 209 genes were downregulated (**Supplementary Table S4**). Based on these DEGs, analyses of GO functional annotation and KEGG pathway enrichment were performed. The DEGs were mainly enriched in immune biology processes such as neutrophil activation/degranulation, neutrophil-mediated immunity, and regulation of trans–synaptic signaling in GO analysis (**Figure 6A**). In the KEGG pathway enrichment analyses, we identified DEGs involved in the Phagosome, Focal adhesion, Proteoglycans in cancer, ECM–receptor interaction, Coronavirus disease—COVID-19, ECM–receptor interaction, and Cell adhesion molecules (**Figure 6B**). To find out the relationship between CR-Score and immune infiltrations, the scores of 16 immune cells and 13 immune-related functions were assessed using the ssGSEA method in the GSVA package. Remarkably, the scores of the immune cell types (including aDCs, B_cells, CD8+_T_cells, Macrophages, Neutrophils, T-helper-cells, TIL, and Treg) were considerably different between these two risk groups (**Figures 6C–E**). In addition, all 13 immune-related signaling pathways also differed between the low- and high-risk groups (**Figures 6D–F**).

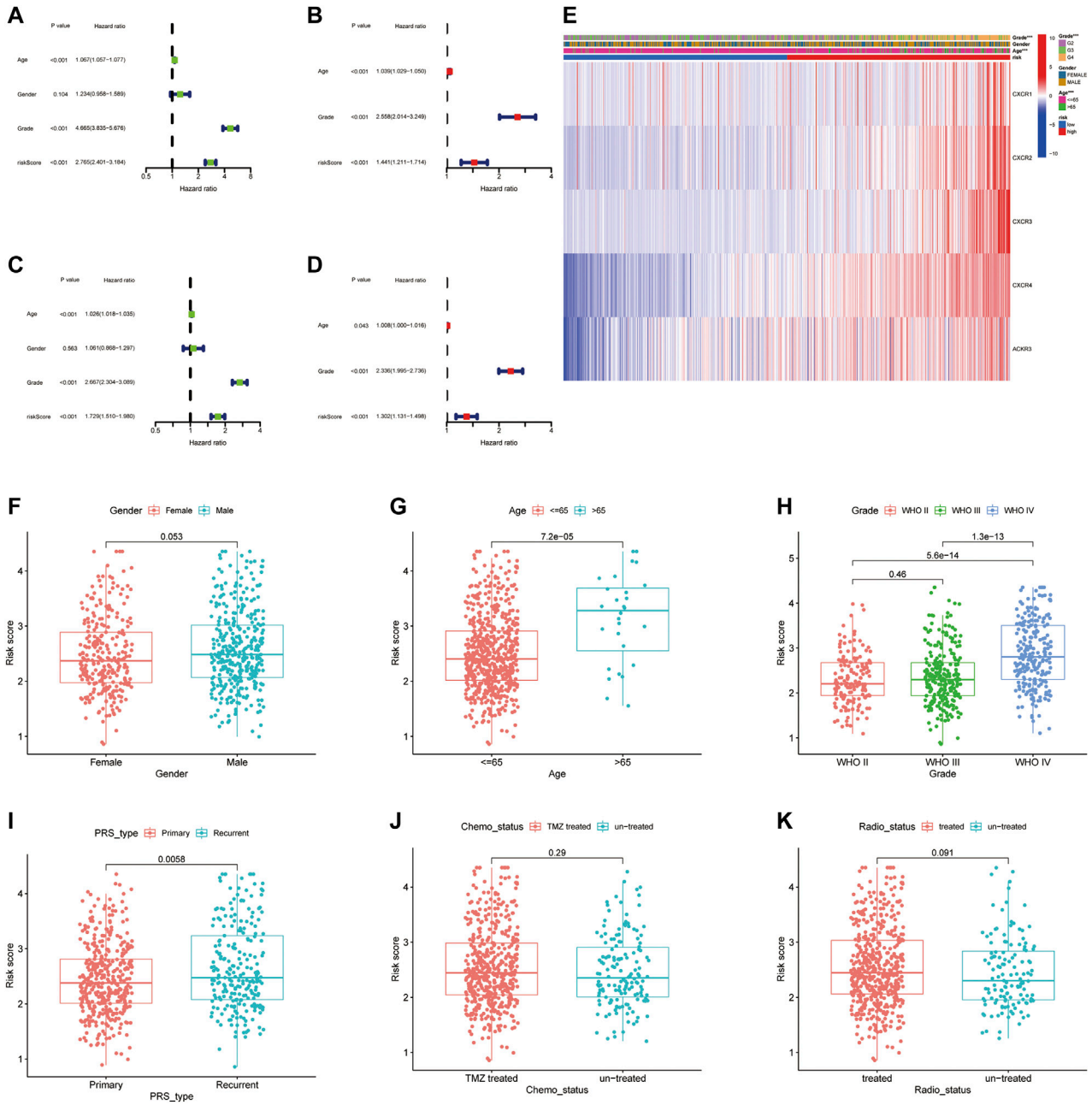

FIGURE 5 | Independent prognostic analysis of CR-Score and clinicopathological parameters. Forrest plot of univariate (**A**, Green) and multivariate (**B**, Red) Cox regression analysis in the TCGA cohort. Univariate **(C)** and multivariate **(D)** Cox regression analysis in the CGGA cohort. **(E)** The relationship between CR-Score and clinicopathologic indicators. **(F–K)** Combination of CR-Score with gender, age, grade, primary/recurrent status, chemotherapy status, radiation therapy.

Variation in the Infiltration Profiles of Tumor Microenvironment cells

We use Timer, Cibersort, Quantiseq, Mcpcounter, Xcell, and Epic to estimate the abundances of immune cells infiltrating in glioma samples using mRNA-Sequencing data. Patients with high CR-Score accumulated more tumor-infiltrating immune cells such as T cell $CD8^+$, neutrophil, macrophage, and myeloid dendritic cells (**Figure 7A**).

The relationship between the expression of five genes of the proposed model and infiltrating immune cells was also investigated. We observed that Neutrophils, NK cells activated, and Macrophages M2 were significantly related to CXCR genes

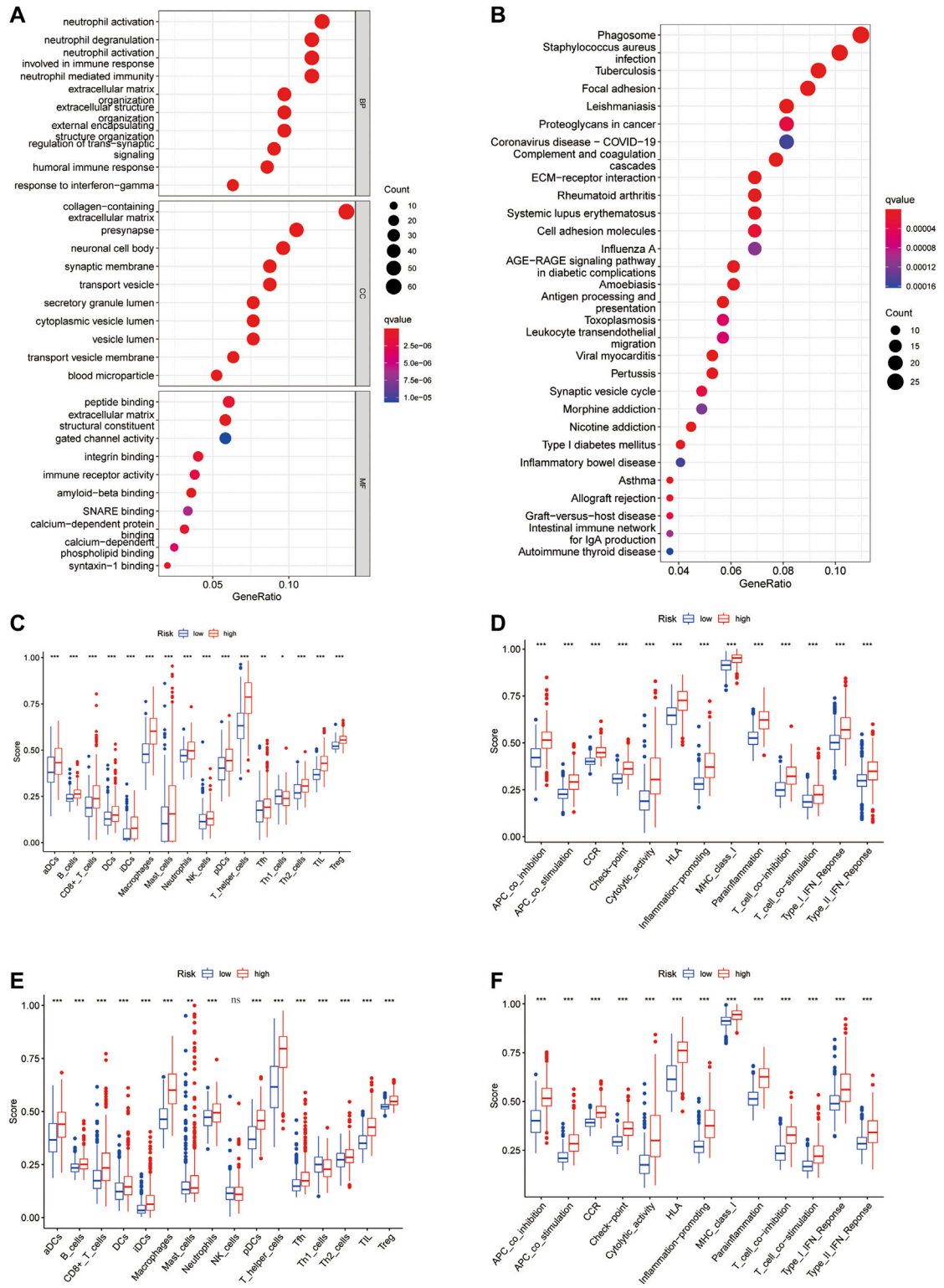

FIGURE 6 | Functional annotation enrichment analysis and comparison of immune cell infiltration between CR-Score subgroups. **(A)** GO functional enrichment analysis. **(B)** KEGG functional enrichment analysis. Bubble size and color correspond to the differentially enriched gene number and *p*-value for the significance of the enrichment. Boxplots of ssGSEA results for 16 immune cells **(C)** and 13 immune-related functions **(D)** in the TCGA cohort. The scores of 16 immune cells **(E)** and 13 immune-related functions **(F)** in the CGGA cohort. Data are shown as the mean ± SD; *t* test, $^{*}p < 0.05$, $^{**}p < 0.01$ and $^{***}p < 0.001$ compared to the high-risk group in **(C–F)**; ns, no significance.

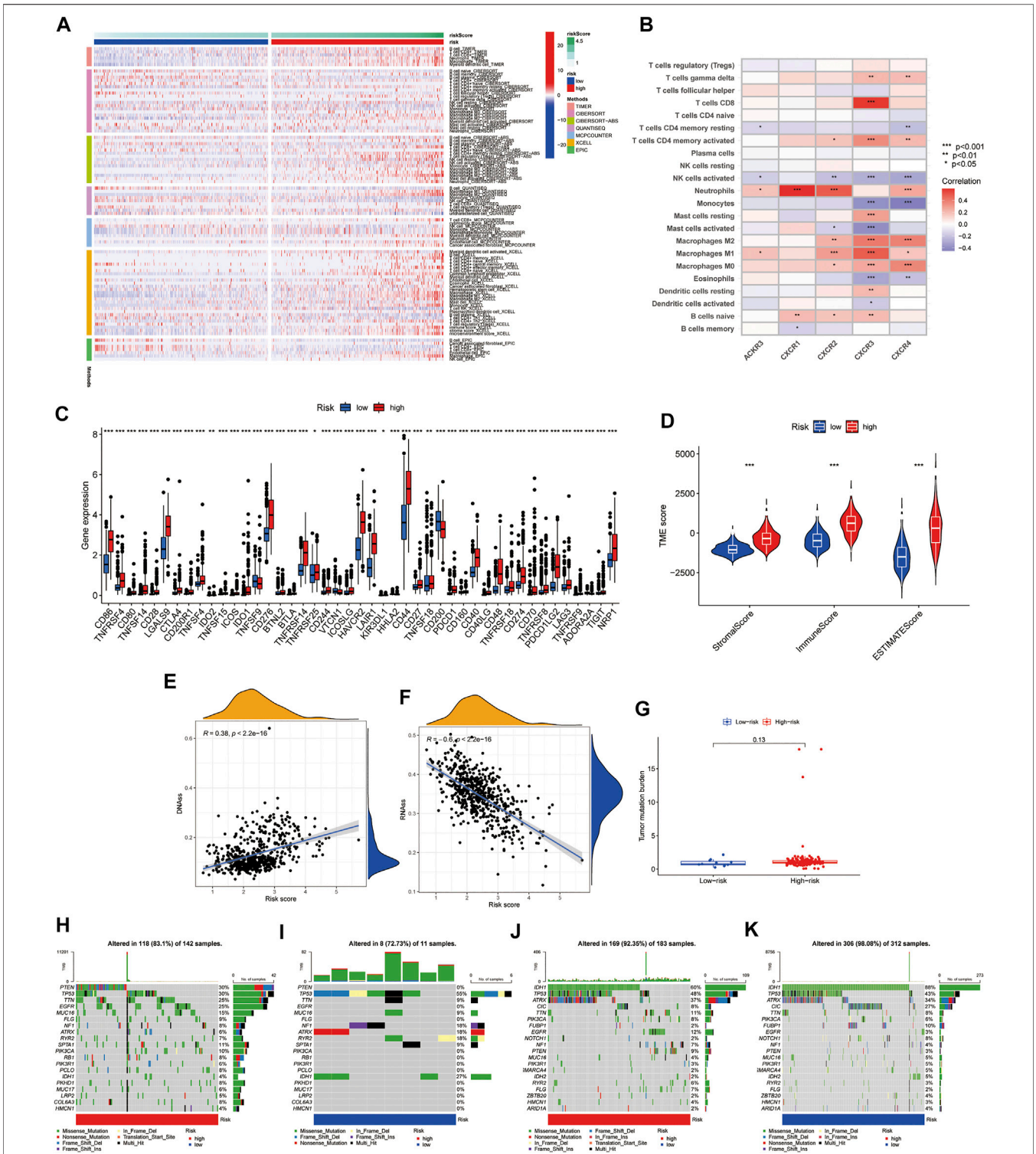

FIGURE 7 | Correlation of CR-Score and with TME, CSC index, immune checkpoints, and mutation. **(A)** The thermogram indicates the frequency of TME infiltrating cells among high- and low-risk group. **(B)** Relationships between the infiltrating levels of 22 immune cell types and the differentially expressed genes. **(C)** The expression of immune checkpoint genes. **(D)** Associations between the CR-Score and TME score. Relationships between CR-Score and CSC index. **(E)** DNAss. **(F)** RNAss. **(G)** Correlations between CR-Score and TMB. **(H–K)** Waterfall plot of somatic mutation profiles established with high and low CR-Scores in each sample. Data are shown as the mean ± SD; t test, $^{*}p < 0.05$, $^{**}p < 0.01$ and $^{***}p < 0.001$ compared to the high-risk group in **(B–D)**.

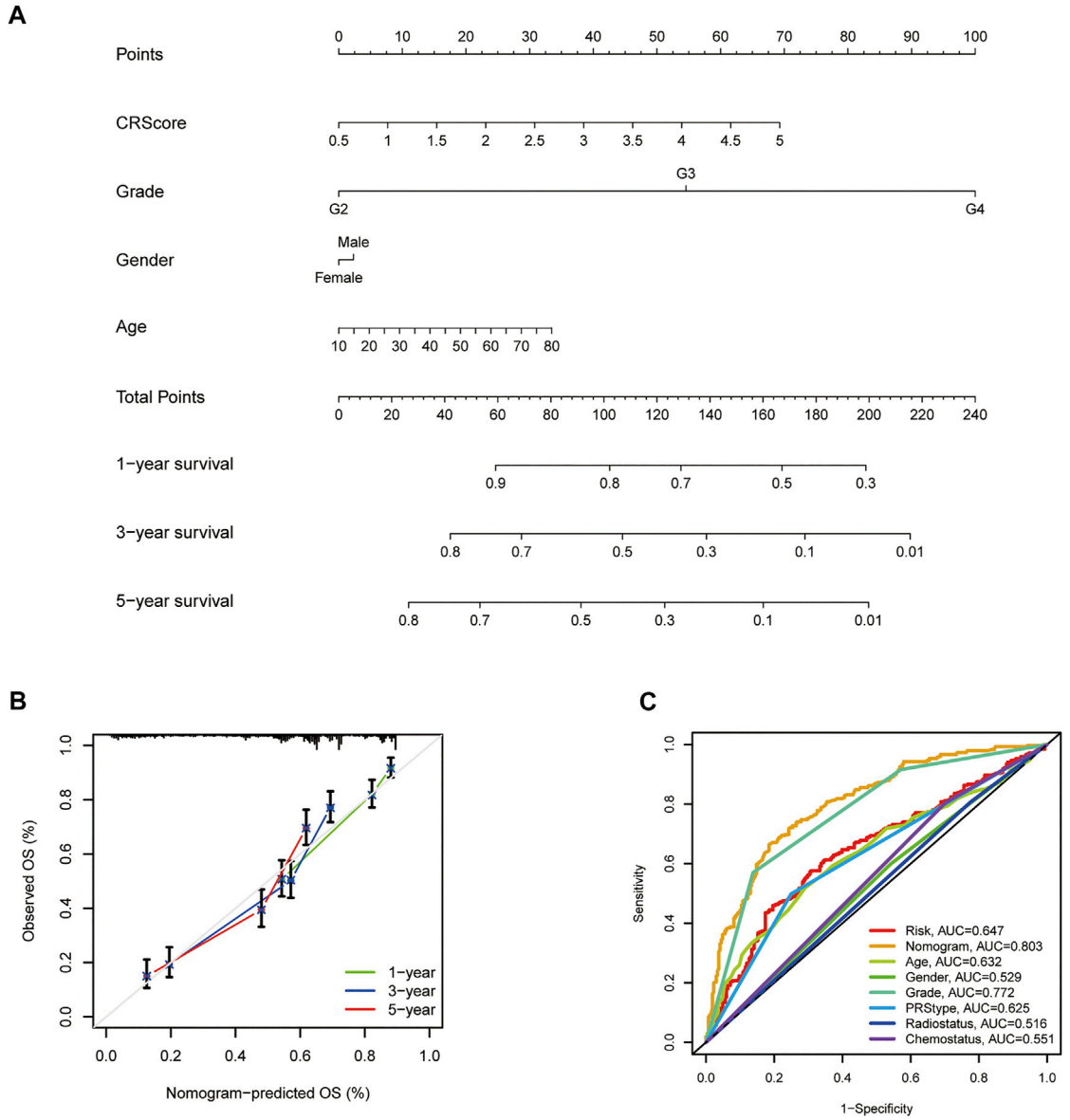

FIGURE 8 | Establishment and application of the scoring model in the external validation cohort. **(A)** Nomogram for the prediction of OS at 1, 3, and 5 years. **(B)** The calibration curves for external validation of the nomogram. **(C)** The clinical ROC curves of the CXCR-related nomogram at 3-year OS.

(**Figure 7B**). In addition, we found that immune checkpoint-related genes, including PD-1, PD-L1, and CTLA-4, were overexpressed in high-risk patients compared to low-risk patients (**Figure 7C**). Tumor microenvironment analysis was also performed, the higher the StromaScore or ImmuneScore, the higher the relative content of stroma or immune components in the immune microenvironment, and the ESTIMATEScore represented the accumulation of stroma or immune cells. We found that subtype C2 had higher TME scores than subtype C1 (**Figure 7D**). **Figures 7E,F** showed the linear correlation between the CSC index and the CR-Score in glioma. We found that the CR-Score correlated positively with the DNAss index (R = 0.38, $p < 0.001$), while the RNAss index correlated negatively with the CR-Score (R = −0.6, $p < 0.001$), indicating that glioma cells with a higher CR-Score had a higher degree of differentiation and more stem cell characteristics (**Figures 7E,F**).

Accumulating evidence suggested that patients with high TMB status may benefit from preventive immunotherapy due to a higher proportion of tumor-specific neoantigens. However, a pooled analysis of TMB showed no significant difference between the two risk groups (**Figure 7G**). GBM patients with high CR-Scores had significantly higher frequencies of PTEN, TTN, and EGFR mutations compared with patients with low CR-Scores. However, the mutation levels of TP53 and NF1 were the exact opposite (**Figures 7H,I**). The somatic mutation features of

LGG established with high and low CR-Score were shown in **Figures 7J,K**.

Establishment of a Nomogram Model for the Prognosis of Glioma.

Given the inconvenience of CR-Score in the clinical application, a prognostic nomogram model was established to predict the probability for glioma patients (**Figure 8A**). The predictors included CR-Score, tumor grade, patient age, and gender. The calibration plot of the nomogram showed that the 1-year, 3-years, and 5-year OS rates can be better predicted in the CGGA cohort (**Figure 8B**). Next, clinical ROC curves were performed to assess the sensitivity and specificity of the nomogram. The AUC of this nomogram at 3- year survival reached 0.803, indicating the potential clinical values of the nomogram model (**Figure 8C**).

DISCUSSION

Increasing evidence suggests the crucial role of CXCR in anti-tumor immunity, however, the underlying molecular mechanism of glioma is still not fully understood. In this research, we explored the transcriptional and genetic heterogeneity of seven CXCR molecules in both tumor tissues and normal tissues and found that the regulation of genome variation may not be related to the degree of CXCR expression. Then we identified two distinct molecular subtypes of CXCR in glioma. Significant differences in the immune cell infiltration level and clinical characteristics among different clusters were observed. The success of ICI depends on prior recruitment of the TILs, particularly the existence of CD8 + T cells, in the TME. It is generally believed that the extent of PD-L1 and PD-1 expression correlates with better immunosuppressive therapy (Topalian et al., 2012). In our research, the group with a high CR-Score had more checkpoint molecular expression and ESTIMATE score. The results show that there is a significant correlation between CXCR and tumor immunity in glioma. Consequently, we confirmed that the combination of CXCR inducers and ICI has great potential for the development of new combined therapeutic strategies. In addition, compared with PD-L1 protein expression detected by immunohistochemical, a high TMB is more significantly associated with better response to PD-1/PD-L1 blockades (Luchini et al., 2019). However, we did not detect any significant differences in the TMB between the two risk groups.

We focused on five CXCR genes, CXCR1/2/3/4/7, which have a significant impact on the overall survival rate of glioma. There is a high degree of homology between CXCR1 and CXCR2, studies from Lee et al. showed that knockdown of CXCR1 or CXCR2 was effective in inhibiting neutrophilic infiltration and tumor growth *in vitro* and *in vivo* (Lee et al., 2012). CXCR3 is a CXC chemokine receptor dominated by IFN-γ, which interacts with CXCL9, CXCL10, and CXCL11 to regulate tumor progression and cytokine secretion (Singh et al., 2013). This is consistent with the results of our current study. Recently, Saahene et al. showed that CXCL4 interaction with CXCR3b might be associated with poor prognosis in breast cancer (Saahene et al., 2019). Among the CXCRs, CXCR4 is the most studied in gliomas. Over-expression of CXCR4 has been identified as a promising prognostic biomarker for gastrointestinal and acute myeloid leukemia, among many other tumor types (Du et al., 2019; Jiang et al., 2019). High expression of CXCR4 in glioma was modulated through Akt/mTOR signaling by Notch1, which promotes the migration of glioma-originating cells (Zheng et al., 2018). In the nervous system, the CXCR7/CXCL12 signaling pathway regulates the differentiation and growth of astrocytes, Schwann cells as well as glioma cells (Odemis et al., 2010; Ödemis et al., 2012). Previous studies have indicated that CXCR7 antagonists could suppress tumor activation in animal models (Burns et al., 2006). So far, little was known about the role of CXCR5 in glioma. Studies carried out by Zheng et al. reported that the CXCR5-CXCL13 axis promotes the growth of colorectal cancer and clear cell renal cell carcinoma (ccRCC) *via* activating PI3K/Akt/mTOR signaling (Zhu et al., 2015; Zheng et al., 2018). In this study, the results indicated that the mRNA expression of CXCR5 in glioma was higher than that in normal samples. However, CXCR5 was not correlated to the prognosis of glioma. Similarly, CXCR6 is highly expressed in multiple tumor types, and the CXCR6-CXCL16 axis is mainly related to NF-κB and PI3K/Akt signaling pathways. Lepore et al. reported that CXCR6 knockout greatly prolonged survival in mice (Lepore et al., 2018). Unfortunately, the underlying mechanism of CXCR6 is still unknown. In the present study, we found that the expression of CXCR6 between glioma and normal brain tissue did not show any significant difference.

Considering the intratumoral heterogeneity of CXCR phenotypes in individuals with glioma, we established a clinical risk scoring system, CR-Score, to evaluate the value of CXCR molecules in glioma patients. There is a significant positive correlation between the CR-Score and immune cell infiltration level in glioma. In clinical practice, CR-Score can be used to selectively evaluate the immune cell infiltration of TME and the corresponding expression pattern of CXCR-related molecules in glioma patients, confirm the tumor immunophenotype, predict the prognosis of individual patients, and inform the medication properly. In summary, our research explored genetic and transcriptional levels of CXCR-related molecules in glioma and showed that CXCR molecules play a significant role in the remodeling of the tumor microenvironment. These results have strengthened our understanding of the tumor immune microenvironment, improved the response of patients to immunotherapy, identified two distinct tumor immunophenotypes, and promoted precise cancer immunotherapy in the future.

We recognize that our study has some limitations. This is a two-center retrospective study. Although we have corrected the batch effect to a large extent and conducted independent cohort experiments, the current research still has some impact. Further in-depth experimental studies are needed. Our results indicate that CXCR1/2/3/4/7 may play a significant role in glioma, but there is still a lack of investigation on the exact molecular mechanism of oncogenes involved. We are currently collecting samples in a multicenter clinical cohort for further verification and analysis.

DATA AVAILABILITY STATEMENT

The datasets presented in this study can be found in online repositories. The names of the repository/repositories and accession number(s) can be found in the article/**Supplementary Material**.

ETHICS STATEMENT

Written informed consent was obtained from the individual(s) for the publication of any potentially identifiable images or data included in this article.

AUTHOR CONTRIBUTIONS

JH and MZ designed the study and carried out experiments. JH, ZJ, JL, and YC analyzed the data. JH, ZJ, WZ, and BL wrote the draft of the manuscript. MZ edited the manuscript. All the authors read and approved the final version of the manuscript.

FUNDING

This work was funded by the Natural Science Foundation of Hunan Province, China (Grant No. 2019JJ40417), the Fundamental Research Funds for the Central Universities of Central South University (Grant No. 208211114), and the Scientific Research Project of Hunan Provincial Health Commission (Grant No. 202104040152).

ACKNOWLEDGMENTS

The authors would like to thank all members of the Laboratory of Neurosurgery at the Second Xiangya Hospital for technical assistance.

SUPPLEMENTARY MATERIAL

The Supplementary Material for this article can be found online at: https://www.frontiersin.org/articles/10.3389/fgene.2022.787141/full#supplementary-material

REFERENCES

Burns, J. M., Summers, B. C., Wang, Y., Melikian, A., Berahovich, R., Miao, Z., et al. (2006). A Novel Chemokine Receptor for SDF-1 and I-TAC Involved in Cell Survival, Cell Adhesion, and Tumor Development. *J. Exp. Med.* 203 (9), 2201–2213. doi:10.1084/jem.20052144

Conesa, A., Madrigal, P., Tarazona, S., Gomez-Cabrero, D., Cervera, A., McPherson, A., et al. (2016). A Survey of Best Practices for RNA-Seq Data Analysis. *Genome Biol.* 17, 13. doi:10.1186/s13059-016-0881-8

Cristescu, R., Mogg, R., Ayers, M., Albright, A., Murphy, E., Yearley, J., et al. (2018). Pan-Tumor Genomic Biomarkers for PD-1 Checkpoint Blockade-Based Immunotherapy. *Science* 362 (6411), 362. doi:10.1126/science.aar3593

Curran, M. A., Montalvo, W., Yagita, H., and Allison, J. P. (2010). PD-1 and CTLA-4 Combination Blockade Expands Infiltrating T Cells and Reduces Regulatory T and Myeloid Cells within B16 Melanoma Tumors. *Proc. Natl. Acad. Sci. U.S.A.* 107 (9), 4275–4280. doi:10.1073/pnas.0915174107

Du, W., Lu, C., Zhu, X., Hu, D., Chen, X., Li, J., et al. (2019). Prognostic Significance of CXCR4 Expression in Acute Myeloid Leukemia. *Cancer Med.* 8 (15), 6595–6603. doi:10.1002/cam4.2535

Fanelli, M. F., Chinen, L. T. D., Begnami, M. D., Costa, W. L., Fregnami, J. H. T., Soares, F. A., et al. (2012). The Influence of Transforming Growth Factor-α, Cyclooxygenase-2, Matrix Metalloproteinase (MMP)-7, MMP-9 and CXCR4 Proteins Involved in Epithelial-Mesenchymal Transition on Overall Survival of Patients with Gastric Cancer. *Histopathology* 61 (2), 153–161. doi:10.1111/j.1365-2559.2011.04139.x

Hattermann, K., Held-Feindt, J., Lucius, R., Müerköster, S. S., Penfold, M. E. T., Schall, T. J., et al. (2010). The Chemokine Receptor CXCR7 Is Highly Expressed in Human Glioma Cells and Mediates Antiapoptotic Effects. *Cancer Res.* 70 (8), 3299–3308. doi:10.1158/0008-5472.can-09-3642

Hu, M., Li, K., Maskey, N., Xu, Z., Yu, F., Peng, C., et al. (2015). Overexpression of the Chemokine Receptor CXCR3 and its Correlation with Favorable Prognosis in Gastric Cancer. *Hum. Pathol.* 46 (12), 1872–1880. doi:10.1016/j.humpath.2015.08.004

Jiang, Q., Sun, Y., and Liu, X. (2019). CXCR4 as a Prognostic Biomarker in Gastrointestinal Cancer: A Meta-Analysis. *Biomarkers* 24 (6), 510–516. doi:10.1080/1354750x.2019.1637941

Jin, L., Tao, H., Karachi, A., Long, Y., Hou, A. Y., Na, M., et al. (2019). CXCR1- or CXCR2-Modified CAR T Cells Co-opt IL-8 for Maximal Antitumor Efficacy in Solid Tumors. *Nat. Commun.* 10 (1), 4016. doi:10.1038/s41467-019-11869-4

Lee, Y. S., Choi, I., Ning, Y., Kim, N. Y., Khatchadourian, V., Yang, D., et al. (2012). Interleukin-8 and its Receptor CXCR2 in the Tumour Microenvironment Promote Colon Cancer Growth, Progression and Metastasis. *Br. J. Cancer* 106 (11), 1833–1841. doi:10.1038/bjc.2012.177

Lepore, F., D'Alessandro, G., Antonangeli, F., Santoro, A., Esposito, V., Limatola, C., et al. (2018). CXCL16/CXCR6 Axis Drives Microglia/Macrophages Phenotype in Physiological Conditions and Plays a Crucial Role in Glioma. *Front. Immunol.* 9, 2750. doi:10.3389/fimmu.2018.02750

Luchini, C., Bibeau, F., Ligtenberg, M. J. L., Singh, N., Nottegar, A., Bosse, T., et al. (2019). ESMO Recommendations on Microsatellite Instability Testing for Immunotherapy in Cancer, and its Relationship with PD-1/pd-L1 Expression and Tumour Mutational Burden: A Systematic Review-Based Approach. *Ann. Oncol.* 30 (8), 1232–1243. doi:10.1093/annonc/mdz116

Marin-Acevedo, J. A., Chirila, R. M., and Dronca, R. S. (2019). Immune Checkpoint Inhibitor Toxicities. *Mayo Clinic Proc.* 94 (7), 1321–1329. doi:10.1016/j.mayocp.2019.03.012

Mollica Poeta, V., Massara, M., Capucetti, A., and Bonecchi, R. (2019). Chemokines and Chemokine Receptors: New Targets for Cancer Immunotherapy. *Front. Immunol.* 10, 379. doi:10.3389/fimmu.2019.00379

Newman, A. M., Liu, C. L., Green, M. R., Gentles, A. J., Feng, W., Xu, Y., et al. (2015). Robust Enumeration of Cell Subsets from Tissue Expression Profiles. *Nat. Methods* 12 (5), 453–457. doi:10.1038/nmeth.3337

Odemis, V., Boosmann, K., Heinen, A., Küry, P., and Engele, J. (2010). CXCR7 Is an Active Component of SDF-1 Signalling in Astrocytes and Schwann Cells. *J. Cel Sci* 123 (Pt 7), 1081–1088. doi:10.1242/jcs.062810

Ödemis, V., Lipfert, J., Kraft, R., Hajek, P., Abraham, G., Hattermann, K., et al. (2012). The Presumed Atypical Chemokine Receptor CXCR7 Signals Through Gi/o Proteins in Primary Rodent Astrocytes and Human Glioma Cells. *Glia* 60 (3), 372–381. doi:10.1002/glia.22271

Park, S. H., Das, B. B., Casagrande, F., Tian, Y., Nothnagel, H. J., Chu, M., et al. (2012). Structure of the Chemokine Receptor CXCR1 in Phospholipid Bilayers. *Nature* 491 (7426), 779–783. doi:10.1038/nature11580

Pitt, J. M., Marabelle, A., Eggermont, A., Soria, J.-C., Kroemer, G., and Zitvogel, L. (2016). Targeting the Tumor Microenvironment: Removing Obstruction to Anticancer Immune Responses and Immunotherapy. *Ann. Oncol.* 27 (8), 1482–1492. doi:10.1093/annonc/mdw168

Pozzobon, T., Goldoni, G., Viola, A., and Molon, B. (2016). CXCR4 Signaling in Health and Disease. *Immunol. Lett.* 177, 6–15. doi:10.1016/j.imlet.2016.06.006

Richardson, P. J. (2016). CXCR4 and Glioblastoma. *Anticancer Agents Med. Chem.* 16 (1), 59–74. doi:10.2174/1871520615666150824153032

Romani, M., Pistillo, M. P., Carosio, R., Morabito, A., and Banelli, B. (2018). Immune Checkpoints and Innovative Therapies in Glioblastoma. *Front. Oncol.* 8, 464. doi:10.3389/fonc.2018.00464

Rooney, M. S., Shukla, S. A., Wu, C. J., Getz, G., and Hacohen, N. (2015). Molecular and Genetic Properties of Tumors Associated with Local Immune Cytolytic Activity. *Cell* 160 (1-2), 48–61. doi:10.1016/j.cell.2014.12.033

Saahene, R. O., Wang, J., Wang, M.-L., Agbo, E., and Song, H. (2019). The Role of CXC Chemokine Ligand 4/CXC Chemokine Receptor 3-B in Breast Cancer Progression. *Biotech. Histochem.* 94 (1), 53–59. doi:10.1080/10520295.2018.1497201

Singh, A. K., Arya, R. K., Trivedi, A. K., Sanyal, S., Baral, R., Dormond, O., et al. (2013). Chemokine Receptor Trio: CXCR3, CXCR4 and CXCR7 Crosstalk via CXCL11 and CXCL12. *Cytokine Growth Factor. Rev.* 24 (1), 41–49. doi:10.1016/j.cytogfr.2012.08.007

Sung, H., Ferlay, J., Siegel, R. L., Laversanne, M., Soerjomataram, I., Jemal, A., et al. (2021). Global Cancer Statistics 2020: GLOBOCAN Estimates of Incidence and Mortality Worldwide for 36 Cancers in 185 Countries. *CA A. Cancer J. Clin.* 71 (3), 209–249. doi:10.3322/caac.21660

Topalian, S. L., Hodi, F. S., Brahmer, J. R., Gettinger, S. N., Smith, D. C., McDermott, D. F., et al. (2012). Safety, Activity, and Immune Correlates of Anti-PD-1 Antibody in Cancer. *N. Engl. J. Med.* 366 (26), 2443–2454. doi:10.1056/NEJMoa1200690

Wang, Q., Hu, B., Hu, X., Kim, H., Squatrito, M., Scarpace, L., et al. (2017). Tumor Evolution of Glioma-Intrinsic Gene Expression Subtypes Associates with Immunological Changes in the Microenvironment. *Cancer Cell* 32 (1), 42–56. doi:10.1016/j.ccell.2017.06.003

Yang, J.-k., Liu, H.-j., Wang, Y., Li, C., Yang, J.-p., Yang, L., et al. (2019). Exosomal miR-214-5p Released from Glioblastoma Cells Modulates Inflammatory Response of Microglia After Lipopolysaccharide Stimulation Through Targeting CXCR5. *Cnsnddt* 18 (1), 78–87. doi:10.2174/1871527317666181105112009

Zheng, Z., Cai, Y., Chen, H., Chen, Z., Zhu, D., Zhong, Q., et al. (2018). CXCL13/CXCR5 Axis Predicts Poor Prognosis and Promotes Progression Through PI3K/AKT/mTOR Pathway in Clear Cell Renal Cell Carcinoma. *Front. Oncol.* 8, 682. doi:10.3389/fonc.2018.00682

Zhou, Y.-Q., Liu, D.-Q., Chen, S.-P., Sun, J., Zhou, X.-R., Xing, C., et al. (2019). The Role of CXCR3 in Neurological Diseases. *Cn* 17 (2), 142–150. doi:10.2174/1570159x15666171109161140

Zhu, Z., Zhang, X., Guo, H., Fu, L., Pan, G., and Sun, Y. (2015). CXCL13-CXCR5 Axis Promotes the Growth and Invasion of Colon Cancer Cells via PI3K/AKT Pathway. *Mol. Cel. Biochem.* 400 (1-2), 287–295. doi:10.1007/s11010-014-2285-y

Conflict of Interest: The authors declare that the research was conducted in the absence of any commercial or financial relationships that could be construed as a potential conflict of interest.

Publisher's Note: All claims expressed in this article are solely those of the authors and do not necessarily represent those of their affiliated organizations, or those of the publisher, the editors and the reviewers. Any product that may be evaluated in this article, or claim that may be made by its manufacturer, is not guaranteed or endorsed by the publisher.

frontiers | Frontiers in Cell and Developmental Biology

ORIGINAL RESEARCH
published: 17 May 2022
doi: 10.3389/fcell.2022.839986

Integrative Analysis of KCNK Genes and Establishment of a Specific Prognostic Signature for Breast Cancer

Yutian Zou†, Jindong Xie†, Wenwen Tian†, Linyu Wu, Yi Xie, Shanshan Huang, Yuhui Tang, Xinpei Deng, Hao Wu and Xinhua Xie**

Department of Breast Oncology, Sun Yat-sen University Cancer Center, State Key Laboratory of Oncology in South China, Collaborative Innovation Center for Cancer Medicine, Guangzhou, China

OPEN ACCESS

Edited by:
Christiane Pienna Soares, Sao Paulo State Universty, Brazil

Reviewed by:
Igor Pottosin, University of Colima, Mexico
Xiaowei Qi, Army Medical University, China

***Correspondence:**
Hao Wu
wuhao1@sysucc.org.cn
Xinhua Xie
xiexh@sysucc.org.cn

†These authors have contributed equally to this work

Specialty section:
This article was submitted to Epigenomics and Epigenetics, a section of the journal Frontiers in Cell and Developmental Biology

Received: *20 December 2021*
Accepted: *29 March 2022*
Published: *17 May 2022*

Citation:
Zou Y, Xie J, Tian W, Wu L, Xie Y, Huang S, Tang Y, Deng X, Wu H and Xie X (2022) Integrative Analysis of KCNK Genes and Establishment of a Specific Prognostic Signature for Breast Cancer. Front. Cell Dev. Biol. 10:839986. doi: 10.3389/fcell.2022.839986

Two-pore domains potassium channel subunits, encoded by KCNK genes, play vital roles in breast cancer progression. However, the characteristics of most KCNK genes in breast cancer has yet to be clarified. In this study, we comprehensively analyzed the expression, alteration, prognosis, and biological functions of various KCNKs in breast cancer. The expression of KCNK1/4/6/9/10/13 were significantly upregulated, while KCNK2/3/5/7/17 were downregulated in breast cancer tissues compared to normal mammary tissues. Increased expression of KCNK1/3/4/9 was correlated with poor overall survival, while high expression of KCNK2/7/17 predicted better overall survival in breast cancer. Eight KCNK genes were altered in breast cancer patients with a genomic mutation rate ranged from 1.9% to 21%. KCNK1 and KCNK9 were the two most common mutations in breast cancer, occurred in 21% and 18% patients, respectively. Alteration of KCNK genes was associated with the worse clinical characteristics and higher TMB, MSI, and hypoxia score. Using machine learning method, a specific prognostic signature with seven KCNK genes was established, which manifested accuracy in predicting the prognosis of breast cancer in both training and validation cohorts. A nomogram with great predictive performance was afterwards constructed through incorporating KCNK-based risk score with clinical features. Furthermore, KCNKs were correlated with the activation of several tumor microenvironment cells, including T cells, mast cells, macrophages, and platelets. Presentation of antigen, stimulation of G protein signaling and toll-like receptor cascaded were regulated by KCNKs family. Taken together, KCNKs may regulate breast cancer progression via modulating immune response which can serve as ideal prognostic biomarkers for breast cancer patients. Our study provides novel insight for future studies evaluating their usefulness as therapeutic targets.

Keywords: breast cancer, KCNK, biomarker, prognostic signature, tumor microenvironment

INTRODUCTION

According to the estimates of global cancer statistics, breast cancer is known as the most common cancer and the second leading cause of cancer-related death among women (Kuang et al., 2015). In the United States, approximately 268,600 new cases and 42,260 deaths due to female breast cancer are expected to occur in the year 2019 (Heurteaux et al., 2004). Although surgery, radiation, and chemotherapy vastly improve the prognosis of patients with breast cancer, residual tumor cells may contribute to metastatic recurrence and death (Rolfsen et al., 2014). Potassium ion channels are the most widely distributed types in ion channels and are found in most cell types with multiple cellular functions. There are four major types of potassium channels: 1) Calcium-activated potassium (KCa) channels which turn on according to the presence of calcium ions or other signaling molecules. 2) Inwardly rectifying potassium (Kir) channels that pass current more easily in the inward direction. 3) Two-pore domain potassium (K2P) channels that are constitutively open or possess high basal activation. 4) Voltage-gated potassium (KV) channels, which can be switched on or off in response to changes in transmembrane voltage (Kuang et al., 2015).

As an important member of the potassium channel family, K2P channels (encoded by KCNK genes) have been studied and identified to be associated with a range of physiological and pathological processes, including neuroprotection, cardiac activity regulation, anesthesia, depression, and cancer (Heurteaux et al., 2004; Heurteaux et al., 2006; Lalevée et al., 2006; Devilliers et al., 2013; Innamaa et al., 2013). Moreover, the KCNK channels have been divided into six categories, including TWIK (tandem of P domains in weak inward rectifying K+ channels), TREK (TWIK-related K+ channels), TASK (TWIK-related acid-sensitive K+ channels), TALK (TWIK-related alkaline pH activated K+ channels), THIK (tandem-pore domain halothane inhibited K+ channels), and TRESK (TWIK-related spinal cord K+ channels) (Sauter et al., 2016).

The potential importance of KCNK genes in cancer has become of great interest in recent years. For example, KCNK2/10 were overexpressed in ovarian cancer, and KCNK2 regulators played an important role in cell proliferation and apoptosis. TREK-1(KCNK2) may be a promising novel target for pancreatic ductal adenocarcinoma (Sauter et al., 2016). The TREK2 channel was present in bladder cancer cell lines and may contribute to cell cycle-dependent growth (Park et al., 2013). TASK-1 Regulates Apoptosis and Proliferation in a Subset of Non-Small Cell Lung Cancers (Leithner et al., 2016). TASK3 was significantly up-regulated whereas TASK1 and TRESK were both significantly down-regulated in advanced, poorly differentiated oral squamous cell carcinoma (Zavala et al., 2019). Overexpression rather than mutation of KCNK9 may contribute to the development of colorectal cancer (Kim et al., 2004). Knockdown of TREK-1 significantly inhibited the proliferation of prostate cancer cells both *in vitro* and *in vivo* (Zhang et al., 2015). Due to the increase in apoptosis, knocking down of TASK-3 reduced cell proliferation and vitality (Cikutović-Molina et al., 2019). Lower expression of KCNK 2/15/17 in liver cancer and overexpression of KCNK9 were associated with better prognosis in hepatocellular carcinoma (Li et al., 2019).

Several studies have focused on the role of KCNK genes in tumor treatment and prevention strategies for breast cancer (Wallace et al., 2011). E2 induced the overexpression of KCNK5 in luminal breast cancer cells through ERα+, and KCNK5 played an important role in regulating cell proliferation (Alvarez-Baron et al., 2011). Increased TASK-3 expression, which could be modulated by PKC activation, reduced cell migration and invasion in triple-negative breast cancer cells (Lee et al., 2012). Overexpression of KCNK5, KCNK9, and KCNK12, as well as reduced expression of KCNK6 and KCNK15, was significantly correlated with triple-negative subtype in breast carcinoma (Dookeran et al., 2017). In this study, we comprehensively analyzed the expression, alteration, prognosis, and biological functions of various KCNKs in breast cancer. A specific prognostic signature with seven KCNK genes was established using machine learning method. This constructed model manifested accuracy in predicting the prognosis of patients with breast cancer.

MATERIALS AND METHODS

Data Collection

The 15 members of the KCNK gene family were acquired from reported literature. The mRNA expression matrix of KCNK genes and corresponding clinical data of breast cancer patients were downloaded from the TCGA database (https://portal.gdc. cancer. gov/). Only samples with complete prognostic data were included.

General Assessment and Visualization of KCNK Genes

To investigate the clinical correlation of KCNK genes, boxplots and heatmaps were used to display the distribution of KCNK gene expressions and their relationship with various clinic features in breast cancer patients. Wilcoxon test was applied to calculate statistical significances between groups. The position and expression levels of 15 KCNK genes were shown with a circos plot by applying the "RCircos" R package (Zhang et al., 2013). The correlation of each KCNK gene was shown utilizing the "corrplot" R package. Genomic alteration landscape and biological function enrichment of KCNK gene family in breast cancer in breast cancer was explored in the cBioPortal website (http://www.cbioportal.org/).

Survival Analysis

To better evaluate the prognostic value of the differentially expressed KCNK genes, we obtained the best cutoff value by the "survminer" R package. all samples were divided into high and low expression groups with the automatically selecting cutoff. Kaplan-Meier analysis was performed with the "survival" R package.

Construction and Validation of the KCNK Gene Signature

7 KCNK genes, including KCNK1, KCNK2, KCNK3, KCNK4, KCNK7, KCNK9, and KCNK17, were included to construct a risk signature for their significant effects on overall survival (OS) in breast cancer patients. The "sample" function in R was used and the TCGA dataset was then randomly separated into a training dataset and a validation dataset with the split ratio of 55% and 45%. Based on the LASSO regression analysis, we determined the coefficients and calculated the risk score of each patient with the formula as follows:

$$Risk\ score = \sum_{i=1}^{7} Coef i * Expi \quad (1)$$

Coefi denote the risk coefficient and Expi refer to the expression of each gene, respectively. To make plots more intuitionistic, we used a linear transformation to adjust the risk score. The calculated risk score minus the minimum and divided it by the maximum, which mapped these exponentials to the range of 0–1 (Xie et al., 2021).

According to the median value of the risk score, patients were divided into high- and low-risk groups, and the OS of the two subgroups were compared by Kaplan-Meier analysis with the log-rank test. Similarly, these analyses described above were also conducted in the validation set.

Establishment of a Predictive Nomogram

Univariate and multivariate cox regression analyses were utilized to identify independently prognostic factors in breast cancer patients of the training set. The nomogram was constructed and shown with the "regplot" R package. Then, calibration plots were plotted to evaluate the reliability of the nomogram, and the decision curve analysis (DCA) was performed to investigate the clinical net benefit of the nomogram (R package "caret" and "rmda").

Estimation of Immune Microenvironment

Tumor Immune Estimation Resource (TIMER) (Li et al., 2020) and CIBERSORT (Newman et al., 2015) algorithms were applied to compare the infiltration levels of various immune cells between KCNKs, as well as the high-risk and low-risk groups.

Construction of PPI Networks

The protein-protein interaction (PPI) network of every candidate KCNK gene was built based on the STRING database (Szklarczyk et al., 2015) and rebuilt with Cytoscape software (Shannon et al., 2003).

UALCAN Analysis

UALCAN (http://ualcan.path.uab.edu) is an online tool for in-depth analysis of gene expression differences between various cancers and normal samples (Chandrashekar et al., 2017). In this study, we reviewed the relationship between the expression levels of each model gene and the breast cancer subtypes, histological subtypes, and pathologic stages.

Collection of Clinical Samples

Fresh breast cancer tissues and adjacent mammary tissues were collected from breast cancer patients who received surgery in Sun Yat-sen University Cancer Center (SYSUCC). All resected samples were immediately stored in RNAlater (Ambion, TX). This study was approved by the Ethics Committee of SYSUCC. Written informed consent was collected from all patients.

Cell Lines and Cell Culture

Human breast cancer cell lines were purchased from the American Type Culture Collection. All cell lines were cultured following standard guidelines. All cell lines were maintained without antibiotics in an atmosphere of 5% CO_2 and 99% relative humidity at 37°C. Cell lines were passaged for fewer than 6 months and were authenticated by short tandem repeat analysis. No *mycoplasma* infection was found for all cell lines.

RNA Isolation and Quantitative Real-Time PCR Analysis

Total RNA of cells was extracted with RNA-Quick Purification Kit (ES-RN001, Shanghai Yishan Biotechnology Co.). The primer sequences are provided in **Supplementary Table S1**. The quantitative real-time PCR (qRT-PCR) plate was employed from NEST NO.402301. RNA levels were determined by qRT-PCR in triplicate on a Bio-Rad CFX96 using the SYBR Green method (RR420A, Takara). The RNA levels were normalized against β-actin RNA using the comparative Ct method.

RESULTS

Aberrant Expression of KCNK Gene Family in Breast Cancer

To understand the mRNA expression of KCNK genes in breast carcinoma samples, we reviewed KCNK mRNA levels of 1,097 tumors and 113 normal tissues in the TCGA database. Totally, fifteen genes in the KCNK family were analyzed (KCNK1, KCNK2, KCNK3, KCNK4, KCNK5, KCNK6, KCNK7, KCNK9, KCNK10, KCNK12, KCNK13, KCNK15, KCNK16, KCNK17, KCNK18). Heatmap depicts the expression of different KCNK genes and clinical information in each breast cancer patient (**Figure 1A**). We found that twelve genes in the KCNK family were differentially expressed in normal and breast cancer tissues. Among them, KCNK1/4/6/9/10/13/15 were upregulated in breast tumor samples compared to normal mammary tissues. Additionally, KCNK2/3/5/7/17 were significantly downregulated in breast cancer samples (**Figure 1B**). The RNA expression level of KCNK2, KCNK5, KCNK9, KCNK13, and KCNK15 were validated in human breast cancer cell lines (**Supplementary Figure S1**). Our results revealed that KCNK9, KCNK13, and KCNK15 was significantly upregulated in breast cancer cell lines including MDA-MB-231 and SK-BR-3 cell lines, while KCNK2 and KCNK5 was downregulated in breast cancer cell lines comparing with breast epithelial cell line MCF-10A (**Supplementary Figure S1A**). To further validate their expression patterns in clinical specimens, we detected the expression level in breast cancer tissues and adjacent normal

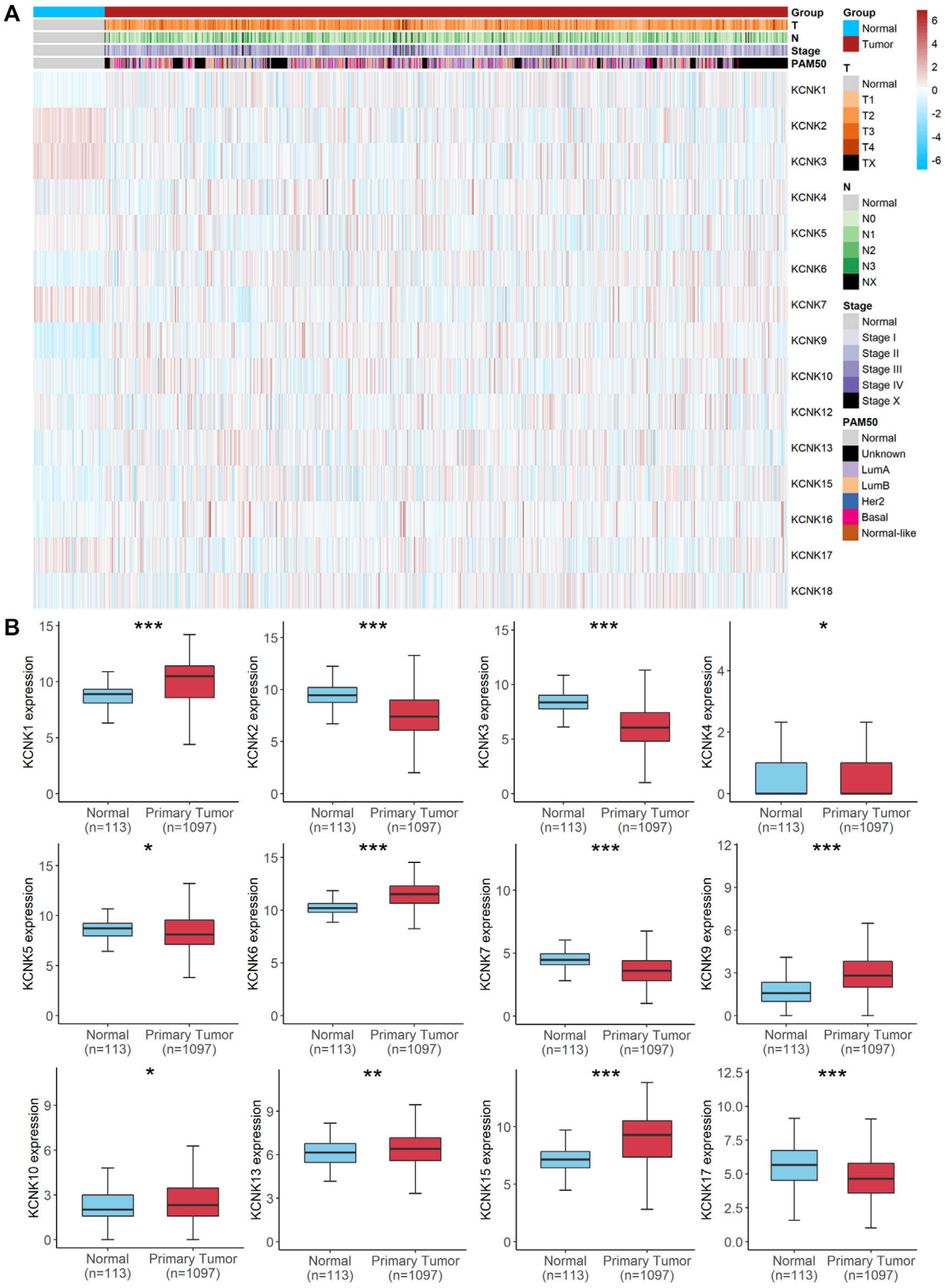

FIGURE 1 | Aberrant expression of KCNK gene family in breast cancer. **(A)** Heatmap of the expression of 15 KCNKs and corresponding clinical information of patients with breast cancer according to the TCGA database. **(B)** Boxplots of the differently expressed KCNKs in normal mammary and breast cancer tissues.

tissues. We found that KCNK2 and KCNK5 was downregulated in breast cancer, while KCNK9, KCNK13, and KCNK15 was upregulated in breast cancer (**Supplementary Figure S1B**). In addition, we found that breast cancer patients with metastasis disease have low expression of KCNK2 and KCNK13 (**Supplementary Figure S1C**).

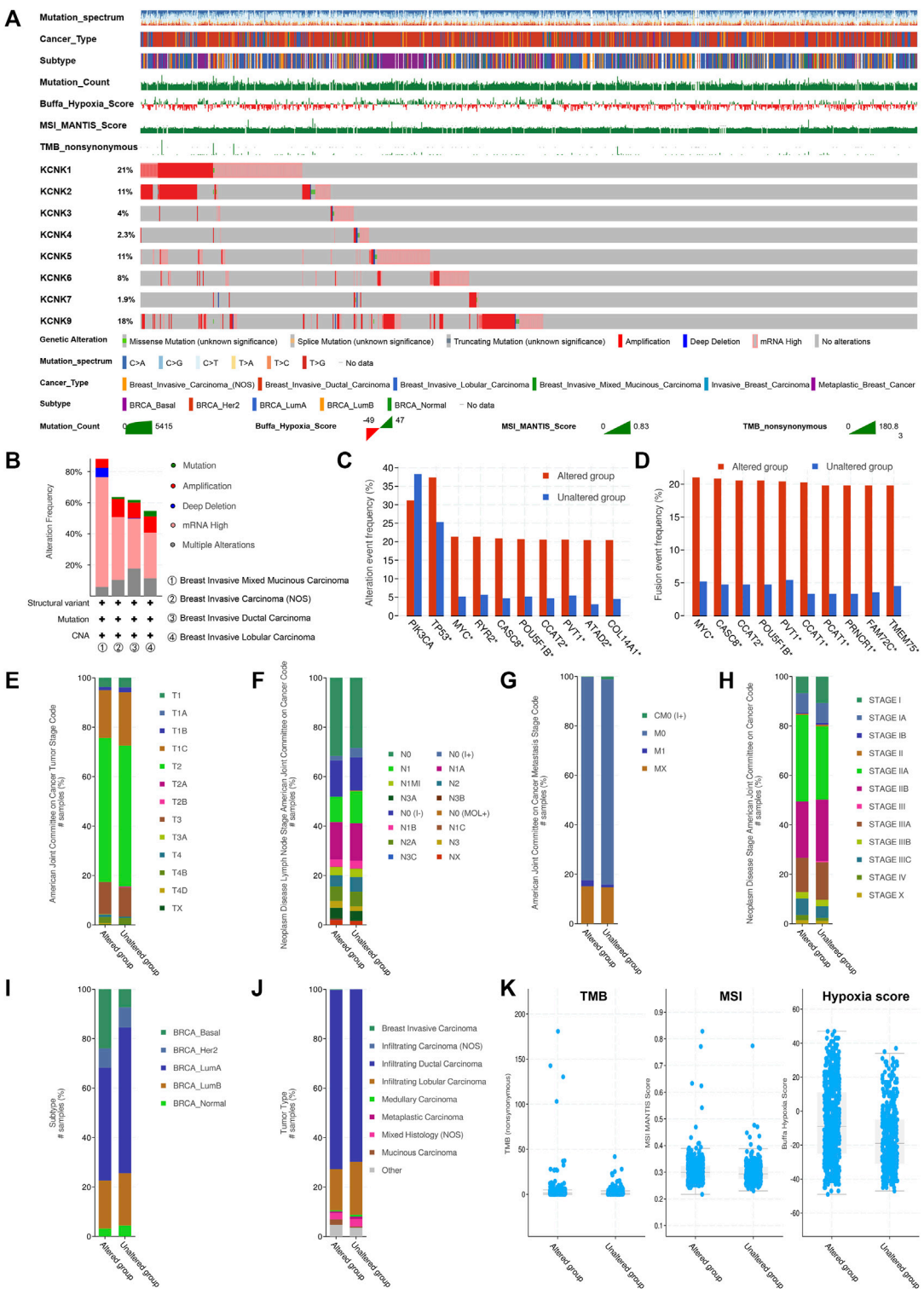

FIGURE 2 | Genomic alteration landscape of KCNK gene family in breast cancer. **(A)** The genomic alteration of KCNK genes in TCGA cohort. Oncoplot was used for display. **(B)** The alteration frequency of KCNKs in different breast cancer pathology types. **(C)** The correlation between the alteration of KCNKs and the alteration of several robust oncogenes in breast cancer development. **(D)** The correlation between KCNKs and fusion genes. **(E–J)** The relationship between the alteration of KCNK genes and the clinical characteristics of breast cancer. **(K)** The relationship between the alteration of KCNK genes and tumor mutation burden (TMB), microsatellite instability (MSI), and hypoxia score in breast cancer.

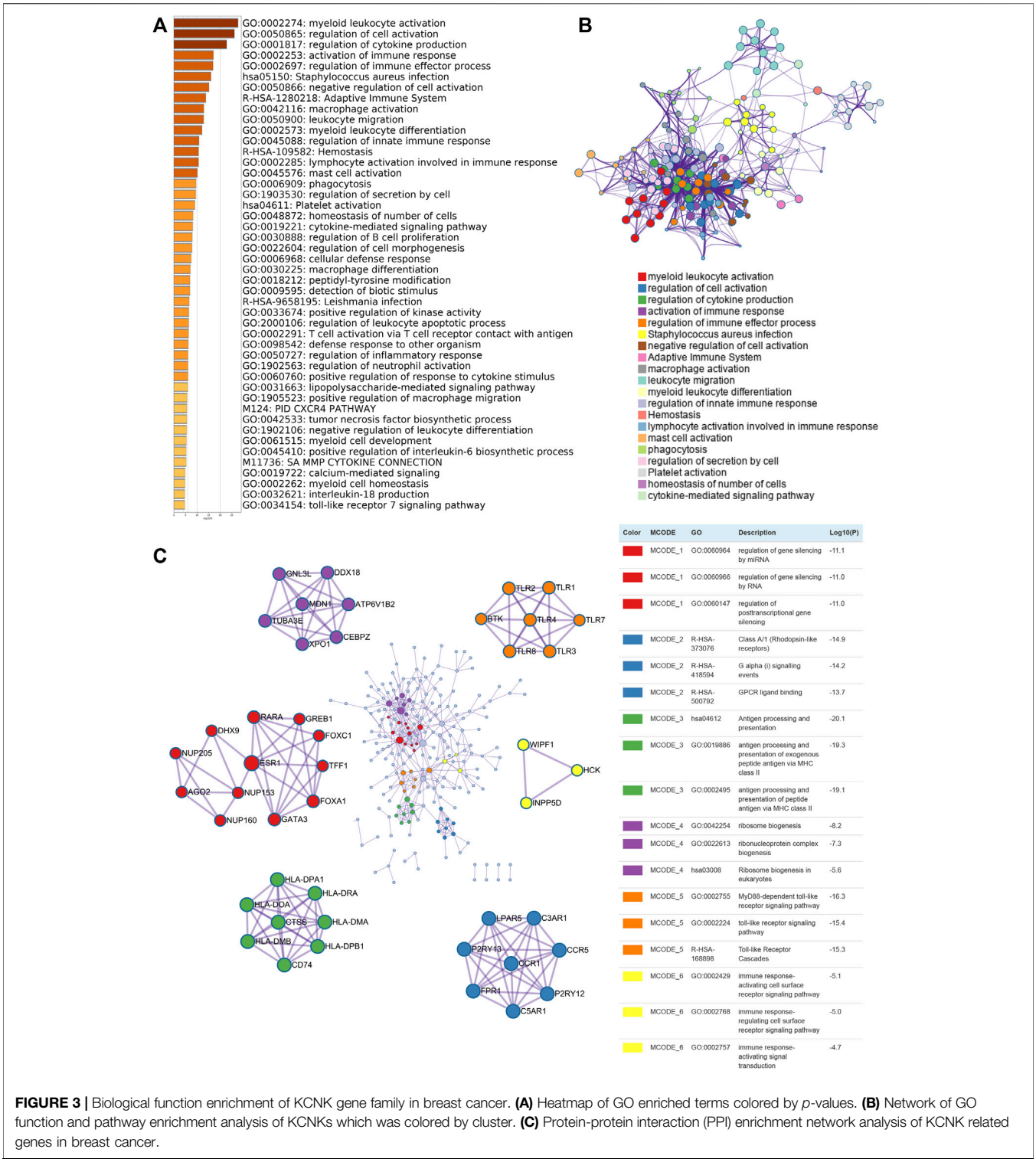

Color	MCODE	GO	Description	Log10(P)
	MCODE_1	GO:0060964	regulation of gene silencing by miRNA	-11.1
	MCODE_1	GO:0060966	regulation of gene silencing by RNA	-11.0
	MCODE_1	GO:0060147	regulation of posttranscriptional gene silencing	-11.0
	MCODE_2	R-HSA-373076	Class A/1 (Rhodopsin-like receptors)	-14.9
	MCODE_2	R-HSA-418594	G alpha (i) signalling events	-14.2
	MCODE_2	R-HSA-500792	GPCR ligand binding	-13.7
	MCODE_3	hsa04612	Antigen processing and presentation	-20.1
	MCODE_3	GO:0019886	antigen processing and presentation of exogenous peptide antigen via MHC class II	-19.3
	MCODE_3	GO:0002495	antigen processing and presentation of peptide antigen via MHC class II	-19.1
	MCODE_4	GO:0042254	ribosome biogenesis	-8.2
	MCODE_4	GO:0022613	ribonucleoprotein complex biogenesis	-7.3
	MCODE_4	hsa03008	Ribosome biogenesis in eukaryotes	-5.6
	MCODE_5	GO:0002755	MyD88-dependent toll-like receptor signaling pathway	-16.3
	MCODE_5	GO:0002224	toll-like receptor signaling pathway	-15.4
	MCODE_5	R-HSA-168898	Toll-like Receptor Cascades	-15.3
	MCODE_6	GO:0002429	immune response-activating cell surface receptor signaling pathway	-5.1
	MCODE_6	GO:0002768	immune response-regulating cell surface receptor signaling pathway	-5.0
	MCODE_6	GO:0002757	immune response-activating signal transduction	-4.7

FIGURE 3 | Biological function enrichment of KCNK gene family in breast cancer. **(A)** Heatmap of GO enriched terms colored by *p*-values. **(B)** Network of GO function and pathway enrichment analysis of KCNKs which was colored by cluster. **(C)** Protein-protein interaction (PPI) enrichment network analysis of KCNK related genes in breast cancer.

Genomic Alteration Landscape of KCNK Gene Family in Breast Cancer

We next evaluated the genomic mutations of KCNKs and their correlation with other clinical characteristics in breast cancer. A total of 1,082 patients were included for analysis on the TCGA PanCancer accessed by the cBioPortal tool (**Figure 2A**). The genomic mutation rate ranged from 1.9% to 21% among four different breast cancer subtypes. We found that KCNK1 and

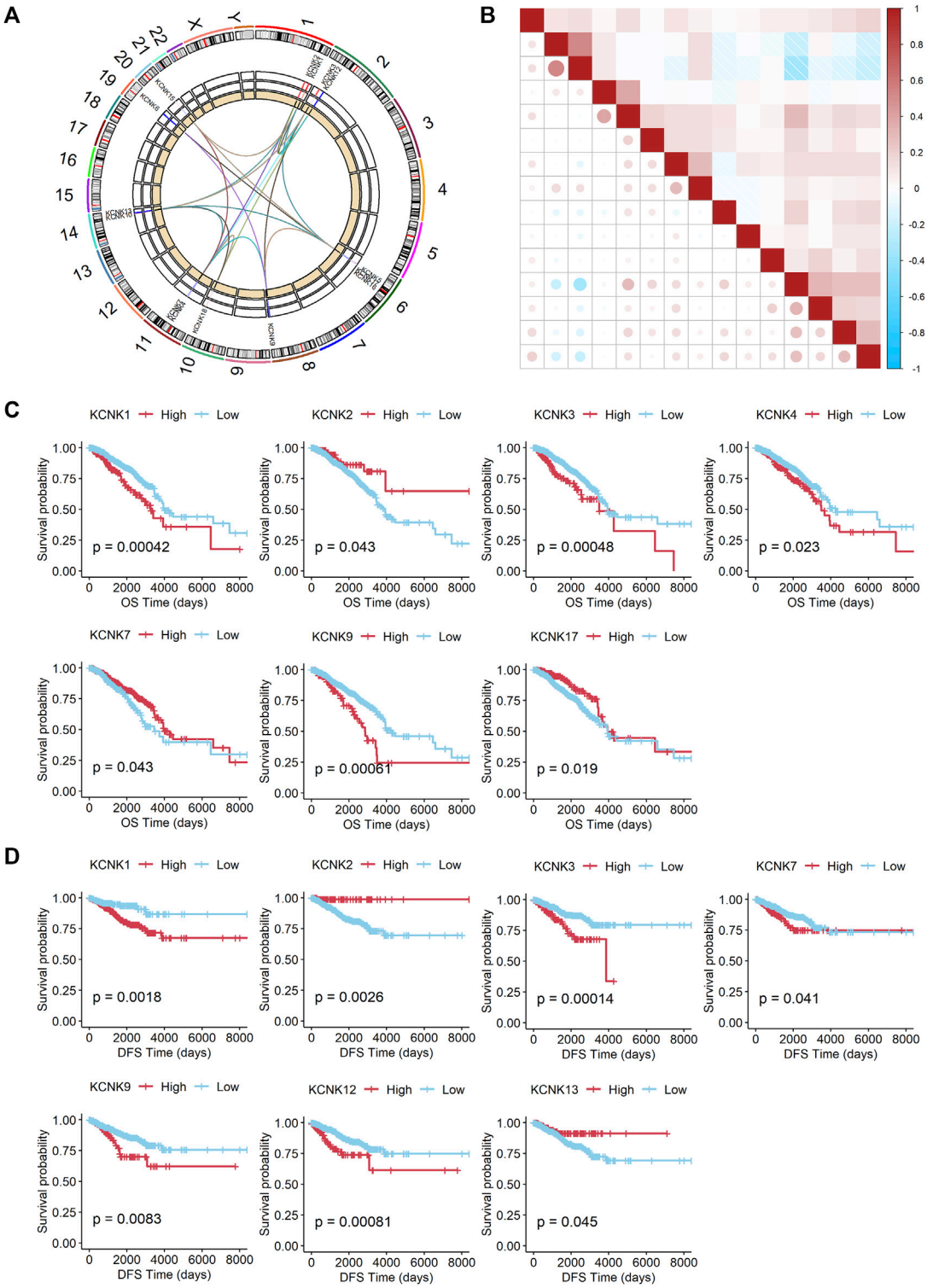

FIGURE 4 | Prognostic value of the expression of KCNK gene family in breast cancer. **(A)** Circos plot displaying the position of KCNK genes on chromosomes. **(B)** The correlation of each KCNK gene according to the TCGA database. **(C)** K-M analysis of the overall survival (OS) of breast cancer patients with high or low expression of each KCNK gene according to the TCGA database. **(D)** K-M analysis of the disease-free survival (DFS) of breast cancer patients with high or low expression of each KCNK gene according to the TCGA database.

KCNK9 were the two most common mutations in breast cancer, occurring in 21% and 18% of patients, respectively (**Figure 2A**). The alteration frequency of KCNKs in different breast cancer pathology types was analyzed, in which breast invasive mixed mucinous carcinoma had the highest mutation rate of KCNK family genes (**Figure 2B**). Moreover, the rate of KCNK gene alteration was significantly correlated with the alteration of several robust oncogenes in breast cancer development (PIK3CA, TP53, MYC, PVT1, etc.) (**Figure 2C**). The correlation between KCNKs and fusion genes was further analyzed. We found that the frequency of several fusion genes was higher in the altered group of KCNK genes (**Figure 2D**). In addition, mutation of KCNK genes was associated with the clinical characteristics (T status, N status, M status, clinical stage, molecular subtype, and pathological type) in breast cancer (**Figures 2E–J**). Patients with high TMB, MSI score or hypoxia score had an increased rate of KCNK alteration (**Figure 2K**).

Biological Function Enrichment of KCNK Gene Family in Breast Cancer

To investigate the potential biological function of KCNKs in breast cancer development and progression, we conducted function and pathway enrichment analysis. Genes correlated with KCNKs were identified by Spearman's test ($|r|>0.3$, $p < 0.05$), which were included for further functional and pathway enrichment analysis in Metascape. We found that KCNKs were mainly associated with the regulation of tumor immune response (**Figure 3A**). KCNKs were involved in the activation of several tumor microenvironment components, including T cells, mast cells, macrophages, and platelets. Pathway enrichment analysis identified that KCNKs family might modulate immune response via regulating presentation of antigen, stimulation of G protein signaling, and toll-like receptor cascaded (**Figure 3B**). Furthermore, protein-protein interaction enrichment analysis was performed to figure out the hub genes of each biological function module (**Figure 3C**).

Prognostic Value of the Expression of KCNK Gene Family in Breast Cancer

Firstly, the position and expression of KCNK genes were analyzed (**Figure 4A**), and the correlation of KCNK genes is also shown in **Figure 4B**. We next explored the prognostic predictive value of KCNK genes for patients with breast cancer by using the TCGA database. High expression of KCNK1/3/4/9 was correlated with a poor overall survival in patients with breast cancer (**Figure 4C**). Patients with higher KCNK2/7/17 expression were associated with better overall survival (**Figure 4C**). In addition, we found that KCNK1/3/7/9/12 was negatively correlated with disease-free survival in patients with breast cancer (**Figure 4D**). High expression of KCNK2 and KCNK13 levels were associated with favorable disease-free survival in patients with breast cancer (**Figure 4D**).

Construction and Validation of a KCNK-Based Prognostic Signature for Breast Cancer

A 7-gene signature was constructed by performing the LASSO Cox regression analysis (**Figures 5A,B**). The risk score was calculated by the formula as follows. risk score = (0.002199218 * KCNK1 exp.) + (−0.027946148 * KCNK2 exp.) + (0.060471745 * KCNK3 exp.) + (0.068412510 * KCNK4 exp.) + (−0.077890308 * KCNK7 exp.) + (0.120687908 * KCNK9 exp.) + (-0.096099063 * KCNK17 exp.).

Based on the median risk score, 588 patients in the training cohort were classified into low- and high-risk groups. We found that patients in the high-risk group were harder to survive as risk scores increased (**Figures 5C,D**). An obvious difference was detected in OS time between these two groups, that is, patients in the low-risk group were more likely to lower death rate ($p = 0.012$, **Figure 5E**). Subsequently, we utilized the validation cohort. Based on the median risk score, 482 patients were also divided into two groups. It also showed that high risk score resulted in poor survival time (**Figures 5C,D**). K-M analysis also showed that patients in the high-risk group were more likely to have shorter OS time and higher death rate ($p = 0.038$, **Figure 5E**).

Establishment and Assessment of the KCNK-Based Nomogram Survival Model for Breast Cancer

Univariate and multivariable Cox regression analyses were performed to explore whether the risk score could be an independent prognostic factor. The univariate Cox regression analysis showed that, compared with other features, the risk score was obviously regarded as a risk factor (HR = 3.984, 95% CI: 2.061–7.700, and $p < 0.05$, **Figure 6A**). After adjusting for other confounding factors, the multivariate analysis also indicated that the risk score was still an independent prognostic factor (HR = 4.442, 95% CI: 2.329–8.474, and $p < 0.05$, **Figure 6A**). Besides, the relationship between the expression levels of each model gene and the breast cancer subtypes, histological subtypes, and pathologic stages were also analyzed in **Supplementary Figure S1**. Stage and risk score were selected to establish a KCNK-based nomogram model in the training cohort (**Figure 6B**). Calibration curves showed the accuracy of this model in predicting the 2-, 3-, and 5-years survival rate is favorable (**Figure 6C**). Moreover, we performed DCA and found that the nomogram model was apparently better than any other predictor applied in this study (**Figure 6D**).

Relationship Between KCNK-Based Risk Model and Tumor Microenvironment Components in Breast Cancer

To validate the function of KCNKs in regulating the tumor microenvironment, we compared the infiltrated level of several immune and stromal cells between high and low-risk groups by using

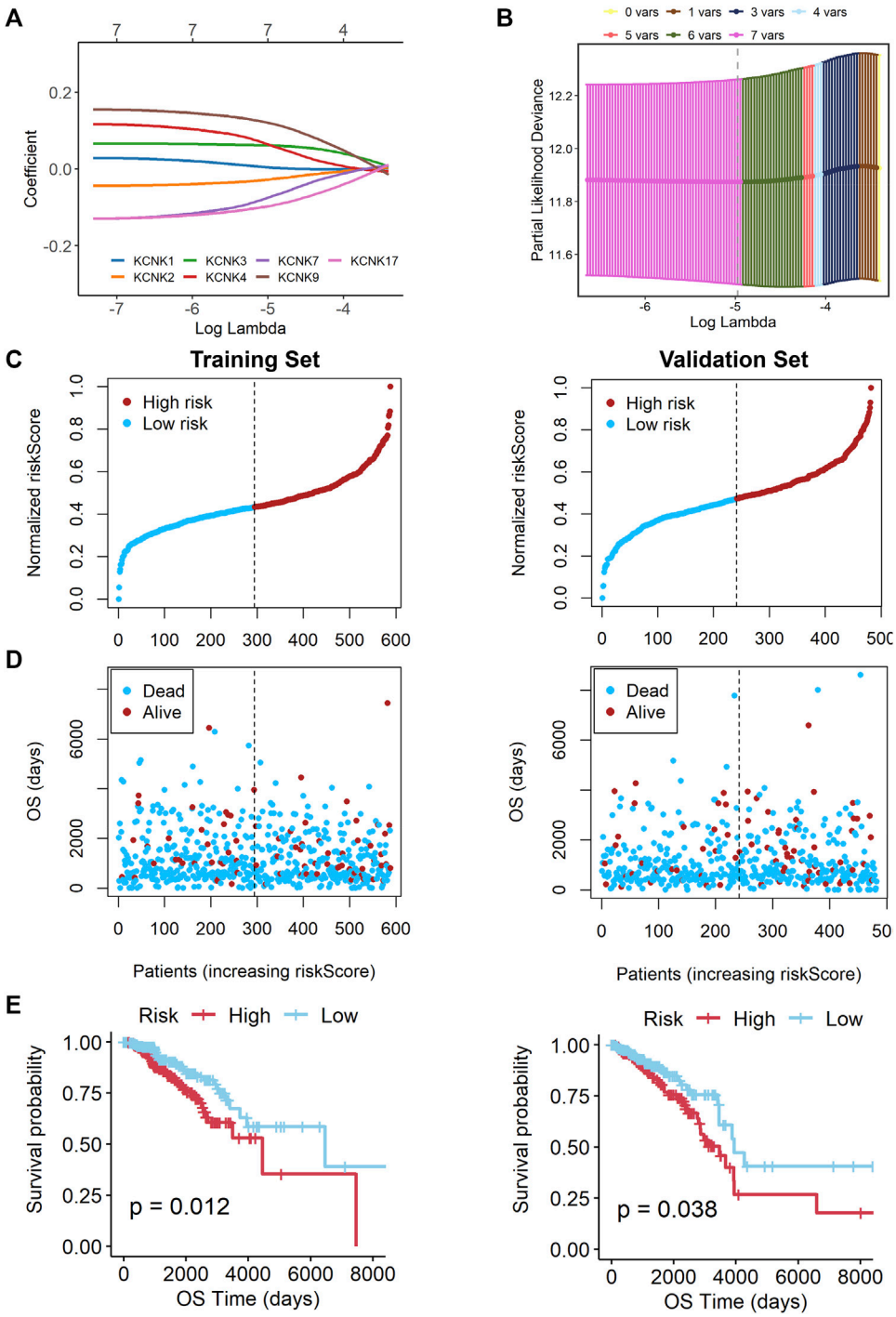

FIGURE 5 | Construction of a KCNK-based prognostic signature for breast cancer. **(A)** Selection of the seven model KCNK genes in lasso regression model. **(B)** Cross-validation of the constructed signature. **(C,D)** Distribution of adjusted risk score in the training and validation cohorts. **(E)** Overall survival (OS) in the low- and high-risk group patients in the training and validation cohorts. The specific prognostic signature with seven KCNK genes was established, which manifested accuracy in predicting the prognosis of breast cancer in both training and validation cohorts.

the CIBERSORT algorithm. We found that the KCCK-based risk score was correlated with the proportion of several tumor microenvironment components, including memory B cell, helper T cell, activated NK cell, M1 macrophage, and activated dendritic cell (**Figure 7A**). Moreover, the correlation between seven modeling genes and tumor microenvironment cells was analyzed. High expression of KCNK1 and KCNK2 was

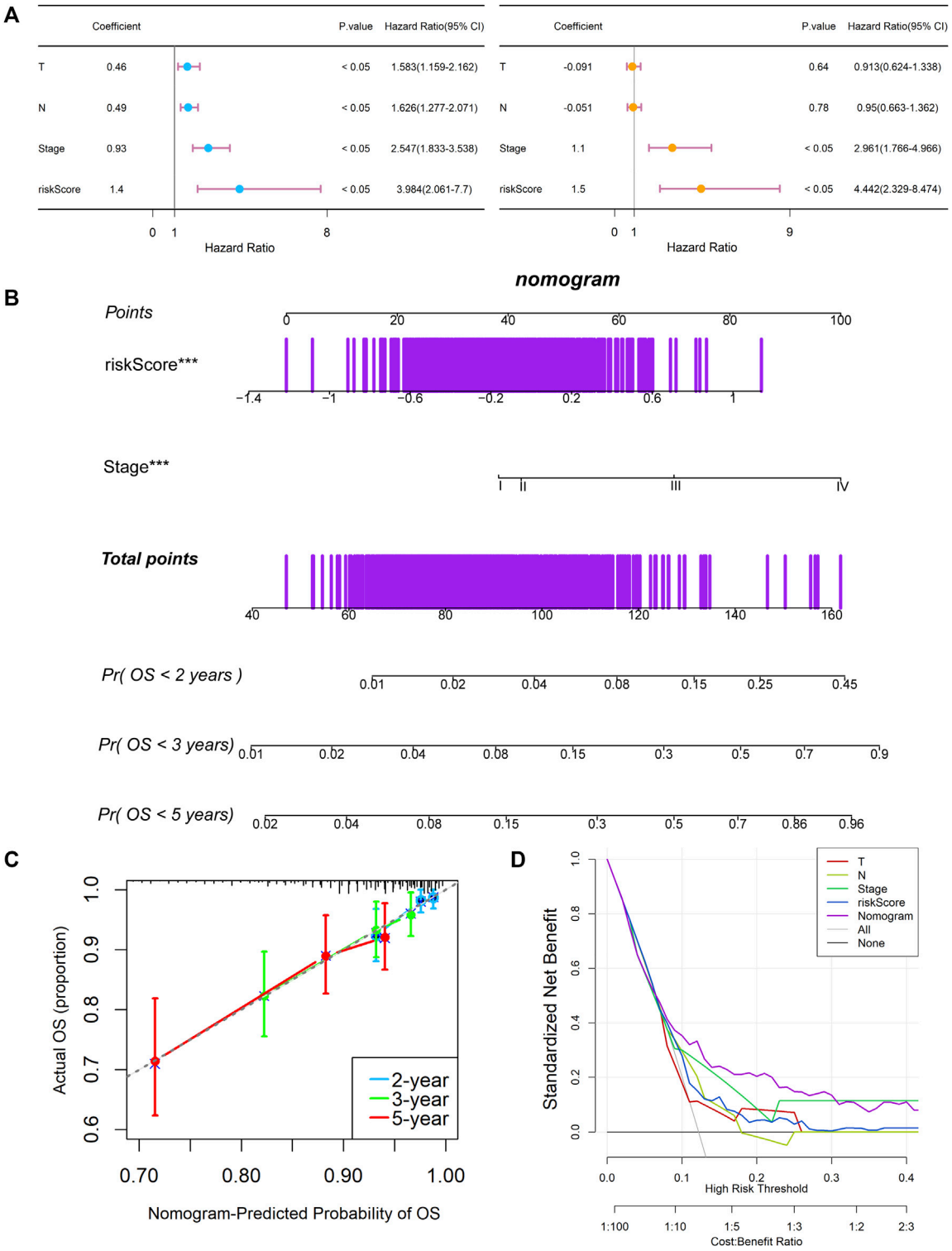

FIGURE 6 | Establishment and assessment of the KCNK-based nomogram survival model for breast cancer. **(A)** Univariate and multivariate analysis for the training cohort. **(B)** The nomogram for predicting the overall survival of the patients with breast cancer. **(C)** Calibration plots showed the probability of 2-, 3-, and 5-years overall survival in training cohort. **(D)** DCA of nomogram predicting 2-, 3-, and 5-years overall survival.

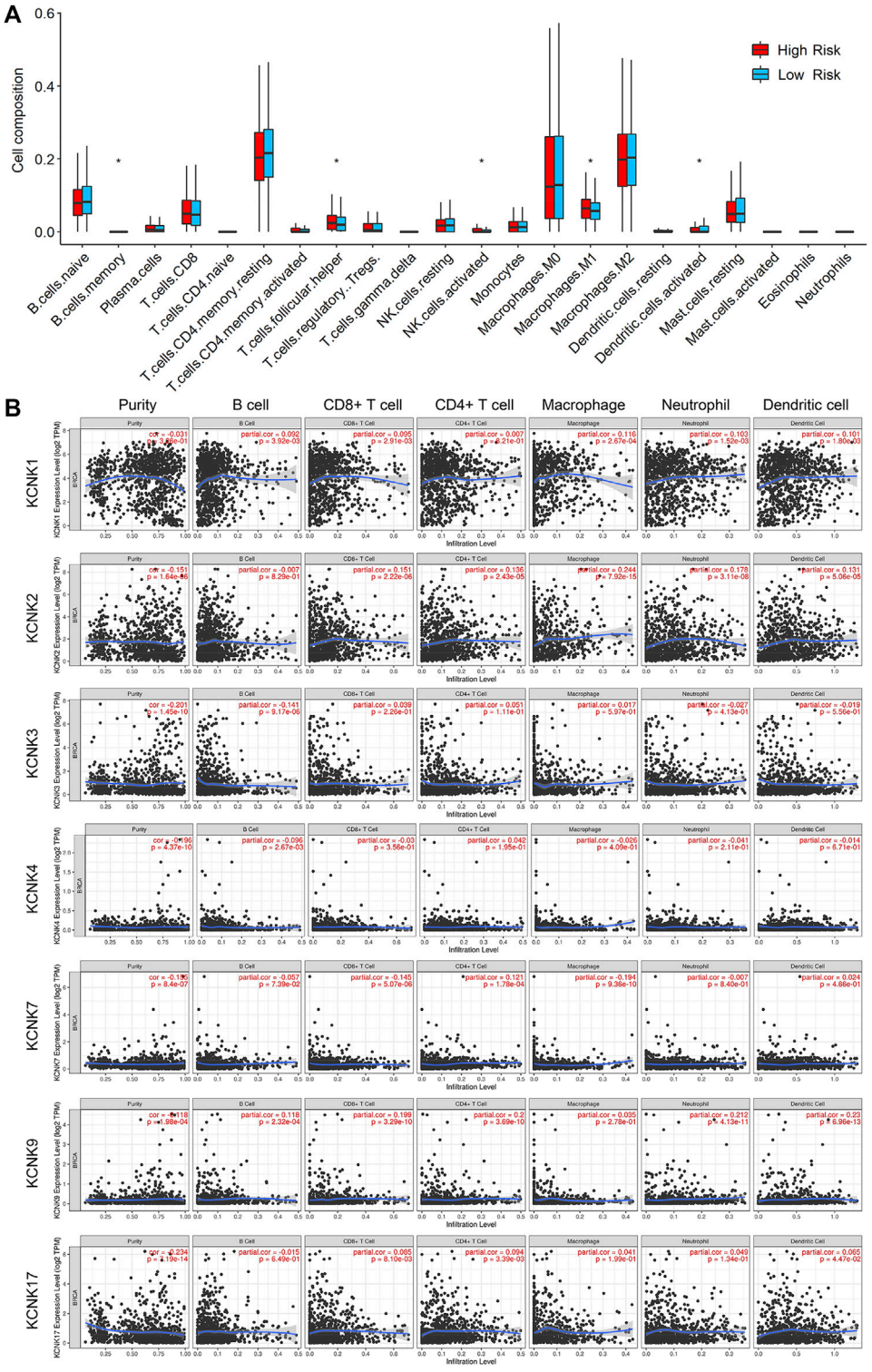

FIGURE 7 | Relationship between KCNK-based risk model and tumor microenvironment components in breast cancer. **(A)** Boxplots of the infiltrated level of immune or stromal cells in the tumor microenvironment between high- and low-risk groups according to the TCGA cohorts. **(B)** The correlation between seven modeling KCNK genes and the infiltrated level of immune or stromal cells in the tumor microenvironment.

associated with increasing macrophage in breast cancer. Expression of KCNK7 was negatively correlated with $CD8^+$ T cell level, while KCNK9 expression was positively correlated with $CD8^+$ T cell level in breast cancer (**Figure 7B**). Furthermore, the relationship between copy number variation of KCNKs and tumor microenvironment components was also analyzed (**Supplementary Figure S2**).

DISCUSSION

The two-pore domain (K2P) potassium channel family encoded by KCNK genes has been reported to be involved in the development of breast cancer (Kindler and Yost, 2005). Our study was the first systematic and comprehensive analysis of all fifteen KCNK genes expression, alteration, prognostic value, and their potential biological functions in breast cancer. Through bioinformatics analysis, we found that twelve KCNKs were differentially expressed between normal mammary and breast cancer tissues. Moreover, eight mutations of KCNK genes were identified which were associated with more advanced clinical characteristics according to the TCGA database. Expression of KCNK1/2/3/4/7/9/17 and KCNK1/2/3/7/9/12/13 were the prognostic factor for overall survival and disease-free survival in patients with breast cancer, respectively. Though function enrichment analysis, we found that KCNKs were mainly associated with the regulation of tumor immune response. The immune system can recognize and destroy tumor cells, preventing them from growing and spreading (da Silva et al., 2013). Several tumor microenvironment cells were activated by KCNKs, including T cells, mast cells, macrophages, and platelets. Presentation of antigen, stimulation of G protein signaling, and toll-like receptor cascaded were regulated by KCNKs family. A specific prognostic signature with seven KCNK genes was established using machine learning method. This constructed model manifested accuracy in predicting the prognosis of breast cancer in both training and validation cohorts. Afterwards, a nomogram with great predictive performance was constructed through incorporating KCNK-based risk score with clinical features. In consist with the functional enrichment analysis, the established risk score was correlated with the infiltrated level of several immune and stromal cells in the tumor microenvironment.

Several KCNK genes were included in the specific prognostic model, which have been reported as important oncogenes or tumor suppressors in multiple malignancies. KCNK1, also called TWIK-1, was cloned from the human kidney and was the first K2P channel identified (Zhang et al., 2015). In our study, mRNA expression level of KCNK1 was upregulated in breast cancer tissues with poor overall survival and disease-free survival. However, further research was necessary to test whether KCNK1 could be a targeted signature in breast cancer therapy. KCNK2, also known as TREK-1, expressed highly in central nervous system and was found to be responsible for temperature, mechanical stretch (Bockenhauer et al., 2001). KCNK2 was detected as a prognostic factor in breast cancer, which was similar with previous study (Li et al., 2019). The KCNK9 gene, commonly referred to as TASK-3, was associated with cancer due to its overexpression in human tumors and its ability to promote tumor survival and growth (Zavala et al., 2019). Base on the previous research, KCNK9 was overexpressed in rectal cancer, melanoma, and adrenal cortical adenocarcinoma (Sun et al., 2016). KCNK9 has been identified as an oncogene to promote cell migration and invasion in breast cancer cells, which was consistent with our result that increased KCNK9 mRNA expression had worse disease-free survival (Rusznák et al., 2008). Besides, several previous studies regarding the impact of KCNKs in breast cancer focused on certain subtypes such as luminal and triple-negative subtype, which are different from all-subtype breast cancer studies.

Taken together, we determined KCNKs as ideal prognostic biomarkers for patients with breast cancer. Our results also provided more evidence for discovering potential therapeutic targets for breast cancer patients.

DATA AVAILABILITY STATEMENT

The datasets presented in this study can be found in online repositories. The names of the repository/repositories and accession number(s) can be found in the article/**Supplementary Material**.

ETHICS STATEMENT

The studies involving human participants were reviewed and approved by the SYSUCC. The patients/participants provided their written informed consent to participate in this study.

AUTHOR CONTRIBUTIONS

Conception and design, XX and HW; Development of methodology, YZ, JX, and WT; Acquisition of data, YZ, JX, WT, LW, YX, SH, YT and XD; Formal Analysis, YZ, JX, WT, LW, YX, SH, YT and XD; Writing, YZ, JX, and WT; Reviewing and Editing, XX and HW All authors read and approved the final manuscript.

FUNDING

This study was funded by the National Natural Science Foundation of China (81974444, XX).

SUPPLEMENTARY MATERIAL

The Supplementary Material for this article can be found online at: https://www.frontiersin.org/articles/10.3389/fcell.2022.839986/full#supplementary-material

REFERENCES

Alvarez-Baron, C. P., Jonsson, P., Thomas, C., Dryer, S. E., and Williams, C. (2011). The Two-Pore Domain Potassium Channel KCNK5: Induction by Estrogen Receptor α and Role in Proliferation of Breast Cancer Cells. *Mol. Endocrinol.* 25 (8), 1326–1336. doi:10.1210/me.2011-0045

Bockenhauer, D., Zilberberg, N., and Goldstein, S. A. N. (2001). KCNK2: Reversible Conversion of a Hippocampal Potassium Leak into a Voltage-dependent Channel. *Nat. Neurosci.* 4 (5), 486–491. doi:10.1038/87434

Chandrashekar, D. S., Bashel, B., Balasubramanya, S. A. H., Creighton, C. J., Ponce-Rodriguez, I., Chakravarthi, B. V. S. K., et al. (2017). UALCAN: A Portal for Facilitating Tumor Subgroup Gene Expression and Survival Analyses. *Neoplasia* 19 (8), 649–658. doi:10.1016/j.neo.2017.05.002

Cikutović-Molina, R., Herrada, A. A., González, W., Brown, N., and Zúñiga, L. (2019). TASK-3 Gene Knockdown Dampens Invasion and Migration and Promotes Apoptosis in KATO III and MKN-45 Human Gastric Adenocarcinoma Cell Lines. *Int. J. Mol. Sci.* 20 (23). doi:10.3390/ijms20236077

da Silva, G. B., Silva, T. G., Duarte, R. A., Neto, N. L., Carrara, H. H., Donadi, E. A., et al. (2013). Expression of the Classical and Nonclassical HLA Molecules in Breast Cancer. *Int. J. Breast Cancer* 2013, 250435. doi:10.1155/2013/250435

Devilliers, M., Busserolles, J., Lolignier, S., Deval, E., Pereira, V., Alloui, A., et al. (2013). Activation of TREK-1 by Morphine Results in Analgesia without Adverse Side Effects. *Nat. Commun.* 4, 2941. doi:10.1038/ncomms3941

Dookeran, K. A., Zhang, W., Stayner, L., and Argos, M. (2017). Associations of Two-Pore Domain Potassium Channels and Triple Negative Breast Cancer Subtype in the Cancer Genome Atlas: Systematic Evaluation of Gene Expression and Methylation. *BMC Res. Notes* 10 (1), 475. doi:10.1186/s13104-017-2777-4

Heurteaux, C., Guy, N., Laigle, C., Blondeau, N., Duprat, F., Mazzuca, M., et al. (2004). TREK-1, a K+ Channel Involved in Neuroprotection and General Anesthesia. *EMBO J.* 23 (13), 2684–2695. doi:10.1038/sj.emboj.7600234

Heurteaux, C., Lucas, G., Guy, N., El Yacoubi, M., Thümmler, S., Peng, X.-D., et al. (2006). Deletion of the Background Potassium Channel TREK-1 Results in a Depression-Resistant Phenotype. *Nat. Neurosci.* 9 (9), 1134–1141. doi:10.1038/nn1749

Innamaa, A., Jackson, L., Asher, V., van Schalkwyk, G., Warren, A., Keightley, A., et al. (2013). Expression and Effects of Modulation of the K2P Potassium Channels TREK-1 (KCNK2) and TREK-2 (KCNK10) in the normal Human Ovary and Epithelial Ovarian Cancer. *Clin. Transl. Oncol.* 15 (11), 910–918. doi:10.1007/s12094-013-1022-4

Kim, C. J., Cho, Y. G., Jeong, S. W., Kim, Y. S., Kim, S. Y., Nam, S. W., et al. (2004). Altered Expression of KCNK9 in Colorectal Cancers. *APMIS* 112 (9), 588–594. doi:10.1111/j.1600-0463.2004.apm1120905.x

Kindler, C., and Yost, C. (2005). Two-Pore Domain Potassium Channels: New Sites of Local Anesthetic Action and Toxicity. *Reg. Anesth. Pain Med.* 30 (3), 260–274. doi:10.1016/j.rapm.2004.12.001

Kuang, Q., Purhonen, P., and Hebert, H. (2015). Structure of Potassium Channels. *Cell. Mol. Life Sci.* 72 (19), 3677–3693. doi:10.1007/s00018-015-1948-5

Lalevée, N., Monier, B., Sénatore, S., Perrin, L., and Sémériva, M. (2006). Control of Cardiac Rhythm by ORK1, a Drosophila Two-Pore Domain Potassium Channel. *Curr. Biol.* 16 (15), 1502–1508. doi:10.1016/j.cub.2006.05.064

Lee, G.-W., Park, H. S., Kim, E.-J., Cho, Y.-W., Kim, G.-T., Mun, Y.-J., et al. (2012). Reduction of Breast Cancer Cell Migration via Up-Regulation of TASK-3 Two-Pore Domain K+channel. *Acta Physiol. (Oxf)* 204 (4), 513–524. doi:10.1111/j.1748-1716.2011.02359.x

Leithner, K., Hirschmugl, B., Li, Y., Tang, B., Papp, R., Nagaraj, C., et al. (2016). TASK-1 Regulates Apoptosis and Proliferation in a Subset of Non-Small Cell Lung Cancers. *PLoS One* 11 (6), e0157453. doi:10.1371/journal.pone.0157453

Li, T., Fu, J., Zeng, Z., Cohen, D., Li, J., Chen, Q., et al. (2020). TIMER2.0 for Analysis of Tumor-Infiltrating Immune Cells. *Nucleic Acids Res.* 48 (W1), W509–W514. doi:10.1093/nar/gkaa407

Li, W.-C., Xiong, Z.-Y., Huang, P.-Z., Liao, Y.-J., Li, Q.-X., Yao, Z.-C., et al. (2019). KCNK Levels Are Prognostic and Diagnostic Markers for Hepatocellular Carcinoma. *Aging* 11 (19), 8169–8182. doi:10.18632/aging.102311

Newman, A. M., Liu, C. L., Green, M. R., Gentles, A. J., Feng, W., Xu, Y., et al. (2015). Robust Enumeration of Cell Subsets from Tissue Expression Profiles. *Nat. Methods* 12 (5), 453–457. doi:10.1038/nmeth.3337

Park, K.-S., Han, M. H., Jang, H. K., Kim, K.-A., Cha, E.-J., Kim, W.-J., et al. (2013). The TREK2 Channel Is Involved in the Proliferation of 253J Cell, a Human Bladder Carcinoma Cell. *Korean J. Physiol. Pharmacol.* 17 (6), 511–516. doi:10.4196/kjpp.2013.17.6.511

Rolfsen, G. B., Castelli, E. C., Donadi, E. A., Duarte, R. A., and Soares, C. P. (2014). HLA-G Polymorphism and Breast Cancer. *Int. J. Immunogenet.* 41 (2), 143–148. doi:10.1111/iji.12092

Rusznák, Z., Bakondi, G., Kosztka, L., Pocsai, K., Dienes, B., Fodor, J., et al. (2008). Mitochondrial Expression of the Two-Pore Domain TASK-3 Channels in Malignantly Transformed and Non-Malignant Human Cells. *Virchows Arch.* 452 (4), 415–426. doi:10.1007/s00428-007-0545-x

Sauter, D. R. P., Sørensen, C. E., Rapedius, M., Brüggemann, A., and Novak, I. (2016). pH-Sensitive K+ Channel TREK-1 Is a Novel Target in Pancreatic Cancer. *Biochim. Biophys. Acta (Bba) - Mol. Basis Dis.* 1862 (10), 1994–2003. doi:10.1016/j.bbadis.2016.07.009

Shannon, P., Markiel, A., Ozier, O., Baliga, N. S., Wang, J. T., Ramage, D., et al. (2003). Cytoscape: A Software Environment for Integrated Models of Biomolecular Interaction Networks. *Genome Res.* 13 (11), 2498–2504. doi:10.1101/gr.1239303

Sun, H., Luo, L., Lal, B., Ma, X., Chen, L., Hann, C. L., et al. (2016). A Monoclonal Antibody Against KCNK9 K+ Channel Extracellular Domain Inhibits Tumour Growth and Metastasis. *Nat. Commun.* 7, 10339. doi:10.1038/ncomms10339

Szklarczyk, D., Franceschini, A., Wyder, S., Forslund, K., Heller, D., Huerta-Cepas, J., et al. (2015). STRING V10: Protein-Protein Interaction Networks, Integrated Over the Tree of Life. *Nucleic Acids Res.* 43 (Database Issue), D447–D452. doi:10.1093/nar/gku1003

Wallace, J. L., Gow, I. F., and Warnock, M. (2011). The Life and Death of Breast Cancer Cells: Proposing a Role for the Effects of Phytoestrogens on Potassium Channels. *J. Membr. Biol.* 242 (2), 53–67. doi:10.1007/s00232-011-9376-4

Xie, J., Zou, Y., Ye, F., Zhao, W., Xie, X., Ou, X., et al. (2021). A Novel Platelet-Related Gene Signature for Predicting the Prognosis of Triple-Negative Breast Cancer. *Front. Cell Dev. Biol.* 9, 795600. doi:10.3389/fcell.2021.795600

Zavala, W. D., Foscolo, M. R., Kunda, P. E., Cavicchia, J. C., and Acosta, C. G. (2019). Changes in the Expression of the Potassium Channels TASK1, TASK3 and TRESK in a Rat Model of Oral Squamous Cell Carcinoma and Their Relation to Malignancy. *Arch. Oral Biol.* 100, 75–85. doi:10.1016/j.archoralbio.2019.02.007

Zhang, G.-M., Wan, F.-N., Qin, X.-J., Cao, D.-L., Zhang, H.-L., Zhu, Y., et al. (2015). Prognostic Significance of the TREK-1 K2P Potassium Channels in Prostate Cancer. *Oncotarget* 6 (21), 18460–18468. doi:10.18632/oncotarget.3782

Zhang, H., Meltzer, P., and Davis, S. (2013). RCircos: An R Package for Circos 2D Track Plots. *BMC Bioinformatics* 14, 244. doi:10.1186/1471-2105-14-244

Conflict of Interest: The authors declare that the research was conducted in the absence of any commercial or financial relationships that could be construed as a potential conflict of interest.

Publisher's Note: All claims expressed in this article are solely those of the authors and do not necessarily represent those of their affiliated organizations, or those of the publisher, the editors and the reviewers. Any product that may be evaluated in this article, or claim that may be made by its manufacturer, is not guaranteed or endorsed by the publisher.

frontiers | Frontiers in Cell and Developmental Biology

ORIGINAL RESEARCH
published: 08 June 2022
doi: 10.3389/fcell.2022.879057

Inhibition of the Protein Arginine Methyltransferase PRMT5 in High-Risk Multiple Myeloma as a Novel Treatment Approach

Philip Vlummens[1,2], Stefaan Verhulst[3], Kim De Veirman[1], Anke Maes[1], Eline Menu[1], Jérome Moreaux[4,5,6], Hugues De Boussac[4], Nicolas Robert[4], Elke De Bruyne[1], Dirk Hose[1], Fritz Offner[2], Karin Vanderkerken[1] and Ken Maes[1,7]**

[1]Department of Hematology and Immunology, Vrije Universiteit Brussel (VUB), Brussels, Belgium, [2]Department of Clinical Hematology, Ghent University Hospital, Ghent, Belgium, [3]Liver Cell Biology Lab, Vrije Universiteit Brussel (VUB), Brussels, Belgium, [4]CHU Montpellier, Laboratory for Monitoring Innovative Therapies, Department of Biological Hematology, Montpellier, France, [5]Department of Biological Hematology, CHU Montpellier, Montpellier, France, [6]Institut Universitaire de France, IUF, Paris, France, [7]Center for Medical Genetics, Vrije Universiteit Brussel (VUB), Universitair Ziekenhuis Brussel (UZ), Brussels, Belgium

OPEN ACCESS

Edited by:
Daniela Trisciuoglio,
Italian National Research Council, Italy

Reviewed by:
Nicola Amodio,
Magna Græcia University, Italy
Barbara Illi,
Italian National Research Council, Italy
Maciej Tarnowski,
Pomeranian Medical University, Poland

***Correspondence:**
Ken Maes
Ken.Maes@vub.be
Philip Vlummens
Philip.Vlummens@vub.be

Specialty section:
This article was submitted to Epigenomics and Epigenetics, a section of the journal Frontiers in Cell and Developmental Biology

Received: 18 February 2022
Accepted: 06 May 2022
Published: 08 June 2022

Citation:
Vlummens P, Verhulst S, De Veirman K, Maes A, Menu E, Moreaux J, De Boussac H, Robert N, De Bruyne E, Hose D, Offner F, Vanderkerken K and Maes K (2022) Inhibition of the Protein Arginine Methyltransferase PRMT5 in High-Risk Multiple Myeloma as a Novel Treatment Approach. Front. Cell Dev. Biol. 10:879057. doi: 10.3389/fcell.2022.879057

Multiple myeloma (MM) is an incurable clonal plasma cell malignancy. Subsets of patients have high-risk features linked with dismal outcome. Therefore, the need for effective therapeutic options remains high. Here, we used bio-informatic tools to identify novel targets involved in DNA repair and epigenetics and which are associated with high-risk myeloma. The prognostic significance of the target genes was analyzed using publicly available gene expression data of MM patients (TT2/3 and HM cohorts). Hence, protein arginine methyltransferase 5 (PRMT5) was identified as a promising target. Druggability was assessed in OPM2, JJN3, AMO1 and XG7 human myeloma cell lines using the PRMT5-inhibitor EPZ015938. EPZ015938 strongly reduced the total symmetric-dimethyl arginine levels in all cell lines and lead to decreased cellular growth, supported by cell line dependent changes in cell cycle distribution. At later time points, apoptosis occurred, as evidenced by increased AnnexinV-positivity and cleavage of PARP and caspases. Transcriptome analysis revealed a role for PRMT5 in regulating alternative splicing, nonsense-mediated decay, DNA repair and PI3K/mTOR-signaling, irrespective of the cell line type. PRMT5 inhibition reduced the expression of upstream DNA repair kinases ATM and ATR, which may in part explain our observation that EPZ015938 and the DNA-alkylating agent, melphalan, have combinatory effects. Of interest, using a low-dose of mTOR-inhibitor, we observed that cell viability was partially rescued from the effects of EPZ015938, indicating a role for mTOR-related pathways in the anti-myeloma activity of EPZ015938. Moreover, PRMT5 was shown to be involved in splicing regulation of MMSET and SLAMF7, known genes of importance in MM disease. As such, we broaden the understanding of the exact role of PRMT5 in MM disease and further underline its use as a possible therapeutic target.

Keywords: myeloma, PRMT5, DNA repair, RNA splicing, epigenetics

INTRODUCTION

Multiple myeloma (MM) is a clonal B-cell malignancy characterized by the proliferation of malignant plasma cells in the bone marrow. The disease is characterized by marked complexity of genomic defects, which is believed to trigger the progression from monoclonal gammopathy of undetermined significance (MGUS), a pre-malignant stage, towards florid MM disease (Joseph et al., 2017; Binder et al., 2019). Moreover, high-risk genomic defects can already be seen in clonal plasma cells in the MGUS stage, thus leading to high-risk disease even at the MGUS and smoldering MM (SMM) stage (Keuhl and Bersagel, 2012; Hajek et al., 2013). In recent years, emerging evidence has shown that epigenetic alterations are involved in MM pathogenesis and disease progression. Moreover, targeting of several epigenetic modifiers such as DNA methyl transferases and histone deacetylases has shown to be able to exhibit anti-MM effects (Caprio et al., 2020). As relapse in high-risk patients cannot be avoided with current treatment options, despite availability of novel agents and monoclonal antibodies, additional treatment strategies that focus on novel targets are needed. Therefore, a deeper understanding of MM disease biology focusing on epigenetic targets is of high value because this can lead to novel therapeutic options.

One important mechanism of epigenetic and post-translational modifications in cancer cells is arginine methylation (Gulla et al., 2018). As such, it was identified that protein methyltransferases (PRMT) play a role in the modulation of gene transcription and protein function and play critical roles in regulatory pathways leading to cancer development and therapy resistance (Kim and Ronai, 2020). One of these is PRMT5, a type II PRMT enzyme which has been shown to play a role in tumour development and progression in solid cancer (Tan et al., 2020; Banasavadi-Siddegowda, 2017). PRMT5 is involved in lymphomagenesis through the inhibition of p53-dependant tumour suppression in response to oncogenic events (Li et al., 2015). It was also shown that MYC directly upregulates the transcription of the core small nuclear ribonucleoprotein particle assembly genes, including PRMT5, regulating splicing machinery with an essential role in lymphomagenesis (Koh et al., 2015). Moreover, its role in MM pathogenesis has been reported by Gulla et al. (Gulla et al., 2018). They showed that PRMT5 has a prognostic role in MM patients and that it is implicated in NF-kB signaling in MM cells.

Here, we report the independent identification of PRMT5 using large public datasets and further elucidate the role in MM disease, focusing on pathophysiology and therapeutic implications. In detail, we implicate PRMT5 as an important driving force in MM cell signaling, showing its involvement in DNA damage repair, mTOR signaling and mRNA splicing.

MATERIALS AND METHODS

Bioinformatical Analysis and PRMT5 Identification

Publicly available data sets were used to evaluate the prognostic significance of 457 selected genes, known to be involved in epigenetic regulation. The University of Arkansas for Medical Sciences (UAMS) cohort consists of 345 MM patients treated with thalidomide versus placebo combined with 4 cycles of chemotherapy (Total Therapy 2/3 protocol or TT2/3). Data can be accessed through the Gene Expression Omnibus, accession number GSE2658. (Zhan et al., 2007; Barlogie et al., 2006). Normalised gene expression data was used for further analysis and coupled with patient survival data when available. The second dataset used for identification was the Heidelberg-Montpellier cohort, an independent MM patient cohort consisting of 206 patients for whom complete survival data was available. This cohort also includes 7 bone marrow plasma cell (BMPC) samples from healthy donors, which were not used in our analysis. These data are publicly available through ArrayExpress database (E-MTAB-372) (Hose et al., 2009; Hose et al., 2011). Subsequent validation of withheld candidate genes was performed in 2 independent cohorts. The GMMG-HD4/HOVON-65 cohort consists of gene expression data of 320 newly diagnosed MM patients for which survival data is available (Broyl et al., 2010). The Mulligan patient cohort, consisting of 264 bone marrow aspirate samples of patients with relapsed multiple myeloma, treated with dexamethasone versus bortezomib, was used for validation (GEO accession number GSE9782) (Mulligan et al., 2007; Weinhold et al., 2016). PRMT5 was selected out of the prognostic gene list because of the potential druggability and unexplored mode of action. Validation of PRMT5 as a candidate gene was performed using the Relating Clinical Outcomes in MM to Personal Assessment of Genetic Profile (CoMMpass) trial release IA14, launched by the MMRF. Normalized FPKM gene expression values, generated using RNA-sequencing, were downloaded alongside clinical data through the MMRF research portal (https://research.themmrf.org). Collected baseline data included the presence of chromosomal abnormalities and patient survival data. Gene expression levels were correlated with patient survival data using the MaxStat R package as previously described, as such analysing the prognostic value of the genes of interest.

Cell Lines and Cell Culture

Human MM cell lines (HMCLs) OPM2, JJN3 and AMO1 obtained from ATCC (Molsheim, France). The XG7 HMCL was kindly provided by Jérôme Moreaux (University of Montpellier) (Moreaux et al., 2011; Vikova et al., 2019). JJN3 have a del17p with deletion of one p53 locus whereas OPM2 cells harbour a p53 mutation (Moreaux et al., 2011). Cells were cultured in RMPI1640 medium (Lonza, Basel, Switzerland) supplemented with 10% fetal bovine serum (FBS) (Hycone, Logan, United States), 2 mM L-glutamin and 1% penicillin/streptomycin (Thermo Fisher Scientific, Waltham, United States) at 37°C in a 5% CO_2 enriched atmosphere. As the XG7 cell line is interleukin 6 (IL6) dependent, recombinant IL6 (R&D Systems, Minneapolis, United States) was added at a concentration of 2 ng/ml for this cell line specifically. All HMCLs were regularly tested for *mycoplasma* contamination and checked for authenticity by STR profiling.

Treatment Schedules

PRMT5 inhibition was performed by culturing HMCLs (0.1 × 10^6 cells/ml) with or without EPZ015938 (Selleckchem, Munich,

Germany) at a concentration of 5 or 10 μM. DMSO at a concentration of 1 % was added to the control sample. Refreshing the cells: cells were gently harvested, counted and replated at the initial cellular concentration (0.1×10^6 cells/ml) on day 3 and 6 by in fresh mediumto which either DMSO or EPZ015937 was added. Cells were collected at indicated timepoints for subsequent analysis. Combination experiments were performed with melphalan (Selleckchem, Munich, Germany) and the mTOR-inhibitor KU-0063794 (Selleckchem, Munich, Germany). For combination experiments with melphalan, HMCLs were exposed to EPZ015938 for 3 days (OPM2, AMO1, JJN3) or 1 day (XG7) prior to adding melphalan at different concentrations (5 or 10 μM) for two additional days. Combination experiments with KU-0063794 were performed by exposing HMCLs to EPZ015938, KU-0063794 or the combination for 6 days (OPM2, AMO1, JJN3) or 4 days (XG-7). Concentration of the mTOR-inhibitor (0.5 up to 10 μM) and time of analysis (day 4 or 6) was determined according to basal HMCL susceptibility to the drug.

Treatment of Primary MM Cells

Bone marrow of MM patients (n = 7) was obtained at the university hospital of Montpellier after patients' written informed consent in accordance with the Declaration of Helsinki and agreement of the Montpellier University Hospital Centre for Biological Resources (DC-2008-417). Mononuclear cells (MMC) were treated with or without EPZ015938 (2 μM) and MMC cytotoxicity was evaluated using an anti-CD138-phycoerythrin monoclonal antibody (Immunotech, Marseille, France) as described previously (De Boussac H et al., 2020).

Growth Assessment, Apoptosis Assay and Cell Cycle Analysis

Cell growth was assessed on day 3 by manual trypan blue counting. Viability and apoptosis were assessed at predefined timepoints. Briefly, cells were analysed using AnnexinV/FITC-staining (BD Biosciences, Belgium) and 7-AAD staining (BD Biosciences) by flow cytometry on a BD FACSCanto Clinical Flow Cytometry System using the manufacturer's instructions. Cell cycle analysis was performed on day 3 or 4 of treatment according to cell line type. Cells were stained for 5 min with a PI solution containing 1 mg/ml sodium nitrate (Merck, Darmstadt, Germany), 0.1% Triton-X (Merck), 100 μg/ml RNase A (Boehringer, Ingelheim, Germany) and 50 μg/ml PI (Sigma-Aldrich, Overijse, Belgium). Analysis was subsequently performed using flow cytometry (BD FACSCanto Clinical Flow Cytometry System).

Western Blot Analysis

Cells were harvested and lysed prior to western blotting as previously described (De Bruyne et al., 2010). Analysis was performed using chemiluminescent detection using Li-Cor Odyssey Fc (Li-Cor Biosciences, Lincoln, United States). Antibodies used were targeted against PRMT5 (#79998), SDMA (#13222), Beta-actin (#4967), caspase-9 (#9502), caspase-3 (#9662), PARP (#9542), p-Ser15-p53 (#9286), p53 (#9282), p27 (#3688), p21 (#2974), ATM (#2873), p-ATM (#4526), FANCA (#14657S), ATR (#2792), p-ATR (#2853), tubulin (#2144), p-AMPK (#2535), AMPK (#5831), p-4EBP1 (#2855), 4EBP1 (#9644), MMSET (#65127), HELLS (#7998) and SLAM7 (#98611). HRP-linked anti-mouse IgG (#7076S) and anti-rabbit IgG (7074S) were used for primary antibody detection. Antibodies were purchased from Cell Signaling Technology (Leiden, the Netherlands). Densitometric analysis of western blot data was perfomed using Image Studio (Li-Cor Biosciences).

Immunofluorescent Staining and Microscopy

Cells were plated as described above. After 3 days, cytospins were made and stored at -20°C. Cytospins were subsequently stained for gamma-H2AX as previously described (Maes et al., 2014). Immunofluorescence was observed using a Nikon Eclipse 90i with a ×40 objective magnification and ×10 ocular magnification. Pictures were taken using a Nikon DS-Ri1.

RNA Sequencing and Bioinformatical Analysis

Selected HMCLs were cultured for 3 days with either EPZ015938 or placebo (DMSO). RNA was extracted as previously described (Vikova et al., 2019). Sample quality was checked by calculating the RNA integrity number (RIN value). RNA-seq library preparation was done with 150 ng of input RNA using the Illumina TrueSeq Stranded mRNA Library Prep Kit (Illumina, Cambridge, UK). Paired-end RNA-seq was performed on an Illumina sequencing instrument (Helexio, Clermond-Ferrand, France). Read pairs were mapped to the human reference genome (version GRCh38) using the STAR alignment algorithm. Differential expression analysis was performed using the R/BioconductorDESeq2 package with p-value adjustment for multiple comparisons using the default option (Love et al., 2014). Genes were considered differentially expressed when having a p-value ≤ 0.05 and a fold change of 1.5 in either direction. Intron retention analysis was performed using the R/Bioconductor IRFinder package according to the package vignette (Middleton et al., 2017). Geneset annotation and pathway enrichment analysis were performed using the R/Bioconductor ReactomePA package (Yu and He, 2016). PCA analysis was performed using R/Bioconductor Rtsne package (van der Maaten and Hinton, 2008).

qPCR Analysis

Total RNA was extracted using the Nucleospin RNA plus kit (Macherey-Nagel, Düren, Germany), including gDNA removal. Reverse transcription was performed using the Verso cDNA synthesis kit (ThermoFisher Scientific, Gent, Belgium), both according to manufacturer's instructions. Quantitative real-time PCR was performed as previously described (Oudaert et al., 2022). Primers were purchased from IDT (Leuven, Belgium). Primers were designed to target the intronic region of the gene of interest. Sequences are shown in **Supplementary Figure S13**.

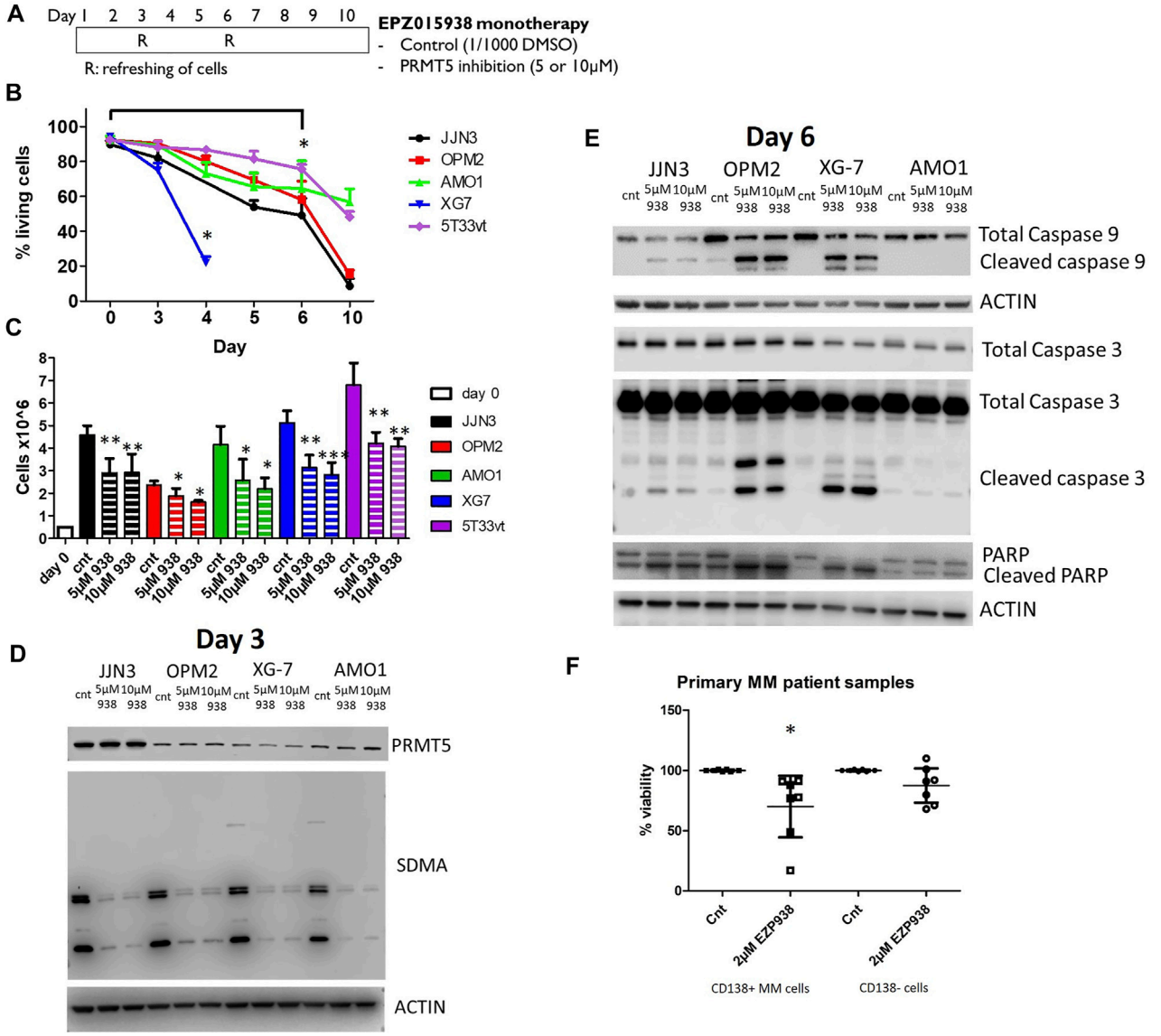

FIGURE 1 | (A): Schematic representation of EPZ01938 therapy in HMCLs. Cells were incubated with either compound or DMSO as placebo. Cells were refreshed at predetermined intervals. At timepoints R cells were gently harvested, counted and replated at the initial cellular concentration (0.1 × 106 cells/ml) on day 3 and 6 by in fresh medium to which either DMSO or EPZ015938 was added. **(B)**: Viability assay of HMCLs upon treatment with EPZ015938. Viability was assessed by trypane blue staining at depicted timepoints for the selected HMCLs. Treated samples were compared against control samples. Error bars depict mean values ± SD; * denotes $p < 0.05$ ($n > 3$) **(C)**: Cumulative cell counts of living cells for each HMCL when cultured with or without 5 and 10 μM EPZ015938 after 3 days of treatment. Treated samples were compared against control samples. Error bars depict mean values ± SD; */**/*** denotes $p < 0.05$, $p < 0.01$ and $p < 0.001$ respectively ($n > 3$) **(D)**: Western blot staining for PRMT5 and SDMA protein levels was performed after 3 days of EPZ015938 treatment on JJN3, OPM2, XG7 and AMO1 cells. Actin was used as a loading control. One experiment representative of 3 experiments performed is shown ($n = 3$). **(E)**: Western blot of pro-apoptotic proteins caspase 9, 3 and PARP after 3 days of treatment with EOZ015938. Actin was added as loading control. One representative experiment is shown ($n = 3$). **(F)**: Effect of PRMT5 inhibitor treatment on primary human CD138 + MM cells and CD138- microenvironment. Mononuclear cells from 7 MM patients were treated with the indicated concentration for 4 days, and the percentage of viable CD138 + plasma cells and CD138- cells were determined by flow cytometry. Results are expressed as the relative viability compared with control. * denotes $p < 0.05$ compared to control cells.

Statistical analysis

Prognostic significance of gene expression levels was calculated as indicated above. Overall survival (OS) is defined as the time from trial inclusion until death from any cause or until the time point the patient was last known to be alive. In the latter case patients were censored. Progression free survival (PFS) delineates the time from treatment initiation until relapse or death from any cause. Statistical analysis was performed using the IBM SPSS software package, v. 26 (Chicago, IL, United States). Survival curve estimates were generated using the Kaplan-Meier method and statistical significance was calculated using the log-rank test. Statistical significance was determined using a Mann-Whitney

(two conditions) or one –way ANOVA with Bonferroni's multiple comparison test for selected pairs paired T-test (multiple conditions). Correlation coefficients of RNAseq data were calculated by using the Pearson method. Reported *p*-values are 2-sided and a conventional significance level of 5% was used. Combination index (CI) values were calculated for the EPZ015938—melphalan combination experiments by the Chou and Thalalay method using CompuSyn 1.0 software.

RESULTS

Bioinformatical Analysis Identifies PRMT5 as a Gene Linked to Poor Prognosis Gene in MM

A total of 457 candidate genes, involved in epigenetic regulation and DNA-repair, were identified for further analysis (**Supplementary Table S1**). MaxStat analysis was performed in both the TT2/3 and HM patient cohorts thus generating a list of genes being prognostic in both cohorts internally (Hothorn and Lausen, 2003). Using this approach, a common set of 45 poor and 17 good prognostic genes were identified (**Supplementary Table S1**). To exclude the effect of known prognostic drivers in MM, WHSC1 was excluded from this analysis (data not shown). Performing unsupervised hierarchical clustering of the TT2/3 and HM cohort using these common genes lead to a clear delineation of a high-risk MM population. A clear increase in hazard rate was seen in both cohorts; HR = 2.86 with $p = 0.0017$ in the HM and HR 2.22 with $p = 0.0032$ in the MMRF cohort (**Supplementary Figure S1**). Subsequent analysis of the HOVON and Mulligan cohort revealed similar OS results, as a HR = 2.5 with $p < 0.0001$ and HR = 2.04 with $p = 0.0025$ was seen respectively (**Supplementary Figure S2**). Lastly, our signature retained its prognostic value in an RNA-seq based cohort (MMRF), both at the level of PFS (HR = 2.13, p-value < 0.0001) and OS (HR = 2.92, $p < 0.0001$) (**Supplementary Figure S3**). From the 45 candidate genes, we chose PRMT5 for which the biological function is partially known, and clinical grade inhibitors are available for further study (**Supplementary Figure S4**).

PRMT5 Inhibition in HMCLs Leads to Decreased Cellular Growth and Increased Apoptosis

We inhibited PRMT5 function in 4 HMCLs using the EPZ015938 compound. EPZ015938 is an orally active and selective inhibitor of PRMT5 which is currently also being used in clinical trials (clinicaltrials.gov, accessed 04-Apr-22). Cells were exposed to different concentrations of EPZ015938 for up to 10 days according to the refreshment scheme (**Figure 1A**). A clear decrease ($p < 0.05$) in cell viability could be seen using Annexin-V/7AAD staining, with XG-7 cells being the most susceptible to EPZ015938 induced apoptosis with a significant decrease in cellular viability becoming apparent at day 4. In other HMCLs, a similar effect was observed after 6 days of treatment. AMO1 cells were shown to be the most resistant to effects of PRMT5 inhibition (**Figure 1B**). Moreover, significantly ($p < 0.05$) decreased cellular growth was observed in all cell lines from day 3 (**Figure 1C**). To further evaluate this observation, cell cycle analysis was performed. A cell line dependent effect on cell cycle could be seen (**Supplementary Figure S5A**). In both JJN3 and OPM2 cells, an increase in G2 was observed, while in AMO1 an increase in G1 could be seen. Both AMO1 and OPM2 cells showed decrease cell numbers in S-phase was seen alongside an increase of cells in the G2-phase. In XG-7 cells a significant increase in sub-G1 was observed, because of increased cell death already visible at this time point. On a protein level, an increase in both phosphorylated and unphosphorylated p53 levels were seen in all but JJN3 cells, which have a known bi-allelic deletion of the p53 gene. Only a slight increase could be seen in AMO1 cells. Effects on p21 and p27, G1-checkpoint cyclin-dependant kinase inhibitors involved in p53-mediated apoptosis differed between cell lines as a decrease in p21 levels was observed in JJN3 and OPM2 cells whereas an increase was observed in XG7 and AMO1 cells. p27 levels showed a relative increase after PRMT5 inhibition in AMO1 cells but not in the other HMCLs studied (**Supplementary Figure S5B**). We also evaluated the effect of EPZ015938 treatment on global symmetrical di-methylated arginine (SDMA) residues as well as PRMT5 protein levels to ensure inhibitor target function and exclude autoregulation of PRMT5. Western blotting of cell lysates showed a decrease in SDMA levels, suggestive of on target effects of EPZ015938, alongside unaltered PRMT5 levels (**Figure 1D**). The presence of apoptosis, in view of prior observations of the effect of PMRT5 inhibition on cellular survival, was also confirmed on the protein level as an activation of the pro-apoptotic proteins caspase 3, caspase 9 and PARP could be objectified (**Figure 1E**). The least activation could be seen in AMO1 cells, which corroborates with the observation of lowered sensitivity to EPZ015938. Treatment of primary human MM samples (n = 7, clinical data **Supplementary Table S1**) showed a similar variability in response upon exposure to EPZ015938 but a significant decrease in MM cell viability could also be observed (**Figure 1F**). Additionally, no significant effect was observed on the CD138- negative cellular fraction from the bone marrow microenvironment (**Figure 1F**).

RNA-Sequencing Identifies PRMT5 as a Modulator of DNA Repair, mTOR Signaling and Alternative Splicing in MM

To molecularly assess the impact of PRTM5 inhibition, we performed RNA-seq on OPM2, JJN3 and XG7 cells with and without the addition of EPZ015938 ($n = 2$ for each condition). Primary analysis of sequencing data confirmed an influence of HMCL type on normalized counts (**Supplementary Figure S5**). DESeq2 analysis per cell line was used to identify differentially expressed genes (**Supplementary Table S2**). A common set of 20 up- and 222 downregulated genes could be identified alongside HMCL specific gene sets (**Figures 2A,B**; **Supplementary Table S2**). To identify common pathways where PRMT5 is involved, further analysis was performed on the common gene set only. Reactome gene set enrichment revealed that EPZ015938 treatment influenced mRNA splicing pathways, mTOR signalling and DNA repair mechanisms in all 3 HMCLs

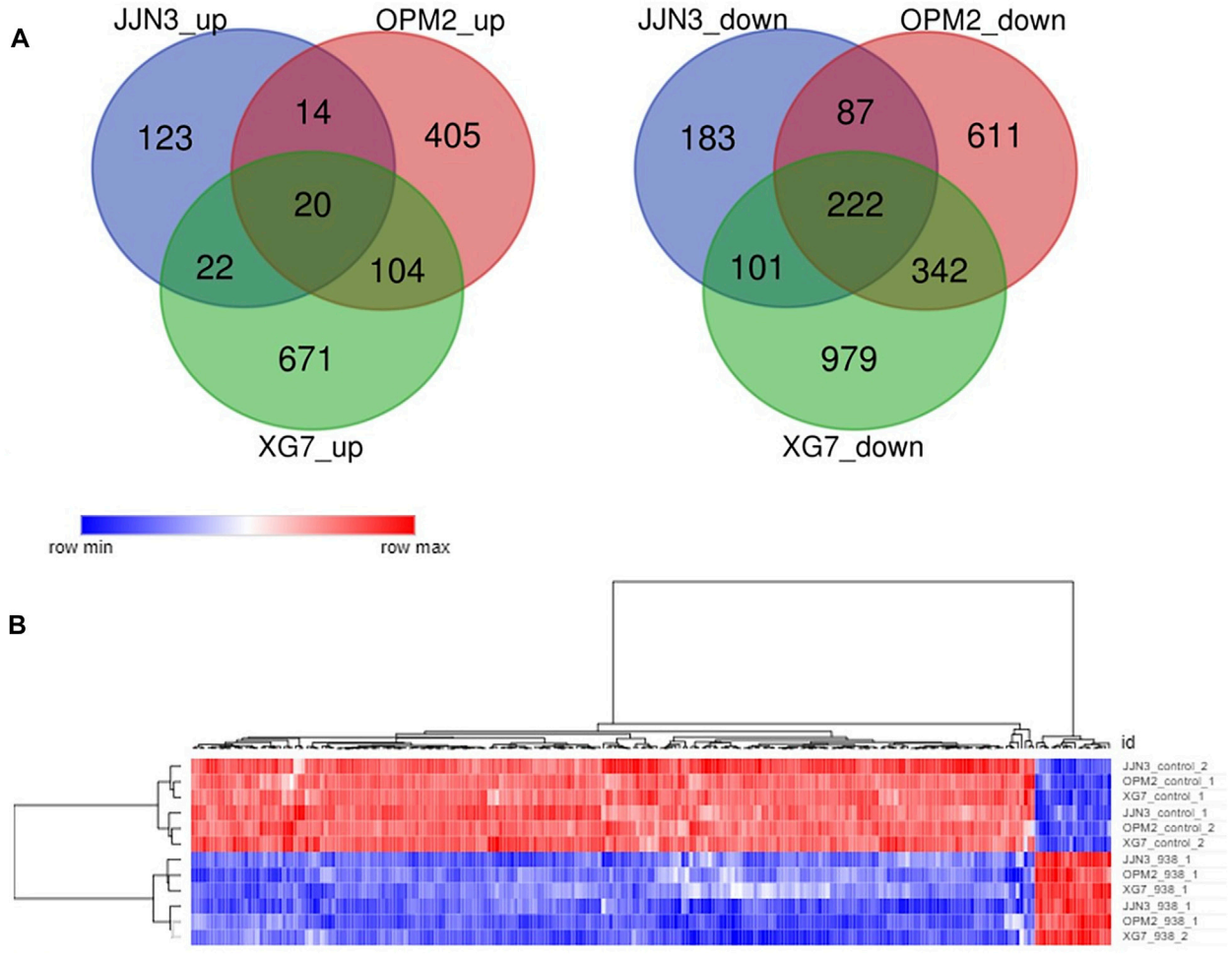

C

Reactome pathways	Fold	P-value
mRNA splicing	26,34	1,45E-05
mRNA decay	22,1	4,50E-02
Metabolism of RNA	11,25	8,99E-06
mTOR signaling	5,84	4,94E-02
Homology Directed Repair	3,85	1,12E-02
Nucleotide Excision Repair	2,74	2,74E-02

FIGURE 2 | (A): Deregulated genes after PRMT5 inhibition were identified using RNA-seq and analysed for JJN3, OPM2 and XG7 cells separately due to possible cell type specific events. Venn diagram analysis shows the presence of a specific set of common up- (left) or downregulated (right) genes per cell line type ($n = 2 \times 2$ per cell type/treatment). **(B)**: Unsupervised clustering of analysed samples used for RNA-seq based on common deregulated genes ($n = 242$), clearly segregating according to treatment type. **(C)**: Overview of reactome pathway analysis output (selected pathways are shown) with fold changes and *p*-values per pathway, after multiple testing correction.

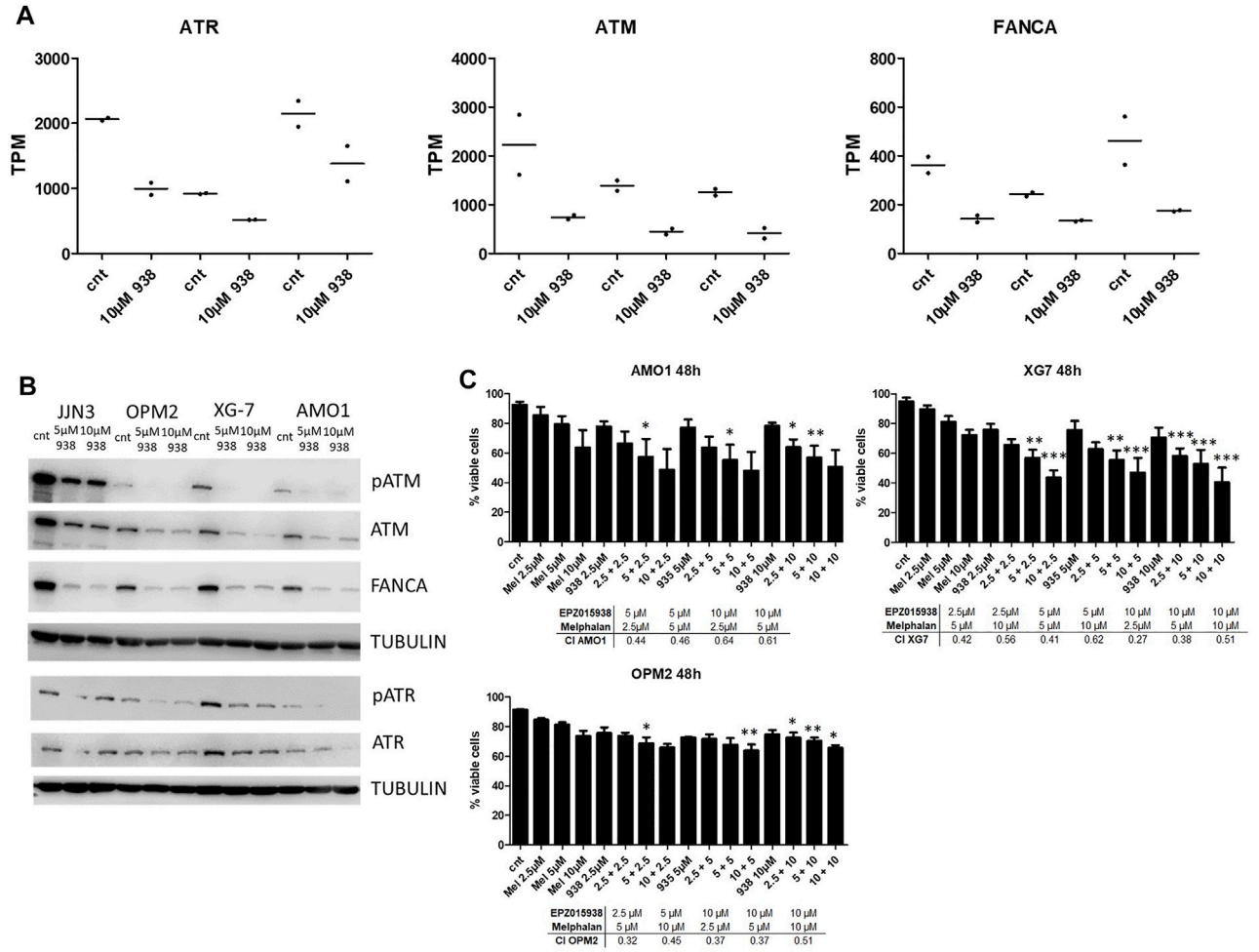

FIGURE 3 | (A): TPM values for ATR, ATM and FANCA for both control and EPZ015938 cells, showing decrease in transcript abundancy following PRMT5 inhibition in all 3 cell lines studied ($n = 2$ for each cell line and condition, no error bars are shown). **(B)**: Western blot analysis was performed on JJN3, OPM2, XG7 and AMO1 cell lysates to evaluate ATM/ATR and FANCA protein levels upon PRMT5 inhibition for 3 consecutive days. Tubulin was used as a loading control. One experiment representative of 3 experiments performed is shown ($n = 3$). **(C)**: Viability assay using Annexin/7AAD-staining of HMCLs after treatment with EPZ015938, melphalan or combination therapy at depicted concentrations. Samples were analysed using an ANOVA selected pairs test. to evaluate differences between different treatment settings and against control samples and samples treated with only EPZ015938 or melphalan. Error bars represent mean +SD; */**/*** denotes $p < 0.05$, $p < 0.01$ and $p < 0.001$ respectively ($n = 3$). Synergy was evaluated for between both compounds by calculation of the combination index (CI) for significant combinations, with a CI < 1 showing a synergistic effect.

(**Figure 2C**). We subsequently selected these pathways for further functional investigation.

PRMT5 Inhibition Modulates DNA Repair Mechanisms in MM and Leads to Increased Cell Death When Combined With Melphalan

To further evaluate the impact of EPZ01598 treatment on DNA repair pathways on a protein level, we performed western blotting for the cell cycle checkpoint kinase Ataxia Telangiectasia Mutated (ATM), the DNA damage sensor ATR Ataxia Telangiectasia And Rad3-Related Protein (ATR) and Fanconi Anemia complementary group A (FANCA) known to play roles in DNA damage repair and shown to be affected by PRMT5 inhibition at the RNA-level (**Figure 3A**). As such, we saw a decrease of these targets upon PRMT5 inhibition (**Figure 3B**, **Supplementary Figure S7**). This result could indicate that HR/FA repair pathways functionality is decreased upon PRMT5 inhibition. In agreement, an increase in gamma-H2AX foci, a biomarker for DNA double strand breaks, was seen upon EPZ015938 treatment (**Supplementary Figure S8**). Moreover, PRMT5 expression levels were also shown to be significantly correlated with genes involved in HR/FA in MM patients, further strengthening the suggestion that there is cross-talk between PRMT5 function, expression of HR/FA-related genes and DNA damage occurrence (**Supplementary Figure S9**). We subsequently treated HMCLs with both EPZ015938 and melphalan, an alkylating standard of care agent in MM, to evaluate any potential combinatory effect. We established a sub-lethal dose of melphalan per HMCL prior to combination

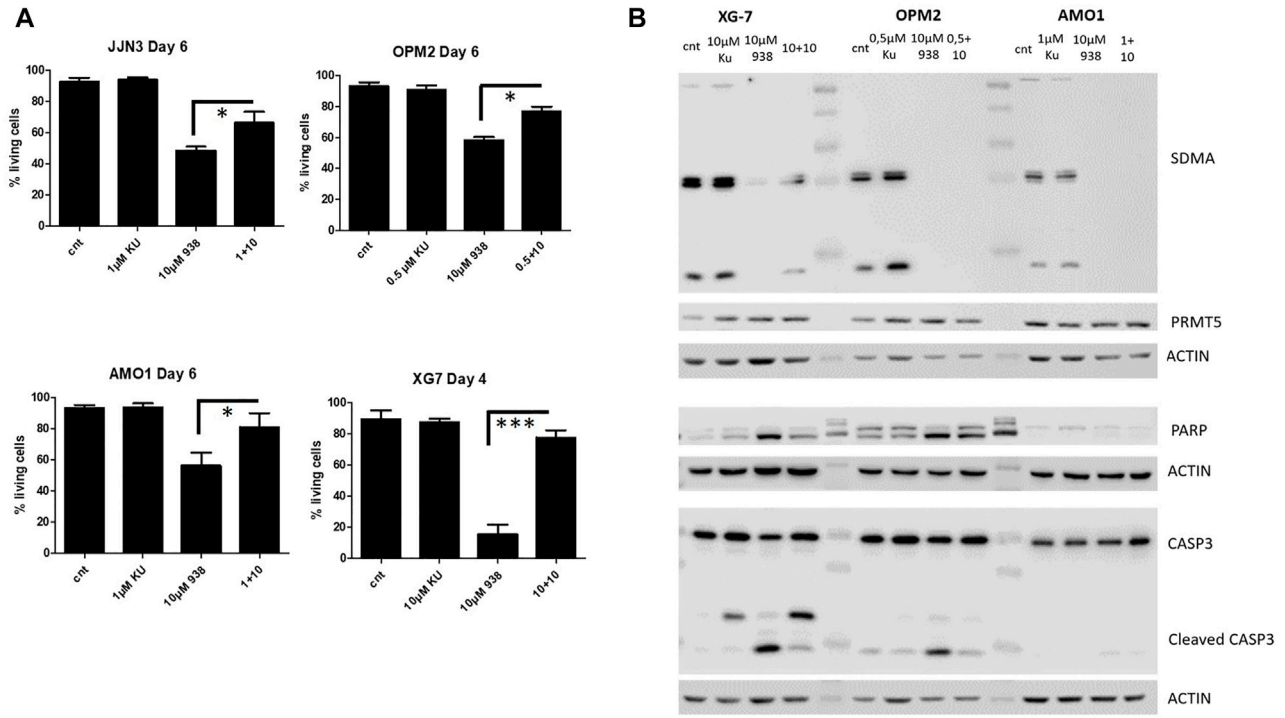

FIGURE 4 | (A): Viability assay of HMCls upon treatment of JJN3, OPM2, AMO1 and XG7 cells with EPZ015938, KU-0063794 or combination therapy after predefined timepoints. Cellular viability was assessed using AnnexinV/7AAD staining. Samples were analysed using an T—test with selected pairs test, significance was evaluated between different treatment settings and compared to control. Error bars depict mean ± SD; */**/*** denotes $p < 0.05$, $p < 0.01$ and $p < 0.001$ respectively ($n = 3$). **(B)**: Western blot analysis of SDMA levels, global PRMT5 levels and pro-apoptotic proteins caspase 9, 3 and PARP in XG7, OPM2 and AMO1 cells. Cells were treated with EPZ015938, KU-0063794 or combination therapy. Control samples were included for comparison. Actin was used as a loading control. One experiment representative of 3 experiments performed is shown ($n = 3$).

experiments (data not shown), after which cells were cultured according to methods described above. Using this approach, a statistically significant effect of combination therapy on HMCL survival could be seen in all cell lines used. Cells treated with both compounds had higher levels of cellular death upon AnnexinV/7AAD-staining when compared to control or both compounds in monotherapy. Also, the effect on cellular survival could be seen in HMCLs with a defective p53 state, suggesting the presence of regulatory effects that are irrespective of the genomic status of p53. Calculation of the combination index revealed a synergistic effect between EPZ015938 and melphalan (**Figure 3C**).

mTOR Signalling is Important for the Anti-Myeloma Effects of PRMT5 Inhibition in HMCLs

A similar approach was used to evaluate whether manipulation of mammalian target of rapamycin (mTOR) signalling, which has been known to play a role in B-cell malignancies, could impact cellular survival when combined with PRMT5 inhibition. We first determined sub-lethal doses of KU-0063794 for each cell line, ranging between 0.5 and 10 μM (data not shown). KU-0063794 reversed EPZ015938 anti-apoptotic effects, leading to diminished cellular toxicity when HMCLs were treated with a combination of both compounds (**Figure 4A**). We observed a decrease in SDMA levels and decreased caspase cleavage on WB, when cells where exposed to both mTOR- and PRMT5-inhibition. mTOR-inhibition thus leads to the decreased effect of PRMT5 inhibition in HMCL cells (**Figure 4B**). No significant different increase of PRMT5 on both the RNA or protein levels were seen upon treatment, (**Figure 4B**; **Supplementary Figures S10A,B**). Treatment of HMCLs with KU-0063794 alone or in combination with EP2015938 also leads to an increase in AMP-activated protein kinase (AMPK) phosphorylation in XG7 and OPM2 cells whereas monotherapy with EPZ015938 did not, further implicating the interplay between PRMT5 and mTOR/autophagy pathways (**Supplementary Figure S11**). During exploration of downstream effects, we observed that phosphorylation of 4EBP1 is seen upon treatment with KU-0063794, showing that this compound inhibited mTOR activity in MM cells. Moreover, this observation was also observed in the combination treatment. Effects were less marked in AMO1 cells, potentially due to a more intrinsic resistance (**Supplementary Figure S11**).

PRMT5 Inhibition Leads to Defective Splicing in HMCLs and Targets Known MM Pathways

We next assessed RNA metabolism and splicing. To evaluate the presence of intron retention, RNA-seq output data was re-

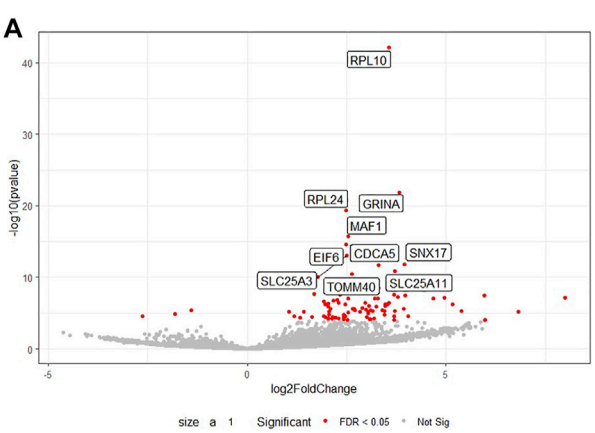

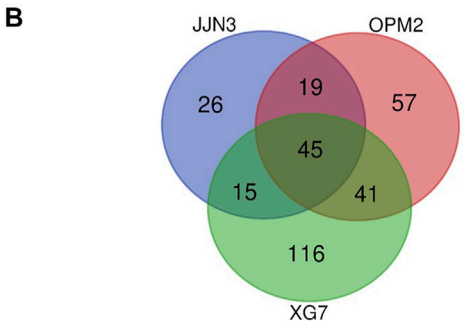

C

Pathway	p-value	FDR
Cap-dependent Translation Initiation	3.94E-07	4.17E-05
Nonsense Mediated Decay (NMD) independent of the Exon Junction Complex (EJC)	4.81E-06	3.25E-04
Chromatin organization	9.41E-03	1.03E-01
Regulation of Apoptosis	1.36E-02	1.03E-01
p53-Dependent G1 DNA Damage Response	2.67E-02	1.07E-01
G1/S DNA Damage Checkpoints	2.87E-02	1.15E-01
Mitophagy	3.30E-02	1.30E-01
mRNA Splicing	3.45E-02	1.30E-01

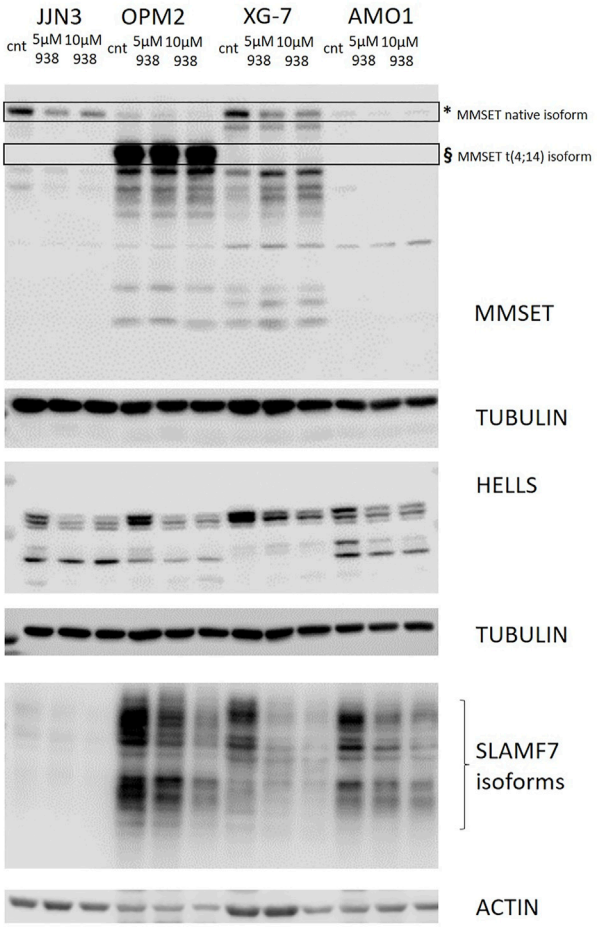

FIGURE 5 | (A): Intron retention due to PRMT5 inhibition was evaluated by re-analysis of RNA-seq data (as described earlier) using IRFinder (n = 2 for each condition and per cell line). Volcano plot shows IRFinder output in JJN3 cells, identifying different gene targets affected by intron retention. Only the plot for JJN3 is shown here, other plots are shown in the supplementary data. **(B)**: Venn diagram presentation of common genes affected by intron retention (n = 2 × 2 per HMCL/treatment condition). A set of 45 common affected genes were identified. Samples were analysed per cell line type to account for cell type specific effects. **(C)**: Reactome enrichment analysis was subsequently performed using the 45 common genes. Selected pathways that were deregulated are shown. **(D)**: Western blot analysis of identified targets MMSET/WHSC1 HELLS and SLAMF7 in JJN3, OPM2, XG7 and AMO1 cells. For MMSET, * depicts the wild type MMSET isoform where § depicts the aberrant MMSET protein affected by t (4; 14), which is present in OPM2 cells. Tubulin and actin were used as loading control. One experiment representative of 3 experiments performed is shown (n = 3).

analysed using IRFinder. Aberrant RNA transcripts could indeed be identified in OPM2, JJN3 and XG-7 cells (**Figures 5A–C**, **Supplementary Figure S12**, **Supplementary Table S3**). When comparing the sets of affected transcripts, a total set of 45 affected genes were shown to be shared between all 3 cell lines studied. Of note, 3 genes of interest were identified as having intron retention in both OPM2 and XG7 cells: 1) HELLS, encoding a lymphoid-specific helicase involved in chromatin remodelling, 2) SLAMF7, encoding the CD319 surface antigen which is targeted by the anti-MM drug elotuzumab and 3) WHSC1/MMSET, involved in the chromosomal translocation t (4; 14). HELLS was also part of our initial high-risk gene signature (**Supplementary Table S1**). Validation of IRFinder results were performed for HELLS, WHSC1 and SLAMF7. As such, we were able to confirm enrichment for gene transcripts with intron retention for WHSC1 in OPM2 and XG7 cells and for SLAMF7 in OPM2, AMO1 and XG7 cells. A statistical non-significant trend towards upregulation of WHSC1 transcripts was seen in AMO1 cells. Significant intron retention of HELLS gene transcripts was only seen in XG7 cells (**Supplementary Figure S13**). As intron retention can activate the process of nonsense-mediated decay of RNA transcripts, we evaluated the presence of these proteins, with and without EPZ015938 treatment, showing a decrease in expression levels upon PRMT5 inhibition (**Figure 5D**). MMSET/WHSC1 levels were less affected in OPM2 cells, which could be due to the presence of the t (4; 14) translocation in these cells. The

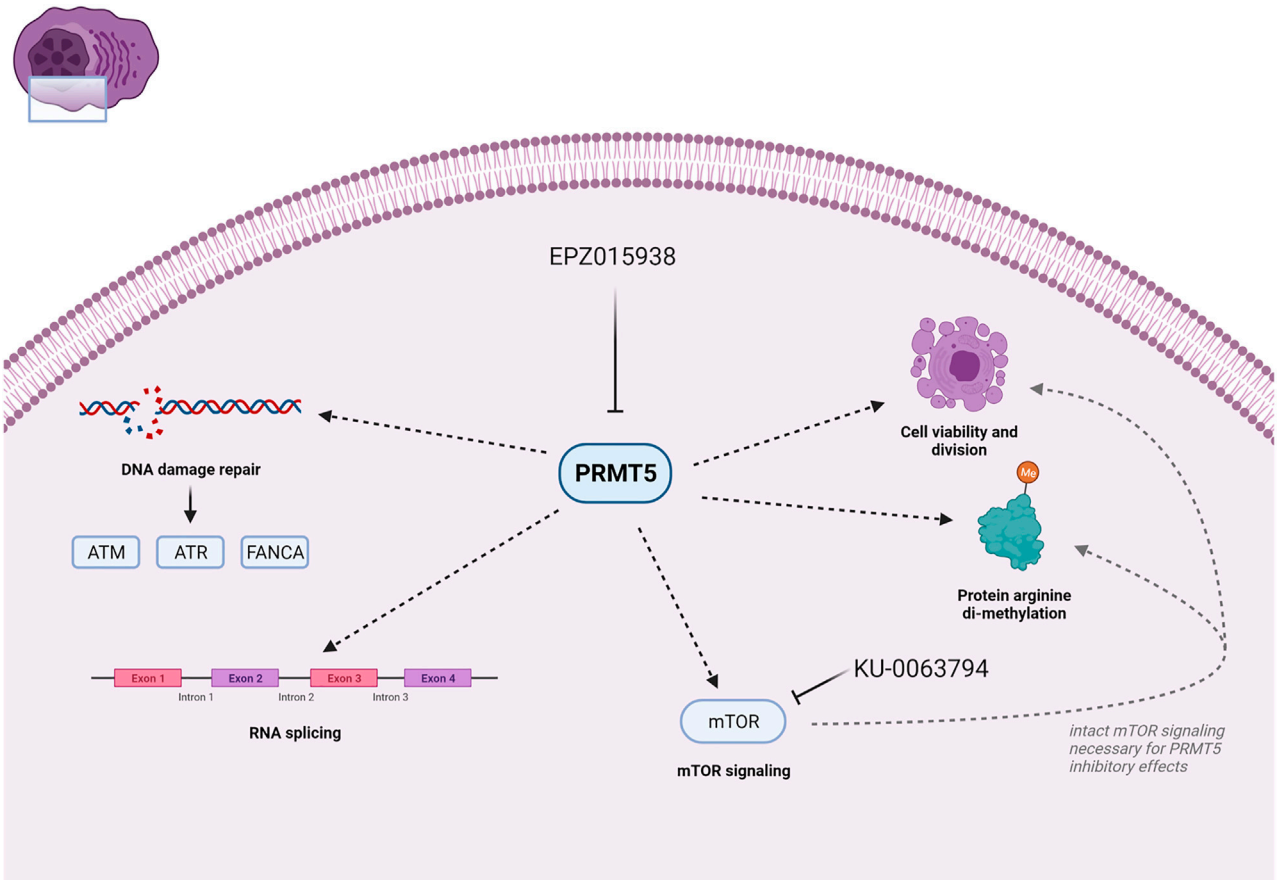

FIGURE 6 | Schematic representation of PRMT5 function and effects upon treatment as evaluated in this study. PRMT5 inhibition by using i.e., EPZ015938 leads to decreased DNA damage repair through a decrease in ATM/ATR and FANCA transcript and protein levels. Moreover, the function of PRMT5 as a regulator of mRNA splicing also plays a role in MM cellular processes and survival. Lastly, our study shows that mTOR signalling is important for PRMT5 function and has effects on cell viability, division and overall arginine di-methylation. Created with BioRender.

native WHSC1 isoform was downregulated by PRMT5 inhibition, whereas an additional unaffected protein was observed in OPM2 cells (**Figure 5D**, * and §, respectively). These findings show that WHSC1 protein levels, in the presence of t (4; 14), are less susceptible to PRMT5 inhibition. This however also suggests a t (4; 14) independent mechanism by which PRMT5 inhibition exerts its function.

DISCUSSION

In our present study, we were able to confirm that PRMT5 gene expression is associated with adverse PFS and OS in MM patients. Using the PRMT5 inhibitor EPZ015938, we show PRMT5 inhibition to decrease MM cell growth rate, cell count, and increase apoptosis both in HMCLs and in primary human MM samples depicting different of the known molecular defects. Although prior research (Hamard et al., 2018) has identified PRMT5 as being a regulator of p53, we observed that PRMT5 acts in both a p53 dependent mechanism alongside p53 independent mechanisms, as HMCLs harbouring a p53 mutation or del (17p) also displayed increased levels of apoptosis despite the absence of augmented p53 activity. As such, PRMT5 inhibition is of interest in the treatment of MM patients independent of p53 status. Gulla et al. showed that p53 knockdown using shRNA in AMO1 cells could not abrogate the sensitivity to the PRMT5 inhibitor EPZ015666, whereas OPM2 cells, harbouring a gain-of-function mutation in the p53 gene, displayed a resistance to this inhibitor, we saw that EPZ015938 was able to overcome this resistance (Gulla et al., 2018). This difference could be explained by the improved efficacy of EPZ015938 when compared to EPZ015666, as shown by a biochemical IC50 of 6.2 ± 0.8 nmol/L for EPZ0159838 versus 22 ± 14 nmol/L for EPZ015666 (Vinet et al., 2019). Although PRMT5 inhibition has been shown to lead to a G1-arrest in solid cancers such as bladder urothelial cancer and glioblastoma (Banasavadi-Siddegowda et al., 2018; Tan et al., 2020), our data suggests that the mechanism of decreased cellular growth is more complex in MM: CCA profiles could not show G1-arrest in all HMCLS, as thus suggesting the presence of other pathways. NF-κB was already identified as playing a role in PRMT5 inhibition in MM (Gulla et al., 2018). We aimed to further unravel the role of PRMT5 in MM by performing transcriptome

analysis. We were able to identify PRMT5 function as being involved in DNA damage repair pathways, mTOR signalling and RNA metabolism. As the alkylator melphalan is a standard of care drug e.g., in autologous stem cell transplantation, we assessed whether melphalan activity could be enhanced by addition of EPZ015938. We found a potentiating effect of PRMT5 inhibition on melphalan treatment, irrespective of p53 status, and potentially caused by modulation of the ATM/ATR and FANCA pathways. As p53 −/− cells have been shown to lose sensitivity to melphalan and other classical chemotherapeutic regimens, this observation creates a rationale for evaluating the role of PRMT5 inhibitors in MM patients harbouring p53 defects (Drach et al., 1998; Munawar et al., 2019). The added benefit of PRMT5-inhibition during treatment with melphalan could as such provide evidence to explore whether pre-treatment of MM patients with a PRMT5 inhibitor prior to exposure to melphalan in a transplant setting would have an added benefit in patients with high-risk MM such as del (17p). Additional evidence for the clinical use of PRMT5 inhibitors has been generated by the results of the METEOR-1 trial, a phase 1 study showing safety and tolerability of the compound in patients with advanced solid tumours (Siu et al., 2019). Moreover, additional clinical trials are currently actively evaluating the clinical use of EPZ015938. Secondly, we observed deregulation of mTOR signalling by PRMT5 inhibition. The mTOR pathway is a critical pathway in cancer cell survival, proliferation and invasion and inhibition of mTOR activity has been shown to lead to decreased MM cell survival (Li et al., 2020). Interplay between mTOR and PRMT5 has already been identified in different cell types, including T-lymphocytes B-cell lymphoma and glioblastoma (Holmes et al., 2019; Webb et al., 2019; Zhu et al., 2019). We observed an opposite phenomenon in MM cells than previously described by Holmes et al. in glioblastoma, an aggressive type of brain malignancy (Holmes et al., 2019). Whereas they saw an increase in PRMT5 function upon mTOR inhibition, our data suggest that PRMT5 activity needs mTOR signalling to exert its function in MM. Secondly, no significant decrease in PRMT5 protein levels was observed upon treatment with an mTOR inhibitor in MM, whereas this was previously reported in T-cell expansion in a murine multiple sclerosis model (Webb et al., 2019). On the contrary, we observed a trend towards upregulation upon mTOR inhibition which is in line with the findings of Holmes et al. in both glioblastoma cell lines and primary patient material. Our observations thus suggest a different relationship between PRMT5 and mTOR signalling, and warrants caution when exploring the options of PRMT5 targeting in clinical practice. Also, the loss of PRMT5 function on EPZ015938 treatment upon mTOR inhibition provides evidence that mTOR pathway modulation could be responsible in part for the observed p53-independent effects on HMCL survival (Yan et al., 2021). A potential explanation in MM specifically could however be the functional effects of cereblon (CRBN) in MM cells and its effects on mTOR signalling. Previous research has shown that deficient CRBN function impacts protein synthesis through the AMPK-mTOR cascade (Lee et al., 2014). Moreover, CRBN is an important target in MM cells and interaction with AMPK has also been seen in HMCLs (Zhu et al., 2011; Zhu et al., 2013). As such, further research towards the interaction between PRMT5 and CRBN would be of special interest, as it is important to evaluate whether PRMT5 inhibition would negate the potential effects of immunomodulatory drugs such as thalidomide and lenalidomide or vice versa (Zhu et al., 2013). A further pathway of interest was the implication of PRMT5 in RNA metabolism and transcript splicing in MM cells. Although PRMT5 has been implicated in spliceosome regulation in other cancers, we provide evidence that intact PRMT5 function is also important for spliceosome function in MM (Rengasamy et al., 2017; Radzisheuskaya et al., 2019). *In silico* analysis was used to identify possible targets of interest of PMRT5 in MM. We saw PRMT5 to be involved in the correct splicing of MMSET/WHSC1, SLAMF7 and HELLS, thus possibly leading to decreased protein levels due to nonsense mediated decay. Subsequent qPCR analysis indeed showed that a significant enrichment of gene transcripts with intron retention were present for SLAMF7 and WHSC1. Aberrant HELLS transcripts were only seen to be enriched in XG7 cells. The presence of a statistically significant downregulation in AMO1 cells upon treatment could also suggest the presence of other mechanisms concerning this gene. 1) MMSET/WHSC1 is aberrantly expressed in MM cells harbouring the translocation t (4; 14) (Keats et al., 2005; Xie and Chng, 2014; Xie et al., 2019). Moreover, it is a high-risk disease marker (Keats et al., 2003; Shah et al., 2016). We observed decreased levels of MMSET protein in HMCLs upon PRMT5 inhibition. In OPM2 cells, a less clear decrease was seen for several isoforms. As these cells harbour the translocation t (4; 14), with marked MMSET overexpression under the IgH promotor in these cells, more discrete alterations at the protein level could however be obscured. 2) SLAMF7, was further assessed due to its implications for possible combination therapy with elotuzumab, a monoclonal antibody targeting SLAMF7 which is already used in MM patient care (Gentile et al., 2021). A decrease in the different isoforms of the SLAMF7 protein could be seen, aside from a marked HMCL specific expression pattern. 3) Lastly, our study identified HELLS, a gene encoding a lymphoid-specific helicase involved in chromatin remodelling, as being processed by PRMT5 during intron removal. It has an important function in B-cell maturation and germline mutations have been shown to cause a severe immunodeficiency syndrome (He et al., 2020). To conclude, we show that the role of PRMT5 in MM disease is much more complex as thought and involves the regulation of DNA damage repair and correct intron removal during gene transcription in MM cells. Moreover, intact mTOR signalling seems to be required for proper PRMT5 inhibitor effects (**Figure 6**). As such, it is important that PRMT5 is further validated as a potential therapeutic target in a preclinical setting.

DATA AVAILABILITY STATEMENT

The datasets presented in this study can be found in online repositories. The names of the repository/repositories and accession number(s) can be found below: https://www.ebi.ac.uk/arrayexpress/, E-MTAB-11489 https://www.ebi.ac.uk/arrayexpress/, E-MTAB-372 https://www.ncbi.nlm.nih.gov/geo/

, GSE2658 https://www.ncbi.nlm.nih.gov/geo/, GSE19784 https://www.ncbi.nlm.nih.gov/geo/, GSE9782.

ETHICS STATEMENT

The studies involving human participants were reviewed and approved by Montpellier University Hospital Centre for Biological Resources (DC-2008-417). The patients/participants provided their written informed consent to participate in this study.

AUTHOR CONTRIBUTIONS

PV and KM conceived the study. PV, KM, KDV, HDB, NR, JM, DH and AM performed experiments. PV, KM, and SV performed bioinformatical analysis. PV and KM analyzed the data. PV and KM wrote the draft manuscript. All authors contributed to data interpretation, revising the manuscript and approved the final manuscript.

FUNDING

This work was funded by FWO-Vlaanderen (1503619N) and Vrije Universiteit Brussel under the strategic research program scheme SRP48.

ACKNOWLEDGMENTS

These data were generated as part of the Multiple Myeloma Research Foundation Personalized Medicine Initiatives (https://research.themmrf.org and http://www.themmrf.org).

SUPPLEMENTARY MATERIAL

The Supplementary Material for this article can be found online at: https://www.frontiersin.org/articles/10.3389/fcell.2022.879057/full#supplementary-material

REFERENCES

Banasavadi-Siddegowda, Y. K., Welker, A. M., An, M., Yang, X., Zhou, W., Shi, G., et al. (2018). PRMT5 as a Druggable Target for Glioblastoma Therapy. *Neuro Oncol.* 20 (6), 753–763. doi:10.1093/neuonc/nox206

Barlogie, B., Tricot, G., Rasmussen, E., Anaissie, E., van Rhee, F., Zangari, M., et al. (2006). Total Therapy 2 without Thalidomide in Comparison with Total Therapy 1: Role of Intensified Induction and Posttransplantation Consolidation Therapies. *Blood* 7(7), 2633–2638. doi:10.1182/blood-2005-10-4084

Binder, M., Rajkumar, S. V., Ketterling, R. P., Dispenzieri, A., Lacy, M. Q., Gertz, M. A., et al. (2019). Substratification of Patients with Newly Diagnosed Standard-risk Multiple Myeloma. *Br. J. Haematol.* 185 (2), 254–260. doi:10.1111/bjh.15800

Broyl, A., Hose, D., Lokhorst, H., de Knegt, Y., Peeters, J., Jauch, A., et al. (2010). Gene Expression Profiling for Molecular Classification of Multiple Myeloma in Newly Diagnosed Patients. *Blood* 116 (14), 2543–2553. doi:10.1182/blood-2009-12-261032

Caprio, C., Sacco, A., Giustini, V., and Roccaro, A. M. (2020). Epigenetic Aberrations in Multiple Myeloma. *Cancers* 12 (10), 2996. doi:10.3390/cancers12102996

de Boussac, H., Bruyer, A., Jourdan, M., Maes, A., Robert, N., Gourzones, C., et al. (2020). Kinome Expression Profiling to Target New Therapeutic Avenues in Multiple Myeloma. *Haematologica* 105 (3), 784–795. doi:10.3324/haematol.2018.208306

De Bruyne, E., Bos, T. J., Schuit, F., Van Valckenborgh, E., Menu, E., Thorrez, L., et al. (2010). IGF-1 Suppresses Bim Expression in Multiple Myeloma via Epigenetic and Posttranslational Mechanisms. *Blood* 115 (12), 2430–2440. doi:10.1182/blood-2009-07-232801

Drach, J., Ackermann, J., Fritz, E., Krömer, E., Schuster, R., Gisslinger, H., et al. (1998). Presence of a P53 Gene Deletion in Patients with Multiple Myeloma Predicts for Short Survival after Conventional-Dose Chemotherapy. *Blood* 92 (3), 802–809. doi:10.1182/blood.v92.3.802

Gentile, M., Specchia, G., Derudas, D., Galli, M., Botta, C., Rocco, S., et al. (2021). Elotuzumab, Lenalidomide, and Dexamethasone as Salvage Therapy for Patients with Multiple Myeloma: Italian, Multicenter, Retrospective Clinical Experience with 300 Cases outside of Controlled Clinical Trials. *haematol* 106 (1), 291–294. doi:10.3324/haematol.2019.241513

Gullà, A., Hideshima, T., Bianchi, G., Fulciniti, M., Kemal Samur, M., Qi, J., et al. (2018). Protein Arginine Methyltransferase 5 Has Prognostic Relevance and Is a Druggable Target in Multiple Myeloma. *Leukemia* 32 (4), 996–1002. doi:10.1038/leu.2017.334.Epub.2017Nov21

Hajek, R., Okubote, S. A., and Svachova, H. (2013). Myeloma Stem Cell Concepts, Heterogeneity and Plasticity of Multiple Myeloma. *Br. J. Haematol.* 163 (5), 551–564. doi:10.1111/bjh.12563.Epub.2013.Sep20

Hamard, P.-J., Santiago, G. E., Liu, F., Karl, D. L., Martinez, C., Man, N., et al. (2018). PRMT5 Regulates DNA Repair by Controlling the Alternative Splicing of Histone-Modifying Enzymes. *Cell Rep.* 24 (10), 2643–2657. doi:10.1016/j.celrep.2018.08.002

He, Y., Ren, J., Xu, X., Ni, K., Schwader, A., Finney, R., et al. (2020). Lsh/HELLS Is Required for B Lymphocyte Development and Immunoglobulin Class Switch Recombination. *Proc. Natl. Acad. Sci. U.S.A.* 117 (33), 20100–20108. doi:10.1073/pnas.2004112117

Holmes, B., Benavides-Serrato, A., Saunders, J. T., Landon, K. A., Schreck, A. J., Nishimura, R. N., et al. (2019). The Protein Arginine Methyltransferase PRMT5 Confers Therapeutic Resistance to mTOR Inhibition in Glioblastoma. *J. Neurooncol* 145 (1), 11–22. doi:10.1007/s11060-019-03274-0

Hose, D., Reme, T., Hielscher, T., Moreaux, J., Messner, T., Seckinger, A., et al. (2011). Proliferation Is a Central Independent Prognostic Factor and Target for Personalized and Risk-Adapted Treatment in Multiple Myeloma. *Haematologica* 96, 87–95. doi:10.3324/haematol.2010.030296

Hose, D., Rème, T., Meissner, T., Moreaux, J., Seckinger, A., Lewis, J., et al. (2009). Inhibition of Aurora Kinases for Tailored Risk-Adapted Treatment of Multiple Myeloma. *Blood* 113, 4331–4340. doi:10.1182/blood-2008-09-178350

Joseph, N. S., Gentili, S., Kaufman, J. L., Lonial, S., and Nooka, A. K. (2017). High-risk Multiple Myeloma: Definition and Management. *Clin. Lymphoma Myeloma Leukemia* 17, S80–S87. doi:10.1016/j.clml.2017.02.018

Keats, J. J., Maxwell, C. A., Taylor, B. J., Hendzel, M. J., Chesi, M., Bergsagel, P. L., et al. (2005). Overexpression of Transcripts Originating from the MMSET Locus Characterizes All T(4;14)(p16;q32)-Positive Multiple Myeloma Patients. *Blood* 105 (10), 4060–4069. doi:10.1182/blood-2004-09-3704

Keats, J. J., Reiman, T., Maxwell, C. A., Taylor, B. J., Larratt, L. M., Mant, M. J., et al. (2003). In Multiple Myeloma, T(4;14)(p16;q32) Is an Adverse Prognostic Factor Irrespective of FGFR3 Expression. *Blood* 101 (4), 1520–1529. doi:10.1182/blood-2002-06-1675

Kim, H., and Ronai, Z. e. A. (2020). PRMT5 Function and Targeting in Cancer. *Cst* 4 (8), 199–215. doi:10.15698/cst2020.08.228

Koh, C. M., Bezzi, M., Low, D. H. P., Ang, W. X., Teo, S. X., Gay, F. P. H., et al. (2015). MYC Regulates the Core Pre-mRNA Splicing Machinery as an Essential Step in Lymphomagenesis. *Nature* 523, 96–100. doi:10.1038/nature14351

Kuehl, W. M., and Bergsagel, P. L. (2012). Molecular Pathogenesis of Multiple Myeloma and its Premalignant Precursor. *J. Clin. Invest.* 122 (10), 3456–3463. doi:10.1172/JCI61188.Epub.2012.Oct.1

Lee, K. M., Yang, S.-J., Choi, J.-H., and Park, C.-S. (2014). Functional Effects of a Pathogenic Mutation in Cereblon (CRBN) on the Regulation of Protein

Synthesis via the AMPK-mTOR Cascade. *J. Biol. Chem.* 289 (34), 23343–23352. doi:10.1074/jbc.M113.523423

Li, L., Zheng, Y., Zhang, W., Hou, L., and Gao, Y. (2020). Scutellarin Circumvents Chemoresistance, Promotes Apoptosis, and Represses Tumor Growth by HDAC/miR-34a-mediated Down-Modulation of Akt/mTOR and NF-Kb-Orchestrated Signaling Pathways in Multiple Myeloma. *Int. J. Clin. Exp. Pathol.* 13 (2), 212–219.

Li, Y., Chitnis, N., Nakagawa, H., Kita, Y., Natsugoe, S., Yang, Y., et al. (2015). PRMT5 Is Required for Lymphomagenesis Triggered by Multiple Oncogenic Drivers. *Cancer Discov.* 5 (3), 288–303. doi:10.1158/2159-8290.CD-14-0625

Love, M. I., Huber, W., and Anders, S. (2014). Moderated Estimation of Fold Change and Dispersion for RNA-Seq Data with DESeq2. *Genome Biol.* 15 (12), 550. doi:10.1186/s13059-014-0550-8

Maaten, L. V. D., and Hinton, G. (2008). Visualizing Data Using T-SNE. *J. Mach. Learn Res.* 9 (86), 2579–2605.

Maes, K., Smedt, E. D., Lemaire, M., Raeve, H. D., Menu, E., Van Valckenborgh, E., et al. (2014). The Role of DNA Damage and Repair in Decitabine-Mediated Apoptosis in Multiple Myeloma. *Oncotarget* 5 (10), 3115–3129. doi:10.18632/oncotarget.1821

Middleton, R., Gao, D., Thomas, A., Singh, B., Au, A., Wong, J. J.-L., et al. (2017). IRFinder: Assessing the Impact of Intron Retention on Mammalian Gene Expression. *Genome Biol.* 18 (1), 51. doi:10.1186/s13059-017-1184-4

Moreaux, J., Klein, B., Bataille, R., Descamps, G., Maiga, S., Hose, D., et al. (2011). A High-Risk Signature for Patients with Multiple Myeloma Established from the Molecular Classification of Human Myeloma Cell Lines. *Haematologica* 96 (4), 574–582. doi:10.3324/haematol.2010.033456

Mulligan, G., Mitsiades, C., Bryant, B., Zhan, F., Chng, W. J., Roels, S., et al. (2007). Gene Expression Profiling and Correlation with Outcome in Clinical Trials of the Proteasome Inhibitor Bortezomib. *Blood* 109 (8), 3177–3188. doi:10.1182/blood-2006-09-044974

Munawar, U., Roth, M., Barrio, S., Wajant, H., Siegmund, D., Bargou, R. C., et al. (2019). Assessment of TP53 Lesions for P53 System Functionality and Drug Resistance in Multiple Myeloma Using an Isogenic Cell Line Model. *Sci. Rep.* 9 (1), 18062. doi:10.1038/s41598-019-54407-4

Oudaert, I., Satilmis, H., Vlummens, P., De Brouwer, W., Maes, A., Hose, D., et al. (2022). Pyrroline-5-Carboxylate Reductase 1: a Novel Target for Sensitizing Multiple Myeloma Cells to Bortezomib by Inhibition of PRAS40-Mediated Protein Synthesis. *J. Exp. Clin. Cancer Res.* 41 (1), 45. doi:10.1186/s13046-022-02250-3

Radzisheuskaya, A., Shliaha, P. V., Grinev, V., Lorenzini, E., Kovalchuk, S., Shlyueva, D., et al. (2019). PRMT5 Methylome Profiling Uncovers a Direct Link to Splicing Regulation in Acute Myeloid Leukemia. *Nat. Struct. Mol. Biol.* 26 (11), 999–1012. doi:10.1038/s41594-019-0313-z

Rengasamy, M., Zhang, F., Vashisht, A., Song, W.-M., Aguilo, F., Sun, Y., et al. (2017). The PRMT5/WDR77 Complex Regulates Alternative Splicing through ZNF326 in Breast Cancer. *Nucleic Acids Res.* 45 (19), 11106–11120. doi:10.1093/nar/gkx727

Shah, M. Y., Martinez-Garcia, E., Phillip, J. M., Chambliss, A. B., Popovic, R., Ezponda, T., et al. (2016). MMSET/WHSC1 Enhances DNA Damage Repair Leading to an Increase in Resistance to Chemotherapeutic Agents. *Oncogene* 35 (45), 5905–5915. doi:10.1038/onc.2016.116.Epub.2016.Apr.25

Siu, L. L., Rasco, D. W., Vinay, S. P., Romano, P. M., Menis, J., Opdam, F. L., et al. (2019). METEOR-1: A Phase I Study of GSK3326595, a First-In-Class Protein Arginine Methyltransferase 5 (PRMT5) Inhibitor, in Advanced Solid Tumours. *Ann. Oncol.* 30 (S5), v159. doi:10.1093/annonc/mdz244

Tan, L., Xiao, K., Ye, Y., Liang, H., Chen, M., Luo, J., et al. (2020). High PRMT5 Expression Is Associated with Poor Overall Survival and Tumor Progression in Bladder Cancer. *Aging* 12 (9), 8728–8741. doi:10.18632/aging.103198

Vikova, V., Jourdan, M., Robert, N., Requirand, G., Boireau, S., Bruyer, A., et al. (2019). Comprehensive Characterization of the Mutational Landscape in Multiple Myeloma Cell Lines Reveals Potential Drivers and Pathways Associated with Tumor Progression and Drug Resistance. *Theranostics* 9 (2), 540–553. doi:10.7150/thno.28374

Webb, L. M., Narvaez Miranda, J., Amici, S. A., Sengupta, S., Nagy, G., and Guerau-de-Arellano, M. (2019). NF-κB/mTOR/MYC Axis Drives PRMT5 Protein Induction after T Cell Activation via Transcriptional and Non-transcriptional Mechanisms. *Front. Immunol.* 10, 524. doi:10.3389/fimmu.2019.00524

Weinhold, N., Ashby, C., Rasche, L., Chavan, S. S., Stein, C., Stephens, O. W., et al. (2016). Clonal Selection and Double-Hit Events Involving Tumor Suppressor Genes Underlie Relapse in Myeloma. *Blood* 128 (13), 1735–1744. doi:10.1182/blood-2016-06-723007

Xie, Z., and Chng, W. J. (2014). MMSET: Role and Therapeutic Opportunities in Multiple Myeloma. *BioMed Res. Int.* 2014, 1–5. doi:10.1155/2014/636514

Xie, Z., Chooi, J. Y., Toh, S. H. M., Yang, D., Basri, N. B., Ho, Y. S., et al. (2019). MMSET I Acts as an Oncoprotein and Regulates GLO1 Expression in T(4;14) Multiple Myeloma Cells. *Leukemia* 33 (3), 739–748. doi:10.1038/s41375-018-0300-0

Yan, J., Xie, Y., Si, J., Gan, L., Li, H., Sun, C., et al. (2021). Crosstalk of the Caspase Family and Mammalian Target of Rapamycin Signaling. *Ijms* 22 (2), 817. doi:10.3390/ijms22020817

Yu, G., and He, Q.-Y. (2016). ReactomePA: an R/Bioconductor Package for Reactome Pathway Analysis and Visualization. *Mol. Biosyst.* 12 (2), 477–479. doi:10.1039/c5mb00663e

Zhan, F., Barlogie, B., Arzoumanian, V., Huang, Y., Williams, D. R., Hollmig, K., et al. (2007). Gene-expression Signature of Benign Monoclonal Gammopathy Evident in Multiple Myeloma Is Linked to Good Prognosis. *Blood* 109 (4), 1692–1700. doi:10.1182/blood-2006-07-037077

Zhu, F., Guo, H., Bates, P. D., Zhang, S., Zhang, H., Nomie, K. J., et al. (2019). PRMT5 Is Upregulated by B-Cell Receptor Signaling and Forms a Positive-Feedback Loop with PI3K/AKT in Lymphoma Cells. *Leukemia* 33 (12), 2898–2911. doi:10.1038/s41375-019-0489-6

Zhu, Y. X., Braggio, E., Shi, C.-X., Bruins, L. A., Schmidt, J. E., Van Wier, S., et al. (2011). Cereblon Expression Is Required for the Antimyeloma Activity of Lenalidomide and Pomalidomide. *Blood* 118 (18), 4771–4779. doi:10.1182/blood-2011-05-356063

Zhu, Y. X., Kortuem, K. M., and Stewart, A. K. (2013). Molecular Mechanism of Action of Immune-Modulatory Drugs Thalidomide, Lenalidomide and Pomalidomide in Multiple Myeloma. *Leukemia Lymphoma* 54 (4), 683–687. doi:10.3109/10428194.2012.728597

Conflict of Interest: The authors declare that the research was conducted in the absence of any commercial or financial relationships that could be construed as a potential conflict of interest.

Publisher's Note: All claims expressed in this article are solely those of the authors and do not necessarily represent those of their affiliated organizations, or those of the publisher, the editors and the reviewers. Any product that may be evaluated in this article, or claim that may be made by its manufacturer, is not guaranteed or endorsed by the publisher.

frontiers | Frontiers in Genetics

TYPE Review
PUBLISHED 09 August 2022
DOI 10.3389/fgene.2022.921972

OPEN ACCESS

EDITED BY
Ângela Sousa,
University of Beira Interior, Covilhã, Portugal, Portugal

REVIEWED BY
Buddolla Viswanath,
Dr. Buddolla's Institute of Life Sciences, India
Mehdi Mahdavi,
Motamed Cancer Institute, Iran

*CORRESPONDENCE
Marcos Pileggi,
mpileggi@uepg.br

SPECIALTY SECTION
This article was submitted to Epigenomics and Epigenetics, a section of the journal Frontiers in Genetics

RECEIVED 17 April 2022
ACCEPTED 13 July 2022
PUBLISHED 09 August 2022

CITATION
Schemczssen-Graeff Z and Pileggi M (2022), Probiotics and live biotherapeutic products aiming at cancer mitigation and patient recover. *Front. Genet.* 13:921972. doi: 10.3389/fgene.2022.921972

Probiotics and live biotherapeutic products aiming at cancer mitigation and patient recover

Zelinda Schemczssen-Graeff[1] and Marcos Pileggi[2]*

[1]Comparative Immunology Laboratory, Department of Microbiology, Parasitology and Pathology, Federal University of Paraná, Curitiba, Brazil, [2]Environmental Microbiology Laboratory, Structural and Molecular Biology and Genetics Department, Life Sciences and Health Institute, Ponta Grossa State University, Ponta Grossa, Brazil

Molecular biology techniques allowed access to non-culturable microorganisms, while studies using analytical chemistry, as Liquid Chromatography and Tandem Mass Spectrometry, showed the existence of a complex communication system among bacteria, signaled by quorum sensing molecules. These approaches also allowed the understanding of dysbiosis, in which imbalances in the microbiome diversity, caused by antibiotics, environmental toxins and processed foods, lead to the constitution of different diseases, as cancer. Colorectal cancer, for example, can originate by a dysbiosis configuration, which leads to biofilm formation, production of toxic metabolites, DNA damage in intestinal epithelial cells through the secretion of genotoxins, and epigenetic regulation of oncogenes. However, probiotic strains can also act in epigenetic processes, and so be use for recovering important intestinal functions and controlling dysbiosis and cancer mitigation through the metabolism of drugs used in chemotherapy, controlling the proliferation of cancer cells, improving the immune response of the host, regulation of cell differentiation and apoptosis, among others. There are still gaps in studies on the effectiveness of the use of probiotics, therefore omics and analytical chemistry are important approaches to understand the role of bacterial communication, formation of biofilms, and the effects of probiotics and microbiome on chemotherapy. The use of probiotics, prebiotics, synbiotics, and metabiotics should be considered as a complement to other more invasive and hazard therapies, such chemotherapy, surgery, and radiotherapy. The study of potential bacteria for cancer treatment, as the next-generation probiotics and Live Biotherapeutic Products, can have a controlling action in epigenetic processes, enabling the use of these bacteria for the mitigation of specific diseases through changes in the regulation of genes of microbiome and host. Thus, it is possible that a path of medicine in the times to come will be more patient-specific treatments, depending on the environmental, genetic, epigenetic and microbiome characteristics of the host.

KEYWORDS

metabolomics, metagenomics, proteomics, epigenetics, chemical signaling, dysbiosis, gut microbiome, bacterial diversity

Overview

The most obvious perception that people have about microorganisms since the 19th century is that they are mostly pathogens for humans. In more recent years, molecular biology techniques, mainly cloning and sequencing, brought to light the ideas of healthy microbiomes, while studies using analytical chemistry, as Liquid Chromatography and Tandem Mass Spectrometry, showed the existence of a complex communication system among bacteria, signaled by quorum sensing molecules. The ability to chemically communicate among host cells and their microorganisms was, then, the next scientific achievement, with the definition of the gut-brain axis microbiome. The development of metabolome and metagenomic, combined with traditional genetic and microbiological techniques, allowed the concept of dysbiosis to be developed, in which imbalances in the diversity of the human microbiome could lead to the constitution of different diseases, such as diabetes, allergies, autoimmune, autism, Alzheimer's and cancer. Evolutionarily, microbiomes can be passed between generations, from mothers to children, considered as epigenetic inheritances since they can regulate the expression of genes in the hosts. The earlier and more effective this transference from mothers to children is, the more effective the epigenetic imprint can be. Advent such as the use of antibiotics, environmental toxins, processed foods, lead to the loss of diversity in the gut microbiome, causing dysbiosis. In this context, the use of probiotic bacterial strains, such as those of the *Lactobacillus* and *Bifidobacterium* genera, has the objective of recovering important intestinal functions and controlling dysbiosis. The understanding that the metabolites of these strains, and others not yet considered as probiotics, the next-generation probiotics, can have a controlling action in epigenetic processes, has enabled the use of these bacteria not only as food additives capable of improving general human health, but as Live Biotherapeutic Products, with the objective of mitigating specific diseases through changes in the regulation of microbiome and host genes. Colorectal is one of the most well-studied types of cancer in terms of its relationship microorganisms. The gut microbiome, in dysbiosis configuration, is involved with tumor by the biofilm formation, the production of toxic metabolites or inducing DNA damage in intestinal epithelial cells through the secretion of genotoxins. However, healthy gut microbiota has been used in therapeutic drugs metabolism for chemotherapy, radiotherapy response modulation, and targeted immunotherapy. There are distinct levels of epigenetic control by probiotic strains or Live Biotherapeutic Products possible to be envisioned in controlling the proliferation of cancer cells, as the inactivation ratios of cancerogenic compounds; improving the immune response of the host; antiproliferative effects*via*regulation of cell differentiation and apoptosis; inhibition of tyrosine kinase; and inflammatory cell infiltration among malignant and stromal cells. As an example, gut bacteria can metabolize fiber into butyrate, a short-chain fatty acid and a histone deacetylase inhibitor, that upregulates tumor-suppressor genes epigenetically in cancer cells and anti-inflammatory genes in immune cells. Not just in cancer, probiotic bacteria are also associated with DNA methylation and the induction of regulatory T-cells, that normally suppress inflammatory, opening the possibility of immunologic diseases treatment, as allergic and autoimmune disorders. A relationship between dysbiosis and microbiome can also be found for breast cancer. Both the gut microenvironment and breast tissue participate in this system. Epigenetics is associated with cancer development in postmenopausal women, through the regulation of steroid-hormone metabolism, mainly estrogens. In contrast, the gut resident microbiome can modulate mucosal and systemic immune responses. There are still gaps in studies on the effectiveness of the use of probiotics strains and Live Biotherapeutic Products in cancer treatments because the metabolic interrelationships among resident microbiome, environmental factors and genetic/epigenetic determinants of the vulnerable host are complex. Metabolome, metagenomics, transcriptome, and analytical chemistry are important approaches to understand the role of bacterial communication*via*quorum sensing, formation of biofilms, and the interference of microbiome and probiotics on chemotherapy. The metabolic and epigenetic interactions between colorectal cancer and resident microbiome are robust experimental model for studies in diverse types of cancer. The use of probiotics, prebiotics, synbiotics, and metabiotics should be considered as a complement to other more invasive and hazard therapies, such chemotherapy, surgery, and radiotherapy. Thus, it is possible that a path of medicine in the coming times will be more specific treatment for the patient, depending on the environmental, genetic, epigenetic and microbiome characteristics of the host. For this, it is necessary to have a better detail of the regulation of genes associated with specific tumors, of metabolites associated with down and up regulation of these genes, and, finally, which bacterial strains are candidates to produce these substances efficiently within the intestinal system.

Literature review

Microbiomes and host genes in chemical communication

For most people microorganisms are primarily pathogens for humans. This is a concept supported since the 19th century with the germ theory of disease and Koch's postulates, therefore the view of the nascent discipline of microbiology focused on the pathogenic potential of microorganisms. A

classic example of this postulate is the association of *Helicobacter pylori* with peptic ulcers recurrence and gastric cancer (Chen et al., 2019).

The concept of healthy microbiomes playing an important role in human physiology has been built more recently in the history of Science, thanks to molecular biology techniques, mainly cloning and sequencing. Strain-level differences in microbiomes has allowed a better understanding of disease associations, not only with cancer, but with a host of diseases, and this have been achieved with a more detailed study in metagenomic sequencing and, therefore, access to complete genomes, as was the case with *Propionibacterium acnes,* being able to compare healthy skin microbiomes and those linked to acne, at strain level (Bangayan et al., 2020). Studies using analytical chemistry showed the existence of a complex communication system among bacteria, signaled by quorum sensing molecules, a population density-dependent characteristic, and that can allow adaptations to environmental conditions, such those involving bioluminescence, antibiotic biosynthesis, plasmid conjugation and virulence (Kiymaci et al., 2018). *Pseudomonas aeruginosa* is an example of an opportunistic human bacterium that causes devastating infections in patients with compromised immune systems, and its ability to form antibiotic-resistant biofilms it is probably the reason for the persistence in clinical settings (Thi et al., 2020). Novel approaches have shown the interference of quorum sensing molecules in other functions, such as coordinate response systems, as antioxidative enzymes production or biofilm formation to tolerate herbicides (Freitas et al., 2021). There is great diversity in communication networks mediated by quorum sensing signals, including in virulence modulation, therefore have become a promising target for mitigating pathogens (Contreras-Ramos and Mansell, 2021).

The ability to chemically communicate among host cells and their microorganisms was, then, the next scientific achievement, with the definition of the gut-brain axis microbiome, which can be defined as the bidirectional chemical communication among the gut, its microbiome, and the nervous system (Bengesser et al., 2019; Osadchiy et al., 2019; Doenyas, 2021). The understanding of communication exclusively between bacteria through quorum sensing signaling molecules possibly inspire studies of communication between bacteria and their eukaryotic hosts, which be conducted through other signaling molecules such as butyrate, propionate, and acetate, related to epigenetic and cancer. These relationships will be exemplified throughout this review. Intestinal neurons can sense bacteria independently of the host immune system, as the mediators with neuromodulatory properties produced by *Staphylococcus aureus*, which increase the membrane permeability in cultured sensory neurons, and change intestinal motility and secretion through the induction of biphasic response in extrinsic sensory afferent nerves (Uhlig et al., 2020). The dysfunction of the brain-gut-microbiome axis is the most important etiological factor for the irritable bowel syndrome, with the neurotransmitter serotonin taking a particularly significant role in the pathology. Thereby, susceptible genes for this disease are related to serotonergic signaling pathways (Mishima and Ishihara, 2021). Long-term treatment with multispecies probiotics attenuated the memory dysfunction through the decreased of trimethylation of histone H3 Lys 27 in lead-exposed rats (Xiao et al., 2020).

The development of metabolome and metagenomic, combined with traditional genetic and microbiological techniques, allowed the concept of dysbiosis to be developed, in which imbalances in the human microbiome diversity could lead to the constitution of different diseases. The identification of obesity-associated gut microbial species, as the glutamate-fermenting commensal *Bacteroides thetaiotaomicron*, was achieved by metagenome sequencing and serum metabolomics profiling in a cohort of lean and obese (Liu et al., 2017). Primary bile acids, through bacterial metabolism, produces secondary bile acids, as in *Ruminococcaceae* and is associated with ulcerative colitis in colectomy-treated patients (Sinha et al., 2020). Gut microbiota dysbiosis can be associated with chronic heart failure. Particularly, *Faecalibacterium prausnitzii* was found at lower population levels and *Ruminococcus gnavus* was found higher in affected patients' gut microbiota than in controls (Cui et al., 2018). Parkinson's disease can be characterized by the accumulation of intracellular aggregates of misfolded *a*-synuclein along the cerebral axis, and this was associated with a reduction of bacteria *Butyrivibrio*, *Pseudobutyrivibrio*, *Coprococcus*, and *Blautia*, belonging to the Lachnospiraceae family, linked to anti-inflammatory/neuroprotective effects (Vascellari et al., 2020). The increased risk of colorectal cancer is associated with dietary fat intake, with the increase of specific strains of bacteria *Alistipes* sp. And gut metabolite alteration, including elevated lysophosphatidic acid, which promotes cell proliferation and impair cell junction (Yang et al., 2022).

Evolutionarily, microbiomes can be passed among generations, from mothers to children, considered as epigenetic inheritances since they can regulate the expression of genes in the hosts (Figure 1). The earlier and more effective this transference from mothers to children is, the more effective the epigenetic imprint can be. Neonatal supplementation in adult mice with p40, a probiotic functional factor, protect the gut against inflammation, and protection against colitis, through an epigenetic imprint on anti-transforming growth factor *ß* TGFβ, leading to long-lasting production by intestinal epithelial cells to expand Tregs (Deng et al., 2021).

Dysbiosis, probiotics, epigenetics in colorectal cancer

The metabolic and epigenetic interactions between colorectal cancer and resident microbiome are well-studied, even because gut microbiomes are most studied so far, able to serve as an

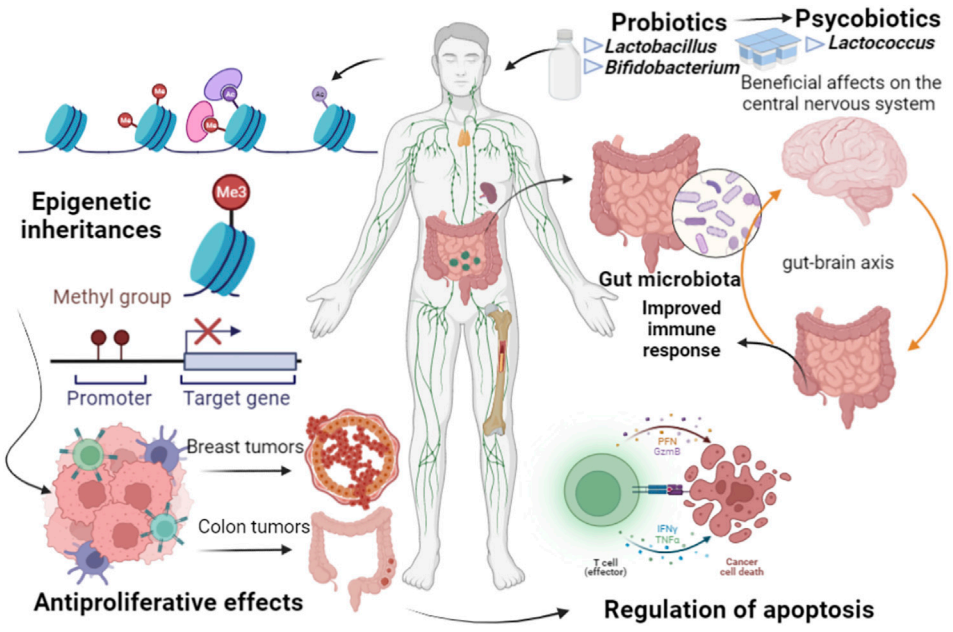

FIGURE 1
Epigenetic inheritances can be passed among host generations, regulated by gut microbiome. Several factors can cause dysbiosis, characterized by changes in microbiome diversity, related to initiation and promotion of chronic inflammatory pathways, promotion of genetic and epigenetic alterations, leading to tumor origin and development, as in breast and colorectal cancer. Nevertheless, probiotic bacteria, as *Lactobacillus* and *Bifidobacterium,* can induce specific mechanisms against various infections, including diverse types of cancer, through apoptosis, antioxidant activity, immune response induction, and epigenetics regulation.

experimental model for diverse types of cancer and other diseases. Advent such as the use of antibiotics, environmental toxins, processed foods, lead to the loss of diversity in the gut microbiome, causing dysbiosis, which can be related to several diseases, from obesity to colorectal cancer. Gut-derived lipopolysaccharide, gut microbiota-associated bile acids, tryptophan, and short-chain fatty acids are dynamically involved in liver regeneration after partial hepatectomy. However, these processes depend on the composition of gut microbiota, which was molded by antibiotics or probiotics (Zheng and Wang, 2021). The interaction between microbiota and the genetic processes that cause the tumors can be exemplified by serrated adenocarcinoma and sporadic colorectal carcinoma, which have histological and molecular characteristics of microsatellite instability and are associated with changes in methylation patterns, whose specificity in epigenetic regulation may help define the key molecules responsible for the weak immune response in these tumors, and identify potential targets for treatment. The work by García-Solano et al., 2018 validated HLA-DOA and CD14 in DNA, mRNA and protein level, as CD14 is related to the mediation of the innate immune response induced by bacterial lipopolysaccharide, while HLA-DOA is found in lysosomes in B cells and peptide regulation mediated by HLA-DM loading on MHC class II molecules. In this context, the use of probiotic bacterial strains, such as those of the *Lactobacillus* and *Bifidobacterium* genera, has the objective of recovering important intestinal functions and controlling dysbiosis (Figure 1). High-fat/carbohydrate diet in obesity cases is characterized by a gut microbiota with a predominance of Firmicutes (*Clostridium*), *Prevotella* and *Methanobrevibacter* but deficient in beneficial bacteria such as *Bacteroides*, *Bifidobacterium*, *Lactobacillus* and *Akkermansia* (Amabebe et al., 2020). Treatment with B6 vitamin and probiotic strains, as *B. longum* and *L. rhamnosus*, may alleviate symptoms in lactose intolerant patients through the increase in acetic acid, 2-methyl-propanoic acid, nonenal, and indolizine 3-methyl, and decrease in phenol (Vitellio et al., 2019). *Lactobacillus*, *Lactococcus* and *Bifidobacterium* can improve the host's immune system through the regulation of brain pathways and serotonin production (Magalhães-Guedes, 2022). Infections caused by *C. butyricum*, *C. difficile*, and *C. perfringens* may originate in conditions of host dysbiosis. *L. plantarum* can be used to restore microbiota after antibiotic treatments to eliminate those opportunist bacteria (Monteiro et al., 2019).

The symbiotic relationship between eukaryotes and microbiomes has been described and might explain some transgenerational inheritance. The epigenetic modulation occurs from the first years of life, occurring even in adulthood, and can be altered with changes in eating habits

and the use of antibiotics, which can lead to dysbiosis (Flandroy et al., 2018). The understanding that the metabolites of microbiomes can repair these conditions, the use of strains such as probiotics and others not yet considered as probiotics, the next-generation probiotics, can have a controlling action in epigenetic processes, has enabled the use of these bacteria not only as food additives capable of improving general human health, but as Live Biotherapeutic Products, with the objective of mitigating specific diseases through changes in the regulation of Microbiome and host genes. The Food and Drug Administration of US Government has defined the category of "live biotherapeutic products" and constituting objectives and regulations for pharmaceutical uses and quality requirements, so these products could reach the market and registered as medicinal products (Cordaillat-Simmons et al., 2020).

Epigenetic mechanisms driven by gut microbiome are more relevant in early childhood and related to the type of delivery, breastfeeding, introduction of solid food, infections, and antibiotic treatments. Short-chain fatty acids, produced by fermentative metabolism of gut microbiome can inhibit histone deacetylase activity and modulate host gene expression involved in cellular lipid metabolism and satiety, may lead to obesity. These are characteristic situations of reduced microbial diversity. The presence of abundant Firmicutes in pregnant women produce a pattern of differentially methylated promoters, which is associated to lipid metabolism, inflammatory response, and risk of obesity (Cuevas-Sierra et al., 2019).

Colorectal is one of the most well-studied types of cancer, being that surgery, radiotherapy, and chemotherapy are the normally used treatments, but presenting side effects as systemic toxicity, resistance, and recurrence (Sharma and Shukla, 2016). Colorectal cancer is also well-studied in terms of its relationship with microorganisms. *Fusobacterium nucleatum* and specific strains of *Escherichia coli* and *Bacteroides fragilis* were related to colorectal carcinogenesis, using DNA sequencing and functional studies in animal models (Wong and Yu, 2019). The gut microbiome, in dysbiosis configuration, is involved with tumor by the biofilm formation, the production of toxic metabolites or inducing DNA damage in intestinal epithelial cells through the secretion of genotoxins. However, healthy gut microbiota, or the use of probiotics strains, has been related to drugs metabolism used in chemotherapy, in modulation of radiotherapy responses, and targeted immunotherapy. For example, dysbiosis can enhance the amount of *F. nucleatum*, which was associated with high microsatellite instability and methylation status of proto-oncogen BRAF, consequently promoting colorectal tumor growth through the inhibition of T-cell-mediated immune responses. This situation results in shorter survival of cancer patients (Figure 2). In contrast, mice submitted to therapy based on anti-programmed cell death 1 and then treated with probiotics showed a lower frequency of interferon-γ-positive

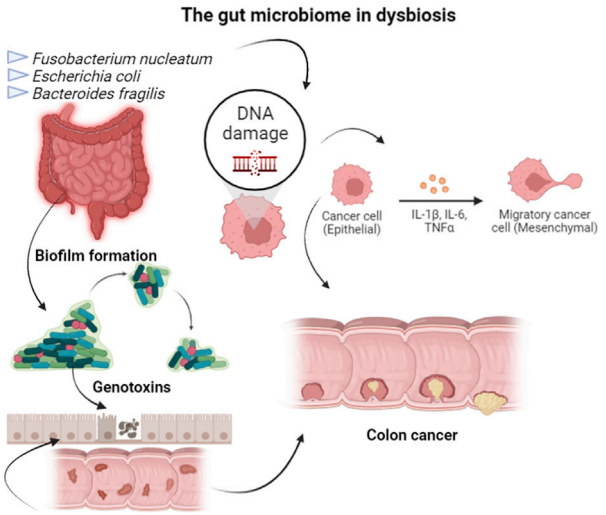

FIGURE 2
Bacteria, as *F. nucleatum* and specific strains of *E. coli* and *B. fragilis*, in dysbiosis configuration of the gut microbiome, is involved with colorectal cancer by the host epigenetic regulation, biofilm formation, toxic metabolites production, DNA damage induction in intestinal epithelial cells through the secretion of genotoxins, or induction of T-cell-mediated immune responses against colorectal tumors.

cytotoxic T cells in the tumor microenvironment (Spencer et al., 2021). Cancer prevention and treatment strategies can be achieved through diet, probiotics, and antibiotics (Mima et al., 2016). A study conducted in colorectal cancer patients with colon resection showed that *Saccharomyces boulardii* deregulated pro-inflammatory cytokines (Consoli et al., 2016).

Loss of beneficial microorganisms is a crucial element for the origin of dysbiosis, in which pathogens and pathobionts have harmful configurations for hosts in different constituents of microbiome diversity (Silva et al., 2021). Therefore, dysbiosis may be related to initiation and promotion of chronic inflammatory pathways and promotes the colorectal cancer through genetic and epigenetic changes, which lead to dysplasia, clonal expansion, and cell malignant transformation (Figure 1).

Probiotic bacteria can mitigate the initiation of the carcinogenic process and the effects of the already established disease, through its metabolism and chemical communication, with systemic effects on the host, as cancerogenic compounds inactivation; competition with putrefactive and pathogenic microbiome; improvement of the immune response of the host; antiproliferative effects *via* regulation of cell differentiation and apoptosis; undigested food fermentation; tyrosine kinase inhibition; reduction of enteropathogenic complications related to colon cancer surgery. Probiotics strains can also improve diarrhea but affecting peristalsis and, therefore, the efficient functioning of the intestine and promoting

the integrity of gut mucosal. This chain of effects culminates with the stimulation on the immune system and prevention of the metastasis in colorectal cancer (Eslami et al., 2019). Microbiome, probiotic strains, and colorectal cancer can be linked through quorum sensing, biofilm formation, sidedness, and effects/counter effects on chemotherapy. Studies on genomics and metabolomics targeting the gut microbiome will uncover important linkages between microbiome and intestinal health (Raskov et al., 2017). Gut microbiome, depending on the bacterial biodiversity, can secrete genotoxins that lead to DNA damage in intestinal epithelial cells and initiate a tumor. The efficacy of chemotherapy, radiotherapy and immunotherapy also will depend on microbiome diversity, and this may vary from patient to patient (Silva et al., 2021). This specific host-microbiome relationship creates an opportunity to control the health of an individual by manipulating the composition of the gut microbiota, which can be achieved through the administration of probiotics, prebiotics, symbiotics, fecal microbiota transplantation, but with generic effects. Thus, new commensal strains, or the next-generation probiotics, have been sought as promising prophylactic and therapeutic agents (Singh and Natraj, 2021). In my opinion, this is the foundation of a new philosophy of patient-specific precision medicine. In addition to these approaches, metabiotics, or probiotic derived factors, which have epigenetic, antimutagenic, immunomodulatory, apoptotic, and antimetastatic effects, can optimize host physiological functions and be used in immunosuppressed individuals (Sharma and Shukla, 2016). Gut bacteria can be exploited in other therapies, such as immune cell boost, and oncolytic bacteria (Silva et al., 2021). One of these approaches is possible with the bacteria *B. animalis*, whose growth is stimulated by the dietary herbal medicine *Gynostemma pentaphyllum*, which has a prebiotic action in this case. This bacterium has enhanced expressions of genes encoding for biogenesis and metabolic pathways of short-chain fatty acid and medium-chain fatty acids, and these molecules are related to host responses in different cellular processes, as RNA processing, *a*-amino acid biosynthesis and metabolism, anion transmembrane activity, and transferase activity. These connected actions reduce polyps in laboratorial mice affected by colorectal cancer (Liao et al., 2021). Another possibility is engineered bacterial immunotherapy, using natural or engineered bacterial strains to deliver antitumor products or drugs, enhance both adaptive and innate immunity. For example, bacterial outer membrane vesicles can generate anticancer cytokines with few side effects (Zhou et al., 2021). In any case, there is still much to be studied in this area. For example, although the modulation of the immune system, targeting neoplasms, by the gut microbiome has improved the survivability of many individuals, predicting post-therapy outcomes is still difficult due to the insufficiency of predictive biomarkers. Thus, the study of the structure of bacterial species associated with tumors and their recovery, and inflammatory indicators,*via via*metagenomics, is fundamental in these predictive studies. *Bifidobacterium* spp. for example, has been used efficiently for treating susceptibility to colitis after treatment with immune checkpoint inhibitors (Schwartz et al., 2019). In addition to *Bifidobacterium* spp. such as *B. pseudolongum*, *L. johnsonii* and *Olsenella* spp. they are related to the significantly increased efficacy of immune checkpoint inhibitors in colorectal cancer mouse models (Wu et al., 2021).

The use of probiotics, prebiotics, synbiotics, and metabiotics should be considered as a complement to other more invasive and hazard therapies, such chemotherapy, surgery, and radiotherapy. 5-fluorouracil is an important drug used in systemic chemotherapy treatment for colorectal cancer, but this therapy has been compromised by the development of chemoresistance, probably due to genetic and epigenetic factors of the patients. *L. plantarum* produces gamma-aminobutyric acid and GABAB receptor-dependent signaling pathway, which can be used as a treatment option for 5-fluorouracil-resistant cells because gamma-aminobutyric acid activates antiproliferative, anti-migration, and anti-invasion effects on the resistant cells. Activated GABAB receptor induces the inhibition of cAMP-dependent signaling pathways and cellular inhibitor of apoptosis protein 2 expression. This system has a predictive biomarker, adjuvant treatment for chemotherapy-resistant cancer cells, chemoprevention, and colon cancer-related diseases treatments potential (An et al., 2021).

Western diets influence colorectal cancer through the modulation of the composition and function of gut microbiome, which can produce oncometabolites or tumor-suppressive metabolites depending on the characteristic of gastrointestinal tract. Energy metabolites for the gut microbiome are essential cofactors for epigenetic enzymes, and they come from the available food to the hosts. Transcriptome profiles can show aberrant epigenetic marks that accumulate during colorectal cancer, indicating the epimutations that drive tumorigenesis. Nevertheless, healthy eating habits, as through dietary fiber, allow them to be metabolized by colonic bacteria into butyrate, short-chain fatty acid and histone deacetylase inhibitor. Butyrate epigenetically upregulates tumor-suppressor genes in colorectal cancer cells and anti-inflammatory genes in immune cells (Bultman, 2017). Anti-cancer drugs, based on histone deacetylase inhibitors, could inhibit tumor cell proliferation or apoptosis. Acetylation marks could be eliminated by the influence of gut microorganisms, featuring an essential epigenetic change in cancer cells (Salek Farrokhi et al., 2020). Patients with active Celiac Disease, carriers of the HLA DR3/DQ2 or HLA DR4/DQ8 haplotypes, show significant increases in the gene expression of several members of the NOD-like receptor family in a gluten-free diet. The regulator of these receptors, NLRX1, was exclusively down-regulated during active disease, allowing for inflammation-induced dysbiosis. These changes were accompanied by changes in the production of

short- and medium-chain fatty acids (Morrison et al., 2022). Food and plant extracts that were fermented by gut microbiome, producing short-chain fatty acids, which act in epigenetics, immunological and molecular signaling pathways, thus playing protective role in colorectal cancer (Shuwen et al., 2019). Colorectal cancer has a genesis related to genetic predisposition and epigenetic events, under heavy influence of gut microbiome. Thus, probiotics, prebiotics and symbiotics can have a potentially positive effect on modulate the host inflammatory response and prevention and treatment of tumor proliferation, metastasis, and cancer inhibition. Galdeano and Perdigon, 2006 highlighted the importance of dosing the use of probiotics, about 10^8 colony forming unit-CFU/day, and the time of intestinal permanence, ranging between 48 and 72 h, characteristics that optimally induce immunostimulation in the host. Metabolites produced in cancer cells environment can induce a chronic inflammatory response by the inflammatory cells and then the predisposing condition for cancer retention. The chronic inflammatory condition is strongly modulated by diet and gut microbiome (Almeida et al., 2019). The next-generation whole-genome sequencing, transcriptome sequencing, and big-data mining pharmacogenomics approaches can make it prospect for new experimental trials specifically for each patient, considering the clinical and pathological history. Therefore, only positive results could be obtained from the administration of probiotics individually for patients, based on their genetic structure, lifestyle, and environmental particularities and seeking to recover the host microbial homeostasis (Vivarelli et al., 2019; Sehrawat et al., 2021).

Dysbiosis, probiotics, epigenetics in diverse types of cancer

There are various levels of epigenetic control by probiotic strains or Live Biotherapeutic Products possible to be envisioned in controlling the proliferation of cancer cells. Gut bacteria can metabolize fiber into butyrate, a short-chain fatty acid and a histone deacetylase inhibitor, that epigenetically upregulates tumor-suppressor genes in cancer cells and anti-inflammatory genes in immune cells.

Supplementation with bacterial mixture composed by *B. longum*, *B. breve*, *B. infantis*, *L. acidophilus*, *L. plantarum*, *L. casei*, *L. bulgaricus*, and *Streptococcus thermophilus*, changed the gut bacterial composition, the abundance of *Lachnospiraceae*, *Streptococcus*, and *Lachnoclostridium*, and could attenuate lung metastasis of melanoma in mice. These effects were achieved through the production of short-chain fatty acids in the gut, as propionate and butyrate, which promote the expression of chemokine ligand 20 in lung endothelial cells and the recruitment of T helper 17, decreasing the number of tumor foci in lungs (Chen et al., 2021).

Not just in cancer, probiotic bacteria are also associated with DNA methylation and the induction of regulatory T-cells, that normally suppress inflammatory, opening the possibility of treatment of allergic and autoimmune disorders, for example. *B. longum* subsp. *Infantis* and *L. rhamnosus* with DNA methylation properties, for example, have a regulatory T cells-inducing capacity, that normally suppress inflammatory events. The methylated CpG oligodeoxynucleotide from *B. longum* could be used as therapeutic vaccine for treating of immunologic diseases, such as the allergic and autoimmune disorders, in which Treg populations are diminished (Li et al., 2020).

A relationship between dysbiosis, microbiome and epigenetic reprogramming can also be found for breast cancer. Both the gut microenvironment and breast tissue participate in this system. In postmenopausal women, an important risk factor for the breast cancer development is the regulation of steroid-hormone metabolism, as estrogens, by the gut microbiome. Thus, diet, probiotics and prebiotics could affect the metabolism of drugs used in immunogenic chemotherapy, which may have an anticarcinogenic action. The gut microbiome produces low molecular weight bioactive substances such as folates, short-chain fatty acids, as butyrate and acetate, and biotin, and contributes to absorption and excretion of zinc, iodine, selenium, cobalt, and others, which are cofactors of enzymes participating in epigenetic processes (Figure 1). For example, butyrate to activate epigenetically silenced genes in cancer cells such as p21 and BAK. In view of these epigenetic processes, probiotic strains can be used in the mitigation of breast cancer, promoting effects in the immune response, leading also to breast tumor cell inhibition (Laborda-Illanes et al., 2020). Epigenetics is possibly associated with the regulation of steroid-hormone metabolism in postmenopausal women, as estrogens, for example, and then be involved in cancer development. In contrast, the gut resident microbiome can modulate mucosal and systemic immune responses.

There are still several gaps in studies on the effectiveness of the use of probiotics strains and Live Biotherapeutic Products in cancer treatments because the metabolic interrelationships among resident microbiome, environmental factors and genetic/epigenetic determinants of the vulnerable host are complex. *Lactobacillus* and other probiotic bacteria can induce specific mechanisms against various infections including cancers through apoptosis, antioxidant activity, immune response, and epigenetics regulation (Figure 1). *L. acidophilus* and *B. longum*, for example, are capable to reduce diarrhea after radiation treatment in cancer patients (Demers et al., 2014). However, further investigations must analyze more data to show the efficiency and type of contribution in mitigating diverse types of cancer using probiotics in clinical practice (Dasari et al., 2017; Drago, 2019). There is no consensus among researchers about the human commensal microbiome is a key determinant in the etiopathogenesis of cancer, but large longitudinal, cohort studies should be a future research priority. However, the microbiome, the environmental factors, and an epigenetically/genetically vulnerable

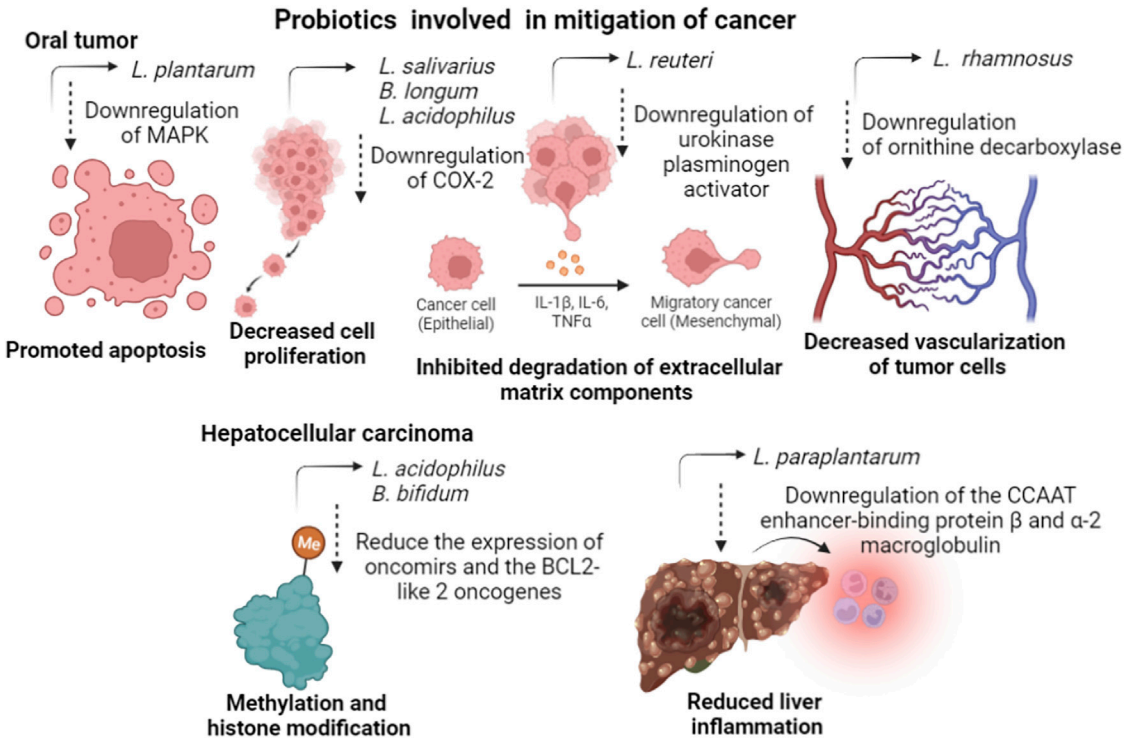

FIGURE 3
The mechanisms of action of some probiotic strains, cited in this review, in mitigating different types of cancer.

host, indicates that multidirectional interactome drives carcinogenesis (Scott et al., 2019). A reliable source of information should be obtained through the metabolome, metagenomics, transcriptome, and analytical chemistry, which are important approaches to understand the role of bacterial communication and the effects of microbiome and probiotics on cancer chemotherapy. For example, the role of the gut microbiome in epithelial tumors, including non-small cell lung, kidney cancer, and melanoma, is done by blocking anti-programmed cell death. Protein 1 or the ligand of these immunotherapy drugs since the use of broad-spectrum antibiotics was associated with the immunotherapy failure. Another example is the fecal microbiota transplantation in mice, in which the level of antitumor $CD8^+$ T cells was increased in immunotherapy responders, while the level of immunosuppressive $CD4^+$ T cells was lower in non-responder's mice (Wan et al., 2021).

Epigenetics mechanistic approaches of probiotics for colorectal cancer mitigation

The effects of using probiotic strains and gut microbiomes in preventing human health are well known and several articles have been published on this subject. These are effects on the immune system, host metabolism, nutrient absorption and vitamin synthesis, increased resistance to opportunistic strains and production of short-chain fatty acids, which are crucial in epigenetic systems, the subject of this review. It is necessary to make it clear that the antitumor mechanisms presented by probiotics are not fully understood.

Different species of *Lactobacillus* are related to upregulate the B-cell lymphoma 2-associated X/B-cell lymphoma 2 ratio, increasing apoptosis in colon cancer cell lines. *L. casei* is also involved with an apoptosis through the upregulated expression of the tumor necrosis factor -related apoptosis-inducing ligand, which was induced by tumor necrosis factor *a*-mediated apoptosis. *L. paracasei* subsp. *Paracasei* and *Bacillus polyfermenticus* can reduce the expression of genes from the cyclin group of cell cycle regulators, associated with tumor development. The use of the probiotic *L. plantarum* inhibits the development of gastric cancer cell lines through the downregulation of the Murine Thymoma Viral Oncogene and upregulation of the phosphatase and tensin homolog, B-cell lymphoma 2-associated X, and toll-like receptor 4. Different species of *Lactobacillus* inhibit the production of interleukin-8 and interferon gamma, attenuating inflammation in gastric epithelial cells and inhibit the adhesion of the bacterium *H. pylori*, linked to the initiation of gastric and colorectal cancer. (Davoodvandi et al., 2021).

TABLE 1 Summary of the performance of probiotic strains evaluated in clinical and laboratory trials, with the references cited in this review.

Cancer	Agent probiotics	Function	Model	References
Colorectal tumor	*Saccharomyces boulardii*	Deregulated pro-inflammatory cytokines	Human	Consoli et al. (2016)
	Bifidobacterium animalis	Biogenesis and metabolic pathways of short-chain fatty acids and medium-chain fatty acids related to RNA processing, biosynthesis and metabolism of *a*-amino acids, transmembrane anionic activity, and transferase activity. These actions reduced polyps	Mice	Liao et al. (2021)
	Lactobacillus plantarum	Produced gamma-aminobutyric acid and GABAB receptor-dependent signaling pathway, which can be used as a treatment option for 5-fluorouracil-resistant cells because gamma-aminobutyric acid activates antiproliferative, anti-migration, and anti-invasion effects on the resistant cells	Human	An et al. (2021)
	Bifidobacterium spp. *Bifidobacterium pseudolongum, Lactobacillus johnsonii Olsenella* spp. *Lactobacillus paracasei* ssp. *Paracasei. Bacillus polyfermenticus*	Related to the increased efficacy of immune checkpoint inhibitors	Mice	Wu et al. (2021a)
		Reduction in the expression of genes from the cyclin group of cell cycle regulators associated with tumor development	Human	Davoodvandi et al. (2021)
Melanoma tumor	*Bifidobacterium longum Bifidobacterium breve Bifidobacterium infantis Lactobacillus acidophilus Lactobacillus plantarum Lactobacillus casei Lactobacillus bulgaricus Streptococcus thermophilus*	Related to the production of short-chain fatty acids in the gut, as propionate and butyrate, which promote the expression of chemokine ligand 20 in lung endothelial cells and the recruitment of T helper 17, decreasing the number of tumor foci in lungs	Mice	Chen et al. (2021)
Breast tumor	*Lactobacillus* spp.	Induced specific mechanisms against various infections including cancers through apoptosis, antioxidant activity, immune response, and epigenetics regulation	Human	Laborda-Illanes et al. (2020)
Colon tumor	*Lactobacillus*	Increased apoptosis	Human	Davoodvandi et al. (2021)
	Lactobacillus casei	Apoptosis through the upregulated expression of the tumor necrosis factor-related apoptosis-inducing ligand, which was induced by tumor necrosis factor *a*-mediated apoptosis	Human	Davoodvandi et al. (2021)
Gastric tumor	*Lactobacillus* spp.	Inhibited the production of interleukin-8 and interferon gamma, attenuating inflammation in gastric epithelial cells and inhibit the adhesion of the bacterium *Helicobacter pylori,* linked to the initiation of gastric and colorectal cancer	Human	Davoodvandi et al. (2021)
	Lactobacillus plantarum	Inhibited the development of cancer cell lines through the downregulation of the Murine Thymoma Viral Oncogene and upregulation of the phosphatase and tensin homolog, B-cell lymphoma 2-associated X, and toll-like receptor 4	Human	Davoodvandi et al. (2021)
Oral tumor	*Lactobacillus plantarum*	Reduced mitogen-activated protein kinase expression and reduced the homeostatic and pathological sequelae caused by intracellular responses under the control of this enzyme	Human	Davoodvandi et al. (2021)
	Lactobacillus salivarius	Decreased the expression level of cyclooxygenase-2 and proliferating cell nuclear antigen, decreasing the effects of the disease	Human	Davoodvandi et al. (2021)
	Lactobacillus rhamnosus	Inhibited of ornithine decarboxylase and decrease the vascularization of tumor cells	Human	Davoodvandi et al. (2021)
	Lactobacillus reuteri	Downregulated the expression level of the urokinase plasminogen activator/urokinase plasminogen activator receptor gene, which is related to the degradation of extracellular matrix components and to cancer metastasis and invasion	Human	Davoodvandi et al. (2021)
	Bifidobacterium longum Lactobacillus acidophilus	Expression level of Interleukin-18 was enhanced, inhibiting the proliferation of cancer cells	Human	Davoodvandi et al. (2021)
Hepatocellular carcinoma	*Lactobacillus acidophilus Bifidobacterium bifidum*	Reduced the expression of oncomirs and the oncogenes BCL2-like 2 and Kristen rat viral sarcoma homolog oncogene through methylation and histone modification processes	Human	Thilakarathna et al. (2021)
	Lactobacillus paraplantarum	Reduced liver inflammation and fibrogenesis by downregulating the CCAAT enhancer binding protein *ß* and *a*-2 macroglobulin expressions	Human	Thilakarathna et al. (2021)

Probiotics may play an important role in the prognosis of tumors, based on the concept that the intestinal microbiota can regulate the immune balance and the "tumor of an organic environment" (TOE), which is related to the tumor microenvironment, and which involves tumor cells, fibroblasts, intratumoral microorganisms and metabolites in the local lesion. TOE also involves the immunity, circulation, metabolism, and gut microbiota closely related to tumor development (Wu et al., 2021). In this context, not so much probiotic strains, but next-generation probiotics and live biotherapeutic products may play an important role in tumor prognosis since they have a more detailed genetic and metabolic relationship with their hosts.

Epigenetics mechanistic approaches of probiotics for mitigation of diverse types of cancer

L. plantarum reduced the expression of mitogen-activated protein kinase in oral cancer cell lines, reducing homeostatic and pathologic sequelae caused by intracellular responses under the control of this enzyme. Still in oral cancer, *L. salivarius* can decrease the expression level of cyclooxygenase-2 and proliferating cell nuclear antigen, decreasing the effects of the disease. Another gene whose inhibition is important for decreasing the vascularization of tumor cells is ornithine decarboxylase, induced by *L. rhamnosus*. The probiotic strain *L. reuteri* can downregulate the expression level of the urokinase plasminogen activator/urokinase plasminogen activator receptor gene, which is related to the degradation of extracellular matrix components and to cancer metastasis and invasion. *B. longum* and *L. acidophilus* treatment of Barrett's esophagus cells downregulated the expression of caudal type homeobox 1, cyclooxygenase-2, tumor necrosis factor α, and phosphoprotein. 53, while the expression level of Interleukin-18 was enhanced, inhibiting the proliferation of cancer cells (Davoodvandi et al., 2021).

Hepatocellular carcinoma is a type of cancer associated with dysbiosis, and its mitigation can go through treatment with probiotic strains capable of regulating cancer suppressor genes. For example, combinations of different species of probiotic strains can upregulate the expression of anti-inflammatory cytokines, such as interleukins 10, 13, and 27; and downregulation of the angiogenic factors and receptors, vascular endothelial growth factor α, Fms related receptor tyrosine kinase 1, angiopoietin 2, and kinase insert domain receptor, contributing to the reduction of tumor growth. Dysbiosis in the gut microbiome disturbs the gut epithelial integrity and promotes the leakage of opportunistic-associated molecular patterns into the hepatic portal circulation. Reaching the liver promotes inflammation by stimulating the immune cells to produce cytokines and chemokines through Toll-like receptors. In this way, the effects of carcinoma can be attenuated through the downregulation of these genes by the action of probiotic strains (Thilakarathna et al., 2021). Probiotic bacteria *L. acidophilus* and *B. bifidum* can reduce the expression of oncomirs and the oncogenes BCL2-like 2 and Kristen rat viral sarcoma homolog oncogene through methylation and histone modification processes. *L. paraplantarum* reduced liver inflammation and fibrogenesis by downregulating the CCAAT enhancer binding protein *ß* and *a*-2 macroglobulin expressions. The probiotic and prebiotic mixture prevented liver fibrosis by the activation of silent information regulator 1 in hepatocytes. (Thilakarathna et al., 2021). Figure 3 presents a summary of the mechanisms of action of probiotic strains in mitigating different types of cancer.

Perspectives

The level of knowledge about the mechanisms of action of probiotic strains in the mitigation of different types of cancer has evolved. The use of probiotics, mainly associated with food, was mostly associated with acting on the immune system and decreasing tumor growth, but with less detailed data on the mechanisms. There is already greater detail at the molecular level, mainly in the communication between host cells and the associated microbiomes*via* chemical signaling, particularly in the regulation of host gene expression, as demonstrated in this review article. Probiotic products have already been used as drugs for treating damage caused by chemotherapeutic drugs, such as gastrointestinal mucositis associated with the use of oxaliplatin. Here, the probiotic mixture BIO-THREE, produced by the Toa Pharmaceutical Co., Ltd. containing the bacterial strains *C. butyricum*, *Bacillus mesentericus*, and *Streptococcus faecalis* was used (Yuan et al., 2022). It is to be expected that probiotic strains with more specific action in metabolic pathways and regulation of genes associated with tumor processes will be used as drugs in precision medicine, not only for the large market that this represents, but for the possibility of developing an effective mitigation system of different types of cancer. Table 1 contains a summary of the performance of probiotic strains evaluated in clinical and laboratory trials, with the references cited in this review.

Conclusion

Dysbiosis is characterized as imbalances in the diversity of the human microbiome, which can lead to the constitution of different diseases, such as diabetes, allergies, autoimmune, autism, Alzheimer's, and cancer. Advent such as the use of antibiotics, environmental toxins, processed foods, led to the loss of diversity in the gut microbiome, causing dysbiosis. A

consequence of dysbiosis could be the epigenetic inheritances, coordinated by gut microbiome, related to cancer inducing. Therefore, the use of probiotic bacterial strains can recover important intestinal functions and controlling dysbiosis. Furthermore, metabolites of these strains, and of next-generation probiotics, can control epigenetic processes. Bacteria able to improve general human health and to mitigate specific diseases through changes in the regulation of microbiome and host genes are characterized as Live Biotherapeutic Products. These bacteria can induce responses in gut microbiome with implications in chemotherapy, radiotherapy, and immunotherapy, through bacterial metabolism of drugs used in therapeutic. The epigenetic control by probiotic strains or Live Biotherapeutic Products is related to the control of proliferation of cancer cells, inactivation ratios of cancerogenic compounds, improvement of the immune response, antiproliferative effects, inhibition of tyrosine kinase, and inflammatory cell infiltration to malignant and stromal cells. There are still several gaps in studies efficiency of the use of probiotics strains and Live Biotherapeutic Products in cancer treatments because the metabolic interrelationships among resident microbiome, environmental factors and genetic/epigenetic determinants of the vulnerable host are complex. Therefore, metabolome, metagenomics, transcriptome, and analytical chemistry are important approaches to understand the role of bacterial metabolism and chemical communication with cancer predisposition and treatments. The use of probiotics, prebiotics, synbiotics, and metabiotics should be considered as a complement to other more invasive and hazard therapies, such chemotherapy, surgery, and radiotherapy. Thus, it is possible that a path of medicine in the times to come will be more patient-specific treatments, depending on the environmental, genetic, epigenetic and microbiome characteristics of the host.

Author contributions

All authors listed have made a substantial, direct, and intellectual contribution to the work and approved it for publication.

Acknowledgments

The author thanks Christiane Pienna Soares for the invitation to participate in this Frontiers collection title “Epigenetic Therapy Against Cancer: Toward New Molecular Targets and Technologies."

Conflict of interest

The authors declare that the research was conducted in the absence of any commercial or financial relationships that could be construed as a potential conflict of interest.

Publisher’s note

Supplementary material

The Supplementary Material for this article can be found online at: https://www.frontiersin.org/articles/10.3389/fgene.2022.921972/full#supplementary-material

References

Almeida, C. V., Camargo, M. R., Russo, E., and Amedei, A. (2019). Role of diet and gut microbiota on colorectal cancer immunomodulation. *World J. Gastroenterol.* 25 (2), 151–162. doi:10.3748/wjg.v25.i2.151

Amabebe, E., Robert, F. O., Agbalalah, T., and Orubu, E. S. F. (2020). Microbial dysbiosis-induced obesity: role of gut microbiota in homoeostasis of energy metabolism. *Br. J. Nutr.* 123 (10), 1127–1137. doi:10.1017/S0007114520000380

An, J., Seok, H., and Ha, E. M. (2021). GABA-producing *Lactobacillus plantarum* inhibits metastatic properties and induces apoptosis of 5-FU-resistant colorectal cancer cells*via*GABAB receptor signaling. *J. Microbiol.* 59 (2), 202–216. doi:10.1007/s12275-021-0562-5

Bangayan, N. J., Shi, B., Trinh, J., Barnard, E., Kasimatis, G., Curd, E., et al. (2020). MG-MLST: characterizing the microbiome at the strain level in metagenomic data. *Microorganisms* 8 (5), 684. doi:10.3390/microorganisms8050684

Bengesser, S. A., Mörkl, S., Painold, A., Dalkner, N., Birner, A., Fellendorf, F. T., et al. (2019). Epigenetics of the molecular clock and bacterial diversity in bipolar disorder. *Psychoneuroendocrinology* 101, 160–166. doi:10.1016/j.psyneuen.2018.11.009

Bultman, S. J. (2017). Interplay between diet, gut microbiota, epigenetic events, and colorectal cancer. *Mol. Nutr. Food Res.* 61 (1), 1500902. doi:10.1002/mnfr.201500902

Chen, C. C., Chen, Y. N., Liou, J. M., and Wu, M. S. (2019). Taiwan Gastrointestinal Disease and *Helicobacter* Consortium. From germ theory to germ therapy. *Kaohsiung J. Med. Sci.* 35 (2), 73–82. doi:10.1002/kjm2.12011

Chen, L., Zhou, X., Wang, Y., Wang, D., Ke, Y., and Zeng, X. (2021). Propionate and butyrate produced by gut microbiota after probiotic supplementation attenuate lung metastasis of melanoma cells in mice. *Mol. Nutr. Food Res.* 65 (15), e2100096. doi:10.1002/mnfr.202100096

Consoli, M. L. D., da Silva, R. S., Nicoli, J. R., Bruña-Romero, O., da Silva, R. G., de Vasconcelos Generoso, S., et al. (2016). Randomized clinical trial: impact of oral administration of Saccharomyces boulardii on gene expression of intestinal cytokines in patients undergoing colon resection. *JPEN. J. Parenter. Enter. Nutr.* 40 (8), 1114–1121. doi:10.1177/0148607115584387

Contreras-Ramos, M., and Mansell, T. J. (2021). Leveraging quorum sensing to manipulate microbial dynamics. *Curr. Opin. Biomed. Eng.* 19, 100306. doi:10.1016/j.cobme.2021.100306

Cordaillat-Simmons, M., Rouanet, A., and Pot, B. (2020). Live biotherapeutic products: the importance of a defined regulatory framework. *Exp. Mol. Med.* 52 (9), 1397–1406. doi:10.1038/s12276-020-0437-6

Cuevas-Sierra, A., Ramos-Lopez, O., Riezu-Boj, J. I., Milagro, F. I., and Martinez, J. A. (2019). Diet, gut microbiota, and obesity: links with host genetics and epigenetics and potential applications. *Adv. Nutr.* 10 (1), S17–S30. doi:10.1093/advances/nmy078

Cui, X., Ye, L., Li, J., Jin, L., Wang, W., Li, S., et al. (2018). Metagenomic and metabolomic analyses unveil dysbiosis of gut microbiota in chronic heart failure patients. *Sci. Rep.* 8 (1), 635. doi:10.1038/s41598-017-18756-2

Dasari, S., Kathera, C., Janardhan, A., Praveen Kumar, A., and Viswanath, B. (2017). Surfacing role of probiotics in cancer prophylaxis and therapy: a systematic review. *Clin. Nutr.* 36 (6), 1465–1472. doi:10.1016/j.clnu.2016.11.017

Davoodvandi, A., Fallahi, F., Tamtaji, O. R., Tajiknia, V., Banikazemi, Z., Fathizadeh, H., et al. (2021). An update on the effects of probiotics on gastrointestinal cancers. *Front. Pharmacol.* 12, 680400. doi:10.3389/fphar.2021.680400

Demers, M., Dagnault, A., and Desjardins, J. (2014). A randomized double-blind controlled trial: impact of probiotics on diarrhea in patients treated with pelvic radiation. *Clin. Nutr.* 33 (5), 761–767. doi:10.1016/j.clnu.2013.10.015

Deng, Y., McDonald, O. G., Means, A. L., Peek, R. M., Jr., Washington, M. K., Acra, S. A., et al. (2021). Exposure to p40 in early life prevents intestinal inflammation in adulthood through inducing a long-lasting epigenetic imprint on TGFβ. *Cell. Mol. Gastroenterol. Hepatol.* 11 (5), 1327–1345. doi:10.1016/j.jcmgh.2021.01.004

Doenyas, C. (2021). Potential role of epigenetics and redox signaling in the gut–brain communication and the case of autism spectrum disorder. *Cell. Mol. Neurobiol.* 42, 483–487. doi:10.1007/s10571-021-01167-3

Drago, L. (2019). Probiotics and colon cancer. *Microorganisms* 7 (3), 66. doi:10.3390/microorganisms7030066

Eslami, M., Yousefi, B., Kokhaei, P., Hemati, M., Nejad, Z. R., Arabkari, V., et al. (2019). Importance of probiotics in the prevention and treatment of colorectal cancer. *J. Cell. Physiol.* 234 (10), 17127–17143. doi:10.1002/jcp.28473

Flandroy, L., Poutahidis, T., Berg, G., Clarke, G., Dao, M. C., Decaestecker, E., et al. (2018). The impact of human activities and lifestyles on the interlinked microbiota and health of humans and of ecosystems. *Sci. Total Environ.* 627, 1018–1038. doi:10.1016/j.scitotenv.2018.01.288

Freitas, P. N. N., Rovida, A. F. D. S., Silva, C. R., Pileggi, S. A. V., Olchanheski, L. R., and Pileggi, M. (2021). Specific quorum sensing molecules are possibly associated with responses to herbicide toxicity in a *Pseudomonas* strain. *Environ. Pollut.* 289, 117896. doi:10.1016/j.envpol.2021.117896

Galdeano, C. M., and Perdigon, G. (2006). The probiotic bacterium Lactobacillus casei induces activation of the gut mucosal immune system through innate immunity. *Clin. Vaccine Immunol.* 13 (2), 219–226. doi:10.1128/CVI.13.2.219-226.2006

García-Solano, J., Turpin, M. C., Torres-Moreno, D., Huertas-López, F., Tuomisto, A., Mäkinen, M. J., et al. (2018). Two histologically colorectal carcinomas subsets from the serrated pathway show different methylome signatures and diagnostic biomarkers. *Clin. Epigenetics* 10 (1), 141. doi:10.1186/s13148-018-0571-3

Kiymaci, M. E., Altanlar, N., Gumustas, M., Ozkan, S. A., and Akin, A. (2018). Quorum sensing signals and related virulence inhibition of *Pseudomonas aeruginosa* by a potential probiotic strain's organic acid. *Microb. Pathog.* 121, 190–197. doi:10.1016/j.micpath.2018.05.042

Laborda-Illanes, A., Sanchez-Alcoholado, L., Dominguez-Recio, M. E., Jimenez-Rodriguez, B., Lavado, R., Comino-Méndez, I., et al. (2020). Breast and gut microbiota action mechanisms in breast cancer pathogenesis and treatment. *Cancers (Basel)* 12 (9), 2465. doi:10.3390/cancers12092465

Li, D., Cheng, J., Zhu, Z., Catalfamo, M., Goerlitz, D., Lawless, O. J., et al. (2020). Treg-inducing capacity of genomic DNA of *Bifidobacterium longum* subsp. *infantis*. *Allergy Asthma Proc.* 41 (5), 372–385. doi:10.2500/aap.2020.41.200064

Liao, W., Khan, I., Huang, G., Chen, S., Liu, L., Leong, W. K., et al. (2021). *Bifidobacterium animalis*: the missing link for the cancer-preventive effect of *Gynostemma pentaphyllum*. *Gut Microbes* 13 (1), 1847629. doi:10.1080/19490976.2020.1847629

Liu, R., Hong, J., Xu, X., Feng, Q., Zhang, D., Gu, Y., et al. (2017). Gut microbiome and serum metabolome alterations in obesity and after weight-loss intervention. *Nat. Med.* 23 (7), 859–868. doi:10.1038/nm.4358

Magalhães-Guedes, K. T. (2022). Psychobiotic therapy: method to reinforce the immune system. *Clin. Psychopharmacol. Neurosci.* 20 (1), 17–25. doi:10.9758/cpn.2022.20.1.17

Mima, K., Nishihara, R., Qian, Z. R., Cao, Y., Sukawa, Y., Nowak, J. A., et al. (2016). *Fusobacterium nucleatum* in colorectal carcinoma tissue and patient prognosis. *Gut* 65 (12), 1973–1980. doi:10.1136/gutjnl-2015-310101

Mishima, Y., and Ishihara, S. (2021). Enteric microbiota-mediated serotonergic signaling in pathogenesis of irritable bowel syndrome. *Int. J. Mol. Sci.* 22 (19), 10235. doi:10.3390/ijms221910235

Monteiro, C. R. A. V., do Carmo, M. S., Melo, B. O., Alves, M. S., Dos Santos, C. I., Monteiro, S. G., et al. (2019). *In vitro* antimicrobial activity and probiotic potential of *Bifidobacterium* and *Lactobacillus* against species of *Clostridium*. *Nutrients* 11 (2), 448. doi:10.3390/nu11020448

Morrison, H. A., Liu, Y., Eden, K., Nagai-Singer, M. A., Wade, P. A., and Allen, I. C. (2022). NLRX1 deficiency alters the gut microbiome and is further exacerbated by adherence to a gluten-free diet. *Front. Immunol.* 13, 882521. doi:10.3389/fimmu.2022.882521

Osadchiy, V., Martin, C. R., and Mayer, E. A. (2019). The gut-brain Axis and the microbiome: mechanisms and clinical implications. *Clin. Gastroenterol. Hepatol.* 17 (2), 322–332. doi:10.1016/j.cgh.2018.10.002

Raskov, H., Burcharth, J., and Pommergaard, H. C. (2017). Linking gut microbiota to colorectal cancer. *J. Cancer* 8 (17), 3378–3395. doi:10.7150/jca.20497

Salek Farrokhi, A., Mohammadlou, M., Abdollahi, M., Eslami, M., and Yousefi, B. (2020). Histone deacetylase modifications by probiotics in colorectal cancer. *J. Gastrointest. Cancer* 51 (3), 754–764. doi:10.1007/s12029-019-00338-2

Schwartz, D. J., Rebeck, O. N., and Dantas, G. (2019). Complex interactions between the microbiome and cancer immune therapy. *Crit. Rev. Clin. Lab. Sci.* 56 (8), 567–585. doi:10.1080/10408363.2019.1660303

Scott, A. J., Alexander, J. L., Merrifield, C. A., Cunningham, D., Jobin, C., Brown, R., et al. (2019). International Cancer Microbiome Consortium consensus statement on the role of the human microbiome in carcinogenesis. *Gut* 68 (9), 1624–1632. doi:10.1136/gutjnl-2019-318556

Sehrawat, N., Yadav, M., Singh, M., Kumar, V., Sharma, V. R., and Sharma, A. K. (2021). Probiotics in microbiome ecological balance providing a therapeutic window against cancer. *Seminars Cancer Biol.* 70, 24–36. Academic Press. doi:10.1016/j.semcancer.2020.06.009

Sharma, M., and Shukla, G. (2016). Metabiotics: one step ahead of probiotics; an insight into mechanisms involved in anticancerous effect in colorectal cancer. *Front. Microbiol.* 7, 1940. doi:10.3389/fmicb.2016.01940

Shuwen, H., Miao, D., Quan, Q., Wei, W., Zhongshan, Z., Chun, Z., et al. (2019). Protective effect of the "food-microorganism-SCFAs" axis on colorectal cancer: from basic research to practical application. *J. Cancer Res. Clin. Oncol.* 145 (9), 2169–2197. doi:10.1007/s00432-019-02997-x

Silva, M., Brunner, V., and Tschurtschenthaler, M. (2021). Microbiota and colorectal cancer: from gut to bedside. *Front. Pharmacol.* 12, 760280. doi:10.3389/fphar.2021.760280

Singh, T. P., and Natraj, B. H. (2021). Next-generation probiotics: a promising approach towards designing personalized medicine. *Crit. Rev. Microbiol.* 47 (4), 479–498. doi:10.1080/1040841X.2021.1902940

Sinha, S. R., Haileselassie, Y., Nguyen, L. P., Tropini, C., Wang, M., Becker, L. S., et al. (2020). Dysbiosis-induced secondary bile acid deficiency promotes intestinal inflammation. *Cell Host Microbe* 27 (4), 659–670. e5. doi:10.1016/j.chom.2020.01.021

Spencer, C. N., McQuade, J. L., Gopalakrishnan, V., McCulloch, J. A., Vetizou, M., Cogdill, A. P., et al. (2021). Dietary fiber and probiotics influence the gut microbiome and melanoma immunotherapy response. *Science* 374 (6575), 1632–1640. doi:10.1126/science.aaz7015

Thi, M. T. T., Wibowo, D., and Rehm, B. H. (2020). *Pseudomonas aeruginosa* biofilms. *Int. J. Mol. Sci.* 21 (22), 8671. doi:10.3390/ijms21228671

Thilakarathna, W. P. D. W., Rupasinghe, H. P. V., and Ridgway, N. D. (2021). Mechanisms by which probiotic bacteria attenuate the risk of hepatocellular carcinoma. *Int. J. Mol. Sci.* 22 (5), 2606. doi:10.3390/ijms22052606

Uhlig, F., Grundy, L., Garcia-Caraballo, S., Brierley, S. M., Foster, S. J., and Grundy, D. (2020). Identification of a Quorum Sensing-Dependent communication pathway mediating Bacteria-Gut-Brain cross talk. *iScience* 23 (11), 101695. doi:10.1016/j.isci.2020.101695

Vascellari, S., Palmas, V., Melis, M., Pisanu, S., Cusano, R., Uva, P., et al. (2020). Gut microbiota and metabolome alterations associated with Parkinson's disease. *mSystems* 5 (5), e00561–20. doi:10.1128/mSystems.00561-20

Vitellio, P., Celano, G., Bonfrate, L., Gobbetti, M., Portincasa, P., and De Angelis, M. (2019). Effects of *Bifidobacterium longum* and *Lactobacillus rhamnosus* on gut microbiota in patients with lactose intolerance and persisting functional gastrointestinal symptoms: a randomised, double-blind, cross-over study. *Nutrients* 11 (4), 886. doi:10.3390/nu11040886

Vivarelli, S., Falzone, L., Basile, M. S., Nicolosi, D., Genovese, C., Libra, M., et al. (2019). Benefits of using probiotics as adjuvants in anticancer therapy (Review). *World Acad. Sci. J.* 1 (3), 125–135. doi:10.3892/wasj.2019.13

Wan, X., Song, M., Wang, A., Zhao, Y., Wei, Z., and Lu, Y. (2021). Microbiome crosstalk in immunotherapy and antiangiogenesis therapy. *Front. Immunol.* 12, 747914. doi:10.3389/fimmu.2021.747914

Wong, S. H., and Yu, J. (2019). Gut microbiota in colorectal cancer: mechanisms of action and clinical applications. *Nat. Rev. Gastroenterol. Hepatol.* 16, 690–704. doi:10.1038/s41575-019-0209-8

Wu, J., Wang, S., Zheng, B., Qiu, X., Wang, H., and Chen, L. (2021a). Modulation of gut microbiota to enhance effect of checkpoint inhibitor immunotherapy. *Front. Immunol.* 12, 669150. doi:10.3389/fimmu.2021.669150

Wu, M., Bai, J., Ma, C., Wei, J., and Du, X. (2021b). The role of gut microbiota in tumor immunotherapy. *J. Immunol. Res.* 2021, 5061570. doi:10.1155/2021/5061570

Xiao, J., Wang, T., Xu, Y., Gu, X., Li, D., Niu, K., et al. (2020). Long-term probiotic intervention mitigates memory dysfunction through a novel H3K27me3-based mechanism in lead-exposed rats. *Transl. Psychiatry* 10 (1), 25–18. doi:10.1038/s41398-020-0719-8

Yang, J., Wei, H., Zhou, Y., Szeto, C. H., Li, C., Lin, Y., et al. (2022). High-Fat diet promotes colorectal tumorigenesis through modulating gut microbiota and metabolites. *Gastroenterology* 162 (1), 135–149. e2. doi:10.1053/j.gastro.2021.08.041

Yuan, W., Xiao, X., Yu, X., Xie, F., Feng, P., Malik, K., et al. (2022). Probiotic therapy (BIO-THREE) mitigates intestinal microbial imbalance and intestinal damage caused by oxaliplatin. *Probiotics Antimicrob. Proteins* 14 (1), 60–71. doi:10.1007/s12602-021-09795-3

Zheng, Z., and Wang, B. (2021). The gut-liver axis in health and disease: the role of gut microbiota-derived signals in liver injury and regeneration. *Front. Immunol.* 12, 775526. doi:10.3389/fimmu.2021.775526

Zhou, C. B., Zhou, Y. L., and Fang, J. Y. (2021). Gut microbiota in cancer immune response and immunotherapy. *Trends Cancer* 7 (7), 647–660. doi:10.1016/j.trecan.2021.01.010

frontiers | Frontiers in Cell and Developmental Biology

TYPE Review
PUBLISHED 14 February 2023
DOI 10.3389/fcell.2023.1116805

OPEN ACCESS

EDITED BY
Ângela Sousa,
University of Beira Interior, Portugal

REVIEWED BY
Xiaolong Cui,
The University of Chicago, United States
Hao Chen,
Southern University of Science and Technology, China

*CORRESPONDENCE
Cristiana Libardi Miranda Furtado,
clibardim@gmail.com

†These authors have contributed equally to this work and share first authorship

SPECIALTY SECTION
This article was submitted to Epigenomics and Epigenetics, a section of the journal Frontiers in Cell and Developmental Biology

RECEIVED 05 December 2022
ACCEPTED 01 February 2023
PUBLISHED 14 February 2023

CITATION
Costa PMdS, Sales SLA, Pinheiro DP, Pontes LQ, Maranhão SS, Pessoa CdÓ, Furtado GP and Furtado CLM (2023), Epigenetic reprogramming in cancer: From diagnosis to treatment. *Front. Cell Dev. Biol.* 11:1116805. doi: 10.3389/fcell.2023.1116805

Epigenetic reprogramming in cancer: From diagnosis to treatment

Pedro Mikael da Silva Costa[1,2†], Sarah Leyenne Alves Sales[1,3†], Daniel Pascoalino Pinheiro[4], Larissa Queiroz Pontes[4,5], Sarah Sant'Anna Maranhão[1], Claudia do Ó. Pessoa[1,2,3], Gilvan Pessoa Furtado[4,5] and Cristiana Libardi Miranda Furtado[6,7]*

[1]Department of Physiology and Pharmacology, Drug Research and Development Center, Federal University of Ceará, Fortaleza, Ceará, Brazil, [2]Postgraduation Program in Biotechnology Northeastern Network of Biotechnology, Federal University of Ceará, Fortaleza, Ceará, Brazil, [3]Postgraduation Program in Pharmacology, Federal University of Ceará, Fortaleza, Ceará, Brazil, [4]Oswaldo Cruz Foundation, FIOCRUZ-Ceará, Sector of Biotechnology, Eusebio, Ceará, Brazil, [5]Postgraduation Program in Biotechnology and Natural Resources, Federal University of Ceará, Fortaleza, Ceará, Brazil, [6]Drug Research and Development Center, Postgraduate Program in Translational Medicine, Federal University of Ceará, Fortaleza, Ceará, Brazil, [7]Experimental Biology Center, University of Fortaleza, Fortaleza, Ceará, Brazil

Disruption of the epigenetic program of gene expression is a hallmark of cancer that initiates and propagates tumorigenesis. Altered DNA methylation, histone modifications and ncRNAs expression are a feature of cancer cells. The dynamic epigenetic changes during oncogenic transformation are related to tumor heterogeneity, unlimited self-renewal and multi-lineage differentiation. This stem cell-like state or the aberrant reprogramming of cancer stem cells is the major challenge in treatment and drug resistance. Given the reversible nature of epigenetic modifications, the ability to restore the cancer epigenome through the inhibition of the epigenetic modifiers is a promising therapy for cancer treatment, either as a monotherapy or in combination with other anticancer therapies, including immunotherapies. Herein, we highlighted the main epigenetic alterations, their potential as a biomarker for early diagnosis and the epigenetic therapies approved for cancer treatment.

KEYWORDS

epigenetic reprograming, cancer, DNA methylation, histone modifications, non-coding RNAs, epidrugs

Introduction

Epigenetic reprogramming and cancer development

Since first described by Conrad Waddington in 1942 (Waddington, 1959), the epigenetic landscape during the differentiation process, where a totipotent undifferentiated cell acquires specialized characteristics and functions, is still a challenge for modern biology (Hunter, 2017). During early development, the whole genome is reprogrammed through epigenetic modifications such as DNA methylation, histone modification and non-coding RNA interaction, that alter chromatin structure and DNA accessibility by establishing a differential gene expression program in a cell-specific manner, without changes on DNA sequence (Skinner, 2011; Olynik and Rastegar, 2012). Epigenetic reprogramming is essential for normal development, as well as the maintenance of cell type-specific epigenetic patterns

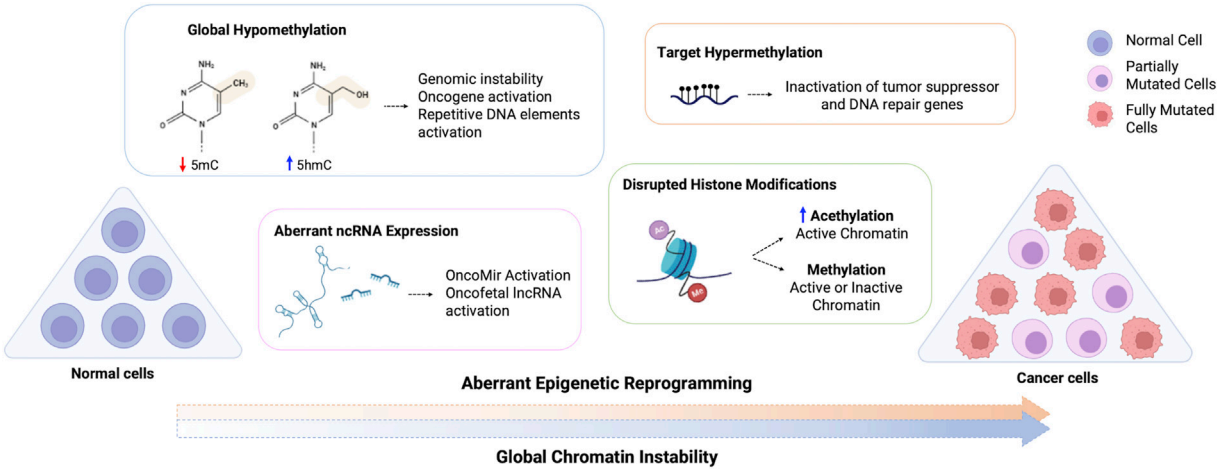

FIGURE 1
Schematic representation of the aberrant epigenetic reprogramming on cancer cells. Normal cells are aberrantly reprogramed through loss of global methylation, altered ncRNA expression, disrupted histone modifications and hypermethylation of target genes, which can inactivate tumor suppressor and DNA repair genes and activate oncogenes, resulting in the global chromatin instability observed in cancer cells. 5mC, 5-methylcytosine; 5hmC, 5-hydroxymethylcytosine.

during cell division. However, given the dynamic and reversible characteristics of the epigenetic modifications, epigenetic reprogramming is strongly affected by environmental factors which play an essential role in the establishment and maintenance of epigenetic markers (Waddington, 1959).

Aberrant epigenetic reprogramming is associated with the etiology of developmental disorders as the imprinting defects (i.e., Beckwith–Wiedemann and Silver–Russell syndromes) (Monk et al., 2019), and complex and multifactorial diseases including metabolic syndrome (Ling and Rönn, 2019), cardiovascular diseases (Handy et al., 2011) and neurological disorders (Chheda and Gutmann, 2017). Due to its ability to regulate cell growth and differentiation pathways, non-mutational epigenetic reprogramming has been added as a hallmark of cancer (Hanahan, 2022) and maybe a driver mutational event in sporadic cancers that promotes genomic instability, tumor initiation and malignant transformation (Feinberg et al., 2006; Feinberg et al., 2016; Hanahan, 2022). These (epi)genetic changes confer a specific phenotype to cancer cells as the uncontrolled growth, resistance to death and increased invasiveness to adjacent tissues and/or spread to other organs (Ilango et al., 2020).

Lifetime disruption in the epigenetic machinery leads to loss of global epigenetic marks, activation of growth-related genes (oncogenes) and silence of cell cycle control genes (tumor suppressor) and DNA repair genes, thereby initiating and propagating tumorigenesis (Figure 1) (Gibney and Nolan, 2010; Feinberg et al., 2016; Hanahan, 2022). These epigenetic features are similar to those observed in early development, where somatic cells are reprogrammed towards a less differentiated state followed by oncogenic reprogramming (Suvà et al., 2013; Feinberg, et al., 2016). The stem-like state or stem progenitor for cancer development is the major challenge in treatment, as it promotes unlimited self-renewal, multi-lineage differentiation and drug resistance (Suvà et al., 2013) Furthermore, alterations in the tumor microenvironment, tumor heterogeneity and regulation of stromal cells are associated with functional abilities acquired through epigenetic reprogramming (Ilango et al., 2020).

Because of the reversible nature of epigenetic changes, the possibility of reprogramming cancer epigenome has become a promising target for both treatment and reversibility of drug resistance (Miranda Furtado et al., 2019). The discovery of chemical compounds that act on the enzymes responsible for the maintenance and establishment of epigenetic mechanisms (epigenetic drugs), changing the epigenetic landscape of a tumor cell, has revolutionized cancer therapy, especially for hematological tumors (Montalvo-Casimiro et al., 2020; Morel et al., 2020). Moreover, the combination of epigenetic drugs with other anticancer therapies, such as chemo, hormonal or immunotherapy has broadened the perspective on the use of these compounds and their effectiveness on treatment. In this review, we present the epigenetic alterations in cancer reprogramming, the main epigenetic drugs and combining therapies for cancer treatment.

Reprogramming DNA methylation in cancer

DNA methylation is an abundant epigenetic marker in the mammalian genome, that is stably maintained during DNA replication. Genome-wide loss of DNA methylation is a recognized epigenetic marker in oncogenic transformation, which is followed by an aberrant reprogramming of the cancer epigenome (Vandiver et al., 2015). The most common DNA modification is the chemical addition of a methyl group to the 5- carbon of the cytosine followed by a guanine (5′CG3′ or CpG, cytosine-phosphate-guanine), giving rise to 5-methylcytosine (5mC) (Geiman and Muegge, 2010). 5mC is a repressive epigenetic mark that aids in maintaining genomic stability as most CpG sequences in the genome are methylated (hypermethylated), except for CpG islands that are hypomethylated and usually encompass

promoters and enhancers (Nishiyama and Nakanishi, 2021). This process is conserved from archaea to eukaryotes, from fertilization to every stage of development, and is carried out by the family of DNA methyltransferases (DNMTs). DNMT1, DNMT3A and DNMT3B are canonical methyltransferase enzymes, while DNMT2 and DNMT3L are non-canonical, without DNMT activity. DNMT1 is involved in the maintenance of DNA methylation, keeping the epigenetic memory in differentiated cells and restoring parental methylation patterns on the nascent DNA strand while DNMT3A and DNMT3B are related to *de novo* DNA methylation (Moore et al., 2013; Lyko, 2018). The role of DNMT2 and DNTM3L are not well understood, but they seem to act on RNA methylation activity and *de novo* DNA methylation, respectively (Schaefer et al., 2010; Veland et al., 2019). DNA methylation during semi-conservative DNA replication occurs with the support of the ubiquitin-like plant homeodomain and RING finger domain 1 (UHRF1) that recognizes CpGs in the hemimethylated DNA, and recruits DNMT1 to restore parental methylation patterns on the nascent strand (Hashimoto et al., 2008).

Global DNA hypermethylation is essential for the maintenance of genome stability, silencing of repetitive elements (transposon and retrotransposons) (Hur et al., 2014) and inactivation of nucleotide-repeat expansion (Poeta et al., 2020). Despite the high stability of DNA methylation, 5mC can be demethylated passively during DNA replication or actively through the oxidation of 5mC to 5-hydroxymethylcytosine (5hmC), with other intermediates (5-formylcytosine, 5fC and 5-carboxylcytosine, 5caC), by the ten-eleven translocated (TET) family of enzymes. The 5hmC is enriched at transcriptionally active regions, such as gene bodies and the borders of promoters and enhancers. The passive process is linked to the absence of DNMT1/UHRF1 which leads to the progressive dilution of cytosine methylation during successive rounds of DNA replication (An et al., 2017). Aberrant active demethylation and increased 5hmC marker at *TOP2A* and *EZH2* genes were associated with poor prognosis in an aggressive subtype of prostate cancer and are related to the activation of oncogenic pathways, such as *MYC* and *E2F*, and TGFβ signaling pathways in metastatic castration-resistant prostate cancer (Palanca-Ballester et al., 2021). On the other hand, loss of 5hmC marker seems to be a common alteration in penile (Rodriguez-Casanova et al., 2021) and oral squamous cell carcinoma (Wang et al., 2017) and myelodysplastic syndrome (MDS) (Cavalcante et al., 2022).

Regions of low CpG density are hypomethylated in cancer, leading to genomic instability thereby facilitating chromosomal rearrangements and DNA damage (Das and Singal, 2004; Baylin and Jones, 2016; Nishiyama and Nakanishi, 2021). However, once carcinogenesis is established, an increased 5mC marker is associated with tumor progression and reduced survival rate (Rodriguez-Casanova et al., 2021). Additionally, site-specific hypomethylation or hypermethylation promotes the activation of proto-oncogenes and the silencing of tumor suppressor genes, respectively (Baylin and Jones, 2011). Among these, genes related to cell cycle progression (e.g., *RB1*, *CDKN2A* and *CDKN2B*), invasion and metastasis (e.g., *CDH1* and *CDH13*) and apoptotic signaling (e.g., *DAPK1*) are hypermethylated in several cancers (Zafon et al., 2019; Nishiyama and Nakanishi, 2021). The transcription factor *MYC*, which is highly expressed during early development and silenced in somatic cells, is overexpressed in almost 70% of cancers (Slamon and Cline, 1984; Madden et al., 2021). Activation of this proto-oncogene by loss of DNA methylation is a common feature of tumor progression and aggressiveness (Souza et al., 2013). Increased chromatin accessibility at *MYC* locus is observed across different cancer types (Corces et al., 2018).

Biallelic expression of imprinted genes or loss of imprinting (LOI) is frequently observed in human cancers (Jelinic and Shaw, 2007), and is an early event for some tumors, such as the childhood Wilms' tumor (WT) (Graf et al., 2021). The imprinting control regions (ICR) are differentially methylated (DMR) in a parent-of-origin manner, resulting in a monoallelic expression of the clustered genes. LOI at the H19/IGF2 locus, for example, is associated with WT in overgrowth syndromes (Graf et al., 2021), and other cancers such as bladder (Byun et al., 2007) and colorectal (Hidaka et al., 2018). LOI of KvDMR1, INPP5Fv2-DMR and RB1-DMR is also implicated in the pathogenesis of cancer (Rumbajan et al., 2013). A comprehensive analysis of The Cancer Genome Atlas showed that the imprinted genes *CDKN1C* and *PEG3* are downregulated in primary tumors, while the *MEST*, *PHLDA2* and *GNAS* were frequently upregulated. As the ICRs are enriched by long ncRNAs (lncRNAs), LOI promotes the overexpression of these regulatory elements during carcinogenesis (Kim et al., 2015).

Loss of function of DNMTs and TETs enzymes during cell differentiation and growth is also related to oncogenic transformation. Mutations in *DNMT3A*, *TET1/2* and *IDH1/2* are recurrent in leukemia and lymphoma (Guillamot et al., 2016). *TET2* mutations are associated with aberrant DNA methylation in a wide spectrum of myeloid malignancies, including myelodysplastic syndrome (MDS), myeloproliferative neoplasms (MPN), myelomonocytic leukemia (CMML), and acute myeloid leukemia (AML). Somatic mutations in *TET* family are linked to changes in the regulation of stem cell differentiation and transformation (Cimmino et al., 2011; An et al., 2017). *DNMT3A* mutations lead to loss of methylation and promote AML transformation, while abnormal CpG island hypermethylation dependent on DNMT3A is observed during AML progression (Spencer et al., 2017). *TET1* and *TET2* reduced expression levels have been frequently observed in hepatocellular carcinoma tissues (Wang P. et al., 2019). Mutational events at chromatin remodeling factors and *Wnt* signaling pathway promote aberrant DNA methylation pattern in human tumors (Saghafinia et al., 2018). Somatic mutations and microsatellite instability also affect cancer epigenome (Velho et al., 2014).

Besides the most common DNA methylation that occurs at CpG sites, non-CpG methylation at CpA and CpT are emerging epigenetic markers in eukaryotes. These modifications, especially the CpA methylation, which gave rise to N6-methyladenine (6mA), were first recognized in embryonic stem cells and seem to be mediated by the DNTM3A (Ramsahoye et al., 2000). Other enzymes may affect 6mA levels, such as the methyltransferase N6AMT1 and the demethylase ALKBH1 (Kweon et al., 2019; Shen et al., 2022). Although the low abundance of 6mA is observed in the mammalian genome under normal conditions, several studies indicated dynamic changes in 6mA levels during development and cancer. A lower abundance of the 6mA marker was observed in glioma cells (Kweon et al., 2019), whereas an increased 6mA was shown in hepatocellular carcinoma (Lin et al., 2022). A decrease of genomic DNA 6mA, accompanied by decreased methyltransferase N6AMT1 and increased demethylase

ALKBH1 levels promotes tumorigenesis and is associated with poor prognosis in cancer patients (Xiao et al., 2018).

DNA methylation can also be detected in liquid biopsies, a minimally invasive procedure that has emerged as a promising element in cancer early detection. Liquid biopsies allow the monitoring of the molecular landscape of circulating tumor elements in body fluids in the search for new biomarkers of cancer diagnosis, prognosis and therapy (Martins et al., 2021; Michela, 2021). Cell-free circulating tumor DNA (ctDNA) exhibits both genetic and epigenetic cancer-related mutations making it possible to detect malignant lesions, monitor tumor evolution, metastasis and recurrence and predict treatment response (Luo et al., 2021; Li et al., 2022). Since aberrant DNA methylation is an early event in carcinogenesis, ctDNA methylation analysis has been used for cancer screening in clinical oncology. Considering that each cell group has a unique epigenetic signature, ctDNA methylation allows to tracing the origin of tissue in cancer patients (Luo et al., 2021).

Circulating SEPT9 methylation assay has been used as a CRC biomarker with increased specificity and sensitivity (DeVos et al., 2009; Church et al., 2014) and was the first blood-based screening approved by the FDA (Luo et al., 2021). *SHOX2* DNA methylation assay was used to distinguish between malignant and benign lung disease from bronchial aspirates (Schmidt et al., 2010). Afterwards, a plasma-based assay was used to detect small cell lung cancer and squamous cell carcinoma with high sensitivity (Kneip et al., 2011). Cell-free DNA (cfDNA) methylation of 15 DMRs allowed the detection and stratification between high and low-risk ovarian cancer (Liang et al., 2022). Similarly, other tumors, as breast, prostate and colorectal used cfDNA methylation to differentiate malignant and normal lesions, and prognosis stratification (Zhang et al., 2021c; Wu Q. et al., 2021; Chen et al., 2022a; Rodriguez-Casanova et al., 2022). Besides target ctDNA methylation, cell-free genome-wide 5hmC has been recently used for cancer diagnosis and prognosis stratification (Song et al., 2017; Xu et al., 2021; Shao et al., 2022). Despite the advances and promising use of cfDNA methylation in clinical oncology, there are some technical limitations that need to be addressed for use in clinical practice as a standard diagnostic tool (Heidrich et al., 2021; Lone et al., 2022).

DNA methylation has been widely investigated in oncology due to its control of time- and tissue-specific gene expression, inactivation of repetitive DNA and the maintenance of genomic stability during cancer initiation and progression. Further, the epigenetic reprogramming of undifferentiated cells through waves of DNA methylation and demethylation, can aberrantly reprogram the stem cell epigenome and promote cancer differentiation, recurrence, and resistance to treatment. Also, 5mC participates in the acquisition of other epigenetic markers as histone modification and ncRNA expression (Das and Singal, 2004; Geiman and Muegge, 2010). Herewith, DNA methylation is an important epigenetic marker for cancer diagnosis, with direct implications for survival rate and an emergent target for drug development.

Aberrant histone modification

Another important epigenetic mark is the chemical modification of histone proteins. Histones assist DNA packaging into a highly organized chromatin structure. DNA is wrapped around a histone octamer (H2A, H2B, H3 and H4), linked by the histone H1 to form the nucleosome, a core structure of the chromatin (Lawrence et al., 2016). The amino-terminal tails of histone proteins are frequently subject to multivalent post-translational modifications (PTM), such as acetylation, phosphorylation, methylation and ubiquitination, altering the degree of local chromatin condensation, and consequently interfering in gene expression and DNA accessibility (Demetriadou et al., 2020). Non-conventional modifications can also occur in histones, such as citrullination/deamination, sumoylation, formylation and propionylation, among others (Tweedie-Cullen et al., 2012).

The most studied histone modifications are methylation and acetylation, however, unlike DNA methylation, histone modifications can either be an active or repressive epigenetic marker, depending on the modification and the modified amino acid group. Many enzymes catalyze methylation at histone protein, such as the histone methyltransferases (HMTs) and demethylase (HDM), lysine methyltransferases (KMTs) and demethylases (KDMs, also known as LSD), protein arginine methyltransferases (PRMTs), among others (Husmann and Gozani, 2019; Wu X. et al., 2021). This modification is frequently observed in lysine (K) and arginine (R) residues and is related to different transcriptional states (active or inactive) (Greer and Shi, 2012). Histone acetylation is a common modification in the lysine amino acid that is catalyzed by histone acetyltransferases (HATs) and histone deacetylases (HDACs). Acetylation, on the other hand, is usually an epigenetic marker of transcriptional activation (Bannister and Kouzarides, 2011).

The combination of these modifications is responsible for maintaining chromatin structure, which is dynamic and plays key role in development and cell differentiation. Aberrant reprogramming of histone modifications is often observed in the pathogenesis of cancer, changing chromatin accessibility, and altering the expression of target genes, subsequently affecting malignant progression (Zhao and Shilatifard, 2019). The imbalance of genome-wide histone methylation changes cell growth and may favor tumorigeneses. The enrichment of the tri-methylation at H3 lysine 9 (H3K9me3) and lysine 27 (H3K27me3), a repressive epigenetic marker found many promoters region, drives oncogenic transformation and chemoresistance (Torrano et al., 2019). Overexpression of *EZH2* (Enhancer of zeste homolog 2), a member of the polycomb proteins which is responsible for the tri-methylation of H3k27 and inactive chromatin state, is a marker of cancer initiation, progression, metastasis and targeted therapy (Chase and Cross, 2011; Duan et al., 2020). Although histone arginine methylation is a less typical and complex marker, increased expression of PRMT and enrichment of methylation at H3 arginine residues (H3R8, H3R3 and H3R2) is observed in digestive cancer cells (Chen et al., 2020).

Monoacetylation at H4K16 (H4K16ac) is a conserved marker that increases chromatin accessibility and gene activation. Reduced levels of the active H4K16ac and H4K20me3 histone modifications are a hallmark of cancer, perhaps by promoting the loss of DNA methylation at repetitive sequences (Fraga et al., 2005). The H3K27ac is often observed in active promoter and enhancer regions and is dysregulated with prognostic value for thyroid tumors (Zhang et al., 2021a). Increased active H3K27ac and

reduced repressive H3K27me3 markers seem to be a driver mutation in high-grade gliomas, which is related to the activation of endogenous retroviruses (EVRs) and promotes therapeutic sensibility to demethylating agents (Krug et al., 2019). Histone H3 and H4 acetylation (H3K9, H3K18 and H4K12) and di-methylation (H4R3 and H3K4), an epigenetic marker of transcriptional activation, predicts molecular heterogeneity in prostate cancer with prognostic value (Seligson et al., 2005).

Post-translational modifications of histones, histone variants and histone-associated DNA modifications can be detected in liquid biopsies using circulating nucleosome (Bauden et al., 2015). Intact nucleosomes are released form cells after death and has been used as a biomarker for early diagnosis and monitoring of various types of tumors (Deligezer et al., 2010; Bauden et al., 2015; Van den Ackerveken et al., 2021). H4K20me3 and H3K27me3 histone modification at circulating nucleosomes is reduced in the plasma of patients with colorectal cancer (Gezer et al., 2015). H3K9me3 marker in the blood plasma was found decreased of patients with colorectal cancer and increased in patients with multiple myeloma (Deligezer et al., 2010). Elevated number of circulating nucleossome have been reported in many tumors (Bauden et al., 2015), and is associated with tumor recurrence and metastasis in breast cancer (Mego et al., 2020b; Mego et al., 2020a). Global analysis of histone PTMs showed 13 modifications specifically related o colorectal cancer and an increasing in methylation of histone H3K9 and H3K27, acetylation of histone H3 and citrullination of histone H2A1R3 (Van den Ackerveken et al., 2021).

The dynamic of histone modifications and modifiers changes chromatin landscape and genomic function and control cancer cell phenotype and promotes disease progression. Although the increased identification of histone modifications and the complex regulatory machinery made possible by the advancement of high-throughput technologies, much still needs to be revealed about the function of each modification and the implications for cancer development. Even though these modifications are predictive of clinical outcomes, targeting histone modifiers is a promising epigenetic therapy in anticancer drug discovery.

Non-coding RNAs as cancer biomarkers

In the human genome, the protein-coding genes represent less than 2%, whereas a large fraction is constituted by regions that are transcribed into non-coding RNAs (ncRNAs), which retain fundamental biological properties within cells, controlling gene expression in a cell-specific manner. Besides its function in the regulation of transcription, ncRNAs also influence the translation as components in the protein synthesis machinery and regulate other ncRNAs function in a complex network (Ratti et al., 2020). Therefore, roles of ncRNAs in physiology and pathology are recognized, including developmental, gametogenesis, stress, immune response, and tumorigenesis (Aprile et al., 2020; Ratti et al., 2020; Taniue and Akimitsu, 2021).

Among ncRNAs, the small ncRNAs (<200 nucleotides, nt) and long ncRNAs (>200 nt) have important roles in cancer development, acting both as oncogenic and tumor suppressor molecules (Ratti et al., 2020). MicroRNAs (miRNA) and small interfering RNA (siRNAs), are small ncRNA duplex, approximately 18–31 nucleotides long, that regulates gene expression at the post-transcriptional level through target block of translation and/or degradation (Zhang et al., 2021b; Torsin et al., 2021). Both miRNA and siRNA have been extensively investigated as molecular markers of cancer and therapeutic agents. The main difference is that the siRNA is highly specific to the target, while the miRNA can target several molecules simultaneously, regulating multiple pathways to maintain physiological homeostasis (Lam et al., 2015; Cuciniello et al., 2021). Aberrant miRNA expression has been reported in several cancer types, inducing cell proliferation, invasion, and resistance to death by activating oncogenes and silencing tumor suppressor genes (Peng and Croce, 2016).

Long non-coding RNAs (lncRNAs, >200 nt) are the most abundant class of ncRNAs in the human genome (Slack and Chinnaiyan, 2019). LncRNAs arise from intergenic regions or are clustered with protein-coding genes (intronic or in gene-dense regions) and like protein-coding genes, their promoter regions are globally enriched with histone modifications, such as H3K27ac, H3K4me3 and H3K9ac (Quinn and Chang, 2016; Taniue and Akimitsu, 2021). The abundant class of lncRNAs modulate gene expression in a complex intracellular network of crossed interactions (competing endogenous RNA networks, or ceRNET) through chromatin remodeling, either as *cis* or *trans* elements, targeting specific sequences at the transcriptional and translational level and participating in post-translational modifications (Engreitz et al., 2016; Yao et al., 2019). Therefore, the lncRNAs, and their protein-and RNA-based regulation, added complexity to the cytoplasmatic post-transcriptional and translation control, orchestrated before by miRNAs and proteins (Aprile et al., 2020).

Many lncRNAs are highly expressed during development and participate in cell growth and differentiation pathways (Cabili et al., 2011). Thus, their modulation in different intracellular pathways, such as cell survival and proliferation, glucose metabolism, apoptosis, metastasis formation, and drug resistance, results in the tumor phenotype (Luo et al., 2018; Hu et al., 2020; Wan et al., 2020; Liang et al., 2022). Disruption of lnRNA expression or stability affects the expression of the neighboring genes (Horlbeck et al., 2020) and promotes chromosomal rearrangements (Yin et al., 2021) modulating several hallmarks of cancer and fostering progression. Moreover, several lncRNAs are transcriptionally regulated by oncoproteins or tumor suppressors, which are directly related to tumorigenesis (Guttman et al., 2009; Taniue et al., 2016).

Other classes of ncRNAs, such as small nucleolar RNA (snoRNAs), involved in RNA modifications and ribosome biogenesis; small nuclear RNAs (snRNAs), involved in pre-mRNA processing; piwi-interacting RNAs (pi-RNAs), which is mainly functional in the germline, inhibiting the transcription and movement of retrotransposons, repetitive sequences, and other mobile elements, have also been implied in cancer development and progression (Zhang et al., 2021b; Xiao et al., 2022). Moreover, circular RNAs (circRNAs), single-stranded covalently closed RNA loops, which act as transcriptional regulators, miRNA sponges and splicing and protein translation regulators, are also abundant in cell cytoplasm, and widely distributed in body fluids and cell-free samples, playing critical roles in tumorigenesis (Zhao et al., 2021).

Besides the main function of ncRNAs in cellular compartments, ncRNAs can also be released from the cell and transported in body fluids through exosomes or RNA binding proteins (RBPs), targeting molecules outside the production site, being a promising minimally invasive cancer biomarker (Qi et al., 2016). Circulating RNAs (as ncRNAs) are easy to be sampled in liquid biopsies and can be used as diagnostic biomarkers in the early detection of cancer, before radiologic and imaging events, as well as for prognosis, monitoring disease evolution and adjustments of treatment (Pardini et al., 2019). Due to their specificity and stability, circulating ncRNAs can provide accuracy and sensitivity for the screening of different human cancers (Slack and Chinnaiyan, 2019). Indeed, there are a large variety of ncRNAs that might be used as cancer biomarkers in liquid biopsies. Among them, the most studied are miRNAs, but more recently also pi-RNAs, circRNAs, and other sncRNAs. The lncRNAs also represent a versatile and promising group of molecules which, besides their use as biomarkers, have also a possible therapeutic role (Pardini et al., 2019).

One of the first described miRNA, and probably the most recurrently detected as a cancer biomarker, is the oncomiR miR-21. This miRNA is implicated in various signaling pathways, and its upregulation results in the inactivation of several tumor suppressors. Altered miR-21 expression is often observed in many cancer types, including digestive, respiratory, hematological, gynecological and brain malignancies (Kumarswamy et al., 2011; Pardini et al., 2019). MiR-21 was also upregulated in serum samples from patients with renal cell carcinoma (RCC), as well as miR-210 and miR-144-3p, and the upregulation of miR-21 was positively correlated to tumor stage (Zhao et al., 2013; Lou et al., 2017; Tusong et al., 2017). On the contrary, miR-508-3p and miR-509-5p were decreased in plasma samples of RCC patients (Zhai et al., 2012). Furthermore, miR-155 has been also reported as dysregulated in serum/plasma samples in gastroenterology malignancies, lung, breast, ovary, and hematologic malignancies (Larrea et al., 2016; Chen et al., 2017; Giannopoulou et al., 2019). Likewise, miR-141 and miR-375 were upregulated in serum and plasma exosomes of patients with metastatic prostate cancer (Hessvik et al., 2013; Samsonov et al., 2016). Although promising, miRNAs are not specific to one type of cancer, therefore understanding the implication of miRNAs in specific pathways and finding the most sensitive and specific ones is still challenging (Pardini et al., 2019).

LncRNAs, particularly circular lncRNAs, are stable circulating ncRNAs used as cancer biomarkers. In this context, overexpression of the oncogenic lncRNA MALAT1 in non-small cell lung cancer (NSCLC) tissue is related to reduced overall survival and could be a potential prognostic biomarker and therapeutic target in early-stage lung cancer (LC) (Gutschner et al., 2013; Huang et al., 2017; Lu et al., 2018). Otherwise, circulating MALAT1 expression is lower in patients with LC when compared to healthy controls (Weber et al., 2013; Guo et al., 2015). Another lncRNA overexpressed in LC is the imprinted gene *H19* which is associated with carcinogenesis from early stages to metastasis, reduced disease-free survival (DFS) time, and poor prognosis. Plasma level of the lncRNA H19 is also increased in NSCLC patients (Ge and Yu, 2013; Luo et al., 2018; Yin et al., 2018). In the same context, the imprinted lncRNA KCNQ1OT1 (LIT1) is dysregulated in human tumors (Nakano et al., 2006), and seems to be related to chemoresistance in tongue squamous cell carcinoma and poor prognosis (Guo et al., 2014).

Wang and collaborators demonstrated that the lncRNA colon cancer-associated transcript 2 (CCAT2) was significantly overexpressed in colorectal cancer (CRC) tissues of CRC patients when compared to healthy controls. Overexpression of CCAT2 was also seen in serum and serum-derived exosomes of the CRC patients (Wang L. et al., 2019). Likewise, in AML, the lncRNAs SBF2-AS1, DANCR, LINC00239, LINC00319, LINC00265 and LEF1-AS1 are overexpressed. Whereas the lncRNA H22954 is downregulated, and its decreased expression is related to a higher risk of relapse (Zimta et al., 2019). In gastric cancer (GC), different lncRNAs are related to drug resistance, by modulating the expression of drug resistance-related genes, such as the oncogenic lncRNAs MACC1-AS1, PVT1 and HAGLR, which are upregulated and promote 5-FU resistance in GC cells (Liu et al., 2022).

CircRNAs have been reported to play important roles in cancer growth, metastasis, and resistance to therapy (Su et al., 2019). In this context, Zhang et al. reported that circUBAP2 was overexpressed in osteosarcoma cells, and its knockdown inhibited cell proliferation and promoted cell apoptosis. CircUBAP2 acts inhibiting the expression of miR-143, thus enhancing the expression of Bcl-2, an important anti-apoptotic molecule (Zhang et al., 2017a). Likewise, circNFIX was found overexpressed in glioma and inhibited apoptosis through sponging miR-34a-5p, regulating NOTCH1 expression (Xu et al., 2018). In NSCLC, circSNAP47 expression, through the miR-1287/GAGE axis, is correlated with metastasis and associated with decreased overall survival (Li et al., 2018). On the other hand, circSHPRH in NSCLC is associated with downregulated metastasis and improved overall survival (Liu et al., 2018).

Due to the important role of ncRNAs in many biological processes through chromatin remodeling, gene expression regulation, protein synthesis and post-translational modifications, these regulatory RNAs have emerged as an important biomarker for cancer diagnosis, with implications in disease prognosis, drug resistance and targeted therapy. Additionally, the possibility to detect small and long ncRNAs in cell-free body fluids and liquid biopsies, circulating ncRNAs represents a new class of minimally invasive biomarkers for the early diagnosis of cancer.

Epigenetic modifications in ncRNAs

RNA modifications have emerged as important post-transcriptional regulators of gene expression patterns and have shown significant implications in several human diseases, including cancer (Barbieri and Kouzarides, 2020; Nombela et al., 2021). These modifications can be divided into two categories: reversible, which include chemical modifications, i.e., the different types of RNA methylation, such as cytosine and adenosine methylation; and non-reversible, i.e., editing and splicing, including the formation of circular RNAs (Esteller and Pandolfi, 2017). Most of the time, those chemical modifications are dynamic, as a result of adaptation to the cell environment, however, they can also be transmitted during mitosis and meiosis.

The epitranscriptome scenery is complex, and more than 170 different types of chemical modifications are described for coding and ncRNAs (Boccaletto et al., 2018). A familiar chemical modification of some RNAs affects its 5′-end, the well-known

"5′cap", and the most characterized cap modification is the addition of an N^7-methylguanosine (m^7G) (Ramanathan et al., 2016). Another frequent modification in RNAs is the 5-methylcytosine (m^5C), first thought to be present only in tRNAs and rRNAs, and later identified in other RNA transcripts, which might have a role in miRNA targeting (Squires et al., 2012). The lncRNA XIST, for example, is regulated by m^5C where cytosine methylation has been shown to interfere with the binding of the histone modifier PRC2 (Amort et al., 2013). Importantly, m^5C is not a static mark of RNA, and can be demethylated to 5-hydroxymethylcytosine. RNA can also be modified at adenosines in the form of N^6-methyladenosine (m^6A) and N^1-methyladenosine (m^1A). m^6A is the most abundant internal modification of mRNA (Lee et al., 2014), but it is also relevant for miRNAs controlling their maturation and expression levels. m^6A is also found in lncRNAs, being required, for example, for the efficient transcriptional repression mediated by the lncRNA XIST and modulating the structure of lncRNA MALAT1, which is associated with cancer malignancy (Patil et al., 2016; Zhang et al., 2017b). Pseudouridylation, the 5′-ribosyluracil isomers of uridine, is a common modification in ncRNAs, including tRNA, rRNA and snoRNAs and lncRNAs (Ge and Yu, 2013; Schwartz et al., 2014).

All those RNA modifications are dynamic, allowing rapid cellular responses to environmental signals, and finely regulating several molecular processes within the cell: altering RNA metabolism, splicing or translation; RNA stability or intracellular localization; binding affinity to RBPs or other RNAs; and finally diversifying (epi)-genetic information (García-Vílchez et al., 2019; Gkatza et al., 2019; Nombela et al., 2021). Although RNA modifications are not alone considered cancer drivers, the resulting ability of them to modulate several processes of RNA metabolism, leads to aberrant expression of important genes functionally related to survival proliferation, self-renewal, differentiation, migration, stress adaptation, and resistance to therapy, all of which are hallmarks of cancer. Alterations in the expression of m^6A writers (i.e. METTL3 and METTL14), erasers (i.e. FTO) or readers (i.e. YTHDC2 and YTHDF1), for example, are associated with tumor-suppressive or tumor-promoting scenarios (Blanco et al., 2016; Cui et al., 2017; Jin et al., 2019; Nombela et al., 2021).

In hepatocellular carcinoma (HCC), for example, the mutation frequency of m^5C regulatory genes is high, and their dysregulation is associated with higher stages of HCC (He et al., 2020). In bladder cancer, NSUN2 and m^5C reader YBX1 are upregulated, which are positively correlated with T and N stages, and poor disease-free survival in those patients (Chen et al., 2019). In breast cancer cell lines, 2′-O methylation appeared to be hypermodified in rRNA and correlated with altered protein translation (Belin et al., 2009). Modifications in tRNA, which includes m^5C or 5-methoxycarbonylmethyluridine (mcm^5U), have been also reported in breast cancer, and correlate with altered translation (Begley et al., 2013; Delaunay et al., 2016; Nombela et al., 2021). In bladder cancer cells, METTL3 promotes the maturation of miR-221/222 in an m^6A-dependent manner, which causes PTEN reduction, leading to cell proliferation and tumor growth (Han et al., 2019). In HCC, METTL14 promotes the m^6A-dependent processing of pri-miR-126, and its depletion reduces m^6A levels and expression of miR-126, leading to cancer cell migration and invasion (Ma et al., 2017). In nasopharyngeal carcinoma (NPC), the oncogenic lncRNA FAM225A stabilized by m^6A modifications serve as a sponge for miR-590-3p and miR-1275, activating the FAK/PI3K/Akt signaling pathway and promoting tumorigenesis and metastasis (Zheng et al., 2019). Therefore, strategies aiming these aberrant post-transcriptional RNA modifications in cancer cells may be an efficient targeted therapy for tumors.

Epigenetic treatment in cancer

Genetic changes, including genetic mutations, are difficult to reverse, unlike epigenetic modifications which are reversible and can be modulated by pharmacological agents (Zhang et al., 2020). The epigenomic´s reprogramming, leading to changes in the cell landscape, reveals a promising therapeutical approach (Miranda Furtado et al., 2019). Many small molecules targeting epigenetic key enzymes, called epigenetic drugs or epidrugs (Table 1), have been discovered and new compounds that modulate epigenetic marks (Figure 2) are being developed focusing on cancer treatment (Xiao et al., 2021) (Jin et al., 2022b). Epidrugs promotes disruption of transcriptional and post-transcriptional modifications, acting manly on tumor suppressor and DNA repair gene activation (Rodríguez-Paredes and Esteller, 2011; Ghasemi, 2020). These drugs are tumor and disease stage specific and the side effects are mostly related to hematologic disorders like leukopenia, neutropenia and thrombocytopenia, and gastrointestinal symptoms as nausea, emesis, diarrhea and constipation (Table 1) (San Miguel Amigo et al., 2011; Bubna, 2015). Most of the side effects are reversed after treatment cessation and taper off with the use of appropriate medicines (Götze et al., 2010; Dong et al., 2012).

The first epigenetic drug approved by the United States Food and Drug Administration (FDA) was azacitidine (Vidaza®) in 2004 for MDS and chronic myelomonocytic leukemia (Kaminskas et al., 2005), followed by decitabine (Dacogen®) approved in 2006 to treat MDS (Steensma, 2009). Both azacitidine and decitabine are two analogues of the cytidine nucleoside in which the carbon atom in position 5, in the pyrimidine ring, has been replaced by a nitrogen (Derissen et al., 2013). Initially, these compounds were planned as cytotoxic agents, but it was found that low dose exposition could cause DNA demethylation by inhibiting the DNMT1 enzyme responsible for maintaining DNA methylation (Stresemann and Lyko, 2008). These so-called 'hypomethylating agents' have been used in myeloid malignancies for more than 1 decade, even though, 50% of patients do not respond initially or during repeated cycles of treatment (Zhao et al., 2021; Šimoničová et al., 2022).

Guadecitabine is a second-generation DNA methylation inhibitor being developed for AML and MDS treatment. It consists of a dinucleotide of decitabine and deoxyguanosine which is resistant to cytidine deaminase, the enzyme which is responsible for decitabine inactivation (Stomper et al., 2021). Guadecitabine might replace azacitidine and decitabine in a near future, due to its higher stability, safety profile and ease of administration (subcutaneous) (Daher-Reyes et al., 2019). Another class of epigenetic drugs are the histone deacetylase inhibitors (HDACi) which increase histone acetylation, an epigenetic mark of transcriptional activation, leading to an

TABLE 1 Epigenetic drugs approved by FDA.

Epigenetic target	Compound	Clinical name	Disease	Administration	Side effects	Company	Approved by (Year)
DNMT1	Azacitidine	Vidaza®	MDS	Intravenous	Neutropenia, thrombocytopenia, nausea, emesis, diarrhea, and constipation	Pharmion Corporation	United States FDA (2004)
	Decitabine	Dacogen®	MDS	Intravenous	Prolonged myelosuppression (neutropenia and thrombocytopenia)	Janssen Pharmaceuticals	United States FDA (2006)
HDACs class I and HDAC6	Suberoylanilide hydroxamic acid (SAHA)	Vorinostat®	CTCL	Oral	Fatigue, nausea, diarrhea, and thrombocytopenia	Merck	United States FDA (2006)
HDAC6	Romidepsin	Istodax®	CTCL	Intravenous	Fatigue, nausea, leukopenia, granulocytopenia, and thrombocytopenia	Celgene	United States FDA (2009)
pan-HDACi	Belinostat	Beleodaq®	T-cell lymphoma	Intravenous	Nausea, vomiting, fatigue, pyrexia, and anemia	Topo Target	United States. FDA (2014)
	Panobinostat	Farydak®	Multiple myeloma	Oral	Diarrhea, peripheral neuropathy, asthenia, fatigue, neutropenia, thrombocytopenia, and lymphocytopenia	Novartis	United States FDA (2015)
HDAC1, HDAC2 HDAC3 and HDAC10	Tucidinostat	Epidaza®	PTCL	Oral	Fatigue, anorexia, thrombocytopenia, leukopenia, neutropenia	Chipscreen Biosciences	China FDA (2014)

DNMT, DNA, methyltransferase; HDAC, histone deacetylases; MDS, myelodysplastic syndrome; CTCL, Cutaneous T-cell lymphoma PTCL, Peripheral T-cell lymphoma; U.S, united states; FDA, Food and Drug Administration.

accessible chromatin conformation and promoting the expression of important genes that controls cell growth and death (Richon et al., 2009; Ramaiah et al., 2021).

The first HDACi was suberoylanilide hydroxamic acid (SAHA, vorinostat®) approved in 2006 by the FDA for the treatment of cutaneous manifestations of T-cell lymphoma (CTCL) (Duvic and Vu, 2007). After SAHA approval, a depsipeptide natural product from the bacterium *Chromobacterium violaceum* named romidepsin was approved in 2006 for CTCL and peripheral T-cell lymphomas (PTCL) treatment (McClure et al., 2018). Belinostat became the third FDA approved HDACi for T-cell lymphoma (Campbell and Thomas, 2017). In 2015, panobinostat arise as the first HDACi approved for a nonlymphoma cancer by FDA and also the European Medicines Agency (EMA). Panobinostat is an oral pan-HDACi recommended for relapsed or refractory multiple myeloma management (Berdeja et al., 2021), the first time that an HDACi was proposed and accepted for non-lymphoma cancer treatment, refreshing the possibility of designing inhibitors for all HDACs bearable enough to benefit humans (McClure et al., 2018).

Tucidinostat (chidamide) is a novel oral subtype of selective HDACi. This drug inhibits class I HDACs (HDAC1, HDAC2, HDAC3) and class IIb (HDAC10). It was approved in 2014 as a second-line therapy for peripheral relapsed or refractory T-cell lymphoma by the China Food and Drug Administration. In Japan, tucidinostat was approved in 2021 for relapsed or refractory adult T-cell lymphoma treatment under the name Hiyasta (Sun et al., 2022). Valproic acid is an FDA-approved antiepileptic drug that also presents inhibitory HDAC class I and II activity (Lunke et al., 2021). Currently, valproic acid is in phase III clinical trial as a potential drug to treat cervical and ovarian malignancies and has been proposed in combination regimens with chemotherapy and radiotherapy (Krauze et al., 2015; Suraweera et al., 2018; Tsai et al., 2021).

Compounds that modulate epigenome are being discovered and currently, there is a race in finding potential inhibitors of epigenetic modifiers. Emerging targets that modulate others DNA-modifying enzymes, as TETs and isocitrate dehydrogenase (IDHs) inhibitors (TETi and IDHi) are in current development for cancer treatment. Likewise, the complex network of histone-modifying enzymes has been added in anticancer therapy, as HMTi, HATi, HDMi, KMTi and PRMTi (Ganesan et al., 2019; Morel et al., 2020). An emerging target therapy for cancer treatment in preclinical studies is the EZH2 lysine methyltransferase inhibitors, with great results especially in combination with radiotherapy or chemotherapy, such as cisplatin, gefitinib and tamoxifen (Duan et al., 2020; Morel et al., 2020). Another class of epidrugs are the inhibitors of bromodomain and extra-terminal domain (BETi), a histone "reader" that recognizes and binds to acetylated lysine and is responsible for the recruitment of transcription machinery and gene activation (Cheung et al., 2021).

The combined use of epigenetic drugs with conventional therapies is gaining prominence due to its potential in increasing tumor cells' sensitivity to classical chemotherapy improving the therapeutical effect. A phase Ib/II clinical trial showed that the small

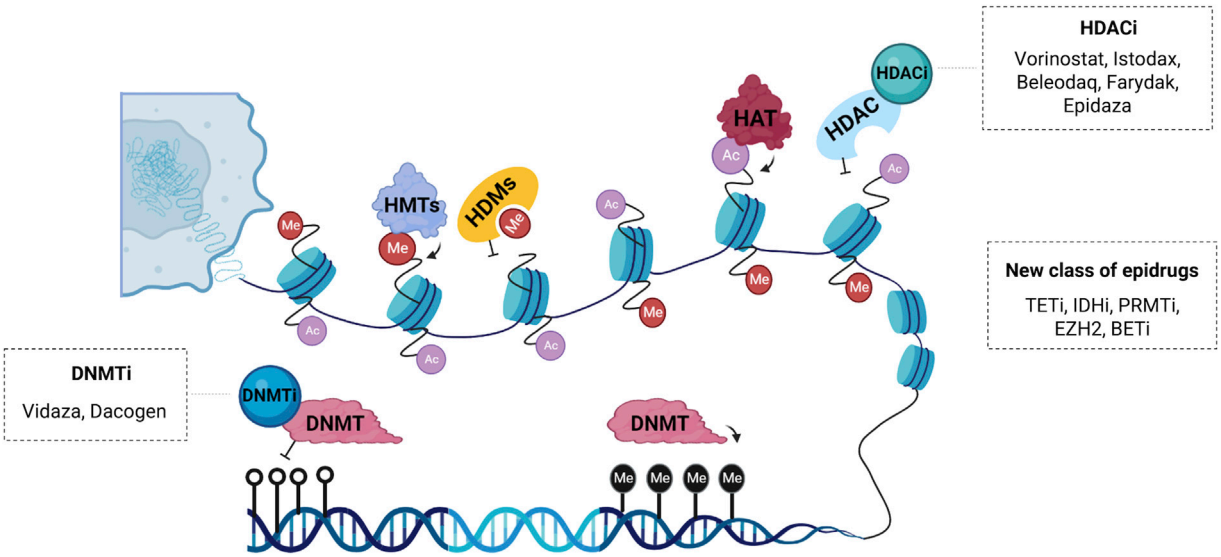

FIGURE 2
Schematic representation of the main epidrugs targets. Histone acetyltransferases (HATs) and deacetylases (HDACs) are enzymes responsible for post-translational acetylation and deacetylation, respectively. HDAC inhibitors (HDACi) such as Vorinostat®, Istodax®, Beleodaq®, Farydak® and Epidaza® induce acetylation thereby promoting transcriptional activation. Histone methyltransferases (HMTs) and demethylases (HDMs) can also be modulated by a new class of epigenetic drugs. DNA methyltransferases (DNMTs) are enzymes responsible for transferring a methyl group to carbon five of cytosine, a repressive epigenetic marker. DNMT inhibitors (DNMTi) like Vidaza® and Dacogen® promote loss of methylation and activation of aberrantly silenced genes. Other compounds with epigenetic activity are inhibitors of the enzyme ten-eleven translocation (TETi), inhibitors of the enzyme isocitrate dehydrogenase (IDHi), inhibitors of the protein arginine methyltransferase (PRMTi), inhibitors of the bromodomain and extra-terminal domain (BETi) and inhibitors of the enhancer of zeste homolog 2 (EZH2i), which is a histone-lysine n-methyltransferase enzyme.

molecule eprenetapopt in combination with azacytidine improved clinical response rates and molecular remissions in patients with *TP53* mutant MDS and oligoblastic AML (Sallman et al., 2021). A selective BCL-2 inhibitor (Venetoclax) has recently been approved for use in combination with hypomethylating agents (Azacitidine or Decitabine), giving promising results for the treatment of acute myeloid leukemia in patients who are ineligible to receive intensive chemotherapy (Manda et al., 2021). The use of decitabine associated with carboplatin has shown greater efficacy in the treatment of ovarian cancer when compared with conventional therapies by increasing the sensitivity of the tumor cells (Fan et al., 2014; Fu et al., 2015).

In the same context, a phase II study showed that patients with AML or MDS who underwent idarubicin therapy with a high-dose continuous infusion of Ara-C (cytarabine) associated with vorinostat® showed an overall response rate of 85%, and a 76% complete response to treatment in association (Garcia-Manero et al., 2012). A multicenter phase 2 trial showed that the combined use of Vorinostat® with Bortezomib and Dexamethasone showed an overall response of 81.3% in patients with relapsed multiple myeloma, although more studies are necessary to further optimize HDACi-based combinations, in order to improve tolerability and increase the efficacy of combination therapy (Brown et al., 2021). A multicenter phase II trial showed that the triple use of belinostat, carboplatin and paclitaxel was well tolerated and demonstrated clinical benefit in patients with recurrent epithelial ovarian cancer (Finkler et al., 2008). Combination therapy of drugs with the ability to modulate the epigenome and conventional therapies demonstrate increased efficacy and tolerability, requiring lower dosages of each agent, and reducing the side effects caused by conventional chemotherapies (Oing et al., 2019).

Recently, ncRNA have been proposed as a target to overcome therapy resistance. The focus of this approach is to inhibit the specific ncRNA molecule if it is overexpressed or restore the normal function of ncRNAs that are downregulated when therapy resistance occurs (Chen et al., 2022b). Inhibition of the microRNA-21 (miR-21) with a locked-nucleic acid-anti-miR resulted in increased apoptosis level in melanoma cell line and reduced tumor growth and volume in mice (Javanmard et al., 2020). Targeted inhibition of miR-221/222 with anti-miR-221 and anti-miR-222 promoted synergetic effects stimulating cell sensitivity to cisplatin in triple-negative breast cancer cell line (Li et al., 2020).

Epidrug-associated immunotherapy

Immunotherapy refers to the treatment in which the patient's immune system is reprogrammed and stimulated to fight defective cells such as those resulting from a tumorigenic process. Its main goal is to empower immunity and modulate the tumor microenvironment by releasing cytokines such as interferons, interleukins, and chemokines, promoting T-cell attack and tumoral cell cleaning (Esfahani et al., 2020).

Monoclonal antibodies have been an important therapeutic agent used in the treatment of several types of cancer. Since the approval in 1997 of Rituximab, the first therapeutic antibody approved for oncology patients and used until the present day

with success in the treatment of B-cell malignancies, dozens of antibodies recognizing a variety of targets have been used successfully in the treatment of both solid and hematological tumors (Zahavi and Weiner, 2020). New antibody formats have emerged such as antibody-drug conjugates (ADCs), bispecific/multispecific binding, nanobodies, antibody fragments, and other engineered molecules (Jin et al., 2022a). In addition to monotherapy, antibodies can be combined with other drugs since multiple treatments can increase their effectiveness and decrease chemoresistance (Miranda Furtado et al., 2019).

Epidrugs are alternative strategies for a more personalized tumor treatment because they might sensitize tumors to immune checkpoint inhibitors and cell therapy, besides their effect on viral mimicry response and immune cell activation. Currently, several clinical trials on different tumor types are ongoing using epidrugs alone or in combination with other immunotherapy drugs (Xu et al., 2022). There are different approaches regarding the use of epidrugs in cancer treatment, such as DNA methyltransferase inhibitors (DNMTi), histone deacetylase inhibitors HDACi, and bromodomain and extra-terminal motif inhibitors BETi.

New combinations of epidrugs and immunotherapeutic molecules have shown potential clinical application for cancer treatment. A study of colorectal cancer in CT26 tumor-bearing mouse model revealed a therapeutic gain when low-dose decitabine was administrated with anti-PD-1 regimen (Yu et al., 2019). Decitabine is a well-known DNMTi and FDA-approved drug. A methylation profile was assessed in decitabine-treated CT26 cells and patient-derived xenografts (PDX) model, and tumor cells were significantly downregulated regarding methylation of promoter regions after decitabine treatment. It was also observed that decitabine in combination with anti-PD-1 antibody administration promoted longer survival in PDX mice than single therapy. These results shed light on the role of decitabine on tumor microenvironment re-modulation of methylation profile of promoter genes and suggest that PD-1 blockade and low-dose decitabine would be effective in future clinical trials.

Huang also correlated decitabine and anti-PD-L1 treatment to colorectal cancer (Huang et al., 2020). Using *in vitro* and *in vivo* models, the study showed that decitabine induces DNA hypomethylation which enhances tumor PD-L1 expression *via* an epigenetic mechanism, improving the therapeutic efficacy of anti-PD-L1 immunotherapy. Besides, decitabine treatment modifies the interferon signaling pathway and remodels the tumor microenvironment, recruiting more immune cells, such as T cells for antitumor immunity (Huang et al., 2020).

An important work performed by Goltz used data from 470 melanoma patients provided by The Cancer Genome Atlas and a cohort of 50 metastatic melanoma patients treated with anti–PD-1 or/and anti–CTLA-4 antibodies, to investigate if *CTLA-4* promoter methylation profile can be used as a biomarker to predict more successful treatment with ICB (immune checkpoint blockage). Methylation levels in patients treated with anti-PD-1 and anti-CTLA-4 were slightly lower when compared to the non-ICB cohort. Low *CTLA-4* methylation levels also play a key role in prolonged overall survival observed in patients (Goltz et al., 2018). The study paves the way for use of demethylating agents to aid the treatment with immune checkpoint inhibitors. Several clinical trials have been performed to evaluate the effects of the combination of epigenetic inhibitors and immunotherapies which creates hope for more efficient treatments and overcomes the limitations of current approaches (Topper et al., 2020; Villanueva et al., 2020; Licht and Bennett, 2021).

Epi-cell therapy

Chimeric Antigen Receptor (CAR-T) cell therapy has revolutionized personalized cancer treatment. Some of the strategies available for this approach target B cell tumors, through molecular markers such as CD19, CD20, and CD22. DNA methylation profiles have been reported to impact outcomes of CAR-T targeting CD19 treatment. A study revealed that the use of the DNA methylation inhibitor 5-Aza-2′-deoxycytidine in the hypermethylated T-cell lines resulted in the downregulation of *INPP5A* and *ECHDC1* expression levels. These genes are involved in intracellular signaling cascades, important to CAR-T Cell therapy. In addition, these T-cell–derived lines also showed that hypermethylation of 5′-end CpG sites was associated with transcript downregulation. An illustrative example is the 5′-UTR CpG hypermethylation of *FOXN3*, a candidate tumor suppressor gene for T-cell acute lymphocytic leukemia which was downregulated in the T-cell-derived lines mentioned (Garcia-Prieto et al., 2022). Wang discussed the influence of decitabine, a DNMTi, on T-cell exhaustion of CAR-T therapy. Decitabine-treated CAR-T cells (dCAR) differentially expressed genes regarding proliferation, cytokine secretion, cytotoxicity and memory *in vitro*. dCAR also presented tumor shrinkage in the acute lymphoblastic leukemia mouse model (Wang et al., 2021). Xu reveal the benefits of priming CAR-T cell therapy mice with 5-azacytidine, a DNMTi. $CD19^+$ B-cell acute lymphoblastic leukemia mouse models were used to perform those experiments. A regimen of 1 day of azacitidine before CAR-T cell infusion expanded $IFN\gamma^+$ effector T cells and promoted CAR-T cell divisions. Azacitidine was related to activating several immune pathways, such as *TNFSF4*, a gene that encodes OX40L which is related to co-stimulatory signals on CAR-T cells. Another interesting finding is that neither PD-L1/PD-L2 expression in leukemia cells nor PD-1 expression in CAR-T cells was affected by pre-treatment with azacitidine, suggesting that azacitidine effects were not mediated through the modulation of the inhibitory PD-1 checkpoint (Xu et al., 2021). Thus, the study of the epigenetics landscape in CART-T-Cells can improve the efficacy of the cellular immunotherapy treatment in patients with B-cell malignancy and expanding its use to other oncological diseases.

Conclusion

Epigenetic reprogramming is the main event to promote cell differentiation, and once cell fate is determined, the epigenetic pattern of genomic function must be stably maintained during DNA replication in cell division. Disruption of the epigenetic landscape of differentiated cells changes cell fate and promotes carcinogenesis and tumor progression. Thought waves of reprogramming cancer cells have the ability to return to a less differentiated state or aberrantly reprogram the stem progenitor.

This stem cell-like phenotype is a challenge in cancer treatment leading to resistance, recurrence, and poor overall survival. Loss of global DNA methylation, aberrant activation/inactivation of growth-related genes, altered chromatin remodeling through histone modifications and ncRNA interaction, as well as disrupted expression of microRNAs and lncRNA, are molecular features of many cancer types. Given the heterogeneity of tumor cells, epigenetic changes have been highlighted as an important diagnostic marker, even in the early stages of cancer development, with great prognostic value. Recently, ncRNAs have an emerging role as a less invasive biomarker for diagnosis since they can be easily detected in body fluid and liquid biopsies. The complex regulatory machinery involved in the establishment and maintenance of epigenetic markers, and the cell-type specific modifications, give an individual variation in oncology, highlighting the importance of precision medicine. In this field, regulating the enzymes that catalyze epigenetic modifications using inhibitors or compounds that target these modifications has been extensively used in cancer therapy, especially for hematological tumors, although some of them are used for solid tumors as combinatory therapy. DNMTi and HDACi are the main epidrugs in clinical use and other new classes of epigenetic modulators are in development. Even though it has great results as monotherapy, the synergic use with other anticancer therapies, such as chemo, hormonal or immunotherapy has expanded the potential and effectiveness of epidrugs on cancer treatment.

Author contributions

PMSC, SLAS and CLMF, designed the manuscript; All authors participated in writing and approved this manuscript's final version and submission.

Funding

Coordenação de Aperfeiçoamento de Pessoal de Nível Superior (CAPES), Programa de Excelência Acadêmica (CAPES-PROEX) and Programa de Apoio à Pós-Graduação (CAPES-PROAP), and Fundação Cearense de Apoio ao Desenvolvimento Científico e Tecnológico Conselho Nacional de Desenvolvimento Científico e Tecnológico (CNPq, Grant Numbers: 437037/2018-5 (CLMF), 439019/2018-4 (GPF) and 434821/2018-7 (CP), besides the research sponsorships of CP(PQ-1B, Process no: 303102/2013-6).

Acknowledgments

The authors are grateful to University of Fortaleza (UNIFOR) for the financial support in the publication; the members of the Experimental Oncology Laboratory (LOE), the Drug Research and Development Center (NPDM) at the Federal University of Ceará (UFC), the Oswaldo Cruz Foundation–Ceara for the support offered.

Conflict of interest

The authors declare that the research was conducted in the absence of any commercial or financial relationships that could be construed as a potential conflict of interest.

Publisher's note

All claims expressed in this article are solely those of the authors and do not necessarily represent those of their affiliated organizations, or those of the publisher, the editors and the reviewers. Any product that may be evaluated in this article, or claim that may be made by its manufacturer, is not guaranteed or endorsed by the publisher.

References

Amort, T., Soulière, M. F., Wille, A., Jia, X. Y., Fiegl, H., Wörle, H., et al. (2013). Long non-coding RNAs as targets for cytosine methylation. *RNA Biol.* 10, 1003–1008. doi:10.4161/rna.24454

An, J., Rao, A., and Ko, M. (2017). TET family dioxygenases and DNA demethylation in stem cells and cancers. *Exp. Mol. Med.* 49, e323. doi:10.1038/emm.2017.5

Aprile, M., Katopodi, V., Leucci, E., and Costa, V. (2020). Lncrnas in cancer: From garbage to junk. *Cancers (Basel)* 12, 3220. doi:10.3390/cancers12113220

Bannister, A. J., and Kouzarides, T. (2011). Regulation of chromatin by histone modifications. *Cell Res.* 21, 381–395. doi:10.1038/cr.2011.22

Barbieri, I., and Kouzarides, T. (2020). Role of RNA modifications in cancer. *Nat. Rev. Cancer* 20, 303–322. doi:10.1038/s41568-020-0253-2

Bauden, M., Pamart, D., Ansari, D., Herzog, M., Eccleston, M., Micallef, J., et al. (2015). Circulating nucleosomes as epigenetic biomarkers in pancreatic cancer. *Clin. Epigenetics* 7, 106. doi:10.1186/s13148-015-0139-4

Baylin, S. B., and Jones, P. A. (2011). A decade of exploring the cancer epigenome-biological and translational implications. *Nat. Rev. Cancer* 11, 726–734. doi:10.1038/nrc3130

Baylin, S. B., and Jones, P. A. (2016). Epigenetic determinants of cancer. *Cold Spring Harb. Perspect. Biol.* 8, a019505. doi:10.1101/cshperspect.a019505

Begley, U., Sosa, M. S., Avivar-Valderas, A., Patil, A., Endres, L., Estrada, Y., et al. (2013). A human tRNA methyltransferase 9-like protein prevents tumour growth by regulating LIN9 and HIF1-α. *EMBO Mol. Med.* 5, 366–383. doi:10.1002/emmm.201201161

Belin, S., Beghin, A., Solano-Gonzàlez, E., Bezin, L., Brunet-Manquat, S., Textoris, J., et al. (2009). Dysregulation of ribosome biogenesis and translational capacity is associated with tumor progression of human breast cancer cells. *PLoS One* 4, e7147. doi:10.1371/journal.pone.0007147

Berdeja, J. G., Laubach, J. P., Richter, J., Stricker, S., Spencer, A., Richardson, P. G., et al. (2021). Panobinostat from bench to bedside: Rethinking the treatment paradigm for multiple myeloma. *Clin. Lymphoma Myeloma Leuk.* 21, 752–765. doi:10.1016/j.clml.2021.06.020

Blanco, S., Bandiera, R., Popis, M., Hussain, S., Lombard, P., Aleksic, J., et al. (2016). Stem cell function and stress response are controlled by protein synthesis. *Nature* 534, 335–340. doi:10.1038/nature18282

Boccaletto, P., MacHnicka, M. A., Purta, E., Pitkowski, P., Baginski, B., Wirecki, T. K., et al. (2018). Modomics: A database of RNA modification pathways. 2017 update. *Nucleic Acids Res.* 46, D303–D307. doi:10.1093/nar/gkx1030

Brown, S., Pawlyn, C., Tillotson, A. L., Sherratt, D., Flanagan, L., Low, E., et al. (2021). Bortezomib, vorinostat, and Dexamethasone combination therapy in relapsed myeloma: Results of the phase 2 MUK four trial. *Clin. Lymphoma Myeloma Leuk.* 21, 154–161. doi:10.1016/j.clml.2020.11.019

Bubna, A. K. (2015). Vorinostat-An overview. *Indian J. Dermatol* 60, 419. doi:10.4103/0019-5154.160511

Byun, H. M., Wong, H. L., Birnstein, E. A., Wolff, E. M., Liang, G., and Yang, A. S. (2007). Examination of IGF2 and H19 loss of imprinting in bladder cancer. *Cancer Res.* 67, 10753–10758. doi:10.1158/0008-5472.CAN-07-0329

Cabili, M., Trapnell, C., Goff, L., Koziol, M., Tazon-Vega, B., Regev, A., et al. (2011). Integrative annotation of human large intergenic noncoding RNAs reveals global properties and specific subclasses. *Genes Dev.* 25, 1915–1927. doi:10.1101/gad.17446611

Campbell, P., and Thomas, C. M. (2017). Belinostat for the treatment of relapsed or refractory peripheral T-cell lymphoma. *J. Oncol. Pharm. Pract.* 23, 143–147. doi:10.1177/1078155216634178

Cavalcante, G. M., Borges, D. P., de Oliveira, R. T. G., Furtado, C. L. M., Alves, A. P. N. N., Sousa, A. M., et al. (2022). Tissue methylation and demethylation influence translesion synthesis DNA polymerases (TLS) contributing to the Genesis of chromosomal abnormalities in myelodysplastic syndrome. *J. Clin. Pathol.* 75, 85–93. doi:10.1136/jclinpath-2020-207131

Chase, A., and Cross, N. C. P. (2011). Aberrations of EZH2 in cancer. *Clin. Cancer Res.* 17, 2613–2618. doi:10.1158/1078-0432.CCR-10-2156

Chen, A., Wang, L., Li, B. Y., Sherman, J., Ryu, J. E., Hamamura, K., et al. (2017). Reduction in migratory phenotype in a metastasized breast cancer cell line via downregulation of S100A4 and GRM3. *Sci. Rep.* 7, 3459. doi:10.1038/s41598-017-03811-9

Chen, B., Dragomir, M. P., Yang, C., Li, Q., Horst, D., and Calin, G. A. (2022a). Targeting non-coding RNAs to overcome cancer therapy resistance. *Signal Transduct. Target. Ther.* 7, 121. doi:10.1038/s41392-022-00975-3

Chen, B., Petricca, J., Ye, W., Guan, J., Zeng, Y., Cheng, N., et al. (2022b). The cell-free DNA methylome captures distinctions between localized and metastatic prostate tumors. *Nat. Commun.* 13, 6467. doi:10.1038/s41467-022-34012-2

Chen, X., Li, A., Sun, B. F., Yang, Y., Han, Y. N., Yuan, X., et al. (2019). 5-methylcytosine promotes pathogenesis of bladder cancer through stabilizing mRNAs. *Nat. Cell Biol.* 21, 978–990. doi:10.1038/s41556-019-0361-y

Chen, Y., Ren, B., Yang, J., Wang, H., Yang, G., Xu, R., et al. (2020). The role of histone methylation in the development of digestive cancers: A potential direction for cancer management. *Signal Transduct. Target Ther.* 5, 143. doi:10.1038/s41392-020-00252-1

Cheung, K. L., Kim, C., and Zhou, M. M. (2021). The functions of BET proteins in gene transcription of biology and diseases. *Front. Mol. Biosci.* 8, 728777. doi:10.3389/fmolb.2021.728777

Chheda, M. G., and Gutmann, D. H. (2017). Using epigenetic reprogramming to treat pediatric brain cancer. *Cancer Cell* 31, 609–611. doi:10.1016/j.ccell.2017.04.008

Church, T. R., Wandell, M., Lofton-Day, C., Mongin, S. J., Burger, M., Payne, S. R., et al. (2014). Prospective evaluation of methylated SEPT9 in plasma for detection of asymptomatic colorectal cancer. *Gut* 63, 317–325. doi:10.1136/gutjnl-2012-304149

Cimmino, L., Abdel-Wahab, O., Levine, R. L., and Aifantis, I. (2011). TET family proteins and their role in stem cell differentiation and transformation. *Cell Stem Cell* 9, 193–204. doi:10.1016/j.stem.2011.08.007

Corces, M. R., Granja, J. M., Shams, S., Louie, B. H., Seoane, J. A., Zhou, W., et al. (2018). The chromatin accessibility landscape of primary human cancers. *Science* 362, eaav1898. doi:10.1126/science.aav1898

Cuciniello, R., Filosa, S., and Crispi, S. (2021). Novel approaches in cancer treatment: Preclinical and clinical development of small non-coding RNA therapeutics. *J. Exp. Clin. Cancer Res.* 40, 383. doi:10.1186/s13046-021-02193-1

Cui, Q., Shi, H., Ye, P., Li, L., Qu, Q., Sun, G., et al. (2017). m6A RNA methylation regulates the self-renewal and tumorigenesis of glioblastoma stem cells. *Cell Rep.* 18, 2622–2634. doi:10.1016/j.celrep.2017.02.059

Daher-Reyes, G. S., Merchan, B. M., and Yee, K. W. L. (2019). Guadecitabine (SGI-110): An investigational drug for the treatment of myelodysplastic syndrome and acute myeloid leukemia. *Expert Opin. Investig. Drugs* 28, 835–849. doi:10.1080/13543784.2019.1667331

Das, P. M., and Singal, R. (2004). DNA methylation and cancer. *J. Clin. Oncol.* 22, 4632–4642. doi:10.1200/JCO.2004.07.151

Delaunay, S., Rapino, F., Tharun, L., Zhou, Z., Heukamp, L., Termathe, M., et al. (2016). Elp3 links tRNA modification to IRES-dependent translation of LEF1 to sustain metastasis in breast cancer. *J. Exp. Med.* 213, 2503–2523. doi:10.1084/jem.20160397

Deligezer, U., Akisik, E. Z., Akisik, E. E., Kovancilar, M., Bugra, D., Erten, N., et al. (2010). "H3K9me3/H4K20me3 ratio in circulating nucleosomes as potential biomarker for colorectal cancer," in *Circulating nucleic acids in plasma and serum* (Berlin, Germany: Springer), 97–103. doi:10.1007/978-90-481-9382-0_14

Demetriadou, C., Koufaris, C., and Kirmizis, A. (2020). Histone N-alpha terminal modifications: Genome regulation at the tip of the tail. *Epigenetics Chromatin* 13, 29. doi:10.1186/s13072-020-00352-w

Derissen, E. J. B., Beijnen, J. H., and Schellens, J. H. M. (2013). Concise drug review: Azacitidine and decitabine. *Oncologist* 18, 619–624. doi:10.1634/theoncologist.2012-0465

DeVos, T., Tetzner, R., Model, F., Weiss, G., Schuster, M., Distler, J., et al. (2009). Circulating methylated SEPT9 DNA in plasma is a biomarker for colorectal cancer. *Clin. Chem.* 55, 1337–1346. doi:10.1373/clinchem.2008.115808

Dong, M., Ning, Z. Q., Xing, P. Y., Xu, J. L., Cao, H. X., Dou, G. F., et al. (2012). Phase i study of chidamide (CS055/HBI-8000), a new histone deacetylase inhibitor, in patients with advanced solid tumors and lymphomas. *Cancer Chemother. Pharmacol.* 69, 1413–1422. doi:10.1007/s00280-012-1847-5

Duan, R., Du, W., and Guo, W. (2020). EZH2: A novel target for cancer treatment. *J. Hematol. Oncol.* 13, 104. doi:10.1186/s13045-020-00937-8

Duvic, M., and Vu, J. (2007). Vorinostat: A new oral histone deacetylase inhibitor approved for cutaneous T-cell lymphoma. *Expert Opin. Investig. Drugs* 16, 1111–1120. doi:10.1517/13543784.16.7.1111

Engreitz, J. M., Haines, J. E., Perez, E. M., Munson, G., Chen, J., Kane, M., et al. (2016). Local regulation of gene expression by lncRNA promoters, transcription and splicing. *Nature* 539, 452–455. doi:10.1038/nature20149

Esfahani, K., Roudaia, L., Buhlaiga, N., del Rincon, S. v., Papneja, N., and Miller, W. H. (2020). A review of cancer immunotherapy: From the past, to the present, to the future. *Curr. Oncol.* 27, S87–S97. doi:10.3747/co.27.5223

Esteller, M., and Pandolfi, P. P. (2017). The epitranscriptome of noncoding RNAs in cancer. *Cancer Discov.* 7, 359–368. doi:10.1158/2159-8290.CD-16-1292

Fan, H., Lu, X., Wang, X., Liu, Y., Guo, B., Zhang, Y., et al. (2014). Low-dose decitabine-based chemoimmunotherapy for patients with refractory advanced solid tumors: A phase I/II report. *J. Immunol. Res.* 2014, 371087. doi:10.1155/2014/371087

Feinberg, A. P., Koldobskiy, M. A., and Göndör, A. (2016). Epigenetic modulators, modifiers and mediators in cancer aetiology and progression. *Nat. Rev. Genet.* 17, 284–299. doi:10.1038/nrg.2016.13

Feinberg, A. P., Ohlsson, R., and Henikoff, S. (2006). The epigenetic progenitor origin of human cancer. *Nat. Rev. Genet.* 7, 21–33. doi:10.1038/nrg1748

Finkler, N. J., Dizon, D. S., Braly, P., Micha, J., Lassen, U., Celano, P., et al. (2008). Phase II multicenter trial of the histone deactylase inhibitor (HDACi) belinostat, carboplatin and paclitaxel (BelCaP) in patients (pts) with relapsed epithelial ovarian cancer (EOC). *J. Clin. Oncol.* 26, 5519. doi:10.1200/jco.2008.26.15_suppl.5519

Fraga, M. F., Ballestar, E., Villar-Garea, A., Boix-Chornet, M., Espada, J., Schotta, G., et al. (2005). Loss of acetylation at Lys16 and trimethylation at Lys20 of histone H4 is a common hallmark of human cancer. *Nat. Genet.* 37, 391–400. doi:10.1038/ng1531

Fu, X., Zhang, Y., Wang, X., Chen, M., Wang, Y., Nie, J., et al. (2015). Low dose decitabine combined with taxol and platinum chemotherapy to treat refractory/recurrent ovarian cancer: An open-label, single-arm, phase I/II study. *Curr. Protein Pept. Sci.* 16, 329–336. doi:10.2174/1389203716041504291557 40

Ganesan, A., Arimondo, P. B., Rots, M. G., Jeronimo, C., and Berdasco, M. (2019). The timeline of epigenetic drug discovery: From reality to dreams. *Clin. Epigenetics* 11, 174. doi:10.1186/s13148-019-0776-0

Garcia-Manero, G., Tambaro, F. P., Bekele, N. B., Yang, H., Ravandi, F., Jabbour, E., et al. (2012). Phase II trial of vorinostat with idarubicin and cytarabine for patients with newly diagnosed acute myelogenous leukemia or myelodysplastic syndrome. *J. Clin. Oncol.* 30, 2204–2210. doi:10.1200/JCO.2011.38.3265

Garcia-Prieto, C. A., Villanueva, L., Bueno-Costa, A., Davalos, V., González-Navarro, E. A., Juan, M., et al. (2022). Epigenetic profiling and response to CD19 chimeric antigen receptor T-cell therapy in B-cell malignancies. *J. Natl. Cancer Inst.* 114, 436–445. doi:10.1093/jnci/djab194

García-Vílchez, R., Sevilla, A., and Blanco, S. (2019). Post-transcriptional regulation by cytosine-5 methylation of RNA. *Biochim. Biophys. Acta Gene Regul. Mech.* 1862, 240–252. doi:10.1016/j.bbagrm.2018.12.003

Ge, J., and Yu, Y. T. (2013). RNA pseudouridylation: New insights into an old modification. *Trends Biochem. Sci.* 38, 210–218. doi:10.1016/j.tibs.2013.01.002

Geiman, T. M., and Muegge, K. (2010). DNA methylation in early development. *Mol. Reprod. Dev.* 77, 105–113. doi:10.1002/mrd.21118

Gezer, U., Yörüker, E. E., Keskin, M., Kulle, C. B., Dharuman, Y., and Holdenrieder, S. (2015). Histone methylation marks on circulating nucleosomes as novel blood-based biomarker in colorectal cancer. *Int. J. Mol. Sci.* 16, 29654–29662. doi:10.3390/ijms161226180

Ghasemi, S. (2020). Cancer's epigenetic drugs: Where are they in the cancer medicines? *Pharmacogenomics J.* 20, 367–379. doi:10.1038/s41397-019-0138-5

Giannopoulou, L., Zavridou, M., Kasimir-Bauer, S., and Lianidou, E. S. (2019). Liquid biopsy in ovarian cancer: The potential of circulating miRNAs and exosomes. *Transl. Res.* 205, 77–91. doi:10.1016/j.trsl.2018.10.003

Gibney, E. R., and Nolan, C. M. (2010). Epigenetics and gene expression. *Hered. (Edinb)* 105, 4–13. doi:10.1038/hdy.2010.54

Gkatza, N. A., Castro, C., Harvey, R. F., Heiß, M., Popis, M. C., Blanco, S., et al. (2019). Cytosine-5 RNA methylation links protein synthesis to cell metabolism. *PLoS Biol.* 17, e3000297. doi:10.1371/journal.pbio.3000297

Goltz, D., Gevensleben, H., Vogt, T. J., Dietrich, J., Golletz, C., Bootz, F., et al. (2018). CTLA4 methylation predicts response to anti-PD-1 and anti-CTLA-4 immunotherapy in melanoma patients. *JCI Insight* 3, e96793. doi:10.1172/jci.insight.96793

Götze, K., Platzbecker, U., Giagounidis, A., Haase, D., Lübbert, M., Aul, C., et al. (2010). Azacitidine for treatment of patients with myelodysplastic syndromes (MDS): Practical recommendations of the German MDS study group. *Ann. Hematol.* 89, 841–850. doi:10.1007/s00277-010-1015-0

Graf, N., Bergeron, C., Brok, J., de Camargo, B., Chowdhury, T., Furtwängler, R., et al. (2021). Fifty years of clinical and research studies for childhood renal tumors within the International Society of Pediatric Oncology (SIOP). *Ann. Oncol.* 32, 1327–1331. doi:10.1016/j.annonc.2021.08.1749

Greer, E. L., and Shi, Y. (2012). Histone methylation: A dynamic mark in health, disease and inheritance. *Nat. Rev. Genet.* 13, 343–357. doi:10.1038/nrg3173

Guillamot, M., Cimmino, L., and Aifantis, I. (2016). The impact of DNA methylation in hematopoietic malignancies. *Trends Cancer* 2, 70–83. doi:10.1016/j.trecan.2015.12.006

Guo, F., Yu, F., Wang, J., Li, Y., Li, Y., Li, Z., et al. (2015). Expression of MALAT1 in the peripheral whole blood of patients with lung cancer. *Biomed. Rep.* 3, 309–312. doi:10.3892/br.2015.422

Guo, X., Xia, J., and Deng, K. (2014). Long non-coding RNAs: Emerging players in gastric cancer. *Tumor Biol.* 35, 10591–10600. doi:10.1007/s13277-014-2548-y

Gutschner, T., Hämmerle, M., Eißmann, M., Hsu, J., Kim, Y., Hung, G., et al. (2013). The noncoding RNA MALAT1 is a critical regulator of the metastasis phenotype of lung cancer cells. *Cancer Res.* 73, 1180–1189. doi:10.1158/0008-5472.CAN-12-2850

Guttman, M., Amit, I., Garber, M., French, C., Lin, M. F., Feldser, D., et al. (2009). Chromatin signature reveals over a thousand highly conserved large non-coding RNAs in mammals. *Nature* 458, 223–227. doi:10.1038/nature07672

Han, J., Wang, J. Z., Yang, X., Yu, H., Zhou, R., Lu, H. C., et al. (2019). METTL3 promote tumor proliferation of bladder cancer by accelerating pri-miR221/222 maturation in m6A-dependent manner. *Mol. Cancer* 18, 110. doi:10.1186/s12943-019-1036-9

Hanahan, D. (2022). Hallmarks of cancer: New dimensions. *Cancer Discov.* 12, 31–46. doi:10.1158/2159-8290.CD-21-1059

Handy, D. E., Castro, R., and Loscalzo, J. (2011). Epigenetic modifications: Basic mechanisms and role in cardiovascular disease. *Circulation* 123, 2145–2156. doi:10.1161/CIRCULATIONAHA.110.956839

Hashimoto, H., Horton, J. R., Zhang, X., Bostick, M., Jacobsen, S. E., and Cheng, X. (2008). The SRA domain of UHRF1 flips 5-methylcytosine out of the DNA helix. *Nature* 455, 826–829. doi:10.1038/nature07280

He, Y., Yu, X., Li, J., Zhang, Q., Zheng, Q., and Guo, W. (2020). Role of m5C-related regulatory genes in the diagnosis and prognosis of hepatocellular carcinoma. *Am. J. Transl. Res.* 12, 912–922.

Heidrich, I., Ačkar, L., Mossahebi Mohammadi, P., and Pantel, K. (2021). Liquid biopsies: Potential and challenges. *Int. J. Cancer* 148, 528–545. doi:10.1002/ijc.33217

Hessvik, N. P., Sandvig, K., and Llorente, A. (2013). Exosomal miRNAs as biomarkers for prostate cancer. *Front. Genet.* 4, 36. doi:10.3389/fgene.2013.00036

Hidaka, H., Higashimoto, K., Aoki, S., Mishima, H., Hayashida, C., Maeda, T., et al. (2018). Comprehensive methylation analysis of imprinting-associated differentially methylated regions in colorectal cancer. *Clin. Epigenetics* 10, 150. doi:10.1186/s13148-018-0578-9

Horlbeck, M. A., Liu, S. J., Chang, H. Y., Lim, D. A., and Weissman, J. S. (2020). Fitness effects of CRISPR/Cas9-targeting of long noncoding RNA genes. *Nat. Biotechnol.* 38, 573–576. doi:10.1038/s41587-020-0428-0

Hu, Y., Zhang, Y., Ding, M., and Xu, R. (2020). Lncrna linc00511 acts as an oncogene in colorectal cancer via sponging mir-29c-3p to upregulate nfia. *Onco Targets Ther.* 13, 13413–13424. doi:10.2147/OTT.S250377

Huang, J. L., Liu, W., Tian, L. H., Chai, T. T., Liu, Y., Feng, Z., et al. (2017). Upregulation of long non-coding RNA MALAT-1 confers poor prognosis and influences cell proliferation and apoptosis in acute monocytic leukemia. *Oncol. Rep.* 38, 1353–1362. doi:10.3892/or.2017.5802

Huang, K. C. Y., Chiang, S. F., Chen, W. T. L., Chen, T. W., Hu, C. H., Yang, P. C., et al. (2020). Decitabine augments chemotherapy-induced PD-L1 upregulation for PD-L1 blockade in colorectal cancer. *Cancers (Basel)* 12, 462. doi:10.3390/cancers12020462

Hunter, P. (2017). Tackling the great challenges in biology: Beyond evolution, defining the greatest challenges in biology is a challenge itself. *EMBO Rep.* 18, 1290–1293. doi:10.15252/embr.201744718

Hur, K., Cejas, P., Feliu, J., Moreno-Rubio, J., Burgos, E., Boland, C. R., et al. (2014). Hypomethylation of long interspersed nuclear element-1 (LINE-1) leads to activation of protooncogenes in human colorectal cancer metastasis. *Gut* 63, 635–646. doi:10.1136/gutjnl-2012-304219

Husmann, D., and Gozani, O. (2019). Histone lysine methyltransferases in biology and disease. *Nat. Struct. Mol. Biol.* 26, 880–889. doi:10.1038/s41594-019-0298-7

Ilango, S., Paital, B., Jayachandran, P., Padma, P. R., and Nirmaladevi, R. (2020). Epigenetic alterations in cancer. *Front. Biosci. - Landmark* 25, 1058–1109. doi:10.2741/4847

Javanmard, S. H., Vaseghi, G., Ghasemi, A., Rafiee, L., Ferns, G. A., Esfahani, H. N., et al. (2020). Therapeutic inhibition of microRNA-21 (miR-21) using locked-nucleic acid (LNA)-anti-miR and its effects on the biological behaviors of melanoma cancer cells in preclinical studies. *Cancer Cell Int.* 20, 384. doi:10.1186/s12935-020-01394-6

Jelinic, P., and Shaw, P. (2007). Loss of imprinting and cancer. *J. Pathology* 211, 261–268. doi:10.1002/path.2116

Jin, D., Guo, J., Wu, Y., Du, J., Yang, L., Wang, X., et al. (2019). M6A mRNA methylation initiated by METTL3 directly promotes YAP translation and increases YAP activity by regulating the MALAT1-miR-1914-3p-YAP axis to induce NSCLC drug resistance and metastasis. *J. Hematol. Oncol.* 12, 135. doi:10.1186/s13045-019-0830-6

Jin, S., Liu, T., Luo, H., Liu, Y., and Liu, D. (2022b). Targeting epigenetic regulatory enzymes for cancer therapeutics: Novel small-molecule epidrug development. *Front. Oncol.* 12, 848221. doi:10.3389/fonc.2022.848221

Jin, S., Sun, Y., Liang, X., Gu, X., Ning, J., Xu, Y., et al. (2022a). Emerging new therapeutic antibody derivatives for cancer treatment. *Signal Transduct. Target Ther.* 7, 39. doi:10.1038/s41392-021-00868-x

Kaminskas, E., Farrell, A., Abraham, S., Baird, A., Hsieh, L. S., Lee, S. L., et al. (2005). Approval summary: Azacitidine for treatment of myelodysplastic syndrome subtypes. *Clin. Cancer Res.* 11, 3604–3608. doi:10.1158/1078-0432.CCR-04-2135

Kim, J., Bretz, C. L., and Lee, S. (2015). Epigenetic instability of imprinted genes in human cancers. *Nucleic Acids Res.* 43, 10689–10699. doi:10.1093/nar/gkv867

Kneip, C., Schmidt, B., Seegebarth, A., Weickmann, S., Fleischhacker, M., Liebenberg, V., et al. (2011). SHOX2 DNA methylation is a biomarker for the diagnosis of lung cancer in plasma. *J. Thorac. Oncol.* 6, 1632–1638. doi:10.1097/JTO.0b013e318220ef9a

Krauze, A. v., Myrehaug, S. D., Chang, M. G., Holdford, D. J., Smith, S., Shih, J., et al. (2015). A phase 2 study of concurrent radiation therapy, temozolomide, and the histone deacetylase inhibitor valproic acid for patients with glioblastoma. *Int. J. Radiat. Oncol. Biol. Phys.* 92, 986–992. doi:10.1016/j.ijrobp.2015.04.038

Krug, B., de Jay, N., Harutyunyan, A. S., Deshmukh, S., Marchione, D. M., Guilhamon, P., et al. (2019). Pervasive H3K27 acetylation leads to ERV expression and a therapeutic vulnerability in H3K27M gliomas. *Cancer Cell* 35, 782–797. doi:10.1016/j.ccell.2019.04.004

Kumarswamy, R., Volkmann, I., and Thum, T. (2011). Regulation and function of miRNA-21 in health and disease. *RNA Biol.* 8, 706–713. doi:10.4161/rna.8.5.16154

Kweon, S. M., Chen, Y., Moon, E., Kvederaviciutė, K., Klimasauskas, S., and Feldman, D. E. (2019). An adversarial DNA N6-methyladenine-sensor network preserves polycomb silencing. *Mol. Cell* 74, 1138–1147. doi:10.1016/j.molcel.2019.03.018

Lam, J. K. W., Chow, M. Y. T., Zhang, Y., and Leung, S. W. S. (2015). siRNA versus miRNA as therapeutics for gene silencing. *Mol. Ther. Nucleic Acids* 4, e252. doi:10.1038/mtna.2015.23

Larrea, E., Sole, C., Manterola, L., Goicoechea, I., Armesto, M., Arestin, M., et al. (2016). New concepts in cancer biomarkers: Circulating miRNAs in liquid biopsies. *Int. J. Mol. Sci.* 17, 627. doi:10.3390/ijms17050627

Lawrence, M., Daujat, S., and Schneider, R. (2016). Lateral thinking: How histone modifications regulate gene expression. *Trends Genet.* 32, 42–56. doi:10.1016/j.tig.2015.10.007

Lee, M., Kim, B., and Kim, V. N. (2014). Emerging roles of RNA modification: M6A and U-tail. *Cell* 158, 980–987. doi:10.1016/j.cell.2014.08.005

Li, P., Liu, S., Du, L., Mohseni, G., Zhang, Y., and Wang, C. (2022). Liquid biopsies based on DNA methylation as biomarkers for the detection and prognosis of lung cancer. *Clin. epigenetics* 14, 118. doi:10.1186/s13148-022-01337-0

Li, S., Li, Q., Lü, J., Zhao, Q., Li, D., Shen, L., et al. (2020). Targeted inhibition of miR-221/222 promotes cell sensitivity to cisplatin in triple-negative breast cancer MDA-MB-231 cells. *Front. Genet.* 10, 1278. doi:10.3389/fgene.2019.01278

Li, Y., Hu, J., Li, L., Cai, S., Zhang, H., Zhu, X., et al. (2018). Upregulated circular RNA circ_0016760 indicates unfavorable prognosis in NSCLC and promotes cell progression through miR-1287/GAGE1 axis. *Biochem. Biophys. Res. Commun.* 503, 2089–2094. doi:10.1016/j.bbrc.2018.07.164

Liang, L., Zhang, Y., Li, C., Liao, Y., Wang, G., Xu, J., et al. (2022). Plasma cfDNA methylation markers for the detection and prognosis of ovarian cancer. *EBioMedicine* 83, 104222. doi:10.1016/j.ebiom.2022.104222

Licht, J. D., and Bennett, R. L. (2021). Leveraging epigenetics to enhance the efficacy of immunotherapy. *Clin. Epigenetics* 13, 115. doi:10.1186/s13148-021-01100-x

Lin, Q., Chen, J., Yin, H., Li, M., Zhou, C., Ren, H., et al. (2022). DNA N6-methyladenine involvement and regulation of hepatocellular carcinoma development. *Genomics* 114, 110265. doi:10.1016/j.ygeno.2022.01.002

Ling, C., and Rönn, T. (2019). Epigenetics in human obesity and type 2 diabetes. *Cell Metab.* 29, 1028–1044. doi:10.1016/j.cmet.2019.03.009

Liu, T., Song, Z., and Gai, Y. (2018). Circular RNA circ_0001649 acts as a prognostic biomarker and inhibits NSCLC progression via sponging miR-331-3p and miR-338-5p. *Biochem. Biophys. Res. Commun.* 503, 1503–1509. doi:10.1016/j.bbrc.2018.07.070

Liu, Y., Ao, X., Wang, Y., Li, X., Wang, J., and Chen, L. (2022). Case report: Condylar metastasis from hepatocellular carcinoma: An uncommon case report and literature review. *Front. Oncol.* 12, 1085543. doi:10.3389/fonc.2022.1085543

Lone, S. N., Nisar, S., Masoodi, T., Singh, M., Rizwan, A., Hashem, S., et al. (2022). Liquid biopsy: A step closer to transform diagnosis, prognosis and future of cancer treatments. *Mol. cancer* 21, 79. doi:10.1186/s12943-022-01543-7

Lou, N., Ruan, A. M., Qiu, B., Bao, L., Xu, Y. C., Zhao, Y., et al. (2017). miR-144-3p as a novel plasma diagnostic biomarker for clear cell renal cell carcinoma. *Urologic Oncol. Seminars Orig. Investigations* 35, e7–e36. doi:10.1016/j.urolonc.2016.07.012

Lu, T., Wang, Y., Chen, D., Liu, J., and Jiao, W. (2018). Potential clinical application of lncRNAs in non-small cell lung cancer. *Onco Targets Ther.* 11, 8045–8052. doi:10.2147/OTT.S178431

Lunke, S., Maxwell, S., Khurana, I., Harikrishnan, K. N., Okabe, J., Al-Hasani, K., et al. (2021). Epigenetic evidence of an Ac/Dc axis by VPA and SAHA. *Clin. Epigenetics* 13, 58. doi:10.1186/s13148-021-01050-4

Luo, H., Wei, W., Ye, Z., Zheng, J., and Xu, R. (2021). Liquid biopsy of methylation biomarkers in cell-free DNA. *Trends Mol. Med.* 27, 482–500. doi:10.1016/j.molmed.2020.12.011

Luo, J., Li, Q., Pan, J., Li, L., Fang, L., and Zhang, Y. (2018). Expression level of long noncoding RNA H19 in plasma of patients with nonsmall cell lung cancer and its clinical significance. *J. Cancer Res. Ther.* 14, 860–863. doi:10.4103/jcrt.JCRT_733_17

Lyko, F. (2018). The DNA methyltransferase family: A versatile toolkit for epigenetic regulation. *Nat. Rev. Genet.* 19, 81–92. doi:10.1038/nrg.2017.80

Ma, J. Z., Yang, F., Zhou, C. C., Liu, F., Yuan, J. H., Wang, F., et al. (2017). METTL14 suppresses the metastatic potential of hepatocellular carcinoma by modulating N6-methyladenosine-dependent primary MicroRNA processing. *Hepatology* 65, 529–543. doi:10.1002/hep.28885

Madden, S. K., de Araujo, A. D., Gerhardt, M., Fairlie, D. P., and Mason, J. M. (2021). Taking the myc out of cancer: Toward therapeutic strategies to directly inhibit c-myc. *Mol. Cancer* 20, 3. doi:10.1186/s12943-020-01291-6

Manda, S., Anz, B., Benton, C., Broun, E. R., Yimer, H., Renshaw, J., et al. (2021). Treatment initiation of venetoclax in combination with azacitidine or decitabine in an outpatient setting in patients with untreated acute myeloid leukemia. *Blood* 138, 1265. doi:10.1182/blood-2021-144886

Martins, I., Ribeiro, I. P., Jorge, J., Gonçalves, A. C., Sarmento-Ribeiro, A. B., Melo, J. B., et al. (2021). Liquid biopsies: Applications for cancer diagnosis and monitoring. *Genes (Basel)* 12, 349. doi:10.3390/genes12030349

McClure, J. J., Li, X., and Chou, C. J. (2018). Advances and challenges of HDAC inhibitors in cancer therapeutics. *Adv. Cancer Res.* 138, 183–211. doi:10.1016/bs.acr.2018.02.006

Mego, M., Kalavska, K., Karaba, M., Minarik, G., Benca, J., Sedlackova, T., et al. (2020a). Plasma nucleosomes in primary breast cancer. *Cancers (Basel)* 12, 2587. doi:10.3390/cancers12092587

Mego, M., Kalavska, K., Karaba, M., Minarik, G., Benca, J., Sedlackova, T., et al. (2020b). Prognostic value of circulating nucleosomes in primary breast cancer. *J. Clin. Oncol.* 38, e12553. doi:10.1200/jco.2020.38.15_suppl.e12553

Michela, B. (2021). Liquid biopsy: A family of possible diagnostic tools. *Diagnostics* 11, 1391. doi:10.3390/diagnostics11081391

Miranda Furtado, C. L., dos Santos Luciano, M. C., Silva Santos, R., Furtado, G. P., Moraes, M. O., and Pessoa, C. (2019). Epidrugs: Targeting epigenetic marks in cancer treatment. *Epigenetics* 14, 1164–1176. doi:10.1080/15592294.2019.1640546

Monk, D., Mackay, D. J. G., Eggermann, T., Maher, E. R., and Riccio, A. (2019). Genomic imprinting disorders: Lessons on how genome, epigenome and environment interact. *Nat. Rev. Genet.* 20, 235–248. doi:10.1038/s41576-018-0092-0

Montalvo-Casimiro, M., González-Barrios, R., Meraz-Rodriguez, M. A., Juárez-González, V. T., Arriaga-Canon, C., and Herrera, L. A. (2020). Epidrug repurposing: Discovering new faces of old acquaintances in cancer therapy. *Front. Oncol.* 10, 605386. doi:10.3389/fonc.2020.605386

Moore, L. D., Le, T., and Fan, G. (2013). DNA methylation and its basic function. *Neuropsychopharmacology* 38, 23–38. doi:10.1038/npp.2012.112

Morel, D., Jeffery, D., Aspeslagh, S., Almouzni, G., and Postel-Vinay, S. (2020). Combining epigenetic drugs with other therapies for solid tumours — Past lessons and future promise. *Nat. Rev. Clin. Oncol.* 17, 91–107. doi:10.1038/s41571-019-0267-4

Nakano, S., Murakami, K., Meguro, M., Soejima, H., Higashimoto, K., Urano, T., et al. (2006). Express ion profile of LIT1/KCNQ1OT1 and epigenetic status at the KvDMR1 in colorectal cancers. *Cancer Sci.* 97, 1147–1154. doi:10.1111/j.1349-7006.2006.00305.x

Nishiyama, A., and Nakanishi, M. (2021). Navigating the DNA methylation landscape of cancer. *Trends Genet.* 37, 1012–1027. doi:10.1016/j.tig.2021.05.002

Nombela, P., Miguel-López, B., and Blanco, S. (2021). The role of m6A, m5C and Ψ RNA modifications in cancer: Novel therapeutic opportunities. *Mol. Cancer* 20, 18. doi:10.1186/s12943-020-01263-w

Oing, C., Skowron, M. A., Bokemeyer, C., and Nettersheim, D. (2019). Epigenetic treatment combinations to effectively target cisplatin-resistant germ cell tumors: Past, present, and future considerations. *Andrology* 7, 487–497. doi:10.1111/andr.12611

Olynik, B. M., and Rastegar, M. (2012). The genetic and epigenetic journey of embryonic stem cells into mature neural cells. *Front. Genet.* 3, 81. doi:10.3389/fgene.2012.00081

Palanca-Ballester, C., Rodriguez-Casanova, A., Torres, S., Calabuig-Fariñas, S., Exposito, F., Serrano, D., et al. (2021). Cancer epigenetic biomarkers in liquid biopsy for high incidence malignancies. *Cancers (Basel)* 13, 3016. doi:10.3390/cancers13123016

Pardini, B., Sabo, A. A., Birolo, G., and Calin, G. A. (2019). Noncoding rnas in extracellular fluids as cancer biomarkers: The new frontier of liquid biopsies. *Cancers (Basel)* 11, 1170. doi:10.3390/cancers11081170

Patil, D. P., Chen, C. K., Pickering, B. F., Chow, A., Jackson, C., Guttman, M., et al. (2016). M6 A RNA methylation promotes XIST-mediated transcriptional repression. *Nature* 537, 369–373. doi:10.1038/nature19342

Peng, Y., and Croce, C. M. (2016). The role of microRNAs in human cancer. *Signal Transduct. Target Ther.* 1, 15004. doi:10.1038/sigtrans.2015.4

Poeta, L., Drongitis, D., Verrillo, L., and Miano, M. G. (2020). Dna hypermethylation and unstable repeat diseases: A paradigm of transcriptional silencing to decipher the basis of pathogenic mechanisms. *Genes (Basel)* 11, 684. doi:10.3390/genes11060684

Qi, P., Zhou, X., and Du, X. (2016). Circulating long non-coding RNAs in cancer: Current status and future perspectives. *Mol. Cancer* 15, 39. doi:10.1186/s12943-016-0524-4

Quinn, J. J., and Chang, H. Y. (2016). Unique features of long non-coding RNA biogenesis and function. *Nat. Rev. Genet.* 17, 47–62. doi:10.1038/nrg.2015.10

Ramaiah, M. J., Tangutur, A. D., and Manyam, R. R. (2021). Epigenetic modulation and understanding of HDAC inhibitors in cancer therapy. *Life Sci.* 277, 119504. doi:10.1016/j.lfs.2021.119504

Ramanathan, A., Robb, G. B., and Chan, S. H. (2016). mRNA capping: Biological functions and applications. *Nucleic Acids Res.* 44, 7511–7526. doi:10.1093/nar/gkw551

Ramsahoye, B. H., Biniszkiewicz, D., Lyko, F., Clark, V., Bird, A. P., and Jaenisch, R. (2000). Non-CpG methylation is prevalent in embryonic stem cells and may be mediated by DNA methyltransferase 3a. *Proc. Natl. Acad. Sci. U. S. A.* 97, 5237–5242. doi:10.1073/pnas.97.10.5237

Ratti, M., Lampis, A., Ghidini, M., Salati, M., Mirchev, M. B., Valeri, N., et al. (2020). MicroRNAs (miRNAs) and long non-coding RNAs (lncRNAs) as new tools for cancer therapy: First steps from bench to bedside. *Target Oncol.* 15, 261–278. doi:10.1007/s11523-020-00717-x

Richon, V. M., Garcia-Vargas, J., and Hardwick, J. S. (2009). Development of vorinostat: Current applications and future perspectives for cancer therapy. *Cancer Lett.* 280, 201–210. doi:10.1016/j.canlet.2009.01.002

Rodriguez-Casanova, A., Costa-Fraga, N., Bao-Caamano, A., López-López, R., Muinelo-Romay, L., and Diaz-Lagares, A. (2021). Epigenetic landscape of liquid biopsy in colorectal cancer. *Front. Cell Dev. Biol.* 9, 622459. doi:10.3389/fcell.2021.622459

Rodriguez-Casanova, A., Costa-Fraga, N., Castro-Carballeira, C., González-Conde, M., Abuin, C., Bao-Caamano, A., et al. (2022). A genome-wide cell-free DNA methylation analysis identifies an episignature associated with metastatic luminal B breast cancer. *Front. Cell Dev. Biol.* 10, 1016955. doi:10.3389/fcell.2022.1016955

Rodríguez-Paredes, M., and Esteller, M. (2011). Cancer epigenetics reaches mainstream oncology. *Nat. Med.* 17, 330–339. doi:10.1038/nm.2305

Rumbajan, J. M., Maeda, T., Souzaki, R., Mitsui, K., Higashimoto, K., Nakabayashi, K., et al. (2013). Comprehensive analyses of imprinted differentially methylated regions reveal epigenetic and genetic characteristics in hepatoblastoma. *BMC Cancer* 13, 608. doi:10.1186/1471-2407-13-608

Saghafinia, S., Mina, M., Riggi, N., Hanahan, D., and Ciriello, G. (2018). Pan-cancer landscape of aberrant DNA methylation across human tumors. *Cell Rep.* 25, 1066–1080. doi:10.1016/j.celrep.2018.09.082

Sallman, D. A., DeZern, A. E., Garcia-Manero, G., Steensma, D. P., Roboz, G. J., Sekeres, M. A., et al. (2021). Eprenetapopt (APR-246) and azacitidine in TP53-mutant myelodysplastic syndromes. *J. Clin. Oncol.* 39, 1584–1594. doi:10.1200/JCO.20.02341

Samsonov, R., Shtam, T., Burdakov, V., Glotov, A., Tsyrlina, E., Berstein, L., et al. (2016). Lectin-induced agglutination method of urinary exosomes isolation followed by mi-RNA analysis: Application for prostate cancer diagnostic. *Prostate* 76, 68–79. doi:10.1002/pros.23101

San Miguel Amigo, L., Franco Osorio, R., Mercadal Vilchez, S., Martínez-Francés, A., and Martinez-FrAnces, A. (2011). Azacitidine adverse effects in patients with myelodysplastic syndromes. *Adv. Ther.* 28, 6–11. doi:10.1007/s12325-011-0024-2

Schaefer, M., Pollex, T., Hanna, K., Tuorto, F., Meusburger, M., Helm, M., et al. (2010). RNA methylation by Dnmt2 protects transfer RNAs against stress-induced cleavage. *Genes Dev.* 24, 1590–1595. doi:10.1101/gad.586710

Schmidt, B., Liebenberg, V., Dietrich, D., Schlegel, T., Kneip, C., Seegebarth, A., et al. (2010). SHOX2 DNA Methylation is a Biomarker for the diagnosis of lung cancer based on bronchial aspirates. *BMC Cancer* 10, 600. doi:10.1186/1471-2407-10-600

Schwartz, S., Bernstein, D. A., Mumbach, M. R., Jovanovic, M., Herbst, R. H., León-Ricardo, B. X., et al. (2014). Transcriptome-wide mapping reveals widespread dynamic-regulated pseudouridylation of ncRNA and mRNA. *Cell* 159, 148–162. doi:10.1016/j.cell.2014.08.028

Seligson, D. B., Horvath, S., Shi, T., Yu, H., Tze, S., Grunstein, M., et al. (2005). Global histone modification patterns predict risk of prostate cancer recurrence. *Nature* 435, 1262–1266. doi:10.1038/nature03672

Shao, J., Wang, S., West-Szymanski, D., Karpus, J., Shah, S., Ganguly, S., et al. (2022). Cell-free DNA 5-hydroxymethylcytosine is an emerging marker of acute myeloid leukemia. *Sci. Rep.* 12, 12410. doi:10.1038/s41598-022-16685-3

Shen, C., Wang, K., Deng, X., and Chen, J. (2022). DNA N6-methyldeoxyadenosine in mammals and human disease. *Trends Genet.* 38, 454–467. doi:10.1016/j.tig.2021.12.003

Šimoničová, K., Janotka, Ľ., Kavcová, H., Sulová, Z., Breier, A., and Messingerova, L. (2022). Different mechanisms of drug resistance to hypomethylating agents in the treatment of myelodysplastic syndromes and acute myeloid leukemia. *Drug Resist. Updat.* 61, 100805. doi:10.1016/j.drup.2022.100805

Skinner, M. K. (2011). Role of epigenetics in developmental biology and transgenerational inheritance. *Birth Defects Res. C Embryo Today* 93, 51–55. doi:10.1002/bdrc.20199

Slack, F. J., and Chinnaiyan, A. M. (2019). The role of non-coding RNAs in oncology. *Cell* 179, 1033–1055. doi:10.1016/j.cell.2019.10.017

Slamon, D. J., and Cline, M. J. (1984). Expression of cellular oncogenes during embryonic and fetal development of the mouse. *Proc. Natl. Acad. Sci. U. S. A.* 81, 7141–7145. doi:10.1073/pnas.81.22.7141

Song, C. X., Yin, S., Ma, L., Wheeler, A., Chen, Y., Zhang, Y., et al. (2017). 5-Hydroxymethylcytosine signatures in cell-free DNA provide information about tumor types and stages. *Cell Res.* 27, 1231–1242. doi:10.1038/cr.2017.106

Souza, C. R. T., Leal, M. F., Calcagno, D. Q., Costa Sozinho, E. K., Borges, B. N., Montenegro, R. C., et al. (2013). MYC deregulation in gastric cancer and its clinicopathological implications. *PLoS One* 8, e64420. doi:10.1371/journal.pone.0064420

Spencer, D. H., Russler-Germain, D. A., Ketkar, S., Helton, N. M., Lamprecht, T. L., Fulton, R. S., et al. (2017). CpG island hypermethylation mediated by DNMT3A is a consequence of AML progression. *Cell* 168, 801–816. doi:10.1016/j.cell.2017.01.021

Squires, J. E., Patel, H. R., Nousch, M., Sibbritt, T., Humphreys, D. T., Parker, B. J., et al. (2012). Widespread occurrence of 5-methylcytosine in human coding and non-coding RNA. *Nucleic Acids Res.* 40, 5023–5033. doi:10.1093/nar/gks144

Steensma, D. P. (2009). Decitabine treatment of patients with higher-risk myelodysplastic syndromes. *Leuk. Res.* 33, S12–S17. doi:10.1016/S0145-2126(09)70228-0

Stomper, J., Rotondo, J. C., Greve, G., and Lübbert, M. (2021). Hypomethylating agents (HMA) for the treatment of acute myeloid leukemia and myelodysplastic syndromes: Mechanisms of resistance and novel HMA-based therapies. *Leukemia* 35, 1873–1889. doi:10.1038/s41375-021-01218-0

Stresemann, C., and Lyko, F. (2008). Modes of action of the DNA methyltransferase inhibitors azacytidine and decitabine. *Int. J. Cancer* 123, 8–13. doi:10.1002/ijc.23607

Su, M., Xiao, Y., Ma, J., Tang, Y., Tian, B., Zhang, Y., et al. (2019). Circular RNAs in Cancer: Emerging functions in hallmarks, stemness, resistance and roles as potential biomarkers. *Mol. Cancer* 18, 90. doi:10.1186/s12943-019-1002-6

Sun, Y., Hong, J. H., Ning, Z., Pan, D., Fu, X., Lu, X., et al. (2022). Therapeutic potential of tucidinostat, a subtype-selective HDAC inhibitor, in cancer treatment. *Front. Pharmacol.* 13, 932914. doi:10.3389/fphar.2022.932914

Suraweera, A., O'Byrne, K. J., and Richard, D. J. (2018). Combination therapy with histone deacetylase inhibitors (HDACi) for the treatment of cancer: Achieving the full therapeutic potential of HDACi. *Front. Oncol.* 8, 92. doi:10.3389/fonc.2018.00092

Suvà, M. L., Riggi, N., and Bernstein, B. E. (2013). Epigenetic reprogramming in cancer. *Science* 339, 1567–1570. doi:10.1126/science.1230184

Taniue, K., and Akimitsu, N. (2021). The functions and unique features of lncrnas in cancer development and tumorigenesis. *Int. J. Mol. Sci.* 22, 632. doi:10.3390/ijms22020632

Taniue, K., Kurimoto, A., Takeda, Y., Nagashima, T., Okada-Hatakeyama, M., Katou, Y., et al. (2016). ASBEL-TCF3 complex is required for the tumorigenicity of colorectal cancer cells. *Proc. Natl. Acad. Sci. U. S. A.* 113, 12739–12744. doi:10.1073/pnas.1605938113

Topper, M. J., Vaz, M., Marrone, K. A., Brahmer, J. R., and Baylin, S. B. (2020). The emerging role of epigenetic therapeutics in immuno-oncology. *Nat. Rev. Clin. Oncol.* 17, 75–90. doi:10.1038/s41571-019-0266-5

Torrano, J., al Emran, A., Hammerlindl, H., and Schaider, H. (2019). Emerging roles of H3K9me3, SETDB1 and SETDB2 in therapy-induced cellular reprogramming. *Clin. Epigenetics* 11, 43. doi:10.1186/s13148-019-0644-y

Torsin, L. I., Petrescu, G. E. D., Sabo, A. A., Chen, B., Brehar, F. M., Dragomir, M. P., et al. (2021). Editing and chemical modifications on non-coding rnas in cancer: A new tale with clinical significance. *Int. J. Mol. Sci.* 22, 581. doi:10.3390/ijms22020581

Tsai, H. C., Wei, K. C., Chen, P. Y., Huang, C. Y., Chen, K. T., Lin, Y. J., et al. (2021). Valproic acid enhanced temozolomide-induced anticancer activity in human glioma through the p53–PUMA apoptosis pathway. *Front. Oncol.* 11, 722754. doi:10.3389/fonc.2021.722754

Tusong, H., Maolakuerban, N., Guan, J., Rexiati, M., Wang, W. G., Azhati, B., et al. (2017). Functional analysis of serum microRNAs miR-21 and miR-106a in renal cell carcinoma. *Cancer Biomarkers* 18, 79–85. doi:10.3233/CBM-160676

Tweedie-Cullen, R. Y., Brunner, A. M., Grossmann, J., Mohanna, S., Sichau, D., Nanni, P., et al. (2012). Identification of combinatorial patterns of post-translational modifications on individual histones in the mouse brain. *PLoS One* 7, e36980. doi:10.1371/journal.pone.0036980

Van den Ackerveken, P., Lobbens, A., Turatsinze, J. V., Solis-Mezarino, V., Völker-Albert, M., Imhof, A., et al. (2021). A novel proteomics approach to epigenetic profiling of circulating nucleosomes. *Sci. Rep.* 11, 7256. doi:10.1038/s41598-021-86630-3

Vandiver, A. R., Idrizi, A., Rizzardi, L., Feinberg, A. P., and Hansen, K. D. (2015). DNA methylation is stable during replication and cell cycle arrest. *Sci. Rep.* 5, 17911. doi:10.1038/srep17911

Veland, N., Lu, Y., Hardikar, S., Gaddis, S., Zeng, Y., Liu, B., et al. (2019). DNMT3L facilitates DNA methylation partly by maintaining DNMT3A stability in mouse embryonic stem cells. *Nucleic Acids Res.* 47, 152–167. doi:10.1093/nar/gky947

Velho, S., Fernandes, M. S., Leite, M., Figueiredo, C., and Seruca, R. (2014). Causes and consequences of microsatellite instability in gastric carcinogenesis. *World J. Gastroenterol.* 20, 16433–16442. doi:10.3748/wjg.v20.i44.16433

Villanueva, L., Álvarez-Errico, D., and Esteller, M. (2020). The contribution of epigenetics to cancer immunotherapy. *Trends Immunol.* 41, 676–691. doi:10.1016/j.it.2020.06.002

Waddington, C. H. (1959). Canalization of development and genetic assimilation of acquired characters. *Nature* 183, 1654–1655. doi:10.1038/1831654a0

Wan, T., Wang, H., Gou, M., Si, H., Wang, Z., Yan, H., et al. (2020). LncRNA HEIH promotes cell proliferation, migration and invasion in cholangiocarcinoma by modulating miR-98-5p/HECTD4. *Biomed. Pharmacother.* 125, 109916. doi:10.1016/j.biopha.2020.109916

Wang, L., Duan, W., Yan, S., Xie, Y., and Wang, C. (2019). Circulating long non-coding RNA colon cancer-associated transcript 2 protected by exosome as a potential biomarker for colorectal cancer. *Biomed. Pharmacother.* 113, 108758. doi:10.1016/j.biopha.2019.108758

Wang, P., Yan, Y., Yu, W., and Zhang, H. (2019). Role of ten-eleven translocation proteins and 5-hydroxymethylcytosine in hepatocellular carcinoma. *Cell Prolif.* 52, e12626. doi:10.1111/cpr.12626

Wang, Y., Hu, H., Wang, Q., Li, Z., Zhu, Y., Zhang, W., et al. (2017). The level and clinical significance of 5-hydroxymethylcytosine in oral squamous cell carcinoma: An immunohistochemical study in 95 patients. *Pathol. Res. Pract.* 213, 969–974. doi:10.1016/j.prp.2017.04.016

Wang, Y., Tong, C., Dai, H., Wu, Z., Han, X., Guo, Y., et al. (2021). Low-dose decitabine priming endows CAR T cells with enhanced and persistent antitumour potential via epigenetic reprogramming. *Nat. Commun.* 12, 409. doi:10.1038/s41467-020-20696-x

Weber, D. G., Johnen, G., Casjens, S., Bryk, O., Pesch, B., Jöckel, K. H., et al. (2013). Evaluation of long noncoding RNA MALAT1 as a candidate blood-based biomarker for the diagnosis of non-small cell lung cancer. *BMC Res. Notes* 6, 518. doi:10.1186/1756-0500-6-518

Wu, Q., Schapira, M., Arrowsmith, C. H., and Barsyte-Lovejoy, D. (2021). Protein arginine methylation: From enigmatic functions to therapeutic targeting. *Nat. Rev. Drug Discov.* 20, 509–530. doi:10.1038/s41573-021-00159-8

Wu, X., Zhang, Y., Hu, T., He, X., Zou, Y., Deng, Q., et al. (2021). A novel cell-free DNA methylation-based model improves the early detection of colorectal cancer. *Mol. Oncol.* 15, 2702–2714. doi:10.1002/1878-0261.12942

Xiao, C., Zhu, S., He, M., Chen, D., Zhang, Q., Chen, Y., et al. (2018). N 6 -methyladenine DNA modification in the human genome. *Mol. Cell* 71, 306–318. doi:10.1016/j.molcel.2018.06.015

Xiao, L., Wang, J., Ju, S., Cui, M., and Jing, R. (2022). Disorders and roles of tsRNA, snoRNA, snRNA and piRNA in cancer. *J. Med. Genet.* 59, 623–631. doi:10.1136/jmedgenet-2021-108327

Xiao, W., Zhou, Q., Wen, X., Wang, R., Liu, R., Wang, T., et al. (2021). Small-molecule inhibitors overcome epigenetic reprogramming for cancer therapy. *Front. Pharmacol.* 12, 702360. doi:10.3389/fphar.2021.702360

Xu, H., Zhang, Y., Qi, L., Ding, L., Jiang, H., and Yu, H. (2018). NFIX circular RNA promotes glioma progression by regulating miR-34a-5p via notch signaling pathway. *Front. Mol. Neurosci.* 11, 225. doi:10.3389/fnmol.2018.00225

Xu, L., Zhou, Y., Chen, L., Bissessur, A. S., Chen, J., Mao, M., et al. (2021). Deoxyribonucleic acid 5-hydroxymethylation in cell-free deoxyribonucleic acid, a novel cancer biomarker in the era of precision medicine. *Front. Cell Dev. Biol.* 9, 744990. doi:10.3389/fcell.2021.744990

Xu, N., Tse, B., Yang, L., Tang, T. C. Y., Haber, M., Micklethwaite, K., et al. (2021). Priming leukemia with 5-Azacytidine enhances CAR T cell therapy. *Immunotargets Ther.* 10, 123–140. doi:10.2147/ITT.S296161

Xu, Y., Li, P., Liu, Y., Xin, D., Lei, W., Liang, A., et al. (2022). Epi-immunotherapy for cancers: Rationales of epi-drugs in combination with immunotherapy and advances in clinical trials. *Cancer Commun.* 42, 493–516. doi:10.1002/cac2.12313

Yao, R. W., Wang, Y., and Chen, L. L. (2019). Cellular functions of long noncoding RNAs. *Nat. Cell Biol.* 21, 542–551. doi:10.1038/s41556-019-0311-8

Yin, T., Zhao, D., and Yao, S. (2021). Identification of a genome instability-associated LncRNA signature for prognosis prediction in colon cancer. *Front. Genet.* 12, 679150. doi:10.3389/fgene.2021.679150

Yin, Z., Cui, Z., Li, H., Li, J., and Zhou, B. (2018). Polymorphisms in the H19 gene and the risk of lung Cancer among female never smokers in Shenyang, China. *BMC Cancer* 18, 893. doi:10.1186/s12885-018-4795-6

Yu, G., Wu, Y., Wang, W., Xu, J., Lv, X., Cao, X., et al. (2019). Low-dose decitabine enhances the effect of PD-1 blockade in colorectal cancer with microsatellite stability by re-modulating the tumor microenvironment. *Cell Mol. Immunol.* 16, 401–409. doi:10.1038/s41423-018-0026-y

Zafon, C., Gil, J., Pérez-González, B., and Jordà, M. (2019). DNA methylation in thyroid cancer. *Endocr. Relat. Cancer* 26, R415–R439. doi:10.1530/ERC-19-0093

Zahavi, D., and Weiner, L. (2020). Monoclonal antibodies in cancer therapy. *Antibodies* 9, 34–20. doi:10.3390/antib9030034

Zhai, Q., Zhou, L., Zhao, C., Wan, J., Yu, Z., Guo, X., et al. (2012). Identification of miR-508-3p and miR-509-3p that are associated with cell invasion and migration and involved in the apoptosis of renal cell carcinoma. *Biochem. Biophys. Res. Commun.* 419, 621–626. doi:10.1016/j.bbrc.2012.02.060

Zhang, H., Hamblin, M. H., and Yin, K. J. (2017b). The long noncoding RNA Malat1: Its physiological and pathophysiological functions. *RNA Biol.* 14, 1705–1714. doi:10.1080/15476286.2017.1358347

Zhang, H., Wang, G., Ding, C., Liu, P., Wang, R., Ding, W., et al. (2017a). Increased circular RNA UBAP2 acts as a sponge of miR-143 to promote osteosarcoma progression. *Oncotarget* 8, 61687–61697. doi:10.18632/oncotarget.18671

Zhang, L., Lu, Q., and Chang, C. (2020). Epigenetics in health and disease. *Adv. Exp. Med. Biol.* 1253, 3–55. doi:10.1007/978-981-15-3449-2_1

Zhang, L., Xiong, D., Liu, Q., Luo, Y., Tian, Y., Xiao, X., et al. (2021a). Genome-wide histone H3K27 acetylation profiling identified genes correlated with prognosis in papillary thyroid carcinoma. *Front. Cell Dev. Biol.* 9, 682561. doi:10.3389/fcell.2021.682561

Zhang, L., Zhang, J., Diao, L., and Han, L. (2021b). Small non-coding RNAs in human cancer: Function, clinical utility, and characterization. *Oncogene* 40, 1570–1577. doi:10.1038/s41388-020-01630-3

Zhang, L., Zhao, D., Yin, Y., Yang, T., You, Z., Li, D., et al. (2021c). Circulating cell-free DNA-based methylation patterns for breast cancer diagnosis. *NPJ Breast Cancer* 7, 106. doi:10.1038/s41523-021-00316-7

Zhao, A., Li, G., Péoc'h, M., Genin, C., and Gigante, M. (2013). Serum miR-210 as a novel biomarker for molecular diagnosis of clear cell renal cell carcinoma. *Exp. Mol. Pathol.* 94, 115–120. doi:10.1016/j.yexmp.2012.10.005

Zhao, G., Wang, Q., Li, S., and Wang, X. (2021). Resistance to hypomethylating agents in myelodysplastic syndrome and acute myeloid leukemia from clinical data and molecular mechanism. *Front. Oncol.* 11, 706030. doi:10.3389/fonc.2021.706030

Zhao, Z., and Shilatifard, A. (2019). Epigenetic modifications of histones in cancer. *Genome Biol.* 20, 245. doi:10.1186/s13059-019-1870-5

Zheng, Z. Q., Li, Z. X., Zhou, G. Q., Lin, L., Zhang, L. L., Lv, J. W., et al. (2019). Long noncoding RNA FAM225A promotes nasopharyngeal carcinoma tumorigenesis and metastasis by acting as ceRNA to sponge miR-590-3p/miR-1275 and upregulate ITGB3. *Cancer Res.* 79, 4612–4626. doi:10.1158/0008-5472.CAN-19-0799

Zimta, A. A., Tomuleasa, C., Sahnoune, I., Calin, G. A., and Berindan-Neagoe, I. (2019). Long non-coding RNAs in myeloid malignancies. *Front. Oncol.* 9, 1048. doi:10.3389/fonc.2019.01048

Frontiers in
Cell and Developmental Biology

Explores the fundamental biological processes of life, covering intracellular and extracellular dynamics.

The world's most cited developmental biology journal, advancing our understanding of the fundamental processes of life. It explores a wide spectrum of cell and developmental biology, covering intracellular and extracellular dynamics.

Discover the latest Research Topics

See more →

Frontiers

Avenue du Tribunal-Fédéral 34
1005 Lausanne, Switzerland
frontiersin.org

Contact us

+41 (0)21 510 17 00
frontiersin.org/about/contact